Polish Academy of Sciences
University of Engineering and Economics in Rzeszów

TEKA

COMMISSION OF MOTORIZATION AND ENERGETICS IN AGRICULTURE

AN INTERNATIONAL QUARTERLY JOURNAL ON MOTORIZATION, VEHICLE OPERATION, ENERGY EFFICIENCY AND MECHANICAL ENGINEERING

Vol. 13, No 1

LUBLIN – RZESZÓW 2013

Editorial Office address

Commission of Motorization and Energetics in Agriculture
Wielkopolska Str. 62, 20-725 Lublin, Poland
e-mail: eugeniusz.krasowski@up.lublin.pl

ISSN 1641-7739

Edition 150+16 vol.

TEKA. COMMISSION OF MOTORIZATION AND ENERGETICS IN AGRICULTURE – 2013, Vol. 13, No. 1, 3–8

Evaluation of changes in traction properties of tyres on selected farming surfaces

Włodzimierz Białczyk, Marek Brennensthul, Anna Cudzik, Jarosław Czarnecki

Institute of Agricultural Engineering, Wroclaw University of Environmental and Life Sciences
ul. Chełmońskiego 37/41, 51-630 Wrocław, e-mail: marek.brennensthul@up.wroc.pl

Received January 5.2013; accepted March 14.2013

Summary. The paper presents the results of tests on two tractor tyres with different designs and external dimensions; these tyres were tested on farming surfaces with various properties. The tests were carried out using a stand operating with a farm tractor. Changes in traction properties were evaluated; values of forces (pulling and traction), rolling resistance, and tractive efficiency were analysed, and the balance of power on the tested wheels was established. It was demonstrated that the two tyres reacted in different ways to the change of surface.
Key words: farm tractor, traction force, tractive efficiency, rolling resistance, power balance

INTRODUCTION

Farm tractors are the main sources of pulling energy in farming. Currently, a substantial group includes multi-purpose tractors with lower pulling classes, one superior feature of these vehicles is variety of application. Such tractors can be used for various field procedures as well as for transportation work, quite often they are also used in other special purpose tasks.

The consequence of farm tractor versatility is the fact that they are used on differentiated surfaces with various properties. The manner of utilisation is connected with different conditions of interaction between the vehicle wheels and the surface. On more deformable surfaces, a bigger immersion of the wheel will occur, as a result of which traction force will be transferred by shearing of the top layer of the surface. On the other hand, on less deformable surfaces, where immersion of the wheel is limited, the phenomenon of friction will prevail during transfer of traction force [15, 22, 25]. It should be mentioned that for economic reasons multi-purpose farm tractors are usually equipped with one set of tyres – tyres are not replaced when the type of surface changes. It is reasonable to ask the question: what type of tyres will be optimal for the multi-purpose farm tractor?

In the literature, studies discussing compatibility of farm vehicle tyres with surfaces of various properties can be found. It was proven that on surfaces with lower strength, greater amounts of wheel rolling resistance and slip occurred, and as a consequence greater losses of energy and lower tractive efficiency [1, 2, 3, 10, 11]. However, tractive efficiency describes only the ratio of power on the outlet and intake of the wheel/surface system, but does not show with what phenomena losses in the system were connected [22, 23]. Bearing this in mind, it seems reasonable to carry out power balancing which will describe in detail what proportion of power is used in the form of pulling force and how much power is lost to rolling resistance and wheel slip [24]. Until now, this issue has been raised in a small number of studies [13, 14, 21]. It is reasonable to examine it with respect to various tyres on different surfaces.

OBJECTIVE, SUBJECT MATTER AND TESTING METHOD

The causes presented in the introduction led to the undertaking of tests the objectives of which were to:
- determine and compare the values of traction force, pulling force, rolling resistance and tractive efficiency of wheels provided with different tyres,
- analyse changes of tractive properties as a result of changes of surface type,
- determine the power of wheels provided with the tested tyres on different surfaces based on the completed energy balance.

Two tyres were accepted for testing differing both in internal design and external dimensions. One common feature of both tyres was the tread type – classic, Mitas was the producer of both tyres. The basic parameters of the tested tyres are presented in Table 1.

Table 1. Parameters of tyres accepted for testing

Tyre identification	Design	External diameter [mm]	Width [mm]	Height of tread protrusions [mm]	Maximum load [kg]	Maximum inflation pressure [MPa]
11.2R24	radial	1060	285	35	1215	0.25
31×15.5-15	diagonal	785	390	25	1400	0.25

According to data presented in the table above, tyre 11.2R24 was characterized by greater external diameter and height of tread protrusions, but lesser width. During testing, one level of static vertical load of wheels was used amounting to 542 kg (5320 N) and falling within the ranges of catalogue loads provided by the producer. Inflation pressure in both tyres was 0.15 MPa – selection of this value was dictated by the fact that it is typical for the multi-purpose nature of the farm tractor operation.

Following acceptance of the concept, the tests were performed on two surfaces with different properties. The first surface was stubble after wheat growth, and the other one – ground forest road. The conditions of both surfaces were characterized on the basis of conducted measurements of moisture, compactness and shearing stresses. The results of these measurements are presented in table 2; the values of compactness and shearing stresses were established using mean values calculated for the measurement depth of 0 – 0,1 m.

Table 2. Parameters of the tested surfaces

Surface	Parameter		
	moisture [%]	compactness [MPa]	shearing stresses [kPa]
Stubble	19	1.46	46
Ground road	7	2.29	91

Tests of tractive properties were conducted using a specialist stand suitable for operation with a farm tractor, class 9,0 kN. This stand is illustrated schematically in Figure 1.

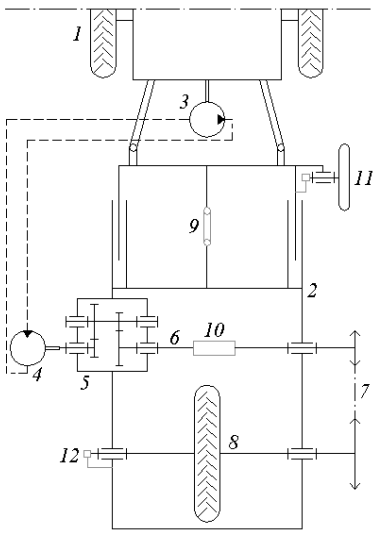

Fig. 1. Scheme of the stand for testing tractive properties (description in the text)

All elements of the stand are placed on a two-part frame (2). Drive for the tested wheel mounted on the shaft (8) was obtained from the power take-off of the tractor (1) through the hydraulic system (hydraulic motor 3, hydraulic pump 4), mechanical gear reducer (5), countershaft (6) and chain drive (7). Measurement of pulling force was carried out using an induction dynamometer (9) with measurement accuracy of 1 N and range of 0 – 20000 N. This dynamometer was located between the front and rear parts of the frame. Measurement of torque was conducted using an induction torque meter placed on the countershaft (10); measurement accuracy was 1 Nm and range 0 – 3000 Nm. For measurement of the actual distance, a potentiometric sensor placed near the additional wheel (11) was used, and the theoretical distance was determined using a sensor (12) placed near the shaft with the tested wheel. All the measured data were transmitted to an electronic registering unit operating with a portable computer.

Testing of traction properties consisted in transmitting drive to the tested wheel and setting the stand and the tractor in motion together. During driving, data measured by the sensors was registered continuously. In the final part of the measurement, the stand was braked using the main brake of the tractor which forced 100% slipping and as a result a full range of slipping for the tested wheel was obtained.

Based on the measured parameters, slip of the tested wheels and values of traction force, pulling force and tractive efficiency were calculated according to formulas 1 – 4:

$$\delta = 100\left(1 - \frac{s_R}{s_T}\right), \quad [1]$$

$$P_T = \frac{M_O}{r_D}, \quad [2]$$

$$P_f = P_T - P_H, \quad [3]$$

$$\eta = \frac{P_H}{M_O} r_D \left(100 - \delta\right), \quad [4]$$

where:
δ – wheel slip [%],
sR – actual distance of the wheel [m],
sT – theoretical distance of the wheel [m],
PT – traction force [N],
MO – wheel torque [Nm],
rD – dynamic radius of the wheel [m],
Pf – rolling resistance [N],
PH – pulling force [N],
η – tractive efficiency [%].

The value of dynamic radius (*rD*) was determined based on the measured value of the distance covered by the wheel during ten full rotations.

Power balancing of wheels equipped with the tested tyres was carried out based on values determined according to formulas 5 – 9:

$$N_k = N_H + N_f + N_\delta, \quad [5]$$

$$N_H = P_H v_R, \quad [6]$$

$$N_f = P_f v_R, \quad [7]$$

$$N_\delta = P_T \left(r_D - \frac{v_R}{\omega_T} \right) \frac{v_T}{r_D}, \quad [8]$$

$$\omega_T = \frac{v_T}{r_D}, \quad [9]$$

where:

Nk – power supplied to the wheel (total) [W],

NH – pulling power [W],

Nf – power lost to overcome rolling resistance [W],

Nδ – power lost to slipping [W],

vR – actual velocity (ratio of actual distance to measurement time) [ms^{-1}],

vT – theoretical velocity (ratio of theoretical distance to measurement time) [ms^{-1}].

TEST RESULTS

Figure 2 presents the courses of traction force as a function of slipping of wheels equipped with the tested tyres, on both types of surface.

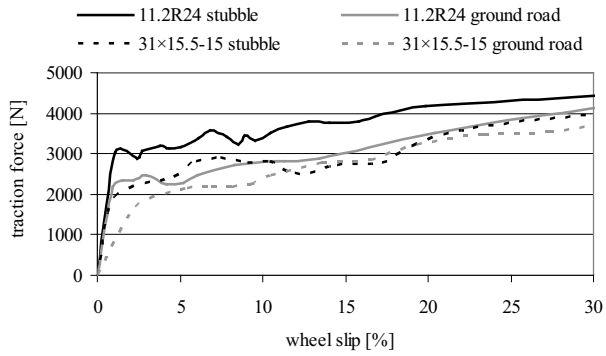

Fig. 2. Courses of traction force of the tested tyres on both tested surfaces as a function of wheel slip

According to the above figure, the largest values of traction force within the entire slip range considered concerned tyre 11.2R24 on the stubble. The greatest growth of this parameter was observed for slip within the range of 0 – 2%. The value of traction force for tyre 11.2R24 on the road and 31×15.5-15 on the stubble were similar. The lowest values of the analysed parameter occurred for tyre 31×15.5-15 on the road; in this case, the lowest growth of traction force with low slip values was also recorded. To some extent, the courses obtained relates to results presented in the literature. It was shown that traction force increases at the highest rate with low slip values [4, 5, 6, 12, 16, 19]. On the other hand, Bashford and others [1] showed that a greater difference in the values of the traction force of tyres with different diameters is associated with more deformable surfaces, which is confirmed in the presented test results.

Since traction force is the sum of pulling force and rolling resistance, it is reasonable to present the proportions of these components. The summary of mean values of these parameters calculated for slip within the range of 0 – 30% is illustrated in figure 3.

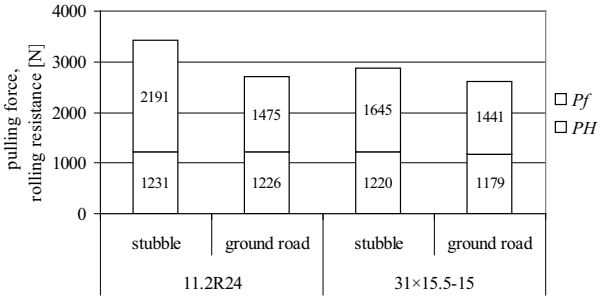

Fig. 3. Summary of mean values of pulling force and rolling resistance for the tested tyres on both surfaces with slips within the range of 0 – 30% (the sum of rolling resistance Pf and pulling force PH is traction force PT)

The analysis of the above summary allows us to conclude that both tyres on various surfaces were characterized by similar values of pulling force (relative difference did not exceed 5%). However, differences in the values of rolling resistance were larger. On both surfaces, higher values of this parameter were obtained by tyre 11.2R14, for this tyre also a higher change in rolling resistance as a result of changing the surface type was observed. Tyre 11.2R24 had smaller width so it should be assumed that the higher rolling resistance is the effect of its greater immersion in the surface. In all cases, values of rolling resistance were higher than values of pulling force – this situation was connected to the method of conducting the measurement; the resistance of motion of the entire stand consisted of rolling resistance of the tested wheel and rolling resistance of the tractor wheels within which the stand was operating. The results presented correspond with the results of other researchers; it was proven that higher values of traction force (that is the sum of pulling force and rolling resistance) were associated with surfaces with lower strength [2, 8, 9]. It was also highlighted that on less resistant surfaces, the values of rolling resistance are higher [3, 5], which also confirms the results of the completed tests.

Another parameter analysed was tractive efficiency. As with traction force, it was presented as a function of slip – the courses are presented in Figure 4.

While analysing the above courses, it can be observed that higher values of tractive efficiency were obtained by both tyres on the ground road. Within the slip range of 0 – 5%, the highest values and growths of the analysed parameter appear for tyre 11.2R24, with higher slips, slightly higher efficiency was obtained by tyre 31×15.5-15. The lowest tractive effi-

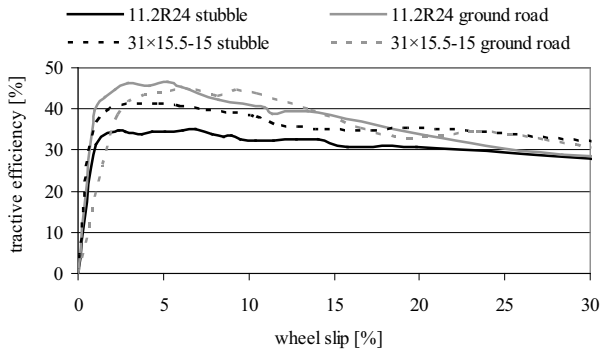

Fig. 4. Courses of tractive efficiency of the tested tyres on both tested surfaces as a function of wheel slip

ciency concerned tyre 11.2R24 on the stubble, and the lowest growth of efficiency occurred in the case of tyre 31×15.5-15 on the ground road. Presumably, lower values of efficiency on the stubble were caused by higher deformability of this surface, and as a consequence higher rolling resistance. In addition, tyre 31×15.5-15, due to greater width, showed a lesser tendency to immerse in the surface, therefore the efficiency of this tyre on the stubble was higher. The character of changes in tractive efficiency as a function of slip relates to results presented in the literature; it was proven that the highest growths of efficiency occurred with low slips, after which stabilization of courses took place [2, 16, 22]. However, in some studies, values of slip at which maximum efficiency occurred were higher than in the obtained test results [17, 18]. It was also demonstrated that tyres with larger external diameters achieved higher tractive efficiencies [8]. The dependency between tyre diameter and values of efficiency on various surfaces is confirmed in the study by Bashford [1].

Tractive efficiency is a parameter which does not describe accurately the type of energy losses that dominate in the wheel/surface system. Hence it is reasonable to perform energy balancing which will show what part of the power supplied to the wheel is used in the form of pulling force and what parts of power are lost to rolling resistance and wheel slip. Figure 5 illustrates courses of power as a function of slip on the stubble.

Based on the courses presented in figure 5, it can be concluded that the character of changes in individual powers as a function of slip was similar for both wheels, however the values of these powers made the difference. Higher values of power were achieved by the wheel with tyre 11.2R24. In both cases, at low slip values (0 – 2%), considerable increases in pulling power, power lost to rolling resistance and total power were observed. After exceeding 2% slip, pulling power and power lost to rolling resistance showed small changes and lack of growth. In both cases, power lost to slip was showed growth proportional to slip, and for the wheel with tyre 31×15.5-15 an increased rate of growth was noticed after exceeding 15% slip.

Figure 6 illustrates courses of power as a function of slip on the ground road.

On the second of the tested surfaces (Fig. 6), the character of courses is slightly different than in the case described previously; for both wheels, fluctuations of power values

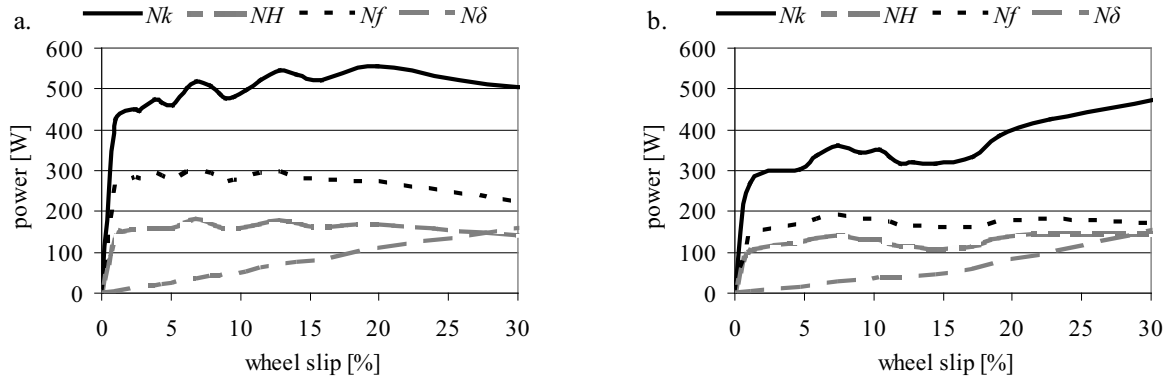

Fig. 5. Courses of power as a function of slip on the stubble: a – wheel with tyre 11.2R24, b – wheel with tyre 31×15.5-15

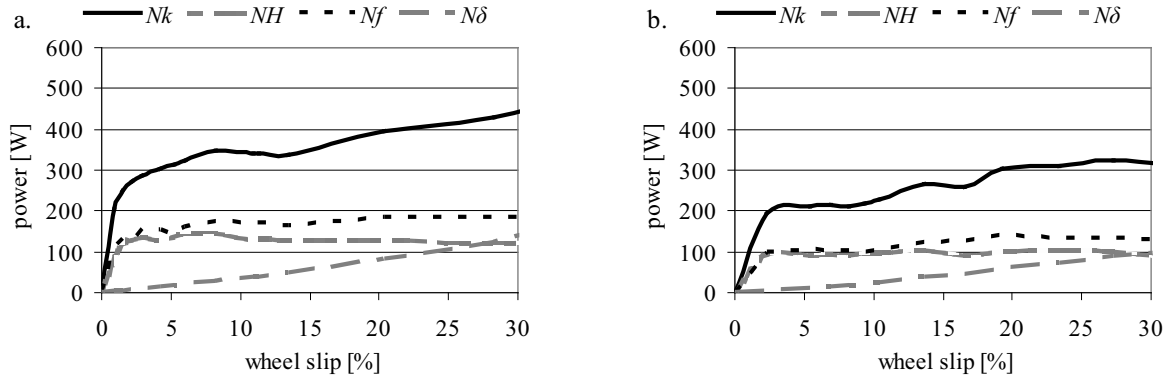

Fig. 6. Courses of power as a function of slip on the ground road: a – wheel with tyre 11.2R24, b – wheel with tyre 31×15.5-15

were lower than on the stubble. The highest increases in total power, pulling power and power lost to rolling resistance occurred at slip within the range of 0 – 3%. For the wheel with tyre 31×15.5-15, it was observed that at slip of 0 – 10%, the values of pulling power and power lost to rolling resistance were maintained at a similar level, when slip was higher, higher values related to power lost to rolling resistance. Power lost to slip for both wheels showed growth proportional to the growth of slip, a slightly higher growth rate was recorded for the wheel with tyre 11.2R24.

The character of changes in power as a function of slip is similar to other test results. It was proven that the greatest increase in pulling power, power lost to rolling resistance and total power occurred at low slips, after which the courses was stabilized, the character of changes in power lost to slip was also similar [9, 13, 14, 20, 21].

In order to determine differences between values of individual powers, mean values of these calculated for slip within the range of 0 – 30% were summarized (Fig. 7). According to this summary, higher values of total power occurred for the wheel with tyre 11.2R24. For both wheels, higher demand for total power appeared on the stubble, and for the wheel with tyre 11.2R24 the difference in the values of power on the two surfaces was higher than for the other wheel. This situation is probably connected with a different degree of deformability for the two tested surfaces and as a consequence different values of rolling resistance. Confirmation of this statement can be the fact that the greatest differences concerned only power lost to wheel rolling resistance.

Since the values of total power presented above differed, comparison of the two wheels on the tested surfaces required presentation of the shares of individual powers in total power. Such summary is illustrated in Figure 8.

Analysing the above summary it can be stated that the proportions of shares of power for the two tyres were different; there was also dissimilarity with respect to various surfaces. The highest shares of pulling for both wheels occurred on the ground road, and the lowest share of this power occurred for the wheel with tyre 11.2R24 on the stubble. In this case, the highest share of power lost to rolling resistance was also observed. Furthermore, it can be observed that tyre 31×15.5-15 was characterized by lower changes of shares of individual powers as a result of change of surface type. Different proportions of power shares on individual surfaces are probably connected with the different degrees of deformability of these surfaces and different values of rolling resistance. A different degree of response of the two wheels to the change of surface type can be the result of the different external dimensions of tyres; tyre 31×15.5-15 was characterized by greater width, hence its immersion effect could be smaller than for tyre 11.2R24. Similar values regarding shares of power lost to slipping for both wheels can be caused by a similar design of tread.

The obtained results were processed using statistical analysis. Since the requirement regarding applicability of the analysis of variance was not fulfilled, a non-parametric Kruskal-Wallis test was used for the evaluation at the significance level of $\alpha = 0{,}05$; results of this test are presented in Table 2. Values of p presented in this table define the probability of accepting the hypothesis that the given factor lacks an essential influence. If value p is lower than the assumed significance level, this hypothesis will be rejected (the factor has an essential effect on the analysed parameter). According to the presented results, no significant effect of the two factors on the value of pulling force and power lost to slipping was found.

CONCLUSIONS

The obtained results enabled formulation of the following conclusions:

1. The tyres reacted to the change of surface in different ways; larger differences in traction properties on different surfaces were present for tyre 11.2R24.
2. Both tyres obtained higher values of tractive efficiencies on the ground road which was the result of the lesser tendency of this surface to deform, and as a consequence lower rolling resistance.

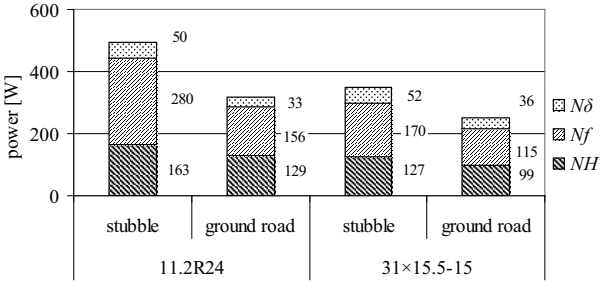

Fig. 7. Summary of mean power values calculated for slip within the range of 0 – 30%

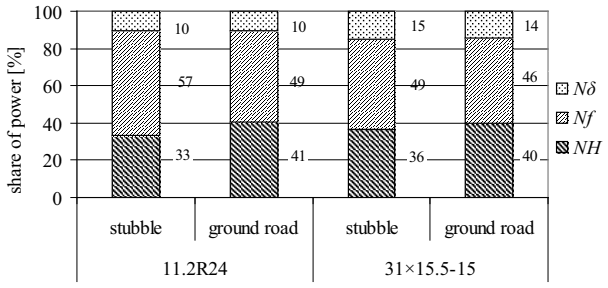

Fig. 8. Summary of shares of pulling power and lost power in total power

Table 2. Results of statistical analysis (p – probability level)

Factor	Values p							
	P_H	P_f	P_T	η	N_k	N_H	N_f	N_δ
Surface type	0,7956	0,0009	0,0427	0,0038	0,0002	0,0003	0,0007	0,2238
Tyre design	0,2112	0,0028	0,0021	0,0124	0,0019	0,0087	0,0039	0,2846

3. The values of pulling force of the tested tyres on both surface were similar, therefore different values of traction force were determined by different values of rolling resistance.
4. Tyre 11.2R24 was characterized by higher tractive efficiency and higher demand for power compared to tyre 31×15.5-15. In the case of this tyre, higher changes in shares of individual powers as a result of the change of surface also occurred.

REFERENCES

1. **Bashford L.L., Al-Hamed S., Jenane C. 1993.** Effects of tire size and inflation pressure on tractive performance. ASAE Paper no 92-1011. 343-348.
2. **Bashford L.L., Kocher M.F., Tibbetts T.S. 1999.** Wide tires, narrow tires. Biological Systems Engineering: Papers and Publications; Paper 174. 1-7.
3. **Botta G.F., Tollon-Becerra A., Tourne M., Lastra-Bravo X., Rivero D. 2012.** Agricultural traffic: Motion resistance and soil compaction in relation to tractor design and different soil conditions. Soil and Tillage Research 120. 92-98.
4. **Diserens E., Battiato A. 2012.** Traction force in arable farming: Agronomic and environmental aspects after field-data acquisition and modeling. International Conference of Agricultural Engineering. CIGR AgEng 8-12 July 2012.
5. **Elwaleed A.K., Yahya A., Zohadie M., Ahmad D., Kheiralla A.F. 2006.** Effect of inflation pressure on motion resistance ratio of a high-lug agricultural tire. Journal of Terramechanics 43. 69-84.
6. **Gholkar M.D., Salokhe V.M., Keen A. 2009.** The Effect of axle load and tyre inflation pressure on the tractive performance of a two wheel drive tractor on soft clay paddy field. An ASABE Meeting Presentation Paper Number 096606. 1-12.
7. **Goering C.E., Hansen A.C. 2004.** Engine and Tractor Power. ASAE Publication, ISBN 1892769425.
8. **Grisso R.D., Taylor R.K., Way T.R., Bashford L.L. 1992.** Tractive performance of 18.4R46 and 18.4R42 radial tractor tires. ASAE Paper no 91-1589. 739-745.
9. **Jenane C. Bashford L.L., Monroe G. 1996.** Reduction of fuel consumption through improved tractive performance. Journal of Agricultural Engineering Research 64. 131-138.
10. **Jenane C., Bashford L.L. 1995.** Field tractive performance comparisons between a tractor operated in the 2WD and 4WD mode. Actes. Inst. Agron. Vet. 15(1). 47-54.
11. **Kolator B. 2006.** Wybrane zagadnienia odkształceń napędowego koła pneumatycznego ciągnika rolniczego. MOTROL – motoryzacja i energetyka rolnictwa. 2006/8, 118-124.
12. **Lyasko M.I. 2010.** Multi-pass effect on off-road vehicle tractive performance. Journal of Terrramechanics 47. 275-294.
13. **Materek D. 2004.** Analiza właściwości trakcyjnych kołowego ciągnika rolniczego w wybranych technologiach uprawy roślin. Zeszyty Naukowe Akademii Rolniczej we Wrocławiu. Rozprawy CCXIX nr 493.
14. **Materek D. 2008.** Analiza wybranych właściwości trakcyjnych ciągnika John Deere 7720. Inżynieria Rolnicza nr 5(103). 127-130.
15. **Renius K.T. 1999.** Tractors: Two Axle Tractors. In: Handbook of Agricultural Engineering vol. III: Plant Production Engineering. ASAE St Joseph Michigan. 115-184.
16. **Rosca R., Rakosi E., Manolanche G. 2004.** Wheel traction prediction – a comparison between models and experimental data. SAE Technical Paper Series 2004-01-2707.
17. **Senatore C., Sandu C. 2011.** Torque distribution influence on tractive efficiency and mobility of of-road wheeled vehicles. Journal of Terramechanics 48. 372-383.
18. **Simikić M., Dedović N., Savin L., Tomić M., Silleli H., Ponjican O. 2012.** Influence of eccentric drawbar force on power delivery efficiency of a wheeled tractor. Turkish Journal of Agricultural and Forestry 36. 1-16.
19. **Smerda T., Cupera J. 2010.** Tire inflation and its influence on drawbar characteristics and performance – energetic indicators of a tractor set. Journal of Terramechanics 47. 395-400.
20. **Turner R.J. 1993.** Single, dual and triple tires and rubber belt tracks in prairie soil conditions. ASAE Paper no 93-1516. 1-18.
21. **Turner R.J. 1995.** Comparison of two and four track machines to rubber tire tractors in prairie soil conditions. SAE Technical Paper Series, Paper no 952097. 1-14.
22. **Wulfsohn D. Way T. R. 2009.** Factors that influence tractive performance of wheels, tracks and vehicles. In: Advances in Soil Dynamics vol. 3. St Joseph Michigan ASABE. 209-252.
23. **Zoz F.M., Grisso R.D. 2003.** Traction and tractor performance. ASAE Distinguished Lecture Series, Tractor Design No 27, publication number 913C0403.
24. **Żebrowski J. 2003.** An analysis of power flowing through the wheel of a running vehicle. Teka Komisji Motoryzacji i Energetyki Rolnictwa III/2003. 271-278.
25. **Żebrowski J. 2004.** Mechatronics in efficiency of tractors in operation. Teka Komisji Motoryzacji i Energetyki Rolnictwa IV 2004.43-48.

OCENA ZMIAN WŁAŚCIWOŚCI TRAKCYJNYCH OPON NA WYBRANYCH PODŁOŻACH ROLNICZYCH

Streszczenie. W pracy przedstawiono wyniki badań dwóch opon ciągnikowych o różnej konstrukcji i wymiarach zewnętrznych; opony te badane były na podłożach rolniczych o różnych właściwościach. Badania wykonywano przy użyciu stanowiska współpracującego z ciągnikiem rolniczym. Oceniano zmiany właściwości trakcyjnych; analizowano wartości sił (uciągu i trakcyjnej), oporu przetaczania, sprawności trakcyjnej, dokonano także bilansu mocy na badanych kołach. Wykazano, że opony odmiennie reagowały na zmianę podłoża.

Słowa kluczowe: ciągnik rolniczy, siła trakcyjna, sprawność trakcyjna, opór przetaczania, bilans mocy

Badania zrealizowano w ramach projektu badawczego MNiSW nr N N 313 146938

TEKA. COMMISSION OF MOTORIZATION AND ENERGETICS IN AGRICULTURE – 2013, Vol. 13, No. 1, 9–14

Evaluation of changes in traction properties of driving tyres on soil covered with turf

Włodzimierz Białczyk, Jarosław Czarnecki, Anna Cudzik, Marek Brennensthul

Institute of Agricultural Engineering, Wrocław University of Environmental and Life Sciences
ul. Chełmońskiego 37/41, 51-630 Wrocław. email: jaroslaw.czarnecki@up.wroc.pl

Received February 15.2013; accepted March 14.2013

Summary. The study presents the results of tests concerning the traction properties of driving tyres with radial and diagonal design on soil covered with turf differing by composition of plant species. It was shown that composition of plant species on the tested grounds had an effect on the traction forces and rolling resistance of tested tyres. Tyre 11.2R24 was characterised by greater pulling forces compared with tyre 9.5-24. However, no effect of the various compositions of species in the soil on the value of tractive efficiency was proven. Tyre 9.5-24 had higher demand for pulling power and power lost on wheel slip compared with tyre 11.2R24.
Key words: tractive abilities, driving tyre, power balance, soil covered with turf.

INTRODUCTION

Farming activities are connected with the operation of technical equipment on various types of soil. The characteristic properties of a given soil determine the tractive abilities of the vehicle, that is, the possibility of moving on it without considerable losses. Most farming work is carried out on deformable grounds which should transfer regular forces resulting from the weight of the vehicle and static forces connected with the applied driving torque of the wheel and the shear strength of the soil [9]. Deformable soils also include soil covered with turf. The research on turf conducted thus far concerns mainly its reaction to intensive utilisation. Changes are shown in the aboveground parts of plants, their root systems and soil environment [4, 14].

It should be stated that the mechanical and traction properties of turf are poorly recognized fields of research [5, 7, 12]. Many publications refer to arable soils. Traction forces are analysed, slip of driving wheels is measured, an energy balance of the driving wheel – soil system is conducted. Many publications refer to the negative effect of tractors on soil. In order to minimize unfavourable changes in soil while maintaining tractive efficiency, structural and operating parameters of tyres are chosen [6, 10, 15, 17, 18]. The specific character of soil covered with turf presented in publications indicates a considerable amount of organic matter covering the soil and the presence of root system of plants. This may have an effect on the tractive abilities of a farming tractor interacting with it. It is also worthwhile adding that tractors working on meadows and pastures in most cases are not equipped with special "grass" type tyres. Use of conventional driving tyres involves the possibility of damaging plants and the appearance of ruts which are the result of considerable unit pressures [13]. However, if usage of these tyres is so common and replacement of them with special tyres is connected with additional costs, the question arises whether other technical solutions limiting the unfavourable phenomena mentioned above are possible? Can such a solution be the replacement of driving tyres of diagonal design with tyres of radial design? The advantages of using these are broadly described in the literature [11, 16].

OBJECTIVE, SUBJECT MATTER AND METHODOLOGY OF TESTS

The analysis of issues connected with traction of farming tractors was the reason for which the research was undertaken, the objective of which was to:

1. Evaluate changes in tractive properties taking into account such parameters as traction forces, efficiency and rolling resistance for tyres of different designs.
2. Analysis of the tractive properties of tested tyres on turf with different composition of plant species.
3. Determination and comparison of the values of power for wheels equipped with the tested tyres for the assumed field conditions.

The research was conducted in autumn 2011 in four sites of the Agricultural Experimental Institute in Swojec

within the Wrocław University of Environmental and Life Sciences. The soil on which the research was conducted was proper alluvial soil made of strong sandy loan. In site I and II a mixture of meadow plants, and in site III and IV a mixture of pasture plants were sown. Composition of species and percentage share of individual mixtures are presented in Table 1.

Table 1. Composition of species and percentage share of sown mixtures

Name of species	Variety	Share [%]
Meadow mixture		
Perennial ryegrass	*Licampo*	30
Meadow fescue	*Limosa*	20
Timothy grass	*Lischka*	10
Red clover	*Nike*	20
White clover	*Hula*	10
Smooth meadow grass	*Bila*	10
Pasture mixture		
Italian ryegrass	*Livictory*	15
English ryegrass	*Licampo*	45
Meadow fescue	*Limosa*	20
Timothy grass	*Lischka*	20

In site I and II, the standard of seed sowing was equal to 30 kg/ha, and in sites III and IV 40 kg/ha was used. No mineral fertilization was used, no pasturage of animals was carried out in the pasture sites. Directly before performance of traction tests, the sites were mowed at the height of 0.07 m and measurements characterizing the condition of the soil i.e. compactness of soil and maximum shear stresses were conducted, soil moisture was also determined.

For measurement of soil compactness, a penetrologger made by Eijkelkamp, with conical penetrometer with vertical angle 60° and field of base 0.0001 m², was used. The additional accessory of this device was the Theta Probe ML2x by means of which soil moisture was measured. Measurement of maximum shear stress was performed using shear Vane H-60 made by Geonor with measurement range from 0 to 260 kPa.

For traction tests, tyres 9.5-24 and 11.2R24 were chosen which were fitted on a special measurement station [1]. The vertical load of the tested wheel was equal to 3300 N. During motion of the wheel, the values of pulling force, driving moment, theoretical and actual route of the tested wheel were registered. The obtained parameters allowed us to calculate the value of traction force, rolling resistance and tractive efficiency [Białczyk and others 2012]. The energy balance of the tested tyres was presented on the basis of calculated powers according to formulas 1-5:

$$N_k = N_H + N_f + N_\delta, \tag{1}$$

$$N_H = P_H \cdot v_R, \tag{2}$$

$$N_f = \left(P_T - P_H\right) \cdot v_R, \tag{3}$$

$$N_\delta = P_T \cdot \left(r_D - \frac{v_R}{\omega_T}\right) \cdot \omega_T, \tag{4}$$

$$\omega_T = \frac{v_T}{r_D}, \tag{5}$$

where:
Nk – power supplied to the wheel [W],
NH – pulling power [W],
Nf – power used to overcome rolling resistance [W],
Nδ – power lost on wheel slip [W],
PT- traction force [N],
PH- pulling force [N],
vR – actual route [m],
vT – theoretical route [m],
rD – dynamic radius of the wheel [m],
ωT – theoretic rotational speed of the tested wheel [s^{-1}].

TEST RESULTS

Table 2 presents the results of parameters characterizing the condition of the tested soils. Values of maximum shear stresses and soil compactness were read out for three depths of soil profile. Growth of the values of these parameters with measurement depth was concluded. In meadow sites (I and II), due to higher soil moisture (20%), lower values of the analysed parameters versus pasture sites were recorded (soil moisture 18%).

Table 2. Values of parameters of the tested soil

	Site I	Site II	Site III	Site IV
Maximum shear stresses [KPa]				
0.05 m	72	70	78	78
0.10 m	98	84	108	118
0.15 m	118	114	126	134
Compactness [MPa]				
0.05 m	2.16	2.15	2.57	2.42
0.10 m	2.95	3.10	3.42	3.76
0.15 m	3.11	3.28	3.33	3.68

Figure 1 presents mean values of traction forces and maximum tractive efficiency calculated for wheel slip within the range of 0-30%. Lower values of traction forces for tyre 9.5-24 were recorded. It is also characteristic that for this tyre no changes in this parameter within sites having the same composition of species were shown. Different standards of seed sowing did not have any effect on traction properties of this tyre. Tyre 11.2R24 made better use of turf properties which was reflected in the values of analysed parameters. Traction forces achieved different values in individual sites. The tractive efficiency of this tyre was characterized by lower dynamics of changes which may indicate low sensitivity of this tyre to varying field conditions.

The highest tractive efficiency was achieved by tyres 9.5-24 in pasture sites. The explanation of this situation can be found in figure 2 presenting pulling force and rolling resistance for the tested tyres. These two parameters are components of the traction force presented above. For this tyre, pulling force remained at a comparable level, and

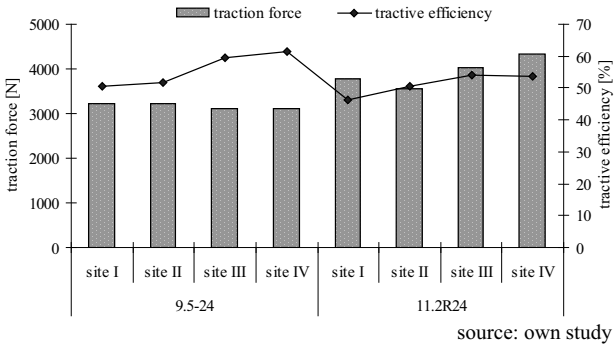

source: own study

Fig. 1. Values of traction forces and efficiency for the tested tyres

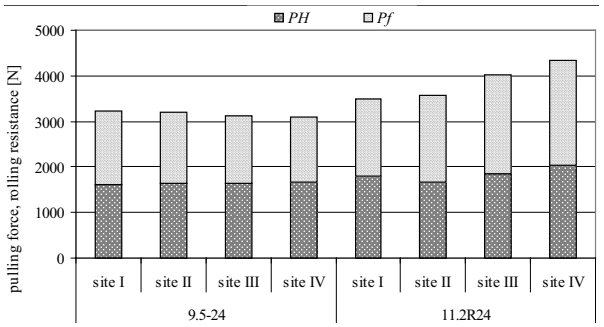

source: own study

Fig. 2. Values of pulling force and rolling resistance for the tested tyres

rolling resistance changed. Lower rolling resistance in sites 3 and 4 allowed us to obtain higher tractive efficiency. This allows us to conclude that in specific field conditions this tyre may achieve better tractive abilities.

A different situation occurred for tyre 11.2R24, whose larger surface of contact with the base enabled it to achieve greater pulling forces, however the values of rolling resistance were (apart from site 1) higher than the generated pulling force. The obtained results are compliant with those received by Wulfsohn and others [19], who proved that design of the tyre had an effect on achieved tractive efficiency, and diagonal tyre had worse tractive abilities.

Figure 3 presented progresses of individual powers in the function of slip for wheel with tyre 9.5-24 in the tested sites. Detailed analysis of the power balance presented in this way allowed us to show what part of supplied power is used for pulling force and what part is lost on rolling resistance and wheel slip. It can be clearly concluded from the presented progresses that the character of changes in analysed powers is comparable for individual sites. Fast growth of power supplied to the wheel (*Nk*) was connected with overcoming initial resistance to motion, and then this power was stabilized and oscillated within the range of 300-450 W, except for site 4 where proportional growth of its value in line with wheel slip is observed. In this site, a higher standard of seed sowing was used which resulted in higher thickness of turf coverage. If this condition is combined with higher values of strength parameters in this site, it can be assumed that the tyre of diagonal design caused more difficult immersion of tread projections as a result of which power lost on wheel slip increased with pulling power maintained at a comparable level.

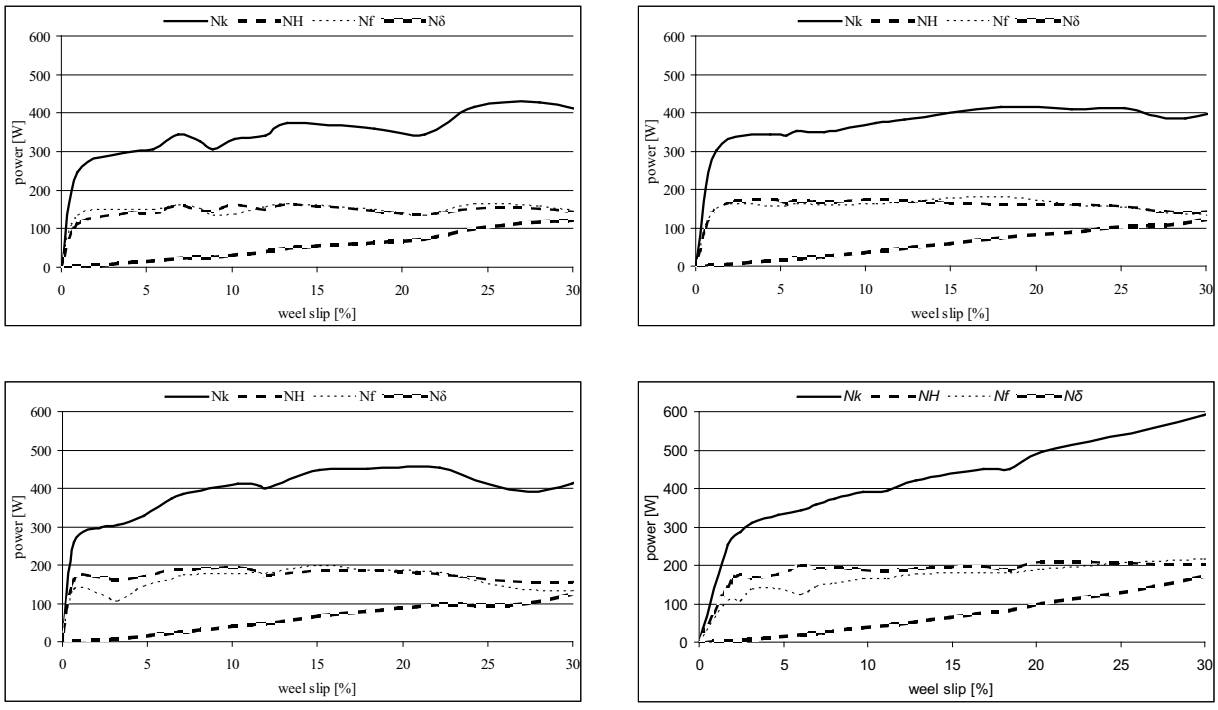

source: own study

Fig. 3. Progresses of power in the function of slip for tyre 9.5-24: a – site I, b – site II, c – site III, d – site IV

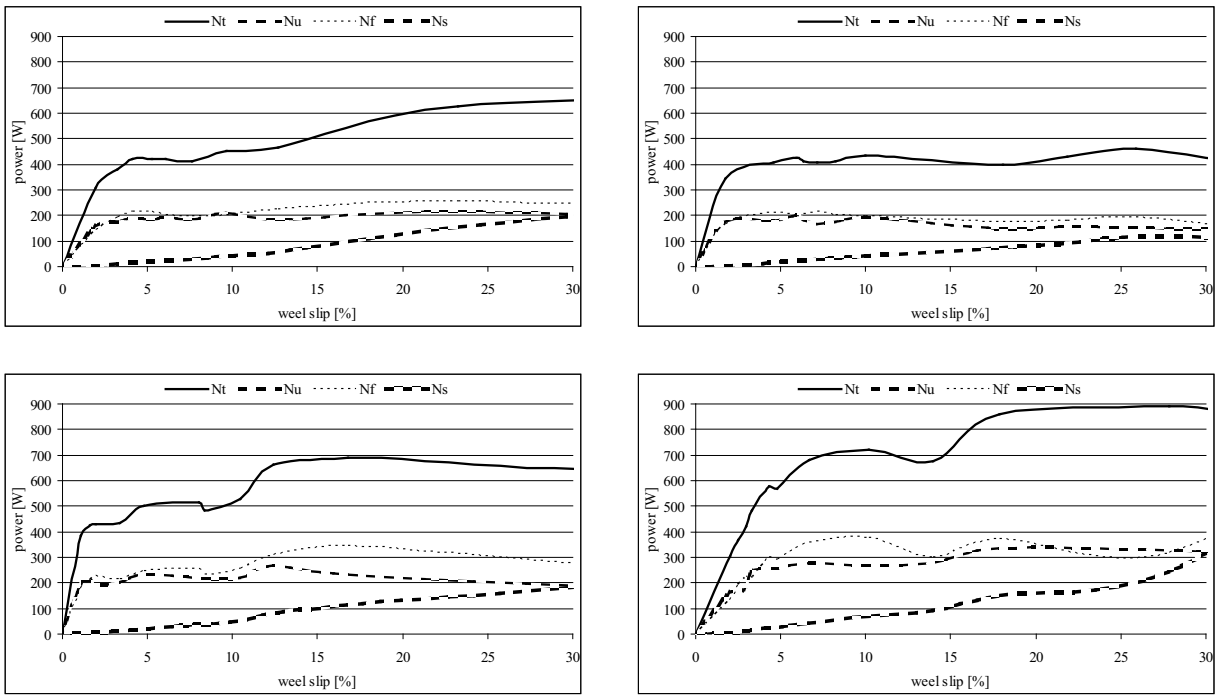

source: own study

Fig. 4. Progresses of power in the function of slip for tyre 11.2R24: a – site I, b – site II, c – site III, d – site IV

Figure 4 presents progresses of individual powers in the function of slip for the wheel equipped with tyre 11.2R24 in the tested sites. The analysed tyre showed higher demand for supplied power if compared with tyre 9.5-24 which allowed increased pulling power. The power needed to overcome rolling resistance also increased. As already mentioned above, the radial tyre better reflects existing field conditions which for sites 1 and 2 allows pulling properties comparable with sites 3 and 4 to be obtained at lower energy expense. This was probably connected with a higher adhesion coefficient for this tyre which was proven also in a study by Gee-Glough and others [8].

Presentation of the above progresses allowed evaluation of the range of changes in the analysed values, however in order to analyse the share of individual powers in total power supplied to the wheel, their percentage share was presented in figure 5. Tyre 9.5-24 showed higher demand for pulling force apparent especially in sites 3 and 4. However, it was not directly reflected in the generated pulling force which in each of the analysed sites had a lower value compared with the pulling force obtained by the radial tyre. Power lost on slip of this tyre in sites 1 and 2 also grew which was probably connected with the presence of white and red clover forming a considerable part of the organic matter reducing the adhesion of this tyre.

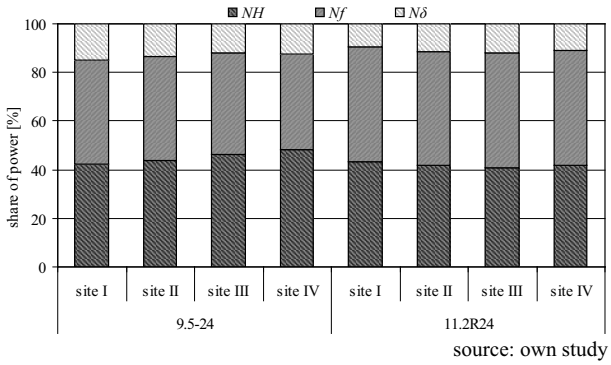

source: own study

Fig. 5. Percentage share of individual powers in total power

In spite of lower demand for pulling power, tyre 11.2R24 was able to generate higher pulling abilities which, however, took place at the expense of a greater share of power lost on rolling resistance. However, this was compensated for by lesser demand for power lost on wheel slip.

Based on the obtained results, multi-factor analysis of variance at the significance level $\alpha = 0.05$ was performed using the Statistica 9.0 package. Different botanical composition of the soil and the type of tyre used have an effect on generation of traction forces with different values. The tested tyres also showed different rolling resistance and tractive efficiency. However, no effect of soil on the value of achieved tractive efficiencies was proven (table 3).

Table 3. Results of statistical analysis (F – test value, p – probability)

Factor	Dependent variable					
	Traction force		Rolling resistance		Tractive efficiency	
	F	p	F	p	F	p
Soil	12,304	<0,0001	10,968	<0,0001	0,530	0,6613
Tyre	41,008	<0,0001	50,212	<0,0001	39,850	<0,0001

source: own study

The results of statistical analysis presented in table 4 allowed it to be proved that both the type of soil and type of tyre used have an effect on total power supplied to the wheel. Different demand for pulling power, power of rolling resistance and power lost on slip were also shown.

Table 4. Results of statistical analysis (F – test value, p – probability)

Factor	Dependent variable							
	Total power		Pulling power		Power lost on Rolling resistance		Power lost on slip	
	F	p	F	p	F	P	F	P
Soil	21,232	<0,0001	27,619	<0,0001	14,336	<0,0001	10,949	<0,0001
Tyre	49,257	<0,0001	28,508	<0,0001	58,405	<0,0001	26,281	<0,0001

source: own source

CONCLUSIONS

1. In the tested sites, the analysed tyres generated traction forces with different values. The completed analysis of components of these forces allowed us to conclude that tyre 11.2R24 showed better pulling abilities, but growth of rolling resistance occurred which resulted in lower tractive efficiency for this tyre.
2. No effect of species-related composition of soil on the tractive efficiency of the tested tyres was shown. Tyre 11.2R24 achieved different pulling forces on turf with the same species-related composition but different seed sowing standards. Due to considerable stiffness resulting from its diagonal design, tyre 9.5-24 achieved pulling forces with comparable values.
3. Tyre 9.5-24 showed higher demand for pulling power which was not directly reflected in growth of pulling forces because higher losses of power on wheel slip occurred. Tyre 11.2R24 lost more power on rolling resistance, but its radial design allowed better use of the strength properties of the soil by reducing wheel slip power.

REFERENCES

1. **Białczyk W., Czarnecki J., Cudzik A., Brennensthul M. 2010:** Ocena właściwości trakcyjnych wybranych opon na podłożach zadarnionych. Inżynieria Rolnicza, 7 (125), 15-22.
2. **Białczyk W., Brennensthul M., Cudzik A., Czarnecki J. 2012:** Ocena trakcyjna opon do uniwersalnego ciągnika rolniczego. Inżynieria Rolnicza. Nr 2 (136). 7-17.
3. **Coates W. 1984:** Comparisons of bias and radial tractor tires on a soft soil. Transactions of the ASAE 28(4). 1090-1093.
4. **Danneberger T., K. 1993:** Turfgrass ecology and Management. Franzak & Foster, div. of G.I.E., Inc. Publishers. Cleveland, OH.
5. **Dąbkowski S., Grabulewski K., Pachuta K. 2004:** Mechaniczne właściwości darni traw. Acta Scientarium Polonorum. Architectura 3 (1), 23-35.
6. **Erbach D., Knoll K. 1992:** Inflation pressure effect on soil compaction. ASAE paper 92-1582. St. Joseph (MI): ASAE.
7. **Ferrero A., Usowicz B., Lipiec J. 2005:** Effects of tractor traffic on spatial variability of soil strength and water content in grass covered and cultivated sloping vineyard. Soil Till. Res. 84, 127–138.
8. **Gee-Clough., Mac Allister D., Everndnen D. 1977:** Tractive performance of tractor drive tyres: a comparison of radial and cross-ply carcas construction. Journal of Agricultural Engineering Research 22, 385-395.
9. **Jakliński L. 2006:** Mechanika układu pojazd – teren w teorii I badaniach. Oficyna Wydawnicza Politechniki Warszawskiej. Warszawa, 18-22.
10. **Jorajuria D., Draghi L., Aragon A. 1997:** The effect of vehicle weight on the distribution of compaction with depth and the yield of Lolium/Trifolium grassland. Soil Till. Res. 41, 1–12.
11. **Materek D. 2006:** Ocena zmian siły uciągu ciągnika rolniczego z radialnymi i diagonalnymi oponami napędowymi. Inżynieria Rolnicza. Nr 3 (78). 321-326.
12. **Minner D., Donn J., Bughrara S., Fresenburg B. 1993:** Traffic tolerance among cultivars of Kentucky bluegrass, tall fescue, and perennial ryegrass. International Turfgrass Society Research Journal. Volume 7, 687-694.
13. **Schäffer B., Attinger W., Schulin R. 2007:** Compaction of restored soil by heavy agricultural machinery – Soil physical and mechanical aspects. Soil Till. Res. 93, 28–43.
14. **Stewart G., Pullin A. 2008:** The relative importance of grazing stock type and grazing intensity for conservation of mesotrophic "old meadow" pasture. Journal for Nature Conservation 16 (3), 175-185.
15. **Szymaniak G., Pytka J. 2003:** Effects of reduced inflation pressure and ride velocity on soil surface deformation. Teka Komisji Motoryzacji i Energetyki Rolnictwa PAN Lublin, III/2003. 236-242.
16. **Tuner R. 1999:** Field performance of Trelleborg and similar size radial tire. ASAE Paper no 99-1038. 1-14.
17. **Tajanowskij G., Taras W., Romashko J. 2009:** Traction dynamics of the all-wheel drive machine tractor unit with hinged soil processing equipment. Teka Komisji Motoryzacji i Energetyki Rolnictwa PAN Lublin, IX/2009. 335-241.
18. **Way T., Kishimoto T. 2004:** Interface pressures of a tractor drive tyre on structured and loose soils. Biosystems Eng. 87 (3), 375–386.
19. **Wulfsohn D., Way T. 2009:** Factors that influence tractive performance of wheels, tracks and vehicles. In: Advances in Soil Dynamics vol. 3. St Joseph Michigan ASABE. 209-252.

OCENA ZMIAN WŁAŚCIWOŚCI TRAKCYJNYCH OPON NAPĘDOWYCH NA PODŁOŻACH ZADARNIONYCH

Streszczenie. W pracy przedstawiono wyniki badań dotyczących właściwości trakcyjnych opon napędowych konstrukcji radialnej i diagonalnej na podłożach zadarnionych różniących się składem gatunkowym roślin. Dokonana analiza sił trakcyjnych oraz oporów przetaczania, wykazała wpływ składu gatunkowego roślin badanych podłoży na zdolności trakcyjne opony 11.2R24, która ponadto cechowała się wyższymi siłami uciągu w porównaniu do opony 9.5-24. Nie wykazano natomiast wpływu odmiennego składu podłoża na wartość sprawności trakcyjnej. Opona 9.5-24 wykazywała większe zapotrzebowanie na moc uciągu oraz moc traconą na poślizg koła w porównaniu do opony 11.2R24.

Słowa kluczowe: zdolności trakcyjne, opona napędowa, bilans mocy, podłoże zadarnione

TEKA. COMMISSION OF MOTORIZATION AND ENERGETICS IN AGRICULTURE – 2013, Vol. 13, No. 1, 15–18

Automatic measurement of time constant for temperature sensors

Artur Boguta, Marek Horyński

Lublin University of Technology, Faculty of Electrical Engineering and Computer Science,
Department of Computer and Electrical Engineering, Nadbystrzycka 38A, 20-618 Lublin, Poland,
phone: (+48 81) 53-84-301, fax: (+48 81) 525-46-01, e-mail: a.boguta@pollub.pl, m.horynski@pollub.pl

Received February 3.2013; accepted March 14.2013

Summary. The importance of temperature measurements is significant in many processes. The accuracy of said measurements is essential for the tasks to be performed by a product and for its compliance with requirements of applicable standards. The maintenance of determined temperature regime in individual production process phases is essential for the quality of obtained product. Apart from temperature measurement accuracy, the time of sensors response to its change is also extremely important. The response time of temperature regulators and controllers which may significantly affect the parameters of finished product, depends on the time of sensor response.

The measurements of time constants for temperature sensors are time consuming and proper equipment and knowledge are also required for this purpose. It is rather unproblematic in case of piece production scale but in case of mass production it is necessary to find a solution enabling the automation of time constant measuring process and ensuring measurements repeatability. The solution presented in this study will make it possible to automate the process and to reduce the time of measurement.

By means of proper software it will be possible to read the time constant from measuring system display.

Key words: time constant, temperature, temperature sensor.

THE STRUCTURE OF A SYSTEM FOR AUTOMATIC MEASUREMENT OF TIME CONSTANT OF PT 100 SENSORS

The system enabling the measurement of time constant for PT100 temperature sensors is illustrated in Fig. 1.

The measurement system consists of a hydraulic assembly ensuring the flow of fluid pre-heating the sensor being tested and changing its flow rate in individual phases of system operation. In the initial phase, the fluid circulates in the circuit consisting of water bath, fluid circulating tubes and check valve. In this operation phase, the fluid flows through the system elements and heats the whole circuit. The purpose of the check valve is to enable the fluid flow while an electro – valve is closed. The latter opens in the second phase and the fluid is supplied to the sensor under test causing a sudden change of sensor temperature. An algorithm recording the sensor temperature change at sudden temperature change is triggered in this operation phase. Temperature changes are recorded by means of one of analogue to digital (A/D) converters of microcontroller. Resistance changes are recorded 25 times/ second by means of the microcontroller [3, 4]. The recording time is equal to 25 s and is completely sufficient to ensure the stabilization of final temperature of the sensor under test. Internal memory of ATmega 64 microcontroller is used to record the values of resistance vs. time. The resistance is recorded as a WORD type variable in the table of variables [18, 19]. An original program has been created, compiled and entered into the microcontroller memory in order to make it possible to determine three time constants T0,50, T0,632, T0,90 [9,16]. The algorithm calculating the time constants performs the analysis of recorded numerical values displayed by A/D converter and determines three values i.e. 0,5, 0,632 and 0,9 for the recorded maximum value. The time elapsed between the system starting and occurrence of determined numerical values is determined on the basis of recorded measurement points (25 times /1s). Corresponding time constants measured by the system are specified on the basis of time elapsed until the recorded maximum value achieved 0,5, 0,632 and 0,9. After START pushbutton is depressed, the signal received from A/D converter is continuously analyzed by the microprocessor triggering the measurement procedure when a positive change of sensor temperature is detected.

Another task of applied microcontroller consists in the measurement of water bath temperature and measuring cylinder temperature. DS18B20 semiconductor sensors have been used for temperatures measurements. The temperatures measurement makes it possible to determine the temperature unit step and to check its conformity with applicable standard [1, 5, 12].

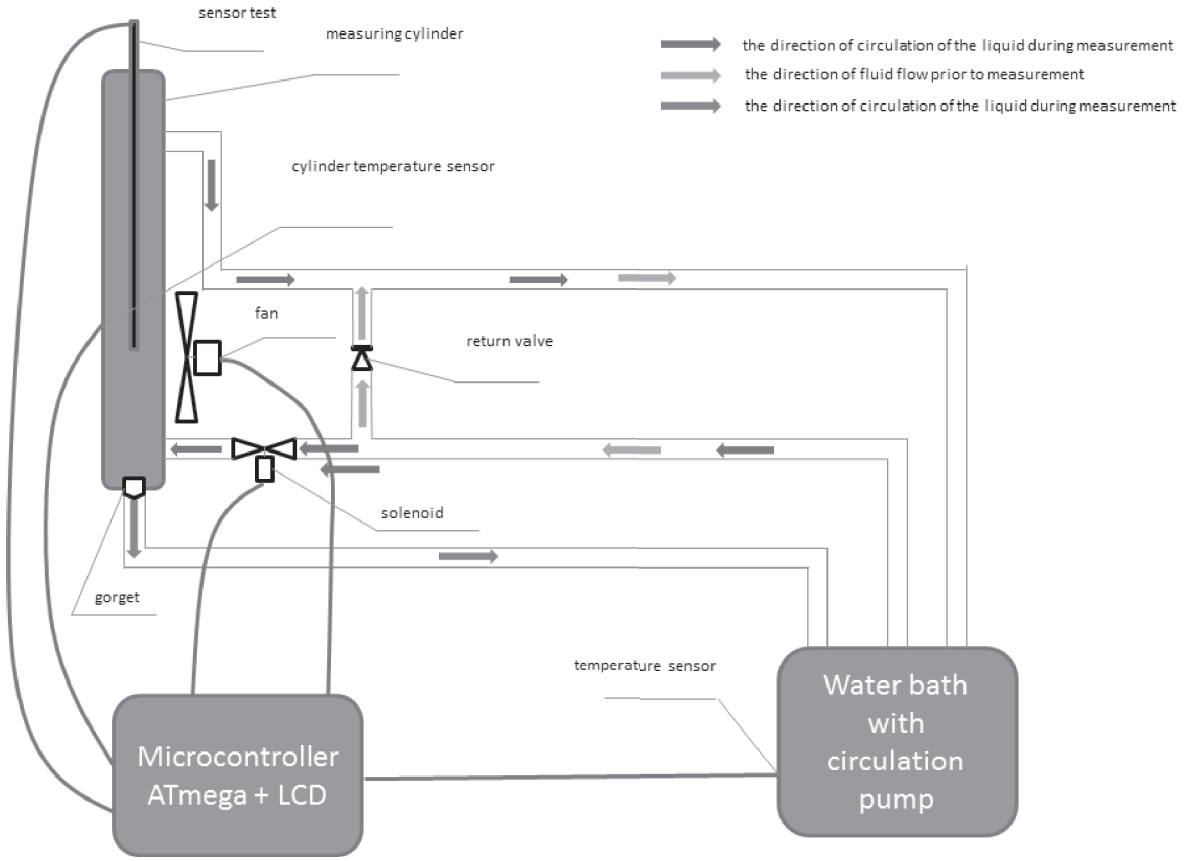

Fig. 1. The system for measurement of time constant for PT100 temperature sensors

After completed measurement, the measured values of time constant are displayed, electro – valve is closed, the fluid is discharged from measuring cylinder into water bath and the fan is turned on in order to cool the system before the next measurement.

The system has been equipped with a function protecting against an erroneous measurement (proper temperature difference, sensor not connected or damaged). In case of possibility of an erroneous measurement, the control system will make it impossible to turn on the system. Information about errors will be shown on LCD display and indicated by means of LED control lights [6, 7, 8].

Figure 2 illustrates the schematic diagram of an electronic system performing the following functions:

– temperatures control in course of system operation;
– control of electro-valve operation,
– control of cooling fan operation,
– measurement of PT100 sensor resistance,
– recording of resistance change vs. time,
– calculation of time constant value for the sensor under tests.

AVR Atmega 64 microcontroller performs the function of a system monitoring the operation of the whole measuring system. Said microcontroller supports an instrumentation amplifier based upon an integrated NE5532 operation amplifier[15]. The purpose of this amplifier is to match the Signac received from PT100 temperature sensor to adequate level required by A/D converter.

Completed measuring system has been tested in laboratory conditions. The tests were carried out on several PT 100 sensors and demonstrated that the time constants for PT 100 platinum temperature sensors are measured correctly by means of designed and completed system.

MEASUREMENTS

Completed system has been used for testing of temperature sensors basing upon PT100 measuring element. The measurements have been performed for more than ten sensors. The results of measurements for four (4) selected sensors have been presented in Table No 1.

Table 1. Time constant T0,5 for PT-100 sensors located in steel jackets with silicone filling

Item	Sensor No 1	Sensor No 2	Sensor No 3	Sensor No 4
	$T_{0,5}$ [s]	$T_{0,5}$ [s]	$T_{0,5}$ [s]	$T_{0,5}$ [s]
1	9,11	11,01	8,95	11,23
2	10,10	10,78	9,56	10,58
3	9,70	10,45	9,87	10,89
4	9,68	09,67	10,23	10,59
5	10,03	10,85	9,68	10,55
6	9,54	10,68	9,89	11,04
7	10,34	11,00	9,45	10,97
8	9,85	10,59	9,78	10,87
9	10,05	10,93	9,83	10,76
10	9,33	10,42	8,97	10,75
Average	9,77	10,63	9,62	10,82

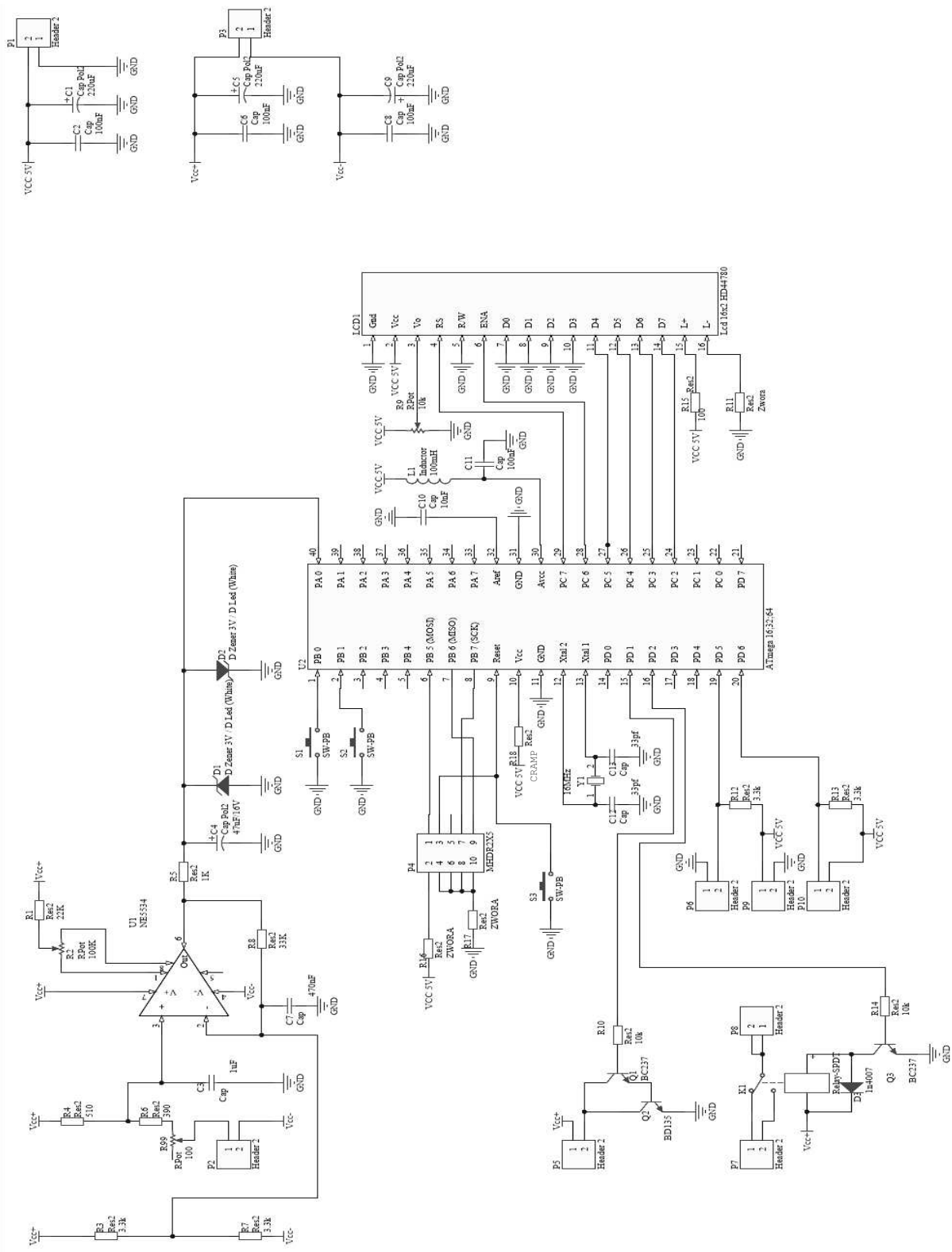

Fig. 2. Schematic diagram of a control and measuring system for determination of temperature sensors time constants

The measurements presented in Table No 1 correspond to measurements performed manually by means of a stop watch and digital multimeter. The results of measurements for individual sensors insignificantly differ from each other. The difference can be caused by an insignificant change of sensor resistance at the time of final temperature stabilization and by limited resolution of A/D converter in applied microcontroller.

CONCLUSIONS

The time constants for the transducers under tests are measured correctly by means of presented system designed for the determination of time constants for PT 100 transducers. Obtained results are conforming with the results obtained by means of manual method. A/D converter with higher resolution (10-bit version has been used in the system) can be used in order to increase the accuracy and repeatability of measurements.

There is a problem in the system being tested due to quick cooling of measuring cylinder. The cylinder consists of a copper tube characterized by good heat conductivity but its heat capacity is high. This significant heat capacity slows down the measuring cylinder process before the next measurement. The application of more efficient measuring cylinder process by means of a fan with increased efficiency or by means of fluid, could significantly reduce the time required to complete next measurements.

REFERENCES

1. **Baranowski R. 2005:** Mikrokontrolery AVR ATmega w praktyce. BTC Legionowo [AVR ATmega microcontrollers in practice].
2. **Brzoza-Woch R. 2010:** Mikroprocesory AT91AM9. BTC Legionowo [AT91AM9 microprocessors].
3. **Doliński J. 2009:** Mikrokontrolery AVR w praktyce. BTC Legionowo. [AVR Microcontrollers in practice].
4. **Doliński J. 2009:** Mikrokontrolery AVR, niezbędnik programisty. BTC Legionowo [AVR microcontrollers, programmer's toolbox].
5. **Górecki P. 2002:** Elektronika dla wszystkich. Mikroprocesorowa ośla łączka. AVT nr: 10, 11, 12 [Electronics for everyone. Górecki P.: An introduction to microprocessors].
6. **Górecki P. 2003:** Elektronika dla wszystkich. Mikroprocesorowa ośla łączka. AVT nr: 1, 2, 3, 4, 5, 6, 7, 10, 11, 12 [Electronics for everyone. Górecki P.: An introduction to microprocessors].
7. **Górecki P. 2004:** Elektronika dla wszystkich. Mikroprocesorowa ośla łączka. AVT nr: 1, 2, 3, 4, 6, 7, 8 [Electronics for everyone. Górecki P.: An introduction to microprocessors].
8. **Górecki P. 2005:** Elektronika dla wszystkich. Mikroprocesorowa ośla łączka. AVT nr: 5 [Electronics for everyone. Górecki P.: An introduction to microprocessors].
9. **Hagel A. 1975:** Miernictwo dynamiczne, WNT Warszawa [Dynamic measurement techniques].
10. **Horyński M. 2011:** Indor Climate Control in EIBSystem, Commission of Motorization and Power Industry in Agriculture TEKA XI/2011.
11. **Jabłoński T. 2010:** Mikrokontrolery PIC16F. BTC Legionowo [PIC16F microcontrollers].
12. **Kapica J. 2011:** Application of Microcontroller in Simulation of the Photovoltaic Generators. Commission of Motorization and Power Industry in Agriculture TEKA XI/2011.
13. **Michalski L, EckersdorfK. 1980:**Pomiary temperatury. WNT Warszawa [Temperature measurements].
14. **Michalski l., Eckersdorf K. 1971:** Pomiary temperatury, WNT Warszawa, Wyd. II [Temperature measurements].
15. **Pawluczuk A. 2006:** Sztuka programowania mikrokontrolerów AVR. BTC Warszawa [The art of AVR microcontrollers programming].
16. Polska Norma 1995- EN 60751+A2.
17. T**ietze U. Schenk CH. 1993:** Układy półprzewodnikowe. WNT Warszawa [Semi-conductor systems].
18. **Wiązania M. 2004:** Programowanie mikrokontrolerów w języku BASCOM. BTC Warszawa. [Microcontroller Programming in BASCOM].
19. **Wiązania M. 2008:** Bascom AVR w przykładach. BTC Legionowo. [AVR in examples].
20. **Wierzbicki S. 2006:** Diagnosing microprocessor-controlled systems, s. 182, TEKA 2006 -, Commission of Motorization and Power Industry in Agriculture.
21. **Wołgajew R. 2010:** Mikrokontrolery AVR dla początkujących. BTC Legionowo. [AVR Microcontrollers for beginners].

Varying of reliability indexes in passively reserved difficult technical systems

Olexander Bondarenko[1], Anatoliy Boyko[2]

[1]Mykolaiv National Agrarian University, Faculty of Farm Mechanization,
Mykolaiv, 17 A Krylova Street, 54038, Ukraine, e-mail: bondarenko–V70@rambler.ru
[2]National University of Life and Environmental Sciences of Ukraine,
Kyiv, 15, Heroyiv Oborony, 03041, Ukraine

Received January 7.2013; accepted March 14.2013

Summary. In the article the passively reserved system working in the mode of gradual damages accumulation is considered. The rules of change of basic reliability indexes, such as the probability of faultless work and mean time of work till renunciation are set.
Key words. Readiness to work, mean work on a renunciation, probability of faultless work, model of fail safety.

INTRODUCTION

Reservation is one of the most effective methods in increase of reliability of the technical systems. Its wider use in engineering is restrained by the necessity of introduction of additional elements (reserve parts), methods and availability of periodic regulations, and also the renewals of details' working capability in the shape of regrinds, use of additional working verges etc [8]. Another reason of insufficient application of the passive reservation is the absence of scientifically-reasonable recommendations on its effective use. This article is directed on the removal of the indicated defects.

RESULTS AND DISCUSSION

Pre-condition for the establishment of main criteria of reliability of the passively reserved system are probabilities of its being in this or that expediently chosen state [5]. The sizes of such probabilities settle accounts in accordance with the rule of Cramer [6]:

$$\varphi_з(S) = \frac{\Delta_i}{\Delta}, \qquad (1)$$

where:

$\varphi_i(S) \leftrightarrow P_i(t)$ – the possibility of i-state in the transformations of Laplas;

Δ_i – determinant of the equation system (7) [1] for the observed unknown authenticity;

Δ – basic determinant of the same equation system.

The choice of the state of the system and corresponding to its determinant are set in obedience to the established task of researches and oriented to one or another studied reliability index. However, in any case it is necessary to find the decision of the determinant which stands in the denominator of formula (1). Its size comes from the general extended matrix of the system of equalizations [1] and makes a basic matrix which is written down as follows:

$$\Delta = \begin{vmatrix} S+\lambda_{00} & 0 & -\mu_{10} & 0 & 0 \\ -\lambda_{00} & S+\lambda_{0'0} & 0 & 0 & 0 \\ S & S & S & S & S \\ 0 & 0 & -\lambda_{10} & S+\lambda_{00'} & 0 \\ 0 & 0 & 0 & -\lambda_{10'} & S+\mu_{11} \end{vmatrix}. \qquad (2)$$

The presented matrix has a fifth grade and needs for a further decision in lowering [7].

Executing the corresponding mathematical operations of grade lowering, by means of algebraic transformations and bringing expressions over, we will get:

$$\Delta = aS^5 + bS^4 + cS^3 + dS^2 + eS,$$

where:

$a = 1;$

$b = (\mu_{11} + \lambda_{10'} + \lambda_{10} + \lambda_{0'0} + \lambda_{00} + \mu_{10});$

$c = (\lambda_{10'}\mu_{11} + \lambda_{10}\lambda_{10'} + \mu_{11}\lambda_{10} + \lambda_{0'0}\mu_{11} + \lambda_{0'0}\lambda_{10'} + \lambda_{0'0}\lambda_{10} + \lambda_{00}\mu_{11} + \lambda_{10}\lambda_{10'} + \lambda_{00}\lambda_{10} + \lambda_{0'0}\lambda_{0'0} - \mu_{10'}\mu_{11} + \mu_{10}\lambda_{10'} + \mu_{10}\lambda_{0'0});$

$d = (\lambda_{0'0}\lambda_{10'}\mu_{11} + \lambda_{0'0}\lambda_{10}\lambda_{10'} + \lambda_{0'0}\mu_{11}\lambda_{10} + \lambda_{0'0}\lambda_{10'}\mu_{11} + \lambda_{00}\lambda_{10}\lambda_{10'} + \lambda_{00}\mu_{11}\lambda_{10} + \lambda_{00}\lambda_{0'0}\mu_{11} + \lambda_{00}\lambda_{0'0}\lambda_{10'} + \lambda_{00}\lambda_{0'0}\lambda_{10} - \mu_{10}\lambda_{00}\mu_{11} - \mu_{10}\lambda_{00}\lambda_{10'} + \mu_{10}\mu_{11}\lambda_{00} + \mu_{10}\lambda_{10'}\lambda_{00} + \mu_{10}\lambda_{10'}\mu_{11} + \mu_{10}\mu_{11}\lambda_{0'0} + \mu_{10}\lambda_{10'}\lambda_{0'0});$

$e = (\lambda_{00}\lambda_{0'0}\lambda_{10'}\mu_{11} + \lambda_{00}\lambda_{10}\lambda_{0'0}\lambda_{10'} + \lambda_{00}\lambda_{0'0}\mu_{11}\lambda_{10} + \mu_{10}\lambda_{10'}\mu_{11}\lambda_{0'0}).$

If to ignore the values of intensities of refuses at triple and more multiplying, as the values of high order of trifle, we will get considerable simplification of mathematical

expressions for determination of matrix decision. Then we get:

$$\Delta = S^3\left(aS^2 + bS + c\right). \quad (3)$$

The numerator of ratio (1) for determination of probability of fully capable working state $\varphi_{00}(S)$ comes from the basic matrix by the substitution of the column of free members of the extended matrix [10] in the column of the found probability of the "00" state. Then we have:

$$\Delta_{00} = \begin{vmatrix} 1 & 0 & -\mu_{10} & 0 & 0 \\ 0 & S+\lambda_{0'0} & 0 & 0 & 0 \\ 1 & S & S & S & S \\ 0 & 0 & -\lambda_{10} & S+\lambda_{10'} & 0 \\ 0 & 0 & 0 & -\lambda_{10'} & S+\mu_{11} \end{vmatrix}.$$

Thus, the components for finding out the probabilities of the first capable working state are set and when we put them according to formula (1) for the state "00" we get:

$$\varphi_{00}(S) = \frac{\left(\begin{array}{l} S^4 + S^3(\mu_{11} + \lambda_{10'} + \lambda_{10} + \lambda_{0'0} - \mu_{10}) + S^2(2\lambda_{10}\mu_{11} + \lambda_{10}\lambda_{10'} + \\ \lambda_{0'0}\mu_{11} + \lambda_{0'0}\lambda_{10'} + \lambda_{0'0}\lambda_{10} - \mu_{10}\lambda_{10'} - \mu_{10}\lambda_{0'0} - \mu_{10}\mu_{11}) + \\ + S(2\lambda_{0'0}\lambda_{10}\mu_{11} - \mu_{10}\lambda_{0'0}\lambda_{10'} - \mu_{10}\mu_{11}\lambda_{0'0}) - \mu_{10}\mu_{11}\lambda_{0'0}\lambda_{10'} \end{array}\right)}{aS^5 + bS^4 + cS^3 + dS^2 + eS}. \quad (4)$$

However, this probability is obtained as a reflection in transformations of Laplace and for passing to the original it needs proper mathematical operations. Such transition becomes possible if to present the function of probability as a sum of vulgar fractions [2]:

$$\varphi_{00}(S) = \frac{A_{00}}{S-S_1} + \frac{B_{00}}{S-S_2} + \frac{C_{00}}{S-S_3} + \frac{D_{00}}{S-S_4} + \frac{E_{00}}{S-S_5}, \quad (5)$$

where:

$A_{00}, B_{00}, C_{00}, D_{00}, E_{00}$ – inserted unknown permanent values, necessary to be set for back transformation of Laplas;

S_1, S_2, S_3, S_4, S_5 – roots of the right part of the equation (3).

The roots come from the equation (3) in the following way:

$$S^3\left(aS^2 + bS + c\right) = 0.$$

It is obvious, that $S_1 = S_2 = S_3 = 0$, but S_3 and S_4 – roots of the right part of the equation, situated in brackets according to the formula [3]:

$$S_{4,5} = -\frac{b}{2} \pm \sqrt{\left(\frac{b}{2}\right) - c}. \quad (6)$$

For determination of the inserted additional permanent values we will make a comparison in the equivalence of numerators of expressions (4) and (5). When denominators are equal, the equivalence of polynomials of numerators is possible as a result of equality of coefficients at the same degrees of the unknown. After inserting of the substitutes $A_{00} + B_{00} + C_{00} = Z_{00}$ it is possible to write down the additional system from three equations:

$$\begin{cases} Z_{00} + E_{00} = 1; \\ (Z_{00} + D_{00})S_5 - (\mathcal{K}_{00} + E_{00})S_4 = \mu_{11} + \lambda_{10'} + \lambda_{10} + \lambda_{00'} - \mu_{10}; \\ -ZS_4S_5 = L, \end{cases}$$

where:

$$L = 2\lambda_{10}\mu_{11} + \lambda_{10}\lambda_{10'} + \lambda_{0'0}\mu_{11} + \lambda_{0'0}\lambda_{10'} + \lambda_{00}\lambda_{10} - \mu_{10}\lambda_{10'} - \mu_{10}\lambda_{0'0} - \mu_{10}\mu_{11}.$$

The received system is solved by the method of successive substitution. From the third equalization we will write down:

$$Z_{00} = -\frac{L}{S_4S_5}.$$

From the second equation we will get:

$$(Z_{00} + D_{00})S_5 - S_4 = \mu_{11} + \lambda_{10'} + \lambda_{10} + \lambda_{00'} - \mu_{10}.$$

And

$$D_{00} = \frac{\mu_{11} + \lambda_{10'} + \lambda_{10} + \lambda_{00'} - \mu_{10} + S_4 - \frac{L}{S_4}}{S_5}.$$

Thus, the permanent values of Z_{00}, D_{00}, E_{00} are obtained and it is possible to conduct reverse transformation of Laplace from the images to the originals. Then we have:

$$P_{00}(t) = Z_{00} + D_{00}\exp(-S_4t) + E_{00}\exp(-S_5t).$$

Inserting the meanings of permanent values we can write down:

$$P_{00}(t) = -\frac{L}{S_4S_5} + \frac{1}{S_5}\left(\mu_{11} + \lambda_{10'} + \lambda_{10} + \lambda_{00'} - \mu_{10} + S_4 - \frac{L}{S_4}\right) \times \exp(-S_4t) + \left(1 - \frac{L}{S_4S_5}\right)\exp(-S_5t). \quad (7)$$

By analyzing the received result it is necessary to notice that the value of probability of $P_{00}(t)$ is determined by three elements. Their signs depend on those components which are included in them, but the general value of probability must not exceed the unit that is the rationed condition. The analysis of the result is complicated by unknown λ, μ – characteristics, included both directly into the formula (7) and into the substitution L, and also roots of S_4 and S_5. That's why in this research it is possible to conduct only the preliminary quality analysis of the change of probability of the working state "00" depending on the time of exploitation of the technical system. It is obvious that independently of its sign the first component is some permanent value which depends on the value of the attended roots of S_4 and S_5 displacing general dependence of $P_{00}(t)$ upwards or downward on a y-axis.

The analysis of behavior of probability function for the state of the system "00" at the time of exploitation of $t \to \infty$ shows that the increase of time diminishes the probability on an exponential law. The final probability in this case is:

$$P_{00}(t \to \infty) = Z_{00}.$$

Or, it is possible on the basis of the value of permanent Z_{00} which has been got before to write down:

$$P_{00}(t \to \infty) = \frac{1}{S_4S_5}(2\lambda_{10}\mu_{11} + \lambda_{10}\lambda_{10'} + \lambda_{0'0}\mu_{11} + \lambda_{0'0}\lambda_{10'} + \lambda_{00}\lambda_{10} - \mu_{10}\lambda_{10'} - \mu_{10}\lambda_{0'0} - \mu_{10}\mu_{11}).$$

Thus, the conducted analysis set, that general character of changing in probability of capable working state "00" of the passively dubbed system is described by a double exponential law. Its chart is presented in Fig. 1. The concrete

form of the curve is greatly dependent on the correlations λ and μ which are descriptions included in the equalization. The double exponential dependence assists at deceleration of loss of capacity by the system while entering the dubbed element.

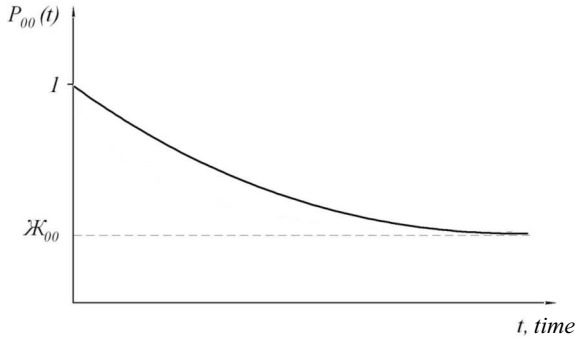

Fig. 1. Changing in the probability of the passively dubbed system in fully capable working state from time of exploitation

Coming from the known determination of mean work on the refuse through the probability of faultless work [4] we can write down:

$$\overline{T} = \int_0^\infty P(t)dt .$$

In detail, to the solving task on determination of mean work in the capable working state "00" it is possible to write down:

$$\bar{t} = \int_{t_1}^{t_2} P_{00}(t)dt .$$

For establishment of mean value of work on the refuse it is expedient to choose the time of domain $t_2 - t_1$, after the period of extra work of the system and its entrance in the mode of exploitation, when aging processes, related to the subsequent loss of capacity, begin gradually show the selves [9].

Putting the value of probability from the expression (7) we have:

$$\bar{t}_{00} = \int_{t_1}^{t_2}\left[-\frac{L}{S_4S_5} + \frac{1}{S_5}(\mu_{11} + \lambda_{10'} + \lambda_{10} + \lambda_{0'0} - \mu_{10} + S_4)\exp(-S_4t) + \right.$$
$$\left. + \left(1 - \frac{L}{S_4S_5}\right)\exp(-S_5t)\right]dt.$$

From where:

$$\bar{t}_{00} = -\frac{L}{S_4S_5}t\Bigg|_{t_1}^{t_2} + \frac{1}{S_5}\left(\mu_{11} + \lambda_{10'} + \lambda_{10} + \lambda_{0'0} - \mu_{10} + S_4 - \frac{L}{S_4}\right)\left(-\frac{1}{S_4}\right)e^{-S_4t}\Bigg|_{t_1}^{t_2} +$$
$$+ \left(1 - \frac{L}{S_4S_5}\right)\left(-\frac{1}{S_4}\right)e^{-S_5t}\Bigg|_{t_1}^{t_2}. \quad (8)$$

For the quality analysis of result the possible dependences of influence of each components of equalization were built (8) on a general result, and the total curve of change of mean time of system staying in the fully capable working state of *t00*. The graphics is represented in Fig. 2.

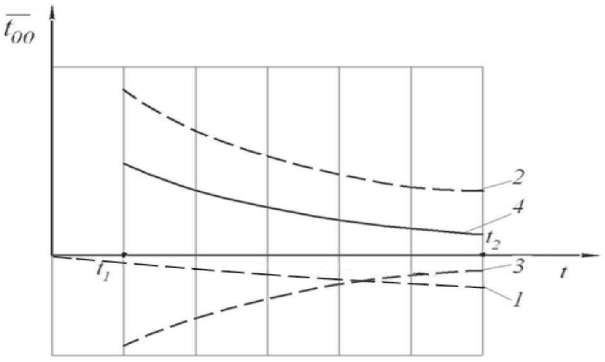

Fig. 2. Dependence of changing of time of the system being in the complete capable working state "00" on the time of its exploitation:
1 – is the first component of equalization (9); 2 – is the second component; 3 – is the third component; 4 – is total resulting dependence

As we can see from the summarizing chart (curve 4), mean time of the system being in the fully capable working state "00", when both basic and reserve elements are in good condition, is gradually going down. It corresponds to the physical essence of the problem of the system's research that it gets older losing the capacity while exploitation.

CONCLUSIONS

1. Passively dubbed technical system losing the capacity as a result of aging has the reliability indexes, depending on the time exploitation according to the double exponential law.
2. The maximally able value of probability of faultless work of the system, when both basic and dubbed elements are in good condition, serves the final (asymptotic) value of this probability.
3. Mean work on the refuse of the system consists of three components, one of those depends on the time of exploitation, and two others change on exponent.

REFERENCES

1. **Boyko A.I. 2010:** Research of function of readiness of the mechanical systems at the accumulation of damages / A.I. Boyko, K.M. Dumenko of // Problem of calculable mechanics and durability of constructions: Bulletin of scientific works, Dnipropetrovsk : Science and education, — /ssue. 14. — 72-78.
2. **Pogorily L.V. 2003:** Harvesting Equipment: problems, alternatives, prognosis / L.V. Pogorily, S.M. Koval // Technika APK. — №7. — 4-7.
3. **Ushakov I.A. 2008:** Theory of Reliability Systems / I.A. Ushakov. — M.: Drofa, — 239.
4. **Nekiporenko V.I. 1977:** Structural Analysis of systems / V.I. Nekiporenko. M. : Sovetskoe radio, — 214.

5. **Gritsishin M. 2003:** Requirements to Combine Harvesters / M. Gritsishin, V. Amons, P. Grinko // Technika APK. – №2, 9-15.
6. **Sudakov P.S. 1988:** Isputaniya sistem: vubor ob′emov i prodolgitelnosti. M.: Mashinostroenie, – 445.
7. **Truhanov V.M. 1995:** Metodu obespecheniya nadegnosti izdeliy mashinostroeniya. M.: Mashinostroenie, – 304.
8. **Truhanov V.M. 1999:** Nadegnost′ v tehnike. M.: Mashinostroenie, – 598.
9. **Truhanov V.M. 1996:** Nadegnost′ izdeliy mashinostroeniya: Teoriya i praktika. M.: Mashinostroenie, – 336.
10. **Hald A. 1956:** Matematicheskaya statistika s tehnicheskimi prilogeniyami. M.: Inostrannaya literatura, – 379.

ВАРЬИРОВАНИЕ ПОКАЗАТЕЛЕЙ НАДЕЖНОСТИ ПАССИВНО РЕЗЕРВИРОВАНЫХ СЛОЖНЫХ ТЕХНИЧЕСКИХ СИСТЕМ

Анотація. У статті розглянута пасивно резервована система працююча в режимі поступового накопичення пошкоджень. Встановлені закономірності зміни основних показників надійності таких як вірогідність безвідмовної роботи і середній час роботи повністю.
Ключові слова: готовність до роботи, середнє напрацювання на відмову, вірогідність безвідмовної роботи, модель надійності системи.

TEKA. COMMISSION OF MOTORIZATION AND ENERGETICS IN AGRICULTURE – 2013, Vol. 13, No. 1, 23–30

Program platform aiding PTZ cameras operator work in CCTV system – improvement in the scope of functionality and ergonomics of system use

Marcin Buczaj[1], *Andrzej Sumorek*[1], *Agnieszka Buczaj*[2]

[1]Department of Computer and Electrical Engineering, Lublin University of Technology, Nadbystrzycka 38A, 20-618 Lublin, email: m.buczaj@pollub.pl; a.sumorek@pollub.pl
[2]Department of Physical Occupational Hazards Institute of Rural Health in Lublin, Jaczewskiego 2, 20-090 Lublin, email: a.buczaj@o2.pl

Received December 15.2012; accepted March 14.2013

Summary. The functionality of control system as well as the ergonomics and intuitiveness of its use are the essential factors, except of system operator experience, affecting CCTV video monitoring system management process. An optimal relationship between system functionality, its ergonomic use and the system operator experience makes it possible to quickly adapt the parameters of recorded image to the needs in the scope of currently performed tasks associated with the observation of assigned area. CCTV video monitoring system management mainly consists in the checking of cameras settings and matching of PTZ cameras parameters to current needs in the scope of observation. The article presents the role of ergonomics of work stations and the technical capabilities of program platforms aiding PTZ cameras operator work in CCTV system. The presented program platform was built as an application basing upon LabView environment. Except of control functions available in standard hardware manipulators for PTZ cameras settings, the program platform enables the visualization of object status on the screen and the performance of pre-set control functions in the form of procedures. Particular emphasis has been placed on the practical capabilities of such systems, operators' work aiding, reduction of operation times in case of performance of a task associated with the change of PTZ cameras settings.
Key words: control and supervision systems, video monitoring, CCTV systems, PTZ cameras, communication protocols, management processes ergonomics.

INTRODUCTION

CCTV video monitoring systems are the components of technical equipment used for property protection. Their basic task is to supply comprehensive information on the current condition of the protected area to the competent organizational sections in the object protection system in the form of images. An essential thing is to configure CCTV system in a manner ensuring that the information received by the user is as complete as possible and suitable to the needs at the point of time. The information can be associated with: protected area checking, confirmation that specified zone has been disturbed, invader identification or occurred danger. The factors specified above affect not only the current safety level in the object being protected but also make it possible for competent organizational sections in the object protection system to early react to specified danger as well as to eliminate thereof or to limit its impact on environment and achieved targets of attack [1, 4, 7, 8, 9, 10, 17, 18].

From presented tasks it appears that a monitoring system shall enable the imaging for the largest possible area in order to perform its task. Therefore, the user is given the possibility of close observation of the object being protected. There are detailed and general surveillance zones in surveillance areas monitored by means of CCTV cameras. The detailed surveillance zones (particularly important sensitive zones) are defined as the locations and areas of importance in view of safety to be maintained in the object. In case of the occurrence of danger, the monitoring shall be commenced as soon as possible by means of maximum possible number of cameras. Rotary cameras controlled by means of special consoles with access to cameras functions and presets are applied in order to get to selected area. The settings of selected rotary camera are controlled by operator by means of a hardware console in order to correct the following parameters: positioning, inclination and zooming. In case of an excessive number of cameras in the system it is possible that the system user is unable to set PTZ cameras parameters, simultaneously tracking the object and properly responding to additional dangers occurring in the object. Too many cameras significantly affect the system operation effectiveness and can even cause the system's dysfunction. It is also associated with increased effort of the user during the system's operation and with reduced comfort at work.

The purpose of the present study is to draw the attention to functional capabilities of CCTV systems and to the impact of algorithmic aiding on the work of system operator and

the reduction of its workload during the process control. The study presents the concept of an universal program platform adapted to specified object and making it possible to supervise selected observation zones and areas. The article presents the technical measures enabling the improvement of ergonomic features of the used system by means of IT solutions. The scope of the study encompasses the presentation and analysis of the technical measures enabling the improvement of the system use ergonomics by means of IT solutions. The *attention* was paid to the possibility of utilizing the algorithms of simultaneous control for PTZ rotary cameras, dedicated for specified object and making it possible to limit the necessary activities of the user in course of the performance of its surveillance tasks in the object being protected. The essence of the algorithm consists in the definition and interrelation of presets for multiple cameras accessible in the system.

FUNCTIONALITY AND ERGONOMICS OF CCTV VIDEO MONITORING OPERATOR

The work performed by hardware and CCTV electronic system operator consists in the achievement of assumed security goals. Particularly, the task of the operator is associated with the management of system elements settings including PTZ rotary cameras parameters control, the reaction to recorded events and the checking of CCTV system operation correctness. The communication between the user and system is possible by means of a screen equipped with proper graphical interface. The working conditions at the station equipped with a Video Display Unit should be sufficient to ensure the safety, convenience and comfort in the course of work performed by the operator in order to avoid errors [5, 6, 7, 8, 10].

Therefore, the task of the person supervising the control process in CCTV system is to check the object condition, to supervise the correctness of registration and control process, to initiate individual phases, procedures and functions and to react in case of any abnormalities. This supervision is particularly characterized by continuous monitoring of instrument readings from images recorded by the cameras and by introduction of corrections in case of deviations from the assumed profile [5, 10].

Computer-aided measuring, control and supervision system enables data acquisition, processing and their presentation to operator through the performance of information and decision making subsystem tasks. The tasks performed by operator consist in monitoring of information occurring on imaging devices screens, in displaying of necessary information about process status, entering supplementary information, evaluation of existing situation, decision making and decision entry into computerized system. The operator's work is aided by the correctly built system performing monotonous repeating activities but the operator is not substituted in the decision making process. The system performs the algorithms and procedures associated with arduous and precisely determined tasks which may take the time of system's operator and divert his attention from the principal goal, i.e. safety management in the supervised object. The information exchange between the operator and system is possible by means of an extended hardware interface (information exchange technology component) supplemented by software creating the graphical user interface (GUI). The work with an incorrectly designed interface can be arduous for the operator and can lead to errors and to non-compliance with requirements in the scope of quality of performed tasks as a result of fatigue or stress perceived after a short period of time [12].

The correctness of decisions made by the operator depends on possibility to receive the signals and ability to understand information contained therein [20]. The purpose of control devices is to make it possible to perform the control process by the operator in an efficient, safe and correct manner through the optimized communication between man and technical system. The operator stations are usually equipped with multiple signalling and control devices. Their correct design solution and working conditions may have significant impact on the number of operator's errors and his fatigue. Currently, control panels have been substituted by computers analyzing the data received from the sensors recording process parameters changes and presenting the information processing results to the operator or correcting the errors basing upon a predetermined program [20].

However, an appropriate manner of information visualization and processes control method is required for operations on synthetic data and processed information. The processes control should not be based upon the regulation of single (partial, detailed) parameters but in the form of determination of resulting (aggregated, total, general) parameters. However the partial parameters should be selected by means of optimizing computer programs. The structures of contemporary testing and measuring systems are characterized by a trend toward the computerization and graphical representation of information. Hence, significant interest has been observed in ergonomic features of the stations provided with visual display terminals (VDT – Visual Display Terminal) [20].

The requirements in the scope of system capability to cooperate with an operator are associated i.a. with the factors resulting from the essence of control process for specified system, tasks to be performed in process control and from established control strategy. Equally essential are the factors associated with man – machine interface design, impact of work station (station layout – i.a. ergonomic features of the devices and their spatial arrangement at the operator station, material environment conditions) and human factors associated with the operator's load in course of work. Therefore, the compliance with requirements in the scope of working conditions may affect the capability of an industrial process control system with the operator [2].

The control room is the basic functional unit in the control centre and in its associated physical structure occupied by operators performing the functions encompassing the centralized control, supervision and guiding. The operator interface located in the vicinity of the equipment or system subjected to supervision and/ or control is called the local control station [3].

The working conditions in the control room shall ensure the safety, human health protection and well being as well as the technical and economical effectiveness. The human factor, machine (hardware and software), working conditions and control functions should be considered in its entirety and subjected to optimization [3, 14].

CAMERAS IN CCTV SYSTEM – FUNCTIONAL MODEL OF PTZ CAMERAS

The camera used in CCTV video monitoring systems are defined as image recording electronic systems. Depending on version, an image converter built in CMOS or CCD technology is their principal element. The cameras can be subdivided into digital cameras (H-264 or MPEG standard) and analogue (TV standard) cameras depending on vision signal transmitted by CCTV camera. Resolution, objective focal range and type of image (monochrome or colour) are the specific features of cameras. There are two types of cameras in view of their construction (Fig. 1): stationary cameras (compact and dome type) and cameras equipped with rotating device (PTZ rotary cameras).

PTZ rotary cameras make it possible to change three settings: P – positioning, T – tilting and Z – zooming. Due to such features, the cameras can record images of various observation areas determined by the operator. The corrections of rotary camera parameters and its setting are most frequently performed by means of a special hardware manipulator. The camera code shall be entered by the operator. It is possible to adapt the image parameters to current requirements and to perform observation tasks by means of special joystick.

Due to possibility of adjustment and changes of image parameters based upon changes of position, tilting and zooming, the functional model of PTZ rotary camera can be described on the basis of spherical coordinate system. The spherical coordinate system is based upon three coordinates f, q, ri making it possible to adapt the regulation parameters of PTZ rotary camera (Fig. 2). The coordinate f corresponds to parameter associated with the camera positioning (*P*), q coordinate – tilting (*T*), and *r* coordinate – zooming (*Z*).

Fig. 2 illustrates the relations making it possible to convert from coordinates in rectangular coordinate system (x, y, z) to spherical coordinate system (f, q, r). The most frequent is the situation when CCTV system operator tracking a moving object (movement in rectangular coordinate system) has to adapt the actions to the specific features of rotary camera control system (spherical coordinate system). Fig. 3 illustrates the situation when the operator is tracking an object moving along a straight line. Attention should be paid to changes of multiple parameters in order to maintain the same image parameters for the object being monitored. Fig. 4 illustrates the situation when an object is moving along a circular path, with constant distance from one of the cameras but it is monitored by two cameras. The necessity of adaptive correction of PTZ rotary camera parameters by the operator in order to achieve the assumed observation goals is also shown in this situation.

The situations presented above have been selected as the examples of problems experienced every day by CCTV video monitoring systems operators operating PTZ rotary cameras in the system. The principal problems experienced by operators and inconveniences resulting from the applied observation method by means of PTZ camera and having essential impact on quality and effectiveness of continued monitoring activities are:

– mismatch between the control system based upon spherical coordinate system (f, q, r) and the behaviour of per-

Fig. 1. Cameras of CCTV system [22] a) compact camera, b) dome camera, c) PTZ rotary camera

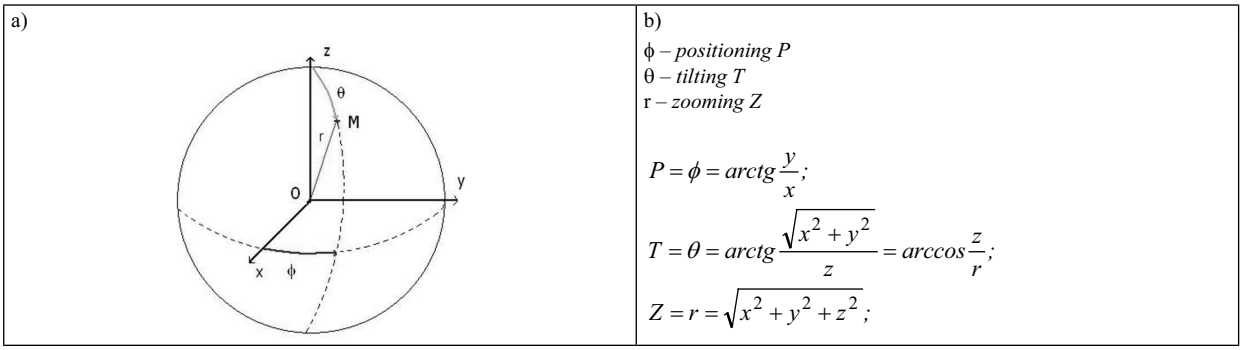

Fig. 2. Functional model of rotary camera a) spherical coordinate system, b) relations between coordinates in spherical coordinate system and in rectangular coordinate system

a)

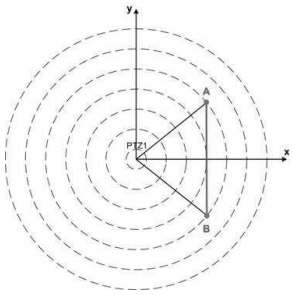

b)

object movement
(rectangular coordinate system)
X = f(x) = const; ΔX = 0;
Y = f(y) = var; ΔY = const;
Z = f(z) = const; ΔZ = 0;

control PTZ 1
(spherical coordinate system)
P = f(ϕ) = var; ΔP=var;
T = f(θ) = var; ΔT=var;
Z = f(r) = var; ΔZ=var;

Fig. 3. Object movement between A and B points – situation 1; a) layout sketch b) description of relations specific for the object movement and corresponding relations of changes of PTZ rotary camera settings

a)

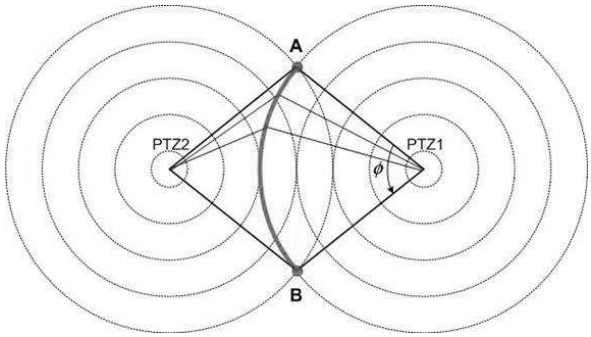

b)

object movement
(rectangular coordinate system)
X = f(x) = var; ΔX = var;
Y = f(y) = var; ΔY = var;
Z = f(z) = const; ΔZ = 0;

control PTZ 1
(spherical coordinate system)
P = f(ϕ) = var; ΔP=const;
T = f(θ) = const; ΔT=0;
Z = f(r) = const; ΔZ=0;

control PTZ 2
(spherical coordinate system)
P = f(ϕ) = var; ΔX=var;
T = f(θ) = var; ΔY=var;
Z = f(r) = var; ΔZ=var;

Fig. 4. Object movement between A and B points – situation 2; a) description of relations specific for the object movement and corresponding relations of changes of PTZ rotary cameras settings

sons moving in the area under observation (rectangular coordinate system x, y, z),
– necessity of continuous switchovers of control options on hardware manipulator in case of supervision over specified zone by means of large number of cameras;
– mismatch between the standard procedures of calling for individual functions and specific features of specified object.

The factors presented above are procedural factors. Therefore, it is possible to improve the operator's activity effectiveness by means of IT tools used in order to make the control process more efficient.

CCTV VIDEO MONITORING SYSTEMS

CCTV (closed circuit television) video monitoring system is defined as the system to be used for observation by means of proper equipment, a determined zone under surveillance [1]. The closed circuit television (Fig. 5) consists of basic system elements used for image recording (video monitoring subsystem), vision signal transmission (signal transmission subsystem) and for its displaying (receiving subsystem) as well as supplementary elements (subsystems) used for archiving of recorded image and controlling of individual system elements settings (cameras, rotary devices etc.)

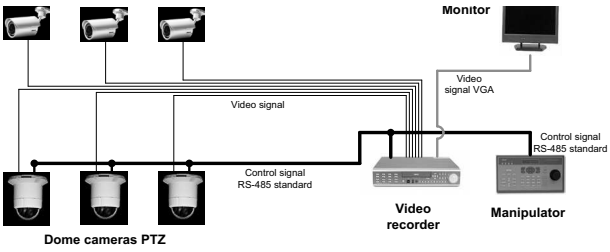

Fig. 5. Diagram of a conventional CCTV video monitoring system

Detailed guidelines for CCTV video monitoring system should encompass the following scope:
– presentation of the required system safety level (assessment of hazards);
– subdivision into zones and determination of manner of surveillance for individual zones (Fig. 6);
– determination of spaces (zones) supervised by the system (coverage);
– characteristics of the range of system operations environment conditions;
– description of tasks and procedures associated with the performance of surveillance functions;
– determination of manner of video signal and control signal transfer;
– presentation of tasks associated with system elements control.

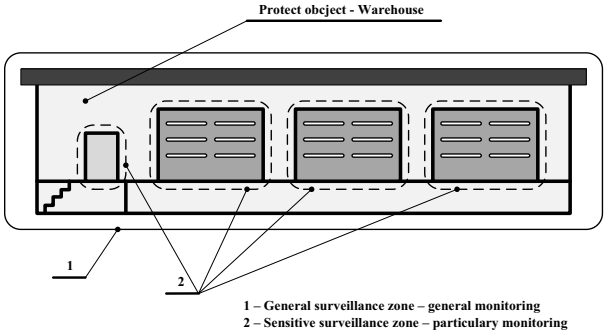

Fig. 6. Subdivision into surveillance zones in the object to be protected

A camera is the basic element of each CCTV system. Two types of cameras can be specified in the view of their functional capabilities, role performed in the system and costs: stationary and rotary cameras. The stationary cameras are usually used for the observation of general surveillance zones and the rotary cameras due to their increased capabilities in the scope of settings are used for the surveillance of particularly important (sensitive) zones in the object being protected. Their functions make it possible, through the change of camera optical parameters and camera position, to match the size of the surveillance zone under observation to current needs of the user.

The video signal in conventional video monitoring systems is transmitted between cameras as well as recording and imaging elements by means of coaxial cables (so called coax). The technical limitations resulting from applied signal transfer medium by means of coaxial cable are associated with the cable length. Maximum recommended lengths of coaxial cables in CCTV systems are included between 250m (RG-59 cable) and 800m (RG-15 cable) [15]. The signal amplifiers are required in case of signal transfer by means of cables with the length exceeding recommend values.

However, in case of control system, the system in RS-485 standard is the most common control signal transfer system. RS-485 standard has been introduced as developed version of RS-422A standard. RS-485 standard consists of a differential (symmetrical) transmitter, dual – circuit transmission path and a differential receiver. It is allowed to connect multiple transmitters and receivers on single line. Due to possibility to transfer only one signal (chain of commands) at the same time, these systems must be equipped with interlocking systems. The systems equipped with so called tri-state gates. In said gates, except of output signals corresponding to the states of logic 1 and logic 0, high impedance state of gate output is possible. The devices in RS-485 system are usually characterized by hierarchy of importance i.e. devices performing master or slave functions to each other [15, 16].

THE CONCEPT OF PROGRAM PLATFORM ENABLING THE CHANGE OF PTZ CAMERAS SETTINGS AIDING CCTV SYSTEM OPERATION WORK

The conventional CCTV video monitoring system illustrated in Fig. 5 is an autonomous system built of elements used only in this type of systems. Exclusive hardware and functional features are a disadvantage of such solutions. The purpose of modernization of a conventional CCTV video monitoring system (Fig. 7) is to increase the system functionality. Therefore, a program platform has been created in LabView environment in the form of an application enabling simultaneous control for multiple rotary PTZ cameras settings. The principal task of this application is to generate a message signal (instruction code string) to the control system. PTZ cameras control is carried out by the calling of procedures triggering predefined presets of cameras. Due to lack of RS-485 interface in standard equipment of PC computers, it is necessary to provide RS-232/RS-485 or USB/RS-48 signal converter in the system.

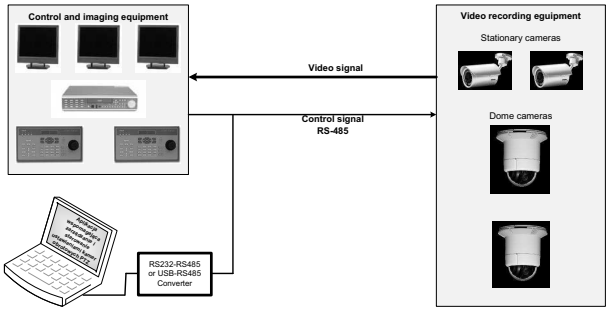

Fig. 7. Schematic diagram of monitoring system with built-in module enabling simultaneous control for multiple rotary PTZ cameras settings by means of computer application

The determination of surveillance of zones in the area of protected infrastructure is an Essentials element of CCTV system designing phase, in the scope of general surveillance zones (Fig. 8) as well as detailed surveillance zones (Fig. 9). The determination of certain sensitive areas shall be based upon analysis of potential hazards occurring therein or upon the performance of control of or supervision over the flow of persons and property. Therefore, it is important to arrange CCTV system elements (particularly rotary cameras) in a manner ensuring the performance of said tasks in the best possible manner. Additional factors limiting excessive extension of CCTV system are the system costs and possibility of transfer of the Signac recorded by camera and its archiving. Not always and additionally simultaneously, it is necessary to provide detailed surveillance for all sensitive zones. Such observation should be carried out in precisely determined conditions only (e.g. as a result of occurred hazard). Therefore, one rotary camera can be used for surveillance of several sensitive zones.

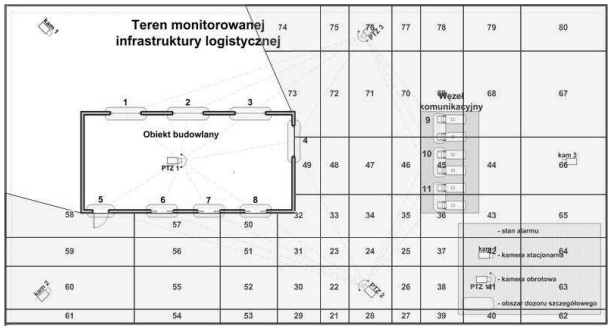

Fig. 8. Field diagram of an object with marked general surveillance zones for PTZ2 camera including their corresponding presets

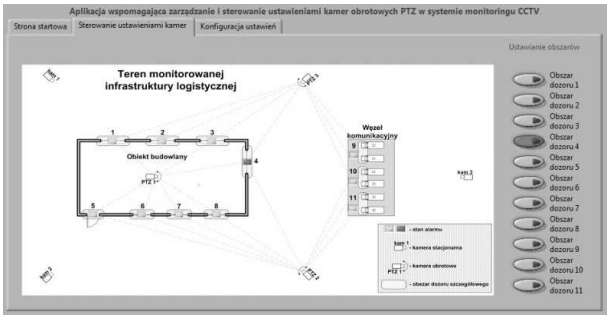

Fig. 9. Field diagram of an object with marked detailed surveillance zones

In a manner identical to the distributions of detailed and general surveillance zones illustrated in Fig. 8 and Fig. 9, the areas associated with presets are created for all PTZ cameras contained in CCTV system. Individual areas are the field areas corresponding to certain areas of dialog window of the system displayed on the screen display. Therefore, to each pixel assigned on the synoptic map (field diagram) of the protected object, there are assigned relations referring to the implementing procedures performing the calling of precisely determined presets for all the cameras contained in CCTV system.

The task of the operator is not to change the settings of successive cameras manually any more but to call corresponding procedure on the screen by means of computer mouse. It is also possible to provide CCTV system operator station with a touch screen. In such case it is possible to call any procedure directly on the screen. The purpose of the presented solution is to support the operator's work. It is possible as a result of his release from arduous manual process associated with calling of successive settings. Individual field areas are called by the operator in presented solution on the synoptic map of the protected object. The areas correspond to real areas in the field. Therefore, an additional advantage of this solution consists in its intuitiveness associated with simple calling of certain functions.

APPLICATION FOR PTZ CAMERAS OPERATION MANAGEMENT IN CCTV SYSTEM

An application aiding PTZ rotary cameras settings management and control in CCTV system has been created on the basis of LabView programming environment. This environment is characterized by large capabilities associated with technological processes support in the scope of checking and control as well as individual approach to the process of creating the system operated by users [9, 11, 13, 19].

The program enabling simultaneous control of settings for PTZ rotary cameras operating in CCTV system in an object under surveillance, contains the following principal elements of the system:

– user interface – enabling (depending on user rights) control, configuration change or checking the system operation;
– organizational diagram – internal relation between individual application elements enabling the performance of tasks assigned by the user on control panel;
– I/0 operation (communication port operation) – system component responsible for generation of actuators operation control signal in PTZ rotary cameras.

In case of a correctly operating system managing the operation and control of settings of individual elements of video monitoring CCTV system, it is necessary to apply a recognizable control protocol. Selected protocol standard does not have to be identical for all the system elements. It is possible to use various protocols in the system. It is important to ensure the correlation (protocol conformity) in the time between the controlling and controlled device. There are many protocol standards applied in practice; but the most popular are PTZ protocols: Pelco-D and Pelco-P. The messages formats (format of generated instruction) in Pelco-D and Pelco-P standard have been presented in Tab. 1 and Tab. 2.

Table 1. Format of message in Pelco-D standard [21]

Bajt 1	Bajt 2	Bajt 3	Bajt 4	Bajt 5	Bajt 6	Bajt 7
Start byte (FF)	Camera No	Instruction code (direction, zoom, sharpness etc.)		Camera movement speed	Camera tilting speed	Checksum

Byte 7 (Checksum) is the result of „modulo 100" operation from logic sum of bytes 2÷6.

Table 2. Format of message in Pelco-P standard [21]

Bajt 1	Bajt 2	Bajt 3	Bajt 4	Bajt 5	Bajt 6	Bajt 7	Bajt 8
Start byte (A0)	Camera No	Instruction code (direction, zoom, sharpness etc.)		Camera movement speed	Camera No	Stop byte (AF)	Checksum

Byte 8 (Checksum) is the result of logic sum XOR operation of byte 1÷7.

The messages (instruction codes) informing about completion of two operations in the system: the first one enabling the movement with maximum speed (Turbo) to the RH side of the camera (rotary device) No 8 and the second one: stopping of the performance of the first operation in Pelco-D and Pelco-P protocol standard (hexagonal code) are presented in Tab. 3.

Table 3. Control messages (instruction codes) in Pelco-D and Pelco-P standard

Operation number	Instruction codes in PelcopD standard	Instruction codes in PelcopD standard
1	FF 08 00 02 FF 00 09	A0 08 00 02 40 00 AF 45
2	FF 08 00 00 00 00 08	A0 08 00 00 00 00 AF 07

The determination of technical possibilities of observation for specified detailed areas by individual cameras is an important element associated with the analysis process for individual capabilities of the system and with the creation of control procedures (generation of control instructions). Therefore, it is necessary to build an individual table of relationships for each object. The table of relationships for presets of PTZ cameras settings making it possible to achieve the observation goals for detailed surveillance zones (Fig. 8) has been presented in Tab. 4. This table illustrates

the relations between presets defined in the system for individual rotary PTZ cameras and detailed surveillance areas.

Table 4. Dome cameras PTZ presets in CCTV system – table of relationships

Survellance areas	1	2	3	4	5	6	7	8	9	10	11
Camera PTZ 1	1	2	3	4	5	6	7	8	-	-	-
Camera PTZ 2	-	-	-	1	2	3	4	5	6	7	8
Camera PTZ 3	1	2	3	4	-	-	-	-	5	6	7

The example of a message (chain of commands) in Pelco-P protocol standard (hexagonal code) generated and sent to the control system (RS-485) by an application aiding the cameras settings management in CCTV system, enabling the setting of all available cameras to the detailed surveillance area No 4, has the following form:
A0 01 00 07 00 04 AF 0D;
A0 02 00 07 00 01 AF 0B;
A0 03 00 07 00 04 AF 0F.

CONCLUSIONS

The correct operation of CCTV video monitoring system is based upon the cooperation between the operator and the system as well as the correct use of available equipment by the system operator. Therefore, the most reasonable solution consists in the best equipment enabling the video data recording and archiving as well as in auxiliary equipment of the system in the form of elements releasing the operator from the execution of unnecessary, complicated or time consuming procedures. In the opinion of authors, such a solution consists in the application of a dedicated program platform matched to object characteristics and making it possible to call assumed procedures and functions directly from the application window. The operator's role is limited to the choice of a function without any analysis of the manner of its performing. In such a case, the operator can engage himself in the object's observation instead of tasks associated with correct execution of control process.

Due to the equipment of conventional CCTV system with the system aiding PTZ, rotary cameras settings management and control in CCTV system, it is possible to achieve a quick and simultaneous preview of a selected sensitive zone in the protected object for all cameras available in the system. The task of the operator is to choose an area of interest in the synoptic map of the object. The change of current settings of cameras to the settings associated with the preview of an area determined in specified preset of camera is carried out in a smooth and unattended manner. Therefore, the time associated with change of system settings is significantly reduced in comparison with manual operation of control devices.

Further integration of PTZ rotary cameras settings control system with other protective systems (Intrusion and Hold-up *Alarm Systems* (*I&HAS*)), access control systems and fire alarm systems, enables automatic change of cameras settings in order to enable the preview to selected zone at the time of hazard occurrence or for the time associated with the performance of assumed procedure.

The use of PTZ rotary cameras in CCTV systems makes it possible to reduce the costs associated with the system installation and video data archiving. In contrast to stationary cameras, the preview of many sensitive zones (obviously not at the same time) is possible by means of single rotary camera. The correct determination of cameras presets makes it possible to achieve the multiplication of rotary cameras capabilities in comparison to stationary cameras.

REFERENCES

1. **PN-EN 50132-7:2003**: Systemy alarmowe. Systemy dozorowe CCTV stosowane w zabezpieczeniach. Część 7: Wytyczne stosowania, PKN, Warszawa.
2. **PN-EN 61069-6:2004:** Pomiary i sterowanie procesami przemysłowymi. Wyznaczanie właściwości systemu w celu jego oceny. Część 6: Ocena współdziałania systemu z operatorem, PKN, Warszawa.
3. **PN-EN ISO 11064-1:2007:** Ergonomiczne projektowanie centrów sterowania. Część 1: Zasady projektowania centrów sterowania, PKN, Warszawa.
4. **Boguta A., 2011:** Zastosowanie monitoringu IP w systemie nadzoru budynku. TEKA Komisji Motoryzacji i Energetyki Rolnictwa PAN, Vol. 11, 9–17.
5. **Bolibok A., 2005:** Ocena stanowisk pracy operatorów komputerowych. Inżynieria Rolnicza. Nr 11 (71). 45–50
6. **Buczaj A., Pawlak H., 2008:** Modelowanie systemu oceny warunków pracy operatorów sterowni. Inżynieria Rolnicza. Nr 7 (105). 31–37.
7. **Buczaj M., Sumorek A., 2010:** Wirtualny system nadzoru sterujący pracą systemu sygnalizacji włamania i napadu. Motrol: Motoryzacja i Energetyka Rolnictwa, t. 12, 46–53.
8. **Buczaj M., Buczaj A., 2011:** Komputerowy system sterowania układem wentylacyjnym i odpylającym w młynie zbożowym. Inżynieria Rolnicza. Nr 1 (126). 15–21.
9. **Buczaj M., Sumorek A., 2011:** Wykorzystanie środowiska LabView do budowy systemu nadzoru kontrolującego parametry klimatyczne i techniczne w pomieszczeniach w gospodarstwie rolnym. TEKA Komisji Motoryzacji i Energetyki Rolnictwa PAN, Vol. 11, 18–28.
10. **Buczaj M., 2012:** Systemy sterowania i nadzoru szyte na miarę. Czasopismo Zabezpieczenia Nr 6(88)/2012. 20–24.
11. **Chruściel M., 2008:** LabView w praktyce, Wydawnictwo BTC, Legionowo.
12. **Donigiewicz A., 2002:** Modelowanie interakcji człowiek-komputer: problemy oceny jakości i niezawodności. WAT, Warszawa.
13. **Horyński M., 2011:** Komputerowe wspomaganie projektowania wirtualnych systemów nadzoru instalacji elektrycznej we współczesnych budynkach. TEKA Komisji Motoryzacji i Energetyki Rolnictwa PAN, Vol. 11. 123–134 .
14. **Horyński M., 2012:** Energy efficient control of lighting in an intelligent building. TEKA Komisji Motoryzacji i Energetyki Rolnictwa PAN, Vol. 12. 61–67.
15. **Kałużny P., 2008:** Telewizyjne systemy dozorowe, Wydawnictwo WKiŁ, Warszawa.

16. **Nawrocki W. ,2006:** Rozproszone systemy pomiarowe, Wydawnictwo WKiŁ, Warszawa.
17. **Okarma K., Lech P., 2010:** A fast image analysis technique for the line tracking robots, ARTIFICIAL INTELLIGENCE AND SOFT COMPUTING, PT II Book Series: Lecture Notes in Artificial Intelligence, Vol. 6114, 329–336.
18. **Okarma K. 2012:** Combined image similarity index, OPTICAL REVIEW Vol. 9, 349–354.
19. **Tłaczała W., 2002:** Środowisko LabView w eksperymentach wspomaganych komputerowo. WNT, Warszawa
20. **Tytyk E., 2001:** Projektowanie ergonomiczne. PWN, Warszawa, Poznań.
21. www.commfront.com
22. cms.cbc-pl.com

PLATFORMA PROGRAMOWA WSPOMAGAJĄCA PRACĘ OPERATORA KAMER PTZ SYSTEMU CCTV – ASPEKT POPRAWY FUNKCJONALONOŚCI I ERGONOMII UŻYTKOWANIA SYSTEMU

Streszczenie: Funkcjonalność systemu sterowania oraz ergonomia i intuicyjność jego użytkowania to obok doświadczenia operatora systemu główne czynniki mające wpływ na proces zarządzania systemem monitoringu wizyjnego CCTV. Optymalne powiązanie funkcjonalności systemu jego ergonomii użytkowania i doświadczenia operatora umożliwia szybkie przystosowanie parametrów rejestrowanego obrazu do potrzeb aktualnie realizowanych zadań związanych z obserwacją zadanego obszaru. Zarządzanie systemem CCTV to w dużej mierze kontrola ustawień kamer oraz dopasowanie parametrów kamer PTZ do aktualnych potrzeb obserwacyjnych. W artykule przedstawiono rolę ergonomii stanowisk pracy oraz technicznych możliwości platform programowych wspomagających pracę operatora kamer PTZ systemu CCTV. Przedstawiona platforma programowa to aplikacja zbudowana na bazie środowiska LabView. Platforma programowa oprócz realizacji funkcji sterowania dostępnych w standardowych, sprzętowych manipulatorów ustawień kamer PTZ umożliwia wizualizację stanu obiektu ma monitorze oraz proceduralne wykonywanie zadanych funkcji sterowania. W artykule szczególny nacisk został położony na praktyczne możliwości takich systemów, na wspomaganie pracy operatorów, zmniejszenie czasów obsługi przy realizacji zadań związanych ze zmianą ustawień kamer PTZ.
Słowa kluczowe: systemy sterowania i nadzoru, monitoring wizyjny, systemy CCTV, kamery PTZ, protokoły komunikacyjne, ergonomia procesów zarządzania.

TEKA. COMMISSION OF MOTORIZATION AND ENERGETICS IN AGRICULTURE – 2013, Vol. 13, No. 1, 31–36

The use of ultrasonic detectors in peripheral object protection for casement windows security

Marcin Buczaj

Department of Computer and Electrical Engineering, Lublin University of Technology,
ul. Nadbystrzycka 38A, 20-618 Lublin, email: m.buczaj@pollub.pl

Received February 14.2013; accepted March 14.2013

Summary. Fast and effective detection of attempted burglary or attack is the essence of alarm systems operation. It becomes necessary to protect not only the inner areas in the building but also the outdoor areas enabling the access to the object. The protection of the window and door openings of the building by means of reed relay sensors or contact sensors often constitutes the only possible method of the peripheral object protection. The purpose of the present paper is to present the concept consisting in the use of Doppler ultrasonic detectors in casement windows as the basic detection element in the peripheral protection circuit for the object. URZ0530 ultrasonic detector has been used for the tests.

Key words: I&HAS, alarm systems, Doppler ultrasonic detectors, peripheral object protection.

INTRODUCTION

The alarm systems are not used to keep the intruder from entering into the object. Their essential task is to detect the hazard and to inform the user about the occurrence of this danger. The time of system response to occurred hazard [6] is the basic parameter characterizing the effectiveness of alarm system. Therefore in view of effective protection of the object, the essential requirement to be met by the system is to enable the detection of attempted invasion of the intruder into the object before the physical protections are forced by this intruder. This solution enables the reaction of the user in order to counteract the hazard or to limit the scale of material damages (theft, devastation) as well as non – material damages (human health and life) which could occur in the protected object.

The hazard detection process is associated with the capabilities of detection elements applied in monitoring system. The time elapsing since the commencement of the attempt to force the protections until this attempt is detected is the crucial factor determining the effectiveness of this process [9]. The principal objectives to be achieved in the course of system designing are:

– to detect the maximum possible number of hazards;
– to minimize the time of system response to the occurrence of hazard.

Owing to the probability level arbitrarily assumed by the designer for the occurrence of determined type of events in the protected object, the hazard detection process is characterized by finite number of hazards causing the response of the system. The number of detected events is closely associated with the number of detection elements in the system. The number of these elements is associated with the system installation cost. The achievement of the second objective consisting in the minimization of the time of system response to the occurrence of hazard depends on the technical parameters of detection element and on the location where this detection element has been installed [6, 9].

The time interval t_r determining the correctly running hazard detection process can be described by means of the following equations:

$$t_r \in (t_1, t_2), \tag{1}$$

$$t_r \geq t_0 = 0, \tag{2}$$

$$t_1 \to 0, \tag{3}$$

where:

t_0 – time of hazard occurrence in the object being protected,

t_1 – minimum time of system response; associated with the least time consuming procedure for anticipated hazard identification,

t_2 – maximum time of system response; associated with the most time consuming procedure for anticipated hazard identification.

Fig. 1 presents running the process of total and correct hazard neutralization in the protected object.

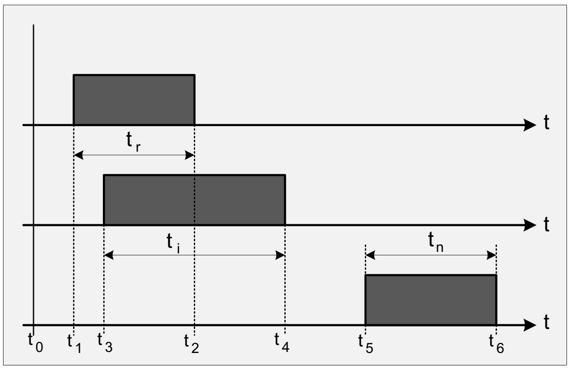

Fig. 1. Running of the procedure of hazard neutralization
t_r – time of hazard detection process
t_i – time of analysis and information relay in the system
t_n – time of physical hazard neutralization

Owing to the duration of the hazard detection process, it is important to provide the system with effective detection provisions functioning inside the object (detection of occurred object penetration) as well as on its periphery (detection of attempted object penetration) in order to enable effective execution of the hazard detection process [10].

Arrangement of the head protection zones in living object is presented in Fig. 2.

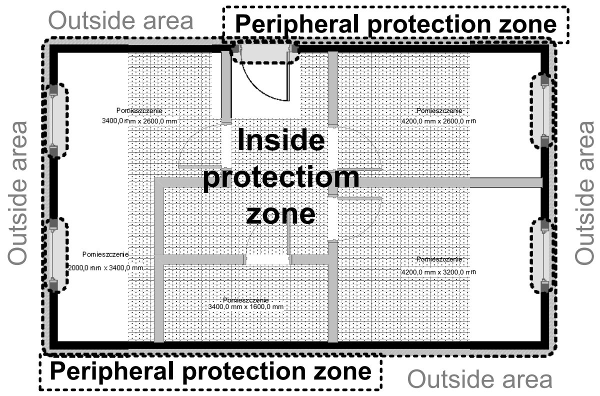

Fig. 2. Arrangement of particular detection zones in living object

The systems protecting the peripheral (circumferential) zones of the building most often are provided in the form of the protections designed for the initiated attempts to enter into the object through the window and door openings. Nowadays these openings are protected by means of reed relay sensors or contact sensors constituting the basic elements of the peripheral protection of the object. The disadvantage of such solutions consists in the possibility to bypass this protection in a simple manner e.g. by window pane breaking. The detection element will not be activated in such case and the responsibility for hazard detection is transferred to detection elements installed inside the protected object.

The purpose of the present paper is to present the concept consisting in the use of ultrasonic motion sensors as the detection elements in specific zones i.e. the spaces between individual layers of casement windows. This type of windows is commonly used in residential buildings. Their effective protection will enable the quick identification of the hazard.

According to the common opinion concerning the possibility of false alarms potentially generated by many external factors and owing to their relatively limited range, the ultrasonic sensors are not widely used in alarm systems of the buildings. However, they are commonly applied in vehicles alarm systems enabling the detection of initiated attempt to enter into the vehicle.

The purpose of the tests will be the analysis in the scope of possibility to detect the attempts to force the area being protected (windows) and the comparison of the effectiveness of ultrasonic sensors with actually applied solutions (reed relay sensors and contact sensors).

Presumably the whole space between window panes will be protected if the ultrasonic sensors are applied for the protection of inner space of the window. Every motion inside the protected object will result in the generation of alarm signal. Owing to insignificant permeability of ultrasonic waves through structural elements of the window (window panes and frames), the advantage of the system will consist in the fact that the area being protected is limited to the inner space of the window only. The possibility of false alarms generated by the sensor will be also minimized owing to the lack of any movable elements in the inner space of the window.

I&HAS ALARM SYSTEMS

Pursuant to the requirements included in the standard PN-EN 50131-1 [1], the monitoring system performing the functions of an intrusion and hold-up alarm system (I&HAS) should contain the provisions enabling the detection, triggering of alarm status, sabotage and identification of damages in the system. Any other functions can be also performed by this systems, unless there is any negative impact of said functions on the basic functions of I&HAS alarm system. The process of the transfer of information about detected hazard in I&HAS systems is carried out between the monitored object and alarm receiving centre by means of alarm transmission system. The signal transmission system should meet determined criteria in the scope of transmission time, maximum value of transmission time, reporting time, accessibility and signal protection; depending on the system protection degree. Detailed guidelines concerning the criteria to be met by the signal transmission systems are determined in the standard PN-EN 50136-1-1 [2].

The contemporary burglary and attack alarm systems (I&HAS) are designed in the form of an electric system ensuring manual or automatic detection of existing hazard (burglary, attack, attempted sabotage of the system) in the object being protected PN-EN 50131-1 [1]. From the technical point of view, the system consists of an assembly of the devices operating together (also combined with the system of conductors) in order to detect the hazards, to generate alarms and to initiate the actions intended to eliminate such hazard. The transmission of information can take place in

many different ways using different media and the use of human factors [4, 5, 7, 8, 9, 12, 14].

As a result of analysis of the functioning of such system, the following interrelated basic function blocks can be determined [8]:

– analytic and decision making (management) block,
– detection (input) block,
– alarming and informing block (actuator),
– power supply block.

Block diagram of the I&HAS alarm system components is shown in Fig. 3.

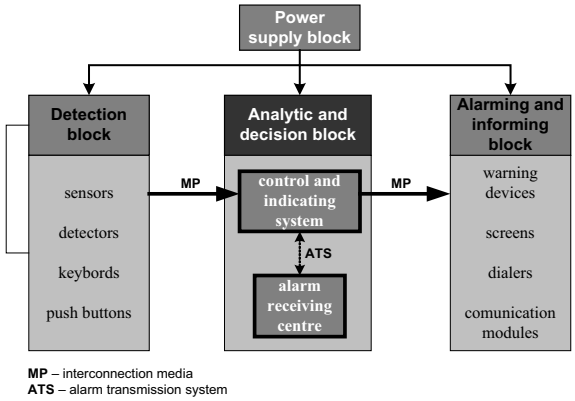

Fig. 3. Organization block diagram of I&HAS

The detection block consists of an assembly of the devices performing the task consisting in the detection of changes occurring in the protected object or in the alarm system (sabotage, failure) and in the information transmission to the control and imaging device (alarm central panel) of the system. The detection block is not responsible for any decision making on alarm triggering but only for the transmission of information about the change of the parameter being measured or controlled (temperature, change of position, sound, image, vibration, sabotage) exceeding permissible range or established value.

Depending on the manner of layout, functioning and the type of individual sensors in detection block, the detection block can be subdivided into designated protection zones (i.e. internal, external, circumferential zone). Every zone will perform different tasks and functions in the hazard detection process.

ULTRASONIC DOPPLER MOTION SENSOR

Doppler motion sensors (motion detectors) are defined as the alarm system elements based upon the phenomenon consisting in change of received wave frequency in comparison with transmitted wave frequency from the object moving in detection field (Doppler effect) and using this phenomenon for the detection of hazard and for generation of alarm signal. All types of motion detectors are classified in active sensors category [3, 13, 14, 16, 18], because their operating principle is based upon the transmission of wave i.e. certain amount of energy into ambient area.

The operating principle of motion sensors is based upon the use of Doppler effect (Fig. 4) i.e. the phenomenon describing the change of wave frequency recorded by the receiver in comparison with standard wave frequency transmitted by the transmitter and occurring when the distance to be covered the wave being transmitted between the transmitter and receiver is changed [11, 14, 18].

The transmitter and receiver remain stationary to each other in the ultrasonic motion sensors used in alarm systems. It this case the presence of Doppler effect is possible in case of change of the distance to be covered by transmitted sound wave reflecting from the object in motion. If all objects existing within the sensor range will remain stationary, the distance to be covered by transmitted sound wave is constant. In such case there will be no change of frequency recorded by the receiver in the relation to standard frequency emitted by the transmitter (Fig. 5). This situation will change in case of the motion of object within the sensor operation area; transmitted wave will be reflected from this object. Then the distance to be covered by the wave and consequently the frequency recorded by the receiver will begin to change (Fig. 6). In this case, for a signal sent from the transmitter and coming to the receiver there are two at the same time following the Doppler effect. The first Doppler effect occurs in system the transmitter – the object, a second Doppler effect is in system the object – the receiver. The mathematical notation of this situation can be described as follows:

– when the object is approaching to the transmitter-receiver system (Fig. 4a),
– the first Doppler effect (between the transmitter and the object):

$$f' = f_0 \cdot \frac{V_0 + V_x}{V_o}, \tag{4}$$

– the second Doppler effect (between the object and the receiver):

$$f'' = f' \cdot \frac{V_0}{V_o - V_X}, \tag{5}$$

– form of the equation determining the frequency of recorded by the receiver,

$$f'' = f_0 \cdot \frac{V_0 + V_x}{V_o} \cdot \frac{V_0}{V_o - V_X} = f_0 \cdot \frac{V_0 + V_X}{V_0 - V_X}, \tag{6}$$

$$f'' = f_0 \cdot \left(1 + \frac{2V_X}{V_0 - V_X}\right) = f_0 + f_0 \cdot \frac{2V_x}{V_0 - V_X}, \tag{7}$$

$$\text{gdy } V \neq 0 \text{ to } f'' > f_0, \tag{8}$$

– when the object is moving away to the transmitter-receiver system (Fig. 4b),
– the first Doppler effect (between the transmitter and the object):

$$f' = f_0 \cdot \frac{V_0 - V_x}{V_o}, \tag{9}$$

– the second Doppler effect (between the object and the receiver):

$$f'' = f' \cdot \frac{V_0}{V_o + V_X}, \tag{10}$$

– form of the equation determining the frequency of recorded by the receiver:

$$f'' = f_0 \cdot \frac{V_0 - V_x}{V_o} \cdot \frac{V_0}{V_o + V_X} = f_0 \cdot \frac{V_0 - V_X}{V_0 + V_X}, \quad (11)$$

$$f'' = f_0 \cdot \left(1 - \frac{2V_X}{V_0 + V_X}\right) = f_0 - f_0 \cdot \frac{2V_x}{V_0 + V_X}, \quad (12)$$

$$\text{gdy } V \neq 0 \text{ to } f'' < f_0, \quad (13)$$

where:

f_0 – frequency of sound wave transmitted by the transmitter,

f' – frequency recorded by the object and frequency emitted by the object,

f'' – frequency recorded by the receiver,

V_X – velocity of object in motion,

V_0 – velocity of sound wave transmitted by the transmitter.

Assuming the following approach:

$V_X > 0$ the situation when the object is approaching to the transmitter-receiver system,

$V_X < 0$ the situation when the object is moving away to the transmitter-receiver system,

equation defining the Doppler frequency value Δf has following form [15]:

$$\Delta f = \frac{2V}{V_0 - \mathrm{V}} \cdot f_0, \quad (14)$$

where:

f_0 – frequency of sound wave transmitted by the transmitter,

V – velocity of object in motion,

V_0 – velocity of sound wave transmitted by the transmitter.

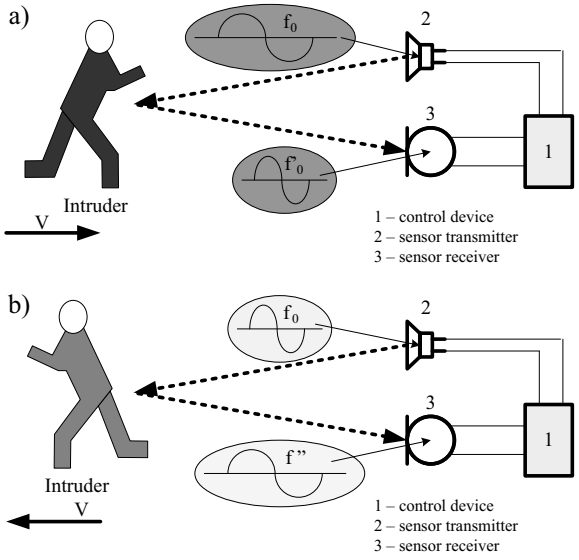

Fig. 4. The principle of ultrasonic motion detector
a – when the object is approaching the transmitter-receiver system,
b – when the object is moving away from the transmitter-receiver system

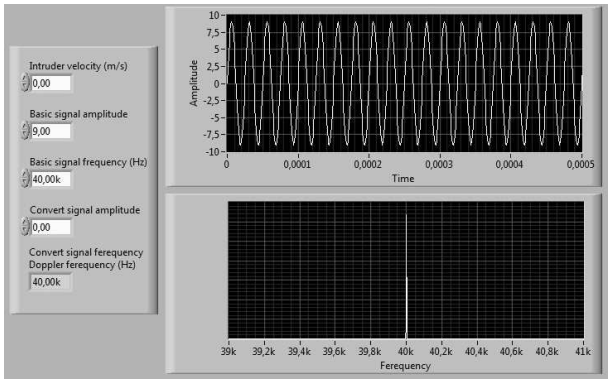

Fig. 5. Waveform chart of recording signal and frequency spectrum for detector in normal state

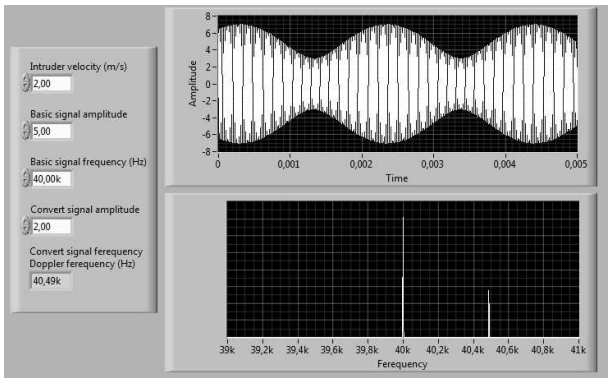

Fig. 6. Waveform chart of recording signal and frequency spectrum in hazard detection state

MODEL OF CASEMENT WINDOWS WITH ULTRASONIC DOPPLER SENSOR

The purpose of performed tests was to present the ultrasonic motion sensors as an alternative solution toward the reed relay sensors or contact sensors actually used for the protection of window openings and constituting the elements of peripheral protection of the object.

The tests associated with the potential applications of the ultrasonic motion sensors for the protection of window openings provided with casement windows have been carried out on the model of such type of the window which was built for this purpose (Fig. 7). This model of the window has been designed in a manner enabling the execution of the tests for the following situations occurring in real alarm systems:

– forcing the window by the force opening of its wing (event 1),
– forcing the window by the opening of its wing (event 2),
– forcing the window through the opening made in a part of this window but without opening of its wing (various variants of the location of openings) (event 3),
– disturbance of alarm system operation by the attempts to generate a false alarm as a result of motions performed on the external side of the window (event 4).

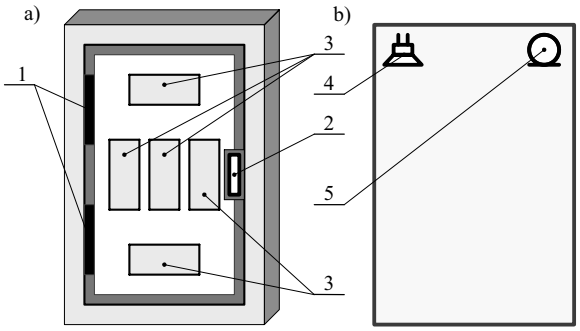

Fig. 7. Model of casement window with an ultrasonic sensor incorporated inside
a) layout of elements enabling the execution of tests on the model, b) layout of ultrasonic motion sensor elements; 1 – hinges; 2 – handle; 3 – openings with diaphragms; 4 – sensor transmitter; 5 – sensor receiver

Additionally the model was equipped with measuring system (Fig. 8). The measuring system consisted of the following elements:
– ultrasonic motion sensor; type URZ0530 (Fig. 9),
– central alarm panel; Integra 32 manufactured by Satel,
– intermediate relay,
– voltmeter and stabilized power pack 12 V.

After its connection to the control system URZ0530 sensor with power supply voltage U=12V, the sensor signal output was characterized by the following levels of voltages:

– in normal condition, in case of normal operation of all sensor elements while the sensor is not excited as a result of detected disturbance – US=6,68 V;

– in alarm condition, in case of normal operation of all sensor elements while the sensor is excited as a result of detected disturbance – US=0 V.

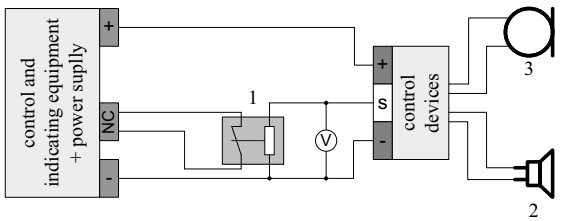

Fig. 8. Connection diagram for devices in the model, 1 – relay, 2 – transmitter of ultrasonic motion sensor, 3 – receiver of ultrasonic motion sensor

Fig. 9. Ultrasonic Doppler motion sensor type URZ0530

The model of casement window has been additionally equipped with a standard reed relay sensor and contact sensor. Their incorporation in the model made it possible to verify the effectiveness of system operation in various hardware configuration. Therefore it will be possible to evaluate the functioning of these elements in various cases.

ANALYSIS OF TEST

The effectiveness of system operation was determined on the basis of the correct (expected) system response in various variants of events. The excitation of alarm system was the result expected in case of three first events. The lack of excitation of alarm system was the result expected in case of the fourth event. The results obtained from performed experiments have been presented in Table 1.

Table 1. Results obtained from test – excitation of alarm system

Event	EXCITATION OF ALARM SYSTEM		
	Ultrasonic sensor	Reed relay sensor	Contact sensor
1	+	+	+
2	+	+	+
3	+	-	-
4	-	-	-

The results presented in Table 1 for individual tests have been obtained from the tests carried out for the conditions without anticipated possibility of sabotage for individual detection systems in course of attempted forcing of the protection. In case of tests in more realistic conditions (allowed penetration of the intruder into the system as attempted sabotage of its operation) for event 2, it was possible to complete the forcing of the protections without generating the alarm for the systems provided with reed relay sensor and particularly with contact sensor. Such attempts were ineffective in case of ultrasonic sensors. The generation of false alarms in the system as a result of ultrasonic sensor excitation was possible only in case of the setting of excessive sensitivity of the ultrasonic sensor detection system.

CONCLUSIONS

The hazard detection time is an important factor deciding on the effectiveness of such system operation. The shorter is the time elapsed between the hazard detection and the reaction of the system user to this hazard, the greater is the chance to limit the damages caused by this hazard. Therefore, it becomes important to provide the monitoring systems with technical equipment ensuring the effective detection of hazards before the intrusion of the intruder into the interior of the object. Consequently, the responsibility for the hazard detection process should be shifted towards the peripheral protection of the objects.

The protections in the form of the reed relay sensors and contact sensors which are actually used for the protection of window and door openings are inefficient in certain cases

(e.g. window pane breaking). The application of active IR barriers for the protection of window and door openings can be used as more effective but very expensive solution. The ultrasonic motion sensors are and equally effective technical solution but their effective functioning is possible in small closed spaces only. In such cases the whole space is protected inside the protected object, i.e. the space enclosed by its structural elements.

The price of the solution associated with the ultrasonic motion sensors is not significantly different from the price of the reed relay sensors and contact sensors. The range of detected events is significantly increased in case of ultrasonic motion sensors (protecting the whole area accessible to potential intruder). Therefore, this solution can be applied as an efficient alternative to the currently used technical solutions.

REFERENCES

1. **PN-EN 50131-1:2009:** Systemy alarmowe. Systemy sygnalizacji włamania i napadu. Część 1: Wymagania systemowe, PKN, Warszawa 2009.
2. **PN-EN 50136-1-1:2001:** Systemy alarmowe. Systemy i urządzenia transmisji alarmu. Wymagania ogólne dotyczące systemów transmisji alarmu, PKN, Warszawa, 2001.
3. **PN-93/E-08390/24:1993:** Systemy alarmowe. Włamaniowe systemy alarmowe. Wymagania i badania ultradźwiękowych czujek Dopplera, PKN, Warszawa 1993.
4. **Boguta A. 2011:** Application of IP monitoring in the supervising system of a building, Teka Komisji Motoryzacji i Energetyki Rolnictwa PAN – 2011, vol. 11, 9÷17.
5. **Boguta A. 2012:** The wireless notification systems used in car alarm systems, Teka Komisji Motoryzacji i Energetyki Rolnictwa PAN – 2012, nr 1, vol. 12, 9÷12.
6. **Buczaj M. 2009:** Czas jako kryterium skuteczności przebiegu procesu neutralizacji zagrożeń w systemach nadzorujących stan chronionego obiektu, Zabezpieczenia nr 6(70)/2009, 56÷61.
7. **Buczaj M. 2010:** Wykorzystanie telefonii mobilnej i Internetu w procesie przekazywania informacji w systemach nadzorujących stan chronionego obiektu, Zabezpieczenia 1/2010, 56÷61.
8. **Buczaj M., Sumorek A. 2010:** Wirtualny system nadzoru sterujący pracą systemu sygnalizacji włamania i napadu, Motrol: Motoryzacja i Energetyka Rolnictwa t.12, Lublin 2010, 46÷53.
9. **Buczaj M. 2011a:** Eliminacja czynnika ludzkiego przez techniczne środki przekazu informacji w systemach nadzoru nad stanem chronionego obiektu, Motrol: Motoryzacja i Energetyka Rolnictwa t.11, Lublin, 34÷42.
10. **Buczaj M. 2011b:** Strefowa organizacja systemów alarmowych w aspekcie realizacji założonych zadań ochrony w obiektach budowlanych. Zabezpieczenia 5/2011, 46÷49
11. **Halliday D., Resnick R., Walker J. 2008:** Podstawy fizyki, T.2, PWN, Warszawa.
12. **Horyński M. 2011:** Computer – aided design of virtual supervision systems for the electric system in contemporary building, Teka Komisji Motoryzacji i Energetyki Rolnictwa PAN – 2011, vol. 11, 123÷134.
13. **Ihara I., 2008:** Ultrasonic Sensing: Fundamentals and its applications to nondestructive Evaluation, Sensors – Lecture Notes in Elecrtical Engineering, 2008, vol. 21, 287÷305.
14. **Jajdek A., Juda Z., 2008:** Czujniki, Wydawnictwo WKiŁ, Warszawa.
15. **Nawrowski R., Skowronek K. 1997:** Systemy alarmowe pojazdów samochodowych, Wydawnictwo Politechniki Poznańskiej, Poznań.
16. **Obraz J. 1983:** Ultradźwięki w technice pomiarowej, WNT, Warszawa.
17. **Resnick R., Halliday D. 2001:** Fizyka cz. 1, PWN, Warszawa.
18. **Śliwiński A. 2001:** Ultradźwięki i ich zastosowania, WNT, Warszawa.

ZASTOSOWANIE ULTRADŹWIĘKOWYCH CZUJEK RUCHU W OKNACH TYPU SKRZYNKOWEGO W OCHRONIE PERYFERYJNEJ OBIEKTU

Streszczenie: Istota działania systemów sygnalizacji włamania i napadu (I&HAS) to szybkie i skuteczne wykrycie zagrożenia dla osób i mienia znajdujących się wewnątrz chronionego obiektu. Aby realizacja tych celów przebiegała prawidłowo konieczne staje się zabezpieczanie nie tylko powierzchni wewnątrz budynku, ale także miejsc umożliwiających dostęp do chronionego obiektu. Zabezpieczenie otworów okiennych i drzwiowych budynku za pomocą czujek kontaktronowych lub stykowych to obecnie podstawowy sposób zabezpieczenia i jedyny element ochrony peryferyjnej obiektu. W artykule zostanie przedstawiona koncepcja wykorzystania w oknach typu skrzynkowego Dopplerowskich czujek ultradźwiękowych, jako podstawowego elementu detekcyjnego w obwodzie ochrony peryferyjnej obiektu. Do badań został wykorzystany czujnik ultradźwiękowy URZ0530.

Słowa kluczowe: ochrona peryferyjna chronionego obiektu, systemy sygnalizacji włamania i napadu, I&HAS, dopplerowskie czujki ruchu.

TEKA. COMMISSION OF MOTORIZATION AND ENERGETICS IN AGRICULTURE – 2013, Vol. 13, No. 1, 37–40

Analysis of energy market using *data mining* methods

*Beata Gołębiewska, Jędrzej Trajer**

Department of Fundamental Engineering, Warsaw University of Life Sciences
Nowoursynowska Str. 166, 02-787 Warsaw, *corresponding author: jedrzej_trajer@sggw.pl

Received January 9.2013; accepted March 14.2013

Summary. The paper compares selected *Data Mining* techniques for forecasting and describes electricity market including the structure and forms of energy trading. One of the goals was to analyze data for electricity production in Poland. The analysis aimed at studying the influence of selected variables on the examined problem and the effectiveness of the proposed models. Four *Data Mining* methods were used to develop the forecast models, namely, regression and time series using *MLP* neural networks as well as Support Vector Machine (*SVM)* and *MARSplines*. Two time horizons of the forecasts, namely, 1 day and 7 days, were studied. The results were used to verify the models and select the best one.
Key words: electricity market, forecast, *Data Mining*.

INTRODUCTION

Electricity market is defined by three key characteristics. One of these characteristics that can be attributed to the specificity of energy, which cannot be stored in large quantities, is the significance of balancing demand and supply, and the fact that electricity overproduction may lead to serious financial losses. Another characteristic is the fact that the energy used by a given consumer cannot be traced back to its source of production. The third characteristic is the variability of demand for energy in time, and its dependence on numerous factors (technology, weather, season of the year, industry).

At present, three types of energy trading can be distinguished on the Polish market:

– *Contract market* is the least complicated in terms of energy trading. It is a place, where contracts between participants of the market are concluded. These contracts specify the price of energy for the period of each day of contract duration. The prices may be fixed, which, in certain situations, may be unprofitable for sellers, or variable, based on demand and instantaneous electricity prices.
– *Exchange market,* where future contracts as well as "day ahead" and "hour ahead" contracts for the purchase and sale of energy are concluded on the Polish Power Exchange (Towarowa Giełda Energii, TGE). Trading is realized on the Day-Ahead Market. Sale and purchase of energy takes place 24 hours before the physical delivery of energy. Orders are placed for the specified hours of the next 24h day. This is the basis for setting hourly electricity prices.
– *Balancing market* is an extremely significant element of the market, whose function is to ensure smooth electricity supply. This function is realized by reacting to demand for energy, and generating the required volume of energy. This sector is managed by the Transmission System Operator – PSE-Operator S.A. – the company which sells or purchases energy to balance supply and demand.

The volume of energy, for which consumers pay, is determined based on forecasts. If the estimated and the actual energy consumption differ, and there is excess of energy, the surplus may be resold on the balancing market. Conversely, in case of deficiency, additional volume of energy may be purchased on the balancing market. Balancing is managed by trading companies and not consumers. Fig. 1 presents a graphical interpretation of this procedure.

The facts presented above clearly show the necessity of developing a model facilitating accurate forecasts of estimated energy consumption, essential for the generation of the required volume of electrical energy, and consequently, more effective balancing of supply and demand [5]. There are various methods to develop forecasting models. New technologies [10], especially neural networks [3, 9] and fuzzy logic [11] are especially useful in this respect. Modifications of currently used forecasting models also contribute to the improvement of forecasts effectiveness [1]. Data Mining methods proved to be an extremely effi-

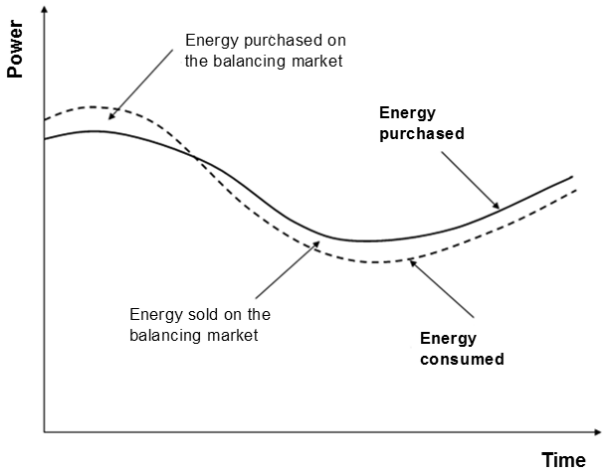

Fig. 1. A graph presenting the dependence of power on time showing how balancing market operates. *Source: www.cire.pl*

cient tool in forecasting, i.a., energy consumption [5]. *Data Mining* methods were used to compare different forecasting models, as they can be applied to on-line analysis of large datasets.

PURPOSE AND METHODS

Data Mining comprises a set of analytical tools and methods that may be applied for various purposes [8]. It relies on computers to discover patterns and regularities in large datasets [2]. These methods can be divided according to a number of criteria. One classification divides data mining methods into supervised learning (learning with a teacher) or unsupervised learning (learning without a teacher) [6]. The first group of methods is used when the situation has been recognized, and the results are included in the training sample. This is the basis for the development of the model, which is then used to classify and categorize new data. The following example might be given to illustrate such a situation: it is necessary to group new consumers according to the criteria specified for each group. Unsupervised methods are used when some data are available but the mechanisms that generate them are unknown. In this case, the goal is to develop the best possible model. These methods, as opposed to supervised methods, are not aimed at discovering relations between variables, but are used to forecast certain values, recognize a situation or present a structure of a phenomenon [7]. An example may be specifying a group of customers according to defined criteria e.g. volume of consumed energy or payment promptness.

The authors analyze the effectiveness of four developed forecasting models that are based on regression and time series using MLP neural networks and support vector machine (*SVM)* as well as *MARSpline*s. The models were developed in the *Statistica 9 Data Miner*. Forecasts for two time horizons were performed for each of these methods, namely, a forecast for the day ahead and day seven. The analysis was performed on the basis of data obtained from *Monthly reports on the operation of the Polish Power System and Balancing Market* (which contain data collected during operative technical planning and during the operation of the system) for the period of five years (2007–2011) The dataset contains 1818 observations (1818 successive days), Fig. 2.

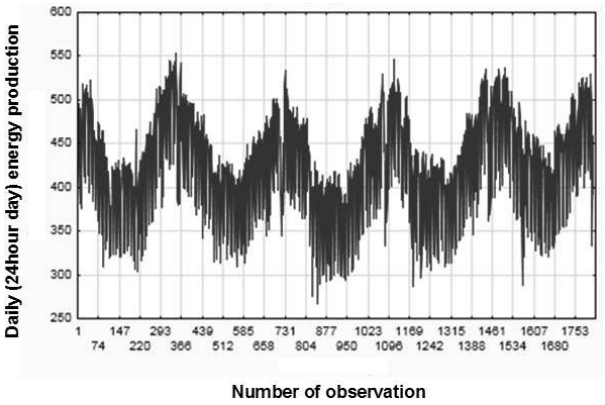

Fig. 2. A plot illustrating variations in daily (24hour day) electricity production [GWh] in the years 2007-2011 *Source: prepared by the authors*

The dataset was divided into two subsets: the training set (80% of cases) and the test set for the verification of the models (20% of cases). The following variables were used to describe these observations:

1. Number of observation (No).
2. Year (Y).
3. Day of year (DY).
4. Number of month (MNo).
5. Number of week (WNo).
6. Day of month (DM).
7. Daily (24hour day) production (DP).
8. Daily production of energy delayed by 1 observation (DP-1).
9. Daily production of energy delayed by 6 observations (DP-6).
10. Daily production of energy delayed by 7 observation (DP-7).
11. Energy production forecast for 1 day ahead (DP+1).
12. Energy production forecast for 7 days ahead (DP+7).
13. A variable informing about holidays (including Sundays) and work days (DS/DR).

The structure of the forecasting models was shown in Fig. 1. Forecasts for all models were prepared for one day and seven days ahead.

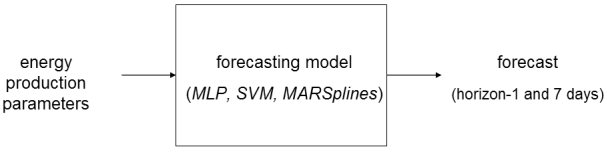

Fig. 3. Structure of forecasting models

Input variables and the structure of each *MLP* model were selected based on the validity analysis (susceptibility analysis) of these models and simulations. In the time series model, only past values for electricity production are

considered, and they are selected depending on the horizon and feasible network structure. In contrast, the *SVM* model aims at finding such a basic function that will predict the values of the dependent variable for new observations with the greatest accuracy. The process involves minimization of the error function using various basis functions (radical functions) and appropriate selection of constants *C* and ε in the process of learning. *MARSpline* (*Multivariate Adaptive Regression Splines*), which belongs to Data Mining methods, is a non-parametric method used for solving classification and regression problems. This method does not require preliminary establishment of assumptions concerning the functional relationship between the independent and dependent variables (e.g. linear or logistic relationship). This relationship is constructed from a set of coefficients and basic functions generated from the available data. MARSplines can be used to solve problems with multiple variables at the input, which is likely to cause problems in other methods. The input space is divided into separate regions, each with its own regression function. *MARSplines* algorithm in the Statistica 9 program permits the use of any number of variables, observations and output variables, and consists of two stages. The first stage involves building a model, i.e. increasing its complexity by adding basis functions, and the second stage, called pruning, involves removal of the least significant basis functions. This procedure stops when the *Generalized Cross Validation error* (GCV) has reached its minimal value. The GCV error is a measure of the goodness of fit of the model that takes into account not only the residual error but the model complexity as well.

RESULTS AND DISCUSSION

Input variables for the time series neural model were 21 past values for the daily energy production. Simulations were performed to construct networks with the optimal structure for forecast horizon 1 – *MLP 21:29:1* and 7 – *MLP* 21:43:1. The forecasting model based on MLP networks was developed for the following input variables: number of month and week of year, daily production of energy – current and delayed by 1 and n days (for forecast horizon 1 – n=6 and 7 – n=7), and the qualitative variable that distinguishes work day from holiday). Optimal network structures were constructed for these variables: for forecast horizon 1 – *MLP 6:3:1*, and 7 – *MLP 6:9:1*. Independent variables for forecast horizons 1 and 7 in the *SVM* networks and in *MARSplines* were assumed analogically as in the previous case. In the *SVM* method, optimal parameters were selected using a cross validation sample. Default regression of type 1 was applied, and optimal parameters were obtained with the following values: capacity C= 3 and ε=0.1. Attempts to construct the model proved that the best results were obtained for the radical basis function *RBF*, where the parameter gamma equaled 0.146. Development of *MARSplines* requires that a number of important parameters be set carefully. For instance, a parameter *Maximum number of basis functions* may be found in the specification of the model. This parameter is best set at maximum possible number of basis functions, so that the program can find all the functions. In this case, the number, determined in the course of model construction, was set to 110. Further increase of model complexity may be achieved by increasing the *Order of interactions* between input variables. Number 2 was selected for the analysis involving forecast of energy for the day ahead, which allowed to take into account not only the results but also the interactions between pairs of variables. This parameter was also determined on the basis of preliminary analyses. With this method, pruning is recommended to limit the complexity of the model. It is performed by selecting the option *Remove the least significant basis functions*. This prevents overfitting. Generalized cross validation errors for the model for time horizon of 1 day and 7 days were equal $GCV_1 = 408.7$ and $GCV_7 = 448.9$, respectively. Table 1 presents the results obtained from MLP time series models, and table 2 shows the results for the other examined MLP models.

The developed models were verified using the generated test set. The values of forecast errors and correlation coefficients indicate the model quality. The forecasting models were verified using the following quality assessment measures: correlation coefficient and the values of forecast errors. To facilitate the model quality assessment, it was assumed that the output variable was within the range 267–553 [GWh] for two horizons. The results of the verification of the models for the test sample are presented in Table 3.

The data show that as the length of forecast horizon increases, the quality of the models decreases. Analyzing the results for forecast horizon equal 7 days it can be observed that the highest correlation coefficient is equal to 0.920 and the smallest forecast errors were for neural networks (solv-

Table 1. Forecast results obtained from MLP time series models.

Forecast horizon	Name of network	Quality (learning)	Quality (testing)	Learning error	Test error	Activation (latent)	Activation (output)
1	MLP 21-29-1	0.960	0.956	110.24	138.86	Exponential	Tanh
7	MLP 21-43 -1	0.890	0.900	297.04	302.30	Logistic	Logistic

Table 2. Forecast results obtained from MLP regression models.

Forecast horizon	Name of network	Quality (learning)	Quality (testing)	Learning error	Test error	Activation (latent)	Activation (output)
1	MLP 6-3-1	0.941	0.934	171.51	193.58	Exponential	Tanh
7	MLP 6-9-1	0.937	0.920	177.83	246.35	Exponential	Tanh

Table 3. Quality measures for each model for the test sample.

	Neural networks (Regression)		Neural networks (Time series)		Support Vector Machine		MARSplines	
Forecast horizon [days]	1	7	1	7	1	7	1	7
Average of squared residuals	387.15	492.6903	266.77	609.64	427.59	518.1768	418.27	643.23
Absolute mean error	13.47	14.9002	11.10	17.50	13.99	15.4277	13.88	16.15
Correlation coefficient	0.932	0.920	0.956	0.900	0.926	0.906	0.926	0.884

ing regression problems). The worst results were obtained using the *MARSplines* method, where the correlation coefficient was equal to 0.884 and the values of forecast errors were the highest.

CONCLUSIONS

Research to develop the most effective forecasting methods, in particular for short forecast horizons, has been conducted by many research centres. *Data Mining* methods are very useful for that purpose, and allow to prepare forecasts of electricity production in a short time. However, the best results (in the two examined horizons) were obtained for regression using MPL neural networks, with the smallest difference between them. Moreover, the results confirm that the developed MLP models yield accurate predictions for new data (small forecast error for the test set).

The advantage of the last studied method, MARSplines, is the fact that it does not require preliminary assumptions. It does well for outlier observations and, consequently, better characterizes the examined phenomenon. It also gives better results in case of higher number of explanatory variables. This method also has its own quality measure (goodness of fit), taking into account the complexity of the model and the residual error. Nevertheless, despite numerous advantages, the interpretation of results in this method is likely to create difficulties. Like in other non-parametric methods, the implementation of the model in this method may cause problems.

REFERENCES

1. **Assimakopoulos V, Nikolopoulos K., 2000:** *The theta model: a decomposition approach to forecasting.* Elsevier – International Journal of Forecasting 16 (2000) 521–530.
2. **Berry M., Linoff G., 2000:** *Mastering Data Mining*. Wiley, Hoboken, New York.
3. **Crone S., Hibon M., Nikolopoulos K., 2011:** *Advances in forecasting with neural networks? Empirical evidence from the NN3 competition on time series prediction.*. International Journal of Forecasting 27, 635–660.
4. **Nęcka K., 2011a:** *Analysis of the Continuity of Electric Energy Supply in Poland.* TEKA Kom. Mot. i Energ. Roln. – OL PAN, 11c, 230–236.
5. **Nęcka K., 2011b:** *Use of Data Mining Techniques for Predicting Electric Energy Demand.* TEKA Kom. Mot. i Energ. Roln. – OL PAN, 2011, 11c, 237–245.
6. **Migut G., 2009:** *Czy stosowanie metod Data Mining może przynieść korzyści w badaniach naukowych*, StatSoft Polska.
7. **Sokołowski A., Pasztyła A., 2004:** *Data mining w prognozowaniu zapotrzebowania na nośniki energii*, Akademia Ekonomiczna w Krakowie, StatSoft Polska.
8. **Tadeusiewicz R., 2006:** *Data mining jako szansa na relatywnie tanie dokonywanie odkryć naukowych poprzez przekopywanie pozornie całkowicie wyeksploatowanych danych empirycznych*. Dostępny w internecie: http://www.statsoft.pl/
9. **Trajer J., Czekalski D., 2011:** *Prognozowanie sum promieniowania słonecznego*. Polska Energetyka Słoneczna,2–4, 39–41.
10. **Trojanowska M., 2008:** *.Alternative Methods of Estimating Rural Consumers' Daily Demand for Electrical Energy*. TEKA Kom. Mot. Energ. Roln. – OL PAN, 8, 287–291.
11. **Trojanowska M.,Małopolski J., 2011:** *Forecast Models of Electric Energy Consumption by Village Recipients over a Long-Term Horizon Based on Fuzzy Logic*. TEKA Kom. Mot. i Energ. Roln. – OL PAN, 2011, 11c, 327–334.
12. Źródło internetowe: *www.cire.pl*

ANALIZA RYNKU ENERGETYCZNEGO Z WYKORZYSTANIEM METOD 'DATA MINING'

Streszczenie. W pracy przedstawiono techniki *Data Mining* służące do prognozowania oraz istotę rynku energii elektrycznej uwzględniająca strukturę i formy handlu energią. Celem pracy była analiza danych dotyczących produkcji energii elektrycznej w Polsce. Analiza miała na celu zbadanie istoty wybranych zmiennych oraz na badane zjawisko oraz skuteczności zaproponowanych modeli. Modele prognostyczne zostały zbudowane za pomocą czterech metod *Data Mining*: regresja i szeregi czasowe z wykorzystaniem sieci neuronowych typu *MLP* oraz metoda wektorów nośnych *SVM* i *MARSplines*. W każdej z metod zostały uwzględnione dwa horyzonty czasowe prognoz 1 i 7 dni. Otrzymane wyniki posłużyły do weryfikacji modeli i wyboru najlepszego.

Słowa kluczowe. rynek energii elektrycznej, prognozowanie, *Data Mining*.

TEKA. COMMISSION OF MOTORIZATION AND ENERGETICS IN AGRICULTURE – 2013, Vol. 13, No. 1, 41–46

Relationships between Common Rail accumulator pressure and vehicle traction properties

Wawrzyniec Gołębiewski, Tomasz Stoeck

Department of Automotive Vehicles Operation, West Pomeranian University of Technology in Szczecin
17 Piastów Ave., 70-310 Szczecin, Poland, tel.+48 91 449 40 45,
e-mail: wawrzyniec.golebiewski@zut.edu.pl, tstoeck@zut.edu.pl

Received February 23.2013; accepted March 14.2013

Summary. This study aimed at presenting the relation between Common Rail accumulator pressure and vehicle traction properties (acceleration capacity and ability to achieve maximum velocity be vehicle). Tests were performed using an engine test bench and a CR pressure testing kit. They were conducted in conformity with engine standards (i.e. the requirements being specified in them), creating the engine torque and engine effective power to CR pressure characteristic curves.

When making the final diagrams for vehicle acceleration (at each gearbox ratio) and vehicle velocity (in the last gear) and accumulator pressure, a significant effect of the latter on traction parameters was found.

Key words: Common Rail, vehicle traction properties, pressure in CR accumulator.

INTRODUCTION

The Common Rail is the fuel supply system most frequently used in direct injection compression-ignition engines in passenger cars at present. Its main advantages are the reduction of noise of working engine and amount of harmful substances emitted to the atmosphere as well as power increase [9,11]. The system is more economical to operate and environmentally friendly (less fuel consumption) in comparison to conventional diesel power systems and power supply systems of TDI.

Its major advantage is the possibility to change and adjust injection pressure and injection time owing to separation of pressure-producing element (high pressure pump) from fuel-injecting elements (fuel injectors) by a container (Rail) acting as a pressure accumulator [10,15]. Pressure in the CR is a dynamic value and, together with injection time and fuel temperature, affects the dose size and the whole characteristic of injection, and the same the engine parameters [2,3,4].

In the paper by Gołębiewski [6], a relationship between CR pressure and these parameters has been presented. A growing non-linear relationship between the pressure p_{rail} and engine effective power was found using graphs. The function of engine torque to Common Rail pressure was similar to that in case of engine rotational speed (curves had very similar courses).

Engine operating parameters (working ability and working ability in time unit) are of importance for vehicle movement potential (accelerations and velocities, thus its dynamics). They define motor car traction properties (presented in Fig. 1) [1,5,7,12,13,14,16,17,18,19].

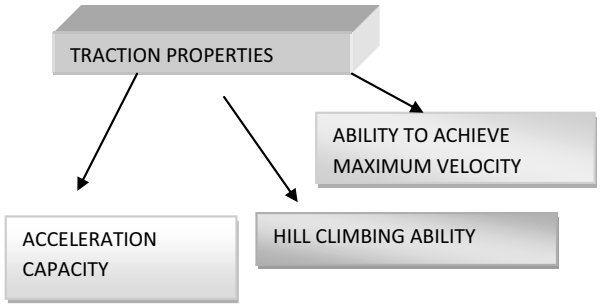

Fig. 1. Division of vehicle traction properties (prepared by the authors)

Acceleration capacity a specified in m/s² has been determined from the following relationship [17,19]:

$$a = \frac{F_N}{m} = \frac{T_{tq\,k}}{mr_k} = \frac{T_{tq} \cdot \eta_{UN} \cdot i_{UN}}{mr_k}, \qquad (1)$$

where :
FN – driving force [N],
m – gross vehicle mass [kg],
T_{tqk} – torque on driving wheels [Nm],
T_{tq} – engine torque [Nm],
η_{UN} – power transmission system efficiency,
i_{UN} – power transmission system ratio,
r_k – wheel kinematic radius [m].

Vehicle linear velocity *v* specified in *m/s* is being defined by the following relation [17,19]:

$$v = \omega_k r_k = \frac{2\pi n_k r_k}{60} = \frac{\pi n r_k}{30 i_{UN}}, \quad (2)$$

where:
ω_k – angular velocity of road wheels [rad/s],
n_k – rotational speed of wheels [min^{-1}],
n – engine rotational speed [min^{-1}].

When changing the velocity units from *m/s* to *km/h*, the result should be multiplied by 3.6.

Article [8] presents the results of traction motor vehicle navigation using techniques designed to determine the characteristics of an external spark-ignition engine is also based on the measurement of the opening of the injector and fuel rail pressure.

The authors of this paper decided to examine a relationship between Common Rail pressure and vehicle traction properties.

OBJECTIVE AND METHODS OF EXPERIMENTS

The objective of this research project was to determine a relation between Common Rail accumulator pressure and vehicle traction properties (acceleration capacity and ability to achieve maximum velocity). In the study, a torque to Common Rail pressure relationship for feeding a direct injection turbocharged compression-ignition engine designed for driving motor cars with a full dose of fuel. Research methods were conducted in conformity with the Polish standard PN-ISO 15550 [21]. Experiments were performed according to the requirements specified in them using an engine test bench.

TEST BED

The test bed consisted of the following components:

a) fuel tank (diesel oil) – a 750 litre fuel tank designed for diesel oil, made of plastic;
b) FIAT Multijet 1.3 JTD engine – a direct injection 4-stroke turbocharged compression-ignition engine with the Common Rail fuel supply system [20];

Table 1. Engine description according to manufacturer's data [20]

FIAT Multijet 1.3 JTD 16 V	unit	value / description
Cylinder diameter	[mm]	69.6
Piston travel	[mm]	82
Compression ratio	-	18.1
Number of cylinders	-	4
Arrangement of cylinders	-	in-line
Injection sequence	-	1-3-2-4
Engine capacity	[cm^3]	1248
Maximum power	[KM/kW]	75/51
Rotational speed at maximum power	[min^{-1}]	4000
Maximum torque	[Nm]	145
Rotational speed at maximum torque	[min^{-1}]	1750

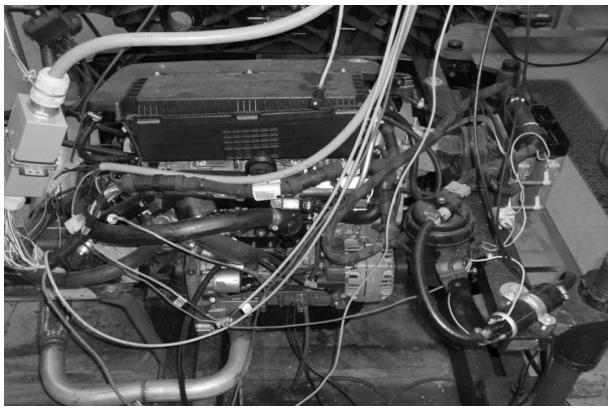

Fig. 2. A view of Fiat Multijet 1.3 JTD 16 V engine

c) EMX 100 eddy current brake manufactured by Elektromex (Poland) – a device for power take off and measurement in combustion engines being placed on test beds;

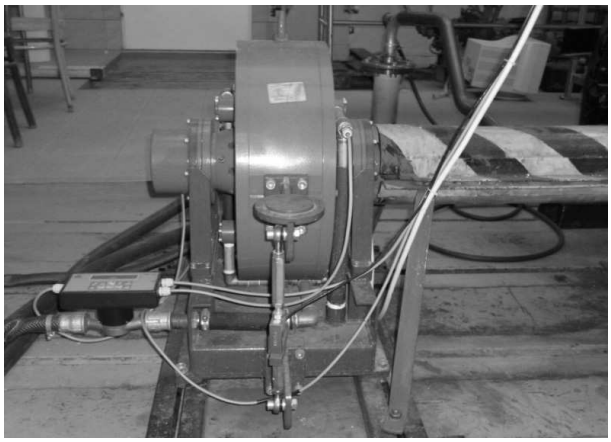

Fig. 3. EMX 100 eddy current brake

d) Common Rail high pressure measurement kit which consisted of: a manometer, a T-connection with nozzles, vent and stopper, a measuring hose, fuel tubbing, a reduction and a venting hose.

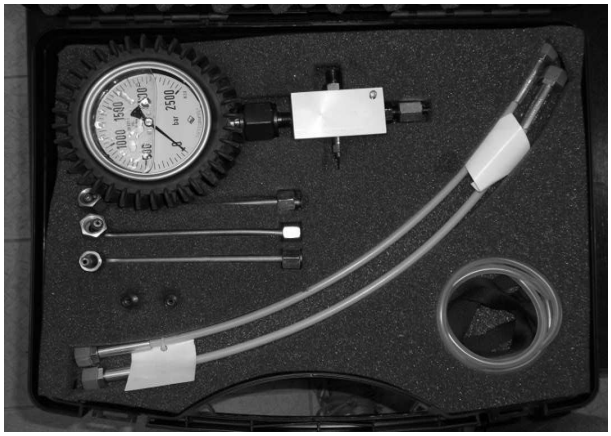

Fig. 4. HP-made Common Rail high pressure measurement kit

COURSE OF TESTS

Results of the measurements being performed are presented in Fig. 5. The engine was fed with a full dose of ON EKODIESEL fuel with the cetane number 51.1. Ambient parameters during the test were as follows:

– ambient temperature T_a = 294 K,
– ambient pressure p_a = 98.5 kPa,
– relative humidity = 40%.

The engine torque and its effective power being measured were corrected according to the relations comprised in the Polish standard PN-ISO 15550 [21]. The use of HP-made high pressure measurement kit allowed creating an engine torque and engine effective power to Common Rail pressure relationship. It is presented below in Fig. 5. The characteristic curves were determined based on measuring points due to very narrow ranges of measurement uncertainties (see section 5). In order to illustrate the relation between CR accumulator pressure and vehicle traction properties, the variables such as vehicle weight, power transmission system efficiency, respective gear ratios and final drive ratio were also necessary.

Table 2. Basic vehicle details

variable	value	unit	where:
m	1932.57	[kg]	gross vehicle mass
η_{UN}	0.9	-	power transmission system efficiency
rk	0.27	[m]	wheel kinematic radius
ibI	3.909	-	first gear ratio
ibII	2.158	-	second gear ratio
ibIII	1.345	-	third gear ratio
ibIV	0.974	-	fourth gear ratio
ibV	0.766	-	fifth gear ratio
ipg	3.438	-	final drive ratio

RANGES OF MEASUREMENT UNCERTAINTIES

The ranges of measurement uncertainties were determined for engine rotational speed, torque and effective power and Common Rail pressure of the engine torque-speed (external) characteristics.

Expanded measurement uncertainty for engine rotational speed was a type B standard uncertainty (depending on the accuracy of measuring device calibration; the experimenter's uncertainty was omitted due to the result self-reading and self-recording measuring system).

Type B standard uncertainty was determined from the following relationship [22]:

$$u_B(n) = \frac{\Delta n}{\sqrt{3}} = \frac{1}{\sqrt{3}} = 0.67[\min^{-1}], \quad (3)$$

where:
Δn – uncertainty of rotational speed sensor calibration = 1 [min^{-1}].

According to the uncertainty propagation law, standard (total) uncertainty was equal to type B standard uncertainty [22]:

$$u_B(n) = u(n) = 0.67[\min^{-1}]. \quad (4)$$

Expanded uncertainty was determined by the following equation [22]:

$$U(n) = k \cdot u(n), \quad (5)$$

where:
k – coverage factor = 2.

$$U(n) = 2 \cdot 0.67 = 1.34[\min^{-1}]. \quad (6)$$

Thus, ultimately, the measurement uncertainty for the whole range of rotational speeds was equal to:

$$U(n) = \pm 2[\min^{-1}]. \quad (7)$$

Expanded uncertainty for corrected engine torque measurement

In the case of type A standard uncertainty, the arithmetic mean of torque was adopted as a measurement result [22]:

$$\overline{T_{tq}} = \frac{1}{n}\sum_{i=1}^{n} T_{tq(i)}, \quad (8)$$

where:
$\overline{T_{tq}}$ – arithmetic mean of engine torque measurement [Nm],
$T_{tq(i)}$ – value of the i-th torque measurement [Nm],
n – number of measurement.

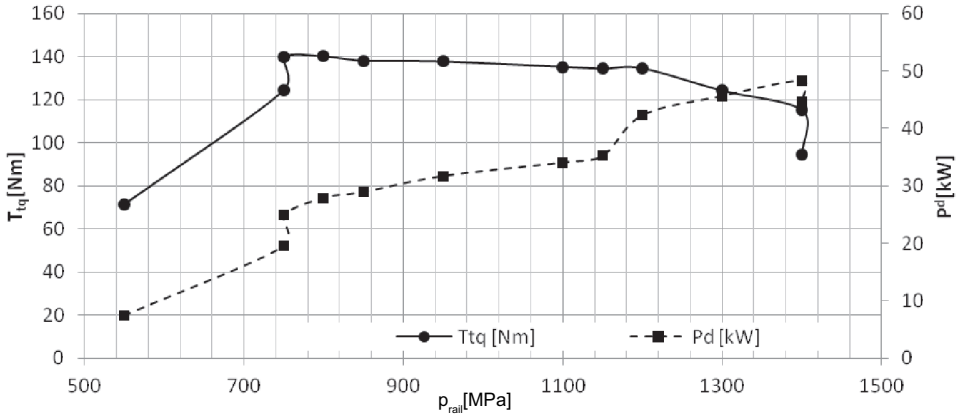

Fig. 5. Engine torque and engine effective power to CR relationship
where: T_{tq} – engine torque, P^d – engine effective power, p_{rail} – Common Rail accumulator pressure

For example for rotational speed n= 1900 obr/min, it was as follows:

Table 3. Calculation table for engine torque measurement

No.	$T_{tq(i)}$	$\overline{T_{tq}}$	$(T_{tq(i)} - \overline{T_{tq}})$	$(T_{tq(i)} - \overline{T_{tq}})^2$
1	140.9	140.1	0.8	0.64
2	140.6		0.5	0.25
3	140.7		0.6	0.36
4	138.3		-1.8	3.24
$\sum (T_{tqi} - \overline{T_{tq}})^2$				**4.49**

Type A standard uncertainty of this result was calculated as a standard deviation [22]:

$$u_A(T_{tq}) = \sqrt{s^2_{\overline{T_{tq}}}} = \sqrt{\frac{1}{n(n-1)}\sum_{i=1}^{n}(T_{tq(i)} - \overline{T_{tq}})^2} = 0.61[Nm]. \quad (9)$$

Type B standard uncertainty was determined from the following relationship [22]:

$$u_B(T_{tq}) = \frac{\Delta T_{tq}}{\sqrt{3}} = \frac{0.1}{\sqrt{3}} = 0.058[Nm], \quad (10)$$

where:

ΔT_{tq} – uncertainty of engine brake calibration = 0.1 [Nm].

According to the uncertainty propagation law, standard (total) uncertainty amounted to [22]:

$$u\ (T_{tq}) = \sqrt{s^2_{\overline{T_{tq}}} + \frac{(\Delta T_{tq})^2}{3}} = 0.62[Nm]. \quad (11)$$

Expanded uncertainty was determined by the following equation [22]:

$$U(T_{tq}) = k \cdot u(T_{tq}), \quad (12)$$

where:

k – coverage factor = 2.

$$U(T_{tq}) = 2 \cdot 0.62 = 1.23[Nm]. \quad (13)$$

Thus, ultimately, the result of engine torque measurement together with measurement uncertainty was written in the following form:

$$T_{tq} = (140.1 \pm 1.3)[Nm]. \quad (14)$$

In the table below, the values of engine torque together with expanded measurement uncertainty are presented for particular rotational speeds. The torque values were calculated as mean values of 4 measurements. The value of coverage factor k was 2, whereas the uncertainty of measurement accuracy for engine brake amounted to 0.1 Nm.

Table 4. Measurement uncertainties for engine torque

	n	$\overline{T_{tq}}$	$u_A(T_{tq})$	$u_B(T_{tq})$	$U(T_{tq})$	$\overline{T_{tq}} \pm U(T_{tq})$
	[min^{-1}]	[Nm]	[Nm]	[Nm]	[Nm]	[Nm]
1	1000	71.4	0.27	0.058	0.56	71.4±0.6
2	1500	124.4	0.38		0.77	124.4±0.8
3	1700	139.6	0.58		1.16	139.6±1.2
4	1900	140.1	0.61		1.23	140.1±1.3
5	2000	138.1	0.32		0.65	138.1±0.7
6	2200	137.7	0.20		0.41	137.7±0.5
7	2400	135.2	0.18		0.38	135.2±0.4
8	2500	134.4	0.06		0.17	134.4±0.2
9	3000	134.6	0.41		0.83	134.6±0.9
10	3500	124.2	0.19		0.40	124.2±0.4
11	4000	115.1	0.13		0.28	115.1±0.3
12	4500	94.6	0.17		0.37	94.6±0.4

Measurement uncertainties for engine effective power were determined in a similar manner.

Table 5. Measurement uncertainties for engine effective power

	n	$\overline{P^d}$	$u_A(P^d)$	$u_B(P^d)$	$U(P^d)$	$\overline{P^d} \pm U(P^d)$
	[min^{-1}]	[kW]	[kW]	[kW]	[kW]	[kW]
1	1000	7.5	0.029	0.058	0.13	7.5±0.2
2	1500	19.5	0.087		0.21	19.5±0.3
3	1700	24.9	0.104		0.24	24.9±0.3
4	1900	27.9	0.112		0.25	27.9±0.3
5	2000	29.0	0.076		0.19	29.0±0.2
6	2200	31.7	0.050		0.15	31.7±0.2
7	2400	34.1	0.029		0.13	34.1±0.2
8	2500	35.2	0.000		0.12	35.2±0.2
9	3000	42.3	0.091		0.22	42.3±0.3
10	3500	45.6	0.065		0.17	45.6±0.2
11	4000	48.3	0.065		0.17	48.3±0.2
12	4500	44.7	0.115		0.26	44.7±0.3

Expanded uncertainty for CR pressure was a type B standard uncertainty (depending on device calibration accuracy).

Type B standard uncertainty was determined from the following relationship [22]:

$$u_B(p_{rail}) = \frac{\Delta p_{rail}}{\sqrt{3}} = 8.34[MPa], \quad (15)$$

where:

Δp_{rail} – uncertainty of CR pressure gauge calibration = 50 [MPa].

According to the uncertainty propagation law, standard (total) uncertainty was equal to type B standard uncertainty [22]:

$$u_B(p_{rail}) = u(p_{rail}) = 8.34[MPa]. \quad (16)$$

Expanded uncertainty was determined by the following equation [19]:

$$U(p_{rail}) = k \cdot u(p_{rail}), \tag{17}$$

where:
k – coverage factor = 2.

$$U(p_{rail}) = 2 \cdot 8.34 = 16.68[MPa]. \tag{18}$$

Thus, ultimately, the measurement uncertainty for the whole range of pressures was equal to:

$$U(p_{rail}) = \pm 50[MPa]. \tag{19}$$

RESULTS

The acceleration values being obtained for each gear were determined using Equation (1) and Table 2. Using the data from Table 2 and Relation (2), the values of vehicle linear velocity in the fifth gear were determined in a similar manner. In Figures 6 and 7 below, the relations between Common Rail accumulator pressure and vehicle traction parameters (acceleration capacity and ability to achieve maximum velocity) are presented. The acceleration values in respective gears themselves depended mainly on the values of selectable ratios, whereas the character of curves showed the vehicle to speed up the best in each gear in the region of Common Rail accumulator pressure being equal to 850 bar. Taking into consideration the range of effective accumulator pressure, it amounted to approximately 40% of the maximum pressure.

The engine torque-speed to CR pressure characteristics pointed to a linear relationship of these parameters. The velocity in the last gear increased together with the increasing value of pressure, which indicates to the fact that the vehicle can be able to achieve maximum velocity at higher values of Common Rail pressure.

CONCLUSIONS

The carried out study allowed drawing the following conclusions:

a) CR pressure affects the course of engine torque characteristic curve and further, which is related to this, the

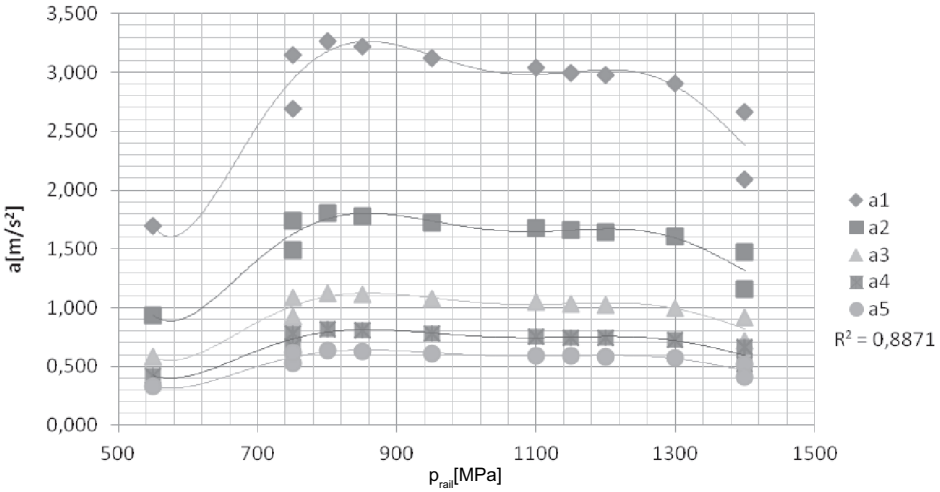

Fig. 6. Relationship between vehicle acceleration and CR pressure:
a – vehicle acceleration, **a1** – vehicle acceleration in first gear, **a2** – vehicle acceleration in the second gear, **a3** – vehicle acceleration in the third gear, **a4** – vehicle acceleration in the fourth gear, **a5** – vehicle acceleration in the fifth gear, $\mathbf{p}_{rail}$ – CR accumulator pressure, $\mathbf{R^2}$ – square of the coefficient of correlation

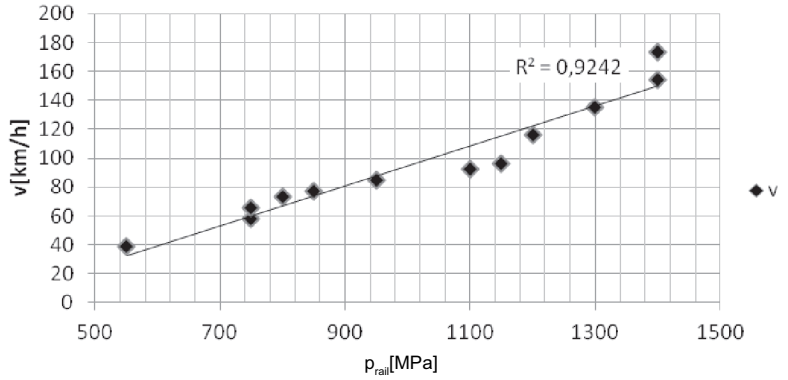

Fig. 7. Vehicle linear velocity (last gear) to CR pressure relationship:
v – vehicle linear velocity (last gearbox ratio), $\mathbf{p}_{rail}$ – CR accumulator pressure

course of vehicle acceleration characteristic curve in respective ratios;
b) it has a significant effect on engine power and thus on the ability of a vehicle to achieve maximum velocity (in the last gear);
c) increase in Common Rail pressure results in better traction parameters but also in higher fuel consumption;
d) it cannot be changed in any range due to durability of engine components (fuel supply system and piston-crank system).

REFERENCES

1. **Arczyński S. 1994:** Mechanika ruchu samochodu. Warszawa, WNT. 45-64, 92-104.
2. **Balawender K. 2007:** Wpływ wybranych parametrów regulacyjnych procesu wtrysku na emisję cząstek stałych w silniku wysokoprężnym typu DI. Rozprawa doktorska, Rzeszów.
3. **Balawender K., Kuszewski H., Lejda K., Ustrzycki A. 2008:** The effect of angle position of main, pilot and preinjection fuel dose on NOx formation in compression ignition engine with Common Rail system. Journal of KONES Powertrain and Transport, Vol. 15, No.3.
4. **Balawender K., Kuszewski H., Lejda K., Ustrzycki A. 2008:** Wpływ wielofazowości wtrysku na wybrane parametry systemu zasilania Common Rail. Silniki spalinowe. Nr 4. Wydawnictwo PTNSS. Bielsko-Biała.
5. **Dębicki M. 1976:** Teoria samochodu. Teoria napędu. WNT. p.19-27, 45-60, 106-120, 161-172.
6. **Gołębiewski W. 2012**: The effect of pressure in a Common Rail accumulator on engine operating parameters. Journal of KONES Powertrain and Transport. Vol. 19 / No. 1. Warsaw.
7. **Gołębiewski W., Stoeck T. 2011:** Traction qualities of a motor car Fiat Panda equipped with 1.3 16 V Multijet engine. TEKA Commission of Motorization and Energetics in Agriculture. Volume XIC. PAN. Lublin.
8. **Grzelka J. 2012:** Determination of specific fuel consumption of IC engine in transient conditions. TEKA Commission of Motorization and Energetics in Agriculture. Vol.12, No.1. PAN. Lublin.
9. **Gunther H. 2011:** Układy wtryskowe Common Rail w praktyce warsztatowej. WKŁ. Warszawa.
10. **Janiszewski T., Mavrantzas S. 2009:** Elektroniczne układy wtryskowe silników wysokoprężnych. WKŁ. Warszawa. 45-53.
11. **Kirichenko I., Strilets O., Koshovy M. 2012:** Piezo actuators injector of Common Rail fuel injection system. TEKA Commission of Motorization and Energetics in Agriculture. Vol.12, No.3.
12. **Lisowski M. 1999**: Ocena własności trakcyjnych samochodu Jelcz 317 wyposażonego w silnik SW-680 z różnymi systemami doładowania. MOTROL. Lublin.
13. **Lisowski M. 2004**: Teoria ruchu samochodu. Teoria napędu. Politechnika Szczecińska. Szczecin. 8-13, 17-19, 43-47, 64-67.
14. **Lisowski M. 2008:** An analysis of fuel consumption by a lorry with the compression ignition dynamic charged engine. TEKA Komisji Motoryzacji i Energetyki Rolnictwa. PAN. Lublin.
15. **Praca zbiorowa 2009:** Zasobnikowe układy wtryskowe Common Rail. WKiŁ. Warszawa.
16. **Prajwowski K., Gołębiewski W. 2011:** Simulative comparison of the traction properties of Daewoo Lublin 3 Mi van with particular types of gearbox. Journal of Kones Powertrain and Transport Vol. 18 / No. 1. Warsaw.
17. **Prochowski L. 2007:** Mechanika ruchu. WKiŁ. Warszawa.
18. **Siłka W. 1997:** Energochłonność ruchu samochodu. WKŁ. Warszawa. 28-36.
19. **Siłka W. 2002:** Teoria ruchu samochodu. WNT. Warszawa. pp. 53-144.
20. **Zembowicz J. 2005:** Fiat Panda. WKiŁ. Warszawa, 12, 50-51, 136-138.
21. **PN-ISO 15550- 2009:** Silniki spalinowe tłokowe. Określenie i metoda pomiaru mocy silnika. Wymagania ogólne. PKN. Warszawa.
22. **Guide to the Expression of Uncertainty in Measurement 1995**, ISO Switzerland.

RELACJE MIĘDZY CIŚNIENIEM W ZASOBNIKU COMMON RAIL A WŁAŚCIWOŚCIAMI TRAKCYJNYMI POJAZDU

Streszczenie. Celem pracy było przedstawienie relacji pomiędzy ciśnieniem w zasobniku Common Rail a właściwościami trakcyjnymi (zdolność do przyspieszania i osiągania prędkości maksymalnej przez pojazd). Badania zostały przeprowadzone przy wykorzystaniu hamowni silnikowej oraz zestawu do sprawdzania ciśnienia w szynie CR. Zostały wykonane zgodnie z normami silnikowymi (wymaganiami w nich określonymi) poprzez utworzenie charakterystyk momentu obrotowego i mocy użytecznej silnika od ciśnienia w szynie CR. Wykonując ostateczne wykresy pomiędzy przyspieszeniem pojazdu (na każdym przełożeniu skrzyni biegów) oraz prędkością pojazdu (na biegu ostatnim) a ciśnieniem w zasobniku stwierdzono o znaczącym jego wpływie na parametry trakcyjne.
Słowa kluczowe: Common Rail, właściwości trakcyjne pojazdu, ciśnienie w zasobniku CR.

TEKA. COMMISSION OF MOTORIZATION AND ENERGETICS IN AGRICULTURE – 2013, Vol. 13, No. 1, 47–52

Injuries sustained by farmers during accidents involving tractors in plain regions

Monika Gorgoń[1], Grzegorz Jordan[2], Witold Jordan[1,3], Andrzej Mruk[1]

[1]Cracow University of Technology, Poland
[2]Jagiellonian University in Cracow, Medical College, Poland
[3]Institute of Forensic Research in Cracow, Poland

Received February 15.2013; accepted March 14.2013

Summary: The work presents the results of research on injuries of farmers, sustained during accidents involving a farm tractor used in plain regions. The analysis was done based on the documentation of Agricultural Social Insurance Fund. The circumstances of accidents were grouped. It was found out that the accidents occurred mostly at an immobile tractor and non-operating tractor engine. The location and severity of injuries sustained by the victims was determined. Most of the accidents happened when leaving the tractor (63%). The body areas mostly injured were lower limbs. The injuries were knee and ankle twists. The average value of permanent damage to health is about 5%.
Key words: tractors, accidents, injuries.

INTRODUCTION

The number of agricultural tractors in the Polish farms amounts to about a million and a half. The data of the Main Statistical Office show that their number is increasing from year to year. It is due both to the widening mechanization of agriculture and to the increasing wealth of the country people. The increase of the tractors number inevitably leads to the increasing number of their accidents. These accidents are special, owing to the character of the works the tractors perform. Getting to know the nature of these accidents will allow for introducing the mechanisms of the accident prevention.

Particular regions of Poland differ both in terms of the percentage of agricultural areas and in terms of the size of individual farms. This determines the number of tractors used in these areas (Fig. 1). The highest number of tractors appears in Mazowsze province (approximately 214 thousands), Lublin province (approximately 174 thousands) and Wielkopolska province (approximately 153 thousands). The least tractors are located in the provinces: Silesian, West Pomeranian, Lubuskie and Pomeranian [10, 14].

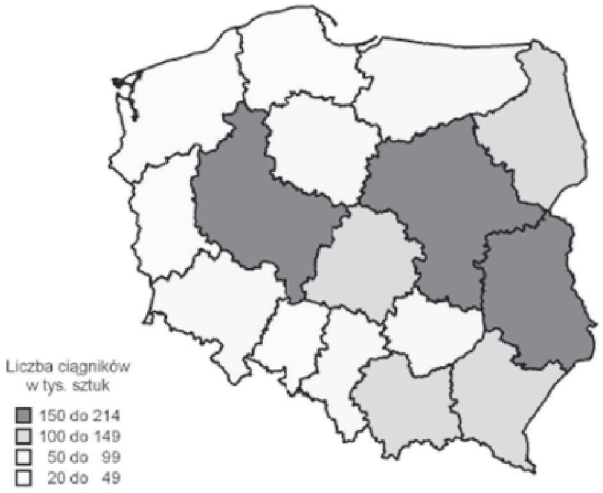

Fig. 1. The number of the tractors used in farms in 2010 in particular provinces of Poland [10]

PURPOSE AND SCOPE OF THE WORK

The work aimed at collection, systematization and analysis of the injuries sustained by the persons using tractors in plain areas. The analysis included the accidents which occurred in 2005 – 2010 in two Małopolska province counties: Proszowice and Miechów. Post-accident documentation of the Agricultural Social Insurance Fund (KRUS) was used in the study. The analysis of the documentation enabled to create the characteristics of the specificity of accidents and damages to the farmers using tractors in plain areas. It also allowed to determine the severity of the damage and to indicate which areas of the body are most vulnerable to damage [9, 10].

DESCRIPTION/PROFILE OF THE ANALYSED AREAS

Proszowice county includes the region called Proszowice Plateau with a plain topography, though there are some hills, ravines and precipices as well. The area of the county is all covered with loess, on which rich soils developed. Owing to the rich soils, the fields dominate the county landscape. There are about 7600 farms in the county; the average farm size is about 4.5 ha.

Miechów county is constituted by Miechów upland. The relief of the land is diversified, though, in general, the landscape appears as a plateau. There are large prominences with flat or undulating surfaces, forming a vast plateau at an altitude of 380-320 m above sea level. Other landforms are the mountains with flat peaks, river valleys, depressions and other denudation forms [10].

Miechów county has excellent soils, mostly of II and III class. There are loess, limestone and fen soils, favourable to agriculture. There are about 9 thousand farms in the county; the average farm size is about 5.3 ha and it is the highest in Małopolska province.

THE SCALE OF THE INJURIES INCURRED DURING ACCIDENTS

The general model of injuries resulting during the accidents is as follows:

accident
↓
mechanical load
measures preventing injuries → ↓
biomechanical response
level of injury tolerance → ↓
injury mechanism

where:

– biomechanical response – every change in time of the human body position and shape, of the body part or tissue during a mechanical load as well as any involved physiological changes;
– injury mechanism – biomechanical response, during which biological tissues are deformed beyond the recoverable limits causing damage to anatomical and functional structures.

The basic classification of human body injuries is penetrating injuries and non-penetrating injuries. Here, we must introduce the notion of injury intensity. It means the importance of the changes involved in damaging anatomical and functional structures of a living organism, resulting from the mechanical force action. The level of the importance of damage to human bodies is not the same for all people. It is due mainly to significant anthropometric differences in body constitution and health condition of individual persons [1, 2, 6, 15, 17].

To estimate quantitatively the level of injury severity, the injury intensity scales are used. We compare the injuries sustained by the accident victims with the given scale injuries and we read the numerical value of the injury intensity level.

There are many scales of injury severity. There are four main groups of scales: anatomical, physiological, combined scales and the scales of invalidity and social losses [16, 17].

The Agricultural Social Insurance Fund – KRUS, estimating the accident consequences, uses the scales of invalidity and social losses. These scales describe not so much the injuries as the long-lasting consequences of the damage and their influence on the injured life quality. When awarding the compensations to persons affected, the impact is estimated of injuries suffered during the accident on their further functioning and quality of life.

THE SCALE OF INJURY SEVERITY APPLIED BY THE AGRICULTURAL SOCIAL INSURANCE FUND

To payment of compensation, for example by the Agricultural Social Insurance Fund, the scale of injury severity applies from the third group of the above classification – the scales of invalidity and social losses. This scale is published in the ordinance of the Minister of Labour and Social Policy of 18 December 2002 on the specified principles of adjudication on permanent or long-lasting damage to health, on the procedure in determining the damage and for payment of a single compensation (Law Gazette of 28 December 2002). "Assessment of the percentage of the

Table 1. Illustrative injuries with percentage assessment of a permanent or long-lasting damage to health

Injury area	Type of injury	Percentage of permanent or long-lasting damage to health
Head	Partial paralysis or radial palsy preventing from independent standing up or walking	100
Upper limb	Brachial bone fracture with a small shift and axe disturbance	Right 5 – 15 Left 5 – 10
Upper limb	Fractures and dislocations of the thumb (the first metacarpal bone and phalanx bone of the thumb) with a shift	Right 5 – 10 Left 3 – 8
Upper limb	Losses within thumb – tip loss	Right 5 Left 3
Lower limb	Lower limb loss	85
Lower limb	Limitation of mobility (as a result of twisting, dislocation, fracture of joint bones, hurting, foreign matter, scars etc.) with and without deformations	1 – 15
Lower limb injuries	Hallux nail bone loss	5

permanent or long-lasting damage to health" is the annex to this ordinance. The annex contains tables with detailed list of body organs (parts) possible injuries. At every item the percentage appears of permanent or long-lasting damage to health, from 0% (no damage to health) to 100%. The degree of permanent or long-lasting damage is determined depending on the effects of an accident/a disease on the organs and systems.

Such a scale is used by a doctor predicate to establish the magnitude of the insurance compensation. The predicate should contain the description of the breach of the body efficiency as well as an establishment of the percentage of permanent or long-lasting damage to health with the number of the item in the percentage assessment. If an accident or an occupational disease has caused the damage to several limbs, organs or systems, the total degree of a permanent or long-lasting damage to health is equal to the sum of damage percentages for particular injuries, according to the percentage assessment procedure, limited to 100% [9].

ACCIDENTS INVOLVING FARM TRACTORS ON THE ANALYSED AREA IN 2005–2010 – RESEARCH METHODOLOGY

The research on the accidents and their consequences was carried out using the documentation of the Agricultural Social Insurance Fund. The research included the accidents occurred in Proszowice and Miechów counties in 2005–2010.

According to the art. 11 of the law of 20 December 1990 on social insurance of farmers, an agricultural accident is a sudden event provoked by an external cause, which occurred during performing agriculture activities or connected with these activities:

1. On the area of the farm run by the insured person or being the place of his/her permanent work, or within a household directly connected with the farm, or,
2. on the way of the insured person from the house to the farm referred to in p. 1, or during his/her way back, or,
3. during the performance beyond the farm referred to in p. 1 of the activities related to agricultural activity, or in connection with the performance of these activities, or,
4. on the way to the place of activities referred to in p. 3, or on the way back.

RESEARCH RESULTS

In 2005–2010, there were 98 accidents with farm tractors – 47 accidents in Miechów county and 52 in Proszowice county.

The accidents occurred mostly at non-operating tractor engine, i.e. during the time when the tractor was immobile. It was so in the case of 81 accidents, which is 82.7% of the total number of accidents with farm tractors in the examined counties Proszowice and Miechów.

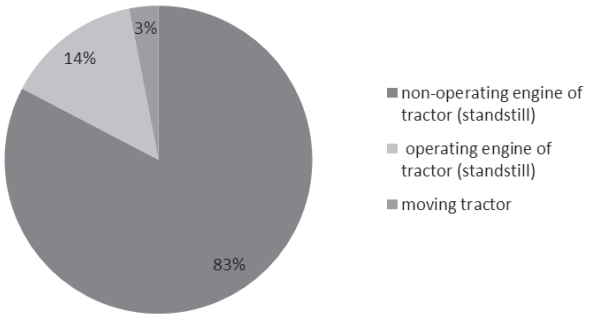

Fig. 2. Accidents involving farm tractors in 2005–2010

The average age of victims is 38 years. Most of them – 88.8% – are men. An escalation of the injuries is within the range from 0 to 23% of permanent damage to health. The average escalation of the injuries is 5%. The average percentage of the permanent damage to health for the accidents with the tractors with non-operating engine is 4.98%, with operating engine – 5%, and with a moving tractor – 5.1%. Translating the percentage values of the permanent damage to health from above accidents to results in AIS scale, we would receive the values from 0 – 2 AIS. It means that the majority of the analysed accidents consequences can be determined as insignificant or average.

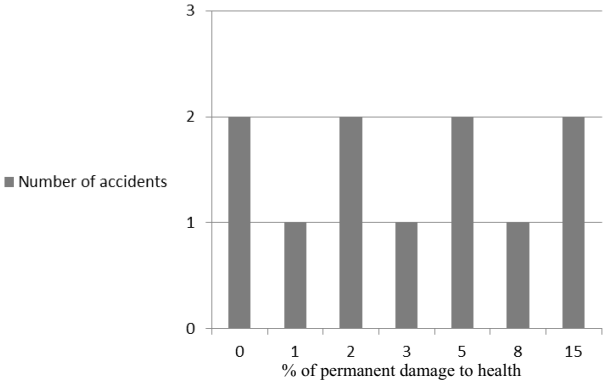

Fig. 3. Percentage values of permanent damage to health in the accidents involving a moving tractor

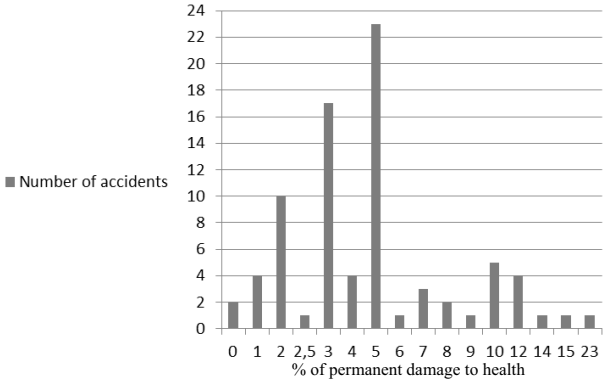

Fig. 4. Percentage values of permanent damage to health in the accidents involving a non-operating tractor

The number of injuries to the particular parts of the body is presented in Table 2.

The most number of injuries in all the accidents involving tractors concerned lower limbs: 63 injuries from the total num-

ber of 100 types of injuries. Damage to upper limbs is 30% of all injuries, damage to thorax – 3%, to head – 2% and to face – 2%.

Table 2. Classification of injuries due to their location

Place of occurrence of injuries	Number of injuries to the given body part			
	Tractor engine non-operating (standstill)	Tractor engine operating (standstill)	Tractor in motion	Total
Upper limbs	21	2	7	30
Lower limbs	56	1	6	63
Thorax	1	-	2	3
Head	1	-	1	2
Face	2	-	-	2
Total	81	3	16	100

Among the accidents, in which the upper limbs were injured, most of them cause 5% of permanent damage to health that is 7 from 28 accidents (Fig. 5). 2% of permanent damage to health is the consequence of 6 accidents. The minimum value of permanent damage to health of the upper limbs is 1%, while the maximum is 15%. The average percentage value of damage is 4.93.

In the case of lower limbs injuries, the most accidents – 17 from 59 – caused 5% of a permanent damage to health. It is the same value as in the case of upper limbs (Fig. 6). 14 accidents resulted in 3% damage, 6 accidents – 2%. The minimum value of a permanent damage to health in the case of lower limbs injuries is 0% (5 accidents). The maximum value is 23% (1 accident). The average percentage value of injuries is 4.78.

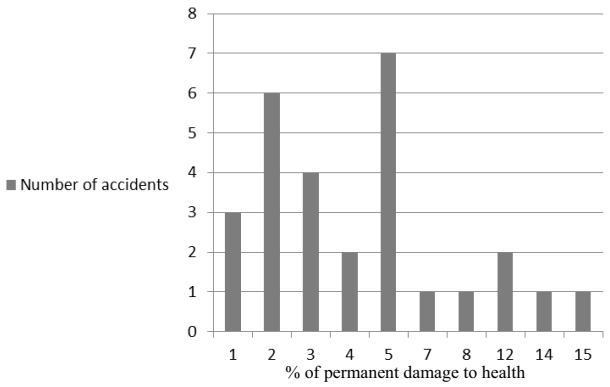

Fig. 5. Percentage of permanent damage to health in the case of accidents with injuries to upper limbs

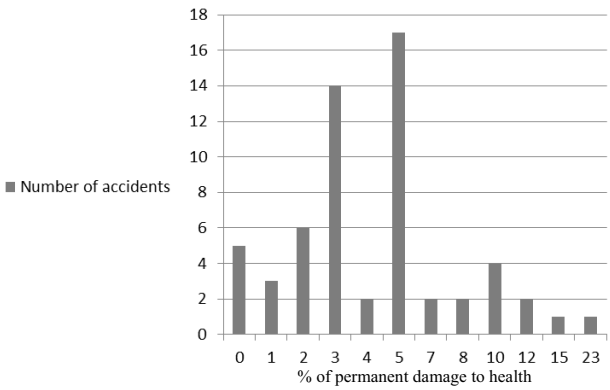

Fig. 6. Percentage of permanent damage to health in the case of accidents with injuries to lower limbs

The analysis of the injuries (Table 2) permits to affirm that a significant part of accidents at non-operating tractor engine occurred while dismounting from the tractor – 51 accidents. There are also the accidents which occurred when repairing a tractor – 11 accidents, the accidents during coupling up/detaching a device/machine with the tractor – 10, 2 accidents when getting into the tractor, 7 accidents qualified as 'others'.

The second largest group are the accidents that occurred while moving the tractor-this is the 14 accidents, i.e. 14.3% of all accidents involving farm tractors. The group includes 7 cases of running on a victim by a tractor, 1 collision with a car when the farmer was coming back home. The remaining 5 accidents are qualified as 'others'.

ANALYSIS OF THE INJURY MECHANISMS

Most accidents – 51 – occurred when dismounting from the tractor. In this group, we can distinguish three types of accident run: slipping on the tractor step and falling on the ground, putting the foot on an unevenness of the terrain, jumping from the tractor on unevenness. By far the majority of these accidents result in ankle (26 cases) or knee twisting (6 cases). The ankle twist consists in damage to the joint soft components. The articular capsule – ligament system is not completely broken, but stretched and a hematoma appears. The ankle twist is the consequence of bad position of the foot on the ground, which happens for example during jumping down, or stepping on an uneven ground as in the accidents when dismounting from the tractor. according to the scale used by KRUS, the degree of the injury intensity in the case of twisting the ankle is from 1 to 10% of the permanent damage to health, depending on the other simultaneous injuries like ankle fracture or shank bruise. If it is only a twisting of the ankle, the permanent damage to health is 1 – 5%.

Another kind of injury occurring when dismounting from the tractor is a knee sprain. The mobility of this joint is limited because of many ligaments and muscles. When our movements are compatible with the direction of the knee joint, the globular surfaces of the joint are rolling smoothly. At every correct movement, the muscles shrink and diastole actively, while the ligaments shrink and diastole passively. The joint structures often twist and turn, which permits to block elastically at the moment of some banned movements appearance. The appropriate structure of the joint allows of a given range of motion, and the other – not allowed – is blocked. If a sudden change of the joint bend direction happens, the correct mechanism will be blocked. A drastic exceeding of the mobility range ends with a damage to knee joint or to its stabilizing system (muscles and ligaments). The knee sprain involves 0 – 12% of permanent damage to health.

The accident resulting in the greatest permanent damage to health – 23% – is located in the group of accidents with non-operating engine of a tractor. The analysis of the accident run is the following: when going down the tractor, the victim foot slips and he falls down. The accident results in fracture of a bone. The consequences of

the remaining accidents were much lighter. There were ankle twists and the permanent damage to health was for instance 3%. The injuries sustained by a man aged 50 were heavier and these sustained by the women aged 33 – 37 were lighter. The age difference and a different structure of the osseous system caused that the injuries to women were lighter. The run of the accident itself influenced the damage as well.

The analysis of the accidents which occurred during motion (Table 2) showed that half of them happened when the tractor ran on a body part of the injured person. The consequences of three of these accidents are unknown. The remained caused 15, 5, 2, and 0% of the permanent damage to health. The fracture of both right forearm bones caused 15% of permanent damage to health. In this case, the arm was run on by a tractor wheel and submitted to high compressing loads from the tractor mass and its charge.

A specific and unique of this kind in the plain regions of Proszowice and Miechów counties is the accident, in which the tractor tipped over and rolled twice. It happened as follows: during going down a steep way, the pressure of the pulled tank trailer makes the tractor tilt and fall on the right side. The tractor rolls ('somersaults') twice with the victim sitting in the cabin. The victim is crushed by the tractor. The effect of the accident is the fracture of V, VI and VII ribs on the left side and 15% of permanent damage to health. The cause of the accident is a sudden shift of the vehicle mass centre (set: tractor and trailer) when the tank trailer leaned.

The farm tractor is a vehicle prone to tipping over because of the high location of its mass centre. A tilt may happen when driving on the curve of the road, on a steep slope or when overcoming different obstacles. Knowing the tractor mass centre position, we can determine the vehicle behaviour during its motion. When loading the trailer or coupling up devices to the tractor, a special attention should be paid to the mass centre location in such a set. The shift of the mass centre beyond the allowable zone may result in tipping over the vehicle. The slope, on which the tractor was moving, is the most important here [3, 4, 11, 12, 19].

CONCLUSIONS

In 2005 – 2010, in the studied area, 98 accidents occurred involving farm tractors – 52 in Proszowice county and 47 in Miechów county. Relating the number of accidents to the number of farms in these counties, about 7500 and about 9000,correspondingly, it is clear that the accidents of this type are rare.

Most accidents involving farm tractors in plain areas occurred at non-operating tractor – 81 accidents. Most accidents in this group – 51 (63%) occurred when leaving the tractor.

The body parts mostly injured in the accidents involving farm tractors are the lower limbs. Among all injuries, the most frequent are the ankle and knee injuries.

The average degree of intensity of the injuries sustained by farmers, according to the scale used by KRUS, is 5% of permanent damage to health.

The cause of the majority of analysed accidents is insufficient attention as well as disregard of general safety principles during the work. Many accidents that occurred during the tractor stoppage were caused by unsuitable shoes of the workers.

REFERENCES

1. **Będziński R.: 1997,** Biomechanika inżynierska, Oficyna Wydawnicza Politechniki Wrocławskiej, Wrocław.
2. **Błaszczyk J.: 2004,** Biomechanika kliniczna, Wydawnictwo PZWL, Warszawa.
3. Bocheński C., Klimkiewicz M.: 1987, Bezpieczeństwo maszyn rolniczych w ruchu drogowym, Przegląd Techniki Rolniczej i Leśnej nr 10.
4. **Cież J.: 1998,** Problemy ergonomii i bezpieczeństwa pracy w sezonowym użytkowaniu urządzeń technicznych w rolnictwie, Prace Komisji Nauk Rolniczych PAN tom 1.
5. **Dajniak H.: 1985,** Ciągniki – teoria ruchu i konstruowanie, WKiŁ Warszawa.
6. **Dziak A., Sanders R.: 2008,** Traumatologia układu ruchu, Elsevier Urban & Partner.
7. **Ekielski A., Skrobacki A.: 2006,** Pojazdy i ciągniki rolnicze, Wieś Jutra.
8. **Gadomski W., Mróz S.: 1983,** Ciągniki rolnicze, Wydawnictwo WSiP, Warszawa.
9. **Gorgoń M.: 2012,** Analiza obrażeń rolników powstałych w czasie wypadków z udziałem ciągników rolniczych na terenach równinnych, Praca dyplomowa inżynierska, Politechnika Krakowska Wydział Mechaniczny.
10. **Kondracki J.: 2009,** Geografia regionalna Polski, Wydawnictwo PWN, Warszawa.
11. **Kruszewski Z., Michalak G.: 1989,** Wybrane zagadnienia z teorii ruchu oraz budowy pojazdów rolniczych, Wydawnictwo Politechniki Warszawskiej, Warszawa.
12. **Nowacki T.: 1963,** Ciągniki rolnicze i samochody, Państwowe Wydawnictwo Rolnicze i Leśne, Warszawa.
13. **Pike J. A.: 1990,** Automotive safety – Anatomy, injury, testing and regulation, Society of Automotive Engineers.
14. **Szeląg Sikora A.: 2012,** Regional differences in equipment of machinery park on farms, Teka Commission of Motorization and Energetics in Agriculture, vol. 12.
15. **Thompson J. C.: 2007,** Atlas anatomii ortopedycznej Nettera, Elsevier Urban & Partner.
16. **Wicher J.: 2006,** Bezpieczeństwo samochodów i ruchu drogowego, Wydawnictwo WKiŁ, Warszawa.
17. **Wismans J. S. i inni: 1994,** Injury biomechanics, Eindhoven University of Technology.
18. **Woźniak W.: 2005,** Ciągniki i maszyny rolnicze – Budowa i przeznaczenie, Wydawnictwo Przemysłowego Instytutu Maszyn Rolniczych, Poznań.
19. **Zalewski P.: 1994,** Bezpieczeństwo kierowcy ciągnika na zboczu jako problem ergonomiczny, Zeszyty Problemowe Postępów Nauk Rolniczych PAN tom 415.

OBRAŻENIA ROLNIKÓW POWSTAŁE W CZASIE WYPADKÓW Z UDZIAŁEM CIĄGNIKÓW NA TERENACH RÓWNINNYCH

Streszczenie: W pracy przedstawiono wyniki badań obrażeń rolników, powstałych w czasie wypadków z udziałem ciągnika rolniczego eksploatowanego na terenach równinnych. Analizę przeprowadzono w oparciu o dokumentację prowadzoną przez Kasy Rolniczego Ubezpieczenia Społecznego. Pogrupowano okoliczności powstania wypadku. Stwierdzono, że największa liczba wypadków nastąpiła gdy ciągnik nie był w ruchu, i przy niepracującym silniku. Ustalono obszar ciał i rodzaje doznanych obrażeń jak i ich ciężkość. Najwięcej wypadków wydarzyło się podczas wysiadania z ciągnika (63%). Obszarem, który najczęściej doznawał obrażeń są kończyny dolne. Obrażenia te to urazy skrętne stawów kolanowego i skokowego. Średnia wartość trwałego uszczerbku na zdrowiu wynosi ok. 5%.
Słowa kluczowe: ciągnik rolniczy, wypadek, obrażenia

The study was performed within the framework of a PK WM M-4/84/2013/DS Project.

TEKA. COMMISSION OF MOTORIZATION AND ENERGETICS IN AGRICULTURE – 2013, Vol. 13, No. 1, 53–56

Analysis of the selected mechanical properties of the root parsley

Gorzelany Józef, Matłok Natalia, Kuźniar Piotr, Zaguła Grzegorz

Department of Engineering in Agricultural Food Production, University of Rzeszów
ul. Zelwerowicza 4, 35-601 Rzeszów, gorzelan@univ.rzeszow.pl

Received February 12.2013; accepted March 14.2013

Summary. Such biological materials as vegetables and fruits are subject to different static and dynamic loads connected with harvesting, loading/unloading, sorting and storage. These processes lead to mechanical damage of vegetables. On the basis of the performed laboratory investigations the measurements have been made of chemical and mechanical properties of the selected varieties of root parsley.

The objective of investigations was to determine the resistance of peel and tissue of the selected varieties of parsley roots against mechanical damage occurring in the process of root penetration by means of a punch and uniaxial tissue compression (free cylindrical sample). Basic elasticity parameters of the parsley roots have been determined in form of destruction stress and apparent Young's modulus. The chemical composition of the investigated parsley varieties has also been determined.

Key words: root parsley, destruction stress, Young's modulus, chemical composition.

INTRODUCTION

Parsley is an edible and ornamental plant and two forms of parsley are cultivated: the root parsley and the leaf one [27]. The parsley, due to its chemical composition, belongs to the vegetable group with high nutritional and health promoting value. 100g of parsley roots contains 4.6 g of sugars, 39 mg of vitamin CD, as well as significant quantities of minerals, especially calcium, phosphorus, magnesium and iron. At the same time the ether oils contained in all plant parts give the parsley its specific flavour [5].

Plant tissues of vegetables and fruits are subject to different static and dynamic loads connected with harvesting, loading/unloading, transportation, sorting and other manipulations necessary in the process of preparation of the final product [16]. Mechanical properties of plant tissues vary not only within species but also within varieties. They depend first of all on the external load [2, 25, 30] and specific properties of tissues, like e.g. the turgor pressure, which varies under the influence of loads [21, 23, 24, 25]. Further, they depend on the soil environment, cultivation technology, as well as on duration and conditions of storage and the part of root selected for sampling [7, 8, 9, 14, 22, 26]. The multi-layered structure of roots of many vegetables creates additional difficulty in mechanical property investigations [1, 4, 5, 28, 29].

Investigation of mechanical properties of vegetables are frequently considered as the addition to biochemical investigations dedicated to quality of particular varieties and their storage durability [26]. Many researchers have carried out investigations connected with rheological characteristics of agricultural products. Investigation objects have comprised such crops as beets [3], potatoes [12, 20], cereal grains [18, 19] and popular vegetables and fruits, like carrots [10, 11, 13], apples [17] soybeans and tomatoes [26].

METHODS AND MEASURING EQUIPMENT

INVESTIGATIONS OF CHEMICAL COMPOSITION OF PARSLEY ROOTS

Calorimetric investigations have been carried out with use of LECO® AC500 calorimeter (Fig. 1). Determination of water and ash contents in the root tissues of the selected parsley varieties has been performed with the use of thermal gravimetric method and LECO® AC500 instrument (Fig. 2). Instead, the analysis of carbon (C), hydrogen (H) and nitrogen (N) contents has been performed with CHN module of True Spec instrument, and sulphur (S) content with the sulphur module.

INVESTIGATION OF MECHANICAL PROPERTIES

Measurements of resistance against mechanical damage have been performed on the strength testing machine *Zwick/Roell* 2010 (fig. 3.).

Fig. 1. LECO® AC500 calorimeter.

Fig. 2. Stand for thermal gravimetric measurements.

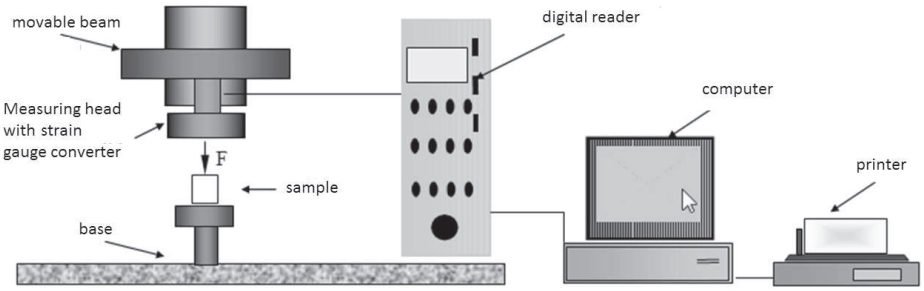

Fig. 3. Scheme of measurement stand – Zwick/Roell strength testing machine.

The investigations have been carried out for the following stationary parameter values:

– F_v = 2N (preliminary load applied to sample);
– $V_{1=}$ 40mm/min (speed of the settling movement of the beam/sensor assembly);
– V_2 = 20mm/min (speed of the beam/sensor assembly during measurement).

The investigations have been carried out with fresh material directly after harvest. Cylindrical samples 10 mm in diameter and 20 mm in height have been cut out from two parts of the parsley roots (the top part and the central one), along the longitudinal root axis and in the transversal direction. Each series of samples comprised 15 samples from each root part and for both directions of sample cutting.

After each series of measurements the results were printed together with calculations of average values of: maximum destruction forces, strains directly before the moment of sample penetration or destruction, energies and at the same time calculations were performed for such parameters as the destruction stresses and Young's modulus.

INVESTIGATION RESULTS

CHEMICAL COMPOSITION OF PARSLEY ROOTS

The average water content for the investigated parsley varieties was equal to 75.22%. The highest water content, equal to 79%, was stated in roots of Wistula variety, while the lowest value of 67.94% has been noted in Ołomuńcka variety. The average water contents in tissues of the investigated parsley varieties, expressed in percentages, are shown in Figure 4.

The ash contents in the investigated parsley varieties were from 1.03 % for Ołomuńcka variety to 1.51 % for Warta variety, while 1.33 % was the average ash content for all the investigated parsley varieties. The average percentage values of ash contents for the investigated parsley varieties are presented in Fig. 5.

It was stated on the basis of the performed investigations of chemical compositions at the angle of carbon (C), hydrogen (H), nitrogen (N) and sulphur (S) contents in parsley roots that the highest share in chemical composi-

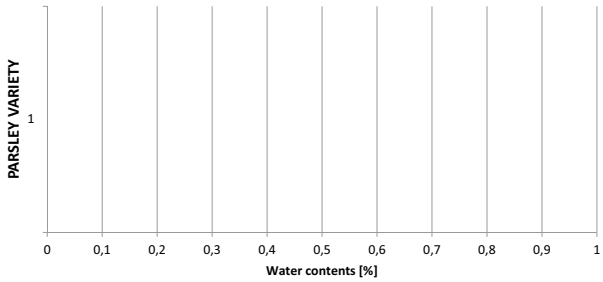

Fig. 4. Average water contents in roots of the investigated parsley varieties OŁOMUŃCKA

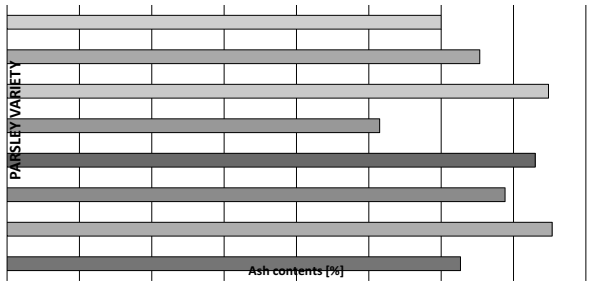

Fig. 5. Average ash contents in roots of the investigated parsley varieties OŁOMUŃCKA

tion is for carbon. The average content of this element in roots of the investigated parsley varieties is 43.79 %. The hydrogen content in parsley roots is significantly lower than for carbon and amounts to 6.42 % in average for all varieties. The nitrogen content in chemical composition of parsley roots is, on average, 1.16 %. The lowest content for this element was stated in Halblange variety, in which the nitrogen constituted only 0.37 %, while the highest content for this element, equal to 1.75 %, was observed in Sonata variety. The average calorific value for all investigated parsley varieties amounted to 3855.7 kcal/g (Table 1).

Table 1. Average contents of C, H, N and S elements and calorific values in the investigated varieties of root parsley

Parsley Variety	Contents of chemical elements [%]				Calorific values [kcal/g]
	C	H	N	S	
Roksana	44,52	6,42	1,34	0,21	3856,1
Cukrowa	42,96	6,33	1,42	0,26	3845,5
Halblange	43,69	6,53	0,37	0,08	3879,7
Ołomuńcka	43,25	6,55	1,07	0,15	3763,3
Sonata	43,44	6,33	1,75	0,32	3860,7
Lenka	43,65	6,27	0,93	0,17	3878,1
Warta	44,42	6,43	1,02	0,14	3900,2
Wistula	44,38	6,49	1,38	0,13	3861,9
x	**43,79**	**6,42**	**1,16**	**0,18**	**3855,7**

MECHANICAL PROPERTIES

PROCESS OF UNI-AXIAL COMPRESSION (FREE SAMPLES)

Table 2 presents the average values of destruction force F_{max} [N], strain directly before the moment of sample destruction L_{max} [mm], work W to F_{max} [Nmm] to the moment of destruction, as well as the destruction stress δ [MPa] and Young modulus E_u [MPa]. On the basis of the obtained results the differentiation was stated in the measured and calculated values of parameters of the investigated root parsley varieties. The highest resistance against mechanical damage was observed in Lenka variety with destruction force of 674.7 N, while the lowest value of 483.7 N was for Cukrowa variety. The lowest average amount of energy needed for destruction of parsley tissuewas stated for Roksana variety – 1485.7 nmm, while the highest amount of 2044 nmm was observed in Ołomuńcka variety. The average strains directly before the moment of sample destruction were stated from 7.3 mm for Lenka variety to 8.1 mm for Ołomuńcka variety. The highest elasticity was noted in Lenka variety with $\mathbf{E}_u$ = 6,5 MPa, and the lowest one – in Roksana variety ($\mathbf{E}_u$ = 5,1 MPa).

Table 2. Average values of mechanical parameters of the investigated varieties of root parsley

Parsley variety	F_{max} [N]	dL for F_{max} [mm]	W to F_{max} [Nmm]	δ [MPa]	ε	E_u [MPa]
Cukrowa	483,7	6,6	1449,1	1,5	0,33	5,2
Halblange	608,0	7,6	1887,2	1,9	0,38	5,6
Lenka	674,7	6,5	1962,5	2,2	0,33	6,5
Ołomuńcka	605,8	7,3	2044,0	1,9	0,37	5,9
Roksana	500,6	6,6	1485,7	1,6	0,33	5,0
Sonata	542,3	6,9	1610,8	1,7	0,33	5,5
Warta	565,2	6,9	1796,6	1,8	0,35	5,6
Wistula	591,6	6,8	1758,9	1,9	0,34	5,9

PARSLEY ROOT RESISTANCE AGAINST PENETRATION

Average values of F_{max} [N] penetration force for root peel and tissue, strain directly before the moment of sample destruction L_{max} [mm], work W to F_{max} [Nmm] to the moment of destruction and the destruction stress δ [MPa] are presented in Table 3.

On the basis of the obtained investigation results and calculations the differentiated values of the analyzed parameters were stated. The highest resistance against penetration of root peel and tissue was noted in Cukrowa variety (77.5 N), while the lowest one for Lenka (67.7 N). The average strain directly before penetration was in the range 4.5-5.5 mm. The average values of penetration energy amounted to 187.9-220.59 Nmm. The average destruction stresses for root peel and tissue were noted from 4.07 MPa (Lenka variety) to 5.40 MPa (Cukrowa variety).

Table 3. Average values of the investigated parameters in the process of penetration of peel and tissue of the root parsley with the punch 5 mm in diameter

Parsley variety	Part of root selected for sampling					
	Top part of the root			Central part of the root		
	Parameters					
	F_{max} [N]	L_{max} [mm]	δ [MPa]	F_{max} [N]	L_{max} [mm]	δ [MPa]
CUKROWA	71,74	4,76	5,29	83,28	4,40	5,52
HALBLANGE	69,19	5,36	4,82	76,71	4,61	5,38
LENKA	65,51	5,19	4,36	69,96	5,69	3,78
OŁOMUŃCKA	68,39	5,37	4,60	79,20	4,95	4,91
ROKSANA	67,60	5,28	4,63	81,70	5,52	4,23
SONATA	64,18	5,37	4,45	71,82	5,33	4,22
WARTA	69,53	5,45	4,72	75,05	5,55	4,12
WISTULA	64,10	5,47	4,22	72,55	5,15	4,30

CONCLUSIONS

- The following factors have the influence on the resistance of parsley roots against mechanical damage:
  - part of root selected for sampling and load applying direction,
  - parsley variety.
- The water contents in fresh parsley roots were differentiated. The highest water content was noted for Wistula variety (79 %), while the lowest – for Ołomuńcka variety (68 %).
- The average values of penetration force of peel and tissue of parsley roots with a punch 5 mm in diameter were within the range from 67.7 N for Lenka variety to 77.56 N for Cukrowa variety. The lowest values of penetration force for peel and tissue were noted for top parts of the root.

– The average values of destruction stress for tissues of the analysed varieties of parsley roots were differentiated and were from 1.5 to 2.2 MPa.
– The average values of Young's modulus were in the range from 5.0 MPa (for Roksana variety) to 6.45 MPa (Lenka), and the relative strains were in the range 0.33-0.38.

REFERENCES

1. **Abbott J.A., Lu R., 1996:** Anisotropic mechanical properties of apples. Transaction of the ASAE 39(4), 1451–1459.
2. **Bajema R. W., Hyde G. M., Baritelle A. L., 1998:** Temperature and strain rate effects on the dynamic failure properties of potato tissue. Trans. ASAE, 41(3), 733–740.
3. **Bentini M., Caprara C., Rondelli V., 2005:** Mechanical properties of sugar beet roots. Transaction of the ASAE, 48(4), 1429–1439.
4. **Bohdziewicz J., 2001a:** Właściwości reologiczne związane z morfologią korzenia marchwi. Inżynieria Rolnicza, 12(32), 51–58.
5. **Bohdziewicz J., 2001b:** Zmienność cech reologicznych korzenia pietruszki. Inżynieria Rolnicza, 12(32), 59–64.
6. **Borna Z. 1997:** Szczegółowa uprawa warzyw. Państwowe Wydawnictwa Rolnicze i Leśne. Warszawa.
7. **Ciupa A., Gładyszewska B., 2011:** Elastic hysteresis determination for the skin of tomato fruit during uniaxial tension test. Teka Kom. Mot. Energ. Roln.- OL PAN, 11, 40–47.
8. **Gładyszewska B., Ciupak A., 2011:** A storage time influence on mechanical parameters of tomato fruit skin. Teka Kom. Mot. Energ. Roln.- OL PAN, 11c, 64–73
9. **Gładyszewska B., Stropek Z., 2010:** The influence of the storage time on selected mechanical properties of apple skin. Teka Kom. Mot. Energ. Roln.- OL PAN, 10, 59–65
10. **Gołacki K., 2001:** Nowe możliwości wykorzystania charakterystyk lepkosprężystych materiałów pochodzenia roślinnego. Inżynieria Rolnicza 2(22), 69–75.
11. **Gołacki K., Obroślak R., 1998:** Wyznaczanie współczynnika Poissona korzeni marchwi. Zeszyty Problemowe Postępów Nauk Rolniczych, 454, 221–227.
12. **Gołacki K., Stankiewicz A., Stropek Z., 2005:** Wpływ prędkości deformacji na wybrane charakterystyki lepkosprężystych materiałów roślinnych. Acta Agrophysica, 5(3), 645– 655.
13. **Gołacki K., Stropek Z., 2001:** Viscoelastic properties of Jonagold apple flesh. Electronic Journal of Polish Agricultural Universities, 4(2), series: Agricultural Engineering.
14. **Guz T., 2008:** Thermal quarantine of apples as a factor forming its mechanical properties. Teka Kom. Mot. Energ. Roln.- OL PAN, 8a, 52–62.
15. **Henry Z.A., Zhang H., Onks D.O., 2000:** New model for elastic behaviour of cellular material. Journal of Agricultural Engineering Research, 76, 399–408.
16. **Kamiński E., Stopa R., Stępień B., 2011:** Zmiana nacisków powierzchniowych korzeni marchwi w funkcji czasu przy stałej wartości przemieszczania początkowego. Inżynieria Rolnicza 4/(129), 105–111.
17. **Kolowca J., 2005:** Właściwości reologiczne miąższu jabłek o zróżnicowanej strukturze. Inżynieria Rolnicza, 6 (66), 355–359.
18. **Kolowca J., 2006a:** Właściwości reologiczne masy ziarna o zróżnicowanej wilgotności. Inżynieria Rolnicza, 12(87), 243–248.
19. **Kolowca J., 2006b:** Wpływ wielokrotnych obciążeń statycznych na stopień zagęszczenia i właściwości reologiczne masy ziarna. Inżynieria Rolnicza, 13(88), 193–199.
20. **Kolowca J., Krzysztofik B., Nawara P., 2006:** Wpływ czasu przechowywania na właściwości reologiczne bulw ziemniaka. Acta Agrophysica, 7(1), 99–104.
21. **Konstankiewicz K., Zdunek A., 2001:** Influence of turgor and cell size on the cracking of potato tissue. Int. Agrophysics, 15, 27–30.
22. **Kuna-Broniowska I., Gładyszewska B., Ciupak A., 2011:** Storage temperature influence of young modulus of tomato skin . Teka Kom. Mot. Energ. Roln.- OL PAN, 11, 218–228
23. **Murase H., Merva G.E., DeBaerdmaeker J.G., Segerlind L.J., 1980:** Importance of the water potential concept in studying physical properties of plant materials. Proceedings of the 2nd International Conference Physical Properties of Agricultural Materials in Godólló, 35, 55–63.
24. **Pitt R.E., 1982:** Models for the rheology and statistical strength of uniformly stressed vegetation tissue. Transactions of the ASAE, 25(6), 1776–1784.
25. **Pitt R.E., Chen H.L., 1993:** Time-dependent aspects of the strength and rheology of vegetative tissue. Transactions of the ASAE, 26(4), 1275–1280.
26. **Stepień B. 2009:** Modyfikacja cech mechanicznych i reologicznych wybranych warzyw pod wpływem różnych metod suszenia. Wydawnictwo Uniwersytetu we Wrocławiu, ISBN 978-83-60574-75-1.
27. **Stępień B., Michalski A., 2006:** Zmiany cech mechanicznych zachodzące w trakcie przechowywania suszonej pietruszki. Inżynieria Rolnicza 4/79,199–206
28. **Szot B., Gołacki K., 1987:** Ocena właściwości mechanicznych korzeni marchwi na podstawie pomiarów podstawowych parametrów wytrzymałościowych. Zeszyty Problemowe Postępów Nauk Rolniczych, 321, 175–183.
29. **Wang J., 2003:** Anisotropic relaxation properties of pear. Biosystems Engineering, 85(1), 59–65.
30. **Zdunek A., Konstankiewicz K., Gancarz M., 2001:** Failure and acoustic emission of potato tuber tissue of selected varieties in compression tests at various strain rates. Electronic of Polish Agricultural Universities. Agricultural Engineering, 4, 2.

ANALIZA WYBRANYCH WŁAŚCIWOŚCI MECHANICZNYCH PIETRUSZKI KORZENIOWEJ

Streszczenie. Celem badań było określenie odporności skórki i tkanki wybranych odmian korzeni pietruszki na uszkodzenia mechaniczne powstałe w procesie przebicia stemplem oraz jednoosiowego ściskania tkanki (walcowa próbka wolna). Wyznaczone zostały podstawowe parametry sprężystości korzeni pietruszki w postaci naprężenia niszczącego oraz umownego modułu Younga. Określono także skład chemiczny badanych odmian pietruszki korzeniowej.

Słowa kluczowe: pietruszka korzeniowa, naprężenie niszczące, moduł Younga, skład chemiczny.

TEKA. COMMISSION OF MOTORIZATION AND ENERGETICS IN AGRICULTURE – 2013, Vol. 13, No. 1, 57–64

Intelligent control for HVAC devices in LCN system

Marek Horyński, Sebastian Styła

Lublin University of Technology, Department of Computer and Electrical Engineering 20 – 618 Lublin, Nadbystrzycka 38A, E-mail: m.horynski@pollub.pl

Received January 26.2013; accepted March 14.2013

Summary: The present paper describes the components of intelligent electric systems used in the building automation systems for HVAC installations control as well as methodology for designing said installations using LCN – Local Control Network system as an example combining the tasks performed by a conventional system and introducing multiple new functionalities making it possible to control individual systems in the building, including HVAC installation.
Key words: heating, control, intelligent, designing, integration, installation.

INTRODUCTION

Electric energy is the most cost-consuming element generating the highest financial burdens in the housing sector [21]. Therefore, newly erected objects are equipped with the systems enabling energy minimization through the cognizant energy management i.e. the systems controlling the devices operation in a manner imposed by operating personnel in order to minimize energy losses [3, 4, 5, 6, 12, 18].

Due to technological development, the contemporary buildings should ensure proper and effective working conditions for their users [14]. It is possible to achieve this goal by means of the state of art, integrated and automated electric installation systems. Therefore, the designers are required to perform a completely new task as a result of such approach to the designing and completion of electrical installations on the basis of technical novelties. In recent years, increased requirements have been observed in the scope of forming a microclimate in rooms. The assurance of proper air quality (described by means of temperature and humidity) becomes an essential task to be performed by an intelligent building. Aforesaid requirements can be met by introduction of modern HVAC systems (Heating, Ventilation, Air Condition), i.e. the heating, ventilation and air – conditioning in the rooms [1, 2, 7, 16, 19, 20].

LCN system has been created and introduced to the market by a German company – ISSENDORFF Mikroelektronik GmbH. The system can be installed in small objects as well as in large buildings, like in case of Main Tower in Frankfurt or F1 racing track in Germany [13].

LCN belongs to leading intelligent control systems worldwide and to the most popular solutions in the scope of buildings automation in global scale. The features of an intelligent building are demonstrated by the degree of integration of installations provided therein. HVAC systems constitute an important element of a modern and fully automated building. The present paper describes the basic elements of LCN system applied in HVAC installation with particular consideration of their programming by means of LCN Pro utility program.

The technological progress in the scope of building sector contributed to the use of more and more new and complex systems dedicated for devices controlling. Due to such complexity and diversity of installations, it was necessary to introduce a system enabling the management of the whole system with all the devices in an integral mode. Another important factor consists in the fact that it is impossible to manage the building energy resources by means of old type installations.

In practice, an intelligent building makes it possible to save 20 up to 30 % of energy; these calculations are realistic even in case of reduced stability of daily and monthly distribution. With increasing speed of our life, we are more interested in the comfort of buildings and in their convenient use. Routine everyday activities can be performed by the building management system to be controlled properly by all of us as the users.

LEGAL AND NORMATIVE REQUIREMENTS IN THE SCOPE OF VENTILATION

Pursuant to building law, the designers of ventilation systems are required to meet determined requirements to ensure proper conditions in the scope of hygiene and energy

consumption. Air change intensity in the building should be modified depending on concentration of the emissions caused by the persons occupying a room and by the devices installed therein.

The amount of air to be removed within one hour from various types of rooms is specified in case of residential buildings. In public utility buildings, the requirements can be met on the basis of fresh air supplied to each person staying in such room.

The issues associated with thermal comfort perceived by the employees in office rooms are governed by PN-EN ISO 7730:2006(U) standard: "Thermal environment ergonomics. Analytical determination of thermal comfort and its interpretation applying the calculation of PMV and PPD indicators and local thermal comfort criterion" and the draft of prEN 15251 standard: "Criteria of indoor environment, encompassing thermal conditions, inside air quality, lighting and noise" [22, 23]. The indicators presented in both documents are used to describe thermal comfort. PMV indicator (Predicted Mean Vote) depends on: activity of an individual, insulation of his / her clothing, air flow velocity as well as its temperature and humidity. The indicator determines the mean vote for thermal environment in the rooms (for a group of persons) in seven step scale: – 3 (cool), 0 (neutral), +3 (hot).

PPD indicator (Predicted Percentage of Dissatisfied (people)) is the next thermal comfort indicator, closely associated with thermal comfort. It must be recognized that owing to individual perception, it is impossible to achieve identical thermal comfort that can satisfy everyone in the same room.

Three basic categories of office rooms are specified in the draft of prEN 15251 standard [7]:

– Class A – PPD < 6%,
– Class B – PPD < 10%,
– Class C – PPD < 15%.

Therefore, it can be concluded that the requirements applicable to class C are met by the majority of objects in Poland and that only a small number can be classified in class B.

REDUCED CONSUMPTION OF ELECTRIC ENERGY AND COMFORT OF USE AS ONE OF ESSENTIAL GOALS OF LCN

We live in times where significant attention is paid to saving of natural resources due to their decreasing amounts and increasing prices. The majority of object resources in the form of thermal and electric energy originates from natural resources processing. Therefore, rational use of electric energy or thermal energy generation became a priority.

Currently, the scope of two principal fields of systems integration encompasses the integration of object security systems as well as building automation systems. The purpose of the first field is to integrate the following systems together: burglary and attack alarm system (SSWN), access control and closed loop control television system (CCTV) in order to enable proper building safety management and to accelerate the support of alarm, emergency and fire signals. The building automation system encompasses the control functions in the scope of heating, ventilation and air-conditioning as well as the control functions in the scope of shutters, lighting, lifts, doors and their power supply system (including holdup systems).

The purpose of the building automation systems integration is the eagerness to achieve savings. A structural network is often used for this task. Simultaneously with increasing prices of electric energy, the reduction of energy consumption in the building causes more and more problems.

Each system makes it possible to reduce the operation costs. For example, the cooperation of systems with each other in the scope of temperature comfort and ventilation in determined room of the building can be commenced at the time of logging in to the system by means of employee's identification card and the temperature will be maintained on an economic level after its logging out. The heating, ventilation and air-conditioning control in the office rooms occupied by several employees increases the comfort of work and is possible by means of simple logical functions AND and OR. The level of saving and safety increase are significantly affected by the number of integrated systems in the building. There are many examples and manners of correct energy management, for instance the heating planning system in the room. Regular working hours for the personnel employed in the specified office are between 8.00AM and 4.00PM. Using the heating electro-valves and temperature sensors connected to LCN network, temperature can be controlled in advance. In order to achieve the temperature of 21°C in the room at 8.00AM, the heating is turned on at 7.00AM and turned out at 3.00PM by the system maintaining the temperature of 15°C. It does not make any big difference but, according to an energy balance, the savings on room heating for the employees are possible. This solution is also comfortable because none of the employees is responsible for heating control [13].

THE EFFECTS OF POOR VENTILATION

Respiratory tract diseases (for instance asthma) are possible as a result of non-compliance with applicable standards and regulations (and consequently poor ventilation and breathing contaminated air) and prolonged stay in the rooms with poor ventilation leads even to cancer cases. The use of gas fired heating equipment in the rooms with inefficient ventilation may lead to carbon monoxide generation.

Carbon monoxide poisoning is most dangerous for humans due to colourless and odourless character of this chemical compound and may lead even to death.

Apart from adverse health consequences for the personnel, the impact of poor ventilation on the building (its structure and appearance) is also unfavourable and leads to heat losses, as shown in Table 1.

Table 1. The effects of poor ventilation (prepared on the basis of [16])

THE EFFECTS OF POOR VENTILATION	
VISIBLE	INVISIBLE
Mildew and mould presence on the lintels, windows framing, under window stools, in the corners of the rooms and behind furniture.	Bad mood, headache and vertigo, tiredness, irritation, irritations of the nasal mucosa, irritations of throat, skin irritation, allergic reactions.
Glasses mist over in windows.	Destruction of building structure, humidity penetration into walls and their gradual reaction.
Condensed water vapour on cool surfaces of walls and objects.	
Air supply through air exhaust grilles in gravity ventilation system.	

THE HEATING, VENTILATION AND AIR-CONDITIONING IN LCN SYSTEM

The central control becomes a necessity in case of lighting, shutters and security system but first of all in case of heating, ventilation and air-conditioning system in many public utility buildings. The main focus is on maintaining the air quality parameters conforming with applicable laws and EU directives in the scope of work conditions. LCN system is selected by many companies in order to meet these expectations. The sensors, actuators and panels are supplied by various manufacturers and selected in a manner ensuring optimal functioning of the whole control system and its economy with consideration of selected transmission medium.

Indoor air quality is measured by means of temperature sensors (thermostats), humidity sensors and carbon dioxide concentration sensors. These values are transmitted to air – conditioning controller ensuring the air – conditioning devices control and to KNX controller ensuring the heating control.

The required data for the system i.e.: wind direction and velocity, daylight intensity are supplied by KNX weather station installed outdoors. KNX/EIB system gives the possibility of remote control and information receiving by means of mobile telephones and the Internet. The settings of heating, ventilation and air-conditioning can be selected automatically, in accordance with the schedule.

It is possible to set „standby" or „comfort" operation mode on the basis of signal informing about open or closed status of the doors locks in a room [8, 9, 10, 11].

LCN system demonstrates its advantages particularly in case of complex control systems, like the heating, ventilation and air-conditioning system. The system simplifies the complex installation enabling the system modifications as well as remote access to the object and measuring data archiving.

SELECTED ELEMENTS AND SENSORS OF LCN SYSTEM VICINITY PARAMETERS

LCN-TSA TEMPERATURE SENSOR

An outdoor temperature sensor equipped with own processor and able to support all modules provided with connection I. The measurement values are directly affected by the installation place. The following factors should be taken into consideration: air flow, solar radiation incidence on the sensor as well as the height of its installation and distance from adjacent heat sources (lamps, ventilation openings). Maximum length of the conductor connecting the sensor with module is equal to 100 m (by means of LCN-IV). After its connection to module, the sensor is identified automatically and its indications are displayed after status checking for the module currently connected with the sensor. Temperature value is specified in the form of four values: LCN value, Kelvin degrees, Celsius or Fahrenheit degrees. After activation, the sensor should be set to determined value of hysteresis associated with its reaction but not exceeding the sensor accuracy. It is also possible to program proper response of module for threshold values contained in the program.

Fig. 1. LCN-TSA sensor [13]

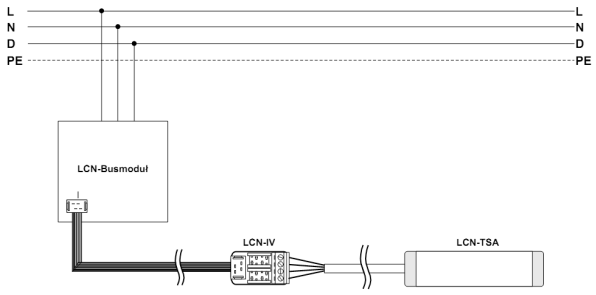

Fig. 2. Sensor connection method [13]

LCN-TS TEMPERATURE SENSOR

Indoor sensor with miniature dimensions enabling its installations. Exactly like outdoor sensor described above, LCN-TS temperature sensor is provided with its own processor establishing gradient dependent noise free values and sending them via port I to specified module. Furthermore, the impact of environment on potentially occurring measurement errors should be taken in account at its installation. The programming is identical to the method applied in case of LCN-TSA sensor.

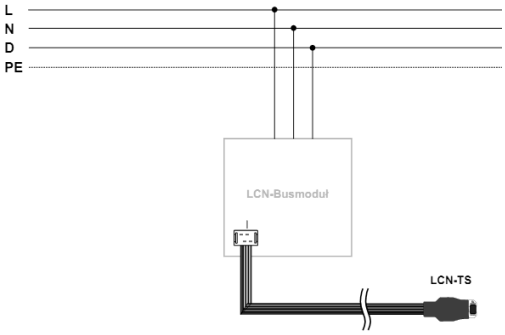

Fig. 3. Sensor connection method [13]

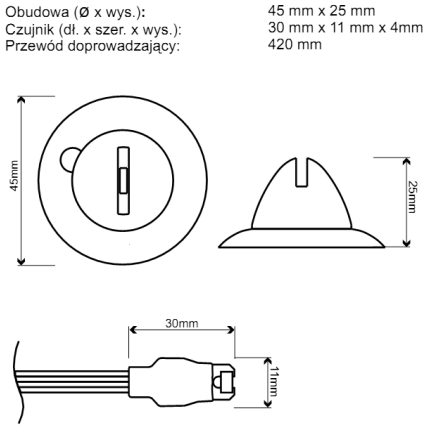

Fig. 4. Sensor dimensions [13]

The sensor is supplied with special holder enabling its installation in any location without excessive jumping out.

LCN-AVC ELECTRO-VALVE FOR HEATING AND AIR – CONDITIONING CONTROL

LCN-AVC is an electronic actuator dedicated for valves setting on central heating radiators. The device is provided with opening angle electronic meter and used for heating control in the rooms instead of conventional radiator shutoff knob. It is possible to connect maximum 5 actuators to one output in the module.

The transparent cover installed on the housing is also used as the lever in order to dismantle the valve from its fastening holder. The flap can be removed in order to prevent any unauthorized flow rate adjustments.

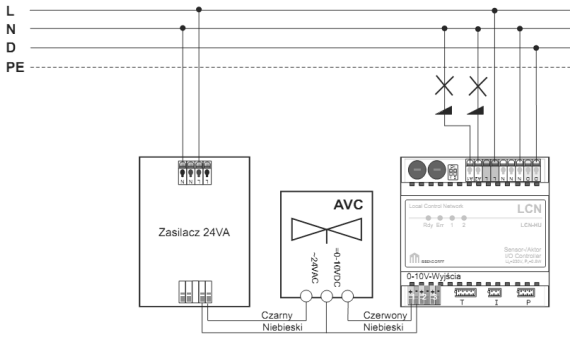

Fig. 5. Sensor connection method [13]

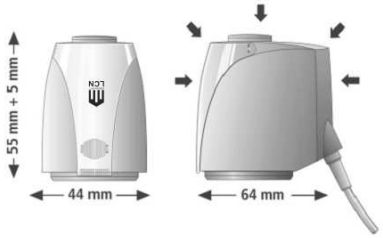

Fig. 6. Sensor dimensions [13]

Fig. 7. LCN-AVC sensor [13]

LCN-WRL65 WEATHER STATION

Weather station consisting of light sensor, rain sensor and wind intensity meter including proper cables. The whole set is contained in two protective boxes which can be installed on the wall or mast. Proper parameters are set by means of appropriate software supplied by the manufacturer. It is possible to change the sensitivity of rain sensor by means of built – in potentiometer. This sensor is subjected to maintenance consisting in contacts cleaning after determined period of use.

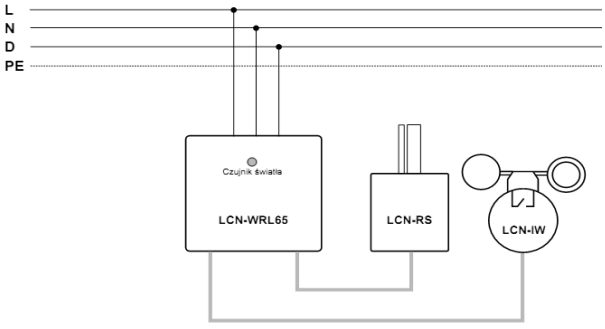

Fig. 8. Sensor connection method [13]

SELECTION OF INTELLIGENT INSTALLATION ELEMENTS

The designing of an intelligent building encompasses the following basic phases:

- Identification of client's needs and presentation of object management system concept.
- Design.
- System installation and programming.
- As-built documentation.
- Warranty and post-warranty service.

In case of incorrect identification of client's needs it is impossible to fully utilize system capabilities. Therefore an audit is necessary to eliminate the differences between client's expectations and system capabilities. Each sensor is less or more necessary, depending on types of objects. It is not required that an object should be provided with all types of specified sensors. All solutions depend on users' needs [16].

An additional data wire and conventional zero wire is used in LCN system for communication. The modules can be provided with 230V power supply or 12 V/ 24 V if required [13].

In designing phase, it is necessary to consider the presence of other systems in the building and to answer the question whether the intelligent network will be integrated with said system and to determine the degree of integration. Furthermore the designer is required to consider the functions which will be performed by the system and to anticipate the use of alternative energy sources.

The models are often created in order to enable the analysis of building installations and to establish the assumptions for energy saving buildings control. The model illustrated in Fig. 8 has been used for testing of installations in an energy saving building.

DESIGN DESCRIPTION

The object has been designed for office functions. The thermostats integrated with electro – valves have been installed in each designed office room in order to ensure the possibility to control and to maintain the temperature in the room on preset level. Windows opening sensors have been installed additionally in order to reduce heat losses and to directly improve rooms heating effectiveness.

Various types of air supply and exhaust elements have been installed in order to ensure proper ventilation in the rooms. Slot diffusers have been mounted in walls or close to the ceiling as well as air supply and exhaust elements i.e. the diffusers mounted in ceiling have been applied in the project in the form of square diffusers. Except of typical gravity ventilation elements, the devices enabling air change control and air temperature control for the air supplied to the rooms have also been installed. Air curtains have also been designed. The principal purpose of an air curtain is to create a visible barrier between the rooms being heated or air – conditioned and its surroundings. These devices are applied in order to improve thermal insulation properties of

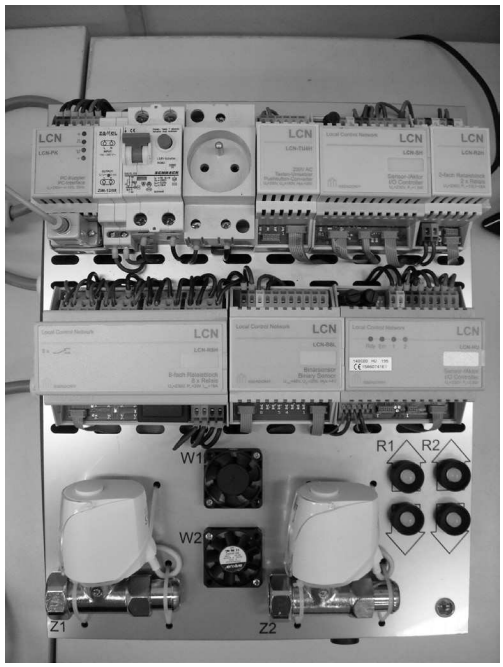

Fig. 9. Switchgear model

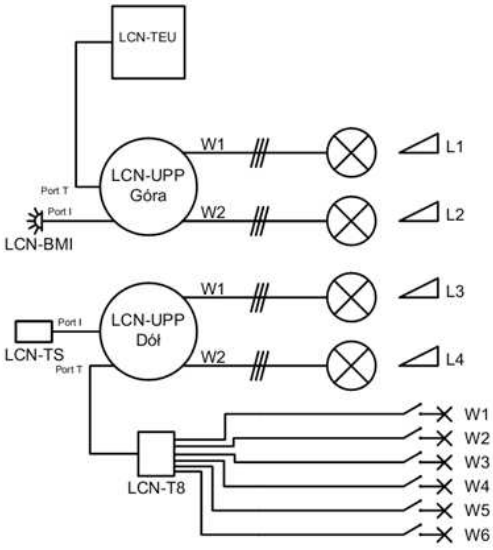

Fig. 10. Electric connection diagram for building modules

the room where they are installed. Therefore, they are usually installed in the areas in vicinity of windows and doors characterized by the highest heat loss. One of the rooms in the building (kitchenette) has been equipped with kitchen extractor hood. This device is usually operated during short period of time but its output is high and air extracted from the rooms contains high amounts of contaminants (mainly fats). Therefore, any connections of kitchen extractor hood with the main ventilation system are avoided.

CONCLUSIONS

The purpose of the present study was to present and analyse HVAC systems integration issue in an intelligent building and to elaborate the installation design for an of-

fice object. In order to achieve this goal, the categories of building automation systems and the concept of intelligent systems integration were first presented. The structure of intelligent installation in LCN system as well as devices contained in these systems, their intercommunication and programming were described thereafter.

The following general conclusions are drawn from the considerations presented in this study:

1. The integration and central control solutions are necessary in many public utility buildings owing to large number of installed building automation systems in case of the following systems: lighting, shutters, safety system but first of all in case of heating, air-conditioning and ventilation system. The main focus is on maintaining the environment quality parameters (e.g. air temperature and humidity) conforming with applicable laws and EU directives in the scope of work conditions.
2. Heat losses and unfavourable impact on the building (its structure and appearance) are possible as a result of non-compliance with applicable standards and regulations. Breathing contaminated air may cause unfavourable health consequences for personnel (e.g. respiratory tract diseases, asthma) and prolonged stay in the rooms with poor ventilation leads even to cancer cases.
3. It is impossible to find one perfectly integrated building automation system meeting all the requirements. All systems, regardless of their capabilities, have their own advantages and disadvantages. Future users of intelligent systems have diversified requirements and needs. Therefore, they will try to find a suitable system in the market; i.e. the system which could attempt to meet their individual needs in the most complete manner.
4. An intelligent installation installed in the building makes it possible to create a place with high comfort, convenience and safety for its users and to improve electric energy quality and its saving. The saving level and safety increase are significantly affected by the number of integrated systems in the building. The tasks associated with LCN system use in an intelligent building are completed in the scope of system operation reliability and its flexible self – adaptation to continuously varying requirements in work and rest environment.
5. Due to low additional expenditures incurred for systems integration, the intelligent building systems become more and more profitable. The investment return period is very short, particularly in case of objects with high energy consumption (e.g.: machine shops, trade and office objects, educational objects). From an economic point of view, the best solution consists in control systems installation in the object already in its construction phase. In such a case, the cost of control systems is equal to only 1-2% of total costs incurred during its whole service life. On the other hand, these systems make it possible to reduce the costs associated with later operation and maintenance of the building by about 75%.
6. Increasingly often, application of intelligent systems in the buildings can bring positive effects in micro scale (residential building, enterprise etc.) as well as in macro scale (whole economy).

REFERENCES

1. **Bogdan A., Chludzińska M., 2008:** Systemy wentylacji i klimatyzacji w budynku inteligentnym, Chłodnictwo i klimatyzacja, Nr 4, 54–57.
2. **Bogdan A., Chludzińska M., 2008:** Zastosowanie wentylacji indywidualnej w pomieszczeniach biurowych, Chłodnictwo i klimatyzacja, Nr 11, 58–62.
3. **Trojanowska M., 2008:** Alternative methods of estimating rural consumers' daily demand for electrical energy. Teka Komisji Motoryzacji i Energetyki Rolnictwa PAN, 8, 287–291
4. **Szymanek M., 2008:** Modeling of demand for energy during sweet corn kernel cutting from the cob. Teka Komisji Motoryzacji i Energetyki Rolnictwa PAN, 247–255.
5. **Boguta A., 2011:** Application of IP monitoring in the supervising system of a building. Teka Komisji Motoryzacji i Energetyki Rolnictwa PAN, vol. XI, 9–17.
6. **Buczaj M., Sumorek A., 2011:** The use of LabVIEW environment for the building of supervision system controlling the climatic and technical parameters in farm rooms. Teka Komisji Motoryzacji i Energetyki Rolnictwa PAN, vol. XI, 18–28.
7. **Chludzińska M., Chojnacka A., 2007:** Wentylacja indywidualna jako rozwiązanie komfortu w pomieszczeniach biurowych, Ciepłownictwo, ogrzewnictwo, wentylacja, Nr 9, 33–36.
8. **Horyński M., 2008:** Heating system control in an intelligent building. Teka Komisji Motoryzacji i Energetyki Rolnictwa, PAN Oddział Lublin, 8, 83–88.
9. **Horyński M., 2010:** Reasonable energy management in an intelligent building. Teka Komisji Motoryzacji i Energetyki Rolnictwa PAN, t. 10C, 87–94.
10. **Horyński M., 2011:** Indoor climate control in EIB system: Sterowanie klimatem pomieszczeń w systemie EIB, Teka Komsji Motoryzacji i Energetyki Rolnictwa PAN, t. 11, 114–122.
11. **Horyński M., 2012:** Energy efficient control of lighting in an intelligent building. Teka Komisji Motoryzacji i Energetyki Rolnictwa PAN, nr 1, vol. 12, 61–67.
12. **Knaga J., 2008:** Energy efficiency of small, compressor assisted air-water type heat pumps. Teka Komisji Motoryzacji i Energetyki Rolnictwa PAN, 8, 99–105.
13. **LCN 2011:** materiały techniczne producenta.
14. **Markiewicz H., 2012:** Instalacje elektryczne. Wydanie VIII, Wydawnictwo Naukowo-Techniczne, Warszawa.
15. **Podosek Z., Włodarczyk J., 2002:** Systemy teletechniczne budynków inteligentnych: okablowanie strukturalne, instalacje elektryczne, systemy alarmowe, systemy kontroli dostępu, sieci domowe, systemy HVAC, systemy przeciwpożarowe. Przedsiębiorstwo Budowlano – Projektowo – Wdrożeniowe Cyber: Bel Studio, Warszawa.
16. **Rusewicz T., 2012:** Wentylacja – podstawa zdrowego budynku, Doradca energetyczny, Nr 2, 20–24.
17. **Styła S., Pietrzyk W., 2011:** The identification of operational failures of the heating, ventilation and air-conditioning circuit in the car by means of thermo-

vision methods. Teka Komisji Motoryzacji i Energetyki Rolnictwa PAN, vol. XI, 354–362.
18. **Gutyrya S., Yaglinsky V., 2006:** System criteria analysis and function optimization of industrial robots. Teka Komisji Motoryzacji i Energetyki Rolnictwa PAN, 6A, 70–81.
19. **Trojanowska M., Szul T., 2006:** Modelling of energy demand for heating buildings, heating tap water and cooking in rural households. Teka Komisji Motoryzacji i Energetyki Rolnictwa PAN, 6A, 184–190.
20. **Trojanowska M., Szul T., 2008,:** Determination of heat demand in rural communes. Teka Komisji Motoryzacji i Energetyki Rolnictwa PAN, 8a, 180–187.
21. **Turzyński J., Czekaj E., 2007:** Implementation of modern materials and foundry techniques in wind power energetic. Teka Komisji Motoryzacji i Energetyki Rolnictwa PAN, 7, 236–242.

Normy:

22. PN-EN ISO 7730:2006(U): „Ergonomia środowiska termicznego. Analityczne wyznaczanie i interpretacja komfortu termicznego z zastosowaniem obliczania wskaźników PMV i PPD oraz kryterium lokalnego komfortu termicznego".
23. Projekt normy prEN 15251: „Kryteria środowiska wewnętrznego, obejmujące warunki cieplne, jakość powietrza wewnętrznego, oświetlenie i hałas".

Streszczenie: Niniejszy artykuł omawia elementy inteligentnych systemów elektrycznych stosowanych w automatyce budynków, w instalacji HVAC. Opisuje również metodykę projektowania tych instalacji w systemie LCN – Local Control Network System, jako przykład łączący zadania wykonywane w ramach tradycyjnej instalacji i systemu inteligentnego budynku.

Słowa kluczowe: ogrzewanie, sterowanie, inteligentne, projektowanie, integracja, instalacja

TEKA. COMMISSION OF MOTORIZATION AND ENERGETICS IN AGRICULTURE – 2013, Vol. 13, No. 1, 65–70

Employing empirical mode decomposition to determine solar radiation intensity curve

Jacek Kapica, Marek Ścibisz

University of Life Sciences in Lublin, Doświadczalna 50A, 20-280 Lublin
email: jacek.kapica@up.lublin.pl, marek.scibisz@up.lublin.pl

Received January 25.2013; accepted March 14.2013

Summary. The paper presents an application of the empirical mode decomposition to filtering of the fast changing components of the solar radiation curve. Results of the measurement of the solar irradiation for a few typical days are presented. The measurements were taken with a frequency of one sample per second, which is a high value as for solar radiation. Then the data were resampled with lower sampling frequencies, directly and after eliminating fast changing components with the use of empirical mode decomposition. For each case a daily solar energy was calculated.
Key words: empirical mode decomposition, signal filtration, solar radiation.

INTRODUCTION

Since the energy crisis in 1970's a constant growth of photovoltaic power production has been observed [6, 12, 16]. One of the areas of solar energy application is agriculture [13, 17]. This kind of energy is sometimes considered as "agro-energy" [14].

The solar radiation, depending on the weather conditions on a particular day, may have various levels of variability. On a cloudless day or when the sky is covered with evenly distributed cloud layer, the insolation changes slowly according to the earth rotation. But on a windy day when the sky is covered with small clouds (for example cumulus clouds), the radiation changes very quickly.

Due to the shape of the current – voltage curve of the photovoltaic (PV) panels, the efficiency of the set PV generator – electrical load depends on how the load matches the source. In systems with battery, instantaneous values of the solar insolation are not that important – presence of the battery stabilizes the working point of the generator. A different situation, due to aforementioned problem of matching between generator and load, occurs in case of a PV island system without battery. It is of special importance in case of applications in agriculture, where this kind of PV system may be employed.

Therefore, when analyzing the operation of systems powered by photovoltaic generators, it often happens that in addition to the sum of energy in a given day the calculations are performed using the data from measurements of the instantaneous values of radiation intensity (as in [15]). The highest accuracy is achieved by using high sampling frequencies, but such an approach generates huge amounts of data which in case of long lasting measurements can be inconvenient because of the storage space required and CPU usage when this data is used in computer simulations. The solution is to properly choose the sampling frequency, however the sampling points are chosen randomly and it may happen that that the sample will be taken in a moment which is not representative for a given period, for example in a temporary, short moment of cloudiness.

An alternative approach is to acquire the data with high frequency, process it in order to eliminate (average) the high volatility and then to resample it with lower frequency for data archiving.

The paper presents application of Empirical Mode Decomposition (EMD) to filter fast changing components of solar radiation curve.

EMPIRICAL MODE DECOMPOSITION

Empirical mode decomposition (EMD) is a novel method which can be applied to any complicated data set in order to decompose it into a finite number of intrinsic mode functions. It is applicable to non-linear and non-stationary processes [1, 4, 5].

According to Huang [8] the decomposition is made on an assumption that any data consists of different simple intrinsic modes of oscillations. Each of the oscillatory modes

is represented by an intrinsic mode function (IMF) with the following definition [7]:

1. in the whole data set, the number of extrema and the number of zero crossings must either be equal or differ at most by one;
   and
2. at any point, the mean value of the envelope defined by the local maxima and the envelope defined by the local minima is zero.

An integral part of the EMD procedure is the sifting process. It can be described by the following steps, assuming that $x(t)$ is the source data:

1. Find all the local extrema (minima and maxima) of $x(t)$,
2. Interpolate the extrema with a cubic spline: the maxima will create the upper envelope $eup\_n(t)$, the minima will create the lower envelope $elo\_n(t)$,
3. calculate the mean value line which lies between the upper and lower envelope according to the following equation:

$$m_n = \frac{e_{up\_n}(t) + e_{lo\_n}(t)}{2}, \tag{1}$$

4. calculate the residue *hn*:

$$h_n = x(t) - m_n, \tag{2}$$

5. the steps 1 to 4 are repeated treating *hn* as the input data until a stoppage criteria is met.

There are two approaches to the stoppage criteria. One is to calculate normalized squared difference between two successive sifting iterations n and n-1 [8]:

$$SD_n = \frac{\sum_{t=0}^{T} \left| h_{n-1}(t) - h_n(t) \right|^2}{\sum_{t=0}^{T} h_{n-1}^2}, \tag{3}$$

and continue the iterations until the *SDn* is small enough. This criterium, however, does not guarantee that the function will have the same number of zero-crossings and extrema, even if the value of *SDn* is lower than a given threshold value.

Another stoppage criterium proposed in [9] is based on the fact whether the signal obtained in the last iteration has the same number of zero-crossings and extrema. With this criteria, the sifting process will stop only after S consecutive times when the number of extrema and zero-crossings differ at most by one. The value of S proposed by Huang et al. is between 4 and 8 for optimal sifting.

If the stopping criteria is met the *hn* will be the first IMF which represents the fastest oscillating component. Subtracting $x(t)$ and *IMF1* gives the residue *r1*:

$$r_1 = x(t) - IMF_1, \tag{4}$$

r1 contains longer oscillations and is treated as input data to the sifting process. In this manner the following IMFs are computed until *IMFn* or *rn* becomes smaller than a predefined value or when *rn* becomes a monotonic function.

Considering equation (4) and iterative nature of the procedure we may write that:

$$x(t) = \sum_{j=1}^{n} IMF_n + r_n. \tag{5}$$

The equation (5) reflects the decomposition process of the given signal $x(t)$ into a series of n IMFs and the residue. Each higher IMF represents longer oscillating component of $x(t)$. The procedure is illustrated on figure 1.

As the intrinsic mode functions of various orders represent different levels of oscillations, eliminating the components with shorter oscillations can be used to filter-out the fast changing components of a given signal.

One big advantage of decomposing the signal using the empirical mode decomposition is that there is no need to decide apriori which function will be used to represent the signal. In contrast, in traditional Fourier transform a sinusoidal function is assumed and in wavelet transform the mother function needs to be chosen prior to the analysis.

Several authors have addressed the usage of the EMD in solar radiation analysis [11, 18, 19, 20]. None of them however uses the EMD to filter solar radiation data. Some attempts are made to employ this procedure to filter other kinds of signals. Fleureau and others [5] use a modified version of EMD to filter ElectroEncephaloGraphic(EEG) sleep recording.

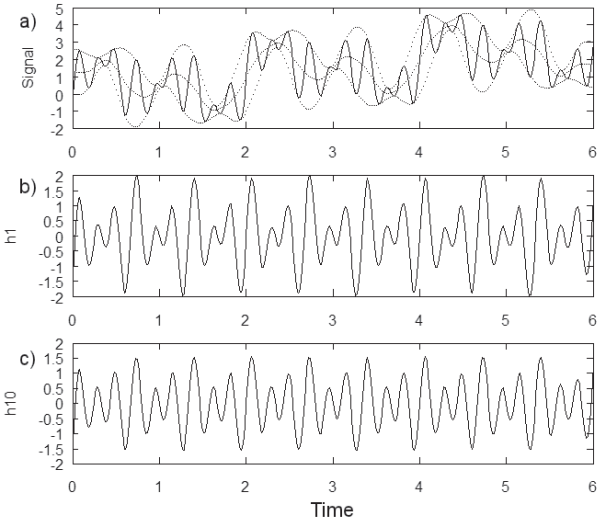

Fig. 1. Example of a sifting process for a simulated signal. a) original signal (solid line), upper and lower envelopes with mean line (dotted lines), b) result of the first iteration of the sifting, c) result of the 10th iteration of the sifting

DATA, METHODS AND TOOLS

The short-circuit current of a photovoltaic cell is directly proportional to insolation [10]. This fact has been used to measure the solar radiation intensity on a PV module plane. The diagram of the measurement circuit is presented on Fig. 2. The sampling frequency was 1 sample per second, which is a high value for solar radiation measures. The measurement was made with help of an application created

in a LabView programming environment which is suitable for measurements both in real and simulated circuits [2, 3].

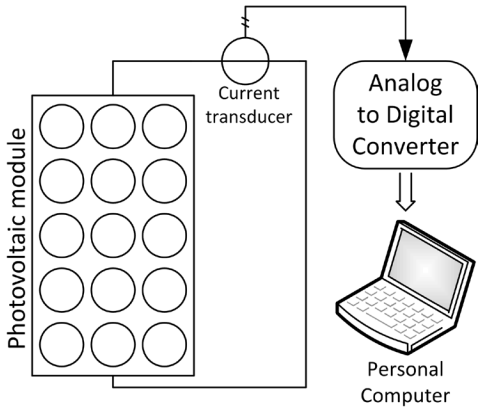

Fig. 2. Diagram of the circuit for solar insolation measurement

The next step was to obtain two types of signals: 1) a signal created by resampling of the original signal with lower frequency, 2) a signal created after filtering the fast-changing components of the originally measured signal and resampling it with the same frequency as the first signal. These steps were performed by a script executed in the GNU Octave programming environment [4]. The script was also calculating the daily amount of solar energy by using a signal acquired with frequency of one sample per second and the two types of signals described previously. Also the absolute and relative errors of daily energy estimation were calculated with an assumption that the original signal is error-free.

The filtering consists of the following steps:

1. Decompose the original signal into set of IMFs,
2. Reconstruct the signal eliminating the IMFs representing faster oscillations.

As a result a new signal is obtained in which the rapid changes of the solar irradiation are removed.

RESULTS

The analyzed data was solar insolation curve registered by the author for selected days of April 2010. Figure 3 presents the instantaneous power of the solar radiation on a PV module plane. On days A and B we can see many rapid changes of the insolation. Day C has significantly less fast components.

The signal was decomposed into 20 intrinsic mode functions plus residue. The filtering was done by reconstructing the signal using higher level IMFs – the IMFs representing faster oscillations were removed. The calculations were done for all the sequences of the IMFs, eliminating the lowest functions gradually (2-20 plus residue, 3-20 plus residue and so on). The results are presented on a 3D chart (Figures 4-6). Additionally, 2D graphs are presented for selected sequences of reconstructed signal (Figures 7-9). For convenience, the residue will be referred as 21st IMF on the charts. On the 3D charts, the presented IMF value is the first IMF included in the signal reconstruction, for example 5 means that the signal is reconstructed from the 5th IMF and higher plus residue.

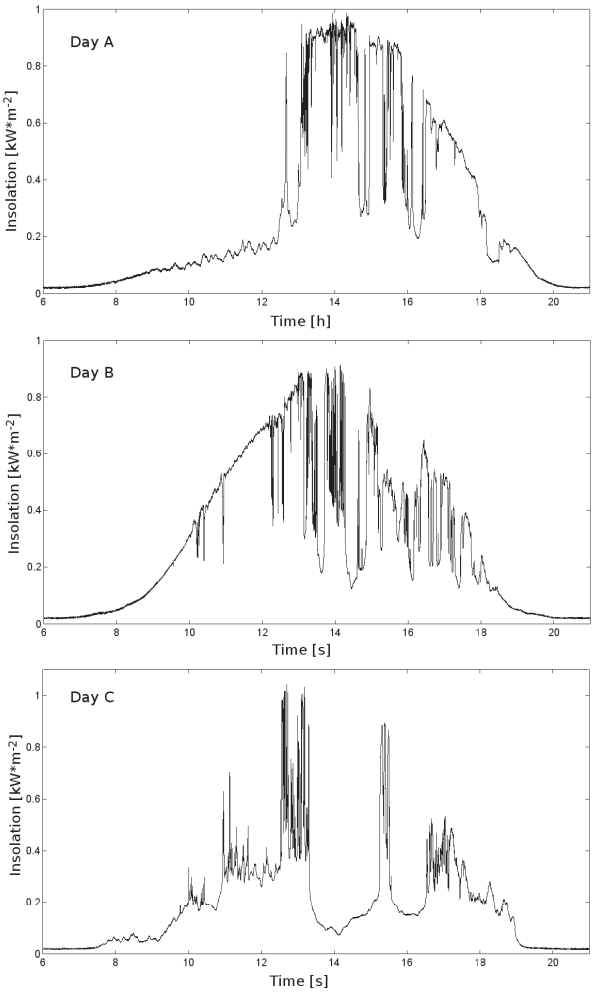

Fig. 3. Solar insolation curve on selected days of April 2010

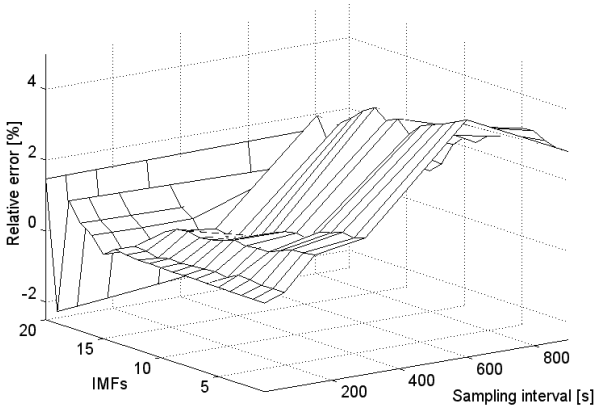

Fig. 4. 3D chart illustrating influence of the IMF components included in the signal reconstruction on the relative error for selected sampling intervals for day A

CONCLUSIONS

The results show that when applying shorter sampling intervals (higher sampling frequency) the error of calculating the daily energy is usually less. There are, however, cases with longer sampling intervals (like 600 and 900 s), in which the relative error is lesser, compared to longer intervals. The

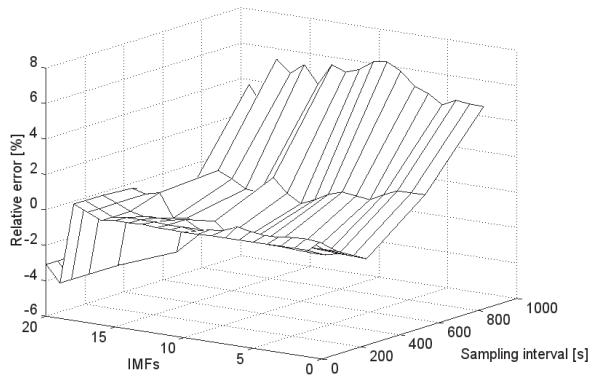

Fig. 5. 3D chart illustrating influence of the IMF components included in the signal reconstruction on the relative error for selected sampling intervals for day B

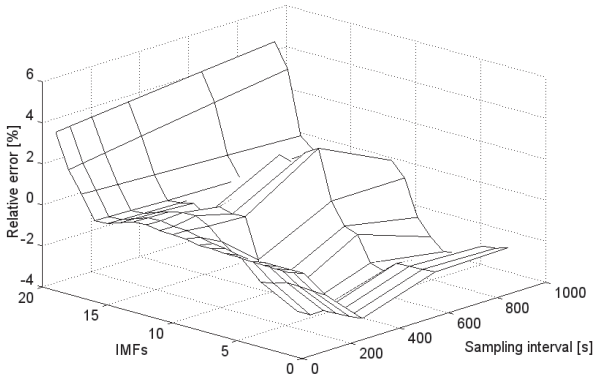

Fig. 6. 3D chart illustrating influence of the IMF components included in the signal reconstruction on the relative error for selected sampling intervals for day C

accuracy of daily energy estimation depends also on the intensity of the irradiation oscillations.

Application of the proposed filtration allowed for an increase of the measurement accuracy. In most cases the error after filtration of the fast-oscillating components is significantly lower than without the filtration, in some cases it is similar. The results show that we should not eliminate too many IMFs – not more than 10 fast oscillating components. Otherwise, the results may become unstable – producing a generally random error.

The relative error values, even without the filtering, are relatively small and not greater than 6 % and if sampling intervals not greater than 3 minutes would be used – not greater than 3,5 %. Nevertheless eliminating faster oscillations with the described procedure decreases the error further.

Applying sampling intervals less than 60 s, even without signal filtering allows for high measurement accuracy. In cases when, due to the amount of the acquired data and calculations performed, it is necessary to use longer sampling intervals it is advisable to perform the measurement with higher frequency, then to remove faster oscillations with the presented method and, before archiving, resample the signal with lower frequency. This will allow for higher accuracy of calculations made using the prepared data.

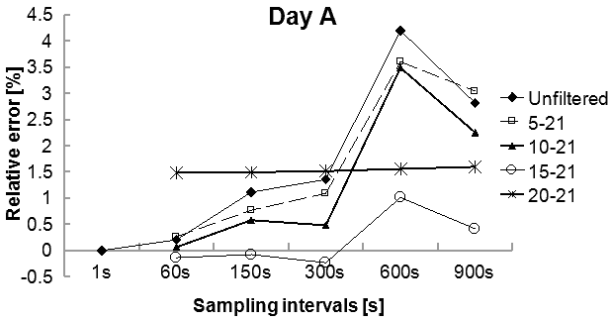

Fig. 7. Illustration of the influence of the IMF components included in the signal reconstruction on the relative error for selected sampling intervals for day A.

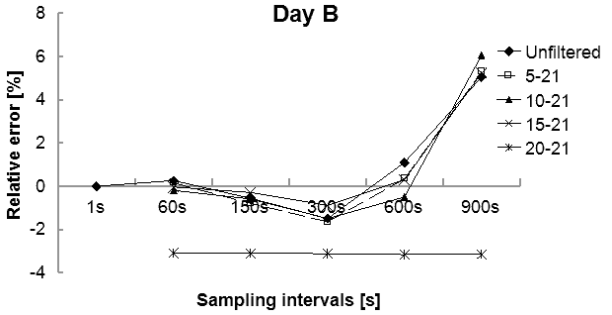

Fig. 8. Illustration of the influence of the IMF components included in the signal reconstruction on the relative error for selected sampling intervals for day B

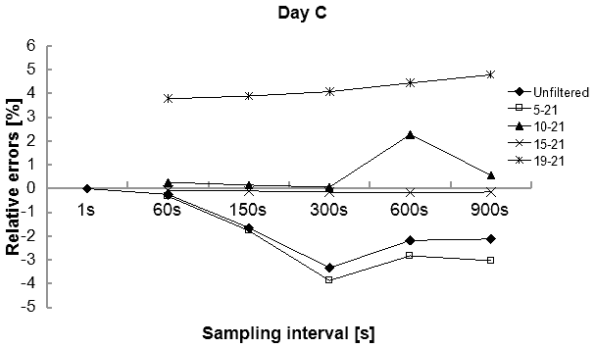

Fig. 9. Illustration of the influence of the IMF components included in the signal reconstruction on the relative error for selected sampling intervals for day C

REFERENCES

1. **Braun S. G., Ewin D. J.; Rao S. S. 2002:** Encyclopedia of Vibration, Volumes 1–3, 647. Elsevier.
2. **Buczaj M., Sumorek A. 2007:** Simulation of motor vehicles instrument panels in LabView environment. Teka Komisji Motoryzacji i Energetyki Rolnictwa VII, 52.
3. **Buczaj M., Sumorek A. 2011:** The use LabView environment for the building of supervision system controlling the climatic and technical parameters in farm rooms. Teka Komisji Motoryzacji i Energetyki Rolnictwa XI, 18.
4. **Eaton J.W., 2000:** GNU Octave Manual, Network Theory Limited, ISBN: 0-9541617-2-6

5. **Fleureau J., Kachenoura A., Albera L., Nunes J.-C., Senhadji L. 2011:** Multivariate empirical mode decomposition and application to multichannel filtering, Signal Processing, Volume 91, Issue 12, 2783–2792
6. **Grubb M., Vigotti R. 1997:** Renewable Energy Strategies for Europe: Electricity systems and primary energy sources. Royal Institute of Internetional Affairs.
7. **Huang, N., Shen, Z., Long, S., Wu, M., & Shih H. 1998:** The empirical mode decomposition and the Hilbert spectrum for nonlinear and non-stationary. Proceedings Mathematical, (454), 903–995.
8. **Huang, Norden E. 2005:** Empirical mode decomposition for analyzing acoustical signals. United States Patent 6862558.
9. **Huang, N. E. 2005:** Introduction to the Hilbert Huang Transform and its related Mathematical problems. (N. E. Huang & S. S. P. Shen, Eds.)Interdisciplinary Mathematics, 5, 1–26.
10. **Kalogirou S. A. 2009:** Solar Energy Engineering – Processes and Systems, 477. Elsevier. ISBN: 978-0-12-374501-9
11. **Lin Z. S., Wang S. G. 2006:** EMD analysis of solar insolation. Meteorology and Atmospheric Physics. Earth and Environmental Science, Volume 93, Numbers 1–2 (2006), 123–128.
12. **Lotsch H.K.V., Goetzberger A., Hoffman V.U. 2005:** Photovoltaic Solar Energy Generation. Springer Series in Optical Sciences Volume 112.
13. **Luque A., Hegedus S. 2003:** Handbook of photovoltaic science and engineering. John Wiley & Sons, 54.
14. **Roszkowski A. 2006:** Agriculture and fuels of the future. Teka Komisji Motoryzacji i Energetyki Rolnictwa VI, 132.
15. **Sarniak M. 2011:** The testing of energy efficiency of a prototype hybrid solar panel. Teka Komisji Motoryzacji i Energetyki Rolnictwa XI, 335–342.
16. **Sinha P.C. 1998:** Energy Crisis. Anmol Publications, 184.
17. **Tiwari G. N., Dubey S. 2010:** Fundamentals of Photovoltaic Modules and their Applications. Royal Society of Chemistry. ISBN: 978-1-84973-020-4, 118.
18. **Xian S., Zhenshan L., Xiaoxia C. Chuangye J. 2008:**Regional features of the temperature trend in China based on Empirical Mode Decomposition, Journal of Geographical Sciences, Volume 18, Number 2 (2008), 166–176.
19. **Yang C X, Wu H F, Hu D T. 2011:** Relationship between air temperature oscillations and solar variability on short and medium time scales. Sci China Earth Sci, Vol. 54, 912–923.
20. **Yong W., Qi-Long M., Chong-Yi E., Jian-Kang H., Yuan-Yuan D. 2010:** Relation between temperature changes of the mid-upper troposphere over Eurasian mid-high latitudes and solar irradiance in the twentieth century. Environmental Earth Sciences, Volume 60, Number 6 (2010), 1257–1266.

ZASTOSOWANIE EMPIRYCZNEJ DEKOMPOZYCJI MODÓW DO WYZNACZANIA KRZYWEJ NATĘŻENIA PROMIENIOWANIA SŁONECZNEGO

Streszczenie: Artykuł przedstawia zastosowanie empirycznej dekompozycji modów do filtrowania szybkozmiennych składowych krzywej natężenia promieniowania słonecznego. Przedstawiono wyniki pomiarów natężenia promieniowania słonecznego dla kilku typowych dni. Pomiary były dokonywane z częstotliwością jednej próbki na sekundę, co jest wartością dużą dla promieniowania słonecznego. Następnie dane zostały ponownie spróbkowane bezpośrednio oraz po wyeliminowaniu szybkozmiennych składowych z wykorzystaniem empirycznej dekompozycji modów. Dla każdego z przypadków została wyznaczona wartość dziennej energii promieniowania słonecznego.

Słowa kluczowe: empiryczna dekompozycja modów, filtracja sygnału, promieniowanie słoneczne.

Prospects of development of bioenergetics in Belarus

Korotinsky Victor, Wojciech Tanas**, Garkusha Karina*, Garkusha Kirill**

*Belarusian State Agrarian Technical University, Minsk
**University of Life Sciences in Lublin

Received February 16.2013; accepted March 14.2013

Summary. The article contains materials on the bio-energetic potential of the Republic of Belarus and prospects of development of bioenergetics. In the area of bio-energetic, technologies which use renewed organic resources, the so-called biomass for energy manufacture, including the electric power, energy of liquid, firm and gaseous kinds of fuel, warmth, chemical substances and other materials were discussed.

Key words: bioenergy, power resources, biomass sources, agricultural production waste, recycling of waste in agriculture.

INTRODUCTION

The Republic of Belarus is located in the eastern part of Europe. It borders Lithuania and Latvia in the north, Ukraine in the south, the Russian Federation in the east and Poland in the west. The territory occupies 207,6 thousand sq. km.

The agricultural soil occupies 44,9%, of the ploughed land – 30% of total area. The weakly utilized soils in the national economy (sands, bushes, swamp so forth) compose 15% of total area [7].

The population of the Republic of Belarus as of 01.02.2012 is 9463 thousand people, 1885 thousand of them live in Minsk.

More than 75% of population live in the cities and there are only 25% rural inhabitants [6].

The dynamics of the population since 1990 is presented in Fig. 1.

The agriculture of Belarus' is specialized in the cultivation of cultures traditional for the temperate latitudes. In the plant growing the predominant grains are barley, rye, wheat, potatoes, feed crops.

In connection with the structural conversions and the orientation to the renewed energy sources in the Republic the volumes of the cultivation of leguminous and oily cultures are enlarged.

In the stock raising in essence large livestock is reared for the production of milk and meat, but also pigs and poultry.

The dynamics of cattle and poultry livestock since 2007 is presented in Tab. 1.

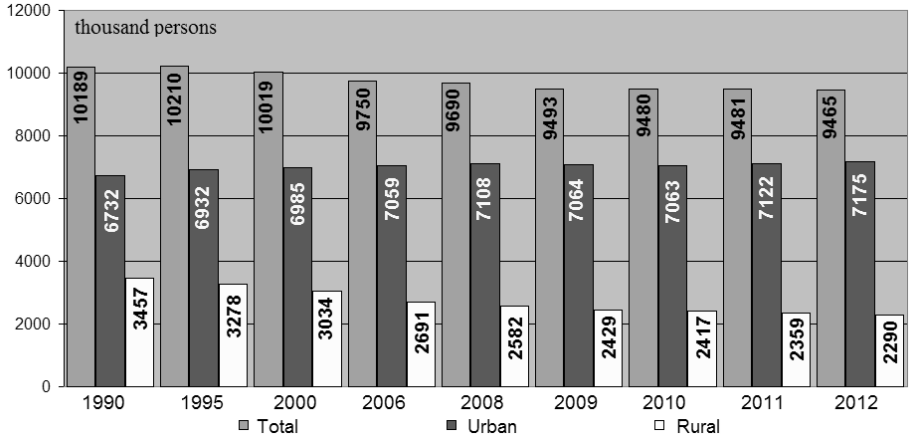

Fig. 1. The rural and urban population of Belarus

Table 1. Cattle and poultry livestock at the beginning of each year

Years	Large horned livestock	Cows of dairy herd	Pigs	Sheep and goats	Horses	Poultry
2007	3989	1506	3642	122	156	28,7
2008	4007	1459	3598	124	147	29,4
2009	4131	1452	3705	126	137	31,2
2010	4151	1445	3782	127	125	34,1
2011	4151	1478	3887	124	113	37,0
2012	4247	1477	3989	125	100	40,0

Note: The poultry is resulted in millions, the others in thousands

THE BASIC PART

According to the Republican program of rational use of power resources for 2011-2015, the total consumption of fuel and energy resources in the Republic in 2015 is predicted at 41 million tons of conditional fuel, in 2020 – 44 million tons of conditional fuel [1]. The forecast of total consumption of fuel and energy resources in Belarus is presented in Tab. 2.

Table 2. The forecast of total consumption of fuel and energy resources in Belarus,%

Fuel and power resources	2010	2015	2020
Natural gas	63,5	56,2	37,3
Coal	0,3	2,4	10,0
Nuclear fuel	0	0	11,4
Mineral oil	18,5	19,7	22,7
Others	17,7	21,7	18,6

The power supply system of Belarus has a difficult character, but it is perfectly integrated into the general uniform electric network in the other states (the scheme of a power supply system of Belarus and the other states is resulted in Fig. 2).

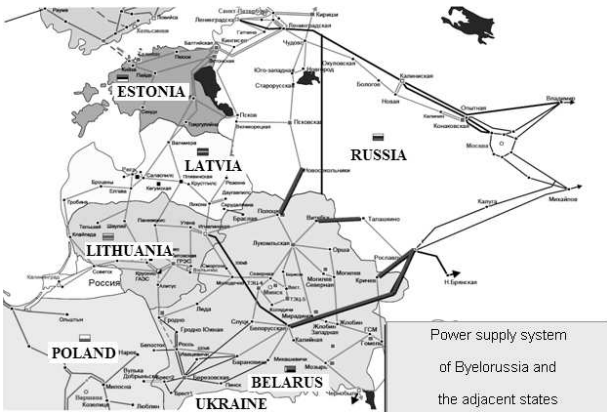

Fig. 2. Scheme of a power supply system of Belarus

Among the power companies of Belarus, Russia, Estonia, Latvia and Lithuania whose electric networks work in a uniform electric ring, the Agreement on parallel work of power supply systems has been in operation since February 7th, 2001.

The specified interstate electric communications of Belarus power supply system not only provides the reliability of electricity supply to consumers of the Republic, but also participate in the realization of steady parallel work of power supply systems of all the region Baltic – Belarus – Russia – Ukraine. Teamwork of a power supply system of Belarus with the CIS countries and Baltics allows to carry out deliveries of the electric power for the purpose of optimization of electric balances of the parties, and also to give reserves of capacity and to render the emergency help in extreme situations [4]. Within the limits of parallel work of power supply systems, Belarus imports the electric power from Russia and Ukraine, exports it to Lithuania, and also carries out electric power transit in energetically scarce regions of Russia and the Baltic State.

The structure of fuel balance of the Belarus power supply system is resulted in Fig. 3.

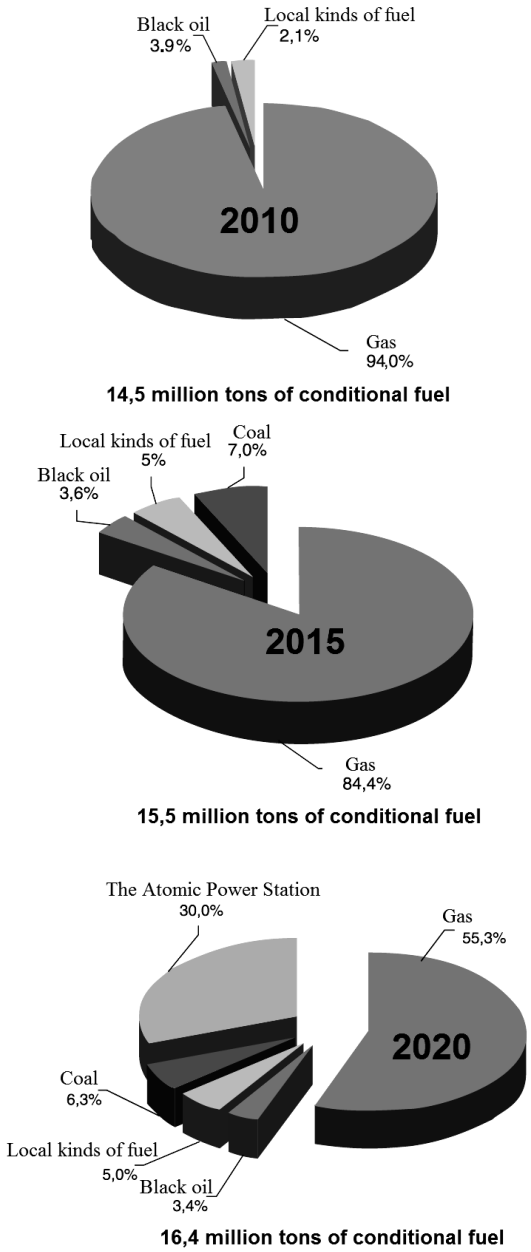

Fig. 3. Structure of fuel balance of the Belarus power supply system on 2010, 2015 and 2020

Bioenergetics – technologies which use renewed organic resources, a so-called biomass for energy manufacture, including the electric power, energy of liquid, firm and gaseous kinds of fuel, warmth, chemical substances and other materials. The bioenergetics after the sun is the most powerful renewed energy source [15].

Fuel from a biomass starts to become more popular because of the growing prices for fossil kinds of fuel. Besides, using biopower sources reduces pollution, helps to supervise emissions of carbon dioxide [14].

What is the biomass and how it can be used for warmth and electricity reception?

Biomass is constituted by any materials of biological origin, products of life processes and various organic waste. The biomass will exist on the Earth until there is life on it. According to the European Economic commission of the United Nations the annual gain of organic substance on the Earth is equivalent to manufacture of such quantity of energy, which is ten times more than annual consumption of energy by all mankind at the present stage [13].

The basic directions of use of biomass for power:

1st group
- Fire wood (coniferous, deciduous breeds and fast-growing trees),
- Manufacture pellets (wood or peat granules),
- Manufacture of combustible briquettes (wood, grassy, peat),
- Manufacture of special wood (for direct burning),
- Straw or grassy bales (in special fire chambers),

2nd group
- Gasification,
- Pyrolysis,

3rd group
- Ethanol manufacture,
- Manufacture of biodiesel fuel,

4th group
- Biohydrogen manufacture,

5th group
- Biogas manufacture.

In the conditions of Belarus, the development of bioenergetics is economically expedient and technically realizable. In Belarus there are in operation over 6300 complexes KPC; over 100 pig-breeding complexes and 60 poultry-farming complexes on which millions of tons of waste (Tab. 3) are annually formed [2].

Table 3. The forecast of an exit of manure and dung in 2012, tons

Animal (birds)	Large horned livestock	Pigs	Birds
Exit of manure (dung)	212 350	79 780	2 400

This waste (practically without their preliminary processing) is dumped on fields as fertilizers. However, besides advantage, they simultaneously cause a considerable ecological damage. Being washed away by snow and storm waters, manure from fields, and also non-neutralized waters of animal industries' enterprises, in particular pig-breeding farms, get to reservoirs. Such sewage contain a considerable quantity of biogenic elements among which there is phosphorus and nitrogen promoting mass development of seaweed.

The potential of biogas from all the sources makes 160 thousand tons of conditional fuel in a year [16].

Biomass sources, characteristic for our republic, can be divided into five basic groups:
- Products of natural vegetation (wood, wood waste, wood dust and peat),
- Photogenes biomass (raps, straw, oil cake, silo, etc.),
- Waste of human life processes (solid household waste, waste of industrial production and deposits of treatment facilities),
- Agricultural production waste (manure, chicken dung, tops of vegetables, etc.),
- Agriculture waste (beetroot, potato waste, beer pellets, technical glycerin, meat waste, milk processing waste, etc.),
- Specially grown up fast-growing agricultures, plants and wood plantings.

In Belarus solid household waste goes to dumps and two waste recycling factories (Minsk and Mogilyov).

Annually there are taken out (thousand ton): paper – 648,6; food waste – 548,6, glass – 117,9; metal – 82,5; textiles – 70,8; wood – 54,2; skin and rubber – 47,2, plastic – 70,8 [3].

The potential energy included in solid household waste, formed on the territory of Belarus, is equivalent to 470 thousand tons of conditional fuel.

At its processing for the purpose of gas obtainment, the efficiency will reach no more than 20–25 %, which is equivalent to 100–120 thousand tons of conditional fuel. Besides, it is necessary to consider long-term stock waste, which is available in all large cities and creates problems with its warehousing. Only in regional cities, the processing of annual municipal waste into gas would allow to receive about 50 thousand tons of conditional fuel, and in Minsk – to 30 thousand tons of conditional fuel energy.

On the whole, in Belarus only 16 % of waste is processed [5].

Efficiency of the given direction should be estimated not only from biogas yield, but also on the basis of the ecological component which will be essential in the given problem.

For obtainment of useful products or substances the biomass demands processing which has complex character and allows to solve a number of extremely important problems:
- Sanitary-ecological (disinfecting of waste);
- Agrochemical (obtainment of effective organic fertilizers);
- Power (obtainment of qualitative fuel, and then thermal and electric energy);
- Social (improvement of working and living conditions, increase in productivity of agricultural crops, increase of efficiency of animals, reduction of poisonous chemicals' application etc.).

At present the following large biogas complexes in agrarian sector are being realized: Open Society «Gomel Integrated Poultry Farm» (340 kw); "The Western" (500 kw); "The Belarussky" (340 kw) and «Agrocombine of Snou» (2 MW, Fig. 4).

Fig. 4. Biocomplex «Agrocombine of Snou»

Understanding the importance of the question of waste recycling, in 2012 in the Belarus Republic it is planned to finish new large projects – seven biogas installations and the complexes working on the waste from agricultural production, with electric capacity 1–3 МВт.

They involve the following: Open Society "Gastellovsky" (electric capacity 3 Mw), Open Society "State Farm Combine" Sozh »(electric capacity 1 Mw), The closed joint-stock company "Lipovcy" (electric capacity 3 Mw), Agricultural production co-operative "Maiak Kommuny" (electric capacity 1 Mw), The republican unitary agricultural enterprise «Sovhoz "Slutck" (electric capacity 1Mw), The republican unitary agricultural enterprise «Pig-breeding Complex "Borisovsky" (electric capacity 1 Mw), Agricultural Production Co-operative "Vishnevetsky" (electric capacity 1 Mw) [6].

Besides, by means of foreign investors, during the same period it is planned to construct six biocomplexes on treatment facilities and 5 biocomplexes on distilleries.

They involve the following: The Municipal Unitary Enterprise «Minskvodocanal» (investments about 20 million $ and 15 million $), The Municipal Unitary Enterprise «Bobruiskvodocanal» (investments about 5 million $ and 4 million $), The Municipal Unitary Enterprise «Baranovichivodocanal» (investments about 5 million $), The Municipal Unitary Enterprise «Slonimvodocanal» (investments about 3 million $), 5 complexes «Belstatefoodprom» (investments about 15 million $) [12].

It is necessary to notice, that the main ecological advantage of the "know-how" of biogas consists of reduction of emissions of methane, carbonic gas and nitrogen oxide in atmosphere. During fermentation process exactly such quantity of carbonic gas which has been absorbed before by plants in the course of photosynthesis is allocated, and methane renders 21 times stronger influence on the hotbed effect than carbonic gas, as it is caught and not dissipated in the environment [9].

State policy realization in the sphere of use of renewed energy sources is carried out according to the following documents:

1. The Law of Belarus «About rational use of power resources» from July, 15th, 1998 №190-З.
2. The Law of Belarus «About renewed energy sources» from December, 27th, 2010 №204-З.
3. The instruction of the President of Belarus «Economy and thrift – primary factors of economic safety of the State» from June, 14th, 2007 №3.
4. The republican program of rational use of power resources for 2011–2015 (it is confirmed by the decision of the Ministerial Council of Belarus from December 24th, 2010 №1882).
5. The national program «Development of local, renewed and nonconventional power sources for 2011–2015».
6. The program of social and economic development of Belarus for 2011–2015.

Among the State's priorities in fuel and energy sphere there is the searching for and commercial operation of alternative energy sources on the basis of modern world technologies. Development of agriculture of Belarus will be carried out according to the Government program of strengthening of agrarian economy and development of rural territories for 2011–2015.

The major problems of development of agriculture are the formation of competitive, ecologically safe manufacture of the agricultural production, fully satisfying the internal requirements of the State, growing export potential as well as an increase in profitability of sales [11].

The prior directions providing an increase of agricultural production concern:

– Creation of highly effective integration structures of corporate type on technological grocery chains from manufacture of initial raw materials till finished goods sale.
– Intensification of an agricultural production on the basis of an effective utilization of industrial and climatic conditions, manpower, infrastructures of sale in the country and abroad with orientation to requirements of the process industry and demand in the foodstuffs world market.
– Modernization of the enterprises processing agricultural raw materials, introduction of new equipment and technologies allowing for deep processing of raw materials, greater assortment, and also the provision of output with high added cost.

The ecological policy of Belarus is directed on the maintenance of ecological safety, effective utilization of natural resources at preservation of integrity of natural complexes, including the unique ones. The basic directions of its realization can result in:

– Considerable improvement of the environmental components quality on the basis of an increase in the technological level of production.
– Reduction of volumes of formation of waste, emissions of polluting substances into the atmospheric air and dumps of polluted sewage in superficial reservoirs, prevention of pollution of underground waters, soils and degradation of agricultural grounds.
– Realization of a complex of actions for the prevention and minimization of the harm caused to the environment by accidents of techno-genic and natural character, at the expense of carrying out of preventive organizational-technical measures in the sphere of manufacture, working out and introduction into practice of modern methods, technologies and equipment for hydro meteorological supervision and preparation of hydro meteorological forecasts.
– Increase in the level of waste involvement in the civil turn, neutralization of the accumulated dangerous production waste.

– Preservation of biological variety, natural landscapes, natural ecological systems by the development of especially protected natural territories network.
– Development of the National system of monitoring of environment on the basis of introduction of progressive technologies of supervision, data gathering, reception and representation of ecological information.
– Formation of ecological culture of the population through the educational system;
– Prevention of the ecological threats connected with the increase in emissions of hotbed gases in atmosphere, anthropogenic change of climate and technology-induced accidents.

Problems in the sphere of efficiency increase, use of local and renewed power resources in Belarus so that:

1. To lower power consumption of gross national product to the level of 2005: not less than 50 % in 2015; not less than 60 % in 2020.
2. To provide economy of power resources (in comparable conditions): not less than 7,1–8,9 million tons of conditional fuel in 2011–2015; not less than 5,2 million tons of conditional fuel in 2016–2020.
3. To provide a share of use of own power resources in the balance of power resources for manufacture of thermal and electric energy: not less than 25,0 % in 2012; not less than 28,0 % in 2015; not less than 32,0 % in 2020.

The financing of actions for the rational use of energy and own power resources in 2010-2015 is presented in Fig. 5. The total amount of financing will make 8 662,5 million $.

The program of building of the power sources working on biogas in 2010–2012 (the purposes and program problems):

– Ecological load decrease in the environment.
– Reception of biogas and its use for the development of electric and thermal energy with the view of replacement of imported fuel and energy resources.
– Obtainment of high-quality organic fertilizers.
– Reduction of the contamination of areas under crops from the use on them of unprocessed organic chemistry.

As a result of realization of this Program in the Republic, 39 biogas installations with the total electric capacity of 40,4 MW will be placed in operation, which will allow for the annual development of about 340 million kWh electric energy and for the replacement of imported natural gas in volume greater than 145 thousand tons of conditional fuel.

Realization of the national program «Development of local, renewed and nonconventional power resources in 2011–2015» assumes:

– Building of 102 biogas complexes in the rural organizations as well as housing and communal services, microbiological industry and on ranges of the municipal and household waste the total electric capacity of 77,8 MW.
– Building wind stations of the total electric capacity 365–385 MW.
– Introduction of 184 solar power plants for the needs of hot water supply.
– Introduction of 166 thermal pumps for the use of low potential secondary power resources and geothermal energy [10].

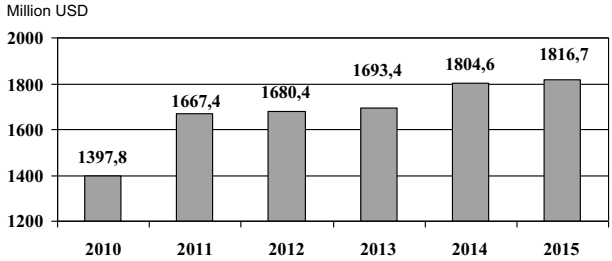

Fig. 5. Financing of actions for rational use of energy

In the conditions of the world's financial crisis and limitation of resource potential, the increase of efficiency of using fuel and energy resources gets the special importance for the Republic. The economy becomes not simply obligatory principle of managing, but the major requirement of maintenance of national safety of the State.

As the basic directions of research and search works for bioenergetics development in Belarus it is possible to consider:

– Reception of new data on resources of biofuel and its characteristics.
– Studying of processes and creation of bases of technologies of preparation, processing and biofuel conversion in power production.
– Studying of accompanying environmental problems, including pollution of surrounding space by production of waste and harmful gas emissions.
– Working out and substantiation of technologies of using materials from waste processing for manufacture of fuel, warmth and electric power.
– Estimation of economically expedient potential of bio-resources for manufacture of fuel, warmth and electric power, including their use in small agricultural towns.

CONCLUSIONS

There is the basic direction in recycling of waste in agriculture, including processing enterprises of an agrarian complex (milk factory, meat-packaging plants, spirit manufactures etc.), old dumps and sewer drains in Belarus.

As to municipal services, both in the industrial and private scale it is still necessary to work intensely. In immediate prospects, the organization of separate collection of food and industrial waste is considered very much as a challenge. As, living in modern high-rise houses (8–16 floors) and having a refuse chute, the population will hardly voluntary carry out waste separation. Besides, the presence of special services (firms) which would be engaged in delivery of the collected waste to destination is very important, and they are not present as yet. All these problems can be solved sooner or later, there would be desires and the will to carry them out. Certainly, the State's support is required.

REFERENCES

1. Building government program in 2011–2015 of hydroelectric power stations in Byelorussia (it is confirmed by the decision of Ministerial council of Byelorussia from December, 17th, 2010 № 1838).

2. Building government program энергоисточников on local kinds of fuel in 2010–2015 (it is confirmed by the decision of Ministerial council of Byelorussia from July, 19th 2010г. №1076).
3. **Busko E. G., Pazniak S. S., Kostukevich S. B., Dudkina L. A. 2012:** Perspectives of renewable energy sources in enhancement of environmental and energy security of Belarus. TEKA commission of motorization and power industry in agriculture. Polish Academy of sciences branch in Lublin, Volume XII, No. 1, 13–20.
4. **Kurpaska S., Latala H. 2012:** Analysis of the influence of variable insulating power of storing tank on energy effects in the conversion system of solar radiation. TEKA commission of motorization and power industry in agriculture. Polish Academy of sciences branch in Lublin, Volume XII, No. 2, 293–299.
5. **Kurpaska S., Latala H., Knaga J. 2012:** Energy efficiency analysis of flat and vacuum solar collector systems. TEKA commission of motorization and power industry in agriculture. Polish Academy of sciences branch in Lublin, Volume XII, No. 1, 115–120.
6. Praca zbiorowa pod red. B. Kołodziej i M. Matyki.: Odnawialne źródła energii. Rolnicze surowce energetyczne. PWRiL Sp. z o.o., Poznań 2012, 616, ISBN 978-83-09-01139-2. I. N.
7. Strategy of development of an energy potential of Byelorussia (it is confirmed by the decision of Ministerial council of Byelorussia from August, 9th, 2010 №1180).
8. The building program of energetic efficiency, working on biogas, for 2010–2015 (it is confirmed by the decision of Ministerial council of Byelorussia from June, 9th, 2010 №885).
9. The instruction of the President of Byelorussia «Economy and thrift – primary factors of economic safety of the state» from June, 14th, 2007 №3.
10. The law of Byelorussia «About rational use of power resources» from July, 15th, 1998 №190-З.
11. The law of Byelorussia «About renewed energy sources» from December, 27th, 2010 №204-З.
12. The national program «Development local, renewed and nonconventional power sources for 2011–2015».
13. The project of cooperation with the World bank «Application of a biomass for heating and hot water supply in Byelorussia» – 3,129 million $ (2003–2008).
14. The project of cooperation with the World bank «Increase of energetic efficiency in Byelorussia» – 125 million $ (2009–2014).
15. The project of cooperation with the World bank «Increase of energetic efficiency residential buildings in Byelorussia» – 4,5 million $. (2012–2016).
16. The republican program of rational use of power resources for 2011–2015 (it is confirmed by the decision of Ministerial council of Byelorussia from December, 24th, 2010 №1882).

PERSPEKTYWY ROZWOJU BIOENERGETYKI W REPUBLICE BIAŁORUŚ

Streszczenie. Publikacja zawiera materiały dotyczące bioenergetycznego potencjału Republiki Białoruś. Przeprowadzono analizę perspektyw rozwoju bioenergetyki. W jej obszarze rozpatrzono technologie wykorzystania odnawialnych organicznych źródeł, w tym biomasy do produkcji energii elektrycznej; energię z ciekłych, twardych i gazowych paliw; energię cieplną związków chemicznych i innych materiałów. W powyższym aspekcie bioenergetyka po słońcu jawi się podstawowym odnawialnym źródłem energii.

Słowa kluczowe: bioenergia, źródła energetyczne, źródła biomasy, odpady rolnicze, przetwórstwo odpadów w produkcji rolniczej.

TEKA. COMMISSION OF MOTORIZATION AND ENERGETICS IN AGRICULTURE – 2013, Vol. 13, No. 1, 77–82

Injuries sustained by victims of road accidents with the participation of farm tractors in mountainous regions

Agnieszka Krasowska[1], Grzegorz Jordan[2], Witold Jordan[1,3], Andrzej Mruk[1]

[1]Cracow University of Technology, Poland
[2]Jagiellonian University in Cracow, Medical College, Poland
[3]Institute of Forensic Research in Cracow, Poland

Received February 8.2013; accepted March 14.2013

Summary: The paper presents the results of investigation of the consequences of accidents involving a farm tractor used in a mountainous region with a specific landform. The injuries sustained by victims of the accidents were analysed. The basis for analyses was the documentation prepared by the Agricultural Social Insurance Fund. The results of the analyses allowed for indicating the specificity of such accidents. The human body parts most exposed to damage and the severity of injuries were determined. The tractor drivers sustain the injuries of a different kind than the other participants of accidents (for example – the passengers). The drivers, apart from the upper and lower limbs injuries, sustain damage to head and trunk. Because of accidents, 2/3 of the victims sustain irreparable damage to the body. In majority, it is 1-5% of permanent damage to health. There are also fatal accidents.
Key words: tractor, accidents, injuries.

INTRODUCTION

The principal element in agricultural engineering is a farm tractor. At present, in the fields of Poland, more than half a million of farm tractors of different types are in operation. They are used for typically agricultural works (tractor + unit) as well as in the transport (tractor + trailer). They are exploited under different conditions resulting from the specificity of agricultural lands where they are used.

In mountainous lands, because of steep slopes, the work of a tractor is difficult as it is necessary to keep its stability. Classic, traditionally designed farm tractors should be able to maintain their stability on a slope of 12º. Special constructions of mountain tractors are designed for working on the slopes of 25-30º. In Poland tractors of traditional designs are used in mountainous regions [5, 8, 11, 12].

The specificity of using tractors in mountainous lands, i.e. on steep slopes, involves the risk of accident if due caution is not observed, when a tractor working with a unit loses its transverse stability. Such accidents usually have considerable effects on mechanical damages of the tractor and the units (or trailers) co-operating with it and on the accident participants [7, 18].

In order to identify and classify the injuries sustained by the persons participating in such accidents, an investigation was performed; the results of the investigation are discussed in this work.

RESEARCH METHODOLOGY

The research included the accidents occurred in Lesser Poland/Małopolska Voivodeship, in the following counties: Limanowa, Nowy Sącz, Nowy Targ, Tatra. The structure of using lands in selected counties is presented in Table 1.

The analysis of the above table comparing the characteristics of examined counties shows that the part of the arable land in these counties amounts to 8% – 31,1%, of the orchards 1,5% – 3,8%, of meadows and pastures 7,4% – 16%, of forests and woodland 36% – 57%.

The accidents were analysed based on the documents of the Agricultural Social Insurance Fund (KRUS) from 2005 – 2010. According to its statute, KRUS keeps the documentation of all accidents that happened in agriculture. Therefore, the accident documentations gathered by KRUS can be used as source material for analysing accidents with the participation of farm tractors. In the paper, we used the materials from KRUS local post in Nowy Sącz, which activity includes the counties of Nowy Sącz, Limanowa, Tatra and Nowy Targ.

From the whole documentation, 46 accidents were selected. The authors assumed these accidents as a representative sample of the accidents with the participation of a farm tractor in the mountain region.

RESEARCH RESULTS

The accidents occurred on the meadows and pastures area – 46%, on the dirt and forest roads – 25%, asphalt

Table 1. Structure of using lands in selected counties of Malopolska Voivodeship [10]

County	Total area [ha]	Arable lands [ha]					Forests and wood-land [ha]	Remained lands and waste land [ha]
		Total	Arable lands	Orchards	Meadows	Pastures		
Tatra	47162	14620	3772	1415	4716	4716	26882	5660
% of total	100	31	8	3	10	10	57	12
Nowy Targ	147466	72996	16221	2212	23594	30968	53088	21382
% of total	100	49,5	11	1,5	16	21	36	14,5
Limanowa	95196	49471	29596	3588	9256	7031	39161	6564
% of total	100	52	31,1	3,8	9,7	7,4	41,1	6,9
Nowy Sącz	155024	72322	36663	5924	16892	12843	69226	13476
% of total	100	46,7	23,6	3,8	10,9	8,3	44,7	8,7
Małopolska	1514410	880807	598159	22599	178406	81643	441642	191961
% of total	100	58,2	39,5	1,5	11,8	5,4	29,2	12,7

roads – 19%, other – 10%. The most frequently participating tractors were: URSUS C-330 – 44%, SAM (individually assembled tractors) – 24%, URSUS C-360 – 13%, others (URSUS, MF, Władymirec) – 19%. None of the farm tractors was a mountain tractor, adapted to work on a land with a steep slope.

The results of research are presented in diagrams. Because of the small sample size, the results give rather quality than quantity information.

The number of accidents in individual counties is presented in Fig. 1

- Limanowa county – 10 accidents
- Nowy Targ county – 13 accidents
- Nowy Sącz county – 17 accidents
- Tatra county – 6 accidents

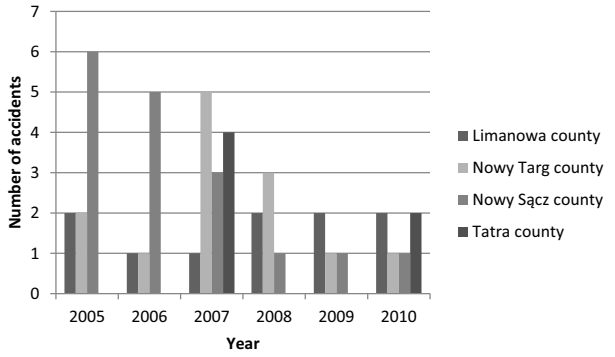

Fig. 1. Number of accidents with the participation of a tractor in individual counties

From the source material it appears that the number of accidents was the highest in Nowy Sącz county (17 accidents), and that it was the lowest in Tatra county (6 accidents). In Limanowa county, 10 accidents took place, while in Nowy Targ county – 13. It is clear that the number of accidents correlates with the surface development in these regions. In Nowy Sącz county, arable lands represent up to 46% of the county area, while in Tatra county only 31% of the county total area.

The most accidents with farm tractors in the mountainous lands happened in 2007 – 13 accidents, the least accidents happened in 2009 – only 4 accidents.

The results of the analysis of the accident participants age groups are presented in Fig. 2.

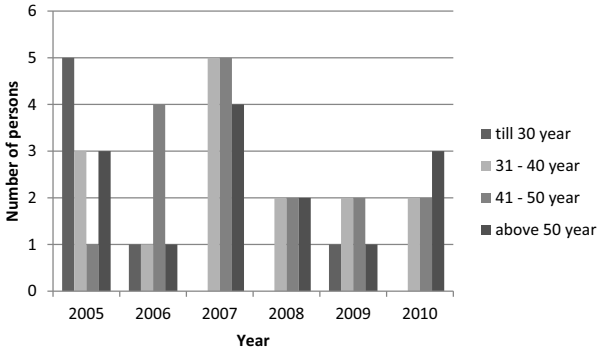

Fig. 2. Age groups of accident participants:
above 51 years – 14 persons
50 – 41 years – 16 persons
40 – 31 years- 15 persons
till 30 years – 7 persons

52 persons participated in 46 accidents. The analysis shows that in a majority of accidents, the participants were more than 31 years old (87%). The most numerous group, that is 28%, in mountainous regions includes the persons from the age interval 41 – 50. The group of people more than 51 years old is also large – 27% of all the participants of accidents with farm tractors. The persons younger than 30 constitute a small group of 7 persons, i.e. 17% of the total number of victims in such accidents. This age structure is presumably the effect of the advantageous opinion on abilities and routine of middle-aged and older people in the works using a farm tractor in mountainous regions. It is notable, at the same time, that the country 'grows old' and elderly people have health problems, which can influence the increase of the number of accidents in country lands.

In 2007, the accidents with the largest group of victims happened. In this period up to 14 persons participated in the accidents with farm tractors, ¾ of whom were the persons above 41 years old.

The analysis of the victims (driver, passenger, observer) of the accidents with farm tractors is presented in Fig. 3.

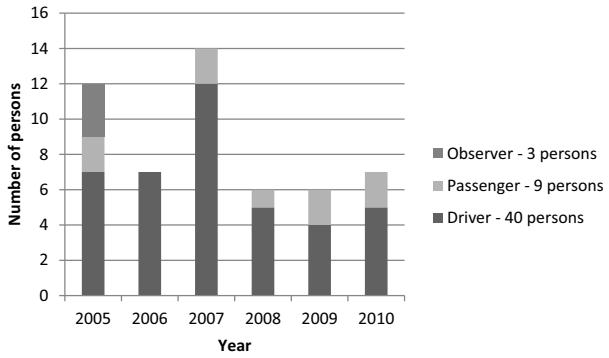

Fig. 3. Victims of agricultural accidents

The analysis shows that not only the persons actively participating in the works with a farm tractor: driver – 77% and passenger – 17%, but also passive observers of the event sustain injuries – 6 %.

Statistical participation of the victims of accidents with farm tractors is as follows: 0.23 passengers and 0.07 observers to one injured driver.

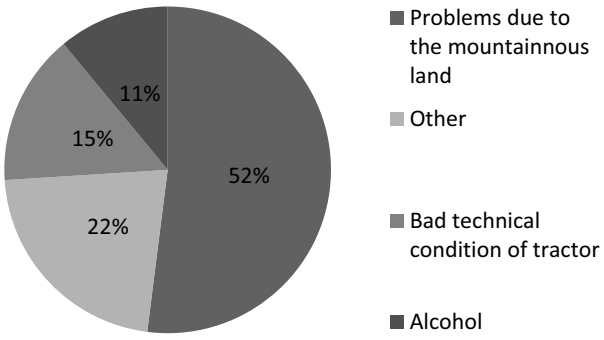

Fig. 4. Cause of accidents

The analysis of the accidents causes demonstrates that more than a half – 52% of accidents is caused by wrong driving technique, not adapted to the current conditions, and by insufficient driver abilities required for operating tractors under heavy mountainous conditions. Bad technical condition of the farm tractors contributes to an increase in the number of accidents, as well. Among 46 analysed accidents with a tractor, only 1/6 of all tractors had been tested. Alcohol and other causes like carelessness or gross negligence are the causes of 1/3 accidents with farm tractors.

The operation of a farm tractor in a mountainous region needs knowing, experience, good equipment and perceptiveness as well as full concentration, because it often happens that some little error involves heavy accidents and injuries. The best solution for the work in mountainous regions is a mountain tractor, which by its design and technology increases the safety and facilitates the work.

INJURIES OF ACCIDENT PARTICIPANTS

It results from the analysis of injuries severity of the victims of accidents with the participation of farm tractors, that within a period of 6 years (2005 – 2010), 50% of victims (27 persons) sustained constant, irreversible damage to health, 16 people sustained prolonged injuries and 8 persons died. Moreover, the attention must be paid to the severity degree of prolonged and constant injuries. The severity of prolonged damages to health, i.e. the percentage of damage to health, is significantly lesser than in the case of constant injuries. From the group of 52 persons, half of them will be disabled for life. The scale of danger involved in the work using a tractor in the regions with significant slopes is very large.

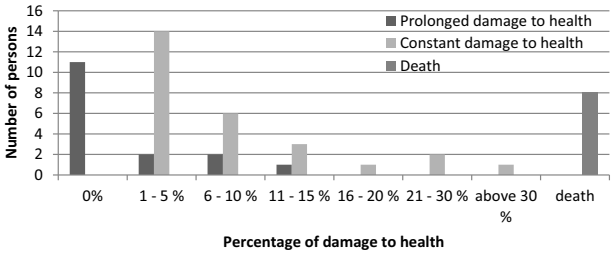

Fig. 5. Injury severity rate of the victims

The location of the post-accident injuries is presented in Fig. 6

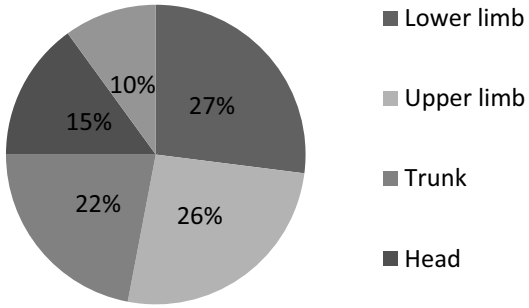

Fig. 6. Location of post-accident injuries

The analysis of the post-accident injuries shows that half of them are the injuries to the limbs: upper (26%) and lower (27%). Trunk injuries are ¼ of all the injuries. Head injuries and multiple-organ injuries are seldom encountered; they represent 25% of all post-accident injuries.

A comparison of injuries sustained by a driver and a passenger is presented in Fig. 7

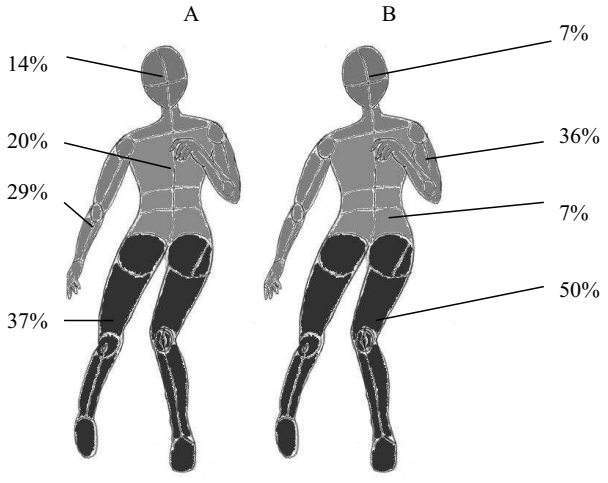

Fig. 7. Comparison of injury location in accident victims: A – driver, B – passenger

It results from the analysis of post-accident injury location in a driver and in a passenger, that the passenger mostly sustains the injuries to a lower limb (50% of all injuries) and to an upper limb (36%). Drivers are often hurt in upper and lower limbs. However, a comparative analysis demonstrates a difference in location of the remaining post-accident injuries; 1/5 injuries of drivers are damages to trunk, a passenger suffers such injuries twice less. It is similar in the case of head injuries – a driver suffers such injuries twice more often than a passenger.

The post-accident injuries to upper (Fig. 8) and lower (Fig. 9) limbs were analysed in detail.

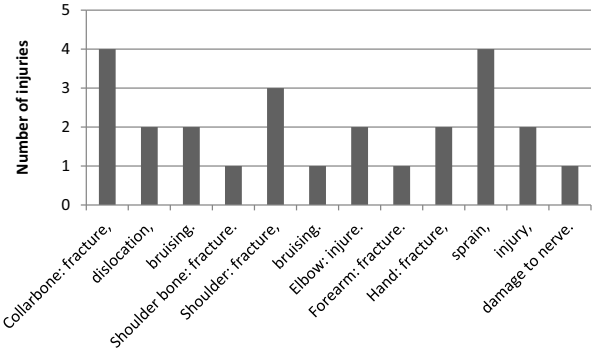

Fig. 8. Post-accident injuries to upper limbs

The analysis shows that 1/3 of all upper limb injuries are the damages to the upper limb pectoral girdle, and 2/3 are the injuries to the upper limb self. The most frequent injury as a result of accidents with a farm tractor in a mountainous region is collarbone fracture and sprain of hand as well as fracture within the shoulder. The most frequent injury is fracture – 45% of injuries, and less serious ones– bruise and damage to the upper limb – constitute 30% of injuries.

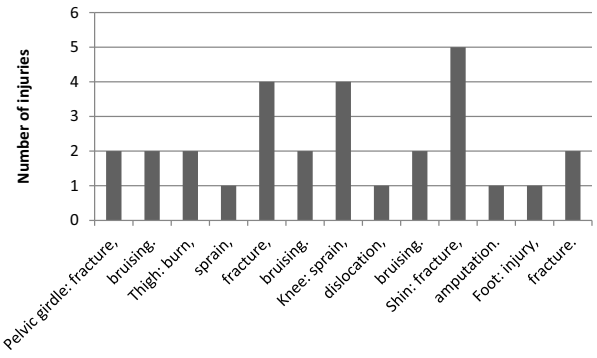

Fig. 9. Post-accident injuries to lower limbs

The analysis of the injuries to a lower limb shows that 86% of injuries were the injuries of the limb itself; other 14% are the injuries to the pelvic girdle. Mostly, as a result of accidents, damages to thigh follow – they constitute 1/3 of all the injuries – next are damages to knee and shank (shin). The most common is the fracture of shin, knee sprain and fracture of thigh. Fracture is the most common injury to a lower limb. It happens in almost half of cases.

Decisive for the extensiveness of injuries are the following factors: place, surface and energy of the vehicle impulse contact between the tractor and the victim. Furthermore, it is notable that the extensiveness as well as the quality of injuries would be dependent on the physical condition (properties) of a particular person. It depends, among other things, on the features like bone and soft tissue elasticity, i.e. damping capacity and energy dissipation [2, 6, 17].

Determinants of the injury type are the kind of the collision, the position occupied by the person and the safety measures used by this person, like safety cabin, safety belts [3, 4, 16, 19].

The collected and analysed source material proves that the most common location of injuries occurring in both tractor drivers and passengers is a lower limb. The type of injury most commonly sustained by the victims is fracture.

Fracture is a break of bone continuity on its whole cross section. It happens under the action of an external force applied to the bone. These forces act on the bone until the moment of surpassing the allowable stress causing destructive deformations – crack and fracture of the bone.

The mechanism of the fracture depends on the position and direction of the force causing the injury. There are two principal mechanisms: direct – when the injury force acts directly on the bone, and indirect – when the injury force acts through another bone, articulation, tendon etc. [6, 15].

In the case of the accidents with a tractor, 2/3 victims are the drivers. The injury type is determined by the accident run, the position occupied by the particular person, as well as the safety measures used by this person, like safety cabin, safety belts.

CONCLUSIONS

- The number of accidents within a representative sample from a mountainous region correlates with the region's development.
- More than 50% of accidents are caused by wrong driving technique, not adapted to the working conditions in a mountainous region and by problems connected with agriculture.
- The injured are mostly (80% of accidents) the drivers. The passengers participate in every fifth accident, and the observers constitute 6% of the injured. The largest age group affected are people after 41 years of age. The 'ageing agriculture', both in terms of technology and humans, influences the increase of the number of accidents.
- In the accidents, the injured drivers and passengers sustain different kind of damages. The passengers are more exposed to the injuries of lower and upper limbs, which may be connected with jumping down the tractor during the accidents. The drivers sustain damages to lower and upper limbs as well, but they are exposed almost as often to head and trunk injuries.
- In the accidents, half of victims sustain irreparable damage to the body, though the severity of these injuries usually is not significant (the largest group within 1% – 5% of permanent damage to health), however a farmer with a leg or hand motor disability would have trouble performing his duties.

– The work with a farm tractor in a mountainous region requires knowledge, experience, good equipment as well as perceptiveness and full concentration on the performed task, because it often happens that some small error or an oversight results in heavy accidents. The best solution for the work in mountainous regions is a mountain tractor, which by its design and technology increases the safety and facilitates the work.

REFERENCES

1. **Będziński R.: 1997,** Biomechanika inżynierska, Oficyna Wydawnicza Politechniki Wrocławskiej, Wrocław.
2. **Błaszczyk J.: 2004,** Biomechanika kliniczna, Wydawnictwo PZWL, Warszawa.
3. **Bocheński C., Klimkiewicz M.: 1987,** Bezpieczeństwo maszyn rolniczych w ruchu drogowym, Przegląd Techniki Rolniczej i Leśnej nr 10.
4. **Cież J.: 1998,** Problemy ergonomii i bezpieczeństwa pracy w sezonowym użytkowaniu urządzeń technicznych w rolnictwie, Prace Komisji Nauk Rolniczych PAN tom 1.
5. **Dajniak H.: 1985,** Ciągniki – teoria ruchu i konstruowanie, WKiŁ Warszawa.
6. **Dziak A., Sanders R.: 2008,** Traumatologia układu ruchu, Elsevier Urban & Partner.
7. **Ekielski A., Skrobacki A.: 2006,** Pojazdy i ciągniki rolnicze, Wieś Jutra.
8. **Gadomski W., Mróz S.: 1983,** Ciągniki rolnicze, Wydawnictwo WSiP, Warszawa.
9. **Krasowska A.: 2012,** Analiza obrażeń rolników powstałych w czasie wypadków z udziałem ciągników rolniczych na terenach górskich, Praca dyplomowa inżynierska, Politechnika Krakowska Wydział Mechaniczny.
10. **Kondracki J.: 2009,** Geografia regionalna Polski, Wydawnictwo PWN, Warszawa.
11. **Kruszewski Z., Michalak G.: 1989,** Wybrane zagadnienia z teorii ruchu oraz budowy pojazdów rolniczych, Wydawnictwo Politechniki Warszawskiej, Warszawa.
12. **Nowacki T.: 1963,** Ciągniki rolnicze i samochody, Państwowe Wydawnictwo Rolnicze i Leśne, Warszawa.
13. **Pike J. A.: 1990,** Automotive safety – Anatomy, injury, testing and regulation, Society of Automotive Engineers.
14. **Szeląg Sikora A.: 2012**, Regional differences in equipment of machinery park on farms, Teka Commission of Motorization and Energetics in Agriculture, vol. 12.
15. **Thompson J. C.: 2007,** Atlas anatomii ortopedycznej Nettera, Elsevier Urban & Partner.
16. **Wicher J.: 2006,** Bezpieczeństwo samochodów i ruchu drogowego, Wydawnictwo WKiŁ, Warszawa.
17. **Wismans J. S. i inni: 1994,** Injury biomechanics, Eindhoven University of Technology.
18. **Woźniak W.: 2005,** Ciągniki i maszyny rolnicze – Budowa i przeznaczenie, Wydawnictwo Przemysłowego Instytutu Maszyn Rolniczych, Poznań.
19. **Zalewski P.: 1994,** Bezpieczeństwo kierowcy ciągnika na zboczu jako problem ergonomiczny, Zeszyty Problemowe Postępów Nauk Rolniczych PAN tom 415.

OBRAŻENIA OSÓB W WYPADKACH Z UDZIAŁEM CIĄGNIKÓW ROLNICZYCH NA OBSZARZE GÓRSKIM

Streszczenie. W pracy przedstawiono wyniki badań skutków wypadków z udziałem ciągnika rolniczego eksploatowanego w specyficznym pod względem ukształtowania terenie górskim. Analizowano obrażenia jakich doznały osoby uczestniczące wypadkach. Podstawą do przeprowadzonych analiz była dokumentacja wypadków prowadzona przez Kasy Rolniczego Ubezpieczenia Społecznego. Wyniki analizy pozwoliły na wskazanie specyfiki takich wypadków. Określono jakie części ciała człowieka są najbardziej narażone na obrażenia oraz ciężkość tych obrażeń. Kierujący ciągnikiem ulegają obrażeniom innego typu niż pozostali uczestnicy wypadku (np. pasażerowie). Kierowcy, obok obrażeń kończyn dolnych i górnych, doznają obrażeń głowy i tułowia. W wyniku wypadków 2/3 poszkodowanych ulega stałemu nieodwracalnemu uszkodzenia ciała. W większości jest to 1%-5% stałego uszczerbku na zdrowiu. Zdarzają się także wypadki ze skutkiem śmiertelnym.
Słowa kluczowe: ciągnik rolniczy, wypadek, obrażenia.

The study was performed within the framework of a PK WM M-4/84/2013/DS Project.

TEKA. COMMISSION OF MOTORIZATION AND ENERGETICS IN AGRICULTURE – 2013, Vol. 13, No. 1, 83–88

The effect of pressure on the compaction parameters of oakwood sawdust enhanced with a binder

Ryszard Kulig[1], Stanisław Skonecki[1], Grzegorz Łysiak[1], Janusz Laskowski[1], Stanisław Rudy[2], Andrzej Krzykowski[2], Rafał Nadulski[3]

[1]Department of Equipment Operation and Maintenance in the Food Industry,
[2]Department of Thermal Technology,
[3]Department of Food Engineering and Machinery,
University of Life Sciences, Doświadczalna 44, 20-280 Lublin, Poland; e-mail:ryszard.kulig@up.lublin.pl

Received January 17.2013; accepted March 14.2013

Summary. This paper presents the results of analyses investigating the effect of specific piston pressure (45 to 113 MPa) and the addition of a calcium lignosulphonate binder (0 to 20%) on the compaction parameters of oakwood sawdust. The experiments were performed with the use of the ZWICK Z020/TN2S universal strength tester and a closed compression die assembly. An increase in pressure led to an increase in material density in the compression chamber and agglomerate density (by 16% on average), and it more than doubled the mechanical strength of the agglomerate. Higher compaction pressure increased the demand for compaction energy by 104%, on average. The addition of binder contributed to agglomerate density and increased the mechanical strength of the agglomerate by 33%, on average.
Key words: compaction, pressure, binder, calcium lignosulphonate, sawdust, biomass.

INTRODUCTION

Solid biofuels manufactured from plant biomass are the main resource in the renewable energy industry [4, 6, 15, 20]. Energy biomass comprises timber processing waste, including sawdust. Those plant resources are characterized by low density and low calorific value (per unit of volume), and they are difficult to transport, store and feed to boilers in unprocessed form [1, 2]. Biomass density has to be increased to make this raw material more suitable for energy production. This is achieved by briquetting or granulating bulk material in the process of pressure agglomeration [5, 13, 21].

In laboratory analyses of the agglomeration process, raw material is compacted in a closed compression chamber with a piston. Process parameters, including energy consumption and raw material's susceptibility to compaction, are determined. Changes which take place in the material during compaction and the quality of the final product have to be closely monitored. The compaction process and agglomerate quality are determined by process parameters as well as by the physical and chemical properties of the compacted material [5, 7].

Compaction pressure (specific piston pressure) significantly affects the compression process and the quality of the resulting agglomerate [3, 11, 14, 17]. Inadequate pressure settings can lead to wasteful energy consumption, and they may lower the strength characteristics of the agglomerate. According to the authors' previous research [8], the use of lignin binders containing calcium lignosulphonate may offer a partial solution to the above problem. Lignin has adhesive properties, and it binds raw material components to improve agglomerate stability and quality [12, 16, 19, 22]. The resulting agglomerates are characterized by greater density and higher mechanical strength which, in turn, lowers energy intensity of the compaction process, decreases storage requirements and facilitates agglomerate transport.

The objective of this study was to determine the effect of specific piston pressure on the compaction parameters of oakwood sawdust containing various quantities of calcium lignosulphonate.

MATERIALS AND METHODS

The experimental material was oakwood sawdust supplied by a sawmill in the Lublin area. The material was obtained by cutting oakwood with a wooden saw with 22.2 mm tooth pitch. The granulometric composition of sawdust was determined in accordance with standard PN-EN 15149-2:2011 using the SASKIA Thyr 2 laboratory sieve. The bulk density of raw material was described in line with standard PN-EN 15103:2010.

A binding agent (calcium lignosulphonate) was added to material samples with 12% moisture content in the amount of 1% and 2%. Material without the added binder served as a control sample.

The pressure compaction methodology was described in the authors' previous study [9]. The experiment was performed with the use of the Zwick Z020/TN2S strength

tester with a closed compression die assembly and a computer-controlled system for monitoring compaction parameters. Test parameters were as follows: chamber diameter – 15 mm, cylinder (compacted material) temperature – 20ºC, piston speed – 10 mm·min^{-1}. Sawdust was compressed at five values of the maximum compaction force: 8, 11, 14, 17 and 20 kN, which corresponded to the following compaction pressure parameters: 45, 62, 80, 96 and 113 MPa. Every compaction process was performed in three replications.

The results were plotted on a compaction curve showing the correlation between compaction force and piston speed. The curve was used to determine process parameters: maximum material density in the chamber ρc, total compaction effort ($Lc = L \cdot m^{-1}$, where : L – compaction effort, m – weight of material sample). The coefficient of material's susceptibility to compaction kc was calculated from the following formula:

$$k_c = \frac{L_c}{(\rho_c - \rho_n)} ((J \cdot g^{-1})/(g \cdot cm^{-3})), \quad (1)$$

where:

ρn – initial density of raw material in the compression chamber, g·cm^{-3}; Lc – specific compaction effort, J·g^{-1}.

Agglomerate density after 48 h of storage (ρa) was determined. The degree of material compaction in the chamber Szm and the degree of agglomerate compaction Sza (volume reduction) were calculated as the ratio of densities ρc and ρa to raw material density in the compression chamber ρn ($Szm = \rho c \cdot \rho n^{-1}$, $Sza = \rho a \cdot \rho n^{-1}$).

The mechanical strength of the agglomerate was determined in a compression test with the use of the ZWICK Z020/TN2S strength tester (piston speed 10 mm·min^{-1}). An agglomerate with diameter d and length l was compressed along the perpendicular axis until damaged, and maximum breaking force Fn was computed. Mechanical strength σn [MPa] of the agglomerate was calculated from the following formula [10, 18]:

$$\sigma_n = \frac{2 \cdot F_n}{\pi \cdot d \cdot l} \text{ (MPa)}. \quad (2)$$

The correlations between binder content and moisture content of the examined material and compaction parameters were analyzed statistically in the STATISTICA application at the significance level of $\alpha_i = 0.05$. Regression equations describing the correlations between compaction and pressure parameters at various binder content levels are shown in Figures 2-5. A regression analysis revealed that the observed correlations can be described by quadratic equations of the second degree or linear equations.

RESULTS

BASIC PHYSICAL PARAMETERS OF THE ANALYZED MATERIAL

An analysis of the granulometric composition of material (Fig. 1) revealed that particles with the size of 0.4 to 1.6 mm were the predominant fraction.

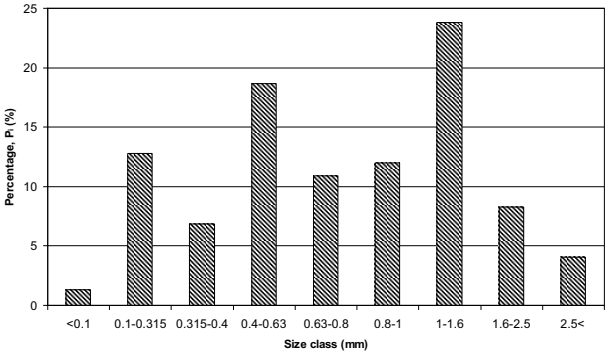

Fig. 1. Particle size distribution (P_i) of the studied raw material

Particle size distribution of the analyzed material was conducive to pressure agglomeration.

The average bulk density of raw material with 12% moisture content was determined at $\rho n = 0.297$ g·cm^{-3}.

RAW MATERIAL DENSITY IN THE COMPRESSION CHAMBER AND AGGLOMERATE DENSITY

The results presented in Figure 2 indicate that the initial density of raw material in the compression chamber ρc increased with a rise in pressure at all binder content levels *zl.* The greatest increase in agglomerate density *ra* was observed in the pressure range of 45–80 MPa. Further pressure increase had no effect on agglomerate density. The highest values of the analyzed parameters were reported for sawdust with the highest binder content, and the lowest – for control material.

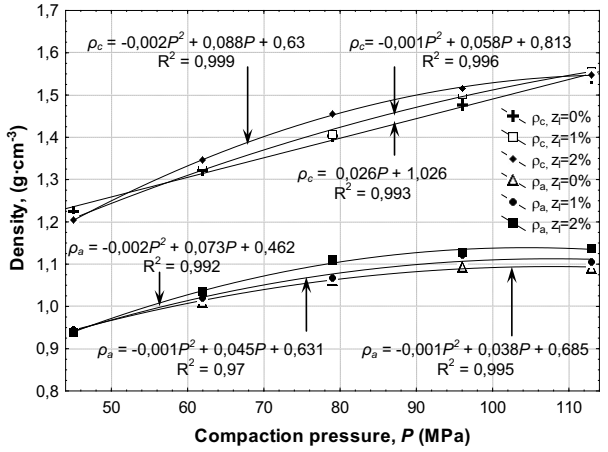

Fig. 2. Correlation between material density in the chamber (ρc), agglomerate density (ρa) and compaction pressure (P) at various binder content levels (zl)

In the pressure range of 45–113 MPa, the density of material with 2% binder content was determined in the range of 1.21 g·cm^{-3} to 1.55 g·cm^{-3} for parameter ρc and 0.92 g·cm^{-3} to 1.11 g·cm^{-3} for parameter ra. The applied binder had the greatest effect on sawdust density within the pressure range of 62– 96 MPa.

DEGREE OF AGGLOMERATE COMPACTION

An analysis of the degree of raw material compaction in the chamber and agglomerate compaction after storage

point to a significant increase in compaction values with an increase in compaction pressure (Fig. 3). Under the pressure of 113 MPa, the maximum material compaction in the chamber ρc was 5.3 times higher on average in comparison with initial density of raw material ρn regardless of its binder content. The addition of binder had the most significant impact on the analyzed parameter within the pressure range of 62–96 MPa.

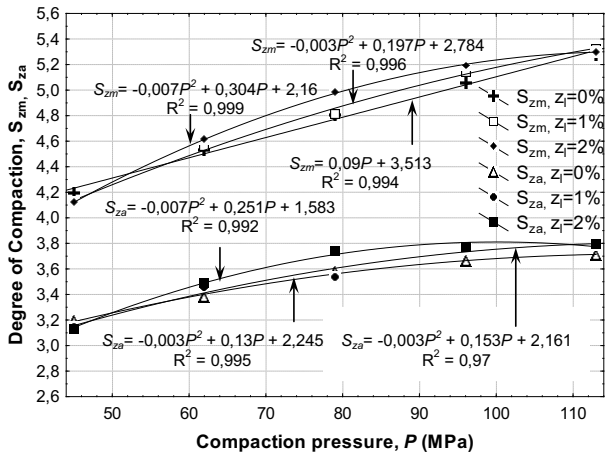

Fig. 3. Correlation between the degree of material compaction *(Szm)*, agglomerate compaction (*Sza*) and compaction pressure (*P*) at various binder content levels (*zl*)

The highest degree of agglomerate compaction *Sza* was reported in sawdust with 2% binder content compressed under the pressure of 80, 96 and 113 MPa (no significant differences in the values of *Sza* were observed under the above pressure settings). Agglomerate density was approximately 3.7 times higher in comparison with the initial density of raw material. Similarly to the reported changes in the value of *ra*, the highest increase in agglomerate compaction was observed in the pressure range of 45–80 MPa in all studied samples.

COMPACTION EFFORT AND SUSCEPTIBILITY TO COMPACTION

The correlations between specific compaction effort *Lc*, coefficient of susceptibility to compaction and compaction pressure *P* are presented in Figure 4. Within the entire range of examined values, the analyzed parameters increased with a rise in compaction pressure. Such a trend was observed in all examined samples. The value of *Lc* was determined in the range of 42.61 to 99.55 $J \cdot g^{-1}$, and the value of *kc* – from 23.01 to 40.11 $(J \cdot g^{-1}) \cdot ((g \cdot cm^{-3}))^{-1}$. The highest values of the analyzed parameters were noted at the maximum compaction pressure (113 MPa) in samples with the highest binder content (2%). This suggests that binder application increases the coefficient of friction between material particles and between particles and the walls of the compression chamber, leading to an increase in compaction effort and the coefficient of susceptibility to compaction (Fig. 4).

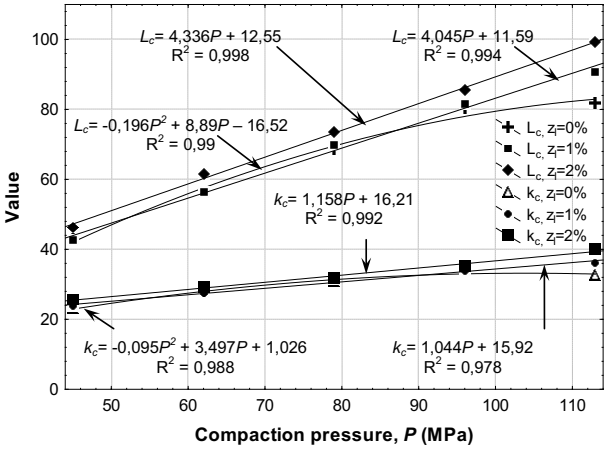

Fig. 4. Correlation between compaction effort (*Lc*), coefficient of susceptibility to compaction (*kc*) and compaction pressure (*P*) at various binder content levels (*zl*)

MECHANICAL STRENGTH OF THE AGGLOMERATE

In all the analyzed samples, the mechanical strength of agglomerate σn increased with a rise in compaction pressure within the range of 45–96 MPa (Fig. 5). A pressure increase to 113 MPa in material samples with 1% and 2% binder content did not lead to a noticeable increase in the mechanical strength of the agglomerate. An insignificant increase in the value of σn was noted only in control material. Mechanical strength values were determined in the range of 0.85 to 2.31 MPa. The agglomerate produced from sawdust with 2% binder content under the pressure of 96 and 113 MPa was characterized by the greatest mechanical strength.

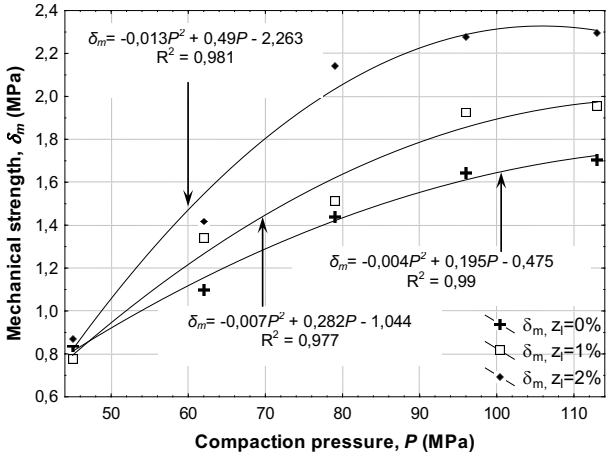

Fig. 5. Correlation between mechanical strength of agglomerate *(δm)* and compaction pressure (*P*) at various binder content levels (*zl*)

Greater variations in the value of σn were reported with an increase in pressure in the range of 45 to 96 MPa due to different binder content of the examined material. Under compaction pressure of 96 MPa, the mechanical strength of material with 2% binder content was 44% higher on average in comparison with control.

CONCLUSIONS

The following conclusions can be drawn from the results of the study:

1. The density of material in the compression chamber, including samples with and without the addition of binder, increased by 18% on average with a rise in compaction pressure. An increase in density within the examined range of values also contributed to an average 16% increase in agglomerate density. The addition of binder had the most significant impact on density within the pressure range of 62–96 MPa.
2. The degree of material compaction in the compression chamber increased by 24% on average within the entire range of tested pressure parameters. The degree of agglomerate compaction increased by 23% on average only within the pressure range of 45–96 MPa.
3. Specific compaction effort and the coefficient of susceptibility to compaction increased with a rise in compaction pressure values. The average increase in the former parameter reached 104% and in the latter – 80%. The addition of binder decreased the analyzed material's susceptibility to compaction.
4. An increase in compaction pressure within the analyzed range of values led to an average 104% increase in the mechanical strength of the agglomerate. In material with 2% binder content, the value of σn increased by 33% on average.

REFERENCES

1. **Adamczyk F., Frąckowiak P., Mielec K., Kośmicki Z., 2005.:** Problematyka badawcza w procesie zagęszczania słomy przeznaczonej na opał. Journal of Research and Application in Agricultural Engineering, 50(4):5–8.
2. **Adamczyk F., Frąckowiak P., Mielec K., Kośmicki Z., Zielnica M., 2006:** Badania eksperymentalne procesu zagęszczania słomy metodą zwijania. Journal of Research and Application in Agricultural Engineering, 51(3):5–10.
3. **Adapa P., Tabil L., Schoenau G., 2009:** Compaction characteristics of barley, canola, oat and wheat straw. Biosystems Engineering 2009, vol.104:335–344.
4. **Busko E. G., Pazniak S. S., Kostukevich S.B., Dudkina L. A., 2012:** Perspectives of renevable energy sources use In enhancement of environmental and energy security of belarus. Teka Commission of Motorization and Energetics in Agriculture, vol. 12: 11–20.
5. **Hejft R., 2002:** Ciśnieniowa aglomeracja materiałów roślinnych. Politechnika Białostocka. Wyd. i Zakład Poligrafii Instytutu Technologii Eksploatacji w Radomiu.
6. **Junginger M., Bolkesjø T., Bradley D., Dolzan P., Faaij A., Heinimö J., Hektor B., Leistad Ø., Ling E., Perry M., Piacente E., Rosillo-Calle F. Ryckmans Y., Schouwenberg P.P., Solberg B., Trømborg E., da Silva Walter A., de Wit M., 2008:** Developments in international bioenergy trade. Biomass and Bioenergy, 32:717–729.
7. **Kaliyan N., Morey V.R., 2009:** Factors affecting strength and durability of densified biomass products. Biomass and Bioenergy, 33:337–359.
8. **Kulig R., Skonecki S. Łysiak G., 2012:** The effect of binder addition on the parameters of compacted POPLAR wood sawdust. Teka Commission of Motorization and Energetics in Agriculture, vol. 12: 87–91.
9. **Laskowski J., Skonecki S., 2001:** Badania procesów aglomerowania surowców paszowych – aspekt metodyczny. Inżynieria Rolnicza, nr. 2(22), 187–193.
10. **Li Y., Wu D., Zhang J., Chang L., Wu D., Fang Z., Shi Y., 2000:** Measurement and statistics of single pellet mechanical strength of differently shaped catalysts. Powder Technology, 113, 176–184.
11. **Li Y., Liu H., 2000:** High pressure densification of wood residues to form an upgraded fuel. Biomass and Bioenergy 2000, vol. 19(3):177–186.
12. **MacMahon M.J., Payne J.D., 1991:** The Pelleting Handbook. Borregaard Lignotech, Sarpsborg Norway.
13. **Mani S., Tabil L., G., Sokhansanj S., 2003:** An overview of compaction of biomass grinds. Powder Handling and Processing, vol.15, 160–168.
14. **Mani S., Tabil L.G., Sokhansanj S., 2006:** Effects of compressive force, particle size and moisture content on mechanical properties of biomass pellets from grasses. Biomass and Bioenergy, 30(7), 648–654.
15. **Redlarski G., Wojdalski J., Kupczyk A., Piechocki J., 2012:** Efficiency of biomass energy used for heating purposes In a residential building In comparison with other energy sources. Teka Commission of Motorization and Energetics in Agriculture, vol. 3: 211–218.
16. **Restolho J.A., Prates A., de Pinho M.N., M.D., 2009:** Sugars and lignosulphonates recovery from eucalyptus spent sulphite liquor by membrane processes. Biomass and Bioenergy, vol. 133, 1558–1566.
17. **Relova I., Vignote S., León M. A., Ambrosio Y., 2009:** Optimisation of the manufacturing variables of sawdust pellets from the bark of Pinus caribaea Morelet: Particle size, moisture and pressure. Biomass and Bioenergy, 33:1351–1357.
18. **Ruiz G., Ortiz M., Pandolfi A., 2000:** Three-dimensional finite-element simulation of the dynamic Brazilian tests on concrete cylinders. Int. J. Numer. Meth. Engng., 48, 963–994.
19. **Sahoo S., Seydibeyo_M.O., Mohanty A.K., M. Misra M., 2011:** Characterization of industrial lignins for their utilization in future value added applications. Biomass and Bioenergy, vol. 135, 4230–4237.
20. **Schenkel Y., Crehay R., Delaunois C., Schummer J., 2003:** The agricultural sector and bioenergy production. Teka Commission of Motorization and Energetics in Agriculture, vol. 3: 228–235.
21. **Sobczyk W., Kowalska A., 2012:** The techniques of producing energy from biomass. Teka Commission of Motorization and Energetics in Agriculture, vol. 3: 257–261.
22. **Van Dam J. E. G., Van den Oever M. J. A., Teunissen W., Keijsers E. R. P., Peralta A. G., 2004:** Process for production of high density/high performance binderless boards from whole coconut husk. Part 1: lignin as intrinsic thermosetting binder resin. Industrial Crops and Products, vol. 19, 207–216.

WPŁYW CIŚNIENIA NA EFEKTYWNOŚĆ ZAGĘSZCZANIA TROCIN DĘBOWYCH Z DODATKIEM LEPISZCZA

Streszczenie. Przedstawiono wyniki badań nad określeniem wpływu jednostkowego nacisku tłoka (od 45 do 113 MPa) i dodatku lepiszcza w postaci lignosulfonianu wapnia (od 0 do 2%) na parametry zagęszczania trocin dębowych. Zagęszczanie przeprowadzano przy wykorzystaniu maszyny wytrzymałościowej Zwick typ ZO2O/TN2S i zespołu prasującego z matrycą zamkniętą. Stwierdzono, że wraz ze wzrostem ciśnienia rośnie gęstość materiału w komorze i gęstość aglomeratu (średnio o 16%) oraz ponad dwukrotnie zwiększa się odporność mechaniczna produktu. Zwiększanie ciśnienia zagęszczania w badanym przedziale, powoduje wzrost zapotrzebowania na energię zagęszczania średnio o 104%. Wykazano, że dodatek lepiszcza zwiększa gęstość aglomeratu oraz powoduje wzrost jego odporności mechanicznej przeciętnie o 33%.

Słowa kluczowe: zagęszczanie, ciśnienie, lepiszcza, lignosulfonian wapnia, trociny, biomasa.

TEKA. COMMISSION OF MOTORIZATION AND ENERGETICS IN AGRICULTURE – 2013, Vol. 13, No. 1, 89–94

Car fleet management problems in enterprises

Kazimierz Lejda, Edyta Zielińska

Rzeszow University of Technology, the Faculty of Mechanical Engineering and Aeronautics

Received January 18.2013; accepted March 14.2013

Summary. The paper presents impact of effective car fleet management on the development of the company. It lists and describes the major problems resulting from the maintenance of vehicles, such as cost of fuel and insurance, expenses related to servicing of vehicles, conducting their periodic inspections and repairs, etc. It also considers the options to acquire savings that can be used for investments that could contribute to the development of the company.

Key words: vehicle fleet management, transport companies, exploitation supervision systems

INTRODUCTION

Dynamic growth of automotive branch enables greater access to means of transport. Most companies have, smaller or larger, vehicle fleet meant to carry out various tasks. In the vehicle fleet, depending on a company, there are cars that enable carrying out transport services related to passenger and cargo transport, personal cars exploited by the management, as well as special, public, fire fighting, military or medical vehicles meant to carry out specific tasks. Cost related to the fleet management, fuel purchase, insurance and service is considerable and significantly influences the company's financial condition [7]. Additionally, in the case of transport companies – the number of which is still increasing and this adds to greater competition on the services market – the clients' expectations pertaining to transport quality and related fees are increasing, too.

In order to decrease the vehicle fleet management-related costs, its proper management is vital [3,6]. Saved financial means resulting from effective vehicle fleet management in a transport company make it possible to lower rates for clients. An attractive price offer for passenger or cargo transport is not only an opportunity for getting regular orders, but also a chance for attracting new clients and developing the transport enterprise. Decreasing the costs resulting from the fleet maintenance in every company means extra financial resources for carrying out various investments having an impact on improved functioning of the company.

OUTSOURCING IN VEHICLE FLEET MANAGEMENT

Vehicle fleet management means proper planning and work organization for means of transport owned by the company. In order to guarantee operational readiness of the fleet its technical condition needs to be controlled during diagnostic tests, it must be serviced at regular intervals, insured, provided with fuel and other materials [1]. Vehicle fleet management means also dealing with all administrative issues related to its maintenance, sale and purchase of cars, coordinating and supervising cooperation with service stations, etc. Duties of the person dealing with the vehicles include negotiating conditions with fleet service providers and insurance companies (Fig.1) [13,17].

Proper vehicle fleet management is a key factor influencing its development and gaining a market position by the company. A crucial element facilitating vehicle fleet management is using telematic technologies [14]. Implementing such solutions and their correct use in transport companies adds to extending the scope of services, lowering the costs and improving the quality of carried out transport tasks. Taking advantage of new technologies and providing the drivers with suitable training packages meant to improve their skills leads to significant savings pertaining to more economic driving style [4,8,12]. Savings resulting from lower fuel consumption and smaller accidents rate add to generating greater profits in the company and creating its own reliable name. Good opinions about a transport company, i.e. reliability, clients' satisfaction, timely execution of tasks are all features of effective vehicle fleet management.

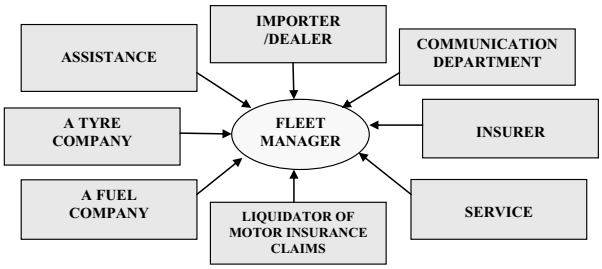

Fig.1. Entities with whom a fleet manager cooperates and deals [21]

More and more companies are aware of the role of proper fleet management. Most companies invest in their own fleet and suitable vehicles management systems. This gives the company's management an opportunity of having complex control over the fleet they operate. Some companies give up their own fleet and decide to make use of external operators specializing in a given field. Delegating some duties to an eternal company (outsourcing) enables better coordination over the remaining tasks.

In many companies vehicle fleet management is worth outsourcing to specialists who can relieve the staff employed by the company owning a vehicle fleet of their workload. They can add to limiting the costs related to vehicles maintenance. In Poland, similarly as in many European countries, functions of fleets managing companies have been taken over by vehicles leasing enterprises [5,20]. Outsourcing a vehicle fleet management has become more and more common practice, both in large corporations and small companies owning just several vehicles. They receive, as a package:

– inspections and repairs in authorised service stations,
– complex scope of insurance services OC, AC, NW and supervision over the liquidation process of motor insurance claims,
– 24-hours Assistance, as well as an opportunity to get an interim vehicle,
– special fuel cards, owing to which fuel costs at petrol stations can be settled in a non-cash way,
– a system monitoring of the vehicle fleet GPS.

Tasks of a fleet managing company include the duty to replace the cars into new ones and disposal of the exploited ones. The client is only to pay a monthly fee related to potential vehicles rental and control over the costs. The fleet managing company also prepares a complex scope of analyses and managerial reports pertaining to exploitation of the client's vehicle fleet. These types of analyses and reports are necessary for costs control and reduction. An appendix to such report can be a list of all transactions realized by particular users, specifying dates, places, fuel type and quantity, and even the vehicle filling up times.

A company deciding to outsource its vehicle fleet management can select one of several options described in Table 1 [21]. There are also solutions meaning partial transfer of duties related to vehicles maintenance to an external partner. This pertains to revolving lease, a service package, insurance lease, as well as lease with a service package. Regardless of the option selected by the company owning a vehicle fleet, taking advantage of outsourcing services has many advantages. It is a perfect solution for enterprises treating their vehicles as business means which, after some period of operation, depreciate and should be replaced into new ones. Also, they do not experience problems related to current exploitation of vehicles.

Table 1. Outsourcing options in vehicle fleet management

Variant		Scope of duties
1.	Full service leasing	– pertains to taking over all duties related to vehicles service maintenance.
2.	Car fleet management	– means current vehicle fleet management, – the entity placing the order remains the vehicle owner, – the outsourcing company is only responsible for current fleet management, – within the scope of the order we provide service, liquidation of claims and other elements that can be offered by an outsourcing company, – the clients purchase vehicles themselves and insure them.
3.	Lease-back	– it means re-sale of the fleet owed by the company to the managing company and then leaseback of the same vehicles, – the offer is addressed mainly to companies owing relatively new vehicle fleet, – taking advantage of this option can improve the flow of documents in the company and simplify settlements.

Selecting a suitable vehicle fleet managing company is crucial. Only an experienced and professional company can add to effective vehicles management, decreasing the costs and generating profits [10, 15]. Thus saving up extra financial means and their proper use can add to each company's development.

COSTS OF VEHICLES FLEET MANAGEMENT

The most important problems related to vehicles maintenance in a company include expenses concerning fuel purchase and their depreciation costs. The costs constitute approx. 57% of general expenses related to owing a vehicle fleet. High depreciation rate has a direct impact on decreasing the vehicles' book value and higher resale value. Compulsory insurances constitute 13% of the fleet maintenance costs. Other elements constituting the fleet-related expenses are: 12% – credit costs, 12% – inspections and tyres replacement, 6% – taxes and administrative costs (Fig.2).

In order to reduce high costs resulting from vehicle fleet maintenance, that significantly influence the company's condition, one should implement various types of economy programs, effective control of all activities and optimization of expenses [2,16,18]. Owing to such activities, monthly expenses can be reduced by as much as 5-10%. Even a more effective way to save up to 10 – 20% is outsourcing the vehicle fleet management to an external company, as mentioned previously. Expenses borne by the company owning

the means of transport, the so-called TCO and ways of their reduction are presented in Tables 2 and 3. All costs related to the owned vehicles and hired drivers should be segregated separately, to know it precisely what specifically the money is spent on and on what one can save. Such accounting restricts undue expenses and individualizes the costs per a specific vehicles/driver.

An important problem in effective fleet management is proper attribution of means of transport to execute a specific task and, resulting from that, determining the required number of drivers. In solving the problem one can take advantage of most recent IT and telematic technologies, such as [11,14]:

– OBD systems diagnosing and informing about vehicles damages,
– satellite navigation systems,
– geographic information systems,
– wireless communication systems.

Applying IT technologies enables continuous vehicles localization online, sending text messages, data collection and administration, time evidence, as well as keeping a route record.

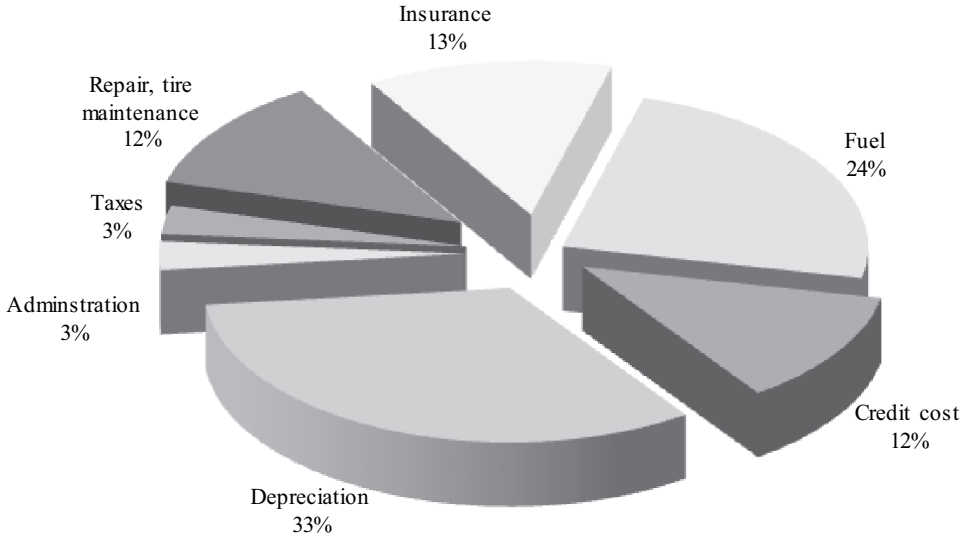

Fig. 2. Cost constituents of maintaining a 50-100 vehicles fleet [21]

Table 2. Ways of reducing costs related to vehicles' purchase and their servicing

Cost	Costs reduction ways	Benefits
Purchase of vehicles	controlling expenses related to the sales offer	paying attention, during vehicles purchase, to: – newest technologies increasing the driver's comfort and safety, – savings related to their exploitation (cars' manufacturers present the total vehicle maintenance cost for some period; the lower CO_2 emission, the less fuel a specific vehicles will consume, and this is related to lower tax rates), – same brand of vehicles – this results in savings related to vehicles' servicing by one service station and thus a possibility of discounts, faster repairs, inspections, tyres replacement, etc.,
Service	analysis of offers from service stations	selection of the best technical and financial offer,
		punctuality and reliability of periodic inspections, pursuant to manufacturers' recommendations and guarantee conditions, because: – an oversight related to this can result in a lost guarantee and generate extra costs (purchase of new spare parts), – an eventual failure may immobilize the vehicle for a longer period and thus reduce its operational ability and value, when intended for sale,
	own repair service	facilitates functioning of a company owing a vehicle fleet and adds to significant savings, because: – it guarantees high quality of performed services, – low inspection and repair costs, – fast and punctual inspections and repairs – this guarantees the vehicle can be timely returned for operation.

Table 3. Ways of reducing costs related to fuel purchase and insurance of a vehicle fleet

Cost	Costs reduction ways	Benefits
Fuel purchase costs	fuel cards	non-cash transactions, owing to which the drives does not have to carry legal tenders (cash, debit card),
		discounts for fuel purchase,
		deferred payments terms,
		unlimited access to on-line systems enabling: – inspection of fuel expenses over a specific period, – having permanent control over transactions realized by means of a fuel card,
		control over drivers working time, since their location and fuel purchase time is known,
		creating monthly reports including all transactions by means of a specific fuel card and submitting them to companies, owing to what detailed fuel purchase costs generated by a specific vehicles are knows,
	change of drivers' habits: – eco driving and defensive driving training sessions, – intelligent systems recording the driving style	improvement of the driving style, increasing safety,
		faster prediction of situations occurring on the road and thus better possibility of avoiding sudden braking and acceleration (also, accidents),
		decreasing fuel consumption (up to 15-20% a year) and fumes emission to the environment,
	selection of the optimum rout and its monitoring	lower fuel consumption,
		control over the driver,
	giving a vehicle at a user's disposal only during business hours	this way one can currently control fuel consumption related to business strips during business hours,
Vehicle insurances	analysis of offers from insurance companies	selection of the best offer,
		insuring the entire fleet in one insurance company, since this enables: – negotiation of the proposed insurance policy terms and conditions, – getting better conditions (more vehicles – better offer),
		selection of an offer with extra options, i.e.: – third-party liability of motor vehicle owners which, in a package, includes also extra voluntary insurance, – an interim vehicle,
	giving up voluntary insurance (eg with AC)	increased awareness of the driver, because he will bear financial consequences related to the vehicle or its equipment damage himself.

On the Polish market modern technologies supporting vehicle fleet management have only been used in approx. 20%. Most Polish companies have purchased such systems mainly to control the drivers and check their location. Meanwhile, the telematic systems offered by manufacturers are used mainly for effective and dynamic management and improved functioning of the entire company. Finder Online (fig.3) and AutoControl are examples of such systems. Characteristic features of the systems are presented in Table 4 [21].

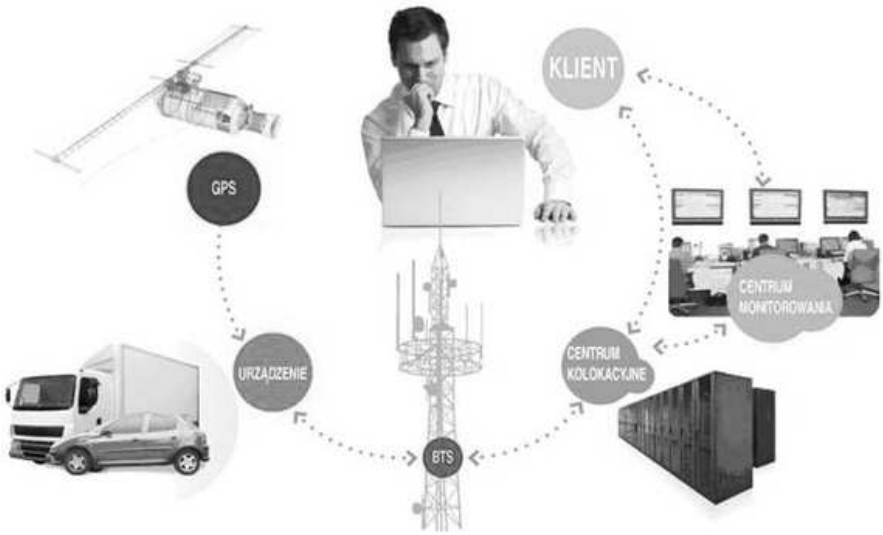

Fig. 3. Diagram of the system Finder On-Line [21]

Table 4. Characteristic features Finder Online i AutoControl

Finder Online	AutoControl
– this is a complex solution addressed to large, medium and small companies who want to increase work effectiveness of their companies, – all data are recorded on a server by means of transmission, – devices installed in vehicles send information to a GSM operator and then the coded data is sent to the server, – when GPRS data transmission is not available, the devices record collected information owing to built-in flash memory, – Finder Pro devices are equipped with a 32-bit processor and an internal battery enabling 48 hours uninterrupted operation without external power supply, – the system is characterised with low current consumption and an aluminium enclosure that guarantees high resistance and aesthetic values.	– data transfer takes place similarly as in Finder system, i.e. by means of GSM network and GPS technology, – the system's operational range includes all European countries, – access to the system is possible through an Internet browser, by means of installing the software on the user's PC, as well as by means of a mobile version available for a mobile phone, – the application is available in 2.0 version and it enables: monitoring the means of transport and fuel consumption, planning the routes, analysis of the travelled route, sending messages and orders, data import from the driver's card and a digital tachograph, supervision of service activities, insurance deadlines, generating reports, creating and mapping own spots and zones, searching for addresses, distance measurement, mobile system management and integration with other systems.

Tests carried out by AutoGuard company show savings caused by implementing IT technologies in a company. Results of the tests are presented in Figure 4.

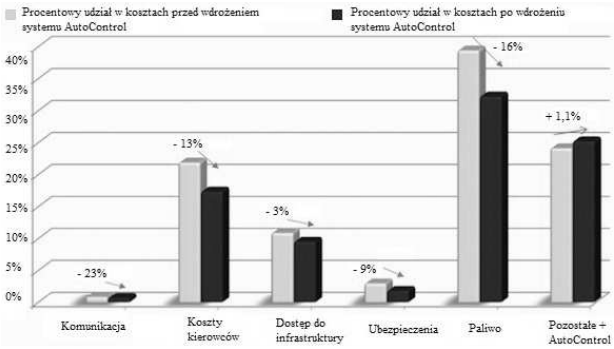

Fig. 4. Percentage costs reduction after the system AutoControl implementation [21]

CONCLUSIONS

Issues related to effective vehicle fleet management require complex and thorough analysis of transport tasks and making rational decisions within that scope. In order to facilitate management of the means of transport one should implement innovative technologies and telematic systems, because they guarantee quality and are a showcase of a modern enterprise. They cause that a company taking advantage of such systems is becoming more competitive on the market [9,19]. Modern technologies and telematic systems make it possible to reduce excessive costs related to vehicles' maintenance and this significantly adds to the company's development, because the saved financial means can be spend on making many investments.

The most recent proposals of companies producing fleet management systems are meant to save many problems that enterprises face. They offer an opportunity of vehicles monitoring, determining optimum routes, constant contact between the employer and the driver, electronic collection of fees resulting from using the road infrastructure. Positioning of facilities on the map, with 1 m accuracy, and using open frequency, will be possible due to the implementing in Poland of a modern and detailed system – Galileo. To collect fees from truck drivers using paid sections of motorways and express roads, the viaTOLL system is used. It also enables weighing the vehicle when in motion and this enables fast and efficient control of its load and thus avoiding penalties resulting from the vehicle's overloading. An important solution for those managing the vehicle fleets is the system implemented by Elte GPS company, which enables authorization and identification of drivers and thus protects the vehicle and the cargo against theft and use by unauthorised parties.

REFERENCES

1. **Abramek K., Uzdowski M. 2009:** Podstawy obsługiwania i napraw. Wydawnictwa Komunikacji i Łączności, Warszawa, 269.
2. **Blaik P. 2013:** Logistyka w systemie zarządzania przedsiębiorstwem: relacje i kierunki zmian. Polskie Wydawnictwo Ekonomiczne, Warszawa, 278.
3. **Chudzicki M. 2004:** Zastosowanie systemu informatycznego zarządzania na przykładzie programu CarRent, wspomagającego proces zarządzania siecią wypożyczalni samochodowych. Zeszyty Naukowe Politechniki Śląskiej, Gliwice, 18, 117–126.
4. **Chudzicki M. 2006:** Zastosowanie SIZ do zarządzania flotą samochodową i wynajmem długoterminowym. Zeszyty Naukowe Politechniki Śląskiej, Gliwice, 35, 43–51.
5. **Chudzicki M., Walaszek-Babiszewska A. 2007:** Model rozmyty dla zadań decyzyjnych w firmie branży zarządzania flotą samochodową. Zeszyty Naukowe Politechniki Śląskiej, Gliwice, 40, 39–49.
6. **Cooke P. 2012:** Zarzadzanie ryzykiem i bezpieczeństwem floty. e-book (plik PDF), 56.
7. **Czekaj J., Dresler Z. 2012:** Zarządzanie finansami przedsiębiorstw: podstawy teorii. Wyd. PWN, Warszawa, 299.
8. **Długosz J. 2009:** Nowoczesne technologie w logistyce. Wydawnictwo Ekonomiczne, Warszawa, 256.

9. **Glinka B., Kostera M. 2012:** Nowe kierunki w organizacji i zarządzania: organizacje, konteksty, procesy zarządzania. Wolters Kluwer Polska, Warszawa, 647.
10. **Griffin R. 2012:** Podstawy zarzadzania organizacjami. Wyd. PWN, Warszawa, 801.
11. **Januszewski A. 2012:** Funkcjonalność informatycznych systemów zarządzania. Wyd. PWN, Warszawa, 250.
12. **Jemielniak D., Koźmiński A., Chrostowski A. 2012:**Zarzadzanie wiedzą. Wolters Kluwer Polska, Warszawa, 496.
13. **Kozina A. 2012:** Planowanie negocjacji w przedsiębiorstwie. Wyd. Uniwersytetu Ekonomicznego w Krakowie, 262.
14. **Wydro K. 2012:** Telematyka – znaczenie i definicja terminu. „Telekomunikacja i Techniki Informacyjne", 1–2.
15. **Zając P. 2003:** Logistyczne zarządzanie flotą pojazdów drogowych. Wyd. Politechniki Wrocławskiej, 145.
16. **Zielińska E. 2011:** Logistyka zarządzania przedsiębiorstwem usług motoryzacyjnych. Monografia, Seria: TRANSPORT nt. „Systemy i środki transportu samochodowego", Rzeszów, 2, 351–358.
17. **Zielińska E. 2012:** Rynek ubezpieczeń komunikacyjnych w Polsce. ВІСНИК, Kijów, 25, 340–345.
18. **Zielińska E., Lejda K. 2010:** Analiza i modelowanie procesów logistycznych w zapleczu technicznym transportu samochodowego w aspekcie problemów ekologicznych. Oficyna Wydawnicza Politechniki Rzeszowskiej, 219.
19. **Zymonik Z., Hamrol A., Grudowski P. 2013:** Zarządzanie jakością i bezpieczeństwem. Polskie Wydawnictwo Ekonomiczne, Warszawa, 333.
20. Czasopismo „Flota", Nr 12/2007, Nr 01/2008.
21. Strony internetowe dotyczące zarządzania flotą samochodową:
   – www.fleetnews.co.uk,
   – www.finder.pl,
   – www.autoguard.pl.

PROBLEMY ZARZĄDZANIA FLOTĄ SAMOCHODOWĄ W PRZEDSIĘBIORSTWACH

Streszczenie. W artykule przedstawiono wpływ efektywnego zarządzania flotą samochodową na rozwój przedsiębiorstwa. Wymieniono i opisano najważniejsze problemy wynikające z utrzymania pojazdów, tj. koszty zakupu paliwa oraz ubezpieczeń komunikacyjnych, wydatki związane z serwisowaniem pojazdów, z przeprowadzaniem ich okresowych przeglądów i napraw itp. Wskazano także na rozwiązania zmierzające do pozyskiwania oszczędności, które mogą być przeznaczone na realizację inwestycji przyczyniających się do rozwoju przedsiębiorstwa.
Słowa kluczowe: zarządzanie flotą samochodową, przedsiębiorstwa transportowe, systemy nadzoru eksploatacyjnego

TEKA. COMMISSION OF MOTORIZATION AND ENERGETICS IN AGRICULTURE – 2013, Vol. 13, No. 1, 95–102

Pressure agglomeration of biomass with additive of rapeseed oil cake or calcium carbonate

Aleksander Lisowski, Magdalena Dąbrowska-Salwin, Adam Świętochowski, Tomasz Motyl, Marcin Pajewski

Warsaw University of Life Sciences – SGGW, 02-787 Warsaw, Nowoursynowska 166, Poland,
Phone: +4822-5934527, Fax: +4822-5934514, E-mail: aleksander_lisowski@sggw.pl
Faculty of Production Engineering, Department of Agricultural and Forest Engineering, Warsaw, Poland

Received February 9.2013; accepted March 14.2013

Summary. The aim of this study was to explain the effect of the 2.5% additive of calcium carbonate or 5% additive of rapeseed oil cake for chopped plant material of topinambour, prairie spartina, multiflora rose, polygonaceous and Virginia mallow (sida) for durability, calorific value and density of the pellets. The additive of calcium carbonate and rapeseed oil cake increased the durability of pellets to 6.1% and 13.6%, respectively, and slightly decreased the density of pellets – 0.7% and 1.7%, respectively. The use of rapeseed oil cake in the pellets improved their calorific value and calcium carbonate had practically no effect on the change in this value. The most marked effect for additives was obtained for topinambour, prairie spartina and Virginia mallow, however for polygonaceous and multiflora rose no significant changes in pellet durability were observed.

Key words: pressure agglomeration, pellet, calcium carbonate, rapeseed oil cake, mechanical durability.

INTRODUCTION

The use of alternative energy sources, including biomass, is becoming wider in recent years [6]. Biomass combustion technology is not complicated and thanks to the availability of cheaper raw material its use for energy purposes is more competitive to currently used conventional fuels [3, 11]. One way of converting biomass is pressure agglomeration, which improves the properties of solid biofuels [4].

One of the stages in the process of pressure agglomeration is conditioning. This covers a range of activities and treatments that are designed to activate natural binders in the material [12]. During conditioning it is possible to add water or steam to the material in order to soften the fiber of densificated particles [20], and particularly the lignin and hemicellulose, which improves the pelletisation process and results in more durability and better physical properties of the obtained pellets [13, 14]. In addition, conditioning also involves adding specific binding agents or other additives.

Although producing pellets without any additives is common [21], there has appeared an interesting possibility to look for a more efficient method of densification of agglomerates improved with appropriately selected binders.

Substances that increase pellet consistency are binders, which means that they support the pressure agglomeration process and, at the same time, they improve their quality and environmental performance [9]. They bind the plant material in a sustainable product that meets standards and does not significantly increase the production cost of the agglomerate , including pellets [1]. Also, binders offer the possibility of developing a new technology and obtaining significantly better agglomerate properties (extra dry, proof against the absorption of moisture from the air, with reduced energy consumption) than before , which may not only affect the combustion process itself, but to a large extent reduce emissions of SO_2, $N2O_5$, dust, CO_2, etc. [8].

Additives, both liquid and solid, produce strong bindings between molecules in the densificated material. Additives are often used in order to improve the quality of pellets according to current standards [10]. Different types of additives are used: binders that improve bindings between particles and those that reduce energy intensity of pellets and improve their combustible properties. There is also an interesting possibility to use waste substances from agricultural production as additives for the production of pellets [15]. In addition to utilising these additives, it can be assumed that rational dosing of those substances can improve physical and chemical parameters of the obtained granules [16, 17].

Adding inert materials, for example, calcium compounds (calcium hydroxide, calcium carbonate) improves plasticity of organic substance which is to undergo pelleting and makes it easier to get forms [19], and a small additive of such a material often significantly reduces dust. In turn, on the basis of agricultural practice, it can be concluded that increasing the participation of protein improves pellet

durability, while a too high proportion of fats significantly worsens it, but positively affects granulate energy [5, 18, 22].

For example, calcium carbonate increases ash melting point and thus reduces the risk of ash pollution on grades [7]. Because it is a mineral, the quantity of ash increases. Such additive absorbs heat to decompose, at the same time decreasing the temperature of combustion, which in consequence leads to a reduction in the amount of NOx. The process of pelletization leads, however, to binding of the water contained in plant material. With little moisture of organic substance, the durability of bond between particles is lower, which results in the reduction of mechanical durability of pellets. In order to compensate for these defects binders that increases the durability of bindings and calorific value, eg. rapeseed oil cake, should be used in the mixtures.

The aim of the study was to determine the impact of the additive of calcium carbonate and rapeseed oil cake into energy plants shredded material on the physical properties of pellets produced from these mixtures in the pressure agglomeration process.

MATERIAL AND METHODS

The research material was obtained from rose multiflora (*Rosa multiflora*), prairie spartina (*Spartina pectinata*), topinambour (*Helianthus tuberosus*), Virginia mallow – sida (*Sida hermaphrodita*) and polygonaceous (*Polygonum sachalinense*) plantations. The raw material moisture content (wet basis) was determined using the dry-and-weighing method according to PN-EN 15414-3: 2011 Standard with accuracy 0.1% (Fig. 1).

The plant material was broken up on a stationary stand by means of a forage harvester and then it underwent pressure agglomeration on the pellet machine ZLSP-200B whose basic parameters are summarized in Table 1.

Table 1. Technical parameters of the pellet machine ZLSP-200B

Efficiency	Power	Weight	Dimensions	Die		
				ø die	ø hole	hole length
[kg·h^{-1}]	[kW]	[kg]	[mm]	[mm]	[mm]	[mm]
80–120	7,5	250	1000/430/950	200	8	20

Tests were carried out for each of the plants without the binder and with 2.5% of calcium carbonate or 5% of rapeseed oil cake. The total final weight of each sample was 2 kg. After each trial the material was cooled to ambient temperature.

Mechanical durability coefficient of pellets was determined at a stand made in accordance with the requirements of the PN-EN 15210-1 Standard. During the tests the bin rotational speed was 50 rpm·min^{-1}, and test time – was 10 min. After the durability test the material was sieved through a sieve with a hole diameter of 3.15 mm and the obtained fractions were weighed with an accuracy of 0.01 g while durability was calculated according to the formula:

$$\Psi = 100\frac{m_{pt}}{m_p}, \tag{1}$$

where:
Ψ – durability coefficient, %,
mp – pellet mass before trial, g,
mpt – pellet mass after trial, g.

Combustion heat was determined by the calorimetric method using KL-10 calorimeter and the calorific value was calculated. Milled samples of 1 g were burned at a pressure of 3 MPa. Taking into account the hydrogen content in the material, which was established in the Analytical Center of Warsaw University of Life Sciences, the calorific value was calculated using the following formula:

$$W_u = W_t - 2454\left(W_w + 9H\right), \tag{2}$$

where:
Wu – calorific value, MJ·kg^{-1},
Wt – combustion heat of sample, MJ·kg^{-1},
Ww – relative moisture of fuel,
H – relative proportion of hydrogen in fuel.

Pellet density measurement was made on a randomly selected representative sample of 10 pellets from each group. Two series of measurements were performed within 1 minute after the agglomeration process as well as after 15 minutes. Pellet diameter was measured in two perpendicular planes in the middle of the pellet length. Linear measurements were made by means of an electronic digital caliper with an accuracy of 0.01 mm, the measurement of mass of each pellet was carried out with an accuracy of

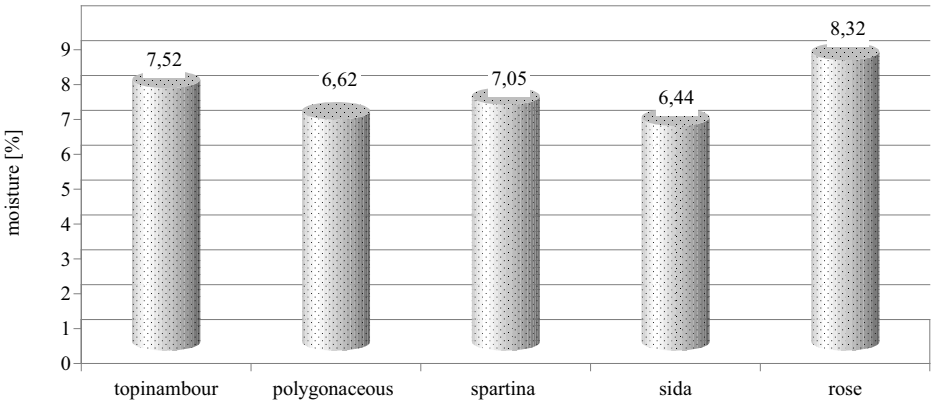

Fig. 1. Moisture content of the material during the tests

0.01 g on laboratory scales RADWAG WPS 600 / C, and the density of the pellets was determined by the formula:

$$\rho = \frac{m}{V}, \quad (3)$$

where:
ρ – pellet density, kg·m^{-3},
m – pellet mass , kg,
V – pellet volume , m^3.

Data analysis was performed using the Statistica computer program version 10, using the procedure of analysis of variance and Duncan's test.

RESULTS AND DISCUSSION

With additives, pellets of similar size and shape changed their colors and appearance (Table 2). Pellets produced with the additive of calcium carbonate were characterized by a slightly cracked outer surface and were matte, rough, without the characteristic glassy surface which is formed as a result of thermal conversion of lignin. Pellets with rapeseed oil cake were characterized by a darker color and a shiny outer surface with burnt lignin. Rapeseed oil cake reduced dust in pressure agglomeration, whereas the additive of calcium carbonate significantly increased dust in that process.

Table 2. Pellets after pressure agglomeration process

Pellets without additive	Pellets with additive of rapeseed oil cake	Pellets with additive of calcium carbonate
topinambour		
		
polygonaceous		
		
sida		
		
spartina		
		
rose		
		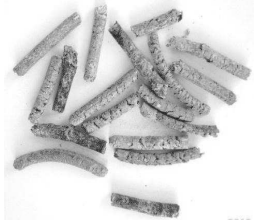

An analysis of variance showed that both the energy plant species, the type of the additive, and their interaction had a statistically significant effect on the pellets mechanical durability, as in all cases, the value of the critical level of significance of $p < 0.0001$ (Table 3). The results of the Duncan test (Table 4) allow the conclusion that in the case of both types of additives and pellets without any additive three distinct homogeneous groups of pellet mechanical durability values were formed.

Table 3. The results of the analysis of variance of factors affecting the mechanical durability of pellets from energy plants material

Source	Sum of squares	Degrees of freedom	Mean square	F factor	p – value
Plant: A	1360.8	4	340.2	311.4	<0.0001
Additive: B	735.6	2	367.8	336.6	<0.0001
Interaction: A x B	472.9	8	59.1	54.1	<0.0001
Error	32.8	30	1.1		

Table 4. The results of the Duncan test of the analysis of mean values of the mechanical durability of pellets for homogeneous groups of plant species and type of additive

Factor	Ψ, %	Homogenous group			
Plant					
Topinambour	73.59	x			
Polygonaceous	74.36	x	x		
Sida	74.78		x	x	
Spartina	75.45			x	x
Rose	88.21				x
Type of additive					
None	72.50	x			
Calcium carbonate	76.96		x		
Rapeseed oil cake	82.38			x	

Plant species formed four homogeneous groups, which included pairs of plant species of mixed system; this means that there were no clear differences between the coefficients of mechanical durability of pellets for the investigational species. Mean values of the mechanical durability, their standard deviations and 95% range of variation are shown in Table 5, a graphic interpretation of the interaction of the durability is shown in Figure 2.

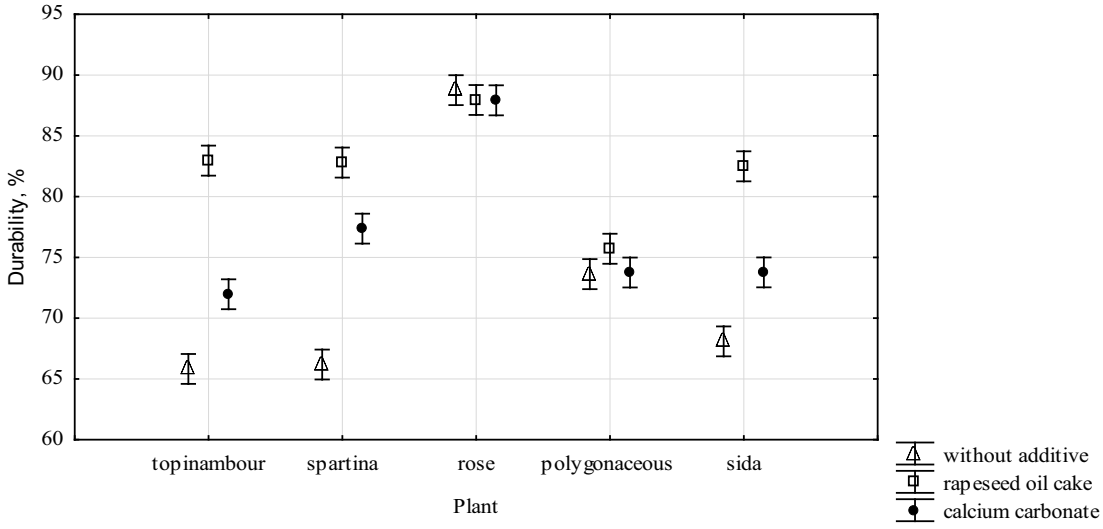

Fig. 2. The interaction of the additive with the species of energy plants on mechanical durability of pellets

Table 5. The average values of mechanical durability, standard deviation, SD and 95% confidence intervals for the plant species and type of additive or its lack

Factor	Ψ, %	SD Ψ, %	-95% Ψ, %	+95% Ψ, %	Population
Plant					
Topinambour	73.59	0.35	72.87	74.30	9
Spartina	75.45	0.35	74.74	76.16	9
Rose	88.21	0.35	87.50	88.92	9
Polygonaceous	74.36	0.35	73.65	75.07	9
Sida	74.78	0.35	74.07	75.50	9
Additive					
None	72.50	0.27	71.94	73.05	15
Rapeseed oil cake	82.38	0.27	81.83	82.94	15
Calcium carbonate	76.96	0.27	76.41	77.51	15

Rose pellets had the highest durability (87%–89%), but the effect of additives on the value rate change of mechanical durability was the lowest and ranged within statistical error (Fig. 2). For other plants, additives improved pellet durability more effectively. The additive of rapeseed oil cake increased durability to a greater extent than the additive of calcium carbonate (Fig. 2). The additive of calcium carbonate and rapeseed oil cake allowed to increase the durability of pellets by 6.1% and 13.6% respectively. To sum up, the greatest effect of additives was obtained for topinambour, spartina and sida, but for rose and polygonaceous practically no change in the pellets durability was recorded. Therefore the durability of the produced pellets was mainly affected by the type of densificated material and type of additive. This observation confirms the inference of Niedziółka et al. [16], who also found that the percentage of additives in prepared mixtures has a significant influence on the durability of pellets. Another factor influencing the value of durability coefficient is also the moisture of material [2]. In our study, material from multiflora rose had relatively the highest moisture (8.32%), but the lowest moisture for sida (6.44%) was not lower significantly enough in this area to draw any conclusions about its impact on the durability of pellets, especially since the moisture content of the material was covariate and was associated with plant species.

Pellet calorific values ranged from 15.1 MJ·kg^{-1} for polygonaceous without an additive to 19.9 MJ·kg^{-1} for spartina without an additive (Fig. 2). For other plants calorific values were similar and were approximately 17 MJ·kg^{-1}. Calcium carbonate had no significant effect on the calorific value of pellets and the additive of rapeseed oil cake generally caused a increase in combustion heat and calorific value.

An analysis of variance showed that pellet density of was affected in a statistically significant way by the main factors: species of energy plants, the type of the additive used, the time of measurement and all of their double and triple interactions with a critical significance level $p < 0.0001$ (Table 6). On the basis of an analysis of the Duncan test (Table 7) four homogeneous groups for the plant species were identified, including a common group created by spartina and rose. An additive of calcium carbonate did not significantly differentiate the density of pellets because it formed homogenous groups with the additive of rapeseed oil cake and without any additive. Table 7 summarizes the mean density of the pellets determined after 1 min and after 15 min from the time of pellet production for comparison purposes only, because for two factor levels variance analysis results are sufficient (Table 6). A smaller value of 2.9% for density of the pellets after 15 min indicates the expansion of the pellets associated with stress relaxation of the material between the particles during their storage. Average densities of pellets with their standard deviations and 95% range of variation are shown in Table 8, and the graphic interpretation of factors interaction on the density of pellets is presented in Figure 4.

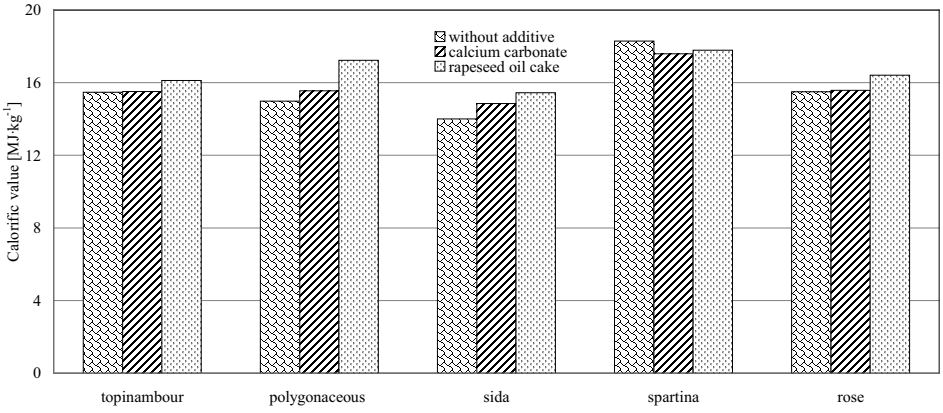

Fig. 3. Calorific values of pellets

Table 6. The results of the analysis of variance of factors affecting the density of the pellets from energy plants material

Source	Sum of squares	Degrees of freedom	Mean square	F factor	p – value
Plant: A	1143889	4	285972	93.6	<0.0001
Additive: B	19681	2	9841	3.2	<0.0001
Time: C	80988	1	80988	26.5	<0.0001
Interaction: A×B	1160604	8	145076	47.5	<0.0001
Interaction: A×C	403876	4	100969	33.0	<0.0001
Interaction: B×C	131004	2	65502	21.4	<0.0001
Interaction: A×B×C	1151864	8	143983	47.1	<0.0001
Error	824974	270	3055		

Table 7. The results of the Duncan test of the analysis of mean values of the density of pellets for homogeneous groups of plant species, type of additive and measurement time

Factor	ρ, kg·m^{-3}	Homogenous group			
Plant					
Spartina	1050.47	x			
Rose	1054.53	x			
Topinambour	1112.61		x		
Polygonaceous	1137.88			x	
Sida	1218.51				x
Type of additive					
Rapeseed oil cake	1104.21	x			
Calcium carbonate	1116.31	x	x		
None	1123.88		x		
Measurement time, min					
1	1131.23	x			
15	1098.37		x		

After 1 min from the pellets production, sida without additive was characterized by the highest density of pellets, whereas spartina with rapeseed cake had the lowest pellet density (Fig. 3). The density of pellets after 15 min was smaller, but more stable than after 1 min. After 1 min from the pellet production, the additive of calcium carbonate increased the density of pellets made of spartina material and after 15 min also of the material of topinambour and sida. Generally, however, the additive of calcium carbonate and rapeseed oil cake contributed to a slight decrease in pellet density, by 0.7% and 1.7% respectively. Confirmation of this inference requires an extension of research on the participation of additives, extended time of stress relaxation in the pellets, increasing the moisture content and diversity of agglomerate pressure.

Table 8. The average values of density, standard deviation, SD and 95% confidence intervals for the plant species, type of additive or its lack and measurement time

Factor	ρ, kg·m^{-3}	SD ρ, kg·m^{-3}	-95% ρ, kg·m^{-3}	+95% ρ, kg·m^{-3}	Population
Plant					
Topinambour	1112.61	7.14	1098.56	1126.66	60
Spartina	1050.47	7.14	1036.42	1064.52	60
Rose	1054.53	7.14	1040.48	1068.58	60
Polygonaceous	1137.88	7.14	1123.83	1151.93	60
Sida	1218.51	7.14	1204.46	1232.56	60
Additive					
None	1123.88	5.53	1113.00	1134.76	100
Rapeseed oil cake	1104.21	5.53	1093.33	1115.10	100
Calcium carbonate	1116.31	5.53	1105.42	1127.19	100
Time					
1	1131.23	4.51	1122.346	1140.12	150
15	1098.37	4.51	1089.485	1107.26	150

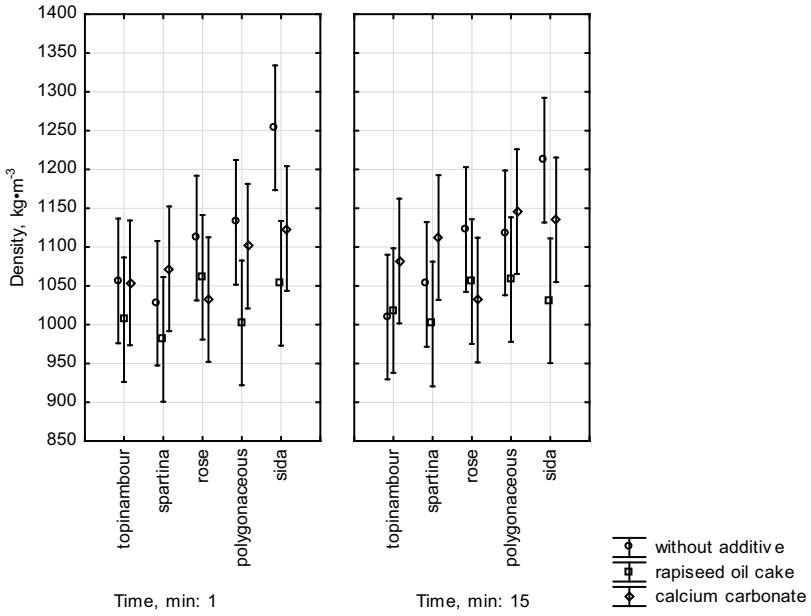

Fig. 4. The interaction of the additive with the species of energy plants and measurement time on the density of pellets

CONCLUSIONS

1. The additive of calcium carbonate or rapeseed oil cake allowed to increase mechanical durability of pellets by 6.1% and 13.6%, respectively, and slightly decreased pellet density by 0.7% and 1.7%, respectively. Also, the calorific value of this solid fuel changed slightly.
2. The density of the pellets after 15 minutes was smaller by 2.9%, but more stable than after 1 minute from production time, which indicates that expansion of the pellets is associated with stress relaxation between the particles of the material during their storage time.
3. The most marked effect of using additives was obtained for topinambour, spartina and sida, but for rose and polygonaceous practically no change in the pellets durability was recorded. However, pellets from rose were characterized by the highest values of the mechanical durability coefficient (87%–89%), which may be due to the structure and physical properties of that material.
4. Pellets produced with the additive of calcium carbonate were characterized by a slightly cracked outer surface and were matte, rough, without the characteristic glassy surface, formed as a result of thermal conversion of lignin. Pellets with an additive of rapeseed oil cake were characterized by a darker color and a shiny outer surface with burnt lignin.

REFERENCES

1. **Borowski G., Kuczmaszewski J. 2005:** Utilization of the fine-grained metal wastes. Monograph. ed. Politech. Lubelska, Lublin, ISBN 83-89246-29-5. (in Polish)
2. **Fiszer A., Dworecki Z. 2012:** Durability test for common reed pellets. J. Res. Appl. Agr. Eng., 57(2), 69–72. (in Polish)
3. **Frączek J. 2010:** Biomass production for energetic purposes. ed. PTIR, Cracow, ISBN 978-83-917053-8-4. (in Polish)
4. **Golubenko A. Tsyvenkova N., Mulyar O., Romanushun O. 2011:** Biomass standardization as a base for its sufficient use. TEKA Kom. Mot. i Energ. Roln. – OL PAN, 11A, 85–91.
5. **Grochowicz J. 1998:** Advanced manufacturing techniques of industrial feed compound. ed. PAGROS s.c., Lublin, ISBN 83-910152-0-3. (in Polish)
6. **Gubacheva L., Andreev A., Shevchenko D. 2011:** Alternative fuels for transport. TEKA Kom. Mot. i Energ. Roln. – OL PAN, 11A, 99–107.
7. **Hartmann H., Turowski P., Robmann P., Ellner-Schuberth F., Hopf N. 2007:** Grain and straw combustion in domestic furnaces – influences of fuel types and fuel pretreatments [In:] Proceedings of the15th European Biomass Conference and Exhibition, Berlin.
8. **Hejft R. 2002:** Pressure agglomeration of plant materials. ed. Politech. Białostocka, Bialystok, ISBN 83-7204-251-9. (in Polish)
9. **Hess R., Kenney K., Wright C. 2010:** A technical review on biomass processing: densification, preprocessing, modeling and optimization, 1–32 [access: 14.02.2013] Available in the Internet: http://www.inl.gov/technicalpublications/documents/ 4559449.pdf.
10. **Kaliyan N., Morey R. 2010:** Natural binders and solid bridge type binding mechanisms in briquettes and pellets made from corn stover and switchgrass. Bioresour. Technol., 101, 1082–1090.
11. **Kowalik P. 2002:** Perspectives of biomass pelletizing in Poland. Czysta Energia, 10, 14–15. (in Polish)
12. **Kulig R. 2007:** Effects of conditioning methods on energy consumption during pelleting. TEKA Kom. Mot. Energ. Roln. – OL PAN, 7A, 52–58.
13. **Kulig R., Laskowski J. 2008a:** Effect of conditioning parameters on pellet temperature and energy consumption in the process of plant material pressing. TEKA Kom. Mot. Energ. Roln. – OL PAN, 8a, 105–111.
14. **Kulig R., Laskowski J. 2008b:** Energy requirements for pelleting of chosen feed materials with relation to the material coarseness. TEKA Kom. Mot. Energ. Roln., 8, 115–120.
15. **Mani S., Tabil L.G., Sokhansanj S. 2006:** Effects of compressive force, particle size and moisture content on mechanical properties of biomass pellets from grasses. Biomass & Bioenergy, 30, 648–654.
16. **Niedziółka I., Szpryngiel M. 2012:** Assessment of quality properties of plant biomass pellets. Inż. Rol., 2(136), 1, 267–276. (in Polish)
17. **Niedziółka I., Szymanek M., Zuchniarz A., Zawiślak K. 2008:** Characteristics of pellets produced from selected plant mixes. TEKA Kom. Mot. Energ. Roln. – OL PAN, 8, 157–162.
18. **Nikolaisen L., Nørgaard-Jensen T., Hjuler K., Busk J., Junker H., Sander B., Baxter L., Bloch L. 2002:** Quality characteristics of biofuel pellets. Aarhus. Danish Technological Institute, 137 + app. 46.
19. **Sedlácek P., Martinek T., Fecko P. 2003:** Ecological pellets from brown coal and biomass. Inżynieria Mineralna, 4(2), 11–17. (in Polish)
20. **Skoch E., Behnke K., Deyoe C., Binder S. 1981:** The effect of steam-conditioning rate on the pelleting process. Anim. Feed Sci. Tech., 6, 83–90.
21. **Sokhansanj S., Mani S., Bi X., Zaini P., Tabil L. 2005:** Binderless pelletization of biomass. ASAE Paper No. 056061. St. Joseph, Mich.: ASAE.
22. **Zawiślak K., Grochowicz J., Sobczak P. 2011:** The analysis of mixing degree of granular products with the use of microtracers. TEKA Kom. Mot. i Energ. Roln. – OL PAN, 11c, 335–342.

AGLOMERACJA CIŚNIENIOWA BIOMASY Z DODATKIEM MAKUCHÓW RZEPAKOWYCH LUB WĘGLANU WAPNIA

Streszczenie. Celem pracy było wyjaśnienie wpływu dodatku 2,5% węglanu wapnia lub 5% makuchów rzepakowych do rozdrobnionego materiału topinambura, spartiny, róży, rdestowca i ślazowca na trwałość, wartość opałową i gęstość peletów. Do-

danie węglanu wapnia i makuchów pozwoliło na zwiększenie trwałości peletów, odpowiednio o 6,1% i 13,6% oraz nieznaczne zmniejszenie gęstości peletów, odpowiednio o 0,7% i 1,7%. Zastosowanie makuchów poprawiło wartość opałową peletów, a węglan wapnia praktycznie nie miał wpływu na zmianę tej wartości. Największy efekt wpływu dodatków uzyskano dla topinambura, spartiny i ślazowca, a dla rdestowca oraz róży praktycznie nie zarejestrowano zmian w trwałości peletów.
Słowa kluczowe: aglomeracja ciśnieniowa, pelet, węglan wapnia, makuchy rzepakowe, trwałość mechaniczna.

TEKA. COMMISSION OF MOTORIZATION AND ENERGETICS IN AGRICULTURE – 2013, Vol. 13, No. 1, 103–108

Polyoptimalization of the construction of subatmospheric pressure press with implementation of the finite element method

Dariusz Lodwik, Włodzimierz Malesa, Zbigniew Wiktorski

KONTENER, Production of Building Elements LLC
8 Kostrogaj Street, 09-400 Płock, Poland, e-mail: polsw@pw.plock.pl

Received February 9.2013; accepted March 14.2013

Summary. In this paper, implementation of CAD systems and the finite element method applied to the parametrization and poyoptimalization process of the test stand of subatmospheric press were discussed. The results, obtained in this way, are presented as electronic maps, tabular listing, charts and graphs. The proposed methodology of research is practically used to place orders for the needs of industry producing agricultural machines and devices, building industry and defense industry.
Key words: computer aided design, finite element method, contact stresses, distribution of stresses in the soil, subatmospheric press, parametrization, polyoptymalization.

INTRODUCTION

The subatmospheric press is intended for cohering large-size, multilayer composite elements. Composite elements are employed for the contraction of, among other things, self-supporting container constructions of various usage. Wall composite elements are also used in agricultural technology for cold store erecting and farm building construction [7].

In this work, practical aspects dealing with polyotimalisation of a digital model of test stand of the large-size press intended for subatmospheric cohering multilayer composite panels were discussed. The work on the project of the test stand of the subatmospheric press is co-supported financially by the European Regional Development Fund as a part of the Innovative Economy Programme [10].

In the project, a parametric digital model of the press (3D) with implementation of solid modeling with CAD system application was created. Sample constructional variants of presses, with different selected geometrical features, were generated [6]. The next stages of work were devoted to carrying on calculations of strength and stiffness for selected constructional cases of main components and parts constituting the supporting structure of modeled test stands with implementation of tools of analytical systems CAD (a frame analyzer, the finite element method). The last element of this work was devoted to finding optimal constructive solution to the problem of press construction, considering adopted scalar criteria [1, 2, 3, 4].

Fig. 1. The test stand of subatmospheric presses

DETERMINATION OF PARAMETRIC CONSTRUCTIONAL FEATURES (DECISION-MAKING VARIABLE) OF THE SUBATMOSPHERIC PRESS

The carrying frame, designed with closed-profile steel sections, is the basic constructive element of subatmospheric press. The frame construction is constituted with two stringers and two outer cross-bars which are connected in a process of welding. The inner construction of the carrying frame's truss was made of cross-bars which are perpendicularly welded to stringers of the frame. Perpendicularly to outer cross-bars and inner cross-bars, struts were welded, placed in two rows in a particular way that they constitute, together with stringers and cross-bars, a uniform surface on which a unit of panels was placed [7].

The features which played the role of parameters were selected in the construction of the subatmospheric press. The assigned parameters were coordinates describing constructive shape of particular constructive features and, determined on a stage of assumptions, values of layout dimensions [15, 17, 18, 19]. Two basic parameters, describing geometry of the carrying frame – ie. the length of the frame LR and its width SR, were determined in the construction of the press. It was presented in Figure 2.

The place for possible constructional solutions was generated, in the design process of the subatmospheric press, based on series of types [5] of the parameters. The determined unit of probable constructional solutions made realization of the assigned task of polyoptimalisation possible. The aim of this action was selection of possible constructional features of the subatmospheric press in order to optimise the basic criteria. The result of polyopimalisation is selection and conceptualisation of the concept of the press to be put into practical realization .

The units of values for the parameters, for which series of types of the construction of the subatmospheric press were set, are presented in Tables 1 and 2.

Table 1. The unit of the value for the L_R parameter [mm]

$L_R(1)$	$L_R(2)$	$L_R(3)$	$L_R(4)$	$L_R(5)$	$L_R(6)$	$L_R(7)$
3400	5200	7000	8800	10600	12400	14200

Table 2. The unit of the values for the S_R parameter [mm]

$S_R(1)$	$S_R(2)$	$S_R(3)$	$S_R(4)$	$S_R(5)$	$S_R(6)$	$S_R(7)$	$S_R(8)$
1380	1680	1980	2280	2580	2880	3180	3480

The whole number of choices for series of types was estimated at 8x7=56, but the number of selected options for the further analysis was limited because of time consuming complexity of calculations for this problem. The need for comparison of options due to technological conditions of cohering process of composite panels, was an additional reason for the choice.

Table 3. Dimensional values of parameters selected from series of types of the optional variety of the subatmospheric press

Working name of optional selection from series of types of the press	L_R [mm]	S_R [mm]
A	8800	2580
B	8800	2280
C	7000	2580
D	7000	2280

DETERMINATION OF QUANTITATIVE CRITERIA FOR POLYOPTIMALISATION OF THE SUBATMOSPHERIC PRESS

The aim of optimization deals with selection, from the unit of acceptable solutions, such a solution for which the objective function (optimisation criteria) reaches the extreme value (minimum or maximum). In case of the task of polyoptimalisation, lots of criteria of optimisation, sometimes opposing one another [12], come into existence.

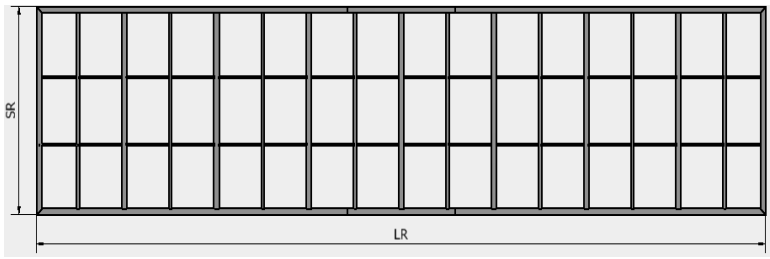

Fig. 2. Constructional parameters for the carrying frame of the subatmospheric press.

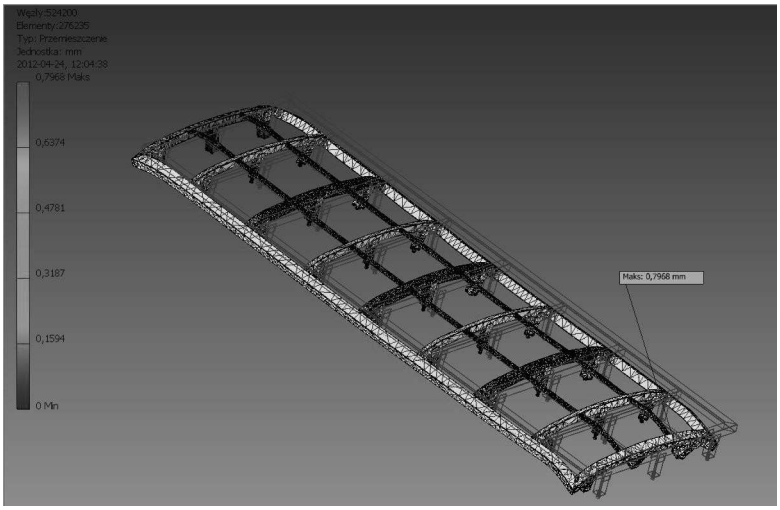

Fig. 3. The numeric map of displacement of the frame of the subatmospheric press formed during the cohering process (subatmospheric pressure of 400 hPa applied) – a view from the side of the supports

Two criteria for the task of polyoptimalisation were set in the discussed case of the construction of the subatmospheric press:

$\mathbf{q}_1$ – the weight of the press (the carrying frame, the support, laminated panels, the rebate) given in [kg],

$\mathbf{q}_2$ – maximal displacement in [mm] of constructive elements of the press operated with implementation of subatmospheric pressure at 400 Pa, determined with the use of the MES calculations [8, 9, 11, 13, 16, 20, 21].

The choice of the presented criteria was introduced due to the following matters:

– reduction of expenses spent on materials used to build the subatmospheric press,
– reduction of costs necessary to build the press (minimisation of weight directly results in the drop of technological expenses, e.g. the welding process),
– reduction of deformations of the carrying frame of the press during cohering process (400 hPascals' worth of subatmospheric pressure applied), due to this fact the circumstances affecting deformation of the formed element (multilayer composite panel) are held down.

The value of the q_1 criterion was determined based on a digital model of the press and qualities of materials used for its construction. This task was completed using the Inventor system by applying appropriate functions of this program (the Proprieties function). The value of the q_2 criterion was determined in a digital model by applying the finite elements method, implemented in the Autodesk Inventor. Pairs of numbers, valued for the q_1, q_2 criteria, were assigned for any constructional variety of series of types of subatmospheric press.

According to the above, for the problem analyzed, the positive cone will have coordinates set down for the a=(a1, a2) point, whose values were determined in the process of polyoptimalisation.

The mathematical notation is recorded as:

$$C_a = \{q = (q_1, q_2): (q_i - a_i) \geq 0, \qquad i = 1{,}2\}.$$

In view of that, the $x_p=(x_{1p}, \dots, x_{np})$ polyoptical element will be such constructive solution (allotted for the Φ unit of possible solutions); it means that for any $x=(x_1, \dots, x_n)\in\Phi$ possible element there will not be any relation of minority according to the partial order set up by the positive cone between the $Q(x)=(q_1(x), q_2(x))$ elements and the $Q(x_p)=(q_1(x_p), q_2(x_p))$ element.

The polyoptimal constructions, which were set up in this way, comprise the Pareto unit for modeled series of types of the subatmospheric press construction.

DETERMINATION OF THE PARETO-OPTIMAL UNIT (UNDOMINATED SOLUTIONS) FOR SELECTED CASES OF THE PARAMETRIC MODEL OF THE SUBATMOSPHERIC PRESS

Two criteria q_1, q_2 were accepted to carry on the task of polyoptimalisation of the subatmospheric press construction. The q_1 criterion means the weight of the construction of the carrying frame of the subatmospheric press, together with supports, whereas the q_2 criterion means the maximal dislocation set up for the construction of the carrying frame and supports.

Four acceptable constructional x_A, x_B, x_C, x_D solutions were examined in the project task and also an appropriate value for quality indicators was calculated for every solution. In the target space, a unit of four $a_A(q_1, q_2)$, $a_B(q_1, q_2)$, $a_C(q_1, q_2)$, $a_D(q_1, q_2)$ points, which comprises quality vector for every constructional solutions, was obtained.

The polyoptical solution, in terms of the Pareto sense, is any acceptable solution, for which any other acceptable dominating solution does not exist. No solution, for which the value of all criteria would be better than any optional polyoptimal solution, exists in the unit of the correct solutions.

The Pareto relation (equal to the relation of partial order specified by the positive cone) is the most frequently met relation which is implemented to defy the polyoptimal solution [12].

In the analyzed task, the following coordinates of the a_A, a_B, a_C, a_D points, in the (q_1, q_2) criterion space, were determined in the process of the MES calculations.

Table 4. Coordinates of the a_A, a_B, a_C, a_D points in the q_1, q_2 criterion space

real results	q_1 [kg]	q_2 [mm]
a_A	1842,74	0,7915
a_B	1707,84	1,3990
a_C	1495,85	0,6801
a_D	1391,18	0,7968

In order to make the values for the points in the criterion space more readable and comprehensive, the subsequent measure was implemented – normalisation of their coordinates in concordance with the following dependence:

$$q_i^N = \frac{q_i}{q^{MAX}},$$

$$where: q^{MAX} = MAX(q_i(a_A), q_i(a_B), q_i(a_C), q_i(a_{AD}))$$

The maximal values for the q_1^{MAX}=1842,74 kg, q_2^{MAX} = 1,3990 mm. criterion function was determined, running Table 4. Based on this action, the normalizing measure of the value for the q_1, q_2 and function was implemented, according to the dependence presented in Table 5.

$$q_i \xrightarrow{normalisation} q_i^N$$

Table. 5. Normalized values for the coordinates of the a_A^N, a_A^N, a_A^N, a_A^N points in the (q_1^N, q_2^N) criteria space.

Normalized results	q_1^N	q_2^N
a_A^N	1,0000	0,5658
a_B^N	0,9268	1,0000
a_C^N	0,8118	0,4861
a_D^N	0,7550	0,5695

In Figure 4, the dimensional graph of the (q_1, q_2) target space was presented, where the unit of four a_A, a_B, a_C, a_D points, or vectors of quality for particular constructional solutions of (A, B, C, D), was also illustrated.

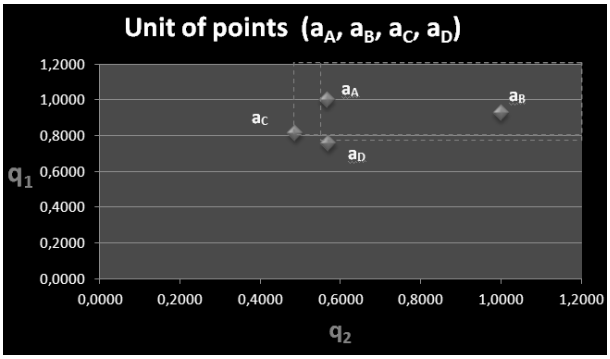

Fig. 4. Graphic illustration of the target space

When investigating into relations between the elements, the Pareto unit was determined, following the dependence:

$$x_p \in \Phi: \bigwedge_{x \in \Phi} \text{does not occur } Q(x) \overset{c}{\prec} Q(x_p),$$

polyyoptimal values were determined in the unit of obtainable targets or a_C and a_D. Consequently, polyoptical constructions are constructions valued by vectors of the x_3, x_4 decision-making variables. The element matched as a_A exists in the space determined by the positive cone of the a_C point, which means that a_C dominates over a_A. The similar situation is observed in the next case, where an element lies in the area of the cones of the aC and aD positive points, and this results that it is dominated by them. On the other hand, the aC and aD points are not dominated by one another, which means that they constitute representation matching the Pareto unit, that is poloptimal constructions. The graphic illustration of this problem is provided in Figure 5.

And subsequently, the task of polyoptimalisation was solved and also "the best element" was determined by the implementation of the target polyoptimalisation method.

DETERMINATION OF THE OPTIMAL SOLUTION WITH APPLICATION OF THE TARGET POLYOPTIMATISATION METHOD

The target method is applied when the target point in the target space, which would be an ideal solution if could be gained, is given. Such a point is always physically unapproachable (utopian) and usually it is the beginning of the co-ordinate system in the target space [12].

The target point forms the $q_1=0$ and $q_2=0$ co-ordinates (zero value for the weight of the frame construction and zero value for displacement), in the discussed problem.

The target polyoptimalisation depends on the searching for such solution of the Pareto unit (the x_3, x_4 constructions), for which the distance, in terms of the selected norm from the target solution, reaches its minimum in the target space. The solution existing in the closest range of the target point is treated as the most optimal.

In this way, a new target function is generated; it is made as the distance between the target state and the optional state in the target space, which can be recorded in the following way:

$$Q^*(x) = \|Q_0 - Q(x)\|,$$

where:

$$Q_0 = (q_{10}, \ldots, q_{s0}).$$

In the discussed case of polyoptimalisation of the construction of the subatmospheric press, when s=2 the Q_0 target point forms the following expression:

$$Q_0 = (q_{10} = 0, q_{20} = 0).$$

The Q*(x) function is a scalar function and determines the distance of the point belonging to the target space from the point at which it is aimed, and its value depends on the decision-making variables making up the $x=(x_1, \ldots, x_n)$. construction. The calculating methods of the one-criterion optimalisation are applied to reduce the Q*(x) function, and finds the .optimal solution in this explicit way.

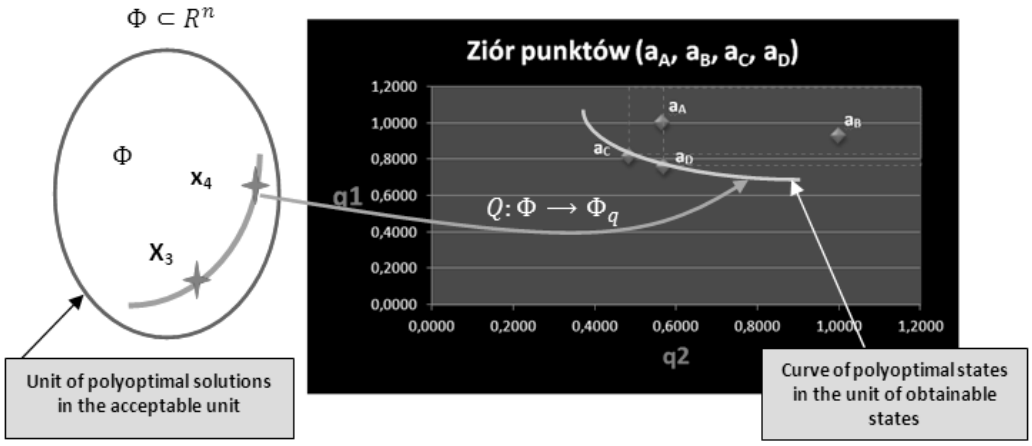

Fig. 5. Graphic illustration of the Pareto unit

The way the Q*(x) function is recorded depends on the accepted norm. In case of the Euclid norm, it forms the following expression:

$$Q(x) = \sqrt{\sum_{i=1}^{i=s} \left(q_{i0} - q_i(x)\right)^2}\,.$$

In case of polyoptimalisation of the subatmospheric press, for the case when s=2 and the qi values were normalised, the $Q_j(x)$ function will form the expression:

$$Q(x) = \sqrt{(q_{10} - q_1)^2 + (q_{20} - q_2)^2}.$$

Because of the fact that, in the discussed case, the co-ordinates of the target point in the target space are equal to zero, the Q(x) function forms the expression:

$$Q(x) = \sqrt{q_1^2 + q_2^2}\,.$$

In the analysed process of polyoptimalisation of the construction of the subatmospheric press, the Pareto unit is constituted of two (x_3, x_4), solutions, for which the values of the functions in the q_i target space as well as the distance from the Q(x) point at which it is aimed is presented in Table 5.

Table 6. Values for the Q(x) function

Normalised results	q_1^N	q_2^N	Q(x)
X_3	0,8118	0,4861	0,9462
X_4	0,7550	0,5695	0,9457

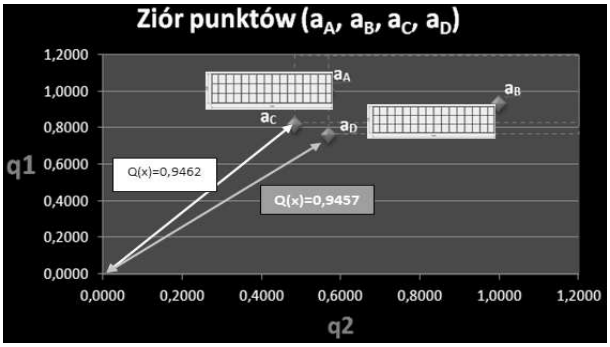

Fig. 6. The selection of the optimal point in the target space

The findings derived from the analysis of the calculations results, presented in Table 6 with graphic representation in Figure 6, lead to the ultimate conclusion that, it is the choice number 4 of the press for the construction of the subatmospheric press which is the optimal solution (the lowest value for the Q(x)=0,9457 function).

CONCLUSIONS

The results of the calculations are presented in the form of numerical maps, tabular listing, charts and graphs. The analysis of theoretical calculations demonstrated the compatibility with the results gained based on empirical research carried on in the "KONTENER" – Production of Building Elements LLC in Płock, Poland. Practical application of the CAD systems and the MES calculations, presented in the discussed matters, gives the following practical benefits:

- vast cut of time of applied researches and designing work due to numerical analysis of many possible options for the press,
- relief given to the investigational team from routines and uncreative working,
- completion of reliable researches with implementation of computer systems, at the project-stage of the press,
- possibility of optimalisation of the construction on the grounds of the chosen criterium.
- proposed methodology of researches was practically used to place orders for the needs of industry producing agricultural machines and devices, building industry and defense industry.

REFERENCES

1. **Branowski B., 1998:** Wprowadzenie do projektowania, PWN.
2. **Chlebus E., 2000:** Techniki komputerowe CAx w inżynierii produkcji, WNT.
3. **Dietrych J., 1978:** System i konstrukcja, WNT.
4. **Encarnacao J.L., Lindner R., Schlechtendahl E.G.,** Computer Aided Design, Springer-Verlag.
5. **Gendarz P., 1998:** Aplikacje programów graficznych w uporządkowanych rodzinach konstrukcji, Wydawnictwo Politechniki Śląskiej, Gliwice.
6. **Jaskulski A., 2009:** Autodesk Inventor 2009PL/2009+ metodyka projektowania, PWN.
7. **Jakliński J., Lodwik D., Malesa W., Wiktorski Z., 2012:** The test stand calculations of the research station of sub-atmospheric pressure press with implementation of the finite element method, TEKA Kom. Mot. I Eng. Roln. OL PAN, Vol 12. No. 2. 81–86.
8. **Król K., 2006:** Metoda elementów skończonych w obliczeniach konstrukcji, Politechnika Radomska, Wydawnictwo.
9. **Kruszewski J., Gawroński W., Wittbrodt E., Najbar F., Grabowski S., 1975:** Metoda sztywnych elementów skończonych, Arkady.
10. **Maksimow V., Galgash R., Synytsya L., 2010:** Information and organizational-economic aspects of innovative development management of regional enterprises, TEKA Kom. Mot. I Eng. Roln. OL PAN, 10D, 184–189.
11. **Niezgodziński M.E., Niezgodziński T., 1996:** Wzory, wykresy i tablice wytrzymałościowe, WNT.
12. **Osiński Z., Wróbel J., 1995:** Teoria konstrukcji, PWN,
13. **Rakowski G., Kacprzyk Z., 2005:** Metoda elementów skończonych w mechanice konstrukcji, OWPW.
14. **Rohatyński R., Miller D., 1994:** Problemy metodologii i komputerowego wspomagania projektowania technicznego, tom 1, Wydawnictwo Politechniki Wrocławskiej.

15. **Sydor M., 2009:** Wprowadzenie do CAD. Podstawy komputerowo wspomaganego projektowania, PWN.
16. **Szmelter J., Dacko M., Dobrociński S., Wieczorek M., 1979**: Metoda elementów skończonych w statyce konstrukcji. Przykłady obliczeń, Arkady.
17. **Szymczak C., 1998:** Elementy teorii projektowania, PWN.
18. **Tarnowski W., 1997:** Podstawy projektowania technicznego, WNT.
19. **Wróbel J., 2004:** Technika komputerowa dla mechaników, OWPW.
20. **Zagrajek. T., Krzesiński G., Marek P. 2006:** Metoda elementów skończonych w mechanice konstrukcji. Ćwiczenia z zastosowaniem systemu ANSYS, OWPW.
21. **Zienkiewicz O.C., 1972:** Metoda elementów skończonych, Arkady.

POLIOPTYMALIZACJA KONSTRUKCJI PRASY PODCIŚNIENIOWEJ Z ZASTOSOWANIEM METODY ELEMENTÓW SKOŃCZONYCH

Streszczenie. W artykule przedstawiono zastosowanie systemów CAD i metody elementów skończonych w procesie parametryzacji i polioptymalizacji stanowiska badawczego prasy podciśnieniowej. Uzyskane wyniki obliczeń przedstawiono w postaci map numerycznych, zestawień tabelarycznych oraz wykresów. Zaproponowana metodyka badań została praktycznie wykorzystana do realizacji zleceń dla potrzeb przemysłu maszyn i urządzeń rolniczych, budownictwa oraz przemysłu obronnego.

Słowa kluczowe: komputerowo wspomagane projektowanie, metoda elementów skończonych, naprężenia kontaktowe, rozkład naprężeń w glebie, prasa podciśnieniowa, parametryzacja, polioptymalizacja.

TEKA. COMMISSION OF MOTORIZATION AND ENERGETICS IN AGRICULTURE – 2013, Vol. 13, No. 1, 109–112

Effect of water content on the strain hysteresis of pea (*Pisum S.*)

Grzegorz Łysiak[1], *Ryszard Kulig*[1], *Stanisław Skonecki*[1], *Janusz Laskowski*[1], *Rafał Nadulski*[2]

[1]Department of Equipment Operation and Maintenance in the Food Industry,
[2]Department of Food Engineering and Machinery,
University of Life Sciences, Doświadczalna 44, 20-280 Lublin, Poland;
e-mail: grzegorz.lysiak@up.lublin.pl

Received December 16.2012; accepted March 14.2013

Summary. The paper presents results of tests on influence of pea moisture on parameters obtained in a test of axial loading and unloading. For the tests pea cv. Fidelia at the moisture ranging from 8 to 18% was used. The measurements were performed on a universal machine Zwick Z020. The load-displacement characteristics recorded using the TestXpert software by Zwick allowed to set out values of elastic and loss energies and corresponding deformations. An increase in seed moisture caused changes in values and relations between the aforementioned parameters. The lowest changes were observed for the elastic strain energy, which changed only slightly with the change of seed moisture. A considerable increase was observed for the lost energy, which also had significant influence on values of the total energy. Similar relations were found while analysing seed deformations.
Key words: compression, hysteresis, moisture, pea

INTRODUCTION

The great interest in studying of mechanical properties of food and agricultural materials is reasoned by fact that the latter have a crucial impact on conditions and outcomes of processing as well as properties of final products. Agricultural materials frequently discover a large variability in the response to mechanical loading. They change from brittle to elasto-plastic, plastic, viscous due to varying moisture, temperature, ripeness, and others [4, 10, 20]. Grace to this, on one hand a large spectrum of products can be obtained and on the other hand strict control of processing conditions is necessary for the optimization of outcomes.

Mechanical properties in relation to their processing and quality is an issue that has been studied with different approaches for years. Within the context, research on a material's elastic or plastic behaviour is one of the most important. Strain hysteresis is one of the available techniques, and addresses the amount of energy dissipated in the loaded body due to friction, internal damage, irreversible deformations etc. [1,7,13]. Thus, it can be used for description of the processes, for which such exchange is relevant. It can be related to a material's resistance to cracking [5,18], susceptibility to reversible deformations and internal damages, grindability and others [2]. Increased plasticity significantly influences breakage mechanisms, which leads to an increase in grinding energy requirements [3,10]. It is necessary in compaction processes, where it causes the agglomerate formation in an easier and more energy-efficient way [8,12,14,15]. In this context, the profound knowledge on materials response to loading is important for agglomeration of foods, feeds, biomass, and others [6,8,9,16,17].

The objective of the study is to focus on examining the effect of moisture content on the response of pea seed to cyclic loading.

MATERIAL AND METHODS

The Polish variety of pea (*Pisum sativum* L.) cv. Fidelia was used in the studies. The moisture content of a batch of seeds sample was determined applying the air oven method and drying three 5 g samples of pre-crushed seeds for over 3 h at a temperature of 105°C according to Polish Standard PN-86/A74011.The batch was subsequently divided into smaller samples, and to each of them, the amount of required water was added (or removed by drying in 40°C) to achieve moisture levels established at 8–18% (wet basis) with 2% increment. The added or removed amounts of water were achieved, according to the mass balance equations. The samples were then tempered in hermetic jars, and stored for 48 hours at ambient temperature.

Testing was carried out on a Zwick Z020 universal testing machine. An intact seed was positioned on the fixed bottom plate, such that the plane splitting two seed cotyledons was parallel to the compressive plates. The seed was then loaded and unloaded with the compression rate adjusted at 10 mm/min. The loading was performed until

a predefined force, set at 200N, was achieved. For each test load–displacement data were recorded using testXpert software by Zwick. On the basis of the strain hysteresis loops, an example of which is presented in Fig.1, partitions of strain energy and deformations were calculated (Fig. 1) [11,12,19]. In the figure, *Et* represents the total amount of strain energy absorbed by a seed during compression, while *En-r* and *Er* correspond to the irrecoverable and released energy respectively. All the experiments were done in 10 repetitions for each moisture level of seeds.

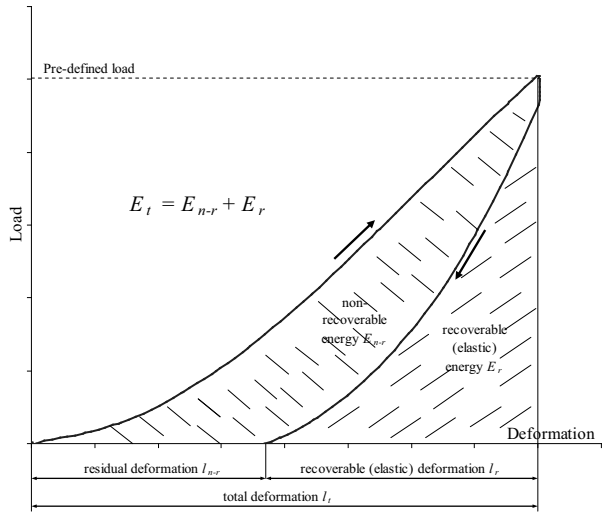

Fig. 1. Typical strain hysteresis curve while loading of a pea seed

Statistical analyses of the obtained parameters were done with a help of Statistica 6.0 software (StatSoft Inc.). Any verification of statistical hypotheses and development of mathematical models were done applying 95% probability level.

RESULTS

General view of the loading-unloading profiles in relation to moisture is given in Fig. 2.

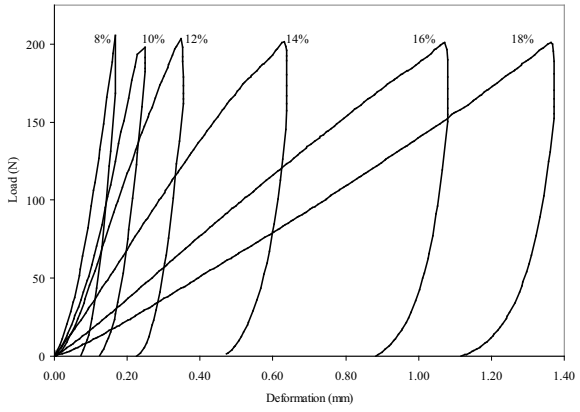

Fig. 2. Examples of hysteresis curves for pea seeds varying in moisture content

It is well noticeable, that the response of an individual seed to the compressive loading was strongly related to the amount of water content. An increase of moisture caused significant changes in the shape of the hysteresis loops. The area enclosed between the loading and unloading parts of the hysteresis curves increased very significantly with the moisture increment. It expresses the increased plasticity of seeds. As the result of it, the response of seed to mechanical loading is prevalently plastic in nature. The strain energy used is mainly released to permanent i.e. non recoverable deformations. They are not accompanied by readable cracking effects, what demonstrates the loss of brittleness and increased toughness of seeds. The results are in agreement with observed for pea [10], and similar to obtained by Łysiak et al. for wheat kernels [11].

A high increase of deformations up to the pre-defined load (200 N) was first and the best visible. The total deformation increased from about 0.20 mm to 1.63 mm. The differences were more considerable for moisture above 12%. This was confirmed by statistical analysis. The analyses applying Tukey procedures discovered that the average deformations obtained for the particular moisture levels were significantly different at 95% probability. It was observed that the increase in total deformation was mainly driven by the level of the permanent one. The latter increased in similar extent from 0.09 to 1.37 mm. The two were closely correlated. The elastic deformation increased with moisture as well, but relatively very slightly (Fig. 3).

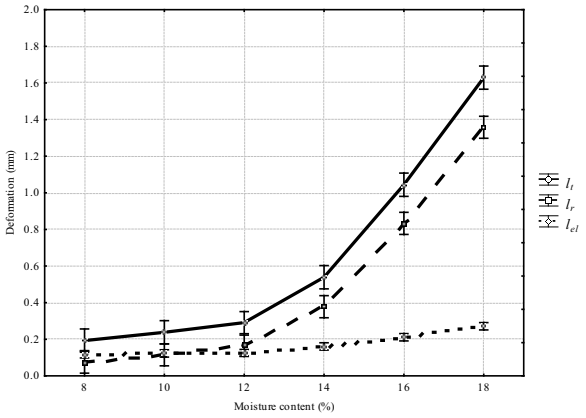

Fig. 3. Influence of seed moisture on values of total, elastic and lost deformations

Moisture content influenced the relative contribution of residual deformation in relation to elastic one (Fig. 4). The share of residual (permanent) deformation increased from 39% up to 83% in the studied moisture range. It was observed that the rate of the increment was higher at lower moisture levels, and slightly decreased above 14-16%. The differences were statistically confirmed at 95% probability.

The above analyzed total, residual and elastic deformations were expressed in function of seed moisture. It was done by means of regression equations and procedures included in a Statistica 6.0 software (Statsoft Inc.). The results are presented in table 1. In each case the best fitting to the experimental data was obtained for polynomial equations of the second degree. The right choice of the mathematical models was confirmed by the high values of

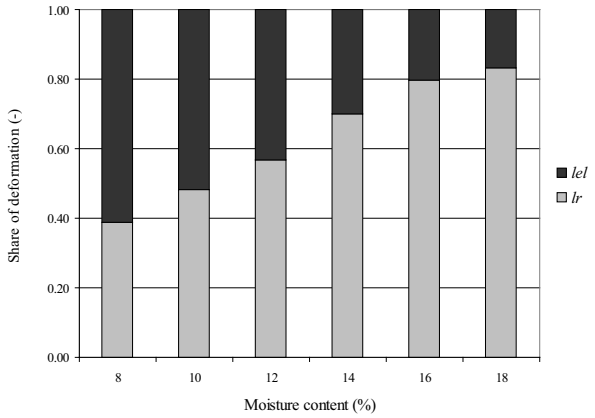

Fig. 4. Share of elastic and permanent deformation as a function of seed moisture

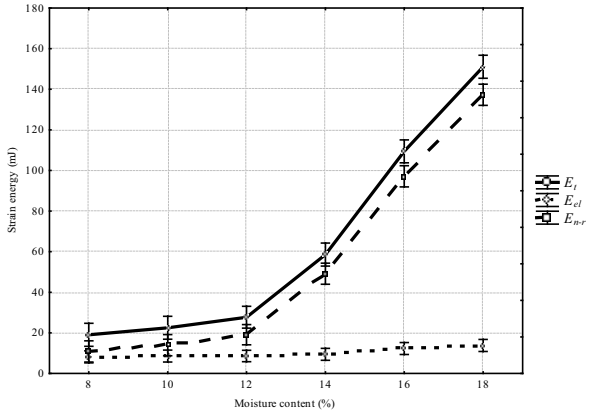

Fig. 5. Influence of seed moisture on values of total, elastic and non-recoverable strain energy

determination coefficients, which were generally higher than 0.99 (on the basis of averages values obtained for particular moisture level)

Table 1. Relations describing the influence of moisture of pea on the deformation during axial loading-unloading

Parameter	Equation form: $y = ax^2 + bx + c$			Determination coefficient R^2
	a	*b*	*c*	
Total deformation, l_t (mm)	0.0201	-0.3826	1.994	0.996
Residual deformation l_r (mm)	0.0180	-0.3438	1.696	0.996
Elastic deformation l_{el} (mm)	0.0021	-0.0388	0.297	0.996
Share of residual deformation (-)	-0.0009	0.0714	-0.137	0.985

x – moisture of pea seeds in % (w.b.)

The effect of moisture on the energies obtained in the hysteresis test was similar to the described above changes in deformations (Fig. 5 and 6). The total strain energy increased from about 20 mJ to 152 mJ. The relatively low increment for the lower moisture range (8-12%) was followed by a considerable increase for the moisture above 12%. It was confirmed that the strain energy inputs were mainly dependent on the energy absorbed for plastic deformations. The irreversible energy increased very significantly, from 0.12 mJ to 1.38 mJ.

The elastic energy changed relatively slightly with moisture, although a rise in this parameter was also observed.

The contribution of non-recoverable energy increased very significantly with the increase in amount of water (Fig. 6). The values ranged from 57% to 90%. The magnitude of changes decreased when moisture crossed 14-16%. The differences were statistically confirmed at 95% probability.

Similarly to the analyses done for the deformations, the strain energy release during the axial loading-unloading was related to the moisture of pea seeds. The results are presented in table 2. The best fitting to the experimental data was also obtained for polynomial equations of the second degree.

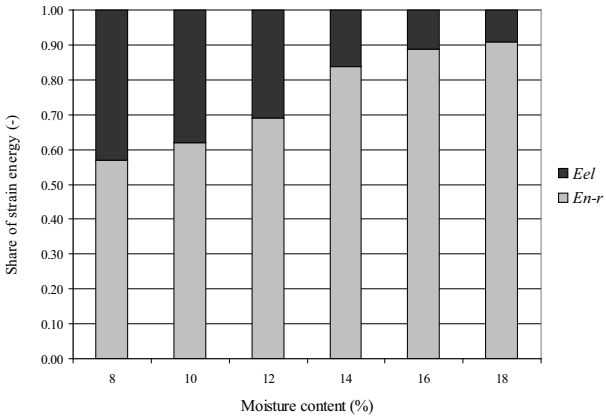

Fig. 6. Share of elastic and permanent energy as a function of seed moisture

The obtained relations were, like previously, characterized by high values of determination coefficients.

Table 2. Relations describing the influence of moisture of pea on the strain energy release during uniaxial loading-unloading

Parameter	Equation form: $y = ax^2 + bx + c$			Determination coefficient R^2
	a	*b*	*c*	
Total strain energy, E_t (mJ)	1.668	-29.77	150.4	0.992
Non-recoverable strain energy E_{n-r} (mJ)	1.592	-28.38	135.8	0.991
Elastic strain energy E_{el} (mJ)	0.0754	-1.387	14.56	0.968
Share of non-recoverable strain energy (-)	-0.0011	0.0657	0.0902	0.9548

x – moisture of pea seeds in % (w.b.)

CONCLUSIONS

1. The differences in water content of seeds were clearly reflected by changes in parameters obtained during cycling loading.
2. The studied increment in moisture resulted in an increase in elastic, permanent and total deformations. The most

significant influence was observed for the residual deformation.

3. The elastic energy changed only slightly with the rise in seed moisture. On the other hand, a considerable increase of the energy absorbed by irreversible processes was observed. It had a major influence on the total strain energy inputs during compression.
4. The share of non-reversible energy and deformation changed significantly with the seed moisture. The effect was observed mainly at lower moisture range.
5. The influence of moisture of pea on the parameters obtained during axial loading-unloading were the best described with the help of polynomial equations of the second degree. It concerns both analyzed deformation and strain energies.
6. The strain hysteresis data will be correlated to grinding and agglomeration, and are expected to be useful for a better understanding of the phenomena accompanying these processes. This is necessary both for of successive energy optimization and improving production quality.

REFERENCES

1. **Baste S.** 2001. Inelastic behaviour of ceramic-matrix composites. Composites Science and Technology, 61, 15, 2285–2297.
2. **Dobraszczyk B.J.** 1994. Fracture mechanics of vitreous and mealy wheat endosperm. Journal of Cereal Science, 19, 273–282.
3. **Dziki D., Laskowski J., Biernacka B., Siastała M.** 2011. Wpływ wilgotności na proces rozdrabniania ziarna pszenicy zróżnicowanego pod względem twardości. Inżynieria Rolnicza, Nr 1 (126), 47–53.
4. **Dziki D., Tomiło J., Różyło R., Laskowski J., Gawlik-Dziki U. 2012**. Influence of moisture content on the mechanical properties and grinding energy requirements of dried quince (Cydonia Oblonga Miller). TEKA Kom. Mot. Energ. Roln. 12, 2 13–18.
5. **Fossdal A., Einarsrud M-A., Grande T.** 2005. Mechanical properties of LaFeO3 ceramics. Journal of the European Ceramic Society, 25, 927–933.
6. **Kaliyan N., Morey R.V.** 2009. Constitutive model for densification of corn stover and switchgrass. Biosystems engineering 104, 47–63.
7. **Kucherskii A.M.** 2005. Hysteresis losses in carbon-black-filled rubbers under small and large elongations. Polymer Testing, 24, 6, 733–738.
8. **Kulig R., Laskowski J.** 2008. Effect of conditioning parameters on pellet temperature and energy consumption in the process of plant material pressing. TEKA Kom. Mot. Energ. Roln. 8a, 105–111.
9. **Kulig R., Laskowski J.** 2006. Effects of conditioning methods on energy consumption during pelleting. TEKA Kom. Mot. Energ. Roln., 6, 67–74.
10. **Łysiak G. 2007.** Fracture toughness of pea: Weibull analysis, Journal of Food Engineering, 83, 436–443.
11. **Łysiak G., Laskowski J., Gawłowski S.** 2006. Wpływ wilgotności na histerezę odkształceń ziarna pszenicy odmiany Kobra. Inżynieria Rolnicza, Nr 13 (88), 333–340
12. **Mohammed H., Briscoe B.J., Pitt K.G.** 2006. The intrinsic nature and the coherence of compacted pure pharmaceutical tablets, Powder Technology, 165 2006 11–21.
13. **Moorcroft C.I., Ogrodnik P.J., Thomas P.B.M., Wade R.H.** 2001. Mechanical properties of callus in human tibial fractures: a preliminary investigation Clinical Biomechanics, 16, 9, 776–782.
14. **Panasiewicz M.** 2009. An influence of kernel conditioning method on energy consumption during flaking process. TEKA Kom. Mot. Energ. Roln., 9, 211–216.
15. **Panasiewicz M., Mazur J., Sobczak P., Zawiślak K**. 2012. The analysis of the influence of initial processing of oat caryopses on the course and energy consumption of the flaking process. TEKA Kom. Mot. Energ. Roln. 12, 1, 195–199.
16. **Roopwani R., Buckner I.S.** 2011. Understanding deformation mechanisms during powder compaction using principal component analysis of compression data, International Journal of Pharmaceutics, 418, 227–234.
17. **Skonecki S., Kulig R., Laskowski J., Potręć M.** 2011. Wpływ wilgotności wiórów drewna sosny i topoli na parametry brykietowania. Inżynieria Rolnicza, Nr 1 (126), 245–252.
18. **Vincent J.F.V.** 1982. Structural Biomaterials. The Macmillan Press Ltd, Hong Kong, 1982.
19. **Wang T.H., Fang T-H., Lin Y-C.** 2007. A numerical study of factors affecting the characterization of nanoindentation on silicon. Materials Science and Engineering A 447, 244–253.
20. **Wójtowicz A.** 2012. Influence of process conditions on selected texture properties of precooked buckwheat pasta. TEKA Kom. Mot. Energ. Roln. 12, 1, 315–322.

WPŁYW WILGOTNOŚCI NA HISTEREZĘ ODKSZTAŁCEŃ NASION GROCHU (*PISUM S.)*

Streszczenie: W pracy przedstawiono wyniki badań nad wpływem wilgotności grochu na parametry uzyskane w wyniku osiowego cyklicznego ściskania. Do badań zastosowano groch odmiany Fidelia o wilgotności w zakresie 8-18%. Badania wykonano na uniwersalnej maszynie wytrzymałościowej Zwick Z020. Na podstawie eksperymentalnych charakterystyk siła-przemieszczenie, uzyskanych przy wykorzystaniu oprogramowania TestXpert firmy Zwick, określono wartości nakładów energii sprężystej, trwałej i całkowitej oraz odpowiadające im deformacje nasion. Wzrost wilgotności nasion powodował wyraźne zmiany w wartościach i wzajemnych relacjach pomiędzy analizowanymi parametrami. Najmniejsze zmiany obserwowano dla nakładów energii sprężystej, które w badanym zakresie wilgotności zmieniały się jedynie nieznacznie. Znaczący wzrost ze zwiększaniem wilgotności nasion odnotowano dla energii odkształceń trwałych, która też wywierała zasadniczy wpływ na wartość energii całkowitej. Podobne zależności stwierdzono w analizach oddziaływania wilgotności na wartości deformacji nasion.

Słowa kluczowe: ściskanie. histereza, wilgotność, groch

TEKA. COMMISSION OF MOTORIZATION AND ENERGETICS IN AGRICULTURE – 2013, Vol. 13, No. 1, 113–118

Modelling of operational cycle of hydraulic drive of lifting mechanism on the basis of axial piston hydraulic machines with discrete control

Ilia Nikolenko, Andrey Ryzhakov

National Academy of Environmental Protection and Resort Development,
181, Kievskaya str. , 95493 Simferopol, Autonomous Republic of Crimea, Ukraine
E-mail: napks@napks.edu.ua

Received January 25.2013; accepted March 14.2013

Summary. The mathematical model of hydraulic drive of lifting mechanism on the basis of discretely controlled bent axial piston hydraulic machines is developed. The model allows investigating of features of transients in hydraulic drive and control unit associated with the change of its operation mode, including physical and mechanical properties of power fluid.
Key words: axial piston hydraulic machines, hydraulic drive, mathematical model, discrete control, transients.

INTRODUCTION

The use of axial piston adjustable pumps and hydraulic motors in hydraulic drives of lifting mechanisms provides an ability of machines operating elements' speed control, with virtually no loss of energy by changing of hydraulic machines displacement. For lifting mechanisms it is enough to ensure the functioning of their operating elements in two modes: speed range operation (for operating element movement without load or with a cargo at the mean phase of lifting) and slow mode (for phases of cargo breakaway and completion of cargo movement). To ensure these two operation modes, one adjustable hydraulic machine with two fixed values of displacement is enough. Application of the second adjustable hydraulic machine in hydraulic drive allows increasing the number of different speeds of lifting mechanism up to four. Thus there is no need for manual or proportional control of lifting mechanism hydraulic drive, that requires rather complicated scheme of automatic control and increases the initial cost of hydraulic equipment and its maintenance and repair. Availability of mechanism's several speeds provides increasing of performance and workmanship of lifting machine, as well as reliability of the hydraulic drive.

Changing time parameters of discrete control of hydraulic drive, one can affect the nature of transients in the hydraulic system [1] arising from a change of APH and reducing the negative impact of pressure fluctuations in the hydraulic system.

Design solution and features of individual devices of APH displacement discrete control system affect the time value change of hydraulic machine displacement and nature of pressure fluctuations in the discharge line and in the line of displacement control system.

STATEMENT OF TASK

The objective of this paper was the creation of a mathematical model of lifting device hydraulic drive which allows carrying out numerical experiments for studying of progress of the transients and stable processes in hydraulic drive depending on its design features, physical and mechanical properties of power fluid and forces acting on the operating element of a lifting machine.

Results of numerical experiments can be used for optimization of discrete control procedure and technical parameters of hydraulic drive elements.

MATHEMATICAL MODEL

Hydraulic drive of lifting device comprises two bent axial piston hydraulic machines (P – Pump and M – hydraulic motor) with discrete two-level control of displacement (Fig. 1.). Pressure value in the discharge line of hydraulic drive is hydraulically controlled by overflow valve with direct action (V), with zero overlap, comprised of throttle (Th1).

Discrete change of displacement of the hydraulic machines P and M [2] is fulfilled by differential connection of hydraulic cylinders Hc, located in the control line (dashed line in Fig. 1.). Connection of hydraulic cylinders Hc is carried out by hydraulic distributors Hd.

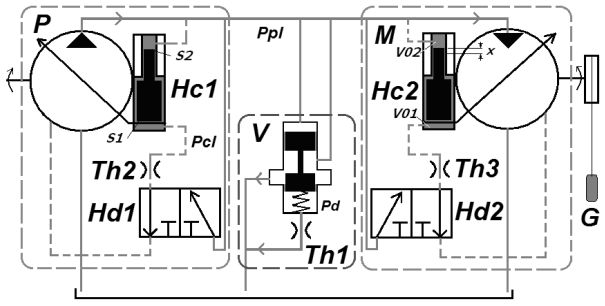

Fig. 1. Basic diagram of hydraulic drive of lifting device on the basis of discrete control axial-piston hydraulic machines

When developing a mathematical model of the hydraulic drive operation [3] it was assumed that:

– wave actions in pipelines are neglected [4] because of the short length of pipelines and minimum pressure loss at power fluid passing,
– no wave actions accompanying the transition of hydraulic cylinders of pumping unit from zone of suction to discharge zone and vice versa,
– little effect of friction forces in the piston supports on dynamics of pumping unit movement.

The following systems of equations are the basis of the mathematical model. Changes of pressure p_{pl} in discharge line of hydraulic drive and hydraulic motor speed w_m are found by simultaneous solving of equation of continuity (1), equation of moments (2), kinematic equations for hydraulic machines (3) and the equations that simulate the operation of overflow valve (4, 5):

$$Q_p - C_{pn}p_{pl} - \frac{V^p + V^{tr}}{E_a\left(p_{pl}, m_0\right)}\frac{dp_{pl}}{dt} - Q_V - Q_{Th1} - \\ -Q_{op} = Q_m + C_{mn}p_{pl} + \frac{V^M}{E_a\left(p_{pl}, m_0\right)}\cdot\frac{dp_{pl}}{dt}, \quad (1)$$

$$C_{p(m)n} = 1{,}23\cdot 10^{-8}\left(W^{p(m)}\right)^{0{,}7}/\mu(p_{pl}),$$

$$\beta = 4{,}2\cdot 10^4\cdot\mu(p_{pl})\cdot\left(W^m\right)^{1{,}6},$$

$$W_0^m p_{pl}\eta_m\eta_g - M_c - \beta\omega_m = J\frac{d\omega_m}{dt}. \quad (2)$$

The meanings of (1) and (2): $V^{p(m)}$ – P (M) hydraulic machine displacement; $C_{p(m)n}$ – leakage factor in P (M); V^{tr} – pressure pipeline volume; β – fluid friction coefficient M; J – integral inertia, reduced to the shaft. M_c – moment of resistance on the shaft M; $\eta_{m,g}$ – mechanical and hydromechanical efficiency coefficient. The model took into account that pump delivery flow Q_p and flow rate of the motor M are time variant in accordance with the kinematic dependencies for axial piston hydraulic machines [6]:

$$Q_{p(m)} = \sum_{i=1}^{k} Q_{ip(m)} = \frac{\pi d_{p(m)}^2}{4}\sum_{i=1}^{k}\frac{dx_{ip(m)}}{dt},$$

$$k = \frac{z\pm 1}{2}; \quad R' = \frac{\beta_{R'}\left(\gamma_{\max}, z\right)\cdot d_{p(m)}}{2}, \quad (3)$$

$$R = k_D\cdot R'; \quad d_{p(m)} = 2\cdot\beta_R\left(\gamma_{\max}, z\right)\cdot\sqrt[3]{V^{p(m)}}.$$

In equations (3): x_i – hydraulic machine i- piston stroke [5]; z – number of pistons of internal cylinder block ; d – diameter of the piston; and coefficient values $\beta_R\left(\gamma_{\max}, z\right)$ and $\beta_{R'}\left(\gamma_{\max}, z\right)$ are given in reference [7, 8].

The model of overflow valve V is given by equations (4):

$$m\frac{d^2z}{dt^2} = \left(p_{pl} - p_d\right)S_V - \left(z + z_0\right)\cdot c - F_{gtr} - F_g, \quad (4)$$

$$F_g = \rho Q_V^2\left(\frac{1}{S_V} - \frac{\cos(\theta/2)}{S_p}\right); S_p = \pi d_p\sin\frac{\theta}{2}\cdot z,$$

$$F_{gtr} = \frac{\left(p_{pl} - p_d\right)}{2}b\delta - \frac{\mu b\left(L + x\right)}{\delta}\cdot\frac{dx}{dt}.$$

In equations (4): p_d – pressure in damping cavity of overflow valve V; z – offset of shut-off-and-regulating element of the valve V; F_{gtr} and F_g – liquid friction forces and hydrodynamic force acting on shut-off-and-regulating element ; c – spring stiffness V; θ – cone angle of shut-off element V. Power fluid flow rates Q_V through the valve V and throttle Th1 are given by the equation (5):

$$Q_V = \pi\mu_{Th1}d_p\sin\frac{\theta}{2}\sqrt{\frac{2p_{pl}}{\rho}}z, \quad (5)$$

$$S_V\frac{dz}{dt} = Q_{Th1} + \frac{V_{Th1}}{E_a}\frac{dp_d}{dt}; \quad Q_{Th1} = \mu_{Th1}S_{Th1}\sqrt{\frac{2p_d}{\rho}}.$$

Hydrodynamic processes of power fluid motion in the control line of hydraulic drive between the discharge line and cavities of hydraulic cylinders Hc, at displacement decreasing, are described by differential equation (6), and at displacement increasing – by the equation (7):

$$Q_{Th} = \mu_{Th}\cdot S_{Th}\cdot\sqrt{\frac{2}{\rho}\left(p_{pl} - p_{cl}\right)} = S_{1Hc}\frac{dy}{dt} + \\ + \frac{V_{01Hc} + S_{1Hc}\cdot y}{E_a}\cdot\frac{dp_{cl}}{dt}, \quad (6)$$

$$Q_{Th} = \mu_{Th}\cdot S_{Th}\cdot\sqrt{\frac{2}{\rho}\left(p_{cl} - p_0\right)} + \frac{dp_{cl}}{dt}\cdot \\ \cdot\frac{V_{01Hc} + S_{1Hc}\cdot y}{E_a} = -S_1\frac{dy}{dt}. \quad (7)$$

Relationship of the mathematical model of the stroker (6, 7) with the equation of continuity of the initial model (1) is carried out by means of equations (8 and 9 – in the cases of displacement increasing and decreasing, respectively) describing the flow rate of power fluid Q_{op} to ensure the operation of the stroker:

$$Q_{op} = Q_{Th} - S_{2Hc} \cdot \frac{dy}{dt}, \quad (8)$$

$$Q_{op} = \frac{V_{02Hc} + S_{2Hc} \cdot (y_{\max} - y)}{E_a} \cdot \frac{dp_{pl}}{dt} - S_{2Hc} \cdot \frac{dy}{dt}. \quad (9)$$

The meanings of (6 – 9): p_{cl} – power fluid pressure in the control line (Fig. 1); y – offset of hydraulic cylinder piston Hc; $S_{1,2Hc}$ - area of larger and smaller sections of hydraulic cylinder piston Hc, respectively; $V_{01,2Hc}$ – appropriate minimum cavity volumes of hydraulic cylinder.

Dynamics of hydraulic cylinder piston Hc of hydraulic machine stroker is described [9, 10] by equations (10):

$$m\frac{d^2y}{dt^2} = -S_{2Hc} \cdot p_{pl} + S_{1Hc} \cdot p_{cl} - F_{gtr} - \\ -sign\left(\frac{dx}{dt}\right) \cdot F_{tr} - F_G - F_{in}, \quad (10)$$

$$F_{gtr} = \mu \frac{S_{tr}}{\Delta} \frac{dy}{dt};\ F_G = Mg \cdot \frac{l}{L} \cdot \cos\gamma,$$

$$F_{tr} = \nu_{tr} \cdot \left(z \cdot S_{bc} - k \cdot S_s\right) \cdot p_{pl},$$

$$F_{in} = \left(m_p + \frac{1}{2} m_{pit}\right) \omega_{P,M}^2 \frac{r}{L} \sum_{j=1}^{k} \left[z_j(t) \cdot \right.$$

$$\left. \cdot \sin\left(\omega_{P,M} \cdot t - \delta_j\right)\right],$$

$$\gamma[\deg ree] = -4.5[\frac{\deg ree}{cm}]y + \gamma_{\max}.$$

The meanings of (10): F_{gtr} – viscous friction force of the hydraulic cylinder piston; F_G – force applied to hydraulic cylinder piston Hc by weight of hydraulic machine pumping unit on the control block; F_{tr} – sliding frictional force of the hydraulic distributor; F_{in} – oscillating inertial force of the pistons of pumping unit; γ – bent angle of cylinder block. S_{bc} – sectional area of the piston of pumping unit; S_s – the effective surface area of the distributor, on which squeezing pressure of discharge line acts; δ – phase shift between the pistons of pumping unit; m_p and m_{pit} – masses of the piston and piston rod of pumping unit, respectively.

For lifting device, external forces of torque value M_c acting on the axis of hydraulic motor M, that is a member of the moment equation (2) is found by solving [11] of equations (11). For generation of the equations (11), as a part of the engineering approach, let us present the hoisting rope as a bar, endowed with longitudinal stiffness k of the rope. Tension in the rope is assumed to be uniformly distributed over its cross-section:

$$\frac{d^2h}{dt^2} = g - \frac{k}{M}h - 2 \cdot \delta \cdot \frac{dh}{dt} + a_i, \quad (11)$$

$$a_i = \frac{d\upsilon}{dt} = \frac{D_b}{2} \cdot \frac{d\omega_M}{dt},$$

$$\omega_0 = \sqrt{k/M},\ 2 \cdot \delta = \tau_{tr} \cdot \omega_0^2,\ k = E_d \cdot S / L,$$

$$E_d = \frac{\rho_L}{S} \cdot a^2,\ M_c = k \cdot y \cdot n \cdot D_b / 2.$$

In the equations (11): h – shifting of cargo with weight $G = Mg$; δ – damping factor; a_i – inertia of acceleration; D_b – diameter of the lifting device unit; τ_{tr} – time constant of internal friction; E_d – dynamic modulus of elasticity; a – wave velocity in spiral ropes. Dependences of main parameters that characterize physical and mechanical properties of power fluid – adiabatic bulk modulus E_a, density – ρ and dynamic viscosity – μ from pressure of power fluid p and percentage of non-dissolved air [12] are given by equations (12):

$$\mu(p) = \mu_0 \cdot \exp\left(\frac{p - p_0}{k_\mu}\right), \quad (12)$$

$$E_a(p) = \frac{kE_a^p\left[\left(E_a^0/E_a^p\right)^{1/A} + \bar{m}\left(p_p^0\right)^{1/k}\right]}{k\left(E_a^0/E_a^p\right)^{1/A} + \bar{m}\frac{E_a^p}{\left(p_i + 1\right)}\left(p_p^0\right)^{1/k}},$$

$$\rho(p) = \rho_0\left(\left(A_a\sqrt{\frac{E_a^0}{E_a^p}} + \bar{m}\sqrt[k]{p_p^0}\right)\left(1 - m_0\right)\right)^{-1},$$

$$E_a^p = A_a p + B_a,\ E_a^0 = A_a p_0 + B_a,$$

$$p_p^0 = \left(p_0 + 1\right)/\left(p + 1\right),\ \bar{m} = \frac{m_0}{1 - m_0},$$

$$k = c_p / c_V.$$

In equations (12): μ_0, E_a^0, ρ_0 – the values of dynamic viscosity, bulk modulus and density of power fluid under pressure p_0. The parameters A_a, B_a и k_μ are determined from experimental data for a particular power fluid.

RESULTS AND DISCUSSION

The system of equations (1 – 12) contains the nonlinear differential equations, which eliminates the possibility of its analytic solving. The system was integrated numerically by Bogacki – Shampine using the program Matlab. The results of numerical experiments allow conducting work analysis of both individual hydraulic drives and the whole hydraulic system. The results of numerical modelling of complete cycle of hydraulic drive operation were obtained that provide two possible speeds of lifting mechanism. Complete cycle of operation of lifting mechanism includes: cargo breakaway at the lowest speed, cargo movement at the maximum speed of movement and the completion of movement at the lowest speed. To analyze the effect of different parameters on the hydraulic drive operation various factors were changed: time change τ_0 of hydraulic drive operation mode and physical

and mechanical conditions of power fluid – viscosity μ, density ρ, adiabatic bulk modulus E_a and percentage of undissolved air in power fluid – m_0. Also different models describing the dependence of values μ, ρ and E_a from pressure were compared. The values of the parameters that were used for graphing in Figures 2 – 4 are shown in Table 1.

Table 1. Model varied parameters values

№	τ_{01}, s	τ_{02}, s	μ, MPa s	ρ, MPa s²/cm²	E_a, MPa	m_0, %
1	1	3.5	$\mu(p)$	$\rho(p)$	$E_a(p)$	0
2	1	3.5	1.78 ^{10}-8	8.9 ^{10}-8	$E_a(p)$	0
3	1	3.5	1.78 10^{-8}	8.9 10^{-8}	1880	0
4	0.25	3.5	$\mu(p)$	$\rho(p)$	$E_a(p)$	0
5	0.25	3.5	$\mu(p)$	$\rho(p)$	$E_a(p)$	5
6	-	-	$\mu(p)$	$\rho(p)$	$E_a(p)$	0

The parameters' values $\mu(p), \rho(p)$ and $E(p)$ are considered as functions of pressure in this part of hydraulic drive and were found by equations (12). Time τ_{01} defines the beginning of hydraulic motor M displacement decrease with values $V_M = 112cm^3$ up to $V_M = 56cm^3$, and time τ_{02} – the beginning of its increase up to the initial value.

In Fig. 1. dynamics of power fluid pressure in discharge line of the hydraulic drive under different operation modes are shown.

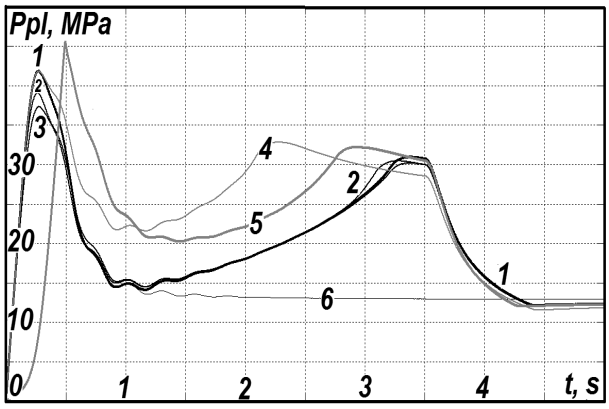

Fig. 2. Pressure in discharge line of lifting device hydraulic drive under different operating conditions

The graph 6 (Fig. 2.) shows the change of pressure in the discharge line of hydraulic drive during the transition process associated with actuation of hydraulic drive. Change of motor displacement for case 6 was not carried out. For transients, shown in Figures 1 – 3 (Fig. 2.), decrease of motor displacement (from value – $V_M = 112cm^3$ up to $V_M = 56cm^3$) began upon expiration of time $\tau_{01} = 1s$ after hydraulic drive starting, the reverse change V_M began in time period $\tau_{02} = 3.5s$ from the moment of process starting. For processes in graphs 4 and 5 displacement decrease V_M began at $\tau_{01} = 0.25s$. Duration of stable process, between changes of displacement V_M, was given as a minimum value in order to reduce computation time.

A given increase of hydraulic motor displacement causes pressure boost in the discharge line of hydraulic drive up to value – $p_{pl} = 3/4 \cdot p_{pl}^{\max}$, where $p_{pl}^{\max}$ – maximum pressure surge at actuation of hydraulic drive without changing of hydraulic motor displacement. In graphs 2 and 3 the results of calculations for the transient process similar to process 1 are shown, but density and viscosity parameters were considered as depended constant values (Table 1.). From these calculations it follows that such a simplification of the model affects only the analysis of non-stable processes and leads to a relative error in the amplitude of pressure pulse, which does not exceed 12%.

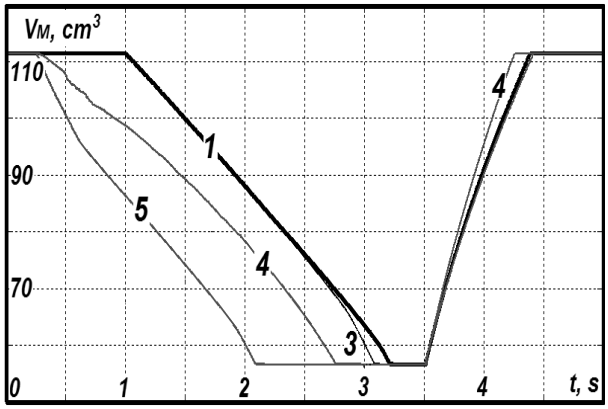

Fig. 3. Changes of hydraulic motor displacement at varying of cargo lifting speed

For processes 1 – 3, two times decrease of displacement motor M takes up some time -about 2.25s. The reverse process is faster – for a period of time about 1s (Fig. 3). The difference in response time of the control system is observed, despite the fact that the differential circuit connection of hydraulic cylinder Hc2, piston sectional area ratio is equal to $S_{2Hc}/S_{1Hc} = 2$. It can be explained if we consider that in the control line P and M the throttle Th is located which slows down pressure increase in the control line at displacement decrease of the hydraulic machine. Dynamics of pressure change in the control line for processes 1 and 5 is shown in Fig. 4. Comparison of graphs 5 in Figures 3 and 4 leads to the conclusion that the high rate of motor displacement decrease, at the initial phase of the process is directly connected with pressure surge of the control line.

Dependencies for the transient process 5, in contrast to previous relationships, were considered the influence of undissolved air bubbles on physical and mechanical properties of power fluid.

This feature leads to increase compressibility of power fluid, time delay in reaching of peak pressure in the transient process (Fig. 2.) and increase the value of pressure starting level in the control line (Fig. 4).

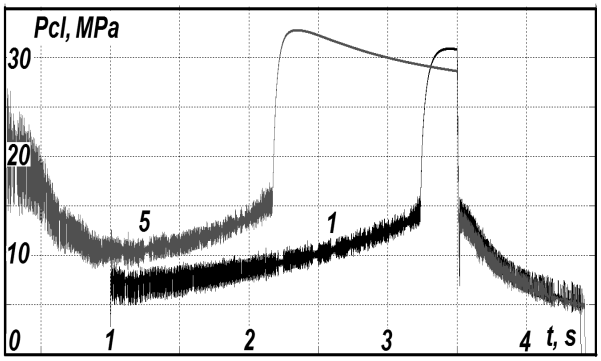

Fig. 4. Pressure change in the control line at hydraulic motor displacement change

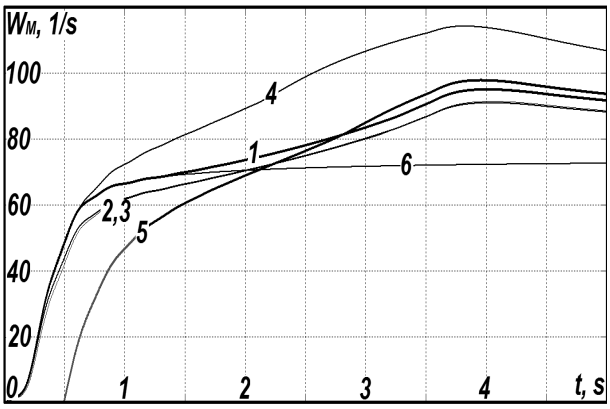

Fig. 5. Dynamics of hydraulic motor shaft acceleration under different operation modes of hydraulic drive of lifting device. Figure 5 shows the time dependence of angular speed of hydraulic motor shaft under different operation conditions of hydraulic drive. By comparison of curves 1 and 6 it can be seen that the expected increase of hydraulic motor shaft speed, at changing its displacement by two, will be resulted in 30%. More significant speed increase at the beginning of cargo lifting can be achieved by use of control 4

CONCLUSIONS

The numerical experiments show the possibility of use of the developed model to simulate the transient and stable state processes in hydraulic drive of lifting mechanism on the basis of discretely controlled bent axial piston hydraulic machines.

The numerical calculations within the framework of the developed model can be used for optimization of the control procedure of lifting mechanism for road building machine for the purpose of decrease of negative impact of pressure fluctuations on the hydraulic system, increase of its performance and workmanship of lifting machine, as well as reliability of the hydraulic drive.

REFERENCES

1. **A. Ryzhakov, I. Nikolenko, K. Dreszer, 2009:** Selection of discretely adjustable pump parameters for hydraulic drives of mobile equipment. – TEKA Kom. Mot. Energ. Roln. – OL. PAN, vol. IX, 267–276.
2. **Nikolenko I. V., Ryzhakov A. N., 2012:** A mathematical model of the control system of displacement of hydraulic drive of axial piston machines of road building machine. – Kiev. – GBDMM. – № 79. 25–30.
3. **Ilya Nikolenko, Eugeniusz Krasowski, 2002:** Tendencies of development in the field of designs and calculation methods of axial piston hydromashines. TEKA Kom. Mot. Energ. Roln. – OL. PAN, vol. II, 149–157.
4. **AndrenkoP.N., Panaiareva O.B., 2012:** Investigation of wave processes in supply hydraulic unit of hydraulic systems. – MOTROL, v.14. – Simferopol – Lublin, 3–10.
5. **Prokofiev V.N., Sinev A.V. 1964:** Kinematic connection in gimballess axial piston hydraulic drives. – Journal of Mechanical Engineering.- № 11. 14–18.
6. **Ryzhakov A. N., Nikolenko I. 2010:** Influence of kinematics of axial piston hydraulic machines with discrete control on the nature of transients.– MOTROL, v. 12D. – Simferopol – Lublin, 110–116.
7. **Nikolenko I.V., 2006:** Determination of geometrical parameters of axial piston hydraulic machine of pumping unit with minimum sizes.– Industrial Hydraulics and Pneumatics. – 4(14) – 75–78.
8. **Ilya Nikolenko, Eugeniusz Krasowski, 2003:** The influence of a bent axis angle on the dimensions of an axial piston hydromashine. – TEKA Kom. Mot. Energ. Roln. – OL. PAN, vol. III, 192–200.
9. **Nikolenko I.V., Ryzhakov A.N., 2012:** Dynamics of stroker of axial piston hydraulic machine with discrete control. Scientific work of Donetsk NTU, series: Mining – and – electromechanical, issue. 23 (196). – Donetsk. 192–203.
10. **Ilya Nikolenko, Eugeniusz Krasowski, Victor Nikolenko, 2003:** Increases of nominal pressure at hydraulic unloading of the of the swinging unit in the axial piston hydromashine. – TEKA Kom. Mot. Energ. Roln. – OL. PAN, vol. VI, 102–108.
11. **Nikolenko I.V., Ryzhakov A.N., 2010:** Influence of dynamic loads in load carrying elements on the nature of transients in hydraulic drive of lifting mechanism.– Kiev. – GBDMM. – № 76. 21–26.
12. **Lurie Z. Ya., Fedorenko I.M. 2010:** Investigation of operation process of mechatronic hydraulic device of lubrication system for metallurgical equipment with consideration of characteristics of two-phase fluid. – MOTROL, vol. 12 C. – Simferopol – Lublin. 10–26.

МОДЕЛИРОВАНИЕ РАБОЧЕГО ЦИКЛА ГИДРОПРИВОДА МЕХАНИЗМА ПОДЪЕМА НА ОСНОВЕ АКСИАЛЬНО-ПОРШНЕВЫХ ГИДРОМАШИН С ДИСКРЕТНЫМ УПРАВЛЕНИЕМ

Аннотация. Разработана математическая модель гидропривода механизма подъема на основе аксиально-поршневых дискретно регулируемых гидромашин с наклонным блоком цилиндров. Модель позволяет исследовать особенности переходных процессов в гидроприводе и блоке управления, связанных с изменением режима их работы, с учетом физико-механических свойств рабочей жидкости.

Ключевые слова: аксиально-поршневые гидромашины, гидропривод, математическая модель, дискретное регулирование, переходные процессы.

TEKA. COMMISSION OF MOTORIZATION AND ENERGETICS IN AGRICULTURE – 2013, Vol. 13, No. 1, 119–126

Casting alloys for agricultural tools operating under the harsh conditions of abrasive wear

Zenon Pirowski[1], *Marek Gościański*[2]

[1]Foundry Research Institute,
Poland, 31-418 Kraków, 73 Zakopiańska Street, pirowski@iod.krakow.pl
[2]Industrial Institute of Agricultural Engineering,
Poland, 60-963 Poznań, 31 Starołęcka Street, margos@pimr.poznan.pl

Received February 19.2013; accepted March 14.2013

Summary. This paper addresses some issues related with the process of tribological wear, focusing on the phenomena that occur during the abrasive wear of parts. Mechanisms of this process were discussed, most important materials resistant to this type of wear were characterised and examples of castings designed for the agricultural sector, developed and manufactured by the Foundry Research Institute in Cracow in collaboration with the Research Institute of Agricultural Engineering in Poznań, were demonstrated. Then the leading methods used in the assessment of abrasive wear resistance of alloys, erosive wear included, were classified and described. The results of own research were quoted as an example. It has been proved that modern casting alloys can successfully compete with the wrought stock.
Key words: tribology, studies, castings, cast alloys, agricultural tools.

INTRODUCTION

Progress in many areas of the economy, the agricultural sector included, is dependent on the development trends in the art of designing machinery and equipment for operation under the increasingly difficult conditions. Technical progress in this area depends on the cooperation of specialists from a variety of industries, and on the close relations between the sphere of scientific research – on the one hand, and the producers of equipment and users of this equipment – on the other. Such interactions should form a type of closed loop. Materials of better performance durability enable the design of advanced structures. Advanced structures increase the efficiency of modern machinery and equipment, but require from materials engineering the development of better materials. Higher efficiency of equipment requires the use of materials more resistant to wear under the increasingly harsh operating conditions. This co-action must be supported by research work in the areas of fundamental theory, experimental trials and field testing of new products (Fig. 1).

Extreme operating conditions of machines and equipment mainly include corrosion with all its variations, the effect of high temperatures, often combined with the need to carry variable stress, and tribological wear. Abrasive wear, which is one of many types of tribological wear, is the subject of this study.

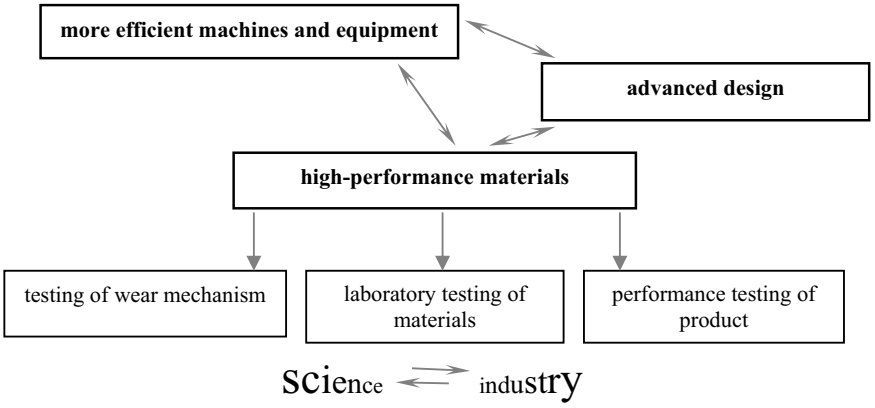

Fig. 1. The interaction of science and practice in improving the competitiveness of machinery and equipment

TRIBOLOGY

Tribology is the science of friction and of the processes accompanying this phenomenon. The name derives from the Greek words tribus – friction, logos – science. Tribology as a science deals with the description of physical, chemical, biological and other related phenomena occurring in the areas of friction. As a science, this field of knowledge was formally established in 1966. Previously, the individual issues of tribology were included in other disciplines.

Tribological wear is an important cause of failure of machinery and equipment. It is caused by the process of friction which leads to a change in weight, structure and properties of the surface layers of contacting bodies. The intensity of wear is a function of different types of interactions and of the resistance of these layers.

Generally speaking, there is no one single type of tribological wear that would have an exclusive influence on the whole process; the decisive effect has the leading mechanism. The elementary tribological processes are:

- loss of material (microcutting, detachment of surface irregularities, brittle cracking, peeling),
- transfer of material (ploughing, polishing, indentation),
- discontinuity of material (surface scratches, dimples)
- accretions (build ups, antibodies, oxide films, deposits),
- changes in geometric structure of the surface (deformation, directional shifting of
- structure, phase transformations),
- changes in chemical composition (new components, surface oxides).

Among the types of tribological wear, the following ones can be identified: abrasive wear, adhesive wear, scuffing, oxidation wear, fatigue wear by spalling (flaking wear), fatigue wear by pitting, fretting. All these types of wear are described in technical publications dealing specifically with the tribological wear [1, 2, 3, 4, 5, 6, 7, 8]. Here only the abrasive wear will be discussed.

ABRASIVE WEAR

Abrasive wear is the most common tribological process of destruction. It arises when the loss of material in the surface layer is caused by the particle detachment due to *microcutting, scratching or ploughing*. This process occurs when within the areas of friction between the mating parts there are loose or fixed abrasive particles or protruding asperities of harder material, which play the role of local micro-edges. In a similar way oxidised products of wear operate within the friction area [1, 2, 3, 4, 5, 6, 7, 8].

Figure 2 presents a dynamic model of the elementary processes of the wear due to abrasion.

As a criterion distinguishing the type of wear, a quotient of the surface area of the cross-sections of the scratch recess (F_2) and swelling of material around the scratch (F_1) was adopted. This is illustrated in Figure 3.

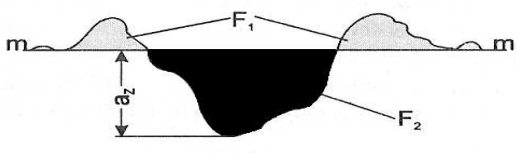

Fig. 3. Criterion distinguishing the types of wear [7]
az – depth of recess, ***m-m*** – reference level

If $F_1/F_2 = 1$, it means that only plastic deformation in the contact areas, or ploughing, occurs. The material indented by protruding asperity or abrasive grain is "pushed" outside the surface (swelling of material on both sides of the scratch).

If $F_1/F_2 = 0$, that is, cross-sectional area of the swollen material is equal to zero ($F_1 = 0$), it means that only microcutting occurs.

If $0 \leq 1 \leq F_1/F_2$, it means that microcutting, plastic deformation and scratching occur.

During scratching, the material within the region of abrasive wear is crushed, upset and cut (chips, other products of wear).

The resistance to abrasive wear depends on many factors such as:

- chemical and fractional composition of loose or fixed abrasive particles,
- relative hardness of abrasive particles compared with hardness of the material exposed to wear,
- specific pressure,
- frequency of the replacement of products in the areas of friction (blowing out, rinsing),
- slip velocity.

Abrasion can take place through:

- grains fixed in mating surfaces,
- single loose abrasive grains,
- abrasive layer that occurs between mating surfaces,
- abrasive jet,
- abrasive environment.

In the case of mating machine parts, due to the impact of mating surfaces, the rubbing grains can execute:

- a translatory motion in direction parallel to the abraded surface,
- a rotary motion in respect of their own axis (rolling).

ploughing *cutting of asperities* *cutting of irregularities with abrasive through protruding asperity* *plastic deformation of material*

Fig. 2. Dynamic model of the elementary wear process types [7]

In the case of grinding, especially crushing of hard materials, the abrasion is characterised by:
– larger dynamics of the effect of forces acting between the abraded surface and grains,
– greater irregularity in the motion of these grains,
– higher proportional share of components normal to the surface, resulting in a dynamic crushing.

Abrasion in an abrasive jet (erosion) means the impact of a jet of fluid or gas, in which the abrasive particles are suspended (e.g. abrasion by sand blasting, abrasive wear by particles suspended in water or other liquids).

Abrasion of metals in an abrasive environment (e.g. caterpillars of vehicles) is characterised by large kinetic energy of the abrasive grains. The grain contact with the abraded surface occurs under the effect of forces performing the work of abrasive wear and crushing of the material. In many cases, the abrasive agent is soil in which there are mineral grains (mainly silica), causing the abrasive effect.

Experimental relationships were obtained between the relative abrasive wear resistance and hardness of metals (Fig. 4).

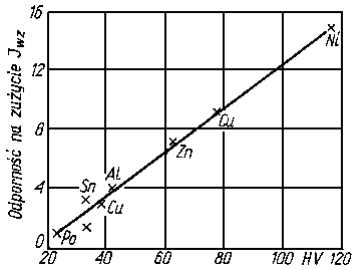

Fig. 4. Relationship between relative abrasive wear resistance ($\mathbf{J}_{wz}$) and Vickers hardness (**HV**) of metals [1]

As follows from this chart, there is a linear relationship between the increase in the relative abrasive wear resistance of metals and hardness (in the case when hardness of the abrasive material is much higher than the hardness of the abraded metal).

Obviously, the relative abrasive wear resistance of steels of different types (steels hardened, tempered, carbon-containing, alloyed, etc.) is also different, but in each case (alloy grade) this resistance is proportional to the hardness of the abraded material. The quotient of the relative abrasive wear resistance of metal (J_{wz}) and its hardness (HV) is for a given family of metals (alloys) constant, that is:

$$J_{wz} / HV = \text{const.}$$

Penetration of abrasive particles into the top layer of the abraded metal often causes serious anomalies in the intensity and mechanism of abrasive wear.

With significant differences in the hardness of mating parts, eventually it is the harder metal that can suffer a more intensive wear. This is due to penetration of a large number of abrasive grains into a softer metal. Due to this, the friction surfaces get coated with a specific kind of abrasive "brush", composed of hard abrasive particles and soft metal layers binding them together.

As a result of this phenomenon, the softer metal becomes a kind of grinding wheel, which causes intense cutting of hard metal.

THE ABRASIVE WEAR OF IRON ALLOYS

In the examination of carbon steel, the results were obtained from which the following general conclusions were drawn:
– pearlitic structures with lamellar pearlite are slightly more resistant to abrasion than structures with spheroidal pearlite (Fig. 5),

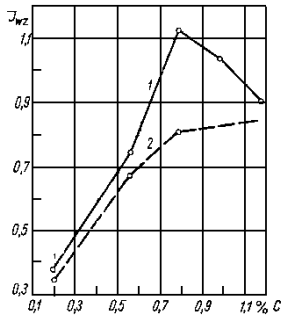

Fig. 5. Effect of pearlite structure on changes in the relationship between hardness and abrasive wear resistance [1];
1 – steel with lamellar pearlite,
2 – steel with spheroidal pearlite

– the wear resistance of hardened steel increases with the increasing carbon content, but starting with 0.8% this increase is gradually becoming less intense, to disappear almost completely at 1% C (Fig. 6).

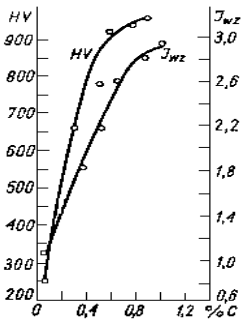

Fig. 6. Relationship between hardness (**HV**) and abrasive wear resistance ($\mathbf{J}_{wz}$) of hardened steels as a function of the carbon content [1]

– in steels quenched and tempered, the abrasive wear resistance decreases with increasing temperature of tempering, but to a lesser extent than the hardness (Fig. 7),
– most abrasion-resistant are non-tempered martensitic structures,
– the increasing content of retained austenite in the structure of martensitic tool steels makes their abrasive wear resistance decrease,
– in hypoeutectoid, annealed, ferritic-pearlitic steels, when the increase in hardness with the increase in carbon content is due only to the increasing content of pearlite of

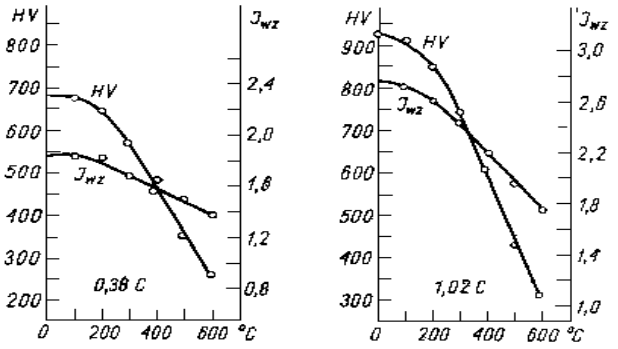

Fig. 7. Relationship between hardness (**HV**) and abrasive wear resistance ($\mathbf{J}_{wz}$) of steel as a function of the tempering temperature [1]

the same structure, i.e. to the change in the phase content ratio without any change in the essential characteristics of the structure, the resistance to abrasion is strongly dependent on the hardness,
- as soon as the eutectoid point is exceeded (according to some studies even a little earlier), and the microstructure of the steel changes quite significantly, the relationship between these parameters, valid for the hypoeutectoid steels, now loses its validity,
- changes in the structure of pearlite also change in both ranges the relationship between hardness and abrasive wear resistance (Fig. 5),
- the relationship between hardness and abrasive wear resistance seems to be valid only for structures of the same type,
- the increase in "natural" hardness, i.e. in hardness of pure metals and annealed steels, is accompanied by much more pronounced increase in the abrasive wear resistance than the increase obtained by quenching and tempering,
- the increase in hardness as a result of cold work, which does not cause any phase transformations in the hardened layer, such as e.g. the transformation of austenite into martensite, gives practically no improvement in the abrasive wear resistance,
- the aforementioned relationships confirm the thesis given previously that only structural changes caused by the heat treatment, mechanical treatment, etc. determine changes in the abrasive wear resistance of a material, and not the associated increase in hardness.

The abrasive wear resistance of cast iron as an alloy of complex multi-phase structure is characterised by the structural features, properties, and percent content of individual phases, the width and shape of the grains and their mutual distribution. One of the characteristics typical of the cast iron abrasive wear is the fact that the constituent undergoing the most intense wear is graphite.

The product of the wear is the graphite powder, which acts as a *lubricant* reducing the coefficient of friction and improving the abrasive wear resistance, especially under the conditions of dry friction. In the mixed mode of friction, the cavities and crevices created by the loss of graphite play the role of "storage tanks" for the lubricant. In those cavities are also accumulated the products of wear, thus reducing the abrasive effect.

On the other hand, graphite inclusions in cast iron act as lubricants of very low resistance, breaking the continuity of the metallic matrix, which can lead to the detachment of metal particles and the related *notch effect*.

The effect of microstructure on the abrasive wear resistance of cast iron depends on:
- content and structure of the metallic layer,
- content, shape and dispersion of graphite inclusions,
- content and shape of the phosphorus eutectic.

The above mentioned microstructural factors are obviously dependent on:
- chemical composition of cast iron,
- the conditions of the casting solidification and cooling,
- possible heat treatment.

The latest generation of casting alloys characterised by high abrasive wear resistance includes ADI and high-alloyed cast steel hardened with nitrogen added as an alloying element. At the Foundry Research Institute in Cracow, for many years, research and implementation works have been conducted on the aforementioned alloys, mainly to explore the possibility of using them for agricultural tools working in the soil [9, 10, 11, 12, 13, 14, 21, 22, 23, 24]. Some examples of castings made for the agricultural sector are shown in the photographs below (Figs. 8 and 9):

WEAR RESISTANCE TESTING

Among various methods to test the tribological wear resistance, three main groups are distinguished:
- field testing,
- bench testing,
- laboratory testing.

High complexity of tribological damage imposes the need to reproduce during testing, as exactly as possible, all conditions under which the wear takes place, and so to ensure exact mapping of the operating conditions of the tested mechanism, machine part or material.

FIELD TESTING

Field tests are carried out on machines or equipment under conditions of their actual operation. The purpose of these tests is, among others, to detect weak parts suffering frequent damage and determine the intensity of their use. Field tests may be carried out as part of research to determine the wear rate of specific components included in a new design and / or made of a new (tested) material.

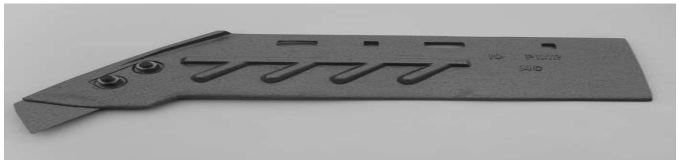

Ploughshare with cutting blade for the reversible and single-sided plough (ADI)

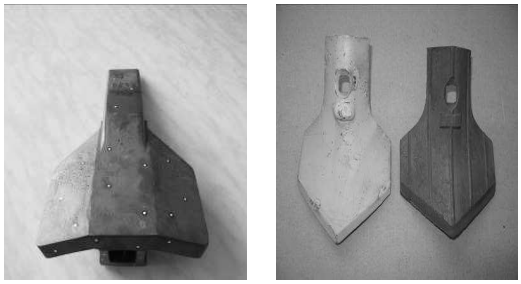

Cast subsoiler coulter. Cast duckfoot for the flexible cultivator teeth

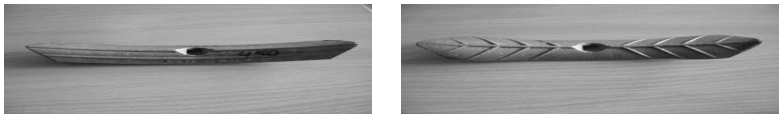

Cast coulters for the flexible cultivator teeth (two types)

Fig. 8. Examples of parts resistant to abrasive wear cast from ADI (own designs)

Casting of rake (left) and part of combine to make compost (right)

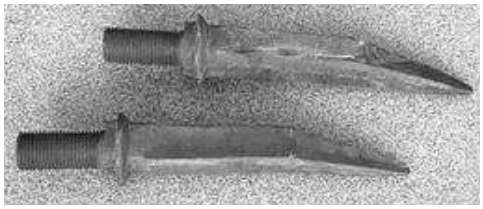

Fig. 9. Examples of parts resistant to abrasive wear made from high-alloyed cast steel with nitrogen

These tests reproduce most fully and faithfully actual operating conditions of parts of the machines and equipment to be evaluated. Since these are usually long-term studies, often, when they are running, narrower operating parameters than under normal operating conditions are applied. However, application of these experimental conditions should not cause changes in the abrasive wear mechanism.

In field testing, the main methods of the measurement of the degree of wear include the measurement of dimensional changes, the method of artificial bases, and isotopic method. Gravimetric method, due to the large mass of the components under inspection, is less useful. Sometimes the weight of the products of wear is determined.

Due to the fact that the operating parameters (load value, ambient temperature, humidity, etc.) under normal conditions vary at random, it is necessary to provide a statistical approach to the results of experiments, which considerably increases both the time and cost of studies.

BENCH TESTING

Bench tests are carried out on entire machines or individual components. They have a control or experimental character. The construction of a stand has to provide conditions similar to the real ones. Compared with field testing, these studies enable wider programming of operating conditions, their exact recording, increasing the number and accuracy of measurements, and high reproducibility of the results. This allows using smaller number of repetitions, which reduces the cost of the experiment.

LABORATORY TESTING

Laboratory tests are carried out for the mating parts of machinery or equipment, or for the mating materials. It is difficult to reproduce in laboratory equipment the real operating conditions such as e.g. the stiffness of structure, the precision of assembly, vibrations, etc.

Therefore, laboratory testing of material wear is most often done for comparative purposes only. These tests are designed to compare the wear resistance of the examined materials with the wear resistance of the adopted reference standard. The studies do not refer to the conditions under which the tested material will be operating, but adopt a simple mechanism of wear for which the comparison is carried out.

Within the framework of materials testing of the developed and implemented casting alloys of a new generation to be used for agricultural tools working in the soil, numerous tests to assess the resistance to abrasive wear have been carried out [15, 16, 17, 18, 19]. For example, Figure 10 compares the erosive wear rate of ADI castings with other selected casting alloys.

Owing to a high content of residual austenite in the matrix, ADI hardens under pressure in a way similar to Hadfield cast steel, offering also similar resistance to erosive wear.

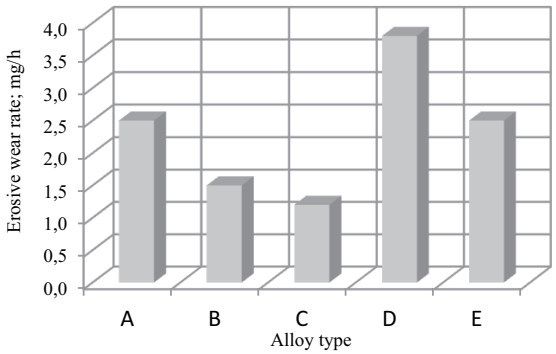

Fig. 10. Erosive wear rate tested in silica sand – water slurry for different ferrous alloys (own studies)
A – Hadfield alloy, B – chromium-nickel cast steel, C – chromium-nickel cast steel with addition of nitrogen, D – ductile iron, E – austempered ductile iron (ADI)

Even more resistant to this type of wear is the high-alloyed, chromium-nickel cast steel, in particular with the addition of nitrogen. High resistance of this alloy to tribological wear was confirmed by comparative bench tests carried out on harrow teeth, shown in Figure 11. Despite a significant increase in the life of harrow teeth cast from the high-alloyed, chromium-nickel steel, compared with forged steel teeth, the rationale of their use must be decided against the background of economic reasons (the cost of production).

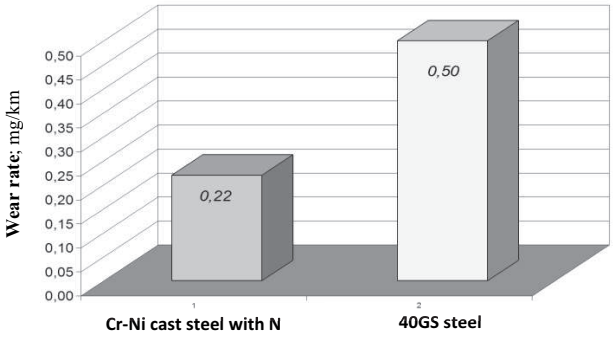

Fig. 11. Abrasive wear rate compared for harrow teeth made from different alloys

In cooperation with the Research Institute of Agricultural Engineering in Poznań, the Foundry Research Institute in Cracow has developed a series of innovative agricultural tools made from the austempered ductile iron (ADI); the developed castings were subjected to a series of laboratory and field tests. Examples of the obtained results are given in Figures 12-15.

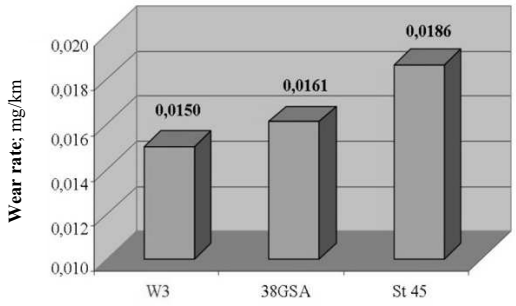

Fig. 12. Wear behaviour of investigated alloys under the conditions of dry friction [own studies]

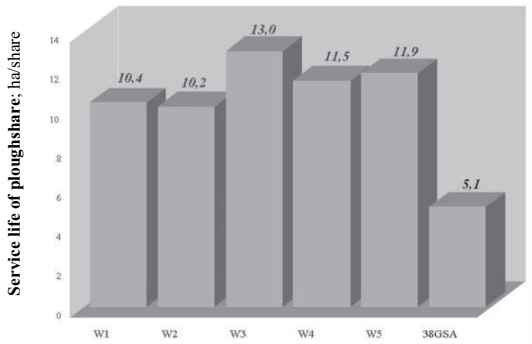

Fig. 13. Service life of ploughshares cast from ADI (designated with symbols W1 – W5) and ploughshares forged from 38GSA steel [own studies]

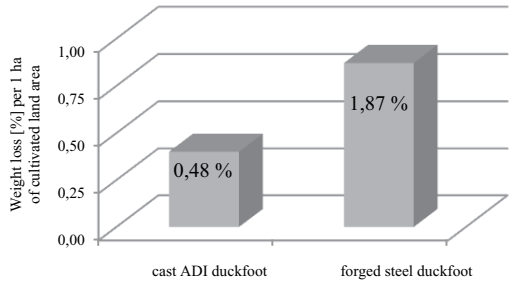

Fig. 14. Weight loss in cultivator duckfoot cast (own studies) and forged [20] calculated per 1ha of the cultivated land area

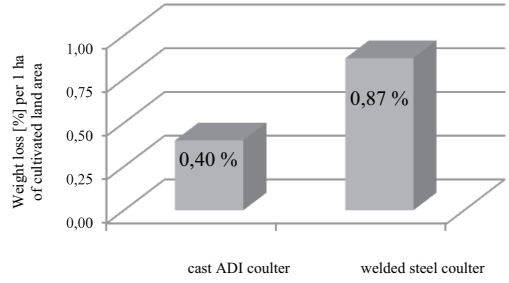

Fig. 15. Weight loss in three-tooth subsoiler coulters cast and welded calculated per 1ha of the cultivated land area (preliminary studies)

CONCLUSIONS

The tests and studies carried out have shown that modern casting materials can in many cases successfully replace the traditional wrought alloys. Sometimes, redesigning of the replaced components is necessary due to changes in production technology, while their introduction to common use requires wide-scale dissemination of innovative solutions wherever it is economically justified.

ACKNOWLEDGMENTS

The study was done within the framework of the EUREKA E! MEDHIAL 4102 project: "The start up of production of castings from iron alloys designed for operation under the extra harsh conditions of abrasive and corrosive wear to replace forged and welded structures", Contract No. E! 4102/11/NCBiR/10

REFERENCES

1. www.radwag.com/e-sklep/pliki/artykuly/pomiary_grawimetryczne_w_badaniach_scieralnosci.pdf
2. **Hebda M., Wachal A.: 1972;** Trybologia; Wojskowy Przegląd Techniczny; nr 8.
3. **Hebda M., Wachal A.: 1971;** Problemy naukowe i techniczne trybologii; Przemysł Chemiczny; nr 6.
4. **Dowson D.: 1967;** Tribologie eine neue wissenschaftliche Dissciplin; Schmiertechnik; Nr 5.
5. **Vogelpohl G.: 1969;** Ober die Ursachen der Unzureichenden Bewertung von Schmierungsfragcn im Vorigen Jahrhundert; Schmiertechnik; Nr 5.
6. **Marczak R., Ziemba S.: 1973;** Trybologia jako nauka – kierunki i perspektywy jej rozwoju; Materiały Szkoły Trybologicznej; Złoty Potok.
7. www.tribologia.org/ptt/try/tr08.htm
8. **Mulhearn T. O., Samuels L. E.: 1962;** The abrasion of metals a model of the processes; Wear; vol. 5.
9. **Pirowski Z., Olszyński J., Gościański M., Tybulczuk J.: 2006;** Innowacyjne tworzywa odlewnicze na elementy maszyn rolniczych podnoszące konkurencyjność wyrobów finalnych; Zeszyty Naukowe Politechniki Rzeszowskiej; MECHANIKA; z. 66.
10. **Pirowski Z., Gwiżdż A., Wodnicki J., Olszyński J.: 2004;** Najnowsze przykłady zastosowania wysokojakościowego żeliwa sferoidalnego w polskim przemyśle maszynowym; Odlewnictwo – Nauka Praktyka; Nr 2 – specjalny.
11. **Pirowski Z., Olszyński J., Gościański M., Turzyński J.: 2006;** Elementy maszyn rolniczych pracujących w glebie wykonane z nowoczesnych tworzyw odlewniczych; MOTROL – Motoryzacja i Energetyka Rolnictwa; t. 8.
12. **Łabęcki M. i inni: 2004;** Laboratory and field testing of chosen agricultural machine elements working in the soil and made of modern cast irons ADI. Part 1. Laboratory resting; Journal of research and applications in agricultural engineering; v. 49 (4).
13. **Pirowski Z., Wodnicki J., Olszyński J., Gościański M., Dudziak B.: 2012;** Wpływ mikrododatku boru na zmiany hartowności w żeliwie sferoidalnym z przemianą izotermiczną w odniesieniu do odlewów grubościennych; Journal of Research and Applications in Agricultural Engineering; vol. 57 (2),
14. **Pirowski Z., Gościański M.: 2009;** Construction and technology of production of casted shared for rotating and field ploughs: TEKA Commission of Motorization and Power Industry in Agriculture Lublin University of Technology the Volodymir Dahl East-Ukrainian National University of Ługańsk: v. IX.
15. **Pirowski Z.: 2006;** Zwiększenie odporności na zużycie erozyjne dwufazowego staliwa Cr-Ni przez dodatek azotu i innych pierwiastków międzywęzłowych; Archiwum Technologii Maszyn i Automatyzacji; t. 26. nr 1.
16. **Pirowski Z., M. Kranc, Olszyński J., Gwiżdż A., Gościański M.: 2012;** Cast agricultural tools for operation in soil; TEKA Commision of Motorization and Energetics in Agriculture; vol. 12; No 2.
17. **Pirowski Z., M. Kranc, Olszyński J., Gwiżdż A., Gościański M.: 2012;** Performance testing of cast agricultural tools operating in soil; TEKA Commision of Motorization and Energetics in Agriculture; vol. 12; No 2.
18. **Pirowski Z., M. Kranc, Olszyński J., Gwiżdż A.: 2012;** Testing ADI propierties when used for cast agricultural tools operating in soil; TEKA Commision of Motorization and Energetics in Agriculture; vol. 12; No 2.
19. **Kapcińska D. i inni: 2006;** Capability of adaptation the new generation ADI cast iron on the building of agricultural machines; Journal of research and applications in agricultural engineering; v. 51 (3).
20. **Kostencki P.: 2005;** Badania odporności ściernej elementów roboczych zębów kultywatora ścierniskowego; Problemy Inżynierii Rolniczej; Nr 1.
21. **Żółkiewicz Z., Żółkiewicz M.: 2009;** Lost Foam Process – The Chance For Industry. TEKA; vol. IX
22. **Karwiński A., Żółkiewicz Z.: 2011;** Application of Modern Ecological Technology Lost Foam For The Implementation Of Machinery. TEKA; vol. XIC.
23. **Gazda A., Żółkiewicz Z.: 2012;** Thermal and physical properties of some refractory layers used in lost foam technology. TEKA; vol. XII.
24. **Żółkiewicz Z., Żółkiewicz M.: 2009;** Lost foam process – the chance for industry. TEKA; vol. IX.

STOPY ODLEWNICZE PRACUJĄCE W TRUDNYCH WARUNKACH ZUŻYCIA ŚCIERNEGO PRZEZNACZONE NA NARZĘDZIA ROLNICZE

Streszczenie. W artykule omówiono wybrane zagadnienia związane z procesami zużycia trybologicznego, koncentrując się na zjawiskach zachodzących w trakcie zużywania się detali w trakcie ścierania. Omówiono mechanizmy takiego procesu,

scharakteryzowano ważniejsze materiały odporne na ten rodzaj zużycia i pokazano przykładowe odlewy przeznaczone dla sektora rolniczego opracowane i wykonane w Instytucie Odlewnictwa w Krakowie we współpracy z Przemysłowym Instytutem Maszyn Rolniczych w Poznaniu. Następnie sklasyfikowano i opisano ważniejsze metody oceny odporności stopów na zużycie ścierne, w tym zużycie erozyjne. Przytoczono przykładowe własne wyniki takich badań. Wykazano, że nowoczesne stopy odlewnicze mogą z powodzeniem konkurować z tradycyjnymi tworzywami przerabianymi plastycznie.

Słowa kluczowe: trybologia, badania, odlewy, stopy odlewnicze, narzędzia rolnicze

TEKA. COMMISSION OF MOTORIZATION AND ENERGETICS IN AGRICULTURE – 2013, Vol. 13, No. 1, 127–132

Innowative construction of agricultural tools from modern casting materials

Zenon Pirowski[1], Marek Kranc[1], Marek Gościański[2], Bartłomiej Dudziak[2]

[1]Foundry Research Institute,
Poland, 31-418 Kraków, 73 Zakopiańska Street, pirowski@iod.krakow.pl
[2]Industrial Institute of Agricultural Engineering,
Poland, 60-963 Poznań, 31 Starołęcka Street, margos@pimr.poznan.pl

Received February 18.2013; accepted March 14.2013

Summary. The article discusses some results of work carried out in the framework of material and technological conversion, which aims to replace with cheaper and / or more durable castings, machine parts and agricultural equipment made so far in the forging and welding technology. The focus is on the agricultural tools working in the soil. The fallowing tools have been created and tested in extreme wear on the field: rotational plowshares, hoes subsoiler, cultivator tooth, cultivator spring, cultivator spring tooth point. Conducted field tests of prototype tools have confirmed the validity of the action taken.
Key words: castings, Austempered Ductile Iron – ADI, agricultural tools, performance tests.

INTRODUCTION

The aim of this study was to increase innovation, modernity and competitiveness of Polish industry in the manufacture of agricultural machinery and equipment.

Prior to the implementation of this work, a study focused on the conversion of agricultural machinery parts previously performed by conventional methods (forging machining, welding, etc.) on the elements made with casting technology, of course, where it seemed to be technically and economically viable.

Foundry is a very extensive industrial branch. It is estimated, according to data from the U.S., that castings are components of up to 90% of final industrial products. In the economies of developed countries there is observed a permanent increase in the production of castings. There are more new applications in the fields of industrial castings such as medicine, energy (including renewable energy), which require a sufficiently high standard, enhanced technical and operating parameters of cast components composing the final product.

It is the quality of the cast components that determines the quality of the final product and, consequently, its price.

Extensive use of castings as components of final products creates opportunities for conversion of various components of machinery and equipment originally performed by other machining technologies such as forging, welding, machining on the parts made with casting technology.

Business practice has shown possibility of replacing these items with casting elements, which often are lighter, more durable, resistant to abrasion, thermal fatigue, etc. [1, 2, 3, 4, 5, 6, 21, 22, 23, 24]. As a result of the conversion work on the material and technology, an experimental series of castings for agriculture have been done. These agricultural tools were made of high-quality ductile iron with alloy additives and heat treatment and they were working in the soil. The fallowing type of tools have been created: blades for rotational plows, subsoiler plough, cultivator points (duckfoot share), tooth for cultivator spring, cultivator spring tooth point [7, 7, 9, 10, 11, 12].

PLOUGH CASTINGS

On the Polish market there are available ploughs made by using two different technologies: bending with welding and stamping. Examples of blades made by using these technologies are shown in Figure 1

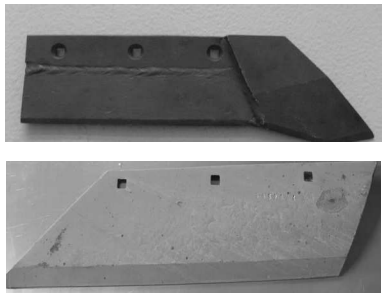

Fig. 1. Polish ploughs: a) plough done by welding, b) plough done by stamping

These ploughs were tested for mechanical and tribological properties. The obtained results were used to determine the material requirements that should be met after the change in the casting plough's material.

During working on the field ploughs of the plow are subjected to a very complex process of destruction. On the one hand there is a strong wear of the soil, on the other hand they are vulnerable to stress cracking due to the presence of high static and dynamic loads. Therefore, the material from which they are made must be very durable and resistant to erosive wear, but sufficiently plastic and able to transmit impact loads (frequently occurring) as a result of stone impact in the soil.

Among the casting materials, properties similar to steel that is plastically processed are possessed only by ductile iron after heat treatment (hardening of isothermal transformation ADI). That ductile iron is resistant to abrasion in different conditions. Its mechanical properties are dependent on the type and quantities of alloying additives, and especially on the parameters of the heat treatment. Such a ductile iron obtained after the isothermal tempering has the tensile strength in the range 800-1500 MPa and elongation up to 18%, depending on the process used. For obtaining the desired properties, the quality is significant of spheroidal graphite iron (particularly the form, size and number of graphite precipitates), and heat treatment parameters. Less significant is the chemical composition of the cast iron. Thus, it can be varied in a very wide range. However, it is necessary to add elements (corresponding to the wall thickness of the casting) to facilitate the hardenability of iron (for example, Ni, Cu).

In order to verify the suitability of the alloy elements of agricultural machinery operating under abrasive wear in direct contact with the cultivated soil, tests have been performed of casting prototype ploughs (shown in Fig. 2).

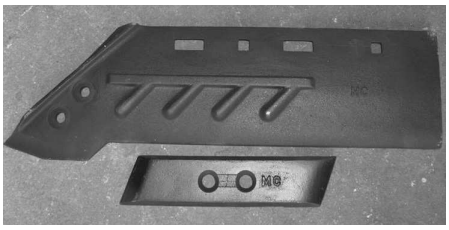

Fig. 2. Share casting and blade for standard and rotational ploughs [own construction]

Abrasion tests have been carried out both in the laboratory and during performance under field conditions. They revealed that the optimum type of ductile iron appears to be a cast (designated as W3) with the following characteristics:
R_m – about 1200 MPa,
A_5 – more than 1.5%,
KCU – over 7 J/cm²,
Hardness – approximately 40 HRC.

As it is shown in Figures 3 and 4, that type of ductile iron can be used successfully on the cast plough's blades in the place of expensive forged and welded blades.

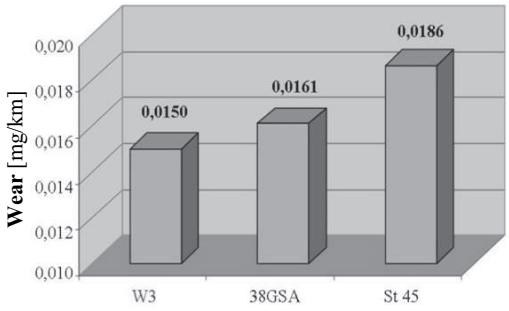

Fig. 3. Wear of alloys tested under dry friction [own research]

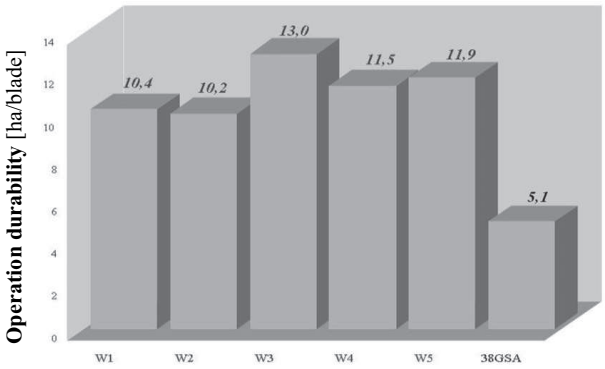

Fig. 4. Operation durability of the castings blades made of cast iron ADI (marked W1 - W5) and forged steel blades made of 38GSA steel [own research]

SUBSOILER PLOUGH CASTINGS

Currently used subsoiler ploughs are made as welded steel structures (Fig. 5). In this paper the conversion of material and technology of these tools have been presented. An innovative design and construction of subsoiler plough have been developed. Also, a short experimental series have been manufactured and tested (Fig. 6).

Manufactured experimental tools were tested in operational condition in the field. During preparation of field research, a study was made concerning the analysis of diversification of agricultural machines used by farmers, including subsoilers. As a result of such an analysis, a general conclusion can be stated that at present the majority of farmers (different acreage) uses a diverse construction machines including cultivation Subsoilers with welded subsoiler ploughs.

At the same time it should be noted that the assortment of soil machinery is constantly changing. Structural modifications of these machines also cause a new, individual for each manufacturer, way of attachment and shape of agricultural tools. Therefore, for the experimental tests were selected only those farms, whose machines can be fitted with the tested elements. The results of wear intensity of casting subsoiler made of ADI were compared with (in similar operating conditions) reference items purchased from a leading Polish manufacturer. Research has been carried out in accordance with the methodology developed in PIMR. Results showed that in the case of casting subsoiler a loss of weight on the 1 ha cultivated area was 58.75 g /ha

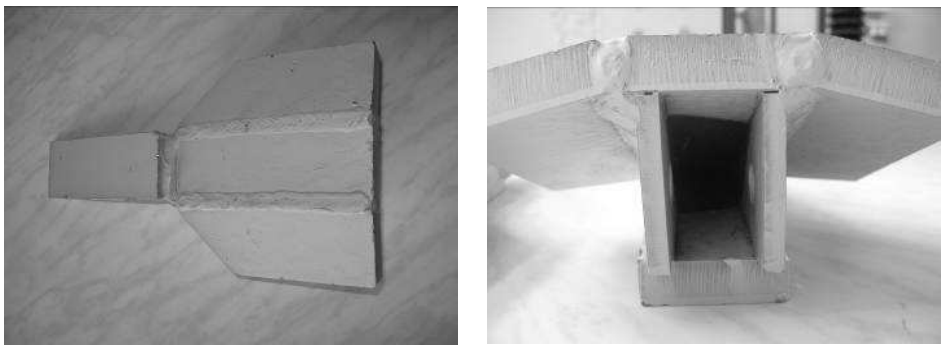

Fig. 5. Subsoiler plough welded from 7 elements

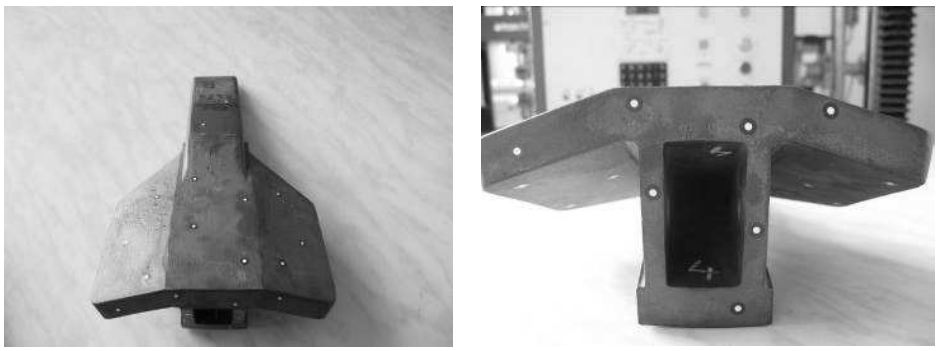

Fig. 6. Casting of subsoiler plough [own construction]

and welded coulter – 45.92 g/ha, and it was larger by the 27%. It should be noted that subsoiler plough has difficult working conditions, which are associated with significant thermal effects occurring in the soil at the depth of about 35-40 cm. These effects could be the cause of structural changes in particularly vulnerable to such changes ADI cast iron (decrease in the ausferrite hardness). Errors that occurred in the internal structure of the thick-walled castings could also contribute to the increased wear intensity of these components.

In the case of casting tools, a much bigger surface area had a contact with the cultivated soil compared to the traditional tools. That suggests a necessity of modification of the castings construction. Rockwell Hardness of reference subsoiler plough made of welded steel with boron is about 40 HRC. The hardness of ductile iron castings after isothermal hardening was also about 40 HRC (according to the technology assumption). Simultaneously, an area of reduced hardness lower than 30 HRC was observed under the gating system. That suggests a necessity of modification in that area: correction of the gate supply system.

Images of scanned subsoiler plough (Figure 7) show the distribution of surface wear intensity. Scanning image of these tools and investigations of surface (tribological aspect), showed no presence of anomalies in the nature of wear intensity and permanent deformation. Only small changes in surface on edges were highlighted.

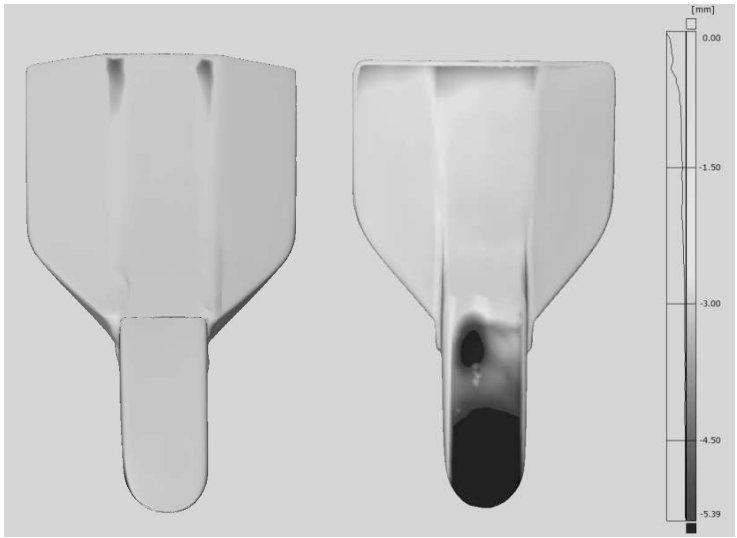

Rys. 7. Comparison of subsoiler plough wear intensity, welded construction (left) and casting (right) [own research]

DUCKFOOT SHARE CASTINGS

As part of the material and technology conversion subject in the field of agricultural tools working in the soil, an innovative variant of casting duckfoot share for spring cultivator teeth has been developed. Currently produced duckfoot share is made from steel by forging and welding. Castings of Duckfoot shares are made of ductile iron tempered with isothermal transformation (ADI). Comparison of construction of an existing one and innovative design of duckfoot share is shown in Figure 8.

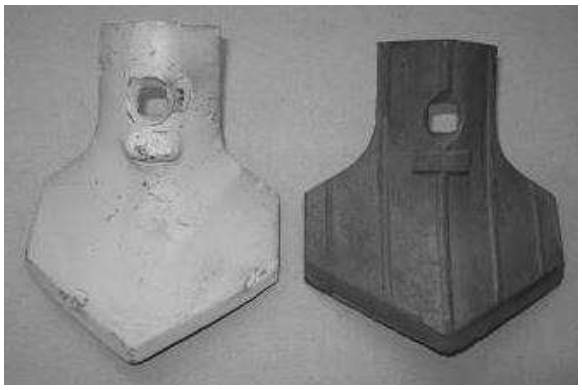

Fig. 8. Duckfoot share for spring cultivator teeth made by forging and welding (left) and as a casting (right (own construction)

In order to assess the operation durability of forged and cast iron duckfoot share, comparative tribological tests were conducted of these tools. They helped to assess their wear intensity in the stochastically varying conditions of operation in the soil. Studies were carried out in accordance with the developed methodology in PIMR and showed that in the case of cast duckfoot share, the average loss of weight per 1 ha of cultivated area was 1.11 g / ha (average from three farms) and was about 31% lower compared to the forged duckfoot share from steel with boron. It should be noted that the Rockwell hardness of cast duckfoot share from ductile iron tempered isothermally (according to the technology assumption) was about 40 HRC, while the hardness of forged steel duckfoot share was higher; approximately 45 HRC. Increased hardness of steel duckfoot share did not translate, therefore, in this case, on direct increase of operational durability of the tool.

Scanning images of duckfoot share after the wear intensity research in the field (Figure 9) showed the distribution of surface defects with a scale of values. Scannig image of these tools and investigations of surface (tribological aspect), showed no presence of anomalies in the nature of wear intensity and permanent deformation. Only small changes in surface on edges were highlighted, dispersion of deviations (losses) in the surface was 2.50 mm for the forged duckfoot share and 3.21 mm for duckfoot share casting.

CULTIVATOR POINT CASTINGS

Cultivator points for spring teeth are interchangeable tool designated for agragates for pre-sowing tillage, working directly in the soil. Current technology of manufacturing cultivator points uses fallowing methods; cutting, hammering, drilling, grinding (Fig. 10). High level of wear intensity of a large scale is one of the most significant premises for an attempt to try to replace steel cultivator points with castings. Therefore, a new design and construction were developed and experimental series of innovative cultivator points were manufactured from ADI ductile iron (Fig. 11).

Operational durability tests of cultivator points confirmed the validity of their implementation in casting variants ver. II and ver. V. Average wear intensity measurements

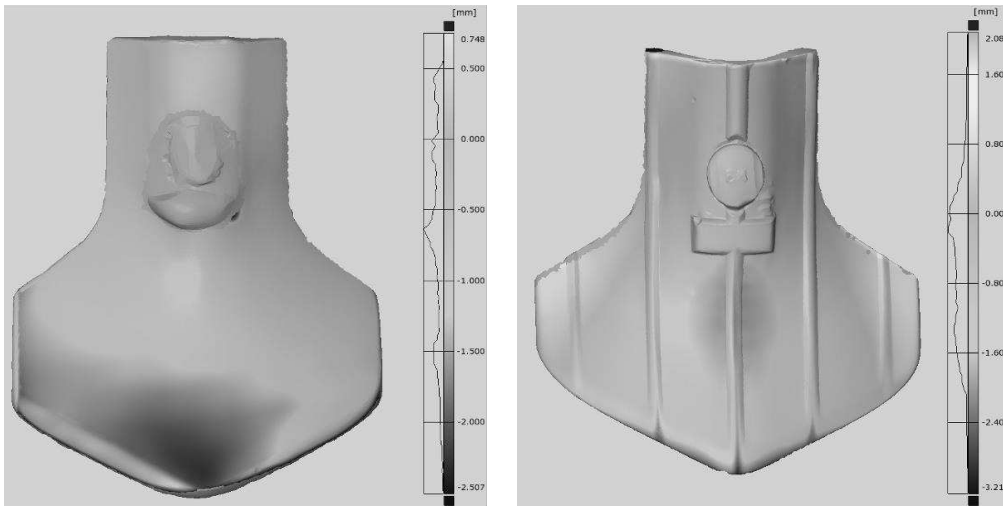

Fig. 9. Comparison of duckfoot share wear intensity, forged construction (left) and casting (right)

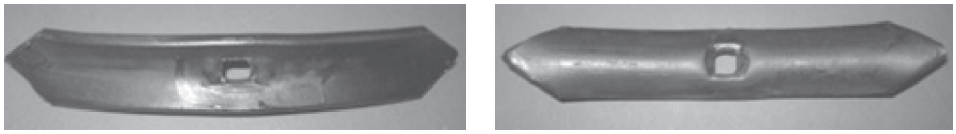

Fig. 10. Cultivator point for spring teeth made from steel

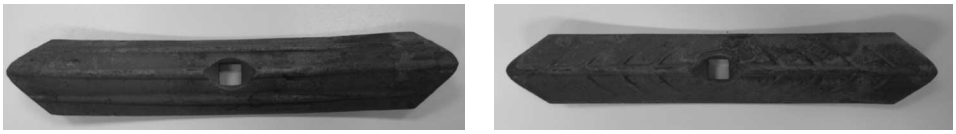

Fig. 11. Cultivator point for spring teeth made from ADI ductile iron (two variants: ver. II on the left, ver. V on the right)

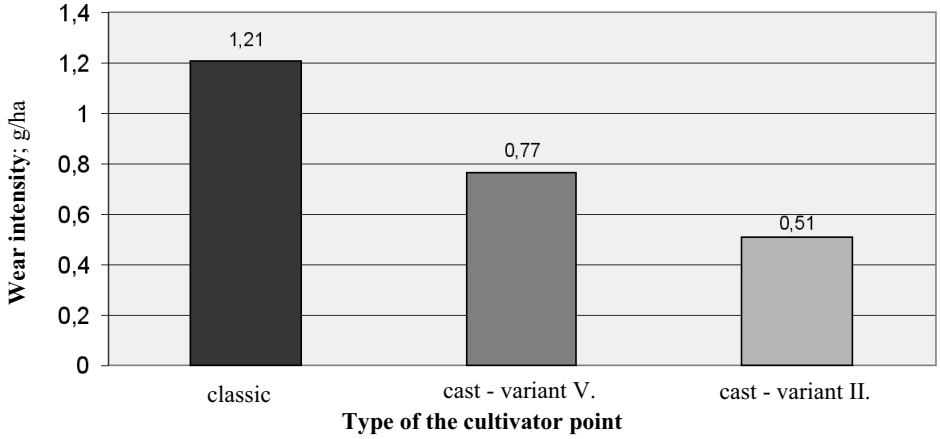

Fig. 12. Graph showing the average wear intensity of cultivator points in different construction variants (operational speed of 6-8 km/h area of 100 ha)

were made of newly developed cultivator points (at the "classical" speed of 6-8 km) in the variant II and V compared with classic cultivator points made from steel. The obtained results showed that there are significant differences in wear intensity (Fig. 12).

The average wear intensity of casting cultivator poins in variant II was 0.51 g/ha, and in variant V 0.77 g/ha, compared to the 1,21 g/ha in the case of classic cultivator point (made by forging). It can be easily calculated that castings are 2-3 times better than the classic equivalent.

CONCLUSIONS

Attempts of material and technological conversion of selected agricultural tools, in most cases provided promising results. Modern materials such as ductile cast iron tempered with isothermal transformation (ADI) can often compete with steel (constructional and tool type) [13, 14, 15].

Scanning images of surface defects on different tools working in the soil showed the most vulnerable places of wear. This will help in the future to improve the technology to increase the operational durability of these tools in key areas (e.g. possible application of laser welding with powder metal alloys – LMD).

The first attempts to use this technology in this field were carried out in the Department of Agricultural Machines Materials Testing and Development in PIMR in Poznan. Research on the effectiveness of laser technology application and laser cladding of metal alloy powders are ongoing, and their results will be subsequently published in scientific journals.

In parallel in the Foundry Research Institute in Cracow work is done on the development of new types of ductile cast iron tempered in isothermal transformation (CADI) [16, 17, 18, 19, 20]. Described in this paper agricultural tools castings working in the soil constructional solutions have been patented or patent pending by cooperating in this area research institutions: PIMR in Poznan and IO in Krakow.

ACKNOWLEDGMENTS

The works presented in this paper have been performed as part of the following research projects:

- project EUREKA E! 4102 MEDHIAL: "The start of production of ferroalloy castings designed for operation under extra-hard conditions of abrasive and corrosive wear to replace forged and welded constructions"; No. of agreement E!4102/11/NCBiR/10,
- research and development project No. N R03 0009 06: "Developing technologies and construction design of elastic elements to a new generation of soil preparation pre-sowing aggregates working with increased operating speeds", financed by the NCBiR in Poland, No. of agrement N R03 0009 06/2009.

REFERENCES

1. **Tybulczuk J., Kowalski A., 2003:** Żeliwo ADI własności i zastosowanie w przemyśle. Atlas Odlewów; Instytut Odlewnictwa.
2. **Pirowski Z., Gwiżdż A., Wodnicki J., Olszyński J., 2004:** Najnowsze przykłady zastosowania wysokojakościowego żeliwa sferoidalnego w polskim przemyśle maszynowym; Odlewnictwo – Nauka Praktyka; Nr 2 – specjalny.
3. **Pirowski Z., Wodnicki J., Olszyński J., 2008:** Physical and Chemical Processes in Metalcasting. Hardenability of austempered ductile iron; Foundry Research Institute, Cracow, 1st Edition.

4. **Pirowski Z., Tybulczuk J., Uhl W., 1999:** Acta Metallurgica Slovaca, vol. 2.
5. **Pirowski Z., i inni: 2003:** Odlewnictwo XXI w. Stan aktualny i kierunki rozwoju metalurgii i odlewnictwa stopów żelaza; Instytut Odlewnictwa.
6. **Pirowski Z., Olszyński J., Gościański M., Tybulczuk J., 2006:** Innowacyjne tworzywa odlewnicze na elementy maszyn rolniczych podnoszące konkurencyjność wyrobów finalnych; Zeszyty Naukowe Politechniki Rzeszowskiej; MECHANIKA; z. 66.
7. **Pirowski Z., Olszyński J., Gościański M., Turzyński J., 2006:** Elementy maszyn rolniczych pracujących w glebie wykonane z nowoczesnych tworzyw odlewniczych; MOTROL – Motoryzacja i Energetyka Rolnictwa; t. 8.
8. **Łabęcki M. i inni: 2004:** Laboratory and field testing of chosen agricultural machine elements working in the soil and made of modern cast irons ADI. Part 1. Laboratory resting; Journal of research and applications in agricultural engineering; vol. 49 (4).
9. **Pirowski Z., Gościański M., 2009:** Construction and technology of production of casted shared for rotating and field ploughs: TEKA Commission of Motorization and Power Industry in Agriculture Lublin University of Technology the Volodymir Dahl East-Ukrainian National University of Ługańsk: vol. IX.
10. **Kapcińska D. i inni: 2006:** Capability of adaptation the new generation ADI cast iron on the building of agricultural machines; Journal of research and applications in agricultural engineering; vol. 51 (3).
11. **Kostencki P., 2005:** Badania odporności ściernej elementów roboczych zębów kultywatora ścierniskowego; Problemy Inżynierii Rolniczej; Nr 1.
12. **Przybył J. i inni: 2009:** Analiza jakości pracy agregatów do uprawy przedsiewnej; Journal of Research and Applications in Agricultural Enginieering; vol. 54 (4).
13. **Pirowski Z., M. Kranc, Olszyński J., Gwiżdż A., Gościański M., 2012:** Cast agricultural tools for operation in soil; TEKA Commision of Motorization and Energetics in Agriculture; vol. 12; No 2.
14. **Pirowski Z., M. Kranc, Olszyński J., Gwiżdż A., Gościański M., 2012:** Performance testing of cast agricultural tools operating in soil; TEKA Commision of Motorization and Energetics in Agriculture; vol. 12; No 2.
15. **Pirowski Z., M. Kranc, Olszyński J., Gwiżdż A., Gościański M., 2012:** Testing ADI propierties when used for cast agricultural tools operating in soil; TEKA Commision of Motorization and Energetics in Agriculture; vol. 12; No 2.
16. **Pirowski Z., Wodnicki J., Olszyński J., Gościański M., Dudziak B., 2012:** Wpływ mikrododatku boru na zmiany hartowności w żeliwie sferoidalnym z przemianą izotermiczną w odniesieniu do odlewów grubościennych; Journal of Research and Applications in Agricultural Engineering; vol. 57 (2).
17. **Guzik E., 2009:** Forum Inżynierskie. Rozwój technologii żeliwa ADI w Polsce. Instytut Odlewnictwa.
18. **Głownia K. i inni., 2010:** Wpływ azotu i boru w żeliwie sferoidalnym na przemiany strukturalne w procesie hartowania z przemianą izotermiczną; Prace Instytutu Odlewnictwa; Kraków; Tom L; Nr 1.
19. **Pirowski Z., Wodnicki J. Olszyński J., 2007:** Microadditions of boron and vanadium in ADI. Part 1. Literature review; Polish Academy of Sciences; vol. 7.
20. **Pirowski Z., Wodnicki J. Olszyński J., 2007:** Microadditions of boron and vanadium in ADI. Part 2. Own investigations; Polish Academy of Sciences; vol. 7.
21. **Żółkiewicz Z., Żółkiewicz M., 2009:** Lost Foam Process – The Chance For Industry. TEKA; vol. IX
22. **Karwiński A., Żółkiewicz Z., 2011:** Application of Modern Ecological Technology Lost Foam For The Implementation Of Machinery. TEKA; vol. XIC.
23. **Gazda A., Żółkiewicz Z., 2012:** Thermal and physical properties of some refractory layers used in lost foam technology. TEKA; vol. XII.
24. **Żółkiewicz Z., Żółkiewicz M., 2009:** Lost foam process – the chance for industry. TEKA; vol. IX.

INNOWACYJNE KONSTRUKCJE NARZĘDZI ROLNICZYCH Z NOWOCZESNYCH TWORZYW ODLEWNICZYCH

Streszczenie. W artykule omówiono wybrane efekty prac prowadzonych w ramach szeroko rozumianej konwersji materiałowo-technologicznej, której celem jest zastąpienie tańszymi i/lub trwalszymi odlewami, elementów maszyn i urządzeń wykonywanych dotychczas w technologii kucia i spawania. Skoncentrowano się na narzędziach rolniczych pracujących w glebie. Wykonano i przebadano narzędzia pracujące w ekstremalnych warunkach zużycia ściernego jak: lemiesze pługów obracalnych, redlice głębosza, gęsiostopki zębów sprężystych kultywatora, redliczki zębów sprężystych kultywatora. Przeprowadzone badania eksploatacyjne wykonanych narzędzi prototypowych potwierdziły słuszność podjętych działań.
Słowa kluczowe: odlewy, żeliwo ADI, narzędzia rolnicze, badania eksploatacyjne.

TEKA. COMMISSION OF MOTORIZATION AND ENERGETICS IN AGRICULTURE – 2013, Vol. 13, No. 1, 133–138

Acquisition and economic use of geothermal energy

Renata Polak, Dariusz Dziki, Andrzej Krzykowski, Stanisław Rudy, Zbigniew Serwatka, Justyna Tomiło

Thermal Engineering Department, University of Life Sciences in Lublin
Doświadczalna 44, 20-280 Lublin, Poland, e-mail: renata.polak@up.lublin.pl

Received January 10.2013; accepted March 14.2013

Summary. Geothermal energy (GE) is heat from within the earth, accumulated inside the Earth in the form of hot water and steam or within hot dry rocks. The total world resources of GE exceed 35 trillion times the current, global demand for energy. GE is renewable, common, clean, abundant and independent of climatic conditions, thus it provides opportunity to be exploited. Resources of GE range from the shallow ground to hot water found a few kilometers beneath the Earth's surface, and deeper to the extremely high temperatures of magma. Many technologies have been developed to take advantage of GE. The paper presents the basic information on GE, ways to obtain and utilize it. The methods of calculation of GE resources were also presented.
Key words: geothermal energy, renewable energy sources.

INTRODUCTION

Over the decades, conventional energy will not be able to meet the growing world energy demands, mainly due to the limited and rapidly dwindling sources of conventional fuels. Renewable energy sources and especially geothermal energy (GE) may be the panacea for the world's energy problems [18, 20, 21, 26].

Geothermal comes from the Greek words "geo" meaning earth and "therme" meaning heat. It is the natural heat of the earth which presents a potentially sustainable and commercial solution to problems of pollution, green house gas emissions, rising prices and long term supply problems associated with fossil fuels. GE is thermal energy generated and stored in the Earth, especially in the magma, rocks and fluids [34]. GE sources are hydrothermal systems, and hot dry rocks [7].

The use of thermal energy stored in hot rocks and groundwater for recreation and therapeutics has been known since ancient times. However, the use of such energy resources to produce heat and electricity began with the development of drilling techniques and modern geology. It has been proved that GE has great potential for supplying many areas with heat and electricity [2].

GE is independent of weather conditions, has a natural ability to accumulate, it is pure energy, contributes to the reduction of harmful combustion products of fossil fuels used for direct application, as well as with other renewable energy sources for electricity generation. Using of GE reduces the deterioration of our land, air, and water, which will allow future generations to live in the clean environment [19, 31].

The aim of the work was to present the basic information on GE. The methods of calculation of GE resources were also showed.

GEOTHERMAL ENERGY RESOURCES

The increased interest in renewable energy sources makes a number of geothermal installations increase rapidly. According to the forecast of the European Renewable Energy Council (EREC), in October 2008, the percentage of the total geothermal renewable energy production will increase from 3.1% in 2005 to 18.5% in 2050 [11].

World geothermal resources are estimated at about $8 \cdot 10^{30}$J. However, only a small part can be used economically, due to the current technical capability and cost-effectiveness [30]. Geothermal resources to the depth of 5000 m (limit of technical feasibility of drilling) are about $1.4 \cdot 10^{26}$ J [21].

According to the way of energy production, there are two basic geothermal system types

– hydro-geothermal resources, which are a two-component mixture of water and steam, at the temperature ranging from 200 to 3000°C, and hot water at temperature of 50 to 70°C, the water being the natural medium in which GE is recovered,
– petro-GE resources – the energy is stored in dry, porous hot rocks and hot salt domes [30], there is no natural medium in these formations and the heating agent in

this case is water which is artificially introduced into the layer of rock and after heating up is turned back to the surface [33].

According to the temperature of water, geothermal resources can be divided into the following classes:
- class I – temperature < 100°C,
- class II – temperature from 100 to 150°C,
- class III – temperature from 150 to 250°C,
- class IV – temperature > 250°C [28].

Taking into account the prospects of geological regions, environmental, technical and economic provisions, operation and use of the potential of geothermal resources, the following categories can be distinguished [1]:
- available geothermal resources,
- static resources of GE,
- static-recoverable resources of GE,
- disposable resources of GE,
- exploitation of GE resources.

Available geothermal resources are defined as part of the total available drilling of geothermal resources. This is the amount of heat energy stored in the Earth's crust to the depth of 3 km or to the ceiling of crystalline substrate, relative to the annual average temperature on the ground surface. Available geothermal resources are calculated as follows [34]:

$$EDZG = VS \times rS \times cS \times (Th_{(3000)} - To)/2A \ \ [J \cdot m^{-2}], \quad (1)$$

where:
VS – volume of rock from the Earth's surface to the depth of 3000 m [m³],
rS – average density of rocks to the depth of 3000 m [kg·m⁻³],
cS – average specific heat of the rock matrix [J/kg°C],
$Th_{(3000)}$ – temperature at the depth of 3000 m [°C],
To – annual average temperature on the Earth surface [°C],
A – surface area calculation [m²].

Static energy resources of hydro-geothermal reservoirs determine the amount of heat accumulated in the volume of free water contained in the pore space or gaps in the rock skeleton of the rock layer, or aquifer. Static resources of GE is the total amount of heat stored in the free water and in the rock matrix with the respect to the computation surface and average Earth surface temperature [34]. Static geothermal resources can be calculated as follows:

$$EZS = A \times mp \times [(1 - pe) \times rS \times cS + pe \times rw \times cw] \times (TS - To) \ \ [J], \quad (2)$$

where:
mp – total volume of aquifers in the reservoir [m],
rS – mean rock density to the depth of 3000 m,
cS – average specific heat of the rock matrix [J/kg°C],
pe – effective porosity,
rw – average density of water [kg·m⁻³],
cw – average density of water [J/kg°C],
A – surface area calculation [m²],
TS – ceiling temperature of geothermal reservoir [°C],
To – annual average temperature on the Earth surface [°C].

The static-recoverable GE resources are part of the static resources of a given level or hydro geothermal layers, which can be extracted to the surface of the Earth, taking into account the specific operating system of using geothermal water (spinner operating system or the operation by using one hole). The recoverable portion of geothermal resources determines the production rate (R_o), described by the formula [4]:

$$Ro = As/Ac[(Ts - Tz)/(Ts - To)], \quad (3)$$

where:
AS – cooled-off operating system [m²],
AC – the total surface area of the operating system [m²],
TS – temperature at the ceiling of hydrothermal reservoir [°C],
TZ – chilled water temperature turned up to the hydrothermal level (usually 25 °C),
To – annual average temperature on the Earth surface [°C].

The static-recoverable resources of GE can be calculated as follows:

$$EZWS = EZS \times Ro \ \ [J], \quad (4)$$

where:
EZS – static resources [J],
Ro – factor of production.

The available resources of GE are determined for those areas that promise hope and possibility of economic use of geothermal heat [4].

The disposable resources of GE are calculated based on the expression:

$$EZdysp = Vw \times (TS - 25) \times rw \times cw \times 8760 \ [J/rok], \quad (5)$$

where:
Vw – nominal capacity of the mining hole [m³·h⁻¹],
TS – temperature at the ceiling of hydrothermal reservoir [°C],
rw – average density of water [kg·m⁻³],
Cw – average specific heat of water [J/kg°C].

Exploitation of GE resources is the amount of free geothermal water possible to obtain under the geological and environmental circumstances with shots of an optimal technical and economic parameters [1, 4].

In order to evaluate the geothermal reservoirs of resources, dimensionless ratio is calculated called the power factor (*F*), which is defined as the ratio of the effective power output (*Pwy*) to efficient power input (*Pwe*):

$$F = Pwy/Pwe. \quad (6)$$

The power factor is an indicator which expresses how many times the output power of geothermal shot exceeds the thermal power, which is an equivalent representation of capital expenditure and operating costs of this shot. It is assumed that *Pwy* – the effective power output corresponds to the average annual intake capacity of geothermal heat:

$$Pwy = 1{,}14 \times 10^{-3} \times Vw \times (TS - TZ) \ \ [W], \quad (7)$$

where:
Vw – the nominal capacity of potential mining hole [m³·h⁻¹],
TS – temperature at the ceiling of hydrothermal reservoir [°C],

TZ – chilled water temperature turned up to the hydrothermal level [°C].

The effective power input (*Pwe*) relates to the capital outlay for the construction of geothermal shot and the costs of its operating, expressed as an equivalent of thermal power. It can be interpreted as the amount of heat that can be obtained per unit of time with an alternative way of financial resources:

$$Pwe = 3{,}17 \times 10^{-8} \times (I/t) + Ka \times W/CP \ \text{[W]}, \quad (8)$$

where:
I – total capital expenditures for construction of intake [zł],
I/t – annual capital expenditures [zł/r],
W – the calorific value of the alternative fossil fuel [MJ/j.p.],
Ka – annual operating costs [zł/r],
CP – alternative of fossil fuel price [zł/j.p.].

ACQUISITION OF GEOTHERMAL ENERGY

Acquisition of GE requires the use of appropriate systems for the extraction of the surface [33]. GE systems can be divided into direct use systems and systems with forced flow of heat-transfer medium [6]:

- the natural geyser system in which heat-transfer medium is extracted to the surface in the form of a geyser,
- the natural hot springs in which heat-transfer medium is extracted to the surface in the form of warm, hot or overheated geothermal water,
- the natural system in which the heat transfer medium is isolated from volcanic outbreaks,
- the artificial system in which the natural heat transfer medium under the effect of artesian hydrostatic pressure is input into the surface to the operating system,
- the artificial system in which the access to the deposit of magma is obtained by artificially made hole ending near the magma,
- the artificial volcanic system in which to the fire of volcanic or magma a smooth shaft or large-diameter hole runs at the bottom of which explosives are placed. As a result of the outbreak a stream of magma comes to the surface and creates a lava lake in a suitably prepared container.

The basic elements of the system's acquisition and development of GE are:

- the geothermal deposit – usually in the form of geothermal aquifer,
- the access channels to the deposit, that connect the operating level with the surface,
- the liquid heat transfer medium,
- the underground equipment such as submersible pumps, heat exchangers,
- a set of devices that enable the use of geothermal water for heating and technological purposes,
- a set of devices capable of converting GE into electricity (for the relevant parameters of geothermal water),
- a set of assistive devices in the case of a low-temperature of thermal energy carrier [6].

An essential part of each mining system is access channels to the bed. There are natural and artificially created channels. Artificial channels make it easy to design the geothermal intake according to the needs of customers.

Among the GE systems using artificially made access channels to geothermal deposits the following can be distinguished:

- the single hole operating system with automatic outflow of geothermal water with low degree of mineralization with artesian pressure,
- the single hole operating system with low degree of water mineralization a low degree of mineralization from the aquifer and by use of submersible pump,
- the single hole open operating system of geothermal with low degree of water mineralization and by use of submersible pump with artificially increased permeability of the deposit near the mining hole,
- the single hole mining and forcing water into the ground system used for the extraction of geothermal water with high degree of water mineralization. In this case it is taken from the field in the lower part of the bed and injected into the bed located above,
- two holes system, which a is closed system used in the case of mineralized geothermal waters with two holes: mining and forcing water into the ground.
- two holes energy receiving system from hot rocks artificially generated water permeability, where heat removal takes place in a forced water circulation [27].

The effectiveness of the construction of the geothermal approach can be determined by cost index (κ), which expresses the ratio of expenditure of underground works (boreholes) to the nominal heat power of geothermal water stream [34]:

$$K = Ko \cdot Nt^{-1} \ \text{[zł/MW]}, \quad (9)$$

where:
Ko – cost of the drilling [zł],
Nt – the nominal heat power of geothermal shot [MW].

The value of *Ko* is dependent on the depth of aquifer and can be expressed as [29]:

$$Ko = a\exp(bH) \ \text{[zł]}, \quad (10)$$

where:
H – hole depth [m],
a and *b* – the cost factors, the value of which depends, among others from the structure and hardness of the rock in a drill place.

The nominal heat power of geothermal shot (geothermal dublet) can be calculated as follows:

$$Nt = V\rho \ cp(T - Tz)2{,}78 \cdot 10^{-7} \ \text{[MW]}, \quad (11)$$

where:
V – the flow of extracted water [$m^3 \cdot h^{-1}$],
ρ – geothermal water density [$kg \cdot m^{-3}$],
cp – the heat of geothermal water [kJ/kgK],
T – temperature of geothermal water [K],
Tz – the temperature of forcing water into the ground [K].

The volume flow of geothermal water possible to extract from a geothermal deposit is calculated from the formula described by Darcy-Dupuita [28]:

$$V = 2\pi kmS/\ln(R/r) \quad [m^3 \cdot s^{-1}], \tag{11}$$

where:
k – bed filtration coefficient [m·s^{-1}],
m – squashing of geothermal deposit [m],
S – depression of water in the hole [m],
r – radius of hole mining near the filter [m],
R – radius of the cone of depression [m].

It follows from the formula that the amount of extracted geothermal water depends on the mining hole design, filtration properties and volume of rocks forming the geothermal water reservoir.

ECONOMIC USE OF GEOTHERMAL ENERGY

GE is used directly and indirectly. The direct, or "non-electric" use of GE is energy used directly (swimming pools and spas, use in agriculture, in water farms, use in industrial, heating and cooling facilities, including district heating and heat pumps) and indirect use of GE is converting it into electricity [2, 13, 24].

The use of geothermal water for spas and recreation goes back to prehistoric times. Warm bath water is one of the oldest procedures used to improve or maintain health [22]. Iceland is well known to be the world leader in the use of geothermal district heating. The island operates 130 pools of the area. 27 tys.m^2, filled with water at the temperature of 35 – 42°C, which are generally available. The most famous ones are Medical Clinic in Hveragerdi and Blue Lagoon Geothermal Spa. Japan has more than 2.200 resorts with hot springs, for example, in the town of Beppu geothermal waters are recommended for diseases of the digestive system, nervous system and skin problems. There are many medical and thermal baths and spas all over Hungary. For example, the thermal spa in Hajduszoblszlo is characterized by a source of geothermal water at the temperature of 73°C, rich in iodine, bromine, sodium chloride, and trace elements. The spa is recommended for musculoskeletal disorders, arthritis, myositis, hypothyroidism, dermatitis. Slovakia has more than 30 resorts with swimming and therapeutics based on geothermal waters, the most famous centers are: Lucky and Oravice of geothermal pools with water temperatures above 30°C.

Spa tourism and balneotherapy are popular in Turkey. There are about 1000 known natural geothermal water sites in Turkey and 194 geothermal spas where geothermal water at the temperature of 36°C are used to treat heart and skin disease and hypertension. In Poland, there are currently 7 spas using geothermal water at temperature from 19 to 45°C form natural sources and wells. They are located in: Ciechocinek, Cieplice Śląskie, Duszniki Zdrój, Iwonicz Zdrój, Konstancin, Lądek Zdrój i Ustroń. The oldest resort in Poland is Lądek Zdrój, the first information comes from 1241. There are six sources of water treatment at the temperature from 20 to 45°C deposited at the depth of 700 m, used in the treatment of the musculoskeletal system, nervous system, skin diseases and respiratory diseases [11]. The seven new swimming and leisure facilities are created In Poland, in the years 2006 – 2011. The most famous of them are located in: Zakopane, Bukowina Tatrzańska, Uniejów and Białka Tatrzańska [15].

GE is used in agriculture for greenhouses heating, soil heating and irrigation, as well as for the decay of biomass. Geothermal heating of greenhouses is practiced in Tunisia, Hungary, Russia, New Zealand, Japan, Iceland, China and the United States. The use of GE for heating reduces the cost of production, which can be as much as 35% of the value of the product. Besides this, GE can be used in colder climate where normal commercial-scale greenhouses would not be cost-effective [25].

GE is directly used in production of mushrooms, fish and animals. There have been successes in water cultures: catfishes, shrimps, eels, trout, snails, alligators conducted in Japan, China, the USA and New Zealand. The use of geothermal heat allows to adjust the temperature of joints, thereby optimizing the growth of breeding material. The use of GE on the farm animals, by adjusting heating and cooling environment stimulates domestic growth, reduces the mortality rate of young, increases litter size, allows to control the disease, facilitates the removal of waste. Geothermal solutions are also used for cleaning, sterilizing and drying facilities for the animals, as well as the alternative in the production of biogas from waste [26].

The geothermal heat is used directly in the industrial scale for drying: agricultural products, fish meal, seaweed, wood construction and dehydration of highly concentrated solutions. Examples of industrial applications of GE are boric acid extraction from geothermal brine (Italy), drying of diatomaceous earth (Iceland), processing of wood and pulp (New Zealand), fermentation of sludge (USA) [26]. GE can also be used directly for the production of drinking water by distillation of sea water [30].

GE is widely used in air conditioning room, which includes both heating and cooling. Heating by the central heating network depends on the delivery hot water or steam from a central source to individual buildings, apartment blocks by the piping network. Supplied thermal energy is used for heating and cooling and for domestic hot water. The primary source of heat is geothermal deposit, but depending on the temperature of the geothermal water and the demand of consumers, district heating can be supplied by the associated system, including fossil fuel and/or heat pumps. Geothermal district heating systems exist in at least 12 countries, including Iceland, France, Poland, Hungary, Turkey and the USA.

Today, in many countries, especially the United States, Switzerland and Germany a lot of heat pump systems are installed with the ground or ground water (groundwater, geothermal heat pumps).

The temperature of groundwater reservoirs and ground use in these systems ranged from 5 to 30°C. Ground source heat pumps use ground water or receive heat through borehole heat exchangers. Geothermal heat pump can be used

for both heating and cooling. Types of heat pumps which can be adapted for use of GE are the water-to-water pumps and water-to-air pumps.

According to Mokrzycki [26], the use of GE in the world is as follows: heating – 37%, spa, swimming pools, baneology – 22%, heat pumps for cooling and heating – 14%, greenhouses – 12%, fish farmers – 8%, industrial – 7%.

Generation of electricity using GE is carried out in 24 countries. The countries which generate more than 15% of the total amount of electricity include: USA, Philippines, Indonesia, Mexico, Italy, Japan, New Zealand, Iceland, El Salvador, Costa Rica, Kenya [3].

There are two basic types of geothermal power plants: steam power plants and binary plants. In steam power station generation of electricity is by using the geothermal water vapor. This system is not widely used, because the use of this solution is limited to the areas of the world where during the extraction of geothermal fluid the dry saturated steam is obtained. In the world there are two such deposits: Larderello in Italy and Geysers in the U.S. [8].

Binary circuit – (two-medium) is used when the geothermal water is highly mineralized, chemically aggressive and its temperature is below 1500°C. In the binary power stations two fluids are working: geothermal water and the working medium with temperature is much lower than temperature of geothermal water. The technological processes used to produce electricity in binary systems are an organic Rankine cycle (ORC) and the Kalina cycle. In both cases, the geothermal water gives off heat in the evaporator, evaporating it at the same time. In the case of ORC, there are organic agents, while in the case of installation based on the Kalina cycle, the ammonia-water mixture [8]. Globally, there are 75 geothermal power plants, where production of electricity is based on the Kalina Cycle or ORC. Especially noteworthy are plants operating in Kalina cycle, since they are characterized by the highest values of electrical power. These are the plants situated in Hsaviku (Iceland), in Unterhaching and Bruchsal (Germany) [10].

THE USE OF GE IN THE WORLD AND IN EUROPE

According to the data presented at the World Geothermal Congress 2010, GE is used directly in 78 countries, and the generation of electricity takes place in 24 countries around the world. At the end of 2009 the total installed capacity for direct use in the world was 50585 MW and heat consumption reached 438073 TJ. The largest share in the world in terms of installed power and consumption of heat belongs to central heating, recreation and therapeutics. In 2009, the total installed capacity for direct use in European countries was 23469 MW and heat consumption 233 737 TJ, representing, respectively, 46.7% and 50.8% share in the world. In terms of total use of geothermal heat, the top five countries are China, the U.S., Sweden, Turkey and Japan, which account for the total of 55% of annual consumption in the world [16].

In 2010, the total installed power of all the geothermal power plants in the world reached the value of 10716 MW and electricity production was 67246 GWh. At the forefront of countries producing electricity in geothermal power plants in the world are: the United States, the Philippines, Indonesia, Mexico and Italy.

In 2010, the total installed capacity of geothermal power plants in Europe amounted to 1553 MW of electricity and the production of electricity had the value of 12372 GWh, making up respectively 14.5% and 18.4% of the "geothermal" generation of electricity in the world [16].

CONCLUSIONS

GE is a renewable source of energy that can be used economically in many parts of the world, both directly and indirectly to generate electricity. It provides not just heat and steam, but electricity itself. Geothermal power generation is completely clean, and releases no harmful gas emissions. GE can be used in aquaculture, horticulture, industry, food processing, and for providing heat for heating buildings.

There is a continuous increase in the development of GE, which could have a significant contribution to mitigating climate change as well as in the implementation of sustainable energy development. In many countries, it is a promising source of renewable energy, which in contrast to other renewable energy sources is available without restrictions throughout the year and not very sensitive to changes in the prices of traditional energy in the world markets.

GE increases local energy security, therefore it is a reliable source of energy and, according to the Declaration of the World Geothermal Congress 2010 – "GE can change the world"

REFERENCES

1. **Bujakowski W., 2003:** Systemy energetyczne wykorzystujące czyste, odnawialne źródła energii. IGSMiE, Kraków, 26–28.
2. **Fridleifsson Ingvar B., 2009:** Energia geotermalna na świecie i jej potencjalna rola w łagodzeniu zmian klimatycznych. Technika Poszukiwań Geologicznych. Geotermia, Zrównoważony Rozwój. 1/2009, Kraków, 3–13.
3. **Gładysz M., 2008:** Elektrownie geotermalne na świecie. GLOBEnergia 2, 14–17.
4. **Górecki W., 2006:** Atlas zasobów geotermalnych formacji paleozoicznych na Niżu Polskim. Goldruk, Kraków.
5. **Górecki W., Hajto M., Sowizdżał A., 2007:** Energia geotermalna energią przyszłości. GLOBEnergia 2, 18–21.
6. **Igliński B., Buczkowski R., Cichosz M., Piechota G., 2010:** Technologie geoenergetyczne. Wydawnictwo Naukowe Uniwersytetu Mikołaja Kopernika, Toruń.
7. **Kaczmarczyk M., 2009:** Podstawy geotermii. GLOBEnergia 2, 13–15.
8. **Kaczmarczyk M., 2009:** Systemy binarne w geotermii. GLOBEnergia 4, 10–13.

9. **Kaczmarczyk M., 2010:** Produkcja prądu elektrycznego. Zastosowanie systemów binarnych w geotermii – przykłady. GLOBEnergia 2, 35–37.
10. **Kaczmarczyk M., 2011:** Wykorzystanie energii geotermalnej do produkcji prądu elektrycznego zastosowaniem Obiegu Organicznego Rankine'a lub cyklu Kaliny – przegląd instalacji działających na świecie. Technika Poszukiwań Geologicznych. Geotermia, Zrównoważony Rozwój. 1–2, Kraków, 131–145.
11. **Kapuściński J., Rodzoch A., 2010:** Geotermia niskotemperaturowa w Polsce i na świecie. Ministerstwo środowiska, Warszawa.
12. **Kępińska B., Łowczowska A., 2002:** Wody geotermalne w lecznictwie, rekreacji i turystyce. Wyd. Instytutu Gospodarki Surowcami Mineralnymi i Energią PAN, Kraków.
13. **Kępińska B., 2007:** Energia geotermalna – wykorzystanie na świecie i w Europie. GLOBEnergia 1, 14–17.
14. **Kępińska B., 2010:** Deklaracja z Bali – Energia geotermalna może zmienić świat. Technika Poszukiwań Geologicznych. Geotermia, Zrównoważony Rozwój. 1–2, Kraków, 187–191.
15. **Kępińska B., 2011:** Energia geotermalna w Polsce – stan wykorzystania, perspektywy rozwoju. Technika Poszukiwań Geologicznych. Geotermia, Zrównoważony Rozwój. 1–2, Kraków, 7–19.
16. **Kępińska B., 2011:** Energia geotermalna na świecie – stan wykorzystania, perspektywy rozwoju. Technika Poszukiwań Geologicznych. Geotermia, Zrównoważony Rozwój. 1–2, Kraków 27–37.
17. **Kotowski W., 2008:** Geotermia: Ogrom energii. Energetyka Gigawat 3, 56–62.
18. **Kowalczuk J., Zarajczyk J., Sobczak P., Mazur J., Rudy S., Cycan D., Winiarczyk M., Jadwisieńczak K, Zalewska K., 2012**. The usefulness of briquettes and pellets from selcted plant materials for energy purposes. TEKA Commission of Motorization and Energetics in Agriculture 12(2): 289–291.
19. **Kowalska A., 2011:** Recruiting and Rusing agricultural biogas. TEKA Commission of Motorization and Power Industry in Agriculture XIC, 118–125
20. **Kowalska A., 2010.:** Overview of technological methods of energy production from biomass. TEKA Commission of Motorization and Power Industry in Agriculture Vol. 10, 88–96.
21. **Kowalska A., 2011:** Recruiting and using agricultural biogas. TEKA Commission of Motorization and Power Industry in Agriculture XIC, 118–125,
22. **Latour T., 2007:** Aktualny stan dalsze możliwości wykorzystania w Polsce wód termalnych do celów leczniczych, profilaktycznych oraz rekreacji. Technika Poszukiwań Geologicznych. Geotermia, Zrównoważony Rozwój. 2, Kraków, 63–69.
23. **Lewandowski W.M., 2007:** Proekologiczne odnawialne źródła energii. WNT, Warszawa 2007.
24. **Lund J.W., 2000:** Sposoby bezpośredniego wykorzystania energii geotermalnej. Technika Poszukiwań Geologicznych. Geosynoptyka i Geotermia. 4, Kraków 2000.
25. **Lund J.W., 2004:** Bezpośrednie zastosowanie ciepła geotermalnego. Technika Poszukiwań Geologicznych. Geosynoptyka i Geotermia. Kraków, 3–19.
26. **Lund J.W., 2004:** Bezpośrednie wykorzystanie energii geotermalnej. Międzynarodowe Dni Geotermalne. Polska 2004, Wyd. Instytutu Gospodarki Surowcami Mineralnymi i Energią PAN, Kraków, 33–50.
27. **Łukasik I.M., 2011:** U źródeł energii odnawialnej – spojrzenie po „horyzont zdarzeń". Rynek energii 6(97), 106–110.
28. **Mokrzycki E., 2005:** Podstawy gospodarki surowcami energetycznymi. RGH Uczelniane Wydawnictwo Naukowo-Dydaktyczne, Kraków 2005.
29. **Nowak W., Sobański R., Kabat M., 2000:** Systemy pozyskiwania i wykorzystania energii geotermicznej. Wyd. Politechniki Szczecińskiej, Szczecin.
30. **Nowak W., Stachel A.A., 2004:** Stan i perspektywy wykorzystania niektórych odnawialnych źródeł energii w Polsce. Wydawnictwo Uczelniane Politechniki Szczecińskiej, Szczecin.
31. **Ney R., 2004:** Rola energii odnawialnej w zrównoważonym rozwoju energetyki. Technika Poszukiwań Geologicznych. Geosynoptyka i Geotermia. 4, Kraków, 35–43.
32. **Pawlikowski M., 2010:** Drinking water production Rusing of geothermal water energy. Technika Poszukiwań Geologicznych. Geotermia, Zrównoważony Rozwój. 1–2, Kraków 2010, 87–90.
33. **Smętkiewicz K., 2010:** Geotermia petrotermalna. GLOBEnergia 1, 30–33.
34. **Sobański R., Kabat M., Nowak W., 2000:** Jak pozyskać ciepło z Ziemi?, Centralny Ośrodek Informacji Budownictwa, Warszawa.

POZYSKIWANIE I GOSPODARCZE WYKORZYSTANIE ENERGII GEOTERMALNEJ

Streszczenie. Energia geotermalna to energia pochodząca z wnętrza Ziemi, zakumulowana w wodzie, parze wodnej oraz gorących suchych skałach. Całkowite zasoby energii geotermalnej przekraczają one 35 bilionów razy obecne, globalne zapotrzebowanie na energię. Energia geotermalna jest odnawialna, występuje powszechnie, jest niezależna od zmieniających się warunków klimatycznych co daje możliwość jej gospodarczego wykorzystania. W artykule przedstawiono podstawowe informacje dotyczące energii geotermalnej, sposobów jej pozyskiwania i wykorzystania. Omówiono również metody obliczania zasobów energii geotermalnej.
Słowa kluczowe: energia geotermalna, odnawialne źródła energii.

TEKA. COMMISSION OF MOTORIZATION AND ENERGETICS IN AGRICULTURE – 2013, Vol. 13, No. 1, 139–144

The study of the rotary cutting process of chosen energy plants

Henryk Rode, Paweł Witkowski

Warsaw University of Technology,
Faculty of Construction, Mechanics and Petrochemistry,
Department of Mechanical Systems Engineering and Automation
Address: Jachowicza 2, 09-400 Płock, Poland, e-mail: hrode@op.pl

Received February 2.2013; accepted March 14.2013

Summary. The article presents a comparison of study results concerning the cutting process of three energy plants: Salix Viminalis, Side Hermaphrodite and Miskanthus Giganteus. The study also presents the influence of the surface area of a stem's cross-section and the speed of rotary disk with knives speed on the unitary energy of the cutting process of stems.

Key words: rotary mower, unitary energy of cutting, rotary cutting process, Salix Viminalis, Side Hermaphrodite, Miskanthus Giganteus, energy plants

INTRODUCTION

The biomass energy can partly replace energy used from fossils. The use of biomass energy protects the environment against greenhouse effect [2,3,6,7]. New technologies for energy plants production need to be effective and cheap. That is why it is important to optimize the harvest, processing and breaking up of these plants [5]. The features influencing the unitary energy of cutting are: plant's dimensions, shear strength, friction factor and moisture [9,11,12]. The studies of the cutting process of energy plants should be useful while designing cutting units and choosing parameters of working units for harvest machines [10,13,21].

The studies of the cutting process of energy plants have been carried out at the Institute of Mechanical Engineering – Warsaw University of Technology in Płock for many years. The research mainly refers to the influence of the cutting process parameters and the plants' constitution on the quality and energy consumption of the cutting process. The previous research had been carried out on a laboratory stand of pendulous type and referred to axe cutting. The new laboratory stand enabled rotary cutting of energy plants' stems.

THE PURPOSE OF RESEARCH

The aim of the research was to determine the influence of selected constructional and functional parameters of the cutting unit on the rotary cutting process of energy plants: Salix Viminalis, Side Hermaphrodite and Miskanthus Giganteus [14,15,23,24,25].

The study was carried out at the research stand for studying energy plants rotary cutting process at the Department of Mechanical Systems Engineering and Automation – Warsaw University of Technology in Płock [16,22].

The research of the energy plants' cutting process included:

– determining unitary energy of the cutting process in the function of surface area of the section of the plant's stem with different diameters
– determining unitary energy of the cutting process in the function of rotary speed of the disk with knives.

The notion of unitary energy means the total energy needed for the realisation of the cutting process falling on the unit area of the section of the cut plant.

THE SUBJECT OF STUDY

Energy plants – in accordance with the UE law – are those which grow on plantations and are processed into biofluel, biocomponents, heat energy or electric energy.

The plants are characterised by quick and high biomass increase, high fuel value, high resistance to frost and pests and low soil requirements – due to which wasteland can be used. Moreover, due to the energy plants features, there is a high vulnerability to mechanized agro-technical activities connected with starting a plantation, running it and harvesting biomass [1,4].

Salix viminalis, Sida hermaphrodita and Miscantus gigantheus were selected for the study. The plants were select-

ed according to their popularity and constitution distinctness. Salix viminalis is an arborescent plant, Sida hermaphrodita is a perennial plant and Miscantus gigantheus is a grass [8,17,18,19,20].

The researched plants came from the Experimental Station at the Faculty of Agriculture and Biology – University of Life Sciences in Skierniewice [The Experimental Station of the Faculty of Agriculture at SGGW].

RESEARCH STAND

The measurement of the unitary energy of cutting was carried out at the research stand for studying energy plants rotary cutting process (Fig.2.). The stand consists of two independently working units (cutting unit and transporting unit) set in a construction frame. The cutting unit consists of inertial knives placed on the circumference of the working plate – diameter 50cm.The working plate is set to the working hub, which is driven by electric motor of the cutting unit. Transporting unit is driven by another electric motor, which pulls a truck along the slide by a line. The truck's construction allows to set the research material of different dimensions and constitutions.

The inverter controls the rational speed of motors. The value of the rational speed of motors is achieved through adequate frequency setting. A required frequency value is put into a computer programme (Drive View), which is designed for LG inverters.

METHODOLOGY AND RESEARCH

For the study of the rotary cutting process, 150mm long samples were prepared. Due to the plants' different constitutions, the samples with the following diameters of stems were prepared: Salix Viminalis (9 – 13,5) mm , Side Hermaphrodite (7,5 – 12) mm, Miskanthus Giganteus (6,5 – 11) mm. The measurement of the diameters was done with the use of a slide calliper in 3 different surfaces. The samples of the researched plants were set on a truck. Its motion imitated the transmission of the cutting unit when used in real condition on plantation farm. The truck's speed was constant, 0,314 m/s, during all the tests. The samples of the plants were set vertically in rows. The measurement was done 3 times for each diameter of the stems. The rotary speed of the working plate, the moisture of the samples and the voltage were constant during the tests. The atmospheric pressure, where the research took place, was equal to 762 mm Hg and the temperature was 20ºC. The cutting process for 3 different rational speeds of the disk with knives was studied: at 1424 r.p.m, 1824 r.p.m and 2108 r.p.m.

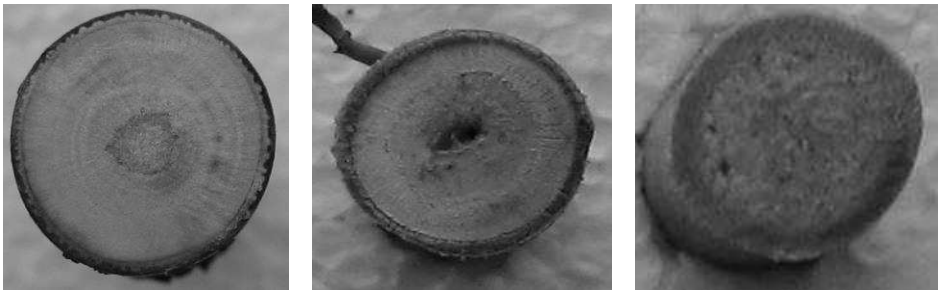

Fig. 1. View of the researched plants' stems in a cross-section: (starting from left) Salix Viminalis, Side Hermaphrodite and Miskanthus Giganteus

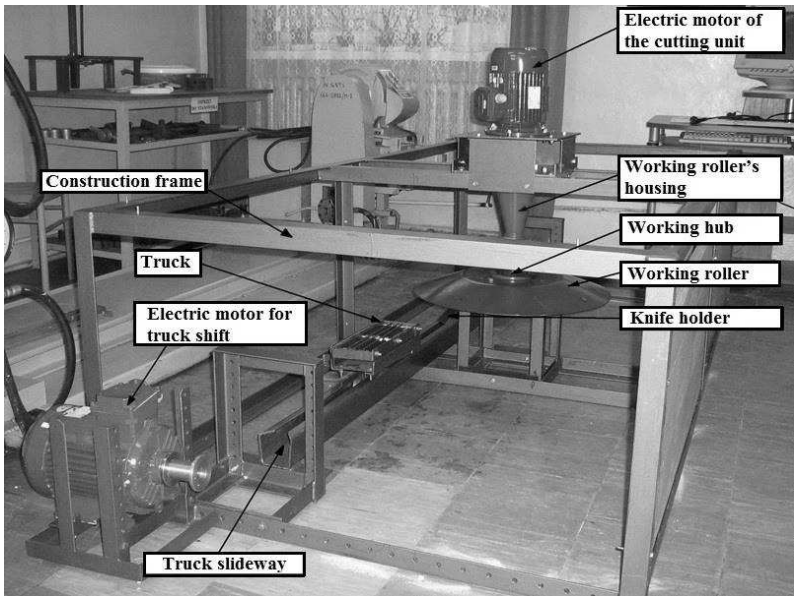

Fig. 2. Station for studying energy plants rotary cutting process

RESEARCH RESULTS AND ANALYSIS

It can be stated, on the basis of the research results, that the unitary energy of Salix Viminalis stems cutting increases together with the cutting surface increase (Fig.3.) and it decreases together with the increase of the rotary speed of the disk with knives from the cutting unit (Fig.4). This tendency is the same for all the tested speeds and diameters. It is connected with the cutting resistance of the plants epidermis. The resistance decreases together with the knife's speed increase.

The unitary energy of cutting Side Hermaphrodite stems decreases together with the cutting surface increase (Fig.5.). This tendency is true for the 2 speeds of the 3 studied. The unitary energy of cutting reaches a significant minimum at the rotary speed of the disk with knives being 1800 r.p.m. (Fig.6.). The tendency is true for all the cut plants' surface areas studied.

The unitary energy of cutting Miskнthus Giganteus stems decreases significantly together with the cutting surface increase (Fig.7.). This tendency is true for the speeds studied. The unitary energy of cutting reaches a significant maximum at the rotary speed of the disk with knives being about 1800 r.p.m. (Fig.8.). The tendency is true for all the cut plants' surface areas studied.

CONCLUSIONS

The study of the rotary cutting process of energy plants is the continuation of studies carried out on the research station of pendulous type. The next step is to carry out a research for chosen energy plants that would determine the influence of some other parameters, e.g.: moisture or the truck's linear velocity on the unitary energy of the cutting process. The research should involve some other energy plants, e.g.:

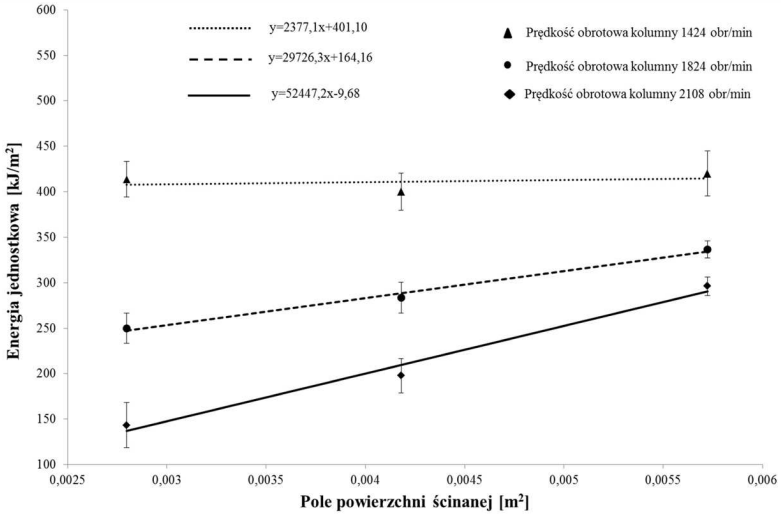

Fig. 3. The course of changes of unitary energy of Salix Viminalis in the cut surface area function
Legend: energia jednostkowa – unitary energy [kJ/m²]; pole ścinanej powierzchni – cut surface area [m²]; ●▲♦ rotary speeds

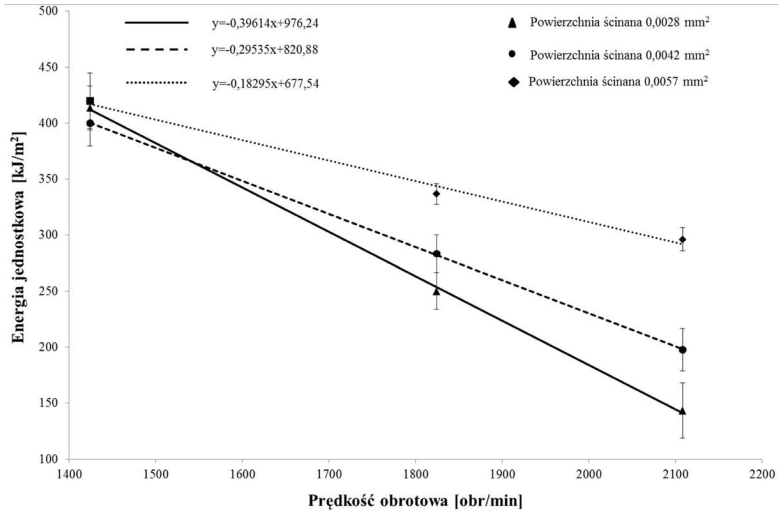

Fig. 4. The course of changes of unitary energy of Salix Viminalis in the function of rotary speed of disk with knives
Legend: energia jednostkowa – unitary energy [kJ/m²]; prędkość obrotowa – rotary speed [r.p.m.]; ●▲♦ the cutting surface

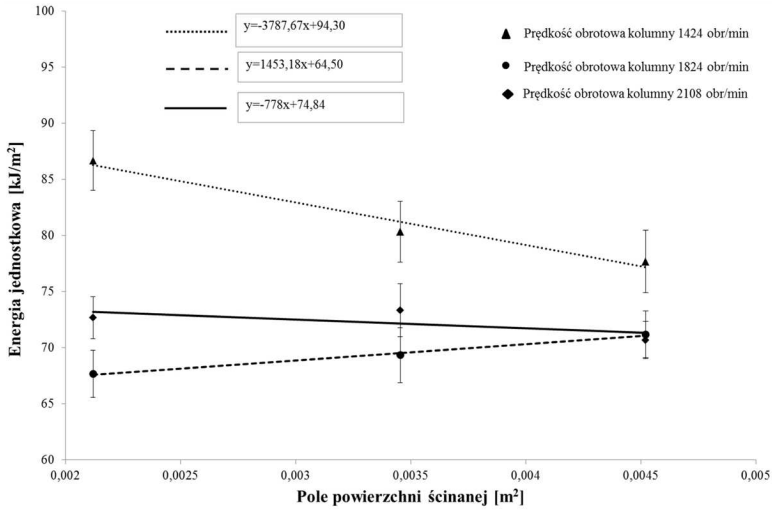

Fig. 5. The course of changes of unitary energy of Side Hermaphrodite in the cut surface area function

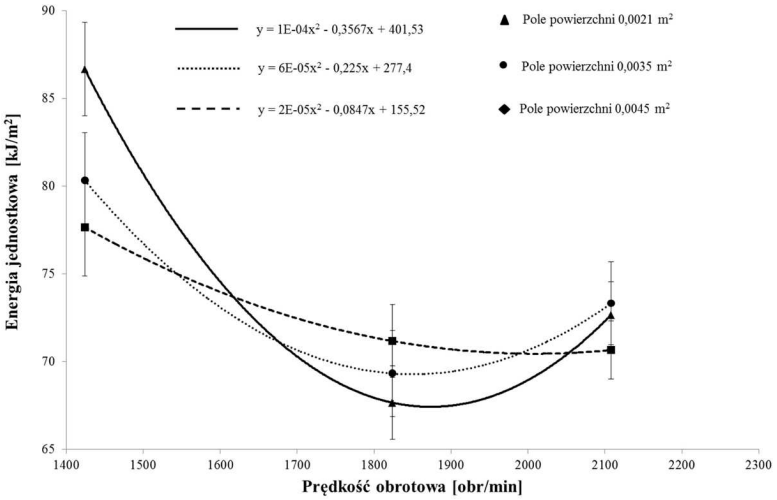

Fig. 6. The course of changes of unitary energy of Side Hermaphrodite in the function of rotary speed of disk with knives.

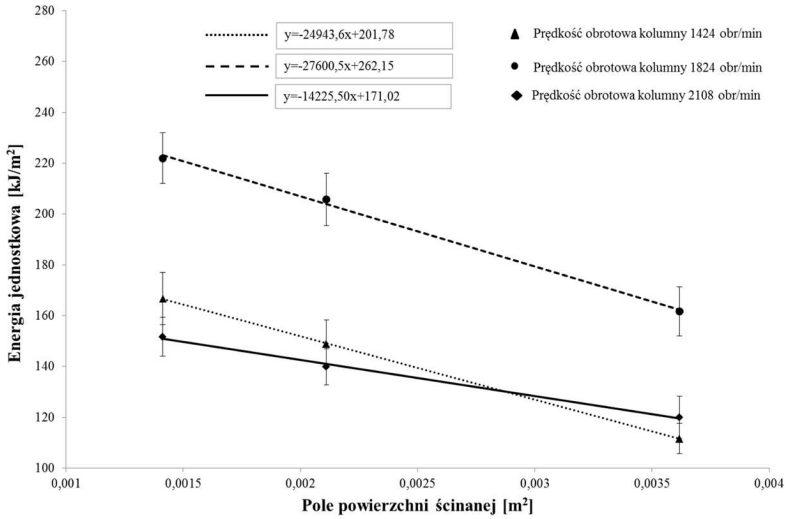

Fig. 7. The course of changes of unitary energy of Miskanthus Giganteus in the cut surface area function

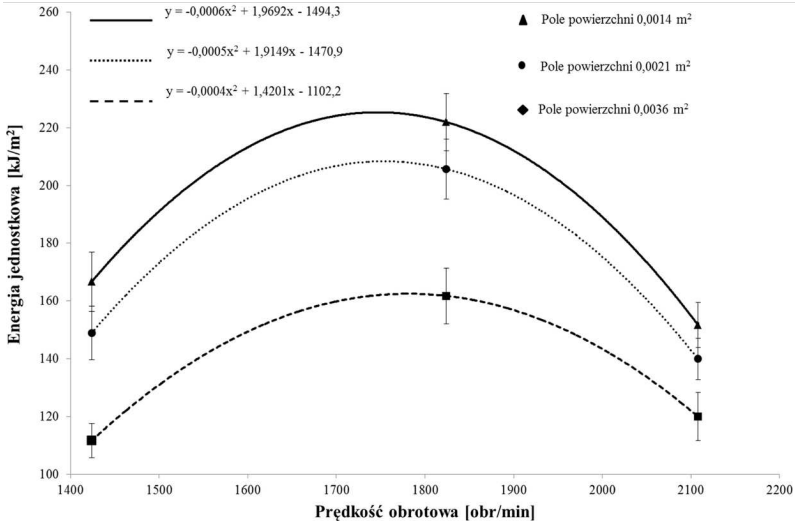

Fig. 8. . The course of changes of unitary energy of Miskanthus Giganteus in the function of rotary speed of disk with knives

a multiflower rose. The cutting process should be studied with the use of flat disk of the cutting unit.

Determining the influence of the cutting unit type on the cutting process energy is another issue. It is necessary to replace the disk with knives with the disk of circular saw.

There is a need to build a new research station equipped with a unit of two cutting disks with adjustable angle of inclination. This should be as close with the construction of a cutting unit of an agricultural machine as possible. An initial design of such a station is being prepared.

REFERENCES

1. **Baran D., Kwaśniewski D., Mudryk K., 2007:** Wybrane właściwości fizyczne trzyletniej wierzby energetycznej. Inżynieria Rolnicza, nr 8(96), 7–12.
2. **Cisek J., Mruk A., Hlavńa V., 2011:** The properties of a HDV diesel engine fuelled by crude rapeseed oil. Teka Komisji Motoryzacji i Energetyki Rolnictwa – OL PAN, XI, 29–39.
3. **Dreszer K., Michałek R., Roszkowski A., 2003:** Energia odnawialna – możliwości jej pozyskiwania i wykorzystania w rolnictwie. Wyd. PTIR, Kraków–Lublin–Warszawa.
4. **Dubas J., Grzybek A., Kotowski W., Tomczyk A., 2004:** Wierzba energetyczna – uprawa i technologie przetwarzania. Wyższa Szkoła Ekonomii i Administracji. Bytom.
5. **Frączek J., Mudryk K., 2006:** Metoda określenia oporów cięcia pędów wierzby energetycznej. Inżynieria Rolnicza, nr 8(83), 91–98.
6. **Gradzik P., Grzybek A., Kowalczyk K., Kościk B., 2003:** Biopaliwa. Warszawa.
7. Grzybek A., 2002: Biomasa jako alternatywne źródło energii. Warszawa.
8. **Juliszewski T., Kwaśniewski D., Baran D., 2006:** Wpływ wybranych czynników na przyrosty wierzby energetycznej. Inżynieria Rolnicza, nr 12(87), Kraków, 225–232.
9. **Kowalczyk-Jusko A., Kulig R., Laskowski J., 2011:** The influence of moisture content of selected energy crops on the briquetting process parameters. Teka Komisji Motoryzacji i Energetyki Rolnictwa – OL PAN, XI, 189–196.
10. **Kowalski S., 1993:** Badania oporów cięcia wybranych roślin. Zeszyt Prob. Post. Nauk Rol. 408, 297–303.
11. **Lisowski A. i inni., 2010:** Technologie zbiorów roślin energetycznych. Wydawnictwo SGGW, Warszawa.
12. **Lisowski A., 2006:** Ścinanie i rozdrabnianie wierzby energetycznej, Technika Rolnicza Ogrodnicza Leśna 4, 8–11.
13. **Popko H., Miszczuk M., 2004:** Badania oporów krajania niektórych produktów spożywczych.. Zeszyt Prob. Post. Nauk Rol. 354.
14. **Rode H., Witkowski P., 2011:** Moisture influence on the unitary energy of a cutting process of selected energy plants. Teka Komisji Motoryzacji i Energetyki Rolnictwa. vol. XI, Lublin, 317–325.
15. **Rode H., 2011:** The energy of a cutting process of a selected energy plant. Teka Komisji Motoryzacji i Energetyki Rolnictwa. vol. XI, Lublin, 326–334.
16. **Rode H., Witkowski P., 2012:** The study of the rotary cutting process of energy plants. Teka Komisji Motoryzacji i Energetyki Rolnictwa. vol. XII, Lublin, 231–235.
17. **Rudko T., Stasiak M., 2004:** Właściwości mechaniczne pędów wierzby energetycznej. III Zjazd Naukowy. Referaty i doniesienia. Dąbrowice 27–29.09.2004.
18. **Rutkowski L., 2006:** Klucz do oznaczania roślin naczyniowych Polski niżowej. Wyd. Naukowe PWN, Warszawa.
19. **Szczukowski S., Tworkowski J., Stolarski M.J., 2004:** Wierzba energetyczna. Wydawnictwo Plantpress Sp. z o.o., Kraków.
20. **Szczukowski S., Tworkowski J., Wiwart M., Przyborowski J., 2002:** Wiklina (Salix Sp.) Uprawa i możliwości wykorzystania. Wydawnictwo Uniwersytetu Warmińsko-Mazurskiego, Olsztyn.
21. **Szymanek M., 2007:** Analysis of cutting process of plant material. Teka Komisji Motoryzacji i Energetyki Rolnictwa – OL PAN, VIIA, 107–113.
22. **Witkowski P., 2011:** Stanowisko do badań procesu cięcia roślin. Rozdział w monografii Inżynieria me-

chaniczna – innowacje dla przedsiębiorstw. 129–132. Politechnika Warszawska, Płock.
23. **Żuk D., 1979:** Określenie koniecznej prędkości elementów tnących w maszynach do ścinania źdźbeł i łodyg. Maszyny i Ciągniki Rolnicze nr 3/1979. Warszawa.
24. **Żuk D., 1986:** Proces cięcia źdźbeł zbóż. Prace Naukowe Politechniki Warszawskiej – Mechanika z. 95. Warszawa.
25. **Żuk D., Rode H., 1992:** Propozycje oceny energetycznej zespołów tnących. Prace Naukowe Politechniki Warszawskiej – Mechanika z. 152. Warszawa.

BADANIE PROCESU CIĘCIA ROTACYJNEGO WYBRANYCH ROŚLIN ENERGETYCZNYCH

Streszczenie. W artykule porównano wyniki badań procesu cięcia trzech roślin energetycznych: wierzby konopianej, ślazowca pensylwańskiego, miskantusa olbrzymiego. Przedstawiono wpływ pola powierzchni przekroju przecinanej łodygi rosliny oraz prędkości obrotowej tarczy z nożami na energię jednostkową procesu ich cięcia.
Słowa kluczowe: kosiarka rotacyjna, energia jednostkowa cięcia, cięcie rotacyjne, wierzba konopiana, ślazowiec pensylwański, miskantus olbrzymi, rośliny energetyczne.

TEKA. COMMISSION OF MOTORIZATION AND ENERGETICS IN AGRICULTURE – 2013, Vol. 13, No. 1, 145–148

Influence of osmotic dehydration on convective drying process of cherries

Stanisław Rudy[1], Dariusz Dziki[1], Andrzej Krzykowski[1],
Renata Polak[1], Beata Biernacka[1], Ryszard Kulig[2]

[1]Thermal Engineering Department, University of Life Sciences,
Doświadczalna 44, 20-236 Lublin, Poland,
[2]Department of Equipment Operation and Maintenance in the Food Industry,
University of Life Sciences, Doświadczalna 44, 20-236 Lublin
e-mail: stanislaw.rudy@up.lublin.pl

Received February 17.2013; accepted March 14.2013

Summary. The paper presents the results of convective drying process of cherries at the temperature of 70°C and at an air flow velocity of 0.5 m×s-1. Fruits were subjected to a pre-osmotic dehydration in 60% sucrose solution for durations from 4 to 24 hours, and the control raw material without dehydration. The results showed that the losses of total weight and water, and the increasing of dry matter during the osmotic dehydration of cherries were the highest at the first five hours of process. The osmotic dehydration over 15 hours had little influence on these parameters. The osmotic dehydration significantly decreases the total energy inputs for the drying of cherries, from 33 to 52% in relation to non-dehydrated raw material.
Key words: osmotic dehydration, convective drying, cherry.

Abbreviations
D*m* – loss of weight [%],
D*mw* – loss of water form dehydrated material [kg],
D*ms* – increase of dry weight (after dehydration) [kg],
mo – initial weight of the raw material [kg],
mt – weight of material after dehydration period *t* [kg],
mso – initial dry weight of the raw material [kg],
mst – dry weight of the raw material after time of dehydration *t* [kg],
u – absolute humidity [$kg_{H2O} \cdot kg_{s.s.}^{-1}$].

INTRODUCTION

Vegetables and fruits are on important aspect of the human diet because of their nutritional value. However they are usually in short supply because they are perishable crops, which deteriorate within a few days after harvest. Preserving these crops in their fresh form for long period has been a problem. A very common method of preservation for these agricultural corps is to dry them in order to conserve the perishable fruits, reduce storage volume and to extend their shelf life beyond the few weeks when they are in season [1]. Longer shelf-life, product diversity and substantial volume reduction are the reasons for popularity of dried fruits and vegetables, and this could be expanded further with improvements in product quality and process applications [14]. Drying can be done by many of methods such as sun drying or industrially through the use hot air drying or freeze drying. The most common drying method employed for food materials to date was hot air drying. However there are many disadvantages of this method. Among these are low energy efficiency and lengthy drying time during the falling rate period. This is mainly caused by rapid reduction of surface moisture and consequent shrinkage, which often results in reduced moisture transfer and, sometimes, reduced heat transfer. Several investigators of drying have reported that hot air drying, hence prolonged exposure to elevated drying temperatures, resulted in substantial degradation in quality attributes, such as colour, nutrients, flavour, texture, severe shrinkage, reduction in bulk density and rehydration capacity, damage to sensory characteristics and solutes migration from the interior of the food to the surface. Thus many of methods are used for pretreatment fruits and vegetables before drying. Before drying fruits and vegetables may be dehydrated or blanched as a pre-treatment to lessen changes in colour and reduce the total number of microorganisms in the food and improve the heat and mass transfer [5].

Food drying is one of the oldest methods of preserving food. Since drying reduces the moisture in foods making them lightweight and convenient to store, it can easily be used in place of other food preservation techniques. Besides, this moisture content decides about physical properties of food and determines the course of many processes [15, 16, 20].

Osmotic dehydration is a pre-treatment method used for food preservation before drying. This process enables fruits and vegetables to be stored for a longer period of time. The mechanism of the osmotic dehydration process is the difference in the concentrations of osmotic substance in the material and in the solution. Osmotic dehydration is a process that entails a partial removal of water from food items

such as vegetables and fruits [2, 4, 11]. Due to the one-side diffusion of water from the drained material to the solution and the osmotic active substance in the opposite direction, the material after osmotic dehydration is characterized by lower absolute humidity and changed chemical composition [17, 18, 22]. Dehydration of sucrose solutions primarily contributes to changes in the surface layer of the material, thus reducing the adverse chemical reactions and losses of water-soluble substances, it also improves the organoleptic characteristics of the raw material [9, 10, 14]. The osmotic dehydration of fruits and vegetables significantly affects the shortening of the drying time, and thus reduces the drying energy requirements [1, 6, 5]. Fruits dried after the initial osmotic dehydration process are characterized by higher ratio of sugars content to organic acids contents in comparison to the raw material without osmotic dehydration. In most cases they retain the natural color and flavor and are preferred by consumers [3, 8, 13, 21].

There are few works concerning the convective drying process of osmotic dehydrated cherries. The aim of the present work was to evaluate the influence the osmotic dehydration time of cherries on the convective drying process. Especially, the indices of osmotic dehydration were determined, the kinetic of the process was presented and the drying energy requirements were evaluated.

MATERIALS AND METHODS

The material for investigation were fruits of cherries (cv. Kelleris) at the stage of full technological maturity. The pits were removed from fruits and the initial moisture content and dry matter were evaluated. Studies of osmotic dehydration of cherries were performed at 20°C for 6 periods (4, 8, 12, 16, 20 and 24 hours). Osmotic dehydration was carried out in a solution of sucrose at the concentration of 60%. The ratio by weight of the raw material to the osmotic agent was 1:4. The process of osmotic dehydration, depending on its duration, was characterized on the basis of the following indices [23]:

– the total weight loss after dehydration:

$$\Delta m = \frac{m_o - m_t}{m_o} \cdot 100\%, \quad (1)$$

– the loss of water from dehydrated material:

$$\Delta m_w = \frac{m_t(100 - m_{st}) - m_o(100 - m_{so})}{m_o \cdot m_{so}} \cdot 100\%, \quad (2)$$

– the increase of dry matter after dehydration:

$$\Delta m_s = \frac{m_t \cdot m_{st} - m_o \cdot m_{so}}{m_o \cdot m_{so}} \cdot 100\%. \quad (3)$$

The convection drying process of cherries was performed at the temperature of 70°C and the air flow velocity of 0.5 ms^{-1}. The convection was conducted using a vertical air-flow dryer. A detailed description of the measuring stand was presented by Krzykowski et al. [7]. The measuring stand was also equipped with a meter of electric power. The specific drying energy was calculated using the numerical integration method changes of power consumption as a function of time, related to the mass of the processed material. The measurements were replicated 5 times. The regression analysis was carried out on these data. All the statistical tests were carried out at the significance level of a = 0.05.

RESULTS

The greatest relative humidity loss was observed at the beginning of the process (the decrease form 85% to 76%, for the first five hours of the process), and then the relative humidity decreased with time (up to 68%). The relative humidity loss during the osmotic dehydration of cherries was described using the polynomial regression equation of the third degree (Fig. 1). The change in relative humidity during the osmotic dehydration results from two opposing processes: 1) passage of water and solutes from the dehydrated material to the solution, 2) passage of osmotic active substance to the dehydrated material.

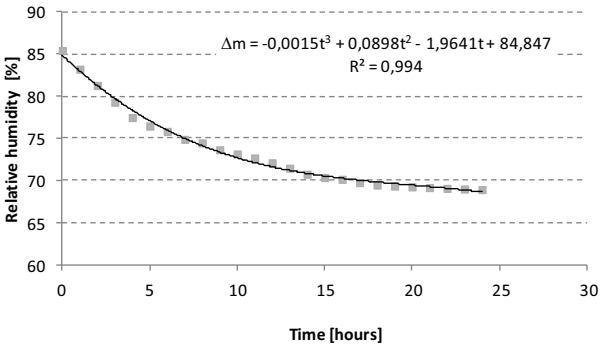

Fig. 1. The relative humidity loss as a function of osmotic dehydration time of cherries

Changes in the mass of water as a function of the duration of the osmotic dehydration process were described using the polynomial regression equation of the fourth degree (Fig. 2).

The largest loss of water by weight, reference on a kilogram of dry substance, occurred during the first five hours of osmotic dehydration. After 24 hours of the process, from the raw material containing one kilogram of dry matter more than 3.5 kilograms of water was discharged.

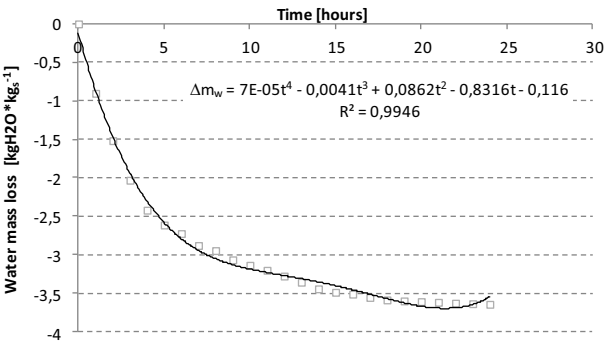

Fig. 2. The loss of water during osmotic dehydration of cherries in relation to time

Figure 3 presents the influence of osmotic dehydration time on an increase of dry matter in cherries. The relation

was described by using the polynomial regression equation of the third degree. The highest increase of dry matter was observed at the beginning of the process (during first five hours of osmotic dehydration). After 24 hours of osmotic dehydration, dry weight of the material more than doubled.

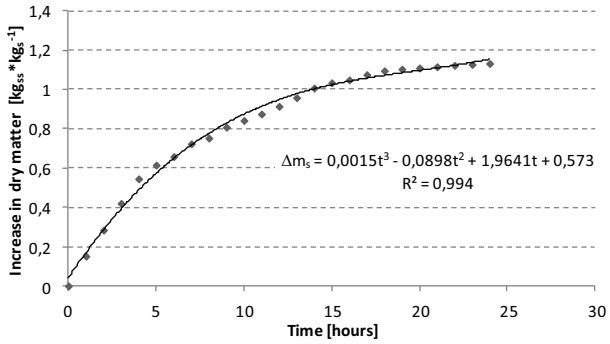

Fig. 3. The increase of dry matter during the osmotic dehydration of cherries

The osmotic dehydrated cherries (from 4 to 24 hours) and the control sample were subjected to convection drying. The drying kinetics of cherries was presented in Fig. 4. The drying curves of dehydrated and non-dehydrated cherries have the characteristic shape for the capillary-porous bodies. Depending on the duration of osmotic dehydration, the material subjected to the drying process was characterized by different initial moisture content. Drying curves of dehydrated material were similar in shape, regardless of the duration of the dehydration process. Drying curves obtained from the material dehydrated for 20 and 24 hours had almost the same characteristics. The regression equations describing the changes of absolute humidity in relation to drying time were of quadratic form (Table 1).

Table 1. The regression equations describing the changes of absolute humidity of dried material in relation to drying time

Dehydration time [h]	Regression equation	R^2
0	u = 2E-05t² – 0,0206t + 5,6131	0,9972
4	u = 2E-05t² – 0,0164t + 3,4007	0,9991
8	u = 2E-05t² – 0,0155t + 2,8867	0,9995
12	u = 2E-05t² – 0,0149t + 2,5756	0,9996
16	u = 3E-05t² – 0,0147t + 2,296	0,9983
20	u = 3E-05t² – 0,0162t + 2,2168	0,998
24	u = 3E-05t² – 0,0161t + 2,192	0,9983

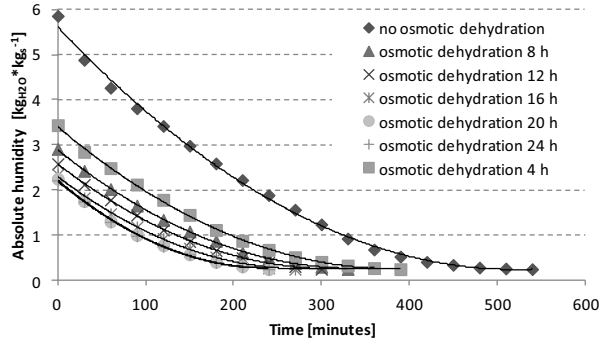

Fig. 4. Convection drying kinetics of osmotic dehydrated cherries and a control sample

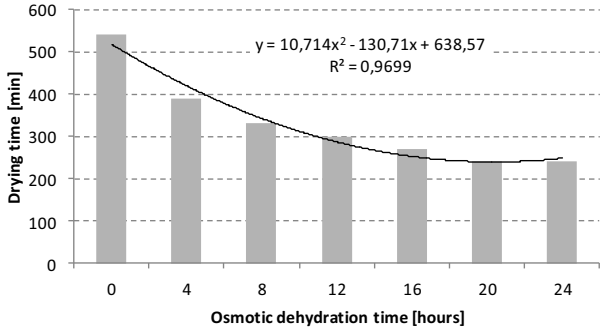

Fig. 5. The convection drying time in relation to osmotic dehydration time of cherries

The relation between the osmotic dehydration time and drying time was presented in Figure 5. The osmotic dehydration significantly decreased the duration of convection drying process. The longest drying time was found for non-dehydrated cherries (540 min). The shortest drying time (240 min) was obtained for fruits dehydrated for 20 and 24 hours.

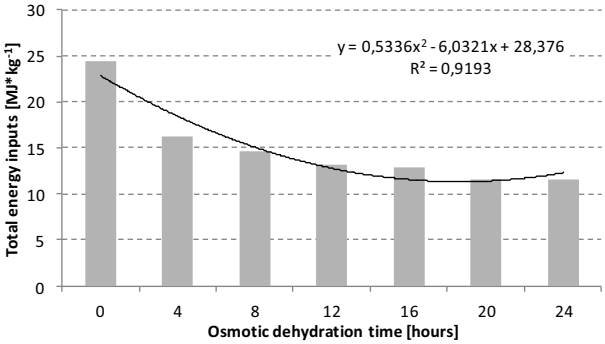

Fig. 6. The total energy inputs for drying of cherries

The total energy inputs required to dry one kilogram of osmotic dehydrated cherries and control sample were presented in Figure 6. The results showed that as the osmotic dehydration time increased, a decrease of total drying energy was observed (average from 24 MJ·kg^{-1} to 12 MJ·kg^{-1}).

CONCLUSIONS

On the basis of the obtained results, the following conclusions can be formulated:

1. The losses of total weight and water, and the increasing of dry matter during the osmotic dehydration of cherries were the highest at the first five hours of process. The osmotic dehydration over 15 hours had little influence on these parameters.
2. The osmotic dehydration caused a decrease of drying time of cherries in comparison to non-dehydrated fruits (from 150 min to 300 min for 4 hours and 24 hours of osmotic dehydration, respectively).
3. The osmotic dehydration caused a decrease of total energy inputs for drying of cherries from 33 to 52% in relation to non-dehydrated raw material.

4. Taking into account the time of drying and the total energy inputs, it is recommended to dry cherries at 70°C after osmotic dehydration in 60% sucrose solution for 20 hours.

REFERENCES

1. **Chua K.J., Mujumdar A. S., Hawlader M.N.A., Chou S. K., Ho J. C. 2001:** Batch drying of banana pieces effect of stepwise change in drying air temperature on drying kinetics and product colour. Food Research International, 34, 721–731.
2. **Corzo O. Go´ mez, E. R. 2004:** Optimization of osmotic dehydration of cantaloupe using desired function methodology. Journal of Food Engineering, 64, 213–219.
3. **Dixon G. M., Jen J. J. Paynter, V. A. 1976:** Tasty apple slices result from combined osmotic-dehydration and vacuum- drying process. Food Process Development., 10, 634-638.
4. **Fito, P. 1994:** Modeling of vacuum osmotic dehydration of food. Journal of Food Engineering, 22, 313–328.
5. **Kozak P., Dziki D., Krzykowski A., Rudy S. 2011:** Optymalization of energy consumption in the freeze drying process of champignon (*Agaricus bisporus* L.). TEKA Commission of Motorization and Energetics in Agriculture nr XIc., 134–141.
6. **Krzykowski A., Rudy S., Kozak P., Dziki D., Serwatka Z. 2011:** Influence of blanching and convective drying conditions of parsley on process energy consumption TEKA Commission of Motorization and Power Industry in Agriculture, XIC., 142-150.
7. **Krzykowski A., Dziki D., Polak R., Rudy S. 2012:** Influence of heating plates temperature on freeze drying energy requirements and quality of dried vegetables. TEKA Commission of Motorization and Power Industry in Agriculture 2(2), 129-131.
8. **Lazarides, H. N., Katsanidis, E., Nickolaidis, A. 1994:** Mass transfer kinetics during osmotic preconcentration aiming at minimal solid uptake. Journal of Food Engineering, 25, 151-166.
9. **Lenart, A, Lewicki P. 1995:** Osmotic dehydration of fruits and vegetables Warsaw: Warsaw Agricultural University Press, 99–111.
10. **Lenart A. 1991:** E€ect of saccharose on water sorption and rehydration of dried carrot. In A. S. Mujumdar, & I. Filkova, Drying'91. Amsterdam: Elsevier, 489–498.
11. **Lenart A. 1995:** Osmotic dehydration of foods before convection drying. In A. Lenart, & P. P. Lewicki, Osmotic dehydration of fruits and vegetables Warsaw: Warsaw Agricultural University Press, (pp. 99–111.
12. **Lenart A., Cerkowniak M. 1996:** Kinetics of convection drying of osmodehydrated apple. Polish Journal of Food and Nutrition Sciences, 5/46, 73–82.
13. **Lenart A., Flink J. M. 1984:** Osmotic concentration of potato. II. Spatial distribution of the osmotic effect. Journal of Food Technology, 19, 65–89.
14. **Lenart A., Lewicki P.P., Mlynarczyk, G. 1987:** Effect of osmotic dehydration on the physico-chemical properties of dried apples. In Annals of Warsaw Agricultural University ± SGGW. Food Technology and Nutrition, 17, 55–63.
15. **Mitrus M., Oniszczuk T., Mościcki L. 2011:** Changes of specific mechanical energy during extrusion-cooking of potato starch TEKA Commission of Motorization and Power Industry in Agriculture, XIC, 200–207.
16. **Mitrus M, Wójtowicz A. 2011:** Extrusion-cooking of wheat starch TEKA Commission of Motorization and Power Industry in Agriculture, XIC, 208–215.
17. **Prokharkar S.M., Prasad S., Das H. 1997:** A model for osmotic concentration of bananas slices. Journal Food Science and Technology, 34, 230–232.
18. **Raoult-Wack A.L. 1994:** Advances in osmotic dehydration. Trends in Food Science and Technology 5, 255–260.
19. **Rastogi N.K., Niranjan K. 1998:** Enhanced mass transfer during osmotic dehydration of high pressure treated pineapple. Journal of Food Science, 63, 508–511.
20. **Rydzak L., Andrejko D. 2011:** Effect of different variants of pretreatment of wheat grain on the particle size distribution of flour and bran. TEKA Commission of Motorization and Power Industry in Agriculture, XIC, 283–290.
21. **Salvatori D., Andres, A. Chiralt A., Fito, P. 1999:** Osmotic dehydration progression in apple tissue. I. Spatial distribution of solutes and moisture content. Journal of Food Engineering, 42, 125- 132.
22. **Simal S., Benedito J., Sa´nchez E.S., Rosello C 1998:** Use of ultrasound to increase mass transport rate during osmotic dehydration. Journal of Food Engineering, 36, 323–336.
23. **Pękosławska A., Lenart A. 2008:** Wpływ powlekania na przebieg odwadniania osmotycznego dyni, Postępy Techniki Przetwórstwa Spożywczego, 1, 9–14.

WPŁYW CZASU OSMOTYCZNEGO ODWADNIANIA NA PROCES KONWEKCYJNEGO SUSZENIA WIŚNI

Streszczenie. W pracy przeprowadzono badania konwekcyjnego suszenia owoców wiśni w temperaturze 70°C i przy prędkości przepływu 0,5 $m \times s^{-1}$. Owoce zostały poddane procesowi wstępnego odwadniania osmotycznego w 60% roztworze sacharozy dla sześciu czasów trwania tego procesu – od 4 do 24 godzin oraz dla surowca nie poddanego zabiegom wstępnym. Na podstawie uzyskanych wyników badań stwierdzono, że całkowite straty masy oraz wody, jak również wzrost suchej substancji były największe przez pierwsze pięć godzin odwadniania osmotycznego wiśni. Po 15 godzinach trwania tego procesu zmiany tych parametrów były już niewielkie. Odwadnianie osmotyczne powodowało skrócenie czasu suszenia oraz zmniejszenie całkowitych nakładów energii na ten proces (od 33 do 52%) w porównaniu do surowca nie poddanego odwadnianiu.
Słowa kluczowe: odwadnianie osmotyczne, suszenie konwekcyjne, wiśnia pospolita.

TEKA. COMMISSION OF MOTORIZATION AND ENERGETICS IN AGRICULTURE – 2013, Vol. 13, No. 1, 149–154

Research into the energy balance of a standalone photovoltaic tracking system

Mariusz Sarniak

Warsaw University of Technology
Faculty of Civil Engineering, Mechanics and Petrochemistry
Department of Mechanical Systems Engineering and Automation
Address: Al. Jachowicza 2/4, 09–402 Płock, e-mail: sarniak@pw.plock.pl

Received January 10.2013; accepted March 14.2013

Summary. The paper presents research into the energy balance of a standalone photovoltaic tracking system. The investigations were conducted on selected days in the months from September until December 2012. A prototype research stand allowed a control of the fixing plane of the photovoltaic modules. The central elements of the PV tracking system was an inverter (TN-1500 212B) and its software. Energy balance was measured for the PV tracking system in both the stationary and tracking modes. Additionally, the authors also measured the energy balance for the configuration of the inverter in the energy saving and in UPS modes.
Key words: photovoltaics, photovoltaic module, PV tracking system, standalone PV system, energy balance.

INTRODUCTION

There are a variety of reasons to begin utilizing renewable sources of energy (RSE). In relevant literature [1, 4, 12, 14, 19] we can find the following observations substantiating the use of RSE:

– depletion of non-renewable energy sources (fossil fuels),
– elimination of destructive impacts on the natural environment related to the excavation and use of fossil fuels,
– a global increase in the human population and a gradually growing level of human quality of life results in an increase in the consumption of energy,
– sometimes statements are made that the XXI century is the age of RSE as compared to previous centuries when the XIX century was named the age of coal and steam and the XX century – the age of crude oil and natural gas).

The phenomenon of photovoltaic conversion is based on a direct conversion of the energy of solar radiation into electrical energy [9, 13, 15, 18]. The amount of energy reaching the photovoltaic module depends on the density of the stream of the solar radiation. In order to use the energy potential of the sun to the maximum, tracker systems are used increasingly. Their task is to set the surface of the photovoltaic modules (referred to as PV) perpendicularly to direct solar radiation.

The most popular PV tracking systems are [10, 11]:

– those controlled by the signals from the radiation sensors,
– those controlled by the theoretically preset sun positions depending on the location of the PV system, date and time,
– hybrid systems being the combinations of the previous two.

The economic aspect of the application of PV tracking systems is also important. On one hand we can analyze the energy-related benefit resulting from the application of PV systems and on the other hand we should mind the consumption of energy needed to control the process. We should also take into account the increased capital expenditure on the construction of a PV tracking system.

THE TEST STAND

For the purpose of the investigations a prototype test stand was constructed whose layout has been shown in Figure 1. The layout presents the possible flows of energy (arrows) among the elements of the PV system.

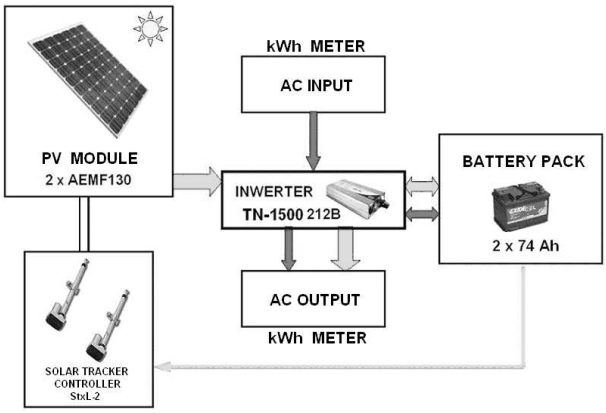

Fig. 1. Layout of the test stand for the investigations of a standalone PV tracking system

The main elements of the experimental standalone PV tracking system are:

– two monocrystalline PV modules – marked AEMF130 – in a parallel connection using special MC4 solar connectors,
– a TN-1500 212B inverter with software supervising the operation of the whole PV system [3],
– tracking system composed of an StxL-2 sensor controller [2], cooperating with two electric Super Power Jack 24'' actuators,
– a set of two acid-lead batteries in a parallel connection of the total nominal capacity of 148 Ah,
– two wattmeters (GREENBLUE GB202) used for the measurement of the energy at the input and output of the PV system.

Figure 2 presents an image of a prototype PV tracking system showing the mechanism realizing the direct sunlight tracking algorithm by the plane fixed to the load bearing section with an asymmetric knuckle joint having four roll encased bearings (UCP204). The control of the tracking system is realized by an StxL-2 controller fitted with a photocell and two Super Power Jack 24" electric actuators independently battery-powered (12V DC – maximum power consumption 1.5A i.e. the maximum power consumption of approximately 18W).

Fig. 2. Image of the prototype PV tracking systems

The working principle of the PV system is that with a frequency of every 5 minutes the direction of the direct sunlight is checked by a controller and actuators are activated to set the PV modules perpendicularly to the sun radiation as needed. The stand can be switched to manual control with electric actuators.

METHODOLOGY AND SCOPE OF RESEARCH

The research was conducted on a prototype research stand being an entirely standalone PV tracking system of the rated power of 260 W_p (W_p – watt of peak power). The prototype PV system is a stationary one and was located in the area of the following geographical coordinates: 52.48 N and 19.67 E (as shown by a GPS device). The tests were carried out from September until December.

The central element of the PV system, as shown in the layout in Figure 1, is the TN-1500 212B inverter. This is a device that replaces several other devices in a conventional standalone PV system. It comprises: charging voltage regulator, sinusoidal DC/AC converter, solar charger and power supply bypass switch. The inverter can be configured with special software and it is connected with the computer through a COM or a USB port.

Figure 3 shows an example screenshot of a system monitoring the functioning of the PV system. The supervising system shows instantaneous basic PV parameters. The inverter can supervise the system in two modes: in the UPS mode and in the energy saving mode. Figure 4 shows a screenshot of a configuration window of INVERTER V.1.38 showing the prototype PV system parameters.

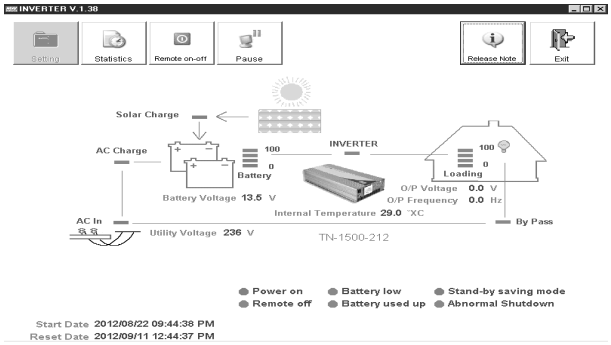

Fig. 3. Example screenshot of the TN-1500 212B inverter software

The above-mentioned two basic operating modes of the inverter (UPS and energy saving) can be supplemented with an additional option of 'inverter off' if no load is detected (below 5W) [2]. The parameters of functioning of the battery chargers (solar chargers and regular – AC chargers) were chosen as per the battery manufacturer recommendations.

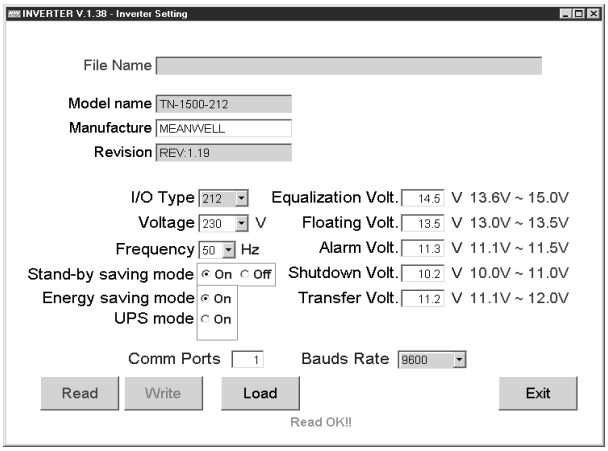

Fig. 4. Configuration window of the INVERTER V.1.38 software with the set parameters of the tested PV system shown

In the UPS mode the inverter controls the PV system similarly to a computer backup power supply (UPS) but for battery charging it uses the solar charger. Figure 5 shows a detailed layout of the functioning of the inverter in the UPS mode. The main objective of this mode is to ensure the longest possible supply of power at the system output. An interruption of the continuity of the power supply takes place only when there is no power in the external AC power supply and the voltage on the battery terminals drops below 10.2 V. Any further operation of the PV system would lead to a critical discharge of the battery and thus its damage. An additional parameter of the inverter operation in this mode is the activation of the AC battery charger only when the charging current drops below 3 A.

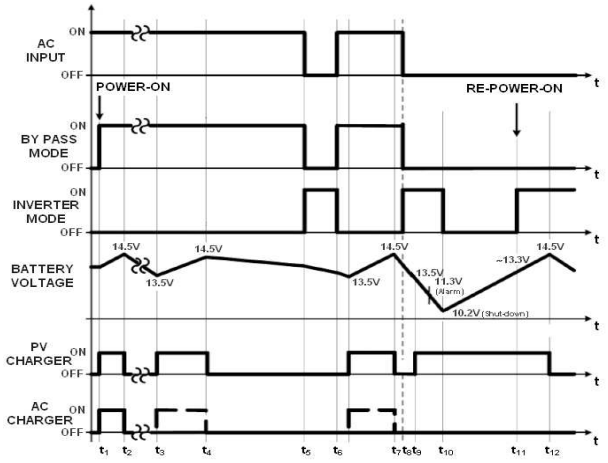

Fig. 5. Characteristics of the TN-1500 212B inverter operation in the UPS mode

In the energy saving mode the inverter controls the PV system so that for the battery charging it chiefly uses the solar charger. Figure 6 presents the details of the inverter operation in this mode.

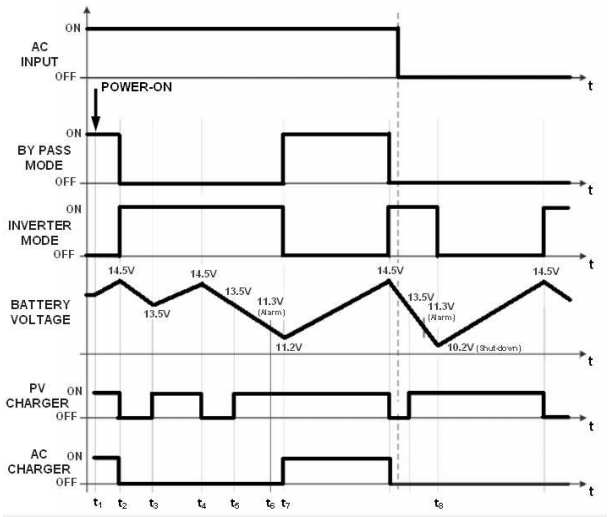

Fig. 6. Characteristics of the TN-1500 212B inverter operation in the energy saving mode

Contrary to the UPS operating mode, in the energy saving mode the inverter uses the solar charger to the maximum, thus reducing the use of the AC charger. Activation of the AC charger in this mode will take place only when the voltage on the battery terminals drops below 11.2 V. The continuity of power supply in this case is a priority in terms of the system operation.

The calculation of the energy balance consisted in the reading the kilowatt-hour meters once per day at 22:00 when the solar charger of the inverter was off. The PV system was under a constant load of 160W automatically activated in the window 22:00÷6:00 in order to unify the obtained results during the performance of the energy balance. This was the method for obtaining of a stable load of the PV system during the tests. The daily energy balance was calculated as an arithmetic average of the value from the kilowatt-hour meters at the input and output of the PV system for the selected three days of a given month. An important issue is that the voltage of the AEMF130 module at the point of maximum power is, according to the manufacturer specifications [6] 17.2 V and the battery charging voltage values shown in figures 5 and 6 are much lower, which leads to losses of the generated power.

RESULTS

Figure 7 shows the energy balance measured at the AC input and output of the TN-1500 212B inverter constituting the central elements of the PV system. The measurements were carried out for a tracking system, and a manually set position of the stationary system, as per the methodology described by the author in [16]. The energy balances for the two basic operating modes of the inverter were also calculated.

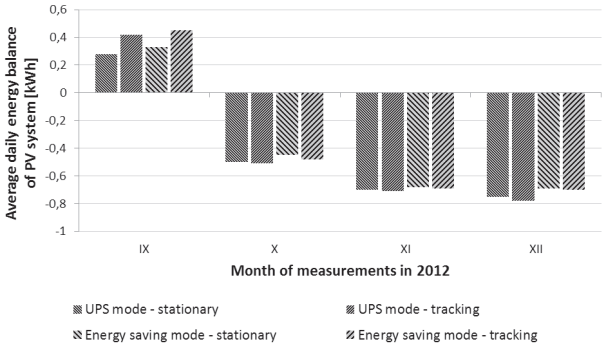

Fig. 7. Energy balance for the prototype PV tracking system

The results obtained in the energy balance for the PV tracking system to some extent confirm the hypothesis that in the winter months the use of tracking solutions in PV systems is unsubstantiated. The PV tracking system can only be construed as a guaranteed power source, assuming that an additional power generator will be the public electricity provider (rather than a combustion engine power generator). The TN-1500 212B inverter is a device that cooperates with the PV modules of the rated voltage of 12 V that is lower than the voltage of the work point of the maximum power. Another reason for the lower system efficiency is the necessity to adapt the PV generator operation to the maximum admissible range of the battery charging voltage [7].

The drawbacks of the standalone system are partly eliminated by the application of an inverter that is capable of tracking the point of the maximum power (MPPT) in a wide voltage range. A modification of the test stand by this element required an increase in the power output of the PV generator (to a minimum of 600 W_p). Inverters are usually fitted with functionalities that monitor the operation of the PV system and, most importantly, do not require the application of batteries.

CONCLUSIONS

1. Due to the necessity of adapting the operating parameters to the characteristics of a system of batteries, standalone PV systems do not usually use the point of maximum power of the generator built from the PV modules.
2. When the batteries reach the maximum admissible voltage (14.5 V – as shown in Fig. 4) the battery solar charger of the inverter is disconnected and the energy potential of the PV modules is not used.
3. In order to make the energy balance of the PV system more precise it would be necessary to develop an additional measuring point of the energy generated in the PV modules on the DC side. This would enable a determination of the indexes of solar fraction (F_{SOL}), performance ratio (P_R) and the final yield (Y_F) that are characteristic of the PV systems [9].
4. The results of the energy balance of the PV tracking system somewhat confirm the theory that in the winter months the use of tracking in PV systems is unsubstantiated. The PV tracking system can only be construed as a guaranteed power source, assuming that additional power generator will be a public electricity provider (rather than a combustion engine generator).
5. Under Polish climatic conditions, designing standalone PV systems operating throughout the year is uneconomical because of the need to select special system subassemblies for winter months characteristic for low sunlight level. If, in the winter months, we change the PV system to function in the UPS mode then the designed system is much smaller. This pertains to both the PV generator and the batteries.

REFERENCES

1. **Chwieduk D., 2006:** Modelowanie i analiza pozyskiwania oraz konwersji termicznej energii promieniowania słonecznego w budynku. Instytut Podstawowych Problemów Techniki PAN. Warszawa.
2. Instrukcja obsługi sterownika StxL-2: http://xlabs.pl/aukcje_pliki/instrukcja_STxL-2.pdf.
3. Instruction Manual. 2012: TS/TN-1500 INVERTER. MEAN WELL ENTERPRISES CO., LTD. http://www.meanwell.com.
4. **Kaiser H., 1995:** Wykorzystanie energii słonecznej. Wydawnictwo AGH. Kraków.
5. **Kapica J., 2011:** Application of a microcontroller in simulation of the photovoltaic generators. TEKA COMMISSION OF MOTORIZATION AND POWER INDUSTRY IN AGRICULTURE. Vol. 11, 173–180. Lublin.
6. Karta produktu modułu AEMF130. 2012: Active Energy: http://www.actionenergy.pl.
7. **Knaga J., Szul T., 2012:** Optimising the selection of batteries for photovoltaic applications. TEKA COMMISSION OF MOTORIZATION AND ENERGETICS IN AGRICULTURE. Vol. 12, No. 1, 73–77. Lublin–Lugansk.
8. **Marecki J., 1995:** Podstawy przemian energetycznych. WNT, Warszawa.
9. **Messenger R. A., Ventre J., 2010:** Photovoltaic Systems Engineering. Third Edition. CRC Press 2010. ISBN: 978-1-4398-0292-2.
10. **Myczko A., Karłowski J., Lenarczyk J., 2010:** Porównanie efektywności energetycznej zestawu modułów fotowoltaicznych stacjonarnych i pracujących w układzie nadążnym w warunkach gospodarstwa rolnego. Problemy Inżynierii Rolniczej nr 4/2010.
11. **Nalepa K., Neugebauer M., Spłowiej P., Chmielewski R., 2009:** Wykorzystanie mikrokontrolera jednoukładowego do sterowania optymalnym ustawieniem płaszczyzny ogniwa fotowoltaicznego w stosunku do słońca. Inżynieria Rolnicza 8(117)/2009.
12. **Nowicki J., 1980:** Promieniowanie słoneczne jako źródło energii. Arkady, Warszawa.
13. **Pluta Z., 2000:** Podstawy teoretyczne fototermicznej konwersji energii słonecznej. Oficyna Wydawnicza Politechniki Warszawskiej. Warszawa.
14. **Roszkowski A., 2006:** Agriculture and fuels of the future. TEKA Komisji Motoryzacji i Energetyki Rolnictwa. Vol. 6, 131–134. Lublin.
15. **Sarniak M., 2008:** Podstawy fotowoltaiki. Oficyna Wydawnicza Politechniki Warszawskiej. ISBN: 978-83-7207-773-8. Warszawa.
16. **Sarniak M., 2012:** The method of selection of optimum fitting parameters for stationary photovoltaic systems and optimum control parameters for tracking photovoltaic systems. TEKA COMMISSION OF MOTORIZATION AND ENERGETICS IN AGRICULTURE. Vol. 12, No. 1, 243–246. Lublin–Lugansk.
17. **Smoliński S., 1998:** Fotowoltaiczne źródła energii i ich zastosowania. Wydawnictwo SGGW. Warszawa.
18. **Szymański B., 2013:** Małe instalacje fotowoltaiczne. Wydanie I. GLOBEnergia. Kraków.
19. **Tymiński J., 1997:** Wykorzystanie odnawialnych źródeł energii w Polsce do 2030 roku. Aspekt energetyczny i ekologiczny. Wydawnictwo IBMER. Warszawa.
20. PN-EN ISO 9488: 2002: Energia słoneczna – Terminologia.
21. PN-EN 60891: 2010: Postępowanie zapewniające korekcję temperatury i natężenia promieniowania do pomierzonych charakterystyk prądowo napięciowych krystalicznych urządzeń krzemowo – fotowoltaicznych.

BADANIA BILANSU ENERGETYCZNEGO NADĄŻNEGO AUTONOMICZNEGO SYSTEMU FOTOWOLTAICZNEGO

Streszczenie. W pracy przedstawiono badania bilansu energetycznego nadążnego autonomicznego systemu fotowoltaicznego. Badania prowadzono w wybranych dniach dla miesięcy od września do grudnia 2012 roku. Prototypowe stanowisko badawcze umożliwiało sterowanie płaszczyzną zamontowania modułów fotowoltaicznych. Centralnym elementem nadążnego systemu PV był inwerter TN-1500 212B z oprogramowaniem. Dla nadążnego systemu PV zmierzono bilans energetyczny w układzie nadążnym i stacjonarnym. Dodatkowo pomierzono również bilans dla konfiguracji inwertera w trybie oszczędzania energii oraz w trybie UPS.
Słowa kluczowe: fotowoltaika, moduł fotowoltaiczny, nadążny system PV, autonomiczny system PV, bilans energetyczny.

TEKA. COMMISSION OF MOTORIZATION AND ENERGETICS IN AGRICULTURE – 2013, Vol. 13, No. 1, 155–160

Attitudes of students towards corporate social and environmental responsibility

Oksana Seroka-Stolka

Department of Public Health, Faculty of Management, Czestochowa University of Technology, Armii Krajowej 36b 42-200 Częstochowa, oksanas@zim.pcz.pl

Received January 25.2013; accepted March 14.2013

Summary. The results of the survey allow to assess the attitudes of students towards the role of the natural environment in the functioning of the company by the concept of social and environmental responsibility which only 1/5 of the respondents are familiar with. Respondents take into account first of all the level of salary and the prospects of their personal development opportunities within the company while choosing the employer. Unfortunately, criteria like the high level of corporate environmental culture and high eco-innovativeness are not important during choosing the employer.

Key words: attitudes, the environment, corporate social responsibility.

INTRODUCTION

Given the growing importance of the environmental aspect, which is global and affects the diversity of enterprises' strategic choices, it becomes ever more substantial to recognize natural environment issues in business[1]. Manufacturers and energy users introduce pro-environmental innovations or seek for such opportunities [6, 7, 8, 10, 12, 17, 19, 27, 33, 34, 36, 38]. Pro-environmental, eco-innovative, or emission-reducing activities, as well as the creation of related databases, are referred to in various publications [11, 15, 16, 21]. The realization of an enterprise's environmental objectives is facilitated by the concept of CSR (Corporate Social Responsibility) in the framework of the so called corporate environmental responsibility (environmental CSR). Successful and effective implementation of this framework is possible only with the change of attitudes towards the environment of all parties of social and economic activity. The environmental knowledge alone is not enough if it is not followed by attitudes changes, that can also be shaped during the didactic process in universities [20, 35]. The economy and the society need employees and citizens who create new knowledge and new pro-environmental and eco-innovative solutions [28]. The development of pro-environmental attitudes requires the increase in the level of environmental awareness, which is a concept combined from psychological, social, and economic elements [13, 22, 24, 37].

The purpose of this study was to learn the attitudes and opinions of young respondents on the subject of the implementation and realization of the concept of Corporate Social Responsibility in relation to the environment. The study purposes also included the recognition of the criteria hierarchy, which is used by future employees when choosing the employer, and the interdependencies among those criteria.

STUDY MATERIALS AND METHODS

A survey questionnaire was used in the course of the study, and it was distributed directly to the respondents (random survey). The study was conducted in 2011 on a sample of 382 University of Technology[2] students, representing following faculties: Management – 73%, Civil Engineering – 9%, Electrical Engineering – 9%, and Materials Processing Technology and Applied Physics – 9%. The purposive sampling was used, and the sample was diverse in terms of age and gender (women – 71%, men – 29%). Average age of respondents was 25 years. The vast majority of the sample were employed individuals (89% of the sample).

Obtained statistics were processed with STATISTICA 9.0 application both in terms of quantity and quality. The

[1] The natural environment concept is recognized by the Author as an equivalent of the environment concept in the management sciences.

[2] The sample is not representative thus the limitations in terms of quantity and sample choice make it impossible to generalize results for all students in Poland. Further studies are planned among students of other Polish universities.

qualitative approach used Mann–Whitney U test and Spearman's rank correlation coefficient.

In the first area of the study respondents answered to the following questions: 1. Are you familiar with the concept of Corporate Social Responsibility (response categories: "yes" or "no")? 2. Where did you encounter the concept of Corporate Social Responsibility for the first time (response options: university classes, the media, Internet, conferences, trainings, workshops, friends, work)? 3. Do you think there is a place for ethics in business? 4. Is it possible to combine pro-environmental activities of enterprises with their financial interests? 5. Pro-environmental activity of an enterprise results in higher or lower profit? (Answers were coded as follows: 1 – "much higher profit", 2 – "higher profit", 3 – "the same profit", 4 – "lower profit", 5 – "much lower profit")? 6. In the future, would you like to run your business, driven by the principle of environmental responsibility? 7. Do you expect enterprises to become more involved in environmental issues. In this part of the study a scale of 1 to 5 was used. In the second part of the first area of the study respondents were asked about the reasons for enterprises undertaking or not undertaking environmental activities (questions 8 and 9) and the activities that an enterprise responsible for the environment should undertake. Those questions 8 to 9 were multiple choice questions. In the second area of the study respondents were asked to rank factors which they took into account when choosing the employer on a scale of 1 to 10[3].

RESULTS AND DISCUSSION

The study conducted among the students indicates that only 21% of the respondents are familiar with the concept of Corporate Social Responsibility, and the sources of knowledge on this subject are primarily university classes (49%), and media (39%). Only 6% of the respondents chose workplace and Internet as sources for developing knowledge on CSR. 81% of the respondents believe that there is a place for ethics in business. 27% of the respondents strongly agree with the statement that it is possible to combine the pro-environmental activities with financial interest of the enterprise. Over 57% of the respondents answered "probably yes", about 13% had no opinion, and only 7% declared that it is impossible to combine pro-environmental activities with the stable financial development of the company. According to less than 27% of the respondents pro-environmental activities result in the higher profit for companies. Over 87% of the respondents declared the will to apply the principles of environmental responsibility in business, and only less than 6% had no opinion. More than half of young consumers (52%) expect greater involvement of enterprises in environmental activities in case of their negative impact on the environment, 26% believe that such activities should be undertaken by all entities, regardless of the type of their business. Pro-environmental management is irrelevant for 10% of the respondents. 7.5% of the respondents have no opinion, and 4.5% do not expect companies to engage in environmental activities at all.

Clearly the most respondents (35% of answers) believe that the main incentive to undertake pro-environmental activities in enterprises is the creation of a positive image and reputation, and is part of the marketing activities (24.6% of answers). The respondents identified the basic factors that determines the lack of pro-environmental activities as: the shortage of financial resources (26% of answers), the desire to make quick and easy profit by companies (22% of answers), the absence of positive role models of shared responsibility for the environment in the society (19% of answers), low environmental culture of companies (16% of answers). The respondents believe that enterprises, which include the principles of sustainable development in their activities (33% of answers) and reduce the acquisition of natural resources (24% of answers) are perceived as entities guided by concern for the natural environment.

In the second area of the study, related to the analysis of the variables affecting the selection of the employer by the respondents, it was found on the basis of the ranking (according to the average rank) that the projected level of proposed salary was the most important criterion (2.47). In second place, the respondents chose the prospects and opportunities for their own development in the company (3.25), and in third – opportunities for promotion (3.83). As another factor the respondents classified the good image of the company in the society (4.94), and following in order: opinions of the company employees about the atmosphere in the company (5.44), prestige (5.51), company size (6.68), and company's involvement in environmental activities (7.34). The last positions of the ranking included high environmental culture (7.57) and high eco-innovativeness of the enterprise (7.98). As far as the hierarchy of the employer selection criteria went it was observed that for women a good image in the society is somewhat more important than for men (Mann-Whitney U test showed a difference on the border of statistical significance ($p = 0.054$; $a = 0.05$).

In the second part of this study area correlations between variables were examined (between employer selection factors). Spearman's rank correlation analysis showed the highest statistically significant positive correlation between the variables 9 and 10 (high eco-innovativeness and environmental culture of the company; $R = 0.38$), which meant that the greater the importance of environmental culture of the company for the respondents, the greater the importance of its high eco-innovativeness. On the other hand the highest statistically significant negative correlation was found for the variables 8 and 5 ($R = -0.40$), 8 and 6 ($R = -0.34$), and 9 and 5 ($R = -0.33$), respectively. The above ratios lead to the following conclusions: the larger the company and its prestige, the less important is the opinion of the company for the respondents; the higher the environmental culture in the company, the less important is its size in terms of the number of employees[4]. Correlation matrix was presented in Table 1.

[3] Where: 1 – is the most important criterion, 10 – is the least important criterion.

[4] The structure of enterprises' size in Poland: small enterprises – 10-49 employees, medium enterprises – 50-249 employees, large enterprises – over 250 employees.

Table 1. Criteria of selecting the employer – matrix of correlations

	1	2	3	4	5	6	7	8	9	10
1. level of proposed salary	1.00									
2. development opportunities (trainings, workshops)	0.17*	1.00								
3. promotion opportunities	0.20*	0.23*	1.00							
4. company's good image in the society	-0.18*	-0.24*	-0.18*	1.00						
5. company's size	-0.14	-0.17*	-0.11*	-0.07	1.00					
6. company's prestige	-0.02	-0.14	-0.11	-0.15	0.26*	1.00				
7. company's involvement in environmental activities	-0.30*	-0.04	-0.21*	-0.04	0.01	-0.24*	1.00			
8. opinions of employees about the atmosphere in the company	-0.15	-0.13	-0.20*	-0.07	**-0.40***	-0.34*	-0.06	1.00		
9. company's high environmental culture	-0.22*	-0.21*	-0.20*	-0.05	-0.33*	-0.17*	0.25*	0.10	1.00	
10. company's high eco-innovativeness	-0.22*	-0.26*	-0.19*	-0.15	-0.26*	-0.17*	0.04	0.16	**0.38***	1.00

An asterisk was used to indicate only statistically significant correlation results with the significance level 0.05; *p < 0.05.
Source: own elaboration.

Most decisions on the implementation and priority of environmental objectives belongs to the competency of managers whose environmental values system influences the development of environmental awareness and attitudes of all employees. Environmental awareness of employees is a strong incentive of organizational nature. It determines the number of environmental instruments used by organizations that promote the reduction of their negative impact on the environment [39]. Pro-environmental attitudes and behaviors contribute to making sustainable and responsible business decisions by employees [5, 25,39]. Employees' attitudes stimulate enterprises to improve the level of environmental culture and environmental responsibility, as the readiness of people for actions and behaviour, showing respect for the environment, [1, 9]. Social responsibility is poorly recognized among the Polish society and university students [29]. The main reasons identified by the students, which drive the enterprises implementing CSR are primarily the positive image and reputation of the company, while the cause of limiting the implementation of that idea is the shortage of financial resources in the company. These opinions are consistent with the opinions of entrepreneurs, mainly from the sector of small and medium-sized enterprises [30, 32].

Enterprises employing people who present pro-environmental attitudes and behaviour can expect the reduction of their negative environmental impact and the increase in the employees' involvement in environmental issues in the long term [2]. Reduction of the negative impact on the natural environment results from the tendency in most entities in the developed economies of the world to replace fossil energy resources with renewable energy sources, that grew into importance after the energy crisis [31]. First generation transport biofuels (produced from edible plants) emit large amounts of CO2. Based on the estimates, it occurs that only bio-ethanol produced from sugarcane complies with the Directive 2009/28/EC on the reduction of CO2 emissions [4]. These requirements are also met by the biofuels of the second and third generation, produced from inedible plants or waste materials.

Production of energy plants is thus a part of the complex system, namely the national economy. It should be considered in multiple aspects, taking into account the assumptions and stages of realization of the strategy of energy production from renewable sources [14]. In Western Europe, more and more of those who look for work take into account Corporate Social Responsibility and the care for the environment as an important criteria in the search for employer [23]. The review of the literature on the subject indicates that the most important factors in selecting an employer include: salary level, reputation of the company, personal development opportunities, positive relationships with colleagues and their expertise, stability of employment, size of the company and the personality and demographic factors [3, 18, 26]. Above conclusions are consistent with the results of the study, as the level of the proposed salary and growth opportunities in the company are the most important determinants for those looking for work. Unfortunately, companies' concern about the natural environment expressed by a high environmental culture that facilitate high eco-innovativeness in enterprises is hardly taken into account by surveyed young future employees, as these two criteria were classified in the last two places in the ranking. Positive image of the enterprise in the society, as part of the social responsibility idea realization was classified by the respondents only in fourth place. Qualitative analysis of the employer selection criteria by gender showed that women pay more attention to the positive image of the company in the society. This finds confirmation in the literature on the subject, which indicates that men are primarily driven by own development opportunities in the company, and woman by good reputation of the company or its convenient location [3].

Analysis of the correlation coefficients for employers selection attributes demonstrated that respondents perceive the relationship between high eco-innovativeness of companies and their environmental culture. It is interesting that the larger the company in terms of the number of employees, the less important for the respondents is its high eco-innovativeness.

CONCLUSIONS

The foundation to build the corporate responsibility for the natural environment consists of the employees of enterprises and their attitudes towards respect for the environment. This study proved that the surveyed young potential employees poorly recognize the idea of Corporate Social Responsibility, even though the vast majority of them believe that there is place for ethics in business nowadays. The optimistic accent of the study was the fact that the majority of respondents was determined to implement the CSR ideas in their future businesses, and believed that it is possible to combine pro-environmental activities of enterprises with their financial interests. Opinions of respondents also indicate the growing environmental requirements of the young generation in the area of the environmental responsibility of business decisions, as the vast majority expect enterprises to care more about the natural environment. Recruiting and retaining the best employees can determine the success of the business through the ability to receive and interpret signals from the surroundings in times of growing social needs in terms of environmental care. Based on the ranking criteria for employer selection it was found that respondents were primarily driven by the level of the proposed salary. Unfortunately, environmental elements related to the responsibility for the natural environment such as high environmental culture and eco-innovativeness were not chosen as criteria of employer selection. After the correlation analysis for the employer selection criteria due to the role of environmental factors, it should be emphasized that the higher the environmental culture of the company, the greater the importance of its eco-innovativeness among respondents. The larger the enterprise in terms of the number of its employees, the less importance is attached by the respondents to the opinion about that enterprise in the society. An important conclusion can be paying greater attention to eco-innovativeness and ethical aspects of the implementation of pro-environmental solutions to business in the study programs at universities.

REFERENCES

1. **Chodyński A., 2007:** Environmental Knowledge and skills in business development strategies. (in Polish Wiedza i kompetencje ekologiczne w strategiach rozwoju przedsiębiorstw), Publisher Diffin, Warszawa.
2. **Daily B., Huang S., 2001:** Achieving sustainability through attention to human resource factors in environmental management. International Journal of Operations & Production Management, 21, 12, 1539–1554.
3. **Dutta A., Punnose E.M. 2010:** Factors Affecting Choice of First Employer. A Study of Indian Management Graduates**.** Global Business Review. October, Vol. 11, 435–448.
4. **Faber A., 2008:** Przyrodnicze skutki uprawy roślin energetycznych [in:] Uprawa roślin energetycznych a wykorzystanie rolniczej przestrzeni produkcyjnej w Polsce, Studia i raporty IUNG – PIB, 11, Puławy 2008, 43–54.
5. **Fryxell G.E., Lo C.W.H., 2003:** The influence of environmental knowledge and values on managerial behaviours on behalf of the environment: an empirical examination of managers in China, Journal of Business Ethics, 46, 1, 445–69.
6. **Grzybek A., 2008:** Zapotrzebowanie na biomasę i strategie energetycznego jej wykorzystania. [in:] Uprawa roślin energetycznych a wykorzystanie rolniczej przestrzeni produkcyjnej w Polsce, Studia i raporty IUNG – PIB, 11, Puławy 2008, 7–9.
7. **Hermosilla J. C., Pablo del Río, Könnölä T., 2010:** Diversity of eco-innovations: Reflections from selected case studies. Journal of Cleaner Production Vol. 18, 1073–1083.
8. H**oryński M., 2011:** Use of unconventional energy sources in modern buildings (In Polish: Wykorzystanie niekonwencjonalnych źródeł energii we współczesnych budynkach). MOTROL, 13, 150–156.
9. **Huczek M., 1999:** A strategy for environmental management in the enterprise, (in Polish: Strategia zarządzania środowiskiem naturalnym), Wyd. BIT, Bielsko-Biala.
10. **Knaga J., Szul T., 2011:** Analysis of water-water type heat pump operation in a building object. TEKA Kom. Mot. i Energ. Roln. – OL PAN, 11C, 100–108.
11. **Kowalska A., 2011:** Recruiting and using agricultural biogas. TEKA Kom. Mot. i Energ. Roln. – OL PAN, 11C, 118–125.
12. **Kozachenko G., Lyashenko O., Bezbozhnyy V., 2010:** Enterprise economic security management conception. TEKA Kom. Mot. i Energ. Roln. – OL PAN, 10A, 263–270.
13. **Kramer M., Urbaniec M., Krynski A., 2005:** International environmental management, Vol. I. Interdisciplinary management of the ecological foundation, (in Polish Międzynarodowe zarządzanie środowiskiem, T. I, Interdyscyplinarne założenia proekologicznego zarządzania przedsiębiorstwem) Wyd. CH Beck Publishing House, Warsaw.
14. **Krasowicz S., 2008:** Wpływ produkcji roślin energetycznych na rynek żywności [in:] Uprawa roślin energetycznych a wykorzystanie rolniczej przestrzeni produkcyjnej w Polsce, Studia i raporty IUNG – PIB, 11, Puławy, 125–132.
15. **Kroyer 1995 G. Th., 1995:** Impact of Food Processing on the Environment an Overview. Lebensm.Wisu.-Technol., 28, 547–552.
16. **Kupczyk A., Borowski P., Powałka M., Ruciński D., 2011:** Transport biofuels in Poland: current status and perspectives. (in Polish: Biopaliwa transportowe w Polsce: stan aktualny i perspektywy). Wyd. WEMA. Warszawa.
17. **Lipski R., 2011:** Using biomass as the renewable energy in polandon the example of the thermal power station heatedwith straw at the Wieniawa commune (in Polish: Wykorzystanie biomasy jako energii odnawialnej w Polsce na przykładzie ciepłowni opalanej słomą w Gminie Wieniawa). MOTROL, 2011, 13, 164–172
18. **Manter, Marcia A. and Y. Benjamin Janice, 1989:** How to hold on to first careerists, Personnel Administration, 34(9): 44–48.
19. **Mysłowski J., 2011:** Negative Impact of Motorization on thr Natural Environment. TEKA Kom. Mot. i Energ. Roln. – OL PAN, 11C, 223–229.

20. **Naffziger D. N. A., Montagno R., 2003:** Perceptions of Environmental Consciousness in US Small Businesses: An Empirical Study. S.A.M. Advanced Management Journal. 68,2, 23–32.
21. **Nęcka K., 2011:** Use of data mining techniques for predicting electric energy demand. TEKA Kom. Mot. i Energ. Roln. – OL PAN, 11C, 237–245.
22. **Nemcsicsne Zsóka, A. 2008:** Consistency and „awareness gaps" in the environmental behaviour of Hungarian companies. Journal of Cleaner Production, 16, 322–329.
23. **Nidumolu R., Prahalad C. K., Rangaswami M. R., 2009:** Why sustainability is now the key driver of innovation, Harvard Business Review, 9, 57–64.
24. **Pawłowski L. 2011:** Idea of sustainable development – real chance for development or utopia (in polish: Idea zrównoważonego rozwoju realna szansa na rozwój czy utopia). MOTROL, 13, 249–257.
25. **Perron, G. M., Cote, R.P. Duffy, J. F., 2006:** Improving environmental awareness in business. Journal of Cleaner Production, Vol. 14, 551–562.
26. **Posner, Barry Z., 1981:** Comparing recruiters, student, and faculty perceptions of important applicant and position/organization characteristics', *Personnel Psychology*, 34(2), 329–40.
27. **Pytel A., Stefański Z., 2011:** An innovative and environmentally safe method to manufacture high-quality iron castings for possible use as elements of agricultural machines. TEKA Kom. Mot. i Energ. Roln. – OL PAN, 11c, 256–263.
28. **Ramus C. A., 2002:** Encouraging innovative environmental actions: what companies and managers must do. Journal of World Business, 37, 151-164.
29. Raport CSR 2011. 2010. Poland vs. Europe. http: http://www.reportingcsr.org [28.12.2012]
30. Raport o stanie sektora małych i średnich przedsiębiorstw w Polsce, Polska Agencja Rozwoju Przedsiębiorczości, Warszawa 2011. http://www.parp.gov.pl [29.12.2012].
31. **Roszkowski A., 2008:** Efektywność energetyczna różnych sposobów produkcji i wykorzystania biomasy [in:] Uprawa roślin energetycznych a wykorzystanie rolniczej przestrzeni produkcyjnej w Polsce, Studia i raporty IUNG – PIB, 11, Puławy 2008, 101-113.
32. **Seroka-Stolka O., Nowakowska-Grunt J., 2012:** Evaluation of the Eco-Effectiveness and the Individual Environmental Awareness of the Częstochowa Region Businessmen in the Light of the Conducted Survey. Polish Journal of Environmental Studies, Vol.21 nr 5A, 206–211.
33. **Stavytskyy V., Nosko P., Fil P., Karpov A., Velychko N., 2010:** Load-independent power losses of gear systems: a review TEKA Kom. Mot. i Energ. Roln. – OL PAN, 10B, 205–213.
34. **Svinoroev Y., Kostrub V., Klimova O., 2010:** New ecological binder materials based on vegetative raw materials processintg products. TEKA Kom. Mot. i Energ. Roln. – OL PAN, 10b, 227–231.
35. **Tkach V., 2010:** The Adaptive Control of Higher Education Process Quality of a University On a "Teacher – Student " Level. TEKA Kom. Mot. i Energ. Roln. – OL PAN, 10B, 241–246.
36. **Voronkov D., Korolevska N., 2010:** Model of potential changes in the enterprise. TEKA Kom. Mot. i Energ. Roln. – OL PAN 10b, 310–315.
37. **Voronkova A., Grynov A., 2010:** Model of human capital company. TEKA Kom. Mot. i Energ. Roln. – OL PAN, 10B, 310–315.
38. **Wojdalski J., Dróżdż B., Powęzka A., 2009:** Efectiveness of energy and water consumption in a poultry processing plant. TEKA Kom. Mot. Energ. Roln. – OL PAN, 9, 395–402.
39. **Zilahy G., 2004:** Organisational factors determining the implementation of cleaner production measures in the corporate sector. Journal of Cleaner Production, Vol. 12, 311–319.

POSTAWY SUDENTÓW WOBEC SPOŁECZNEJ I EKOLOGICZNEJ ODPOWIEDZIALNOŚCI PRZEDSIĘBIORSTW

Streszczenie. Badanie stanowi próbę oceny postaw studentów wobec roli jaką pełni środowisko przyrodnicze w funkcjonowaniu przedsiębiorstwa poprzez koncepcję społecznej i ekologicznej odpowiedzialności przedsiębiorstw, która znana jest zaledwie 1/5 respondentów. Badani stanowiący przyszły potencjał pracowniczy kierują się przy wyborze pracodawcy przede wszystkim wysokością proponowanego wynagrodzenia oraz perspektywami i możliwościami własnego rozwoju w firmie. Wysoka kultura ekologiczna przedsiębiorstwa oraz jej ekoinnowacyjność nie stanowią żadnego kryterium w poszukiwaniu pracodawcy.
Słowa kluczowe: postawy, środowisko, społeczna odpowiedzialność przedsiębiorstw.

TEKA. COMMISSION OF MOTORIZATION AND ENERGETICS IN AGRICULTURE – 2013, Vol. 13, No. 1, 161–168

On determining the nonnegative relaxation spectrum of viscoelastic materials using complementary error functions

Anna Stankiewicz

Department of Mechanical Engineering and Automatics, University of Life Sciences in Lublin
Doświadczalna 50A, 20-280 Lublin, Poland, e-mail: anna.m.stankiewicz@gmail.com

Received February 20.2013; accepted March 14.2013

Summary. The relaxation spectrum is a characteristic quantity describing the viscoelastic properties of many materials. Given the spectrum, it is very easy to convert one material function into another one. The paper deals with the problems of recovery of the spectrum of relaxation frequencies of linear viscoelastic materials from discrete-time noise corrupted measurements of relaxation modulus obtained in stress relaxation test. A new concept of the approximation of continuous relaxation spectrum by the finite series of nonnegative power basis functions is presented. It is proved that the respective model of the relaxation modulus is given by finite series of functions based on complementary error function. The optimal scheme of the least-squares identification of nonnegative definite model of relaxation spectrum is proposed. The validity of the method is demonstrated using simulated data of Gaussian spectrum. Applying the proposed scheme, the relaxation spectrum of a confined cylindrical specimen of the sugar beet root is also determined.
Key words: viscoelasticity, relaxation spectrum, identification, error functions.

INTRODUCTION

The last three decades have witnessed an increasing amount of interest paid to the study on mechanical properties of viscoelastic materials treating it as a separated subject area [11,13]. Viscoelastic models are used before all to modeling of different polymeric liquids and solids [3,11,13], concrete [13], soils and rocks [9], different composite materials [13], metals and their alloys [13,21], foods [13,16] and many biological materials [13,14], in particular fruits and vegetables [7,10,13,14,18]. The need for detailed knowledge of mechanical material functions has been growing with the increased use of accurate engineering methods for rigorous predictions of the materials behavior, such as the finite element method, the boundary element method and the finite difference method [1].

The mechanical properties of linear viscoelastic materials are characterized by relaxation or retardation spectra [3,13]. The spectra are vital not only for constitutive models but also for the insight into the properties of a viscoelastic material, since from the relaxation or retardation spectrum any other linear material functions can be calculated without difficulty. Hence the identification of relaxation spectrum is one of the actual directions of the mathematical modelling of many viscoelastic materials. Since the problem of relaxation spectrum identification is one of the classical ill-posed inverse problems [13,18], an appropriate special identification methods must be find to overcome the mathematical difficulties.

A number of different methods have been proposed during the last two decades for the relaxation spectrum computation using the data from a small-amplitude oscillatory shear experiment. For references and an overview, see Dealy and Larson [3]. However, a classical manner of studying viscoelasticity for many materials is by two-phase stress relaxation test [13,17]. There are a few papers: [5,23] and [18-20] as well as the previous papers by the present author cited therein, that deal with the spectrum determination from stress relaxation data. However, in all the known methods of the relaxation spectrum identification from time-measured data the restriction that the spectrum is nonnegative, which must be given to satisfy the physical meaning is, unfortunately, neglected. The identification scheme presented in this paper overcomes this limitation.

In this paper the spectrum is recovered from discrete-time noise corrupted measurements of relaxation modulus obtained in stress relaxation test. The approach proposed is based on approximation of the spectrum by finite linear combination of the basis exponential functions. A quadratic identification index, which refers to the measured relaxation modulus, is adopted and the nonnegativity constraints on the model parameters are introduced. The stated linear least-squares approximation task with inequality constraints is solved by using the dual approach. The result-

ing identification scheme is presented and verified for numerical data as well as for selected biological material.

RELAXATION SPECTRUM

In the rheological literature it is commonly assumed that the relaxation modulus $G(t)$ of linear viscoelastic material has the following integral representation [13,20]:

$$G(t)=\int_0^\infty H(\nu)\,e^{-t\nu}d\nu\ , \tag{1}$$

where: the nonnegative relaxation spectrum $H(\nu)$ characterizes the distribution of relaxation frequencies $\nu\geq 0$. Throughout we shall be concerned with the case when $H(\nu)$ is completely unknown. The relaxation modulus $G(t)$ can be, however, measured for any time $t\geq 0$.

MODELS

Assume that $H(\nu)\in L_2(0,\infty)$, where $L_2(0,\infty)$ is the space of square-integrating functions in the interval $(0,\infty)$. The set of the linearly independent functions:

$$\left\{e^{-\alpha\nu^2},\nu e^{-\alpha\nu^2},\nu^2 e^{-\alpha\nu^2},\dots\right\},\quad \alpha>0 \tag{2}$$

forms a basis of the space $L_2(0,\infty)$ [2]. Thus the relaxation spectrum can be expressed as $H(\nu)=\sum_{k=0}^{\infty} g_k\,h_k(\nu,\alpha)$, where: g_k are constant model parameters and the basis functions $h_k(\nu,\alpha)=\nu^k e^{-\alpha\nu^2}$, $k=0,1,\dots$. Since for real materials the relaxation spectrum tends to zero as the relaxation frequency approaches zero from above, i.e., the right-sided limit $lim_{\nu\to 0^+}H(\nu)=0$, the first basis function can be neglected. For practical reasons, it is convenient to replace the infinite summation in the above formula with a finite one of K terms of the form: $\sum_{k=1}^{K} g_k\,h_k(\nu,\alpha)$. The norms of the basic functions $h_k(\nu,\alpha)$ are given by:

$$\|h_k\|_2^2=\int_0^\infty \nu^{2k}e^{-2\alpha\nu^2}\,d\nu=\frac{\prod_{j=1}^{k}(2j-1)}{2^{2k+1}\alpha^k}\sqrt{\frac{\pi}{2\alpha}}\ . \tag{3}$$

Here $\|\cdot\|_2$ denotes the square norm in the space $L_2(0,\infty)$. It is easy to check that for any fixed α the sequence of norms (3) increases or decreases very quickly depending on the parameter α. Thus, in order to guarantee the numerical stability of the resulting identification algorithm the basis functions (2) are replaced by following normalized functions:

$$\tilde{h}_k(\nu,\alpha)=\gamma_k(\alpha)\nu^k e^{-\alpha\nu^2}\quad for\quad k=1,2,\dots, \tag{4}$$

where, by virtue of (3), the weights γ_k are defined by:

$$\gamma_k(\alpha)=2^k\sqrt{2\alpha^k}\,\sqrt[4]{\frac{2\alpha}{\pi}}\Big/\sqrt{\prod_{j=1}^{k}(2j-1)}\quad for\quad k=1,2,\dots. \tag{5}$$

Thus the finite sum:

$$H_K(\nu)=\sum_{k=1}^{K} g_k\,\tilde{h}_k(\nu,\alpha) \tag{6}$$

will be used to approximate the relaxation spectrum $H(\nu)$. The lower index of $H_K(\nu)$ is the number of model summands. According to equation (1) the respective model of the relaxation modulus $G(t)$ is described by:

$$G_K(t)=\int_0^\infty H_K(\nu)e^{-t\nu}\,d\nu=\sum_{k=1}^{K} g_k\,\phi_k(t,\alpha), \tag{7}$$

where:

$$\phi_k(t,\alpha)=\int_0^\infty \tilde{h}_k(\nu,\alpha)e^{-t\nu}\,d\nu. \tag{8}$$

The form of the basis functions $\phi_k(t,\alpha)$ (8) is given by the following theorem; the proof is omitted due to space limitations.

Theorem 1. *Let $k\geq 0$, $\alpha>0$ and $t\geq 0$. Then the basis functions $\phi_k(t,\alpha)$ are given by recursive formula:*

$$\phi_{k+1}(t,\alpha)=\frac{2}{\sqrt{2k+1}}\frac{k}{\sqrt{2k-1}}\left[\phi_{k-1}(t,\alpha)-\frac{\sqrt{2k-1}}{2k\sqrt{\alpha}}t\phi_k(t,\alpha)\right],\quad k\geq 1, \tag{9}$$

starting with:

$$\phi_0(t,\alpha)=\sqrt[4]{\frac{\pi}{2\alpha}}\,e^{\frac{t^2}{4\alpha}}\,erfc\left(\frac{t}{2\sqrt{\alpha}}\right), \tag{10}$$

$$\phi_1(t,\alpha)=2\sqrt[4]{\frac{1}{2\alpha\pi}}-\frac{t}{\sqrt{\alpha}}\phi_0(t,\alpha), \tag{11}$$

where: $erfc(t)=\frac{2}{\sqrt{\pi}}\int_t^\infty e^{-x^2}dx$ is complementary error function [4].

Thus, the problem of the continuous relaxation spectrum $H(\nu)$ approximation by finite series $H_K(\nu)$ of the form (6) is reduced to problem of the relaxation modulus $G(t)$ approximation by finite linear combination (7) of the functions $\phi_k(t,\alpha)$ (9)-(11) based on complementary error function $erfc\left[t/\left(2\sqrt{\alpha}\right)\right]$. Error functions are used in signal processing and mathematical modelling of many processes, e.g., [4, 22]. A few first basis functions $\tilde{h}_k(\nu,\alpha)$ (4) are shown in Figure 1 for two different values of the parameter α; the corresponding functions $\phi_k(t,\alpha)$ (9)-(11) are plotted in Figure 2. From the Figure 2, it is evident that the

basis functions $\phi_k(t,\alpha)$ are congruent to the real relaxation modulus obtained in experiment. The positive parameter α is a time-scaling factor.

It is well-known [13,18,19] that for many materials $lim_{t\to\infty} G(t) = G_\infty > 0$, where G_∞ is the long-term modulus (see example 2 below). Thus, instead of the classical model (1), it is convenient to consider the following augmented model:

$$\overline{G}_K(t) = \int_0^\infty H_K(\nu) e^{-t\nu} d\nu + G_\infty = G_K(t) + G_\infty. \quad (12)$$

Then, the relaxation spectrum model takes the form:

$$\overline{H}_K(\nu) = H_K(\nu) + G_\infty \delta(\nu), \quad (13)$$

where: $\delta(\nu)$ denotes the Dirac delta function. Unbounded component $G_\infty\delta(\nu)$ of the relaxation spectrum $\overline{H}_K(\nu)$ (13) corresponds with the infinite relaxation time.

RELAXATION SPECTRUM APPROXIMATION

Suppose, a finite discrete experiment (stress relaxation test [13,17]) performed on the specimen of the material under investigation resulted in a set of measurements of the modulus $\overline{G}(t_i) = G(t_i) + z(t_i)$ at the sampling instants $t_i \geq 0$, $i = 1,\ldots,N$, where $z(t_i)$ is measurement noise. Optimal identification of the relaxation spectrum $H(\nu)$ in the class of models (13) consists of selecting within the given class of models defined by (13), (6) such a model, which ensures the best fit to the measurement results $\{\overline{G}(t_i)\}$. As a measure of the model accuracy the square approximation error is taken:

$$Q_N(\boldsymbol{g}_K) = \sum_{i=1}^{N} \left[\overline{G}(t_i) - \overline{G}_K(t_i)\right]^2, \quad (14)$$

where: $\boldsymbol{g}_K = [g_1 \ \ldots \ g_K \ \ G_\infty]^T$ is the parameter vector of model $\overline{H}_K(\nu)$ (13), (6) or equivalently of the model $\overline{G}_K(t)$ given by (12), (7). Superscript "T" indicates transpose. Using the vector-matrix notation $\overline{\boldsymbol{G}}_N = [\overline{G}(t_1) \ \ldots \ \overline{G}(t_N)]^T$ and:

$$\boldsymbol{\Psi}_{N,K} = \begin{bmatrix} \phi_1(t_1,\alpha) & \ldots & \phi_K(t_1,\alpha) & 1 \\ \vdots & \ddots & \vdots & \vdots \\ \phi_1(t_N,\alpha) & \ldots & \phi_K(t_N,\alpha) & 1 \end{bmatrix}, \quad (15)$$

the model quality index can be rewritten in the compact form as $Q_N(\boldsymbol{g}_K) = \left\|\overline{\boldsymbol{G}}_N - \boldsymbol{\Psi}_{N,K}\,\boldsymbol{g}_K\right\|^2$. Here and further $\|\cdot\|$ denotes the Euclidean norm in the spaces R^N and R^{K+1}. For physically realistic materials the relaxation spectrum $H(\nu)$ is nonnegative definite for any $\nu \geq 0$. Thus, the requirement that the respective model $H_K(\nu)$ (6) is also nonnegative for any $\nu \geq 0$ is natural. The basic functions $\tilde{h}_k(\nu,\alpha)$ (4) are nonnegative. Therefore, if the model parameters are such that $g_k \geq 0$ for any $k = 1,\ldots,K$, then the model $H_K(\nu)$ is also nonnegative definite function. Obviously, the restriction that the model parameters are nonnegative is sufficient, but not necessary condition for

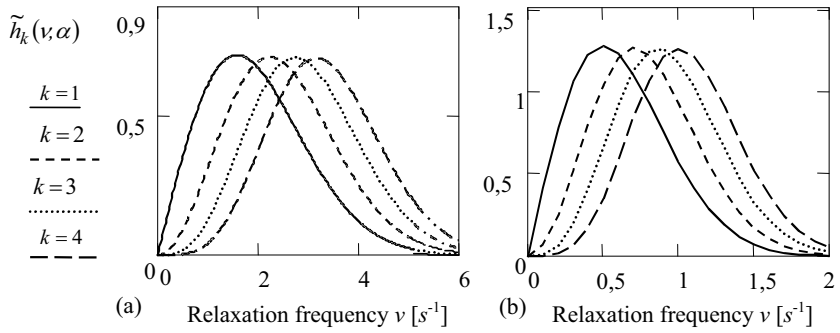

Fig. 1. The basis functions $\tilde{h}_k(\nu,\alpha)$ (4) for parameters: (a) $\alpha = 0{,}2\ [s^2]$ and (b) $\alpha = 2\ [s^2]$, $k = 1,2,3,4$

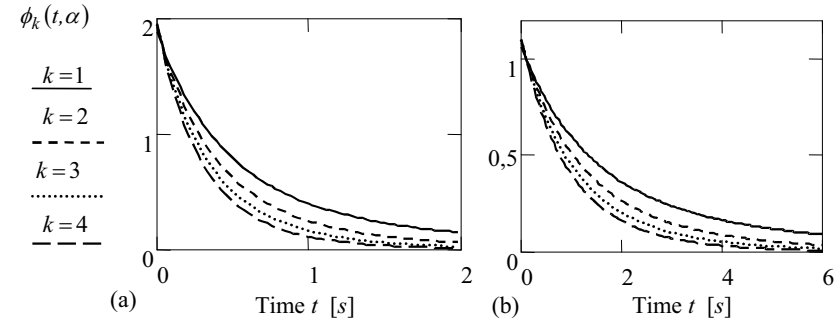

Fig. 2. The basis functions $\phi_k(t,\alpha)$, the parameters: (a) $\alpha = 0{,}2\ [s^2]$ and (b) $\alpha = 2\ [s^2]$, $k = 1,2,3,4$

the non-negation of the spectrum model. Now, the problem of the relaxation spectrum identification reduces to determining the vector of model parameters $\boldsymbol{g}_K$ minimizing the index $Q_N(\boldsymbol{g}_K)$ under the non-negation constraints $g_k \geq 0$ for $k=1,\ldots,K$. Thus, the linear least-squares optimization problem with inequality constraints of the form:

$$\min_{\boldsymbol{g}_K \geq \boldsymbol{0}_K} \quad \left\| \overline{\boldsymbol{G}}_N - \boldsymbol{\Psi}_{N,K}\, \boldsymbol{g}_K \right\|^2, \tag{16}$$

is stated for the optimal identification of the nonnegative relaxation spectrum. $\boldsymbol{0}_K$ is $(K+1)$-dimensional zero vector. The existence and properties of the solution of the above task depends on the properties of the matrix $\boldsymbol{\Psi}_{N,K}$ (15). Unfortunately, $\boldsymbol{\Psi}_{N,K}$ is usually rank- deficient. The linear-quadratic task (16) is still ill-conditioned and when the data are noisy, even small changes of the data $\overline{\boldsymbol{G}}_N$ would lead to arbitrarily large artefact in the optimal model parameters. Therefore, the numerical solution of finite dimensional problem (16) is fraught with the same difficulties that the original continuous ill-posed problem of numerical solution of the Fredholm equation (1). The standard minimization methods may fail. To stabilize the solution an additional "smoothing" constraint will be introduced in the next section.

OPTIMAL IDENTIFICATION PROBLEM

The fluctuations of the solution of optimization task (7) may be reduced by introducing an additional direct constraint on vector $\boldsymbol{g}_K$: $\|\boldsymbol{g}_K\| \leq \beta$, where a constant $0 < \beta < \left\| \overline{\boldsymbol{g}}_K^N \right\|$ estimates the „level of smoothness" assumed for the model parameters. Here $\overline{\boldsymbol{g}}_K^N$ is the normal (minimum Euclidean norm) solution of the original least-squares problem without constraints. In result the modified problem of optimal relaxation spectrum identification is obtained:

$$\min_{\boldsymbol{g}_K \geq \boldsymbol{0}_K} \quad \left\| \overline{\boldsymbol{G}}_N - \boldsymbol{\Psi}_{N,K}\, \boldsymbol{g}_K \right\|^2 \quad \textit{under constraint} \quad \|\boldsymbol{g}_K\|^2 \leq \beta^2. \tag{17}$$

By introducing a vector of prices (Lagrangian multipliers) $\boldsymbol{\lambda} \geq \boldsymbol{0}_K$ and a price $\gamma > 0$ we can define the Lagrangian for the optimization task (17):

$$L(\boldsymbol{g}_K, \boldsymbol{\lambda}, \gamma) = \left\| \overline{\boldsymbol{G}}_N - \boldsymbol{\Psi}_{N,K}\, \boldsymbol{g}_K \right\|^2 - \boldsymbol{\lambda}^T \boldsymbol{g}_K + \gamma\left(\boldsymbol{g}_K{}^T \boldsymbol{g}_K - \beta^2 \right). \tag{18}$$

The prices $\boldsymbol{\lambda}$ aim at providing a fulfillment of the inequality in original optimization task (16). The multiplier $\gamma > 0$ is the price imposed to satisfy the "smoothness" constraint in modified task (17). In order to use the dual approach to solve the optimization task (17) note, that for an arbitrary $\boldsymbol{\lambda} \geq \boldsymbol{0}_K$, $\gamma > 0$ and $\beta > 0$ the Lagrangian $L(\boldsymbol{g}_K, \boldsymbol{\lambda}, \gamma)$ has unique minimum with respect to $\boldsymbol{g}_K$ given by:

$$\hat{\boldsymbol{g}}_K(\boldsymbol{\lambda}, \gamma) = \left[\boldsymbol{\Psi}_{N,K}{}^T \boldsymbol{\Psi}_{N,K} + \gamma\, \boldsymbol{I}_{K,K} \right]^{-1} \left[\boldsymbol{\Psi}_{N,K}{}^T\, \overline{\boldsymbol{G}}_N + \tfrac{1}{2}\boldsymbol{\lambda} \right], \tag{19}$$

where: $\boldsymbol{I}_{K,K}$ is $(K+1)\times(K+1)$ identity matrix. Thus, the dual function defined by:

$$L_D(\boldsymbol{\lambda}, \gamma) = \min_{\boldsymbol{g}_K \in R^{K+1}} L(\boldsymbol{g}_K, \boldsymbol{\lambda}, \gamma) = L(\hat{\boldsymbol{g}}_K(\boldsymbol{\lambda}, \gamma), \boldsymbol{\lambda}, \gamma) \tag{20}$$

can be expressed by convenient analytical formula:

$$L_D(\boldsymbol{\lambda}, \gamma) = \overline{\boldsymbol{G}}_N{}^T \overline{\boldsymbol{G}}_N - \gamma\beta^2 - \left[\boldsymbol{\Psi}_{N,K}{}^T\, \overline{\boldsymbol{G}}_N + \tfrac{1}{2}\boldsymbol{\lambda} \right]^T \boldsymbol{B} \left[\boldsymbol{\Psi}_{N,K}{}^T\, \overline{\boldsymbol{G}}_N + \tfrac{1}{2}\boldsymbol{\lambda} \right], \tag{21}$$

where: symmetric matrix $\boldsymbol{B} = \left[\boldsymbol{\Psi}_{N,K}{}^T \boldsymbol{\Psi}_{N,K} + \gamma\, \boldsymbol{I}_{K,K} \right]^{-1}$ is positive definite for any $\gamma > 0$. It is easy to check that the Hessian matrix of the dual function takes the form:

$$H(\boldsymbol{\lambda}, \gamma) = \begin{bmatrix} -\frac{1}{2}\boldsymbol{B} & \boldsymbol{B}\boldsymbol{B}\left[\boldsymbol{\Psi}_{N,K}{}^T\, \overline{\boldsymbol{G}}_N + \frac{1}{2}\boldsymbol{\lambda} \right] \\ \left[\boldsymbol{\Psi}_{N,K}{}^T\, \overline{\boldsymbol{G}}_N + \frac{1}{2}\boldsymbol{\lambda} \right]^T \boldsymbol{B}\boldsymbol{B} & -2\left[\boldsymbol{\Psi}_{N,K}{}^T\, \overline{\boldsymbol{G}}_N + \frac{1}{2}\boldsymbol{\lambda} \right]^T \boldsymbol{B}\boldsymbol{B}\boldsymbol{B}\left[\boldsymbol{\Psi}_{N,K}{}^T\, \overline{\boldsymbol{G}}_N + \frac{1}{2}\boldsymbol{\lambda} \right] \end{bmatrix}.$$

Since matrix $\boldsymbol{B}$ is positive definite, on the basis of the known result concerning the definiteness of block matrices [12; Theorem $I_{b''}$] the Hessian $H(\boldsymbol{\lambda}, \gamma)$ is negative definite for an arbitrary $\boldsymbol{\lambda} \geq \boldsymbol{0}_K$. Thus the dual function $L_D(\boldsymbol{\lambda}, \gamma)$ is strictly concave function of the arguments $(\boldsymbol{\lambda}, \gamma)$. Taking advantage of the above, it may be proved that the solution to the dual problem:

$$\max_{\boldsymbol{\lambda} \geq \boldsymbol{0}_K,\, \gamma \geq 0} \quad L_D(\boldsymbol{\lambda}, \gamma) = L_D\left(\hat{\boldsymbol{\lambda}}, \hat{\gamma} \right), \tag{22}$$

there exists and the optimal multiplier $\hat{\gamma} > 0$. It is well known that if the saddle point of the Lagrangian $L(\boldsymbol{g}_K, \boldsymbol{\lambda}, \gamma)$ (18) there exists, then the dual approach can be successfully applied to solve (17). In the case considered the existence of a saddle point to the Lagrangian follows immediately from [8; Theorem 1, (ii) and (iii)] due to the uniqueness of (19). Thus the vector $\hat{\boldsymbol{g}}_K\left(\hat{\boldsymbol{\lambda}}, \hat{\gamma} \right)$ is optimal solution of the optimal identification task (17).

IDENTIFICATION SCHEME

The calculation of the relaxation spectrum model involves the following steps.

1. Perform the experiment - stress relaxation test [17] - and record the measurements $\overline{G}(t_i)$ of the relaxation modulus at time instants $t_i \geq 0$, $i = 1,\ldots,N$.
2. Compute $\left\|\overline{\boldsymbol{g}}_K^N\right\|$ (for simple analytical formula see, e.g., [18, eq. (2.24) and the following]) and choose the constant $0 < \beta < \left\|\overline{\boldsymbol{g}}_K^N\right\|$.
3. Solve the dual problem (22) according to the chosen numerical procedure, and determine the multipliers $(\hat{\boldsymbol{\lambda}}, \hat{\gamma})$ maximizing $L_D(\hat{\boldsymbol{\lambda}}, \hat{\gamma})$.
4. Compute the vector $\hat{\boldsymbol{g}}_K = \hat{\boldsymbol{g}}_K(\hat{\boldsymbol{\lambda}}, \hat{\gamma})$ of optimal model parameters using formula (19).
5. Determine the model of the spectrum of relaxation $\hat{H}_K(\nu)$ according to (cf. (6)):
6.

$$\hat{H}_K(\nu) = \sum_{k=1}^{K} \hat{g}_k \, \tilde{h}_k(\nu,\alpha) . \tag{23}$$

Obviously, $\overline{H}_K(\nu) = \hat{H}_K(\nu) + G_\infty \delta(\nu)$ is the relaxation spectrum of the form (13).

Taking advantage of the basic functions $\tilde{h}_k(\nu,\alpha)$ definitions (4), (5) and the properties of the optimal identification problem (17) solution, it may be simply proved that for $\hat{H}_K(\nu)$ (23) the following sequence of estimations hold:

$$\max_{\nu \geq 0} \left|\hat{H}_K(\nu)\right| \leq \sum_{k=1}^{K} \hat{g}_k \max_{\nu \geq 0} \tilde{h}_k(\nu,\alpha) \leq 1{,}084 \sqrt[4]{\alpha}\sqrt{K+1} \sum_{k=1}^{K} \hat{g}_k \leq 1{,}084 \sqrt[4]{\alpha}\sqrt{K+1}\,\beta .$$

Thus the smoothness of the vector $\hat{\boldsymbol{g}}_K$ guarantees that the fluctuations of the respective spectrum of relaxation $\hat{H}_K(\nu)$ are also bounded.

SOME REMARKS

1. For numerical algebraic computations of the scheme the singular value decomposition SVD [15] of the matrices $\boldsymbol{\Psi}_{N,K}$ (15) or $\boldsymbol{\Psi}_{N,K}{}^T \boldsymbol{\Psi}_{N,K}$ may be used - for details see the previous papers [18, 19]. Efficient algorithms for SVD are available nowadays in the form of optimized numerical procedures in most commonly used contemporary computational packets.

2. The matrix $\boldsymbol{\Psi}_{K,K}$ (15) depends on the choice of the basis functions as well as the sampling instants $\{t_i\}$, however, does not depend in the experiment results. Thus, when the identification scheme is applied for successive samples of the same material, the SVD computations have not to be multiple repeated while the same measurement points $\{t_i\}$ are kept.

3. The relaxation modulus basis functions $\phi_k(t,\alpha)$ (9)-(11) are expressed using complementary error function. The function $erfc(t)$ is accessible practically in every computational packets either directly or by error function $erf(t) = 1 - erfc(t)$, where $erf(t) = \frac{2}{\sqrt{\pi}} \int_0^t e^{-x^2} dx$.

4. In the scheme proposed the parameter $\alpha > 0$ is the time-scaling factor. The following rule holds: the lower the parameter α is, the greater are the relaxation frequencies (see Figures 1 and 2). By the optimal choice of the scaling factor, the best fit of the model to the experimental data can be achieved. However, in practice a simple rough rule for choosing α, based on the comparison of a few first functions $\phi_k(t,\alpha)$ for different values of α with the experimentally obtained function $\overline{G}(t)$ is quite enough. In the same manner the number K of the models (6) and (7) summands can be initially evaluated. Thus, the choice both of the number K as well as the parameter α must be done *a posteriori*, after the preliminary experiment data analysis.

NUMERICAL EXAMPLE

To illustrate our approach we consider viscoelastic material whose relaxation spectrum is described by the Gauss distribution:

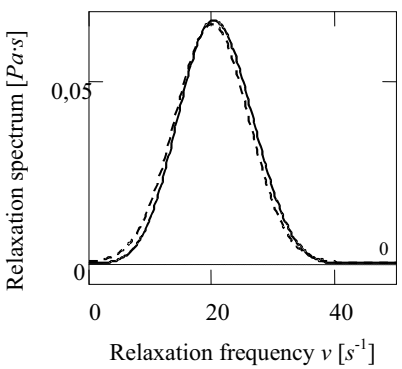

Fig. 3. Relaxation spectrum $H(\nu)$ (24) (dash line) and the nonnegative model $\hat{H}_K(\nu)$ (solid line)

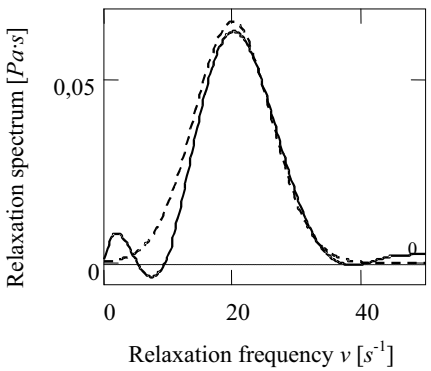

Fig. 4. Relaxation spectrum $H(\nu)$ (24) (dash line) and the least-squares optimal model $\tilde{H}_K(\nu)$ (solid line)

$$H(\nu)=\frac{1}{6\sqrt{2\pi}}e^{-(\nu-20)^2/72}. \quad (24)$$

The relaxation modulus corrupted by additive noises $z(t)$ of the uniform distribution in the interval $[-0{,}02;0{,}02]\,Pa$ has been sampled at $N=200$ sampling instants at the constant period $\Delta t=0{,}003\,[s]$. The parameters $K=8$ and $\alpha=0{,}003\,[s^2]$ are chosen according to the suggestions of Remark 4. Since $\|\bar{\boldsymbol{g}}_K^N\|=8{,}692$, the constant $\beta=0{,}2$ is assumed. Then the vector of the optimal model parameters $\hat{\boldsymbol{g}}_K$ is determined. The "real" relaxation spectrum $H(\nu)$ (24) and the resulting nonnegative definite model $\hat{H}_K(\nu)$ (23) are plotted in Figure 3. For comparison, the model $\tilde{H}_K(\nu)$ of the form (6) determined using the regularized least-squares method without constraints (for detailed description see, e.g., [18,19]) is given in Figure 4.

RELAXATION SPECTRUM OF THE REAL BIOLOGICAL MATERIAL

A cylindrical sample of 20 mm diameter and height was obtained from the root of sugar beet Janus variety [6]. The stress relaxation experiment performed by Gołacki and co-workers is described in details in [6]. The experiment was performed in the state of uniaxial deformation; i.e. the specimen examined underwent deformation in steel cylinder. The modeling of mechanical properties of this material in linear-viscoelastic regime is justified by the research results presented in a lot of works, for references see [6,18]. In the initial phase of the stress relaxation test the strain was imposed instantaneously, the sample was preconditioned at the 0,5 $[m{\cdot}s^{-1}]$ strain rate to the assumed strain. Next, during the second phase at constant strain, the corresponding time-varying force induced in the specimen, which decreases with time, was recorded during the time period $[0{,}5;96{,}2]$ seconds in 958 measurement points with the constant sampling period $\Delta t=0{,}1\,[s]$. The way how the experiment data has been preliminary proceeded is described in [18]. Next the proposed identification scheme was applied. Since $\|\bar{\boldsymbol{g}}_K^N\|=1{,}804E+5$, the constant

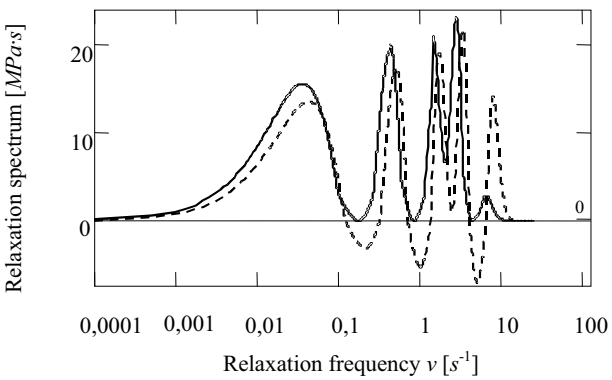

Fig. 5. The models $\hat{H}_K(\nu)$ (solid line) and $\tilde{H}_K(\nu)$ (dash line) of the relaxation spectrum of the sample of beet sugar root

$\beta=50$ is assumed. The parameters $K=8$ and $\alpha=98\,[s^2]$ were chosen. The resulting optimal nonnegative relaxation spectrum $\hat{H}_K(\nu)$ is plotted in Figure 5, where the relaxation spectrum model $\tilde{H}_K(\nu)$ of the class (6) optimal in the sense of regularized least-squares without constrains is also shown. The respective optimal long-term modulus are following: $\hat{G}_\infty=9{,}957\ MPa$ and $\tilde{G}_\infty=9{,}782\ MPa$.

CONCLUSIONS

The problem of the optimal least-squares approximation of the relaxation spectrum by finite series of nonnegative power basis functions is stated. The primary infinite dimensional problem of the relaxation spectrum identification is reduced to the static linear-quadratic programming task with inequality constraints. The dual approach is successfully applied to solved this task and resulting identification scheme is presented. The validity and effectiveness of the method is demonstrated both by numerical example as well as by through the computation of the relaxation spectrum of the specimen of selected biological material.

REFERENCES

1. **Antoun B., Qi H.J., Hall R., G.P., Lu H., Lu Ch. (Eds), 2013:** Challenges in Mechanics of Time-Dependent Materials and Processes in Conventional and Multifunctional Materials. Proceedings of the 2012 Annual Conference on Experimental and Applied Mechanics. Springer, New York London.
2. **Bachman G., Narici L., 1966:** Functional Analysis. Academic Press. New York.
3. **Dealy J., Larson R.G., 2006:** Structure and rheology of molten polymers-from structure to flow behaviour and back again. Hanser, Munich.
4. **Deaño A., Temme N.M., 2010:** Analytical and numerical aspects of a generalization of the complementary error function. Applied Mathematics and Computation, 216, 3680–3693.
5. **Fujihara S., Yamamoto R., Masuda Y., 1995:** Maxwellian Spectra of Stress Relaxation in the Cell Wall and Growth Regulation in Higher Plants. Jiří Blahovec (Ed): Proceedings of International Workshop Stress Relaxation in Solids and Biological Origin, Prague, September 18-19, 1995. Czech University of Agriculture, Prague, 1996, 47–51.
6. **Gołacki K., Kołodziej P., Stankiewicz A., Stropek Z., 2003:** Report of KBN Grant No 5P06F00619: "Mechanical hardiness of sugar beet analysis in the context of practical mechanical loads", 1–214 [in Polish].
7. **Guz T., 2009:** An influence of quarantine conditions on elasticity modulus in apples stored in ulo and regular store. TEKA Commission of Motorization and Power Industry in Agriculture, 9, 69–77.
8. **Hasiewicz Z., Stankiewicz A., 1985:** On Applicability of Interaction Balance Method to Global Identification of

Interconnected Steady-State Systems. IEEE Transaction on Automatic Control, 31(1), 77–80.
9. **Hemmat A., Nankali N., Aghilinategh N., 2012:** Simulating stress–sinkage under a plate sinkage test using a viscoelastic 2D axisymmetric finite element soil model. Soil and Tillage Research, 118, 107–116.
10. **Kobus Z., Kusińska E., 2010:** Effect of temperature and concentration on rheolog1cal properties of tomato juice. TEKA Commission of Motorization and Power Industry in Agriculture, 10, 170–178.
11. **Kontopoulou M. (Ed), 2012:** Applied Polymer Rheology: Polymeric Fluids with Industrial Applications. John Wiley & Sons, New Jersey.
12. **Kreindler E., Jameson A., 1972:** Conditions for nonnegativeness of partitioned matrices. IEEE Transaction on Automatic Control, 17(1), 147–148.
13. **Lakes R. S., 2009:** Viscoelastic Materials. Cambridge University Press, Cambridge.
14. **Prorok B.C., Barthelat F., Korach Ch.S., Grande-Allen J.J., Lipke E., Lykofatitits G., Zavattieri P., (Eds), 2013:** Mechanics of Biological Systems and Materials, Volume 5. Proceedings of the 2012 Annual Conference on Experimental and Applied Mechanics, Springer, New York London.
15. **Schwetlick A.H., 1988:** Numerische lineare algebra. VEB Deutcher Verlag der Wissenschaften, Berlin.
16. **Singh A.P., Lakes R.S., Gunasekaran S., 2006:** Viscoelastic characterization of selected foods over an extended frequency range. Rheologica Acta, 46, 131–142.
17. **Sorvari J., Malinen M., 2006:** Determination of the relaxation modulus of a linearly viscoelastic material. Mechanics of Time-Dependent Materials, 10, 125–133.
18. **Stankiewicz A., 2007:** Identification of the relaxation spectrum of viscoelastic plant materials. Ph. D. Thesis, Agricultural University of Lublin, Poland [in Polish].
19. **Stankiewicz A., 2010:** Identification of the relaxation and retardation spectra of plant viscoelastic materials using Chebyshev functions. TEKA Commission of Motorization and Power Industry in Agriculture, 10, Part I. 363–371; Part II. 372-378; Part III. 396–404.
20. **Stankiewicz A., 2012:** An algorithm for identification of the relaxation spectrum of viscoelastic materials from discrete-time stress relaxation noise data. TEKA Commission of Motorization and Energetics in Agriculture, 12(2), 187–192.
21. **Wang S., Qi J., Yao X., 2011:** Stress relaxation characteristics of warm frozen clay under triaxial conditions. Cold Regions Science and Technology, 69, 112–117.
22. **Yeung A.T., Mitchell J.K., 1993:** Coupled fluid, electrical and chemical flows in soil. Géotechnique, 43(1), 121–134.
23. **Zi G., Bažant Z. P., 2002:** Continuous Relaxation Spectrum for Concrete Creep and its Incorporation into Microplane Model M4. Journal of Engineering Mechanics, ASCE 128(12), 1331–1336.

O WYZNACZANIU NIEUJEMNEGO SPEKTRUM RELAKSACJI MATERIAŁÓW LEPKOSPRĘŻYSTYCH Z WYKORZYSTANIEM FUNKCJI RESZTKOWYCH BŁĘDU

Streszczenie. Spektrum relaksacji naprężeń charakteryzuje lepkosprężyste własności materiałów. Przedmiotem pracy jest problem wyznaczania spektrum częstotliwości relaksacji liniowych materiałów lepkosprężystych na podstawie dyskretnych, zakłóconych pomiarów modułu relaksacji zgromadzonych w teście relaksacji naprężeń. Przedstawiono nową metodę aproksymacji ciągłego spektrum relaksacji skończonym szeregiem nieujemnie określonych wykładniczych funkcji bazowych optymalnej w sensie najmniejszej sumy kwadratów. Pokazano, że funkcje bazowe odpowiedniego modelu modułu relaksacji dane są prostą regułą rekurencyjną i bazują na funkcji resztkowej błędu. Problem optymalnej identyfikacji nieujemnego spektrum relaksacji rozwiązano stosując podejście dualne. Przedstawiono schemat obliczeniowy algorytmu identyfikacji. Metodę zilustrowano przykładem numerycznym. Wyznaczono także spektrum relaksacji próbki buraka cukrowego badanego w stanie jednoosiowego odkształcenia przy zakłóconych pomiarach siły reakcji próbki.
Słowa kluczowe: lepkosprężystość, spektrum relaksacji naprężeń, identyfikacja, funkcje resztkowe błędu.

TEKA. COMMISSION OF MOTORIZATION AND ENERGETICS IN AGRICULTURE – 2013, Vol. 13, No. 1, 169–176

An algorithm for approximate identification of relaxation modulus of viscoelastic materials from non-ideal ramp-test histories

Anna Stankiewicz

Department of Mechanical Engineering and Automatics, University of Life Sciences in Lublin
Doświadczalna 50A, 20-280 Lublin, Poland, e-mail: anna.m.stankiewicz@gmail.com

Received February 20.2013; accepted March 14.2013

Summary. A new fast scheme for approximate identification of linear relaxation modulus of viscoelastic materials on the basis of the discrete stress data from non-ideal ramp-tests, where a time-variable strain rate is followed by a constant strain, is proposed. The approximations of the relaxation modulus in successive time instants are determined on the basis of the stress measurements in only three appropriately chosen sampling points. The numerical simulations are conducted for KWW relaxation modulus, which indicate that the presented approach is suitable for estimating the relaxation modulus. The approximation of relaxation modulus is more accurate than in Sorvari-Malinen method. However, the model errors are greater that in the case of Zapas-Phillips approach and the quality deterioration is acceptable. The noise robustness of the scheme must be noted, especially if compared with Sorvari-Malinen scheme.
Key words: relaxation test, non-ideal ramp-test, relaxation modulus, KWW model, identification method.

INTRODUCTION

Relaxation modulus is probably the most important mechanical characteristic in the framework of linear viscoelastic behavior [1,7,10,11]. The time-variable relaxation modulus $G(t)$, $t \geq 0$, is theoretically the stress that occurs in the material response to a unit step strain $\varepsilon(t)$. However, it is impossible to apply a step strain in experiments. Loading is never done infinitely fast [3,10,16]. In non-ideal stress relaxation tests the strain increases during the loading interval $[0, t_R]$ until a predetermined strain ε_0 is reached at ramp-time t_R, after which that strain ε_0 is maintained constant at that value. In ideal ramp-test [10] the strain increases along a constant strain rate path. However, usually the constant strain rate in the loading phase cannot be achieved experimentally [10,14,22]. Following Flory and McKenna [3], see also [16] and [22], we assume that the strain in non-ideal ramp-test is described by the function:

$$\varepsilon(t) = \begin{cases} 0 & for \ \ t < 0 \\ \frac{a}{3}\left(t - \frac{t_R}{2}\right)^3 + bt + c & for \ \ 0 \leq t < t_R, \\ \varepsilon_0 & for \ \ t \geq t_R \end{cases} \quad (1)$$

where: the strain parameters are: $a = -\frac{3}{4}\varepsilon_0\left(\frac{2}{t_R}\right)^3$, $b = \frac{3}{2}\frac{\varepsilon_0}{t_R}$ and $c = -\frac{1}{4}\varepsilon_0$. The strain $\varepsilon(t)$ (1) is shown in Figure 1, where the ideal step-strain $\varepsilon_0(t)$ and the ideal ramp-test strain $\varepsilon_I(t)$ corresponding to linear loading phase strain, are also plotted.

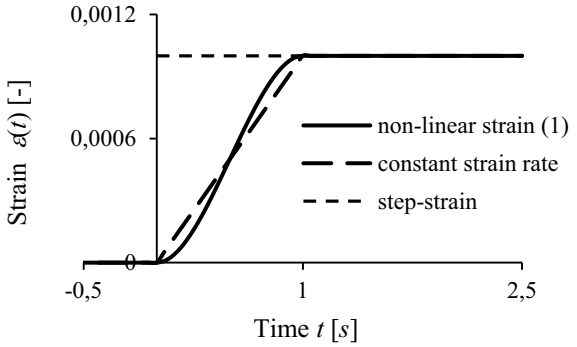

Fig. 1. An ideal and non-ideal ramp strain and step-strain; $t_R = 1\ [s]$, $\varepsilon_0 = 0.001\ [-]$

Different methods [7,10,14-16,18,19,22,23] have been proposed during the last few decades for the relaxation modulus determination using the stress data histories from non-ideal relaxation tests. Most of them are addressed for the case of the linear loading phase strain. Only the classical Zapas-Phillips [23] method and the optimal relaxation modulus identification schemes presented in [15,22] have been designed for non-ideal stress relaxation test with a time variable loading phase strain rate. For detailed references and an overview, see [3] and the recent publication [22].

In the previous paper [20], based on the mathematical properties of the problem of relaxation modulus recovery from time-measurements of the stress $\sigma(t)$ in the non-ideal ramp-test (1), the analytical formulas to approximate the relaxation modulus for an arbitrary time instant have been derived. Under standard and mild assumption concerning the relaxation modulus of the viscoelastic material and the rheological experiment it has been proved, that for noise-free stress measurements the resulting relaxation modulus model is monotonically decreasing continuous function of time with at most one discontinuity point.

To develop a fast algorithm for the relaxation modulus identification using discrete-time stress measurements obtained in the ramp-test $\varepsilon(t)$ (1), in which the relaxation modulus approximations in the successive time instants are calculated on the basis of at most three points of the stress data, is a basic concern. The numerical analysis is performed using the KWW material example both for noise free as well as noise corrupted stress measurements. Comparing the results obtained for the new and two other known algorithms with the true values of the relaxation modulus we will draw conclusions regarding the accuracy and applicability of the method proposed.

MODEL OF THE RELAXATION MODULUS

In the previous paper [20] under standard assumptions concerning the relaxation modulus $G(t)$ of the linear viscoelastic material [20; Assumption (4)] the following formula is derived for $0 < t \le t_R/4$:

$$G^{(NM)}(t) = \frac{{t_R}^3}{12\varepsilon_0(t_R - t)t^2}\sigma(2t), \tag{2}$$

and the next rule is developed for $t > t_R/4$:

$$G^{(NM)}(t) = \frac{8}{3\varepsilon_0}\sigma\left(t + \frac{3t_R}{4}\right) - \frac{7}{3\varepsilon_0}\sigma(t + t_R) + \\ + \frac{2}{3\varepsilon_0}\sigma\left(t + \frac{5t_R}{4}\right), \tag{3}$$

which approximate the modulus $G(t)$. In subsequent sections a complete algorithm for computing the relaxation modulus using discrete-time stress measurements from non-ideal ramp test (1) is presented and examined for simulated KWW model data.

IDENTIFICATION ALGORITHM

The computation of the relaxation modulus according to the above formulas involves the following steps.

1. Design the experiment – ramp-test (1) – with the predetermined constant strain level ε_0 and the ramp-time t_R, i.e., select the sampling instants t_i, $i = 1, \dots, N$, such that $t_1 = h$, $t_{i+1} - t_i = h$ and $t_R = 4i_0h$ for some integer $i_0 \ge 1$.
2. Perform the stress relaxation test (1), record and store the stress measurements $\bar{\sigma}(t_i) = \sigma(t_i) + z(t_i)$, corresponding to the chosen points $t_i, i = 1, \dots, N$, where $z(t_i)$ is additive measurement noise.
3. For $i = 1, \dots, i_0$ calculate the relaxation modulus $G^{(NM)}(t_i)$ according to formula:

$$G^{(NM)}(t_i) = \frac{{t_R}^3}{12\varepsilon_0(t_R - t_i){t_i}^2}\bar{\sigma}(2t_i).$$

4. For $i = i_0 + 1, \dots, N - 5i_0$ determine the relaxation modulus $G^{(NM)}(t_i)$ using the rule:

$$G^{(NM)}(t_i) = \frac{8}{3\varepsilon_0}\bar{\sigma}\left(t_i + \frac{3t_R}{4}\right) - \frac{7}{3\varepsilon_0}\bar{\sigma}(t_i + t_R) + \\ + \frac{2}{3\varepsilon_0}\bar{\sigma}\left(t_i + \frac{5t_R}{4}\right).$$

Remark. Note, that in view of (3), when the equidistant time sampling $t_{i+1} - t_i = h$ is applied, the existence of an integer $i_0 \ge 1$ such that $t_R = 4i_0h$ is obvious applicability condition of the scheme.

OTHER APPROXIMATE METHODS

Zapas and Phillips [23] developed a method, where the correction $t - \frac{t_R}{2}$ of the time is used as follows:

$$G^{(ZP)}\left(t_i - \frac{t_R}{2}\right) = \frac{1}{\varepsilon_0}\bar{\sigma}(t_i),$$

for an arbitrary $t_i \ge t_R$. Thus, the relaxation modulus approximation can be computed for $t_i \ge t_R/2$. For constant loading strain rate Sorvari and Malinen [14] proposed differential formula:

$$G^{(SM)}(t_i) = \frac{1}{\varepsilon_0}\bar{\sigma}(t_i + t_R) - \frac{t_R}{2\varepsilon_0}\,\dot{\bar{\sigma}}\,(t_i + t_R),$$

according to which the approximate value of the relaxation modulus for an arbitrary $t_i \ge 0$ is computed using the stress measurements and their derivatives for $t_i + t_R$. The above methods are used in numerical studies due to their approximate "nature".

NUMERICAL ANALYSIS

Example 1 – noise-free measurements. Consider viscoelastic material whose relaxation modulus is described by KWW (Kohlrausch- Williams-Watts) model of the form [3, 16]:

$$G(t) = G_0 e^{-(t/\tau)^\beta}, \tag{4}$$

where: $G_0 = 10^9\ [Pa]$, the parameter $\beta = 0.5$ [–], and the relaxation times are $\tau = 3\ [s]$ (material A) and $\tau = 100\ [s]$ (material B). The strain $\varepsilon_0 = 0.001$ [–] and the time-horizon $T = 20\ [s]$ are assumed for experi-

ment. The test data was equally spaced in the time interval $[0, T]$. The ramp times: $t_R = 1\ [s]$, $t_R = 2\ [s]$ and $t_R = 5\ [s]$ have been taken in experiment studies. Thus, the condition $t_R \leq 18\tau$ [20, Remark 1] which is sufficient for the monotonicity of the relaxation modulus model determined according to the proposed method is satisfied for material (4) in every case examined. The Zapas-Phillips and Sorvari-Malinen rules and the new method are studied. For any method the number N of sampling points t_i are chosen according to the applicability conditions of the respective scheme. Noise free measurements $\bar{\sigma}(t_i) = \sigma(t_i)$, $i = 1, \ldots, N$, are assumed. To estimate the approximation error of the relaxation modulus (4) for the new method the following mean square relative index is taken:

$$ERRG^{(NM)} = \frac{1}{\bar{N}} \sum_{i=1}^{\bar{N}} \left[\frac{G^{(NM)}(t_i) - G(t_i)}{G(t_i)} \right]^2 100\%,$$

where: $\bar{N} = N - 5i_0$ is the corrected number of sampling instants t_i for which the approximate value of the relaxation modulus $G^{(NM)}(t_i)$ can be determined using the scheme proposed. The indices $ERRG^{(ZP)}$ and $ERRG^{(SM)}$ for Zapas-Phillips and Sorvari-Malinen methods are defined by analogy. The indices $ERRG^{(NM)}$, $ERRG^{(ZP)}$ and $ERRG^{(SM)}$ for noise-free stress measurements are given in Table 1 for material A. For material B the courses of this indices as a function of N are shifted in Figure 2 using the logarithmic axis to obtain the best clearness if this graph.

Table 1. Mean relative errors of the relaxation modulus approximation for the new method and Zapas-Phillips and Sorvari-Malinen rules; material A, noise-free case

Mean relative error	Noise-free case, $t_R = 1\ [s]$					
	$N = 80$	N =160	$N = 240$	$N = 320$	$N = 400$	$N = 480$
$ERRG^{(NM)}$ [%]	4,32E-3	2,46E-3	8,202E-4	4,158E-4	3,038E-4	2,843E-4
$ERRG^{(ZP)}$ [%]	6,39E-4	5,02E-4	4,61E-4	4,415E-4	4,302E-4	4,228E-4
$ERRG^{(SM)}$ [%]	0,273	0,101	0,061	0,044	0,035	0,03
	Noise-free case, $t_R = 2\ [s]$					
	$N = 40$	$N = 80$	$N = 120$	$N = 160$	$N = 200$	$N = 240$
$ERRG^{(NM)}$ [%]	2,77E-3	0,011	3,997E-3	2,204E-3	1,637E-3	1,467E-3
$ERRG^{(ZP)}$ [%]	3,45E-3	2,74E-3	2,533E-3	2,432E-3	2,373E-3	2,335E-3
$ERRG^{(SM)}$ [%]	1,02	0,399	0,247	0,182	0,148	0,127
	Noise-free case, $t_R = 5\ [s]$					
	$N = 32$	$N = 80$	$N = 112$	$N = 160$	$N = 208$	$N = 240$
$ERRG^{(NM)}$ [%]	0,103	0,017	0,013	0,014	0,014	0,015
$ERRG^{(ZP)}$ [%]	0,031	0,027	0,026	0,026	0,026	0,025
$ERRG^{(SM)}$ [%]	2,562	1,057	0,831	0,675	0,597	0,563

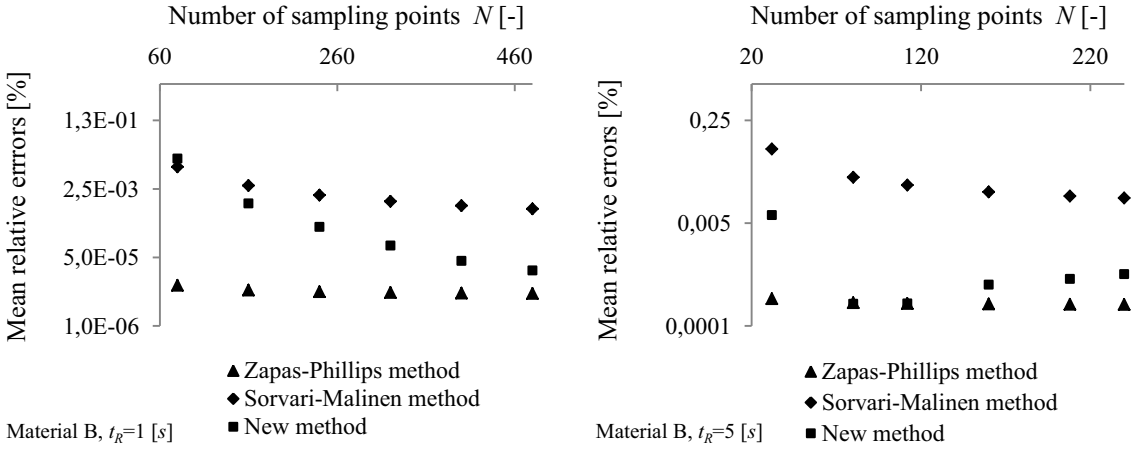

Fig. 2. Mean relative errors of the relaxation modulus approximation for the new method and Zapas-Phillips and Sorvari-Malinen rules; material B, $t_R = 1\ [s]$ and $t_R = 5\ [s]$, noise-free case

It can be seen from the above simulation results that for noise-free stress measurements the new algorithm ensures very good accuracy of the relaxation modulus approximation, which is comparable with the Zapas-Phillips rule and better than for the Sorvari-Malinen method, whenever the number of the measurements is appropriately chosen in accordance with the ramp-time t_R and the relaxation time of the material. The relaxation modulus $G^{(NM)}(t)$, $G^{(ZP)}(t)$ and $G^{(SM)}(t)$ calculated according to the considered methods for time interval $[0; 3{,}75]$ seconds are plotted for $t_R = 2\,[s]$ and $N = 160$ in Figure 3 (material A) and in Figure 4 (material B). The relaxation modulus $G(t)$ (4) is also marked in both figures.

Example 2 – noise robustness. We consider again the materials A and B described by the KWW relaxation modulus (4). In order to model the noise produced by a test machine the noises $z(t_i)$ have been generated independently by random choice with normal distribution with zero mean value and variance equal to 100% and 200% of the mean integral value $\frac{1}{T}\int_0^T \sigma(\lambda)d\lambda$ of the signal $\sigma(t)$ in the time interval $[0, T]$. Such measurement noises are even strongest than the true disturbances recorded for the plant materials (see [17; Chapter 5.5.4]). The experiment and next the computations of the approximate relaxation modulus model have been repeated n=100 times. The mean values $MERRG^{(ZP)}$, $MERRG^{(SM)}$ and $MERRG^{(NM)}$ of the indices $ERRG^{(ZP)}$, $ERRG^{(SM)}$ and $ERRG^{(NM)}$, respectively, obtained for material A are given in Table 2 for the case of weak 100% noises and in Table 3 for 200% strong noises. The Zapas-Phillips relaxation modulus model $G^{(ZP)}(t)$ does not depend essentially on the measurement noises, while

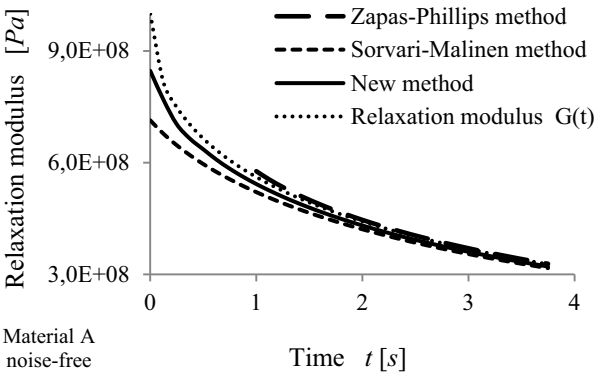

Fig. 3. Approximations $G^{(NM)}(t)$, $G^{(ZP)}(t)$, $G^{(SM)}(t)$ of the relaxation modulus $G(t)$; material A, noise-free case, $t_R = 2\,[s]$

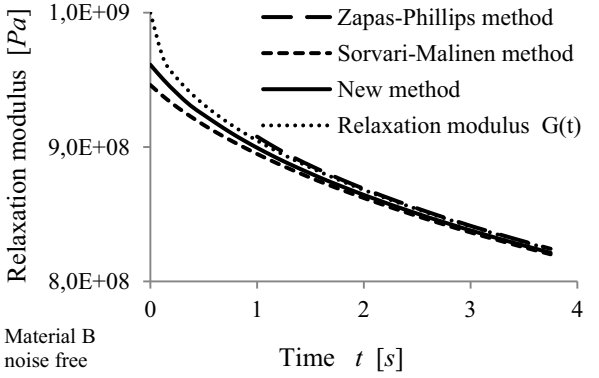

Fig. 4. Approximations $G^{(NM)}(t)$, $G^{(ZP)}(t)$, $G^{(SM)}(t)$ of the relaxation modulus $G(t)$; material B, noise-free case, $t_R = 2\,[s]$

Table 2. Mean relative errors of the relaxation modulus approximation for the new method and Zapas-Phillips and Sorvari-Malinen rules; material A, weak noises 100%

Mean relative errors	Weak noises 100%, $t_R = 1\,[s]$					
	$N = 80$	$N = 160$	$N = 240$	$N = 320$		
$MERRG^{(NM)}$ [%]	0,0474	0,04749	0,04618	0,04602		
$MERRG^{(ZP)}$ [%]	0,004516	0,004493	0,004324	0,004399		
$MERRG^{(SM)}$ [%]	0,3195	0,2425	0,3595	0,5662		
	Weak noises 100%, $t_R = 2\,[s]$					
	$N = 40$	$N = 80$	$N = 120$	$N = 160$	$N = 200$	$N = 240$
$MERRG^{(NM)}$ [%]	0,04374	0,04892	0,04264	0,04122	0,04084	0,04357
$MERRG^{(ZP)}$ [%]	0,007173	0,006491	0,006279	0,006276	0,006211	0,006055
$MERRG^{(SM)}$ [%]	1,057	0,526	0,5102	0,6218	0,83	1,103
	Weak noises 100%, $t_R = 5\,[s]$					
	$N = 32$	$N = 80$	$N = 112$	$N = 160$	$N = 208$	$N = 240$
$MERRG^{(NM)}$ [%]	0,1263	0,04797	0,04636	0,0611	0,07399	0,1013
$MERRG^{(ZP)}$ [%]	0,03425	0,03039	0,02964	0,0292	0,02892	0,0289
$MERRG^{(SM)}$ [%]	2,647	1,526	1,75	2,499	3,65	4,625

the mean value of the noise is zero. Both for the new and Sorvari-Malinen methods the accuracy of the relaxation modulus approximation are dependent on the noises, however, for Sorvari-Malinen method the mean approximation errors are multiple greater than in the case of the new method. Similar simulation results are obtained for material B. An example of the models $G^{(NM)}(t)$, $G^{(ZP)}(t)$, $G^{(SM)}(t)$ and the "true" relaxation modulus of material A are illustrated in Figure 5 for weak 100% noises and in Figure 6 for strong 200% noises; the ramp-time $t_R = 2\ [s]$ and the number of measurements $N = 160$ are applied here. The respective characteristics for material B are given in Figures 7 (weak noises) and 8 (strong noises). The models $G^{(ZP)}(t)$ are generally fairly smooth, however the models $G^{(NM)}(t)$ and especially $G^{(SM)}(t)$ are not.

In turn, the relaxation modulus $G(t)$ (4) of material B and the corresponding models for ramp-times $t_R = 1\ [s]$ and $t_R = 5\ [s]$ are recorded in Figures 9 and 10, respectively, for the case of weak noises; as previously, the number of measurements $N = 160$ is taken. Through a comparison of the Figures 7,9 and 10 we can realize how the accuracy of the relaxation modulus approximation strongly depend on the respective choice of such experiment parameters as the ramp-time t_R and the sampling period h.

Example 3 – Young modulus identification. The identifiability of the constant uniaxial Young modulus $G(0)$ has been also examined. The accuracy of the initial value $G(0)$ identification in the case of the new method has been measured by relative means error $ERR0^{(NM)}$ defined as a mean value of the square relative errors

Table 3. Mean relative errors of the relaxation modulus approximation for the for the new method and Zapas-Phillips and Sorvari-Malinen rules; material A, strong noises 200%

Mean relative error	Strong noises 200%, $t_R = 1\ [s]$			
	$N = 80$	$N = 160$	$N = 240$	$N = 320$
$MERRG^{(NM)}$ [%]	0,097	0,092	0,092	0,09
$MERRG^{(ZP)}$ [%]	8,527E-3	8,283E-3	8,186E-3	8,362E-3
$MERRG^{(SM)}$ [%]	0,363	0,388	0,659	1,053
	Strong noises 200%, $t_R = 2\ [s]$			
	$N = 40$	$N = 80$	$N = 120$	$N = 160$	$N = 200$	$N = 240$
$MERRG^{(NM)}$ [%]	0,082	0,086	0,081	0,078	0,08	0,083
$MERRG^{(ZP)}$ [%]	0,011	0,01	9,96E-3	9,96E-3	9,841E-3	9,797E-3
$MERRG^{(SM)}$ [%]	1,098	0,649	0,794	1,103	1,553	2,077
	Strong noises 200%, $t_R = 5\ [s]$					
	$N = 32$	$N = 80$	$N = 112$	$N = 160$	$N = 208$	$N = 240$
$MERRG^{(NM)}$ [%]	0,15	0,07	0,074	0,108	0,147	0,181
$MERRG^{(ZP)}$ [%]	0,038	0,034	0,033	0,033	0,033	0,032
$MERRG^{(SM)}$ [%]	2,733	2,002	2,717	4,293	6,713	8,776

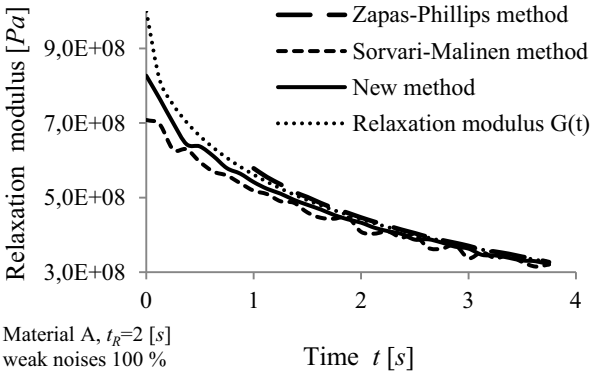

Fig. 5. Approximations $G^{(NM)}(t)$, $G^{(ZP)}(t)$, $G^{(SM)}(t)$ of the relaxation modulus $G(t)$; material A, weak noises 100%, $t_R = 2\ [s]$

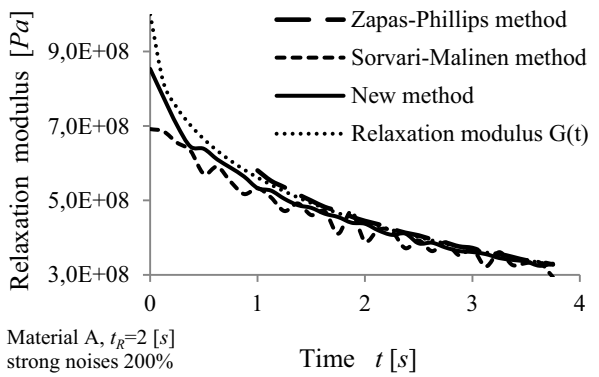

Fig. 6. Approximations $G^{(NM)}(t)$, $G^{(ZP)}(t)$, $G^{(SM)}(t)$ of the relaxation modulus $G(t)$; material A, strong noises 200%, $t_R = 2\ [s]$

$\left[\frac{G^{(NM)}(t_1)-G(0)}{G(0)}\right]^2$ for 100 repetitions of the numerically simulated stress relaxation test (1) in time interval $[0,T]$. The respective indices for the two other methods are defined by analogy. In the case of Zapas-Phillips method the value of $G^{(ZP)}(t_R/2)$ is chosen as a $G(0)$ approximation. The numerical studies results obtained for material A are summarized in Table 4 for weak and in Table 5 for strong noises. Clearly, the Young modulus approximation errors in the case of Zapas-Phillips method is nearly independent of the number of sampling points and the noises intensity, however the errors increases with the ramp-time t_R. For Sorvari-Malinen method the errors decreases with the increasing number of sampling points, but still are unacceptable big. The smallest errors of $G(0)$ approximation are guaranteed by the new method. By respective choice of the experiment parameters t_R and N, the errors can be reduced below 1,5%.

CONCLUSIONS

1. A new fast scheme for approximate identification of linear relaxation modulus of viscoelastic materials using discrete time-measurements of the stress from non-ideal ramp-tests is proposed and analyzed. The approximations of the relaxation modulus in successive time instants are determined on the basis on the stress measurements in only three appropriately chosen sampling points. Numerical results are provided to compare the presented method with two other alternative procedures known in the literature.
2. The model obtained by using Zapas-Phillips method exactly describes the true KWW relaxation modulus, both for noise-free, see Figure 3 and 4, as well as for noise corrupted stress measurements, see Figures 5-10. However, the Zapas-Phillips method fails at the estimating of the initial value of $G(0)$. The approximation accuracy obtained by the new method is worse than that guaranteed by Zapas-Phillips rule, but the applicability for short time interval is an excellent advantage of the new scheme.
3. In Sorvari-Malinen method the relaxation modulus is poorly estimated. The new method provides better approximation accuracy than Sorvari-Malinen method, the more so that the simulation computations indicate that the approximation errors for Sorvari-Malinen method are extremely sensitive to the noises (see Figures 5-10). It seems also reasonable to use the new method to produce a good fit of the constant Young modulus.
4. Both theoretical analysis of the scheme conducted in [20] as well as the results of the numerical studies presented above, especially acceptable noise robustness, suggest

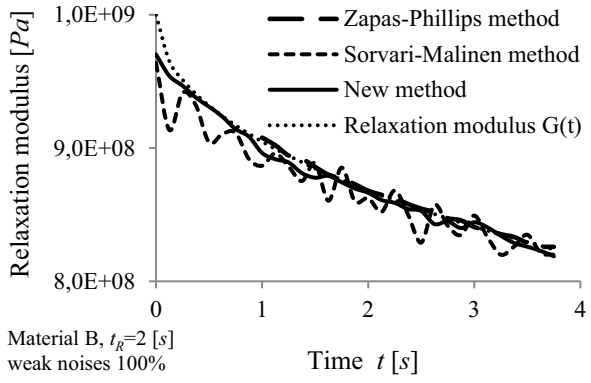

Fig. 7. Approximations $G^{(NM)}(t)$, $G^{(ZP)}(t)$, $G^{(SM)}(t)$ of the relaxation modulus $G(t)$; material B, weak noises 100%, $t_R = 2\ [s]$

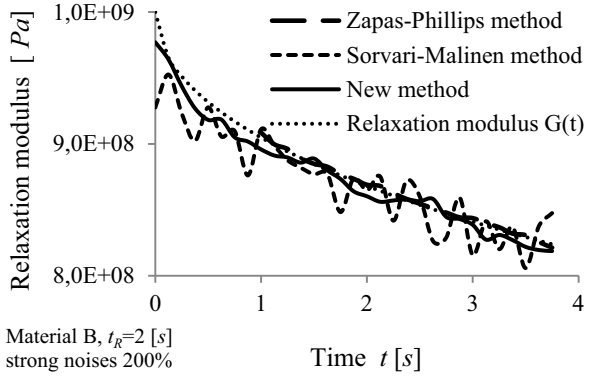

Fig. 8. Approximations $G^{(NM)}(t)$, $G^{(ZP)}(t)$, $G^{(SM)}(t)$ of the relaxation modulus $G(t)$; material B, strong noises 200%, $t_R = 2\ [s]$

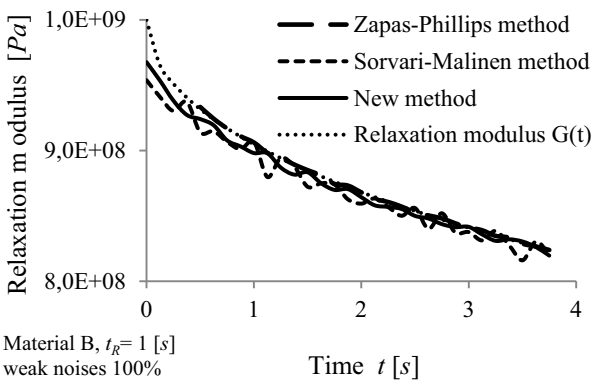

Fig. 9. Approximations $G^{(NM)}(t)$, $G^{(ZP)}(t)$, $G^{(SM)}(t)$ of the relaxation modulus $G(t)$; material B, weak noises 100%, $t_R = 1\ [s]$

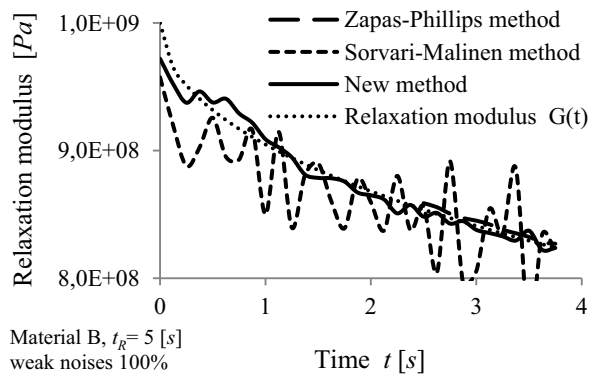

Fig. 10. Approximations $G^{(NM)}(t)$, $G^{(ZP)}(t)$, $G^{(SM)}(t)$ of the relaxation modulus $G(t)$; material B, weak noises 100%, $t_R = 5\ [s]$

Table 4. Mean relative errors of $G(0)$ approximation for the for the new method and Zapas-Phillips and Sorvari-Malinen rules; material A, weak noises 100%

Mean relative errors	Weak noises 100%, $t_R = 1\ [s]$					
	$N = 80$	$N = 160$		$N = 240$	$N = 320$	
$ERR0^{(NM)}$ [%]	8,568	2,858		1,689	1,238	
$ERR0^{(ZP)}$ [%]	10,458	10,474		10,444	10,467	
$ERR0^{(SM)}$ [%]	8,568	5,85		4,938	4,362	
	Weak noises 100%, $t_R = 2\ [s]$					
	$N = 40$	$N = 80$	$N = 120$	$N = 160$	$N = 200$	$N = 240$
$ERR0^{(NM)}$ [%]	12,65	4,906	2,989	2,114	1,742	1,731
$ERR0^{(ZP)}$ [%]	17.892	17.888	17,9	17,88	17,86	17,87
$ERR0^{(SM)}$ [%]	15,36	10,81	9,027	8,239	7,715	7,452
	Weak noises 100%, $t_R = 5\ [s]$					
	$N = 32$	$N = 80$	$N = 112$	$N = 160$	$N = 208$	$N = 240$
$ERR0^{(NM)}$ [%]	9,625	3,909	3,101	4,112	10,79	12,42
$ERR0^{(ZP)}$ [%]	33.263	33,26	33,25	33,24	33,26	33,24
$ERR0^{(SM)}$ [%]	22,64	16,73	15,49	14,9	14,41	13,91

Table 5. Mean relative errors of $G(0)$ approximation for the for the new method and Zapas-Phillips and Sorvari-Malinen rules; material A, strong noises 200%

Mean relative error	Strong noises 200%, $t_R = 1\ [s]$					
	$N = 80$	$N = 160$		$N = 240$	$N = 320$	
$ERR0^{(NM)}$ [%]	8,594	3,17		1,926	1,42	
$ERR0^{(ZP)}$ [%]	10,46	10,46		10,46	10,46	
$ERR0^{(SM)}$ [%]	8,674	5,907		4,804	4,405	
	Strong noises 200%, $t_R = 2\ [s]$					
	$N = 40$	$N = 80$	$N = 120$	$N = 160$	$N = 200$	$N = 240$
$ERR0^{(NM)}$ [%]	12,6	5,138	3,301	2,36	1,74	2,183
$ERR0^{(ZP)}$ [%]	17,87	17,88	17,88	17,89	17,89	17,88
$ERR0^{(SM)}$[%]	15,33	10,85	9,128	8,399	7,632	7,403
	Strong noises 200%, $t_R = 5\ [s]$					
	$N = 32$	$N = 80$	$N = 112$	$N = 160$	$N = 208$	$N = 240$
$ERR0^{(NM)}$ [%]	10,19	4,413	3,544	4,391	9,023	15,64
$ERR0^{(ZP)}$ [%]	33.23	33,26	33,25	33,26	33,24	33,23
$ERR0^{(SM)}$ [%]	22,54	16,78	15,35	14,64	14,42	13,97

that the proposed scheme can be used successfully within a satisfactory range of viscoelastic materials. Moreover, the practical point of view has been specially emphasized while the scheme derivation and because it does not require any other experimental technique more sophisticated than the equidistant sampling of time instants during rheological experiment, the presented algorithm is easy to implement and fast to use since only three measured stress data points are used to evaluate the relaxation modulus at any time instant. Thus the scheme can be easily implemented in an arbitrary computational environment supporting the rheological experiment.

5. The problems of viscoelastic model determination, in which the relaxation test stress history may provide experimental

data for identification, such as that considered in [1,6,9,13] for polymeric liquids and solids, in [12] for metals and their alloys or in [2, 5,8,17,21] for foods and biological materials, constitute the area of applicability of the scheme.

REFERENCES

1. **Doi M., Edwards S.F., 2001:** The Theory of Polymer Dynamics. Oxford University Press, Oxford.
2. **Figiel A., 2008:** Rheological properties of biodegradable material determined on the Basis of a cyclic stress relaxation test Inżynieria Rolnicza, 4 (102), 271–278, [in Polish].
3. **Flory A., McKenna G.B., 2004:** Finite step rate corrections in stress relaxation experiments: a comparison of two methods. Mechanics of Time-Dependent Materials, 8, 17–37.
4. **Gupta H.S., Seto J., Krauss S., Boesecke P., Screen H.R.C., 2010:** In situ multi-level analysis of viscoelastic deformation mechanisms in tendon collagen. Journal of Structural Biology, 169, 183–191.
5. **Guz T., 2009:** An influence of quarantine conditions on elasticity modulus in apples stored in ulo and regular store. TEKA Commission of Motorization and Power Industry in Agriculture, 9, 69–77.
6. **Jerabek M., Tscharnuter D.,·Major Z., Ravi-Chandar K., Lang R.W., 2010:** Relaxation behavior of neat and particulate filled polypropylene in uniaxial and multiaxial compression. Mechanics of Time-Dependent Materials, 14, 47–68.
7. **Knauss W.G., Zhao J., 2007:** Improved relaxation time coverage in ramp-strain histories. Mechanics of Time-Dependent Materials, 11(3–4), 199–216.
8. **Kobus Z., Kusińska E., 2010:** Effect of temperature and concentration on rheological properties of tomato juice. TEKA Commission of Motorization and Power Industry in Agriculture, 10, 170–178.
9. **Kozub Y., 2012:** Deformation of rubber-metal vibration and seismic isolators. TEKA Commission of Motorization and Energetics in Agriculture, 12(4), 96–100
10. **Lee S., Knauss W.G., 2000:** A note on the determination of relaxation and creep data from ramp tests. Mechanics of Time-Dependent Materials, 4, 1–7.
11. **Malkin A.Y., Isayev A.I., 2011:** Rheology: Concepts, Methods and Applications. ChemTec Publishing, Toronto.
12. **Rao G.R., Gupta O.P., Pradhan B., 2011:** Application of stress relaxation testing in evaluation of creep strength of a tungsten-alloyed 10% Cr cast steel. International Journal of Pressure Vessels and Piping, 88, 65–74.
13. **Şerban D.A., Marşavina L., Silberschmidt V.V., 2012:** Response of semi-crystalline thermoplastic polymers to dynamic loading: A finite element study. Computational Materials Science, 64, 116–121.
14. **Sorvari J., Malinen M., 2006:** Determination of the relaxation modulus of a linearly viscoelastic material. Mechanics of Time-Dependent Materials, 10, 125–133.
15. **Sorvari J., Malinen M., 2007:** On the direct estimation of creep and relaxation functions. Mechanics of Time-Dependent Materials, 11, 143–157.
16. **Sorvari J., Malinen M., Hämäläinen J., 2006:** Finite ramp time correction method for non-linear viscoelastic material model. International Journal of Non-Linear Mechanics, 41, 1058–1064.
17. **Stankiewicz A., 2007:** Identification of the relaxation spectrum of viscoelastic plant materials. Ph. D. Thesis, Agricultural University of Lublin, Poland [in Polish].
18. **Stankiewicz A., 2012:** Algorithm of relaxation modulus identification using stress measurements from the real test of relaxation. Inżynieria Rolnicza, 16(4), 389–399 [in Polish].
19. **Stankiewicz A., 2012:** Determination of the relaxation modulus on the basis of the ramp-test stress data. Inżynieria Rolnicza, 16(4), 401–409 [in Polish].
20. **Stankiewicz A., 2013:** Identification of relaxation modulus from non-ideal ramp-test histories. Problem and method. TEKA Commission of Motorization and Energetics in Agriculture (submitted for publication).
21. **Stankiewicz A., Gołacki K., 2008:** Approximation of the Continuous Relaxation Spectrum of Plant Viscoelastic Materials using Laguerre Functions. Electronic Journal of Polish Agricultural Universities, Series: Agricultural Engineering, 11 (1/volome11) #20.
22. **Tscharnuter D., Jerabek M., Major·Z., Lang R.W., 2011:** On the determination of the relaxation modulus of PP compounds from arbitrary strain histories. Mechanics of Time-Dependent Materials, 15, 1–14.
23. **Zapas L.J., Craft T., 1965:** Correlation of large longitudinal deformations with different strain histories. Journal of Research of the National Bureau of Standards, A69(6), 541–546.

ALGORYTM IDENTYFIKACJI MODUŁU RELAKSACJI MATERIAŁÓW LEPKOSPRĘŻYSTYCH NA PODSTAWIE NIEIDEALNEGO TESTU RELAKSACJI NAPRĘŻEŃ O NIELINIOWYM ODKSZTAŁCENIU WSTĘPNYM

Streszczenie. Celem pracy było opracowanie szybkiego algorytmu identyfikacji modułu relaksacji materiałów o własnościach liniowo lepkosprężystych na podstawie dyskretnych pomiarów naprężenia zgromadzonych w rzeczywistym teście relaksacji naprężeń o zmiennej w czasie prędkości odkształcania wstępnego. Zaproponowano prosty schemat identyfikacji, w którym przybliżenie modułu w wybranej chwili czasu wyznaczane jest na podstawie co najwyżej trzech pomiarów naprężenia. Przeprowadzone badania numeryczne wskazują, że opracowana metoda zapewnia lepsze przybliżenie modułu relaksacji niż metoda Sorvari-Malinena oraz akceptowalne pogorszenie jakości jego przybliżenia w porównaniu z regułą Zapasa-Phillipsa. Przewagę nowej metody nad regułą Sorvari-Malinena stanowi także większa odporność na zakłócenia pomiarowe, jej zaletą w porównaniu z regułą Zapasa-Phillipsa jest rozszerzenie zakresu stosowalności o początkowy odcinek czasu. Metoda zapewnia bardzo dobre przybliżenie wartości początkowej modułu relaksacji, a jej prosty algorytm umożliwia zastosowanie w trybie on-line w czasie eksperymentu reologicznego.

Słowa kluczowe: test relaksacji naprężeń, moduł relaksacji, model KWW, algorytm identyfikacji.

TEKA. COMMISSION OF MOTORIZATION AND ENERGETICS IN AGRICULTURE – 2013, Vol. 13, No. 1, 177–184

Identification of relaxation modulus of viscoelastic materials from non-ideal ramp-test histories – problem and method

Anna Stankiewicz

Department of Mechanical Engineering and Automatics, University of Life Sciences in Lublin
Doświadczalna 50A, 20-280 Lublin, Poland, e-mail: anna.m.stankiewicz@gmail.com

Received February 20.2013; accepted March 14.2013

Summary. The identification of the linear relaxation modulus of viscoelastic materials on the basis of the stress data from non-ideal ramp tests where a time-variable strain rate is followed by a constant strain is considered. The loading phase strain is described by the third order polynomial of time. The aim of the paper is to develop a method to approximate identification of relaxation modulus using such ramp strain histories. Middle point rule and generalized Simpson rule are used to derive a new method. The approximations of the relaxation modulus at successive time instants are determined on the basis on the stress measurements in at most three appropriately chosen sampling points. The properties of the relaxation modulus model determined according to the proposed method are examined under standard assumptions concerning the relaxation modulus of the material and the experiment. The method developed is a basis for synthesis of fast identification scheme.

Key words: relaxation test, finite ramp-time, relaxation modulus, identification method.

INTRODUCTION

In current engineering practice it is common to deal with either the uniaxial or shear time-dependent relaxation modulus of viscoelastic materials [1-5,7,9,11,12,15-18,27]. For linear viscoelastic materials the relaxation modulus is the stress, which is induced in the material when the unit step strain is imposed. Unfortunately, that deformation mode cannot be achieved experimentally without invoking stress waves [13]. Thus, the relaxation modulus is not directly accessible by means of straightforward measurement method. It is usually recovered from the experimental data of the stress relaxation process history. A common practice to identify the relaxation modulus is still to compute the modulus from the ideal step-strain case rule. Unfortunately, according to the „ten-times-rule", or equivalently, "factor-of-10'rule", this step-strain assumption is acceptable only if the time is at least ten times larger than the initial loading time, see Example given below. Thus, in practice quite often the first seconds of the relaxation data are ignored to account for the finite loading time of deformation [6].

To take into account the finite initial loading time in the real non-ideal relaxation tests a few methods have been proposed during the last several years [10,13,19-21,24-26,28]. Zapas and Phillips [28] developed a general method, which in the case of linear viscoelasticity takes the form of very simple rule, where the 'true' relaxation time is delayed of half loading time. For the case of constant loading rate a few methods for relaxation modulus identification has been proposed: the backward recursive method developed by Lee and Knauss [13], the differential rule proposed by Sorvari and Malinen [19] and the latest method based on the general trapezoidal rule presented in the papers [23, 24].

In practice, however, to inertia effects the assumption that the ramp loading is approximated to be linear may fail [6, 10, 26]. Following Flory and McKenna [6], see also [21, 26], it is assumed in this paper that the initial loading phase strain of the relaxation test is described by the third order polynomial of the time. To develop a fast method to approximate identification of relaxation modulus on the basis of such non-ideal ramp strain history data, in which the relaxation modulus at arbitrary time instant is determined using only few stress measurements, is the goal of the paper. Based on the mathematical properties of the problem and using two known numerical quadrature rules: midpoint rule and generalized Simpson's rule a new identification method is proposed, in which the approximation of the relaxation modulus at arbitrary time is determined on the basis of the stress measurements in at most three appropriately chosen sampling points. It is proved, under mild assumptions concerning the relaxation modulus

of the material and the experiment that the resulted model is monotonically decreasing function with at most one discontinuity point.

PROBLEM STATEMENT

1. MATERIAL

We consider a linear viscoelastic material subjected to small deformations for which the uniaxial, nonaging and izotropic stress-strain equation can be represented by a Boltzmann superposition integral [11, 14]:

$$\sigma(t) = \int_{-\infty}^{t} G(t-\lambda)\dot{\varepsilon}(\lambda)d\lambda, \tag{1}$$

where: $\sigma(t)$ and $\varepsilon(t)$ denotes the stress and stain, respectively, and $G(t)$ is the time-dependent linear (Boltzmann) relaxation modulus. By assumption, the exact mathematical description of the relaxation modulus $G(t)$ is completely unknown, but the value of $\sigma(t)$ can be measured with a certain accuracy for any given value of the time $t \in \mathcal{T}$, where $\mathcal{T} = [0, T]$ and $0 < T < \infty$.

2. EXPERIMENT

A classical manner of studying viscoelasticity for such materials is by two-phase stress relaxation test, where the strain increases during the loading time interval $[0, t_R]$ until a predetermined strain ε_0 is reached at ramp-time t_R, after which that strain ε_0 is maintained constant at that value [13]. In ideal ramp-test [13] the strain increases along a constant strain rate path. However, the constant strain rate in the loading phase is usually unrealizable due to experimental limitations [19, 26]. Following Flory and McKenna [6], see also [21; Ramp III] and [26], we assume that the strain in non-ideal ramp-test is described by the function:

$$\varepsilon(t) = \begin{cases} 0 & for\ \ t < 0 \\ \frac{a}{3}\left(t - \frac{t_R}{2}\right)^3 + bt + c & for\ \ 0 \le t < t_R \\ \varepsilon_0 & for\ \ t \ge t_R \end{cases}, \tag{2}$$

where: the non-ideal ramp-strain parameters are:

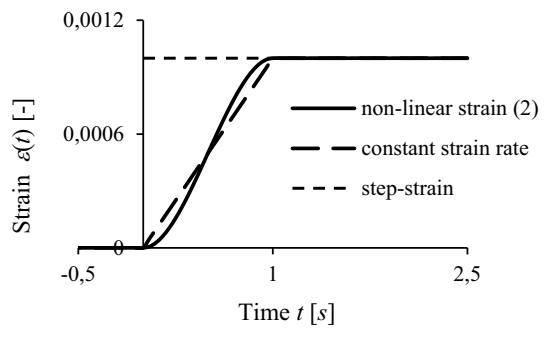

Fig. 1. Step-strain, ideal and non-ideal ramp strain; $t_R = 1\ [s]$, $\varepsilon_0 = 0{,}001\ [-]$

$a = -\frac{3}{4}\varepsilon_0\left(\frac{2}{t_R}\right)^3$, $b = \frac{3}{2}\frac{\varepsilon_0}{t_R}$ and $c = -\frac{1}{4}\varepsilon_0$. The strain $\varepsilon(t)$ (2) is shown in Figure 1, where the ideal step-strain $\varepsilon_0(t)$ and the ideal ramp-test strain $\varepsilon_I(t)$ corresponding to linear loading phase strain, are also depicted.

3. IDENTIFICATION

Suppose that the non-ideal ramp test (2) performed on the real material resulted in a set of the stress measurements. Identification consists in estimating of the relaxation modulus of viscoelastic material described by the equation (1) using the stress measurements. A common practice is to calculate the relaxation modulus by the rule $G(t) = \sigma(t)/\varepsilon_0$, which in view of (1) is valid only for infinitely short initial loading time (for ideal step-strain). According to the „ten-times-rule" that step-strain assumption is acceptable only for $t \ge 10t_R$. Thus, for the times lower than the ten loading time t_R, the classical rule $G(t) = \sigma(t)/\varepsilon_0$ may fail. To illustrate the errors of such approach the following example is considered.

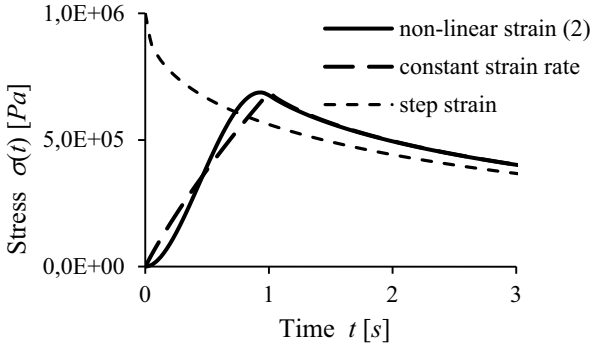

Fig. 2. Stress in ideal and non-ideal ramp-tests and in step-strain relaxation test

Example. Let us consider viscoelastic material whose relaxation modulus is described by the KWW model (Kohlrausch, Williams and Watts) of the form [6, 19]:

$$G(t) = G_0 e^{-(t/\tau)^\beta}, \tag{3}$$

where: following [6] $G_0 = 10^9\ [Pa]$, the dimensionless parameter $\beta = 0{,}5\ [-]$ and the relaxation time $\tau = 3\ [s]$. The strain $\varepsilon_0 = 0{,}001\ [-]$ and the ramp-time $t_R = 1\ [s]$. The stress $\sigma(t)$ resulting for KWW material for non-ideal ramp test (2) is plotted in Figure 2, where the related stress $\sigma_0(t)$ for ideal step-strain relaxation test and the material response $\sigma_I(t)$ after the application of a constant loading strain rate are also given. The differences between the three signals $\sigma(t)$, $\sigma_I(t)$ and $\sigma_0(t)$ are characterized by the relative absolute percent errors summarized in Table 1 for some selected points of time.

The errors are big at short time, and decrease with the time $t > t_R$. The differences for the two signals $\sigma(t)$ and $\sigma_0(t)$ at the time point t_R exceed 20% of the ideal relaxation test stress $\sigma_0(t)$, compare Figure 2, at the

Table 1. Stress differences between the ideal and non-ideal ramp-test and step strain relaxation test

Time t	$t_R/6$	$t_R/4$	$t_R/3$	$t_R/2$	$2t_R/3$	$3t_R/4$	$0{,}95t_R$	t_R	$3t_R$	$5t_R$	$10t_R$	$100t_R$
Errors	Ramp time $t_R = 1\ [s]$											
$\frac{\lvert\sigma(t)-\sigma_0(t)\rvert}{\sigma_0(t)}$ [%]	91,738	82,162	69,844	40,191	9,831	3,165	20,566	20,502	9,296	6,939	4,767	1,458
$\frac{\lvert\sigma(t)-\sigma_I(t)\rvert}{\sigma_I(t)}$ [%]	54,25	35,355	19,313	3,901	14,851	15,602	4,251	1,543	0,118	0,056	0,023	1,64E-3
	Ramp time $t_R = 2\ [s]$											
$\frac{\lvert\sigma(t)-\sigma_0(t)\rvert}{\sigma_0(t)}$ [%]	91,349	81,133	67,844	35,428	1,871	12,511	31,121	30,575	13,45	9,983	6,822	2,07
$\frac{\lvert\sigma(t)-\sigma_I(t)\rvert}{\sigma_I(t)}$ [%]	53,704	34,449	18,085	5,518	16,361	16,813	3,937	2,442	0,199	0,098	0,041	3,13E-3
	Ramp time $t_R = 5\ [s]$											
$\frac{\lvert\sigma(t)-\sigma_0(t)\rvert}{\sigma_0(t)}$ [%]	90,508	78,871	63,377	24,519	16,69	34,432	55,845	53,957	22,271	16,335	11,043	2,07
$\frac{\lvert\sigma(t)-\sigma_I(t)\rvert}{\sigma_I(t)}$ [%]	52,604	32,66	15,667	8,705	19,263	19,063	2,965	4,654	0,417	0,211	0,091	3,13E-3

time $t = 10t_R$ the differences are of 5% degree and they are lesser than 1,5% only at $t > 100t_R$. However, as the two curves approach each other at sufficiently long times greater than $100t_R$, the difference is not negligible as $t \leq 100t_R$. Thus, the „ten-times-rule", according to which the relaxation modulus is calculated as $G(t) = \sigma(t)/\varepsilon_0$ for $t \geq 10t_R$, may fail. The errors for the signal $\sigma_I(t)$ are not as big as for $\sigma_0(t)$, but the accuracy in $\sigma(t)$ approximation is also insufficient, especially in short time region $t < t_R$.

Thus, both using the ramp-test data as ideal step-strain data and calculating the relaxation modulus using the formula $G(t) = \sigma(t)/\varepsilon_0$, as well as even applying the known rules derived for ideal ramp test of ε_0/t_R loading rate, leads to unacceptable errors. What is especially important, these errors are unacceptably big in the time intervals of the greatest dynamics of the stress relaxation process. The presented results convincingly prove, that using the ramp test data $\sigma(t)$ as an ideal step-strain data $\sigma_0(t)$ and even as the ideal ramp test data $\sigma_I(t)$, in many cases fails to give satisfactory approximation of the relaxation modulus of the material.

NEW METHOD

In this paper the following assumption will be taken.

Assumption. The relaxation modulus $G(t)$ is double differentiable function such that:

$$G(t) \geq 0, -\frac{dG(t)}{dt} \geq 0, \frac{d^2G(t)}{dt^2} \geq 0 \quad for \quad t > 0. \tag{4}$$

The above assumption seems to be quite natural. In particular, it takes account of the course of the experimentally recorded relaxation modulus. This assumption, taken for example in [8, 20, 22], is satisfied by commonly used rheological models, such that Maxwell, Zener, KWW and Peleg models. Note also that from (4) it follows immediately that $G(t)$ strictly monotonically non-increasing (decreasing) continuous convex function.

On the basis of (1) and (2), taking into account that $\dot{\varepsilon}(\lambda) = 0$ for any $\lambda < 0$, the stress during the initial loading phase of the stress relaxation test in the interval of time $0 < t < t_R$ is described by the following equation:

$$\sigma(t) = \int_0^t G(t-\lambda)\left[a\left(\lambda - \frac{t_R}{2}\right)^2 + b\right]d\lambda,$$

which, taking into account the definitions of the parameters a and b, can be rewritten as:

$$\sigma(t) = \int_0^t \Phi(\lambda, t, t_R)d\lambda, \tag{5}$$

where the integrand:

$$\Phi(\lambda, t, t_R) = aG(t-\lambda)\lambda(\lambda - t_R), \tag{6}$$

is introduced for brevity. We approximate the integral (6) by respective quadrature. Unfortunately, no general methods can be recommended for numerical integration. The choice of the suitable method must be done on a case-by case basis, depending on the integrand function properties. Let us notice, that $\Phi(0, t, t_R) = 0$, and since $a < 0$, then for an arbitrary $0 < \lambda < t_R$ we have $\Phi(\lambda, t, t_R) > 0$; here $t_R > 0$, $0 < t \leq t_R$. The partial derivative is given by the expression:

$$\frac{\partial\Phi(\lambda,t,t_R)}{\partial\lambda} = -a\dot{G}(t-\lambda)\lambda(\lambda - t_R) + aG(t-\lambda)(2\lambda - t_R).$$

Thus, in view of the Assumption, it is clear that if $\lambda < t_R/2$, then $\partial\Phi(\lambda, t, t_R)/\partial\lambda > 0$ and $\partial\Phi(\lambda, t, t_R)/\partial\lambda \geq 0$ at $\lambda = t_R/2$ for any time variable $0 < t \leq t_R$. Hence, if $t \leq t_R/2$, that is $\lambda \leq t_R/2$, then the integrand $\Phi(\lambda, t, t_R)$ is monotonically increasing function of λ. The course of an exemplary integrand $\Phi(\lambda, t, t_R)$ as a function of the variable $0 \leq \lambda \leq t$ for KWW material (3), ramp-time $t_R = 1\ [s]$ and time instant $t = \frac{2}{5}t_R$ is show in Figure 3(a). Thus the simplest method of numerical integration, the midpoint rule, is appropriate for numerical approximation of the integral

(5) for $t \le t_R/2$. Moreover, it is known that for Volterra's equation of the first kind (1), the midpoint rule is numerically stable. By applying the middle-point rule to integral of the right-hand side of (5) we obtain:

$$\sigma(t) \approx aG\left(\frac{t}{2}\right)\frac{t}{2}\left(\frac{t}{2} - t_R\right)t,$$

whence, for $0 < t \le t_R/2$, the following expression follows immediately:

$$G^{(NM)}\left(\frac{t}{2}\right) = \frac{{t_R}^3}{3\varepsilon_0\left(t_R - \frac{t}{2}\right)t^2}\sigma(t).$$

It is easy to verify that the above implies for $0 < t \le t_R/4$ the rule:

$$G^{(NM)}(t) = \frac{{t_R}^3}{12\varepsilon_0(t_R - t)t^2}\sigma(2t). \tag{7}$$

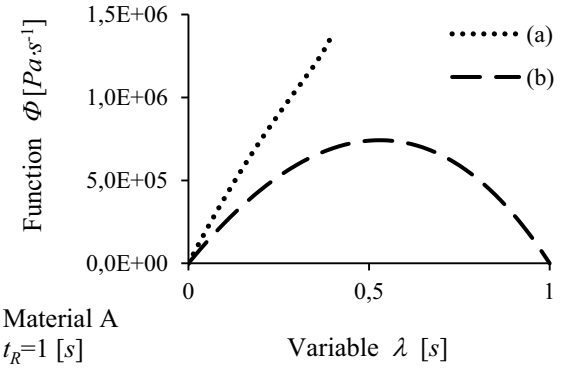

Fig. 3. The function $\Phi(\lambda, t, t_R)$ defined by equation (6) for material (3), $t_R = 1$ [s]: (a) $t = \frac{2}{5}t_R$, (b) $t = 2t_R$, $0 \le \lambda \le t$

We now wish to find the formula for relaxation modulus identification for the time interval $t > t_R/4$. To do this, note that on the basis of equations (1) and (2) in the second constant strain phase of the relaxation test, i.e. for $t > t_R$ the stress is given by the expression:

$$\sigma(t) = a\int_0^{t_R} G(t-\lambda)\lambda(\lambda - t_R)d\lambda, \tag{8}$$

or in equivalent form:

$$\sigma(t) = \int_0^{t_R} \Phi(\lambda, t, t_R)d\lambda, \tag{9}$$

where the integrand $\Phi(\lambda, t, t_R)$ is given by (6). Now, for an arbitrary $t > t_R$ also for the upper limit of integration in (9) we have $\Phi(t_R, t, t_R) = 0$. The function $\Phi(\lambda, t, t_R)$ is continuous and non-negative definite for any $\lambda \le t_R$ and, as it may be easily verified on the basis of the stationary point condition $\dot{G}(t-\lambda)\lambda(\lambda - t_R) = G(t-\lambda)(2\lambda - t_R)$ achieves the maximum for λ_{max} such that $t_R/2 < \lambda_{max} < t_R$. An example of the integrand function $\Phi(\lambda, t, t_R)$ for material (3), the time instant $t = 2t_R$ as a function of variable $0 \le \lambda \le t$ is illustrated in Figure 3(b). The paraboidal nature of this function makes reasonable the choice of Simpson's rule to evaluate the integral (8). We use both the simple three-point and the generalized five-point rule. Applying simple Simpson's rule we obtain the formula:

$$\sigma(t) \approx \frac{4}{3}aG\left(t - \frac{t_R}{2}\right)\frac{t_R}{2}\left(\frac{t_R}{2} - t_R\right)\frac{t_R}{2},$$

and whence:

$$\sigma(t) \approx \varepsilon_0 G\left(t - \frac{t_R}{2}\right), \tag{10}$$

which is the classical Zapas-Phillips formula. By dividing the finite time interval $[0, t_R]$ into four equal subintervals and applying the generalized Simpson's rule, after simple algebraic manipulations we have:

$$\sigma(t) \approx -\frac{a}{48}{t_R}^3\left[3G\left(t - \frac{t_R}{4}\right) + 3G\left(t - \frac{3t_R}{4}\right) + 2G\left(t - \frac{t_R}{2}\right)\right],$$

whence, in view of the definition of the parameter a, we finally obtain:

$$\sigma(t) \approx \frac{1}{8}\varepsilon_0\left[3G\left(t - \frac{t_R}{4}\right) + 3G\left(t - \frac{3t_R}{4}\right) + 2G\left(t - \frac{t_R}{2}\right)\right]. \tag{11}$$

Similar to (11), we have:

$$\sigma\left(t + \frac{t_R}{4}\right) \approx \frac{1}{8}\varepsilon_0\left[3G(t) + 3G\left(t - \frac{t_R}{2}\right) + 2G\left(t - \frac{t_R}{4}\right)\right]. \tag{12}$$

Combining the expressions (10), (11) and (12) treated as the equalities and applying the next equations, which follows from (10):

$$\sigma\left(t + \frac{t_R}{2}\right) = \varepsilon_0 G(t),$$

$$\sigma\left(t + \frac{t_R}{4}\right) = \varepsilon_0 G\left(t - \frac{t_R}{4}\right),$$

after simple algebraic manipulations we obtain:

$$G^{(NM)}\left(t - \frac{3t_R}{4}\right) = \frac{8}{3\varepsilon_0}\sigma(t) - \frac{7}{3\varepsilon_0}\sigma\left(t + \frac{t_R}{4}\right) + \frac{2}{3\varepsilon_0}\sigma\left(t + \frac{t_R}{2}\right), \tag{13}$$

which is the desired result. Thus we have achieved the formula for relaxation modulus approximate identification for $t > t_R/4$.

MONOTONICITY OF THE MODEL

It is assumed here that relaxation modulus is monotonically decreasing function. The monotonicity of the relaxation modulus model obtained by the proposed method is resolved by the two consecutive properties.

Property 1. If the Assumption is satisfied, the stress measurements are noise-free and for any $0 < t \le t_R/2$ the following inequality holds:

$$2\dot{G}(t) + \ddot{G}(t)t \le 0, \quad (14)$$

then the relaxation modulus model $G^{(NM)}(t)$ is monotonically decreasing function in the time interval $0 < t \le \frac{1}{4}t_R$.

Proof. On the basis of (7) we have:

$$\dot{G}^{(NM)}(t) = \frac{{t_R}^3}{12\varepsilon_0}\frac{2\dot{\sigma}(2t)(t_R-t)t-\sigma(2t)(2t_R-3t)}{(t_R-t)^2t^3}. \quad (15)$$

In order to examine the monotonicity of the model $G^{(NM)}(t)$ (7) it is enough to check the sign of the numerator of right-hand side of (15), i.e. of the expression:

$$\Psi(t) = 2\dot{\sigma}(2t)(t_R - t)t - \sigma(2t)(2t_R - 3t). \quad (16)$$

Taking into account (5) and (6), after suitable change of variables, we obtain:

$$\sigma(t) = a\int_0^t G(w)(t-w)(t-w-t_R)dw. \quad (17)$$

Whence, on the basis of known Leibnitz theorem concerning the differentiation of the integral with the limits depending on the variable we have:

$$\dot{\sigma}(t) = a\int_0^t G(w)(2t-2w-t_R)dw. \quad (18)$$

Using (17) and (18) we can rewrite the function $\Psi(t)$ (16) as follows:

$$\Psi(t) = a(4t^3 + 2tt_R^2 - 4t^2t_R)\psi_1(t) + a(7tt_R - \\ -8t^2 - 2t_R^2)\psi_2(t) + a(3t - 2t_R)\psi_3(t), \quad (19)$$

where: $\psi_1(t) = \int_0^{2t} G(w)dw$, $\psi_2(t) = \int_0^{2t} G(w)wdw$ and $\psi_3(t) = \int_0^{2t} G(w)w^2dw$.

By convexity of the function $G(t)$ we have for an arbitrary t and w:

$$G(w) \ge G(t) + \dot{G}(t)(w-t).$$

Hence, the next inequality follows:

$$\psi_1(t) \ge 2tG(t) + \dot{G}(t)\int_0^{2t}(w-t)dw = 2tG(t). \quad (20)$$

In order to estimate the integral $\psi_2(t)$ it is enough to note that under the Assumption the function $G(w)w$ is concave. Thus, for an arbitrary t and w such that $w \le 2t \le t_R/2$ the following inequality holds:

$$G(w)w \le G(t)t + \big[G(t) + \dot{G}(t)t\big](w-t), \quad (21)$$

on the basis of which, we obtain the upper bound:

$$\psi_2(t) \le 2t^2G(t) + \big[G(t) + \dot{G}(t)t\big]\int_0^{2t}(w-t)dw = \\ = 2t^2G(t)$$

and therefore, taking into account the inequality (20), we have:

$$\psi_2(t) \le t\psi_1(t). \quad (22)$$

In a similar fashion, using once more the inequality (21), it may be proved that the next inequality holds:

$$\psi_3(t) \le \frac{4}{3}t^2\psi_1(t). \quad (23)$$

Since the polynomial $(7tt_R - 8t^2 - 2t_R^2)$ of variable t is negative definite for any $0 < t \le t_R/4$ and the expression $4t^3 + 2tt_R^2 - 4t^2t_R = 2t[t^2 + (t-t_R)^2]$ is positive definite for any $t > 0$, taking into account that the parameter $a < 0$, by combining (19), (22) and (23) we obtain for an arbitrary $0 < t \le t_R/4$ the following estimation:

$$\Psi(t) \le \frac{1}{3}at^2t_R\psi_1(t) < 0.$$

Which finally concludes the proof.

Remark 1. It is easy to check that for KWW model (3) the condition (14) takes the form $(t/\tau)^\beta - 1 \le 1/\beta$, therefore is satisfied for every $0 < t \le t_R/2$, whenever $(t_R/2\tau)^\beta \le 1/\beta + 1$. In particular, if $\beta = 0{,}5$ (see Example), then the condition (14) means that $t_R \le 18\tau$, and is not difficult to satisfy.

Remark 2. For Maxwell model $G(t) = G_0e^{-t/\tau}$ we have $\beta = 1$. Thus, the condition (14) is satisfied, whenever $t_R \le 4\tau$.

Having known even rough estimation of the relaxation time of the material we can choose without difficulties the ramp-time t_R so as to satisfy the condition (14).

Property 2. If the Assumption is satisfied and the stress measurements are noise-free, then the relaxation modulus model $G^{(NM)}(t)$ is monotonically decreasing function in the time interval $\frac{1}{4}t_R < t \le T - \frac{5}{4}t_R$.

Proof. Let us first examine the stress derivative $\dot{\sigma}(t)$ for $t > t_R$. On differentiating formula (8) we arrive at the following expression:

$$\dot{\sigma}(t) = a\int_0^{t_R}\dot{G}(t-\lambda)\lambda(\lambda - t_R)d\lambda$$

and then, on differentiating equation (8) with respect to t twice, we obtain:

$$\ddot{\sigma}(t) = a\int_0^{t_R}\ddot{G}(t-\lambda)\lambda(\lambda - t_R)d\lambda.$$

Since the parameter $a < 0$ and the ramp-time $t_R > 0$, in view of the Assumption, the above implies the following inequalities: $\dot{\sigma}(t) < 0$ and $\ddot{\sigma}(t) > 0$. Thus, for any $t > t_R$ the stress derivative $\dot{\sigma}(t)$ is negative definite monotonically increasing function. Since on the basis of (13):

$$\dot{G}^{(NM)}\left(t-\frac{3t_R}{4}\right)=\frac{8}{3\varepsilon_0}\dot{\sigma}(t)-\frac{7}{3\varepsilon_0}\dot{\sigma}\left(t+\frac{t_R}{4}\right)+$$
$$+\frac{2}{3\varepsilon_0}\dot{\sigma}\left(t+\frac{t_R}{2}\right),$$

the above implies:

$$\dot{G}^{(NM)}\left(t-\frac{3t_R}{4}\right)<\frac{8}{3\varepsilon_0}\dot{\sigma}\left(t+\frac{t_R}{4}\right)-\frac{7}{3\varepsilon_0}\dot{\sigma}\left(t+\frac{t_R}{4}\right)+$$
$$+\frac{2}{3\varepsilon_0}\dot{\sigma}\left(t+\frac{t_R}{2}\right)<0,$$

and completes the proof.

FINAL REMARKS

1. Based on the mathematical properties of the considered problem of the relaxation modulus determination using the stress measurements from non-ideal ramp test, new method for approximate identification of relaxation modulus is derived for the case when the time-variable strain in the loading phase of the relaxation test is described by the time polynomial of the third order.
2. It is proved, under quite typical assumptions concerning both the viscoelastic material and the experiment, that for noise-free stress measurements determined model of the relaxation modulus is monotonically decreasing time-function with at most one discontinuity point.
3. For discrete-time experiment the proposed method can be used to develop a new fast identification scheme, in which the approximations of the relaxation modulus in successive time instants are computed using at most three measurements of the stress in appropriately chosen sampling points. Numerical studies of the algorithm, in particular the model error analysis for ideal and noise corrupted stress measurements, is the subject of the forthcoming paper [25].

REFERENCES

1. **Cho J.R., Song J.I., 2007:** Swaging process of power steering hose: Its finite element analysis considering the stress relaxation. Journal of Materials Processing Technology 187–188, 497–501.
2. **Choi S., Cha S.W., Oh B.H., 2010:** Identification of viscoelastic behavior for early-age concrete based on measured strain and stress histories. Materials and Structures, 43, 1161–1175.
3. **Cui T., Chao Y.J., Van Zee J.W., 2012:** Stress relaxation behavior of EPDM seals in polymer electrolyte membrane fuel cell environment. International Journal of Hydrogen Energy, 37, 13478–13483.
4. **Daphalapurkar N.P., Dai C., Gan R.Z., Lu H., 2009:** Characterization of the linearly viscoelastic behavior of human tympanic membrane by nanoindentation. Journal of the Mechanical Behavior of Biomedical Materials, 2, 82–92.
5. **Eitelberger J., Bader T.K., De Borst K., Jäger A., 2012:** Multiscale prediction of viscoelastic properties of softwood under constant climatic conditions. Computational Materials Science, 55, 303–312.
6. **Flory A., McKenna G.B., 2004:** Finite step rate corrections in stress relaxation experiments: a comparison of two methods. Mechanics of Time-Dependent Materials, 8, 17–37.
7. **Gul' Yu.P., Ivchenko A.V., Ambrazhei M.Yu., Tishchenko S.V., 2011:** Influence of Cold Deformation and Aging on the Relaxation of Strengthened Low-Carbon Steel. Stal, 10, 44–47.
8. **Hanyga A., 2005:** Viscous dissipation and completely monotonic relaxation moduli. Rheological Acta, 44, 614–621.
9. **Kawada Y., Nagahama H., Hara H., 2006:** Irreversible thermodynamic and viscoelastic model for power-law relaxation and attenuation of rocks. Tectonophysics, 427, 255–263.
10. **Knauss W.G., Zhao J., 2007:** Improved relaxation time coverage in ramp-strain histories. Mechanics of Time-Dependent Materials, 11(3–4), 199–216.
11. **Kontopoulou M. (Ed) 2012.** Applied Polymer Rheology: Polymeric Fluids with Industrial Applications. John Wiley & Sons, New Jersey.
12. **Kozub Y., 2012:** Deformation of rubber-metal vibration and seismic isolators. TEKA Commission of Motorization and Energetics in Agriculture, 12(4), 96–100.
13. **Lee S., Knauss W.G., 2000:** A note on the determination of relaxation and creep data from ramp tests. Mechanics of Time-Dependent Materials, 4, 1–7.
14. **Malkin A.Y., Isayev A.I., 2011:** Rheology: Concepts, Methods and Applications. ChemTec Publishing, Toronto.
15. **Mirani R.D., Pratt J., Iyer P., Madihally S.V., 2009:** The stress relaxation characteristics of composite matrices etched to produce nanoscale surface features. Biomaterials, 30, 703–710.
16. **Pilipenko V., 2012:** Mathematical model-building of rheological and thermo dynamical processes in modified concrete mix at vibro impact compact method of compression. TEKA Commission of Motorization and Energetics in Agriculture, 12(4), 204–209.
17. **Rault J., 2011:** Relaxation of glasses: The Kohlrausch exponent. Journal of Non-Crystalline Solids, 357, 339–345.
18. **Saksa T., Banichuk N., Jeronen J., Kurki M., Tuovinen T., 2012:** Dynamic analysis for axially moving viscoelastic panels. International Journal of Solids and Structures, 49, 3355–3366.
19. **Sorvari J., Malinen M., 2006:** Determination of the relaxation modulus of a linearly viscoelastic material. Mechanics of Time-Dependent Materials, 10, 125–133.
20. **Sorvari J., Malinen M., 2007:** On the direct estimation of creep and relaxation functions. Mechanics of Time-Dependent Materials, 11, 143–157.
21. **Sorvari J., Malinen M., Hämäläinen J., 2006:** Finite ramp time correction method for non-linear viscoelastic material model. International Journal of Non-Linear Mechanics, 41, 1058–1064.
22. **Stankiewicz A., 2010:** On the existence and uniqueness of the relaxation spectrum of viscoelastic materials. Part

I: The main theorem. TEKA Commission of Motorization and Power Industry in Agriculture, 10, 379–387.
23. **Stankiewicz A., 2012:** Determination of the relaxation modulus on the basis of the ramp-test stress data. Inżynieria Rolnicza, 16(4), 401–409 [in Polish].
24. **Stankiewicz A., 2012:** Algorithm of relaxation modulus identification using stress measurements from the real test of relaxation. Inżynieria Rolnicza, 16(4), 389–399 [in Polish].
25. **Stankiewicz A., 2013:** An algorithm for approximate identification of relaxation modulus of viscoelastic materials from non-ideal ramp-test histories, TEKA Commission of Motorization and Energetics in Agriculture (submitted for publication).
26. **Tscharnuter D., Jerabek M., Major·Z., Lang R.W., 2011:** On the determination of the relaxation modulus of PP compounds from arbitrary strain histories. Mechanics of Time-Dependent Materials, 15, 1–14.
27. **Wang S., Qi J., Yao X., 2011:** Stress relaxation characteristics of warm frozen clay under triaxial conditions. Cold Regions Science and Technology, 69, 112–117.
28. **Zapas L.J., Craft T., 1965:** Correlation of large longitudinal deformations with different strain histories. Journal of Research of the National Bureau of Standards, A69(6), 541–546.

IDENTYFIKACJA MODUŁU RELAKSACJI MATERIAŁÓW LEPKOSPRĘŻYSTYCH NA PODSTAWIE RZECZYWISTEGO TESTU RELAKSACJI NAPRĘŻEŃ O NIELINIOWYM ODKSZTAŁCENIU WSTĘPNYM. PROBLEM I METODA

Streszczenie. W pracy rozważa sie problem wyznaczania modułu relaksacji materiałów liniowo lepkosprężystych na podstawie pomiarów naprężenia zgromadzonych w rzeczywistym teście relaksacji naprężeń o nieliniowym odkształcaniu próbki w fazie wstępnej testu opisanym wielomianem czasu trzeciego stopnia. Celem pracy jest opracowanie metody przybliżonej identyfikacji modułu relaksacji na podstawie danych z takiego testu. Bazując na regule punktu środkowego oraz uogólnionej formule Simpsona opracowano metodę identyfikacji, w której przybliżenie modułu relaksacji w dowolnej chwili czasu wyznaczane jest na podstawie pomiarów naprężenia w co najwyżej trzech wybranych punktach jego próbkowania. Zbadano, przy bardzo ogólnych założeniach dotyczących modułu relaksacji badanego materiału oraz eksperymentu, własności wyznaczonego modelu. Opracowana metoda jest punktem wyjścia dla syntezy szybkiego algorytmu identyfikacji modułu relaksacji podczas trwania eksperymentu.

Słowa kluczowe: test relaksacji naprężeń, skończony czas odkształcania, moduł relaksacji, algorytm identyfikacji.

TEKA. COMMISSION OF MOTORIZATION AND ENERGETICS IN AGRICULTURE – 2013, Vol. 13, No. 1, 185–190

Alternator diagnostics by means of an oscilloscope and infrared radiation – comparison of methods

Sebastian Styła, Katarzyna Wróbel, Artur Boguta

Department of Computer and Electrical Engineering, Lublin University of Technology,
20-618 Lublin, 38a Nadbystrzycka Street; e-mail: s.styla@pollub.pl

Received January 19.2013; accepted March 14.2013

Summary. The article presents an innovative method for testing of the technical condition of an alternator by means of IR camera. Infrared radiation method has been compared with conventional methods, their advantages and disadvantages have been presented herein. ThermaCAM E45 camera manufactured by FLIR has been used for thermovision tests. The tests have been processed by means of FLIR QuickReport software. Furthermore, the article describes the methods of thermovision tests accuracy improvement in order to enable a quick and reliable diagnosis.
Key words: alternative current generator, alternator, diagnostics, thermovision camera, electric power supply circuit.

INTRODUCTION

Alternator is defined as an alternative current generator with electromagnetic or magneto-electric excitation (with permanent magnets) [4]. Its purpose is to supply electrical energy to the battery of motor vehicle and its electric system in the course of combustion engine operation. The power generated by alternator is sufficiently high already at low speeds. It is particularly important in case of motor vehicle operations in idling mode corresponding to about 40% of total operation time in urban traffic [2]. Moreover, the dimensions of alternative current generator are small, its speed range is wide and power-to-mass ratio is high. Currently, the research projects in the scope of design and operational parameters of contemporary alternators are focused on: the reduction of their dimensions and mass, optimization of excitation and cooling circuit and noise reduction [14]. There are many detailed descriptions of design solutions of alternators contained in literature [1, 2, 3]. However, the research methods are significantly facilitated because their operating principle is similar. The modern diagnostic methods most often make it necessary to remove the device from the motor vehicle extending the time required to localize a damage and constituting potential reason of mechanical damages.

ALTERNATOR DAMAGES

The maintenance free operation of alternators application is an argument supporting their application. The scope of periodical maintenance encompasses only the following checks: fastening, cleanness and quality of the conductors and V-belt tension. The alternators damages are divided into mechanical and electrical damages. The first group encompasses the following types of damages: excessively worn brushes, bearings clearances, abrasion of slip rings etc. and are found on the basis of organoleptic tests or as a result of partial disassembly of generator elements. However, further operation of alternator is impossible in case of electric damages. A preliminary evaluation is possible without the necessity to dismantle the unit from the car, but its dismantling is required in order to find a defective element.

In case of an inefficiency, its symptoms can be detected on the basis of indications of dashboard control light (Tab. 1). It is the first diagnostic information indicating the

Table 1. Most frequently occurring symptoms of alternator damages and their reasons

Item	Symptoms	Possible reasons
1.	Control light does not light after the ignition is turned on, with engine not operating	– damaged light – damaged ignition switch – blown fuse – discharged battery – short – circuit of positive diodes

Item	Symptoms	Possible reasons
2.	Low control light after the ignition is turned on, with engine not operating	– discontinuity in rotor winding – worn brushes
3.	Control light does not go off even when ignition switch is turned off	– short – circuit of positive diodes
4.	Control light flashing	– weak tension of V-belt – dirty brushes
5.	Control light does not go off while the engine speed is increased	– damaged regulator – discontinuity or short – circuit in rotor winding of excitation diodes – short – circuit of negative diodes
6.	Low control light with engine operating	– damaged regulator – short – circuit in stator winding – discontinuity in bridge diode – high resistance on contacts – loose conductors

alternator inefficiency. However, no inefficiency is indicated in case of some types of damages, despite the lack of battery charging, e.g. a discontinuity or short – circuit in the regulator circuit of inter-phase short – circuit in stator windings.

CONVENTIONAL TESTS

A quick and reliable diagnosis for damaged machinery is the assumption of primary importance for the creation of new diagnostic procedures for individual equipment elements. As a result of developing technical possibilities, the new methods associated with diagnostic tests quality are created by research centres [9, 10, 11, 17, 20, 21], which directly contributes to repair costs of the operated equipment.

The following checks should be completed in order to enable precise diagnosis for an alternator [19]:
– current efficiency,
– excitation current intensity,
– rectifying diodes,
– regulated voltage,
– alternator leakage current.

Universal meters or oscilloscopes are frequently used in such type of tests. Particular care should be taken in order to prevent any damage of regulator and rectifying diodes as a result of unintended short – circuit or reversal of polarity terminals of the conductors in course of test or when dismantling the device from motor vehicle. The algorithm to be followed in the course of such checks is illustrated in Figure No1.

The rectifying system [15, 16] is the most sensitive part of alternators. The rectifying diodes can be subject to damages occurring mainly when exceeding the rated current values (in conducting direction) and reverse voltage (in reversed direction). A discontinuity or short – circuit, even in one diode, contributes to faster wearing of efficient diodes of the bridge and consequently leads to inefficiency of the whole rectifying system.

The possible reasons of damages in the rectifying system as well as in the electrical systems of the generator (windings) are: reversal of battery polarity or battery disconnection in course of alternator operation, disconnection of B+ (positive) terminal of alternator from the motor vehicle electric system in course of its operation, high environment temperature in course of alternator operation under high load. Furthermore, the mechanical damages are possible in course of repair.

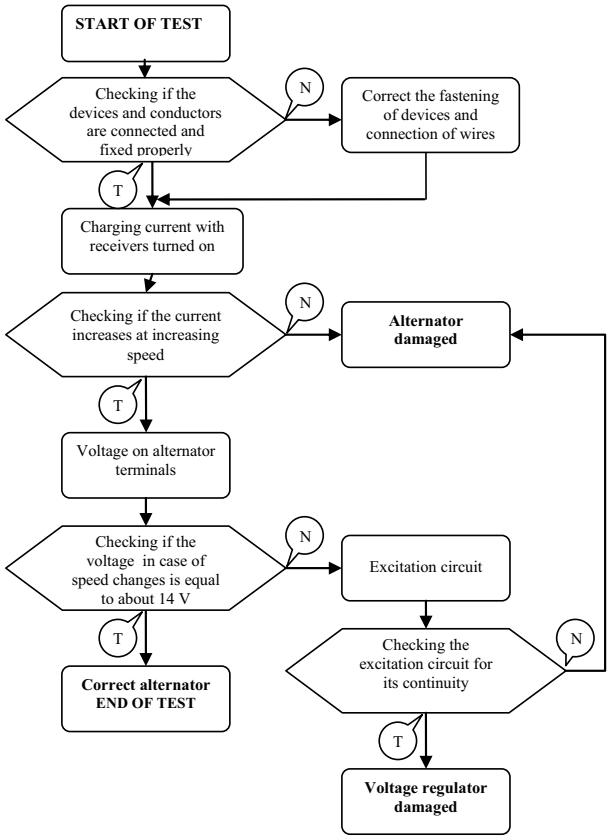

Fig. 1. Alternator checking status algorithm

Oscilloscope is most frequently used for testing of alternator technical condition in workshop practice. The testing consists in comparison of obtained curves with standard oscillograms [15, 16]. Figure 2 illustrates a correct curve occurring between B+ (positive) terminal of alternator and the frame and the curves for typical alternator damages are illustrated in Figure 3a, 3b, 3c, 3d.

The damage illustrated in Figure 3a is caused by the excitation winding discontinuity. However, the identification of this type of inefficiencies is problematic because similar curves occur in case of damages of all negative or positive diodes.

Figure 3c illustrates the curve caused by a damage (discontinuity) in one negative or positive diode and Figure 3d illustrates a curve caused by a damage in two diodes. However, in such cases it is possible to indicate a specific diode causing the inefficiency after the removal of alternator and additional tests.

The thermovision method proposed in the present article makes it possible to eliminate the aforesaid problems. Thanks to their advantages i.e. versatility and possibility of contactless temperature measurement, thermovision tests are perfectly suitable for the analysis of elements generating certain amounts of thermal energy. Therefore, it is possible to indicate the location of damage or an element causing the device inefficiency, i.e. an alternating current generator.

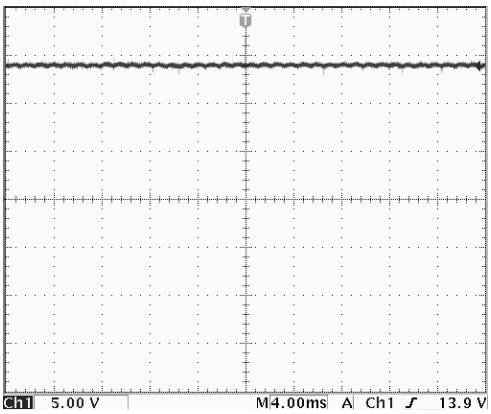

Fig. 2. Voltage oscillogram for an efficient alternator

THERMOVISION TESTS

The tests were carried out for the alternator parts which can be damaged in course of their routine operation as a result of ageing of elements or mechanical and electrical processes described above. The tests were carried out by means of ThermaCAM E45 camera manufactured by FLIR. The following electrical parameters of the alternator were applied in course of tests: U_{B+}=14,8 V, n=3000÷3500 RPM, I_{load}=10 A. The following criteria were followed in order to eliminate "the method errors" of thermovision measurements [5, 6, 7, 8, 12, 13, 18, 22, 23] significantly affecting the obtained results: emission factor was determined individually for each alternator (material) element under test, the impact of external IR radiation (lighting) sources was eliminated, the tests have been performed along alternator axis from the side of rectifying bridge (normal direction).

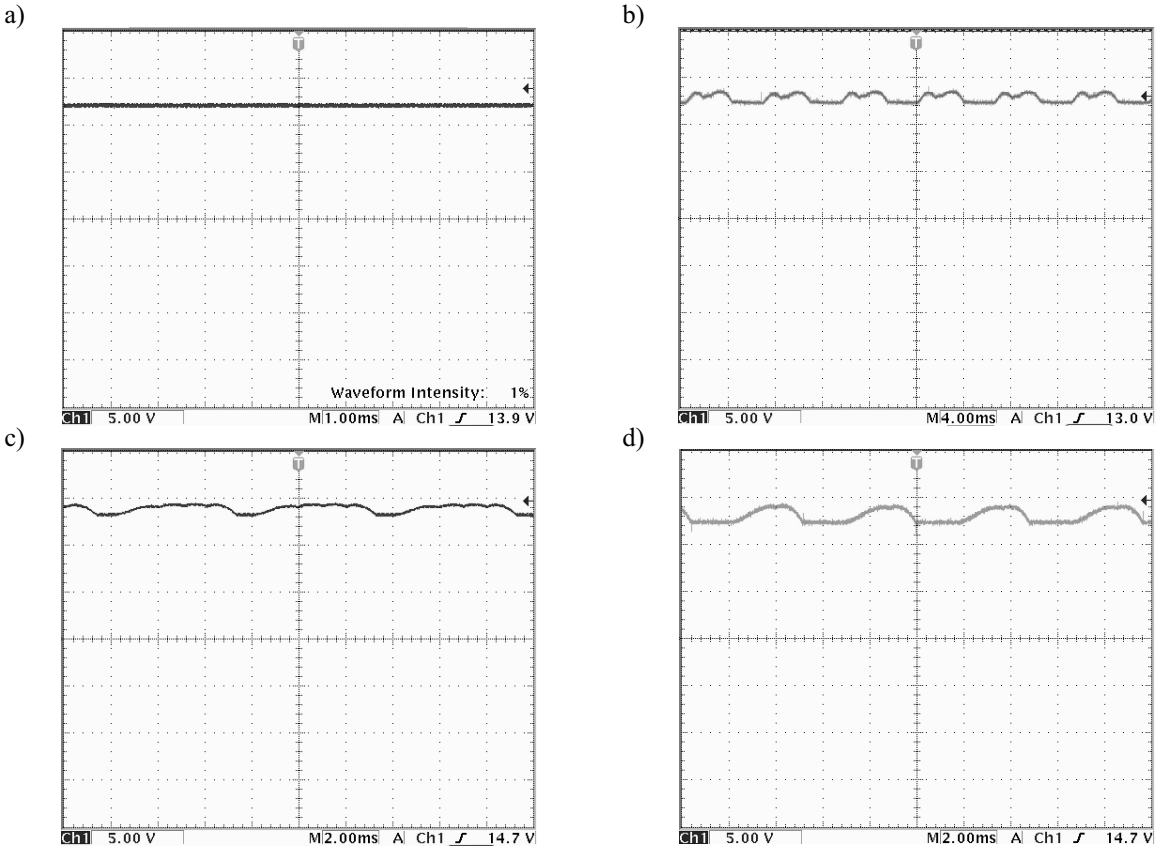

Fig. 3. Voltage oscillograms for a damaged alternator: a) excitation winding discontinuity, b) short – circuit in one bridge diode, c) discontinuity in one negative diode of the bridge, d) discontinuity in two negative diodes of the bridge

Figure 4 illustrates the thermograms obtained in the course of tests. As a result of discontinuity in magnetizing circuit located on the alternator rotor, no electromotive force is generated in the stator (armature). There is no current flow through diodes, therefore they are not heated (Fig. 4b). The temperature of brush holder (No 7, Fig. 4b) should be determined in order to eliminate the diodes damage causing similar diagnostic symptoms. This temperature should be similar to the temperature of the whole alternator. Thermovivion method makes it also possible to evaluate the brushes condition without necessity of their dismantling. When the alternator brushes are worn, their working temperature is reduced due to lack of "brushes – slip ring" contact and reduced value of current flowing through them.

In case of discontinuity in diode (No 6, Fig. 4c), thermovision measurements explicitly indicate the location of inefficiency. Moreover, by means of an appropriate computer assisted analysis, it is possible to determine if a specified diode will be not damaged soon. Table 2 represents the temperature differences for three (3) negative diodes, where: -4- stands for an efficient – brand new diode, -5- an efficient diode with wearing symptoms, -6- damaged diode.

Tab. 2. Temperature distribution in course of operation for individual negative diodes in rectifying bridge

Item	Time	Diode temperature -4-	Diode temperature -5-	Diode temperature -6-
-	(s)	(°C)	(°C)	(°C)
1	60	28,5	28,3	28
2	120	35,4	33,2	29,5
3	180	38,7	36,3	32,8
4	240	40,8	38	34,7
5	300	43	40,2	36,9
6	360	44,7	42,1	38,8
7	420	45,4	42,7	39,6
8	480	46,4	43,8	40,5
9	540	47,5	44,8	41,8
10	600	48,1	45,6	42,3
11	660	48,6	45,8	42,6
12	720	48,9	46,2	43
13	780	49,5	46,9	43,7
14	840	49	45,9	42,9
15	900	49,1	45,9	43

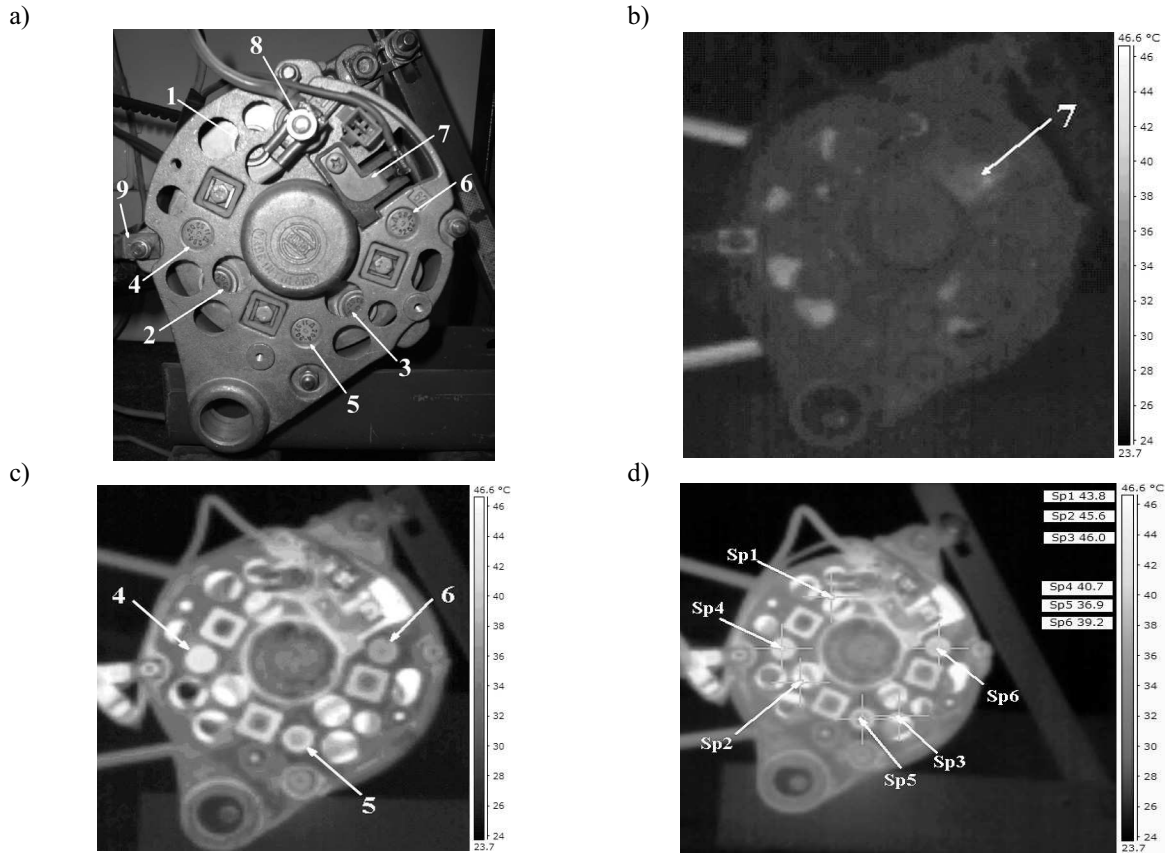

Fig.4. Alternator: a) object of tests, b) thermogram with excitation winding discontinuity, c) thermogram with discontinuity in one negative diode, d) thermogram of an efficient alternator; 1, 2, 3 – positive diodes, 4, 5, 6 – negative diodes, 7 – brush holder, 8 – positive terminal B+, 9 – frame terminal, Sp1-Sp6 – temperatures of main diodes

The difference of temperature achieved in course of operation of an efficient and inefficient diode is used as the criterion in order to qualify the diode as damaged (in course of thermovision measurements). From experimental test it appears that there is no difference in temperatures of efficient diodes exceeding 5%. In case of a damaged diode, regardless of its incorrect operation, the achieved temperature is higher than its value resulting from theoretical considerations as a result of heat exchange in the form of heat conduction and convection between damaged diode and other structural elements of alternator. Nevertheless, the difference of temperature between an efficient and inefficient diode (with discontinuity) is equal to 10% up to 20%. Therefore, it is possible to qualify an alternator diode as damaged.

CONCLUSIONS

Thermovision technique method presented therein can be used as the method supplementing the diagnostics in the scope of alternator technical condition and substituting conventional methods in certain cases. Its advantage consists in the possibility of an objective, non – invasive and contactless measurement. It is decisive criterion for the use of considered diagnostic method owing to difficult access to the generator or to its electric terminals (in some vehicles models). The conducted tests demonstrated that thermovision technique makes it possible to precisely indicate the location of an alternator element and to determine its technical parameters in an easy and quick way. Furthermore, using thorough computer aided analysis of the obtained results, it is possible to create database which could be useful in case of building the new design solutions for alternative current generators, selection of new materials, and consequently contributing to the increase of reliability and efficiency of alternators installed in motor vehicles.

REFERENCES

1. **Dyszy J., 2011:** Techniczne innowacje, Auto Moto Serwis, 6 (2011) , 44–47.
2. **Dziubiński M., Ocioszyński J., Walusiak S., 1999:** Elektrotechnika i Elektronika Samochodowa, WUPL, Lublin.
3. **Herner A., Riehl H. J., 2010:** Elektrotechnika i elektronika w pojazdach samochodowych, WKŁ, Warszawa.
4. **Koziej E., 1986:** Maszyny elektryczne pojazdów samochodowych. WNT, Warszawa.
5. **Madura H., 2004:** Pomiary termowizyjne w praktyce, PAK, Warszawa.
6. **Maldague X., 1993:** Non destructive evaluation of materials by infrared thermography, Springer-Verlag, London.
7. **Minkina W., 2004:** Pomiary termowizyjne – przyrządy i metody, Politechnika Częstochowska, Częstochowa.
8. **Minkina W. A., Rutkowski P., Wild W. A., 2000:** Podstawy pomiarów termowizyjnych. Część II – Współczesne rozwiązania systemów termowizyjnych, błędy metody, PAK 1/2000, Warszawa, 11–14.
9. **Plizga K., 2008:** An evaluation of the technical state of a starter using the hall effect – part I, TEKA Komisji Motoryzacyjnej i Energetyki Rolnictwa PAN o/Lublin, tom VIII ‘2008, 185–196.
10. **Plizga K., 2009:** An evaluation of the technical state of a starter using the hall effect – part II, TEKA Komisji Motoryzacyjnej i Energetyki Rolnictwa PAN o/Lublin, tom IX ‘2009, 244–250.
11. **Plizga K., 2009:** Diagnozowanie stanu rozruszników samochodowych, MOTROL: Motoryzacja i Energetyka Rolnictwa PAN o/Lublin, tom 11, 168–174.
12. **Poloszyk S., Różański L., 1996:** Thermographic Diagnosis Station of Machines, 7th International DAAAM Symposium, Wienna, 351–352.
13. **Poloszyk S., Różański L., 2000:** Termowizyjna diagnostyka maszyn technologicznych, PAK 1/2000, Warszawa, 15–18.
14. **Sęk A., Bogusz R., 2011:** Kryteria projektowania alternatorów samochodowych, Przegląd Elektrotechniczny, 3 (2011), 243–248.
15. **Smolak Ł., Lipiec R., 2006:** Oscyloskop w diagnostyce alternatora cz. 1, Auto Moto Serwis, 10 (2006), 26–27.
16. **Smolak Ł., Lipiec R., 2006:** Oscyloskop w diagnostyce alternatora cz. 2, Auto Moto Serwis, 11 (2006), 20–21.
17. **Styła S., 2012:** Diagnostyka rozrusznika samochodowego w warunkach laboratoryjnych. MOTROL: Motoryzacja i Energetyka Rolnictwa PAN o/Lublin, Tom 14, No. 5, 129–133.
18. **Styła S., Pietrzyk W., 2011:** The identification of operational failures of the heating, ventilation and air-conditioning circuit in the car by means of thermovision methods. TEKA Komisji Motoryzacyjnej i Energetyki Rolnictwa PAN o/Lublin, tom XI ‘2011, 354–362.
19. **Trzeciak K., 2010:** Diagnostyka samochodów osobowych, WKŁ, Warszawa.
20. **Tylicki H., Wilczarska J., Bartol M., 2006:** Metodyka diagnozowania stanu maszyn, MOTROL: Motoryzacja i Energetyka Rolnictwa PAN o/Lublin, tom 8, 230–239.
21. **Walusiak S., Pietrzyk W., Sumorek A., 2003:** Ocena diagnostyczna stanu technicznego pojazdów samochodowych w wybranej stacji diagnostycznej, MOTROL: Motoryzacja i Energetyka Rolnictwa PAN o/Lublin, tom 5, 219–226.
22. **Wesołowski M., Niedbała R., Kucharski D., 2009:** Wiarygodność termowizyjnych technik pomiaru temperatury, Przegląd Elektrotechniczny, 12 (2009), 208–211.
23. **Więcek B., Lis M., Zwolenik S., Danych R., Wajman T., 2002:** Zastosowanie termowizji w badaniach nieniszczących i w mikroelektronice, PAK 11/2002, Warszawa, 8–12.

DIAGNOSTYKA ALTERNATORA Z WYKORZYSTANIEM OSCYLOSKOPU I PROMIENIOWANIA PODCZERWONEGO – PORÓWNANIE METOD

Streszczenie. Artykuł przedstawia nowatorską metodę badania stanu technicznego alternatora z wykorzystaniem kamery na podczerwień. Porównano w nim przedstawioną metodę z wykorzystaniem promieniowania podczerwonego z metodami konwencjonalnymi przedstawiając ich zalety i wady. Do badań termowizyjnych wykorzystano kamerę termowizyjną ThermaCAM E45 firmy FLIR. Badania zostały opracowane z wykorzystaniem oprogramowania komputerowego FLIR QuickReport. W artykule przedstawiono ponadto sposoby poprawy dokładności badań termowizyjnych w celu wykonania szybkiej i pewnej diagnozy.

Słowa kluczowe: prądnica prądu przemiennego, alternator, diagnostyka alternatora, kamera termowizyjna, obwód zasilania w energię elektryczną.

Investigations into the influence of functional parameters of a heat pump on its thermal efficiency

Mariusz Szreder

Warsaw University of Technology
Faculty of Civil Engineering, Mechanics and Petrochemistry
Department of Mechanical Systems Engineering and Automation
Address: Al. Jachowicza 2/4, 09-402 Płock, e-mail: szreder@pw.plock.pl

Received December 19.2012; accepted March 14.2013

Summary. The paper presents some issues related to the selection criteria of a heat pump based on the published research results. The experimental research conducted on a single family house with a floor heating allows an assessment of the influence of individual functional parameters on the heat pump energy performance coefficient.
Key words: ground source heat pump, vertical collector, scroll compressor, evaporator, condenser, lower heat source, coefficient of performance.

1. BACKGROUND INFORMATION

Heat pumps have practically been used in Europe for 25 years now but recently we have been observing a rapid growth in their sales. This partly results from the requirements set by the EU directives whose main aim is to increase the use of RSE in the final energy consumption to 15% in 2020.

According to the data obtained from the Polish Organization for the Development of Heat Pumps (PORT PC) we can state that in 2011 in Poland approximately 10 000 heat pump units were sold [18, 23].

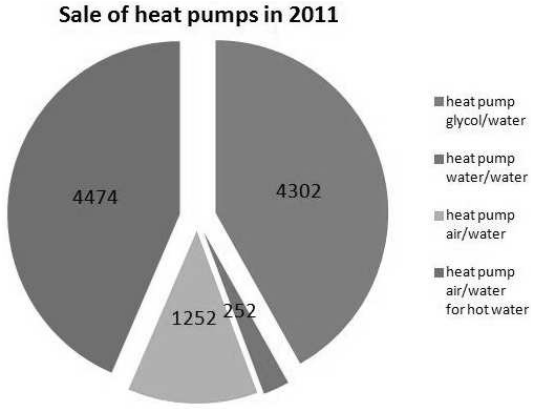

Fig. 1. Statistical data related to the heat pumps installed in 2011

The technology of geothermics, known and developed in the world for over 50 years has gained an increased interest in Poland, too. Unfortunately, it still is a consequence of the efforts of the manufacturers and fans of this type of technology who try to show the invaluable advantages this technology has despite relatively high investment costs. A group of satisfied users also contributes to the growing popularity.

Out of all the installed heat pumps the main share constitute the ground source heat pumps that, due to the cold climate, are preferred by Polish users. In Poland in the sector of ground source heat pumps (41-43% in the years 2008-2009) the most frequently installed are the ones of the power output of up to 10 kW. They are fitted in new single-family houses of the usable area of 150 ÷ 200 m². Such houses constitute 80% of all newly built houses. In recent years a growth in the demand for high power heat pumps has also been observed for the purposes of heating of multifamily houses, office buildings, hotels and buildings undergoing modernizations [7,16].

A dynamically evolving market is the market of air heat pumps used exclusively for the production of hot water. It is mainly caused by their low price and simplicity of fitting. Because of their function they most often compete with solar thermal collectors. Compared to solar thermal systems heat pumps are more cost efficient, capable of producing hot water throughout the year and provide additional ventilation, dehumidification and air conditioning of rooms.

2. CHARACTERISTICS OF THE RESEARCH STAND

INTRODUCTION

At the Institute of Mechanical Engineering of Warsaw University of Technology in Płock for some years now works have been continued in the area of renewable sources of

energy (RSE). Due to a constant decrease of the costs of the installation of renewable sources of energy (RSE) in recent years the interest in these systems has grown significantly. In the current energy-related situation the development of RSE as complementary sources of energy to traditional solutions is a must. To this end, the university team has undertaken to optimize the operating processes of mechanical systems in terms of selected RSE installations. An idea was created to explore fundamental relations between the heat pump parameters in the aspect of minimization of energy consumption. To this end the authors designed and developed a research stand of a ground source heat pump and vertical collectors.

CHARACTERISTICS OF THE RESEARCH STAND

The heating system utilizing a ground source heat pump (brine/water) was installed in a two story single-family house of the total area of **156 m²**. Minding the application of the heat pump a low temperature floor heating system was installed on both stories. The heating circuits on the ground and first floors were supplied independently with circuit pumps, which allowed an easy control of the supply of the heating power to the rooms on the ground and fist floors.

In the blueprint documentation of the building an annual demand for energy of **E=16400 kWh/year** is given. Assuming an average operating time of the heat pump on the level of **1800 h** we can obtain an estimate thermal load of the building on the level of **9.1 kW** [14. 24].

CONSTRUCTION OF THE RESEARCH STAND

The realization of the adopted scope of experimental research and the fulfillment of the basic guidelines as to the construction of the research stand practically excluded serially manufactured heat pumps. The authors decided to build a heat pump basing on generally available construction subassemblies of renowned manufacturers in the refrigeration industry.

It was assumed that the refrigerant would be the widely applied CFC free **R407C.** In the condenser and evaporator plate heat exchangers by WTK were applied and the supplier of the control systems was Danfoss.

Tab. 1. An excerpt from the catalogue data for the C-SBN263H8A compressor

C-SBN263H8A 400V/3f/50Hz / 400В/3ф/50Гц						R407C
Temperatura skraplania / Condensing temperature / Температура конденсации [°C]	Temperatura odparowania / Evaporating temperature / Температура кипения [°C]	-10	-5	0	+5	+10
30	Wydajność / Capacity / Производств, [W] [Вт]	6638	8081	9846	12005	-
	Moc / Power consumption / Потр.мощн. [W] [Вт]	1889	1890	1885	1873	-
	Pobór prądu / Rated current / Потр. ток, [A]	3,7	3,8	3,8	3,8	-
	Współczynnik efektywności / COP / КПД	3,51	4,28	5,22	6,41	-
35	Wydajność / Capacity / Производств, [W] [Вт]	6127	7473	9123	11146	13614
	Moc / Power consumption / Потр.мощн. [W] [Вт]	2079	2080	2076	2064	2044
	Pobór prądu / Rated current / Потр. ток, [A]	4,0	4,1	4,2	4,2	4,2
	Współczynnik efektywności / COP / КПД	2,95	3,59	4,39	5,40	6,66
40	Wydajność / Capacity / Производств, [W] [Вт]	5645	6901	8442	10338	12660
	Moc / Power consumption / Потр.мощн. [W] [Вт]	2310	2313	2309	2298	2279
	Pobór prądu / Rated current / Потр. ток, [A]	4,5	4,5	4,6	4,6	4,5
	Współczynnik efektywności / COP / КПД	2,44	2,98	3,66	4,50	5,56
45	Wydajność / Capacity / Производств, [W] [Вт]	5192	6365	7805	9580	11762
	Moc / Power consumption / Потр.мощн. [W] [Вт]	2583	2587	2584	2574	2556
	Pobór prądu / Rated current / Потр. ток, [A]	5,0	5,0	5,0	5,0	5,0
	Współczynnik efektywności / COP / КПД	2,01	2,46	3,02	3,72	4,60

Due to an even load of the individual phases of the electrical installation and the experimental research performed using an inverter, the authors decided to use a three-phase power supply for the compressor. From the catalogue the authors selected the smallest of the available three phase compressors of the heating power of **9 kW.** For the assumed working parameters (**B0/W35)** it has the coefficient of performance of **COP=4,4.** The catalogue compressor number is C-SBN263H8A.

From the presented catalogue data it results that in the range of evaporation temperatures (-10ºC ÷ +10ºC) the power consumption is on the same level but the compressor efficiency grows, hence the coefficient of performance (COP) is also proportionally higher for higher temperatures. Thus, we need to maintain the highest possible refrigerant evaporation temperature values. The increase in the temperature of the condensation causes significant drops in the coefficient of performance (COP).

Due to limited possibilities related to the organization of the plot and disadvantageous ground conditions (on the depth of 1÷2 m sand deposition was discovered) a lower heat source was performed using a vertical collector.

For the selection of the vertical collector the authors used dedicated **Energeo** software recommended by Aspol – the supplier of the probes of the vertical exchanger. Upon entering of the parameters of the pump to the Energeo software for the assumed coefficient of ground thermal power on the level of **38 W/m** a total required length of the vertical exchanger of **186 m** was calculated (dual pipe probes were applied, filled with a 20% solution of ethylene glycol. Three probes **62 m** each were connected to the wall distributor located in the heater room [8, 12].

Upon installing of the research stand the circuit of the lower heat source was filled with a solution of ethylene glycol of the concentration of 20% (fluid known as Henock 20E15). The circuit of the upper heat source was filled with water. Upon breathing individual circuits, lower heat source circuit pumps were activated for two hours to obtain an even fluid concentration in the whole circuit.

Next, a calibration was performed of the individual measurement chains and a verification of the correctness of the installation of the control circuits was carried out.

3. RESULTS OF THE PRELIMINARY TESTS

The preliminary tests were carried out in November and December in the heating season 2012/2013. For economic reasons the experimental research was carried out in the G12 off peak time of day (night rates applied) [6, 20].

During the tests the basic operating parameters necessary for the determination of the heat balance were recorded.

Symbols adopted in the graphs:

– Tgin – glycol temperature at the inlet from the lower heat source,

– Tgout – glycol temperature at the outlet from the evaporator,
– Thin – return water temperature from the heating circuit,
– Thout – heating circuit water temperature,
– Tco –condensation temperature of the refrigerant,
– Tev – evaporation temperature of the refrigerant,
– Tcwu – water temperature in the hot utility water tank,
– Tcoin – refrigerant temperature at the inlet to the condenser,
– Tevout – refrigerant temperature at the outlet from the evaporator.

Fig. 2 clearly shows that at constant chilling power of the heat pump the increase in the temperature in the hot utility water tank forces an increase in the temperatures of the upper heat source.

From the presented graphs (Fig. 3 and Fig. 4) it results that for a constant temperature difference in the glycol circuit of the lower heat source for the higher preset evaporation temperature, the capability of the takeoff of the refrigerating power by the heat pump decreases.

Additionally, maintaining a higher inlet temperature to the upper heat source causes a much lower value of the coefficient of performance.

Fig. 4 shows that within the first 15 minutes from the pump activation a significant increase in the temperature of the return water was observed in the upper heat source for the floor circuit pump on the ground floor set to speed I. Switching the pumps to speed II causes an abrupt drop in the temperature of the inlet water to the upper heat source. Fig. 5 shows the changes in the temperatures for

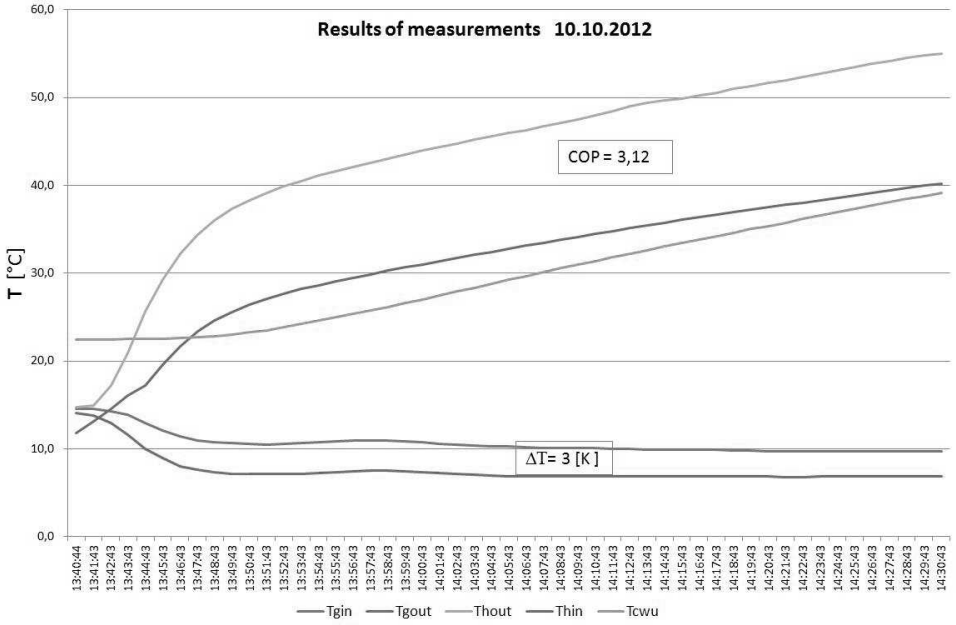

Fig. 2. Changes in the temperatures in the hot utility water tank circuit

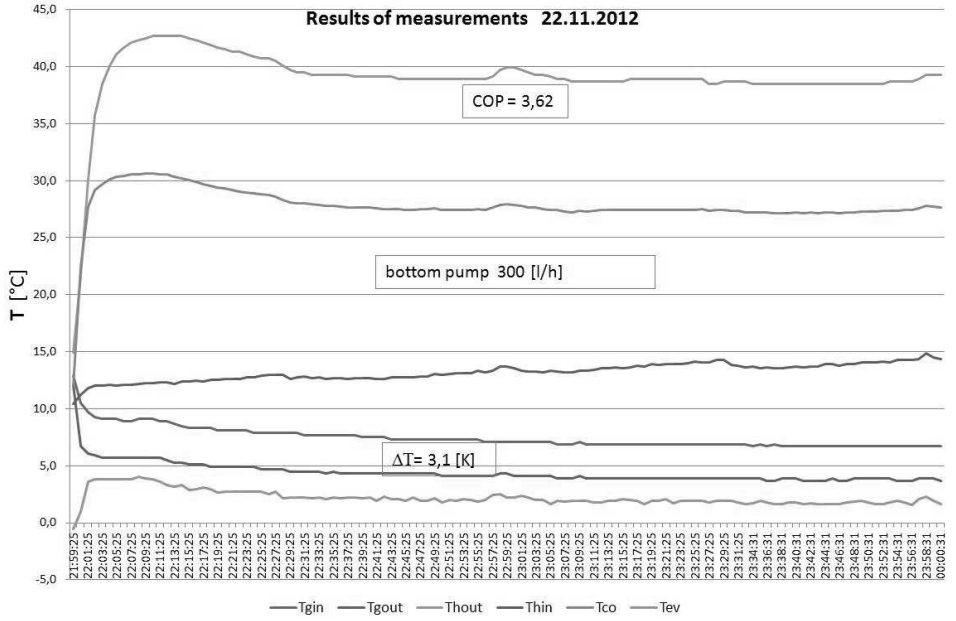

Fig. 3. Changes in the temperatures in the floor circuit for the evaporation temperature of 2°C

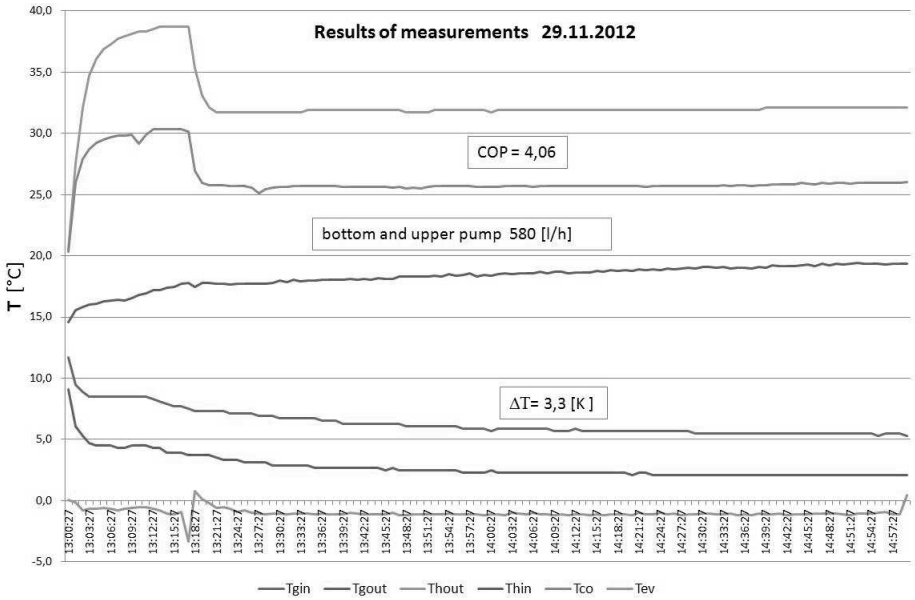

Fig. 4. Changes in the temperatures in the floor circuit for the evaporation temperature of -1°C

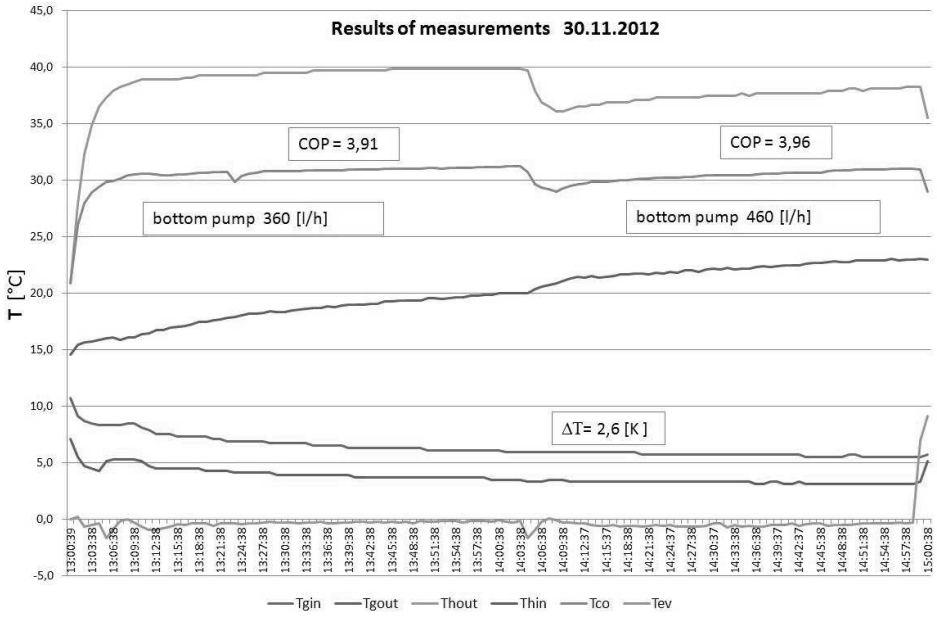

Fig. 5. Changes in the temperatures in the floor circuit for the evaporation temperature of 0°C and circuit pumps in the glycol circuit set to speed II

the case when in the upper heat source circuit only the floor circuit was on and the circuit pumps of the lower heat source were set to speed II. At a constant heat transfer rate in the ground for given conditions, changing the glycol flow rate results in a decrease in the difference in the glycol temperature at the inlet and return of the evaporator.

When only the floor circuit on the ground floor is on, setting the pump to speed II does not result in such a large decrease in the temperature of the inlet water in the upper heat source anymore, as was the case in the example shown in Fig. 4.

In the graph (Fig. 6) we can additionally see the course of the temperature changes in the condenser and evaporator for the CFC circuit.

The temperature of the refrigerant at the outlet from the compressor remains on the level of 60°C irrespective of the operating parameter changes of the upper heat source in the floor heating.

4. CONCLUSIONS

The research was carried out in a single-family house that is not yet in regular use. For purely economic reasons the room temperature was maintained on the level of 16°C, as generated by a heat pump operating in the off peak time of day when night rates for electricity applied. Hence, the pump during the research did not operate under optimal conditions. Nevertheless, from the prelimi-

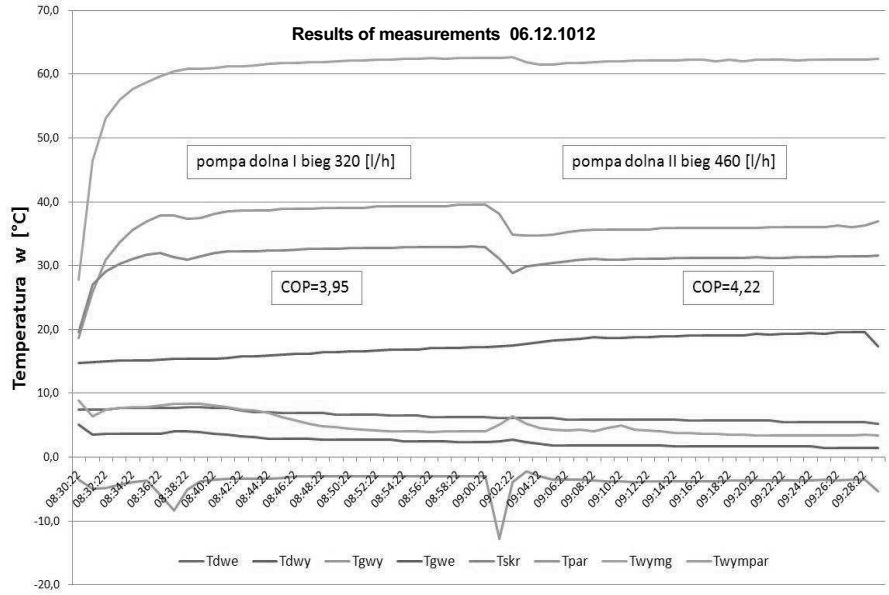

Fig. 6. Changes in the temperatures in the floor circuit for the evaporation temperature of -3°C

nary investigations we were able derive which operating parameters have a significant impact on the heat pump energy performance.

Determining of the fundamental relations of the influence of the operating parameters of the heat pump on the heat pump coefficient of performance will become possible upon a completion of research on the entire range of changes of the operating parameters. A detailed analysis of the obtained results will allow a determination of which of the subassemblies significantly block the possibility of obtaining a better coefficient of performance. The effect of this analysis will be a validation of the correctness of the methodology of selection of the individual heat pump subassemblies.

REFERENCES

1. **Broel-Plater B. 2009:** Układy wykorzystujące sterowniki PLC. Wydawnictwo Naukowe PWN.
2. **Chochowski A., Czekalski D. 2005:** Badania eksploatacyjne hybrydowego systemu zasilania energią z wykorzystaniem układu archiwizacji, transmisji i przetwarzania danych. Inżynieria Rolnicza, Nr 14, Kraków, 45-53.
3. **Ciesielczyk W., Skoneczna J. 2009:** Analiza pracy pompy ciepła z czynnikiem roboczym R407C. Wyd. Politechniki Krakowskiej, Zeszyt nr 4, 128-139.
4. **Jasiński B., Szreder M. 2006:** Microprocessor systems PLC for agricultural machines investigation. X Międzynarodowe Sympozjum im. prof. Cz. Kanafojskiego nt. „Problemy budowy oraz eksploatacji maszyn i urządzeń rolniczych". Płock, 75-76.
5. **Jasiński B., Szreder M. 2008:** Inżynieria mikroprocesorowych systemów monitorowania maszyn rolniczych. Wybrane zagadnienia mechaniki w budowie urządzeń technicznych. Płock, 153-194.
6. **Horyński M. 2008:** Heating system control in an intelligent building. TEKA Kom. Mot. Energ. Roln. – OL PAN, 8, 83-88.
7. **Kapuściński J., Rodzoch A. 2010:** Geotermia niskotemperaturowa w Polsce i na świecie – stan aktualny i perspektywy rozwoju. Wyd. Borgis, Warszawa.
8. **Knaga J. 2007:** Changeability of heat output of heat pump with scroll type compressor. TEKA Kom. Mot. Energ. Roln. – OL PAN, 7A, 41-45.
9. **Knaga J. 2008:** Energy efficiency of small compressor assisted air-water type heat pumps. TEKA Kom. Mot. Energ. Roln. – OL PAN, 8, 99-105.
10. **Kolesnikov A., Dyadichev V. 2010:** Industrial Enterprises Study of Automatic Control Systems. TEKA Kom. Mot. Energ. Roln. – OL PAN, 10A, 126-132.
11. **Kurpaska S. Latała H. 2006:** Analiza wydajności cieplnej gruntowego wymiennika ciepła w instalacjach wykorzystujących pompy ciepła. Inżynieria Rolnicza, Nr 6, Kraków, 251-259.
12. **Kurpaska S. Latała H. 2008:** Efektywność pracy pompy ciepła współpracującej z wymiennikami gruntowymi. Inżynieria Rolnicza, Nr 6, Kraków, 105-111.
13. **Kwaśniewski J. 2008:** Sterowniki PLC w praktyce inżynierskiej. Wydawnictwo BTC.
14. **Miara M. 2008:** Wyniki badań dolnych źródeł ciepła w pompach ciepła typu solanka/woda. InstalReporter nr 6, 11-14.
15. **Miara M. 2011:** Sprawność pomp ciepła w realnych warunkach użytkowania. InstalReporter nr 2, 12-16.
16. **Rubik M. 2006:** Pompy ciepła – poradnik. Wyd. Ośr. Informacji „Technika Instalacyjna w budownictwie", Warszawa.
17. **Sałat R., Korpysz K., Obstawski P. 2010:** Wstęp do programowania sterowników PLC. Wydawnictwo WKiŁ.
18. **Smuczyńska M. 2012:** Rynek pomp ciepła w Polsce. Magazyn instalatora nr 11, 31-33.
19. **Szreder M., Krzywosiński S. 2004:** Implementation of PID controller in the GE FANUC PLC. V International

Scientific Conference on „Microprocessor systems in agriculture”. Płock, 201-205.
20. **Szreder M. 2012:** Hardware configuration of the Unitronics M90 controlers. TEKA Kom. Mot. Energ. Roln. – OL PAN, 12, 289-292.
21. **Wierzbicki S. 2006:** Diagnosing microprocessor-controlled systems. TEKA Kom. Mot. Energ. Roln. – OL PAN, 6, 182-188.
22. **Zbrodowicz K., Dyakowski T. 1990:** Pompy ciepła. PWN, Warszawa.
23. www.viessman.pl. Pompy ciepła, Zeszyty fachowe.
24. www.pompyciepla.danfoss.pl. Poradnik pomp ciepła Danfoss.

BADANIE WPŁYWU PARAMETRÓW FUNKCJONALNYCH POMPY CIEPŁA NA WYDAJNOŚĆ CIEPLNĄ

Streszczenie. W pracy zostały zaprezentowane wybrane zagadnienia dotyczące doboru gruntowej pompy ciepła na podstawie publikowanych wyników badań. Przeprowadzone badania eksperymentalne na stanowisku badawczym (domek jednorodzinny z ogrzewaniem podłogowym) pozwolą oszacować wpływ poszczególnych parametrów funkcjonalnych na współczynnik efektywności energetycznej pompy ciepła.
Słowa kluczowe: gruntowa pompa ciepła, kolektor pionowy, sprężarka spiralna, parownik, skraplacz, źródło dolne, współczynnik efektywności energetycznej.

TEKA. COMMISSION OF MOTORIZATION AND ENERGETICS IN AGRICULTURE – 2013, Vol. 13, No. 1, 197–200

Effect of different rates of nitrogen fertilizer on growth and yield of sweet corn cobs

Szymanek Mariusz, Piasecki Jacek

University of Life Sciences in Lublin, Department of Machines Science
Poniatowskiego 1, 20-060 Lublin

Received February 22.2013; accepted March 14.2013

Summary: The study presents the influence of nitrogen fertilization of sweet corn cobs on yield of kernels and the content of sugar (sucrose) in them. The dose of nitrogen ranged from 60 to 120 kg/ha. There was observed an increase of yield of sweet corn kernels and decrease of content of sucrose in the kernels.
Key words: sweet corn, nitrogen, fertilization.

INTRODUCTION

Sweet corn for processing is harvested at a relatively immature stage as compared to field corn. Processing of corn is used to increase its shelf life but as a consequence, a significant loss of nutrients may occur via heat degradation or leaching [19].

The high yield of suitable quality of sweet corn kernel requires the provision of a lot of nutrient elements to the plant, with nitrogen being the most important element for their growth. It exerts a great influence on the chemical composition, which determines the technological quality [2, 23]. Nitrogen in sweet corn growing is an important component influencing both the yield and aminoacids, which decide on the taste and nutrient value of kernels [4]. Sweet corn cobs constituting raw material for processing must be characterized by the highest quality of kernels. Kernel quality is defined not just by the chemical and sensory properties, but also by the mechanical parameters of kernels. This appears to fully justify joint consideration of all those properties. Sweet corn is probably a mutant of fodder corn [14]. The chemical composition of the kernels is related to the weather conditions, ripeness, and method of storage. According to data from the United States Department of Agriculture [8], the nutritional value of sweet corn kernels is related to the content of water (72,7%) and to the total content of solid parts (27,3%). Solid parts include hydrocarbons (81%), proteins (13%), lipids (3,5%), and others (2,5%). Starch is the dominant hydrocarbon component. Sweet corn has the highest nutritional value in the phase of milk ripeness. With progressing phase of ripeness, in the transition to the phase of wax ripeness the content of sugars decreases, accompanied by an increase in the content of starch [22]. In 100 g of kernels there is about 3,03 g of saccharine, 0,34 g of glucose and 0,31 g 1 of fructose. The content of saccharine increases, and that of reducing sugars decreases as the kernels reach the optimum ripeness . The content of proteins in the kernels decreases from the surface towards the centre of the kernel. The content of proteins, free aminoacids, water-soluble and insoluble hydrocarbons, increases up to the phase of wax ripeness, and then gradually decreases [1]. The amounts of the particular components in various cultivars and in various phases of ripeness variable.

The consumable quality of sweet corn depends on different factors such as: degree of maturity, genotype, variety, isolation of space, length and condition of post harvest storage, weather conditions, fertilization, irrigation and agrotechnics treatment [5, 6, 12, 21, 24].

The new cultivation trend is to balance mineral nutrition, which results in a high yield and reduces to the minimum the negative influence of nitrogen fertilization on the quality of yield and natural environment [9, 13, 15, 16]. In the praxis, nitrogen fertilization should be exactly determined on the basis of chemical sample of soil. It causes many problems because the nitrogen influence on the increase of kernels yield is two-sided and can have a negative influence on the final product [17, 18]. A high dose of nitrogen results in a decrease of the level of sugars in kernels and can cause danger to the natural environment because it is easily rinsed to soil [7, 10].

A high level of nitrogen fertilization creates a series of dangers related with negative influence on plant quality. This problem is especially meaningful in the growing of vegetable plants. Fertilization of nitrogen should be considered in view of a possibility of obtainment of high yield with low content of nitrates [11, 12, 20]. The rational proportion

of nitrogen depends on soil condition, content of available nutrient, humidity and crop rotation [23]. The average provisional portion of nitrogen ranges from 60 to 300 kg/ha. Warzecha [25] stated that the supply of nitrogen should not exceed 90kg/ha. The Miao's study [11] showed that the increase of nitrogen fertilization influenced the increase of cob yield and protein content in kernels and decrease of oil and starch in kernels.

Sweet corn attains consumable maturity when the kernels are at milk stage of maturity and their moisture amount to 70-76%. In this stage, the kernels have the highest level of sugar, especially sucrose which influences the consumable quality of sweet corn kernels [3, 7, 12].

The aim of this study was to determine the influence of nitrogen fertilization of sweet corn on the yield of cut off kernels and their content of sucrose.

MATERIALS AND METHODS

The material was made up by sweet corn cobs of the following three super sweet varieties (*sh2*): Golda, Candle and Helena. Table 1 gives the physical and geometric properties of the sweet corn cobs.

Table 1. Means and standard deviations of physical and geometrical properties of sweet corn cobs.

Specification		Variety		
		Golda	Candle	Helena
Cob mass, g	$x_{śr}$	350,8	327,5	342,1
	SD	18,2	16,9	20,5
Cob lenght, mm	$x_{śr}$	21,7	20,1	20,3
	SD	4,7	3,8	4,2
Cob diameter*, mm	$x_{śr}$	50,2	48,7	49,8
	SD	0,8	1,2	1,0
Kernel length, mm	$x_{śr}$	9,5	8,1	8,7
	SD	1,5	1,2	1,7
Number of kernel per row, pcs.	$x_{śr}$	36,4	32,3	36,2
	SD	5,8	4,3	5,3
Number of kernel rows, pcs.	$x_{śr}$	18	14	16
	SD	2,8	3,3	3,2
Moisture of kernel, %	$x_{śr}$	76,8	73,2	74,4
	SD	2,6	2,1	2,4

$x_{śr}$ – mean value
SD – standard deviation
* measured in central part of cob

The varieties studied were characterized by a relatively low variation of the mean measurement values, which positively assisted the comparison. It was found that an increase in the mean physical and geometrical values of corncobs was related to an increase in their yield.

The fertilizer applied in the experimental was carbamide in the amount of: 0 (control), 60, 90,120 kgN/ha and organic fertilization – 30t/ha. The level of P_2O_5 and K_20 fertilization was constant and amounted to 80 kg P/ha in the form of triple superphosphate and 160 kg K/ha in form of kalium sulphate. The application was realized in two variants:

a) I – all dose of nitrogen fertilization was applied before sowing in amount: 0, 60, 90 and 120 N kg/ha,
b) II -the half of dose of nitrogen fertilization was applied before sowing in amount: 0, 30, 40 and 60 N kg/ha.

The experimental was realized on the plot of 50 m² area in split-block system for three factors: O – variety, N – dose of nitrogen, W – variant.

The yield of cut off kernels (Q_z) was determined according to the following formula:

$$Q_z = \frac{m_k - m_r}{m_k} \cdot Q_k \quad [t/ha]$$

where:
m_k – weight of dehusking cob, t
m_r – weight of cob core, t
Q_k – potential field of dehusking sweet corncob, t/ha.

Kernels were cut from sweet corncob core in the machine Corn Cutter SC-120 FMC FoodTech. The measurements were taken for the angular velocity of the cutter head from 167,5 rad/s and linear velocity of cob feeder 0,31 m/s.

The measurements of sucrose content were realized using hand refractometr with automatic compensation ATC – 1E at measurement range from 0,0 to 32% Brix and accuracy 0,2% according to norm PN-En 12143: 2000.

The yield of cut off kernels was determined on the sample of 100 sweet corncobs, the content of sucrose in 30 sweet corn cobs for each combination of doses of nitrogen and variant.

The measurements results were analyzed statistically at the significance level of a = 0,05.

THE ANALYSIS AND RESULTS

The tree-way analysis of variance to analyze the effect of three qualitative factors: variety (O), dose of nitrogen (N) and variant (W) on the dependent variable of the yield of kernels (Q_z) showed that O, N, W and interaction N-W were statistically significant while interaction O-N, O-W and O-N-W were not statistically significant (Table 1).

Table 1. The analysis of variance to analyze the effect of qualitative factors (O, N, W) on dependent variable (Q_z)

Specification	Sum of square	Degree of freedom	Mean square erroe	Test F	Significance level
O	1,20	2	0,60	14,5	0,00
N	19,29	3	6,43	155,7	0,00
W	22,32	2	11,16	270,2	0,00
O-N	0,41	6	0,07	1,7	0,14
O-W	0,06	4	0,01	0,3	0,84
N-W	1,47	6	0,24	5,9	0,00
O-N-W	0,80	12	0,07	1,6	0,10

The mean value of yield of kernels at first variant at nitrogen fertilization from 0 to 120 N kg/ha ranged from 9,6 to 11,1 t/ha for Golda variety and adequately from 10,3 to 11,3 t/ha for Candle and from 10,2 to 11,4 Helena (Fig. 1). The highest mean value of kernels yield in range of nitrogen fertilization from 0 to 120 kg/N ha were recorded at Golda (14,9%) and the lowest at Candle (9,2%).

At the second variant, the mean value of kernels yield ranged from 10,7 to 11,9 t/ha (Golda), from 11,0 to 12,1 t/ha (Candle) and from 11,5 to 12,5 t/ha (Helena) (Fig. 2). The highest mean value of kernels yield ranged from 11,5% (Golda) to 6,5% (Helena).

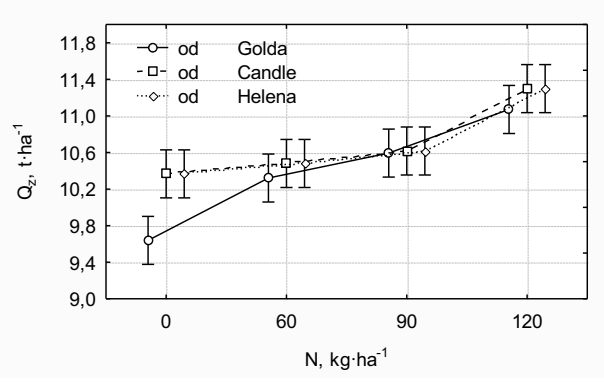

Fig. 1. The mean value of kernels yield (Q_z) with 0,95 confidence interval in relation to dose of nitrogen fertilization (N) at variant I

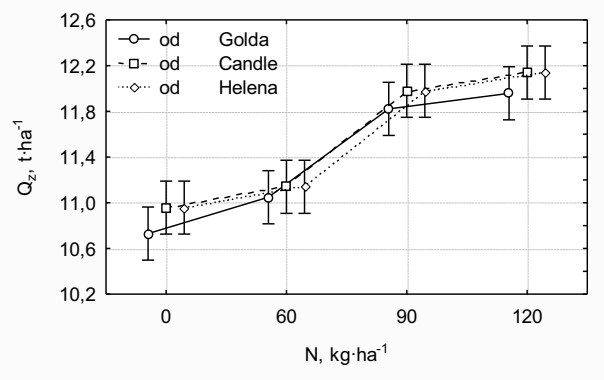

Rys. 2. The mean value of kernels yield (Q_z) with 0,95 confidence interval in relation to dose of nitrogen fertilization (N) at variant II

The analysis of variance to analyze the effect of three qualitative factors: variety (O), dose of nitrogen (N) and variant (W) on one dependent variable: the content of sucrose in kernels (C_s) showed that O, N, N and interaction of O-W were statistically significant while O-N, N-W and O-N-W were not statistically significant (Tab.2).

Table 2. The analysis of variance to analyze the effect of qualitative factors (O, N, W) on dependent variable (C_s)

Specification	Sum of square	Degree of freedom	Mean square erroe	Test F	Significance level
O	7,18	2	3,59	5,45	0,00
N	114,68	3	38,23	58,00	0,00
W	58,54	2	29,27	44,41	0,00
O-N	6,65	6	1,11	1,68	0,13
O-W	11,86	4	2,97	4,50	0,00
N-W	3,36	6	0,56	0,85	0,53
O-N-W	6,18	12	0,52	0,78	0,66

The increase of dose of nitrogen fertilization in the range from 0 to 120 kg N/ha effected the decrease of sucrose in kernels from 19,1 to 16,2% (Golda), from 20,8 to 15,8% (Candle) and from 18,5 to 16,5% (Helena) at the first variant (Fig. 3) and from 19,0 to 16,9%(Golda), from 19,1 to 16,4% (Candle) and from 19,2 to 17,1% (Helena) at the second variant (Fig. 4).

The highest decrease of sucrose content was recorded at Candle variety (24,0%) at first and 14,0% at second variant and the lowest at Helena (10,8%) at first variant and at (Golda and Helena) 11,0%.

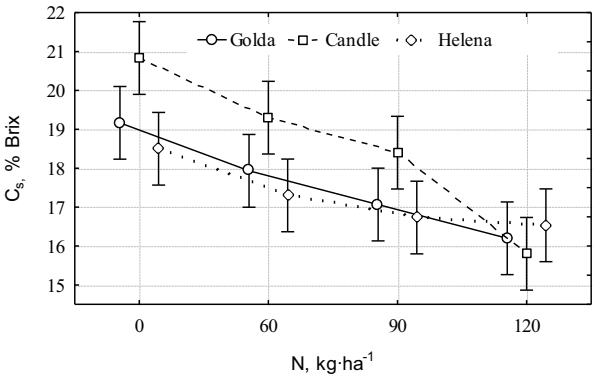

Rys. 3. The mean value of sucrose content (C_s) with 0,95 confidence interval in relation to dose of nitrogen fertilization (N) at variant I

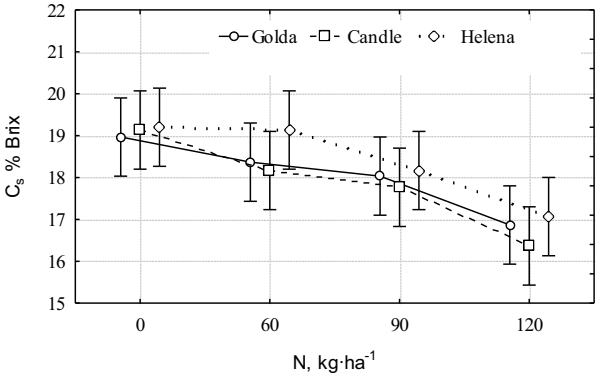

Rys. 4. The mean value of sucrose content (C_s) with 0,95 confidence interval in relation to dose of nitrogen fertilization (N) at variant II

CONCLUSIONS

1. The yield and content of sucrose in kernels are statistically significantly differentiated with regard to the dose of nitrogen fertilization and its variant of application.
2. The change of nitrogen dose from 0 to 120 kg/ha effected the increase of yield kernels in the range from 4,0 (Helena) to 15% (Golda) and decrease of sucrose content in kernels from 24 (Candle) to 11,0% (Helena) at the first variant and, correspondingly, from 10,0 to 12% and from 15,0 to 4%.

REFERENCES

1. **Azanza F.; Tadmor Y. Klein B.P. 1996.** QTL influencing chemical and sensory characteristics of; eating quality in sweet corn. Genome, 39, 40–50.
2. **Ardelean M., Cordea M., Haş V., Bors A. 2010.** Yield and quality performances of five sweet corn hybrids grown in conventional and organic systems of agriculture. Proceedings of ISHS Congres., Lisbon, 174–178.
3. **Cherr C. M., Scholberg J. M. S. McSorley R., Mbuya O. S. 2007.** Growth and yield of sweet corn following green manure in a warm temperate environment on sandy soil. Journal of Agronomy and Crop Science, 193, 1–9.
4. **Dale E.** Sweet corn nitrogen fertilization. 1995. Oswego Country Vegetable Program News, Cornell Cooperative Extension, 25, 6.
5. **Eghball B. 2002.** Soil properties as influenced by phosphorus and nitrogen based manure and compost applications. Agronomy Journal, 94, 128–135.
6. **Eghball B., Ginting D., Gilley J. E. 2004.** Residual effects of manure and compost applications on corn production and soil properties. Agronomy Journal, 96, 442–447.
7. **Hanna H. Y., Story R. N. 1992.** Yield of super sweet corn as affected by N application timing, plant density, tiller removal, and insecticides. Proceedings of the Florida State Horticultural Society, 105, 343–344.
8. **Hardenburg R. E., Watada A. E. 1986.** The Commercial Storage of Fruits, Vegetables, and Florist and Nursery Stocks. U.S. Dept. *Agriultural. Handbook,* 66.
9. **Hochmuth, G. 1997a.** Response of sweet corn and snapbean to Growplex Humate. *Fla. Agr. Expt. Sta. Res. Rep. Suwannee Valley AREC* 97–7.
10. **Hochmuth, G. 1997b.** Snapbean and sweet corn response to N rate and furrow-placed Growplex humate. *Fla. Agr. Expt. Sta. Res. Rep. Suwannee Valley AREC* 97–21.
11. **Miao Y., Mulla D. J., Robert P. C., Hernandez J. A. 1991.** Within-Field variation in corn yield and grain quality responses to nitrogen fertilization and hybrid selection. Agronomy Journal, 98,129–140.
12. **Michałojć Z. 1999.** Wpływ nawożenia i terminu zbioru na plon kukurydzy cukrowej. Hasło Ogrodnicze, 6, 46–48.
13. **Olczyk, T., Y. Li,. Simonne E, R. Mylavarapu. 2003.** Reduced phosphorus fertilization effects on yield and quality of sweet corn grown on a calcareous soil. Proceedings of the Florida State Horticultural Society. 116:95–97.
14. **Orłowski M. 2000.** Polowa uprawa warzyw. Kukurydza cukrowa, 383–386.
15. **Paul J. W., Beauchamp E. G. 1993.** Nitrogen availability for corn in soils amended with urea, cattle slurry and solid and composted manures. Canadian Journal of Soil Science, 73, 253–266.
16. **Sanchez C. A., Porter P. S., Ulloa M. F. 1991.** Relative efficiency of broadcast and banded phosphorus for sweet corn produced on histosols. Soil Science Society American Journal, 55, 871–875.
17. **Salardini, A. A., Sparrow L. A., Holloway R. J. 1992.** Sweet corn response to basal and top-dressed rates and sources of nitrogenous fertilizers. Australian Journal of Agricultural Research 43, 171–180.
18. **Schepers J. S., Frank K. D, Bourg C. 1986.** Effect of yield goal and residual nitrogen considerations on nitrogen fertilizer recommendations for irrigated maize in Nebraska. *J. Fert.* 3, 133–139.
19. **Scott C. E., Eldridge A. L. 2005.** Comparison of carotenoid content in fresh, frozen and canned corn. Journal of Food Comosition and Anaysis, 18, 551–559.
20. **Staggenborg, S.A. Dhuyvetter K.C. Gordon W. B. 2008.** Grain Sorghum and Corn. Efficient use of nutrients in Comparisons: Yield, Economic and Environmental Responses. Agronomy Journal, 100, 1600–1604.
21. **Stoyanowa S.D. 1999.** Influence of nitrogen fertilization on the dynamics of growth and productivity of sweet corn. Acta Horticulturae, 371, 125–131.
22. **Suk S. L., Sang H.Y. 1999.** Sugars, soluble solids and flavor of sweet, super sweet and waxy corns during grain filling. Korean Journal of Crop Science, 44(3), 267–272.
23. **Waligóra H. 1999.** Uprawa i wykorzystanie kukurydzy cukrowej. Hasło Ogrodnicze, 12, 10–12.
24. **Warman P. R, Havard K. A. 1996.** Yield, vitamin and mineral content of four vegetables grown with either composted manure or conventional fertilizer. Journal of Vegetable Crop Production, 2(1), 13–25.
25. **Warzecha R. 2003.** Słodki smak kukurydzy. Owoce warzywa kwiaty, 6, 20–21.

WPŁYW INTENSYWNOŚCI NAWOŻENIA AZOTOWEGO KUKURYDZY CUKROWEJ NA PLON ZIARNA ORAZ ZAWARTOŚĆ W NIM SACHAROZY

Streszczenie. Przedstawiono wpływ nawożenia azotowego kukurydzy cukrowej na plon ziarna oraz zawartość w nim sacharozy. Badania realizowano dla dwóch wariantów nawożenia w zakresie od 0 (kontrola) do 120 kg/ha. W wariancie I aplikowano całą dawkę przed siewem, a w wariancie II połowę dawki przed siewem i połowę pogłównie. W badanym przedziale zmiana dawki nawożenia wpływała na wzrost plonu ziarna od 15% (odmiana Golda) do około 11% (odmiana Helena) oraz spadek zawartości sacharozy od około 31% (Candle) do około 12% (Golda) w pierwszym wariancie i odpowiednio dla II wariantu od 11% (Golda) do 7% (Helena), i od 20% (Candle) do 11%(Helena).

Słowa kluczowe: Słodka kukurydza, azot, nawożenie.

Significance tests uses in material logistics of food company in aspect of process technology

Mariusz Szymanek, Zbigniew Burski***

**Department of Agricultural Machines Science*
***Department of Power Industry and Vehicles*
University of Life Sciences in Lublin

Received February 10.2013; accepted March 14.2013

Summary. In this paper the problems of beer-can in production of beer, the stage of taking and filling as well as problems of the "disappear" in process technology are considered. The estimation of process quality has been performed on the basis of statistical significance tests.
Key words: food company, technology process, pouring of beer, statistical tests

INTRODUCTION

In logistic systems of production company of technical materials [8, 13, 14, 15] of food [1, 2, 3, 4, 7, 10] or mechanization of agricultural production [10, 11, 12] the procedure of evaluation of the technological and working costs has become more and more useful [16].

Traditional methods of the evaluation of the materials requirement have used the analyses of statistical methods (rule Just-in-time, ABC methods, system of materials planning – PPK) and control of technologically and working process [6, 18].

The objective of this work was to show the possibility of using the statistical significance tests in production of beer as the component of material logistics estimation (magazine and technology). It is an attempt at quantity estimation of their significance at the specific level of a company.

MATERIAL AND METHODS

The object was the estimation of beer-can "disappear" in time of process technology process at their taking and filling in aspect of the time of the highest demand of consumption.

The methods took into account:

– Tests of zero hypotheses for variables: taking of beer-can (p.p.), filling of beer-can (n.p.) and beer-can "disappear",
– Total statistical calculation of variables,
– Analysis of variance,
– Multiple tests of Tukey, with confidence interwal of 95%

In the test calculations there were used: the t-student test, sign test and test of ranked sign [20].

Results of calculations:

1. The testing of zero hypothesis and total statistic of variables.

The calculations for p.p. variable in the range of level for factor "group" (month) is shown in Table 1.

The calculations for n.p. variable in the range of level for factor "group" (month) is shown in Table 2.

Table 1. The total statistic for p.p.variable

Contents	Variable– p.p.					
	Number	Mean	Standard deviation	Min	Max	Coefficient of variability
1	20	98614.0	7871.70	75410.0	106660.0	7.98
2	16	99501.3	11270.60	60980.0	113600.0	11.32
3	21	101910.0	7448.90	83787.0	112320.0	7.30
4	22	96302.3	14022.50	54470.0	114280.0	14.56
5	22	104400.0	14009.70	64860.0	125680.0	13.41
6	19	106323.0	30158.70	13140.0	173180.0	28.36
Total	120	101167.0	15945.60	13140.0	173180.0	15.76

Table 2. The total statistic for n.p. variable

Contents	Variable – n.p.					
	Number	Mean	Standard deviation	Min	Max	Coefficient of variability
1	20	9872.0	7848.00	75144.0	106296.0	7.98
2	16	99162.0	11237.30	60768.0	113280.0	11.33
3	21	101404.0	7480.18	83208.0	111860.0	7.37
4	22	95946.5	13997.40	54264.0	113928.0	14.58
5	22	404113.0	13970.30	64680.0	125328.0	13.41
6	19	112118.0	20472.60	84696.0	172656.0	18.25
Total	120	101776.0	13962.30	54264.0	172656.0	13.71

In the Table 3 the results for variable „disappear" is presented.

Table 3. The total statistic for „disappear" variable

Contents	Variable – „disappear"					
	Number	Mean	Standard deviation	Min	Max	Coefficient of variability
1	20	342.20	57.07	264.0	504.0	16.67
2	16	339.25	50.58	212.0	434.0	14.91
3	21	509.90	178.27	240.0	950.0	34.96
4	22	351.60	85.34	160.0	478.0	24.27
5	22	322.00	102.67	180.0	708.0	30.92
6	19	410.31	87.24	272.0	576.0	21.26
Total	120	381.80	120.99	160.0	950.0	31.69

2. The analysis of variance and Tukey HSD test.
   The calculations for p.p. and n.p. variables in the range of level for factor "group" (month) is shown in Table 4.

Table 4. The analysis of variance for n.p. and p.p. variable

Content	Sum of square		Degree of freedom		Mean of square		Test F		Significance level	
	p.p.	n.p.	p.p.	n.p.	p.p.	n.p.	p.p.	n.p.	p.p.	n.p.
Between group	1.4E9	3.2E9	5	5	2.9E8	6.5E8	1.14	3.72	0.32	0.037
Inside group	2.8E10	1.9E9	114	114	2.5E8	1.7E8	-	-	-	-

Results of Tukey test for p.p. and n.p. variables was presented in Table 5a and 5b

Table 5a. Results of Tukey test for p.p. and n.p. variables

Method: 95% interwal confidence of HSD Tukey'a						
Contents	Number		mean		Homogenity group	
	p.p.	n.p.	p.p.	n.p.	p.p.	n.p.
4	22	22	96302.3	95946.5	x	x
1	20	20	98614.0	98272.0	x	x
2	16	16	99501.3	99162.0	x	xx
3	21	21	101910.0	101404.0	x	xx
5	22	22	104400.0	104113.0	x	xx
6	19	19	106323.0	112118.0	x	x

Table 5b. Results of Tukey test for p.p. and n.p. variables according to factors level „group" and LSD

Contrast group	Difference		+/- Limit of LSD	
	p.p.	n.p.	p.p.	n.p.
1-2	887.25	890.00	15487.0	12858.4
1-3	3295.52	3132.38	14398.4	11977.8
1-4	2311.75	2325.45	14237.9	11844.3
1-5	5785.55	5841.00	14237.9	11844.3
1-6	7709.16	13846.10	14763.5	12281.5

2-3	2408.27	2242.38	15292.5	12721.6
2-4	3198.98	3215.45	15141.5	12595.9
2-5	4898.30	4951.00	15141.5	12595.9
2-6	6821.91	12956.10	15636.7	13007.9
3-4	5607.25	5457.84	14059.2	11695.6
3-5	2490.02	2708.62	14059.2	11695.6
3-6	4413.63	10713.70	14591.2	12138.2
4-5	8097.27	8166.45	13894.8	11558.8
4-6	10020.90	16171.60	14432.8	12006.4
5-6	1923.61	8005.11	14432.8	12006.4

The results for "disappear" variable is shown in Table 7a and 7b.

The analysis of equipment, material and production of beer on the basis of significance test was performed.

The statistic results that the nominal capacity uses of pouring line(160 00 pcs per day) e.g. in first day – June (group 1) was exploited in minimum value of 47.13% of their possibility. The maximum day uses in June amount 66.66%. In the next month (group 2) the results were 38.13%, 71.00%, respectively. In the whole period of studies (group 1 – group 2) the lowest (8.2%) and the highest (108.2%) day uses were recorded, the highest use option achieved in December. The coefficient of variability amounts to 28.36%. This value is lower than the highest values (28.36%) achieved in November.

The calculations of next production phase for n.p. showed that e.g. in June the minimum value amounted to 94.7% and the maximum to 99.6% in relation to the number of beer-can taking (p.p.).

In the whole month – June the coefficient amounted to 98.8% at 13.77% of variability coefficient.

The information presented in Table 3, concerning the variable "disppear" of beer-can after filling (n.p.) shows large diversifications in the number of carried out studies.

The nominal value of month "disappear" amounted to160 pcs (October) and the maximum value amounted to 950 pcs (August). As to losses in the final product, they resulted from objective reasons (leakiness, deformation, little pour l) and others. As practice shows, 475 liters of beer goes to sewage.

The analysis of variance for p.p. and factor "group" and Tukey test showed that there are the homogeneity group without significance statistical difference (Tab. 5a). However, for n.p. there are homogeneity group (Tab. 5b). Tables 6 and 7a show that the values of variable "disappear" are differential monthly. The difference between June – August and July – August showed two homogeneity groups.

Table 6. The analysis of variance for variable "disappear" and level factor "group"

Content	Sum of square	Degree of freedom	Mean of square	Test F	Significance level
Between group	494986.0	5	98997.2	9.05	0.000
Inside group	1.24E6	114	10940.9	-	-
Total	1.74E6	119	-	-	-

Table 7a. Tukey test for the variable "disappear" and level factor "group"

Contents	Number	Mean	Homogenity group
5	22	332.00	x
2	16	339.25	x
1	20	342.20	x
4	22	351.63	x
6	19	410.31	x
3	21	509.90	x

Table 7b. Tukey test for the variable "disappear" and level factor "group" for LSD

No.	Contrast „group"	Difference	+/- Limits LSD	No.	Contrast „group"	Difference	+/- Limits LSD
1	1-2	2.95	101.69	9	2-6	71.06	10.87
2	1-3	167.70	94.72	10	3-4	158.26	82.49
3	1-4	9.43	93.67	11	3-5	177.90	92.49
4	1-5	10.20	93.67	12	3-6	99.59	95.99
5	1-6	68.11	97.13	13	4-5	19.63	91.41
6	2-3	170.65	100.61	14	4-6	58.67	94.95
7	2-4	12.38	99.61	15	5-6	78.31	94.95
8	2-5	7.25	99.61	-	-	-	-

CONCLUSIONS

Results of researches, which were limited in this paper, showed the significant possibility of uses in the company of the technical standards of beer-can production at no remittent popularity on the market of wrapping.

The difference between the number of beer-can in day production and after filling, so called "disappear" amounted to 950 pcs. It showed the necessity of production of the highest quality beer-cans from the producer as well as strict formality of standards in pasteurization process as well as proper control of their filling. The coefficient of variability for variable "disappear" amounted to 34.96% (August). The average values amounted to 31.69%.

The research will be continued in the next period of production. The information has been particularly subject to analysis, especially that so far there have been no numerous published papers in this range, and the existing articles have presented the information only on the process of technology in range of biological and chemical changes or the description of a particular machine and its technical and technological aspects [9, 17].

REFERENCES

1. **Burski Z., Bulgakov, V., Reichenbach J. 2005:** The analysis of Raw materials and energy consumption and the costs of their utilization in brewery plants. Zbirnik Nauowych Prac NAU, Wid. NAUU, Kyiv XII, T. II, 82-87.
2. **Burski Z., Burski P., Krasowski E., Skoczylas A. 2005:** Utilization of multiple comparisons HSD Tukey'a in analysis of safety system of cars exploitation in Polish Republic. Zbirnik Naukowych Prac NAU, Wid. NAUU, Kyiv XII, T. II, 320-328.
3. **Burski Z., Krasowski E., Skoczylas R. 2005:** The analysis of costs of energy corers consumption and working capacity in the various technical and technological conditions of brewery plants. Zbirnik Naukowych Prac NAU, Wid. NAUU, Kyiv XII, T. I, 123-128.
4. **Burski Z., Sosnowski S., Reichenbach J. 2005:** Structure analysis of the use of Power transmitters of brewing enterprises in the aspect of products with energy economy. Zbornik Naukowych Prac NAU, Wid. NAUU, Kyiv XII, T. II, 104-109.
5. **Burski Z. Tarasińska J. 2003a:** Application of multifactoral analysis of influence of number piston ring son on the Dynamics of vibracions of tractor's engine. Min. Agrarnoj Politiki Ukraini. Proceedings of Kharkiv State Technical University of Agriculture (KSTUA) No. 20, 269-279.
6. **Burski Z., Tarasinska J. 2003b:** The methodolgical aspects of Rusing multifactor analysis of ariance in the examination of exploatation of engine sets. TEKA Kom. Mot. i Energ. Roln. PAN, Lublin, 45-54.
7. **Burski Z. Zając G., Pawłowski M. 2003:** Analiza sieci teleinformacyjnych w scentralizowanym systemie logistycznym produkcji przedsiębiorstwa spożywczego. Wyd. Kom. Mot. i Energ. Roln., Motoryzacjia i Energetyka Rolnictwa, T. 5, 30-35.
8. **Demuyakor B., Ohta. Y. 1993:** Characteristics of single and mixed culture fermentation of *Pito* beer. J. Sci. Food Agric., vol. 62, 401–408.
9. **European Brewery Convention. 1987:** Free Amino Nitrogen. In: Analytica EBC. 4th ed. Zurich: Brauerei-und Getranke-rundschau, 141–142.
10. **Fernandez S., Machuca N., Gonzalez M., Sierra J. 1985:** Accelerated fermentation of high gravity worts and its effect on yeast performance. Am Soc Brewing Chemists vol. 43, 109–13.
11. **Gestryk V. 2010:** Peculiaries and reference points of machine – building enterprice activities. TEKA Kom. Mot. i Energ. Roln. – Odz. Lublin, 158-164.
12. **Juściński S., Piekarski W. 2009:** Analiza procesu zaopatrzenia w części zamienne do ciągników I maszyn rolniczych w oparciu o "outsourcing" usług logistycznych. Eksploatacja i Niezawodność, vol. 2(42), 63-70.
13. **Krasowski E., Krasowska M. 2001:** Gospodarka energetyczna w rolnictwie. Wyd. AR w Lublinie, Lublin, 60-62.
14. **Lahno V., Petrov A. 2010:** Tasks and methods of the static optimum encoding of service request relative prorities in the information protection system of local area Network. TEKA Kom. Mot. i Energ. Roln. PAN – Odz. Lublin, T. 10a, 215-222.
15. **Niziński S. 1999:** Logistyka. Wyd. ART w Olsztynie, Olsztyn, 251-258.
16. **Niziński S. 2001:** Analiza kosztów eksploatacji obiektów technicznych w rolniczych systemach działania. Motrol, Wyd. AR w Lublinie, Lublin, 287-293.
17. **Praca zbiorowa. 1985:** Poradnik piwowara, Nr 7, Wyd. NOT Sigma, Warszawa, 11-27.
18. **Ramazanow S. 2010:** Innovative Technologies of anticrisis management for production – Transport Complex. TEKA Kom. Mot. i Energ. Roln. PAN – Odz. Lublin, T. 10b, 120-124.
19. **Slobodomyuk M. Nechaev G. 2010:** The evaluation technique efficiency development. TEKA Kom. Mot. i Energ. Roln. PAN – Odz. Lublin, T. 10b, 162-170.
20. **Wesołowska-Janczarek M. , Mikos H. 1995:** Zbiór zadań ze statystyki matematycznej. Wyd. AR w Lublinie, 46-122.

ZASTOSOWANIE TESTÓW ISTOTNOŚCI W LOGISTYCE MATERIAŁOWEJ PRZEDSIĘBIORSTWA SPOŻYWCZEGO W ASPEKCIE PROCESU TECHNOLOGICZNEGO PRODUKCJI

Streszczenie: W artykule przedstawiono problemy związane z puszkami do piwa w produkcji piwa na etapie podnoszenia i napełniania, a także problemy związane ze „znikaniem" w procesie technologicznym. Ocena jakości procesu została przeprowadzona w oparciu o testy statystyczne.

Słowa kluczowe: firma spożywcza, proces technologiczny, nalewanie piwa, testy statystyczne

TEKA. COMMISSION OF MOTORIZATION AND ENERGETICS IN AGRICULTURE – 2013, Vol. 13, No. 1, 205–208

Use of modern techniques to determine porosity of corps casting made of copper alloy

Z. Żółkiewicz[1], A. Gwiżdż[1], S. Pysz[1], M. Nowak[2]

[1,2]Foundry Research Institute, 73 Zakopianska St., 30-418 Krakow, Poland, kzs@iod.krakow.pl
'Fabryka Armatur JAFAR S.A.', 12 Kadyiego St., 30-200 Jasło

Received January 17.2013; accepted March 14.2013

Summary. In the article switched modern methods of analysis system flooding determination type and place of defects in non experimental. Using computer support system Magma Soft defined flow over metal in the form of decomposition temperature, successive phases freezing and cooling metal foundry defects and the location in together corps DN 150. The results have been used to develop simulation technology performed by casting corps DN 150.
Key words: cast, defects, computational simulation, technology.

INTRODUCTION

The simulation processes, using computer programs, is to develop optimal technology implementation casting, with simultaneous eliminating defects foundry. Simulate how flooding test cast has been carried out at an angle saturation forms by verifying the accuracy metal, of knots thermal, effectiveness of their power in areas with will together in which may occur defects type: bladders gas, porosity. For the analysis was used computer support programmes Magma Soft. In order to avoid errors in the design technologies comply with the castings, shortening the time, cost savings investigation for optimal technological solutions, computer simulation process has been carried out flooding, freezing and cooling simulating the technological process has been carried out for founded i.e.: Manner of implementation:

– system flooding,
– plastic casting,
– temperature flooding,
– parameters thermo-physical material form.

The computer simulation de corps casts valve DN 80 and DN 150 (Figure 1) made of bronze working in the environment active chemically, from which is required to pressure tightness 1, 6MPa, at the temperatures from -20 °C to 20 °C.

a)

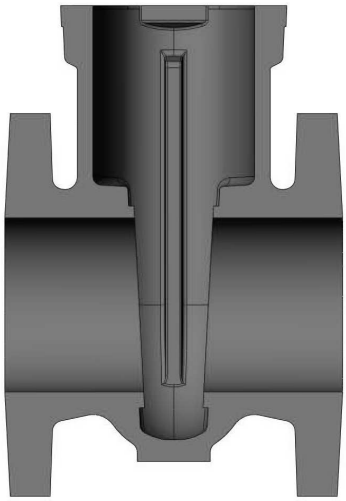

b)

Fig. 1. Corps Valle, a – 3D, b – casting

Via simulation foundry processes occurring in window form has been defined:
- system including the determination flooding movement by metal channels and closing the generation cavity forms, speed over metal in the initial phase,
- freezing, cooling, power supply castings, cooling casting specifying the alterations phase, phenomena contract and the related problems internal defects (porosity),
- stresses and strains and possible cracks both hot and cold,
- shaping bronze structure and its impact on property in the casting of stress in the construction corps, lids and their impact on their integrity.

In the article discussed the impact of flooding in the presence defects in together body DN 150. For the analysis was programme computer simulation MAGMA SOFT.

METHODS RESEARCH

In foundry operations, in the area there is a number of phenomena physico-chemical which affect the process of casting, on its quality [4, 5, 6, 7, 8,10, 13, 14, 17, 19, 20, 21, 22, 24].

An undertaking which carries out repetitive shapes casting, with the same plastic and of the same weight may overcome technological process of implementing them, and to limit the quantity defects.

Once the range of the enlargement cast is growing threat presence carried out in a series non defects the mastery of which is an, sometimes time consuming. Foundry defects may be disclosed in subsequent stages of production:
- after casting,
- carrying mechanical treatment,
- assembly valves.

Therefore the technological process analysis was carried out using:
- classic methods to evaluate quality casting, depicting type defects, place of its occurrence,
- programme computer simulation.

Jafar S.A. unveiled research establishment in the valve body castings DN 80 and DN 150 made of bronze, is intended to work in an environment of increased aggressiveness (chemical sea water). For casts of bodies program was carried out with regard to computer simulation process flow, freezing and metal cools down and broken down by risk areas by the existence of casting defects and voids porosity. Simulations were performed with the help of MAGMASOFT. He wide-ranging analysis and thermal hydraulic processes occurring in space molding. It has enabled a complete study phenomena transiting during the process of casting by:
- predicting quality castings (identify the occurrence of defects and position: i am molding porosity,
- predicting effects of introducing different technologies,
- optimization of filler caps,
- verification of, Shape and layout tabs and related to the increase in yield metal,
- document production process.

Analysis included the process of flow in the metal filler and mold in the bay. By examining metal flow rate verified the flooding and filling geometry as well as its location and layout. The freezing metal after the flooding was fully described by temperature distribution. The primary criterion used in assessing body casting is porosity.

An analysis defects casting has led to the determination of the impact the technological process parameters of their presence. This allows the defects specify the type and location of its place.

This makes it easier to take a decision aimed at implementing casting technological changes parameters or laying down a repair casting so as to achieve implied tightness casting. Freezing analysis (temperature drop in metal on the temperature solidusu) and cooling (lowering the temperature below casting temperature solidusu) has been carried out primarily for directional freezing and speed these solid phase in wall casting.

These direction the solid phase takes place in the first period freezing mainly from the forms which is the external wall casting. As a consequence uneven distribution temperature in the entire together (Fig. 2, 3), in the various elements

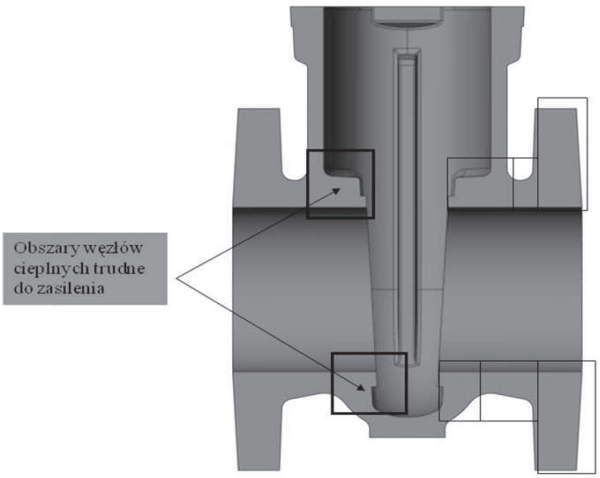

Fig. 2. Areas at risk bringing castingporosity

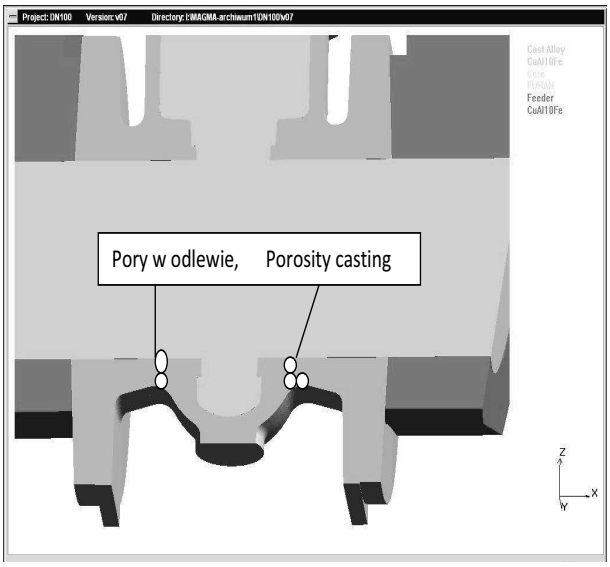

Fig. 3. The expected porosity casting

related to the nierównomierną casting wall thickness, presence knots thermal, there are significant discontinuities or even porosity.

They will be located mainly in the internal walls casting on an overall distribution temperature during flooding, freezing and cooling significant impact on the distribution of this temperature fisheries metal in the form and the way thermal power knots casting (Figure 4).

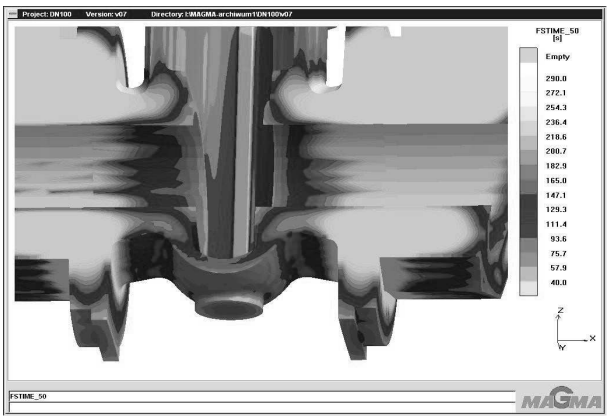

Fig. 4. Computer simulation casting corps power

Distribution of this temperature the liquid phase in together shows that after a specified time temperature metal falls, metal in together is, in together there are places where metal is still liquid, there is this phenomenon loss of power certain elements casting (Fig. 4).

Made simulation flooding, power supply, freezing and cooling casting corps DN 150 showed places at which there is discontinuity material (Figure 5, 6, 7).

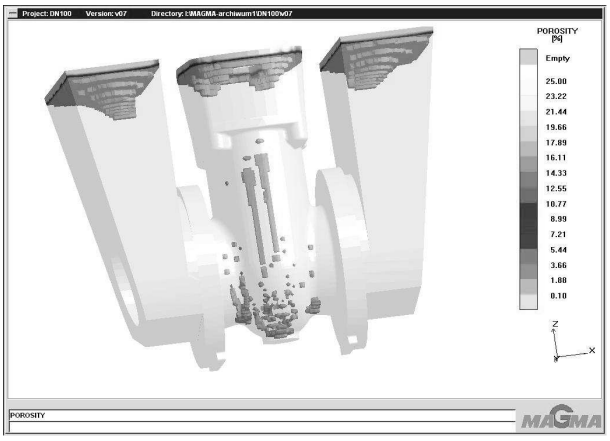

Fig. 5. The location porosity together in body material in the density of 0,1%

Studies have found full fitness used methods of research. In the tests have been used option library data thermo-physical parameters. Test system flooding, freezing and cooling casting corps has shown together in place in which there is a threat of defects iron porosity.

Their elimination can be achieved by changing technology or their repair [1, 2, 3, 12, 15, 16, 18, 23, 25, 27].

Computer simulation has been carried out for various options for casting flooding and freezing. On the basis of

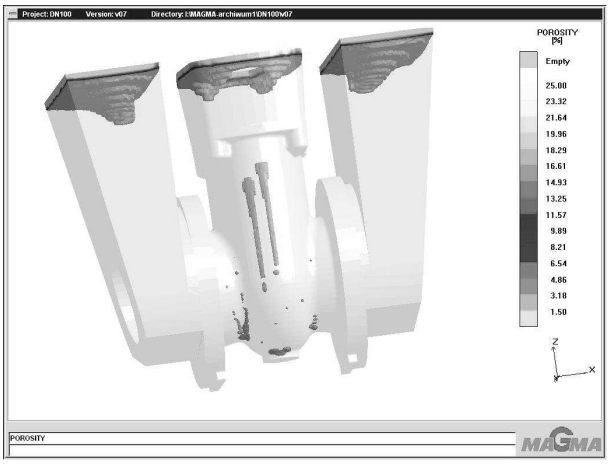

Fig. 6. The location porosity together in body material in the density of 1%

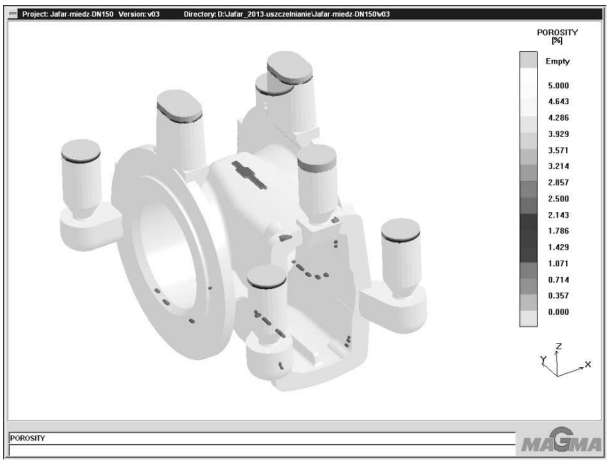

Fig. 7. The porosity in the casting body when technology changes

defects in the test simulations have been applied for position of casting. After examination of the results of simulation decision was taken that the proposed technology provides casting castings without defects

CONCLUSIONS

A simulation casting comply with the technological process has shown that there are in place together with porosity material. Carried out the analysis has led to the risks which creates adopted technology casting.

Enabled t for the development of technology modified castings corps DN 150 while developing methods repair porosity castings corps.

REFERENCES

1. **Allison J.E., 2010**: Integrated Computational Materials Engineering (ICME) for Mg: International Pilot Project. Ford Motor Company, April
2. **Allison J., Backman D., Christodoulou L., 2006**: Integrated Computational Materials Engineering: A New

Paradigm for the Global Materials Profession, JOM, Nov.25-27.
3. **Baliński A., Wisła-Walsh E. 2008**. Fly ash from hard coal combustion as a ceramic base material of moulding sands. "Polish Journal of Environmental Studies," vol.14, no.3 A, 44-
4. **Gazda A., Homa M. 2009**, Określenie przewodnictwa cieplnego wybranych gatunków żeliwa sferoidalnego za pomocą pomiaru przewodnictwa temperaturowego metodą laser-flash. Prace Instytutu Odlewnictwa, t. XLIX, nr 2, 5-18, "Archives of Foundry Engineering", vol.8, no 2, 5-8
5. **Gazda A., Żółkiewicz Z. 2012**. Thermal and physical properties of some refractory layers used in lost foam technology. TEKA , V. 12, 47-
6. **Gazda A., 2007**: Kompleksowa baza danych właściwości termofizycznych metali ,stopów oraz materiałów formierskich i ceramicznych aspekcie projektowania odlewów. Innowacje w Odlewnictwie. Część I. Instytut Odlewnictwa. Kraków,311
7. **Gwiżdż A ., Żuczek R. ,Nowak M.: 2012**. Analiza stanu naprężeń w konstrukcjach odlewu korpusu, pokrywy i klina zasuw klinowych do gazu. Praca I.ODL. Tom LII, nr 4
8. **Gwiżdż A., Żuczek R.: 2012**. Opracowanie modelu 3D zasuw klinowych do gazu, analiza stanu naprężeń w konstrukcjach odlewu korpusu, pokrywy i klina. Sprawozdanie z zadania nr 2 projektu celowego CI NOT ROW-III-209.
9. **Gwiżdż A., Małysza M., Nowak M.: 2012**. Badania modelowe i analiza rozpływu metalu I krzepnięcia w formach odlewniczych. Sprawozdanie z zadania nr 4 projektu celowego CI NOT ROW-III-209
10. **Hindurao D.V., Chavan D.S. 2011**: Optimization of 16" plug valve body using FEA and Experimental Stress analysis method, International Journal of Mechanical Engineering, Vol. 1, No. 1, 79-83
11. **Ignaszak Z., Popielarski. P., Hajkowski, Prunier J.B., 2012**: Problem of Acceptability of Internal Prosity in Semi-Fisnished Cast Product as New Trend –"Tolerance of Damage" Present in Modern Desing Offise. Defect and Diffusion Forum Vols.326-328 (2012) Online available since 2012 Apr /26 at www.sientific.net (2012)Trans Tech Publications, Switzerland. doi:10.4028/www.sientific.nrt.DDF.326-328.612
12. **Karwiński A., Żółkiewicz Z. 2011**. Application of Modern Ecological Technology Lost Foam For The Implementation Of Machinery. TEKA , V. XIC, Lublin
13. **Maj M., Piekło J., 2009**: MLCF-an optimised program of low – cycle fatigue test to determine mechanical properties of cast materials. Archives of Metallurgy and Materials, Vol. 54, No. 2, 393-397
14. **Z. Maniowski , M. Młyński , Z. Sierant, Z. Żółkiewicz. 2010**. Selected aspects of the piece production of iron alloy castings in terms of their environmental impact. Archives of Foundry Engineering. V. 10, nr. 3, 163-166
15. **Pirowski Z., Gościanski M. 2009**. Construction and technology of production of casted shares for rotating and firld plougs, TEKA , vol. . IX, 231-239
16. **Pirowski Z. 2011**. Aplication of Nickiel Superalloys On Castings For Conventional Energy Equimpment Items. TEKA , vol. . XIC, 246-255
17. Problem empirycznych parametrów pre-processingu na przykładzie symulacji krzepnięcia i zalewania odlewów z żeliwa sferoidalnego. 2007: Innowacje w Odlewnictwie .Część I. Instytut Odlewnictwa. Kraków, 301
18. **Pytel A., Stefański Z. 2011**. An Inovattive And Environmentally Safe Method To Manufacture High-Quality Iron Castings For Possible Use As elements Of Agriculture Machines. TEKA , vol. . XIC, 256-263
19. **Pysz S., Żółkiewicz Z., Żuczek R., Maniowski Z., Sierant Z., Młyński M. 2010**. Badanie symulacyjne warunków wypełnienia wnęki formy ciekłym metalem w technologii modeli zgazowywanych. Transactions of the Foundry Research Institute. Volume L, nr 3, 27-37
20. **Pysz S., Karwiński A., Czekaj E. 2009**. An analyysis of the technical state of a stater Rusing the hall efekt-part II, TEKA , vol.. IX, 251-258
21. **Warrick R.J., Althoff P., Druschitz A.P., Lemke J.P., 2000**: Zimmerman K.: Austempered Ductile Iron Castings for Chassis Applications. Society of Automotive Engineers, 2000 World Congress, Detroit, March 6–9,.
22. **Wilk J., Żółkiewicz Z. 2006**. Detrmination of optimum Technology in Respect of the Required Values of Casting Quality Parameters by Aplication of the Weighted Variables Metric. Materials Enginering, vol. 13, nr. 3, 89
23. **Wilk W., Staniewicz-Brudnik B., Żółkiewicz Z.. 2011**. Współczesne tendencje w obróbce ściernej wyrobów odlewanych. INNOWATIVE MSANUFACTURING TECHNOLGY, Kraków, 117-136
24. **Wowra S., 2010**: Obliczenia równoległe w ANSYS. Konferencja ANSYS – Symulacja 2010, Tarnowskie Góry,.
25. **Żółkiewicz Z., Żółkiewicz M. 2009**. Lost Foam Process – The Chance For Industry. TEKA , 2009, vol. IX, 431-436
26. **Żółkiewicz Z., Żółkiewicz M. 2010**. Characteristic properties of materials for evaporative patterns. Archives of Foundry Engineering vol. 10, Special Issue, 3, 289-292
27. **Żółkiewicz Z., Jankowski W., 2012**. Badanie właściwości filtracyjnych doświadczalnych warstw ceramicznych. Transactions of the Foundry Research Institute. Kraków T. LII, 51-62

WYKORZYSTANIE NOWOCZESNYCH TECHNIK DO OKREŚLENIA POROWATOŚCI ODLEWU KORPUSU WYKONANEGO Z STOPU MIEDZI

Streszczenie. W artykule przestawiona nowoczesne sposoby analizy systemu zalewania z określaniem rodzaju i miejsca występowania wad w odlewach doświadczalnych . Wykorzystując system wspomagania komputerowego Magma Soft określono przepływ strugi metalu w formie, z rozkładem temperatury, kolejne fazy krzepnięcia i stygnięcia metalu oraz umiejscowienie wad odlewniczych w odlewie korpusu DN 150. Wyniki symulacji wykorzystano przy opracowaniu technologii wykonaniu odlewu korpusu DN 150.

Słowa kluczowe: odlew, wady, symulacja komputerowa, technologia.

TEKA. COMMISSION OF MOTORIZATION AND ENERGETICS IN AGRICULTURE – 2013, Vol. 13, No. 1, 209–214

Methods of porosity elimination from valve corps casting made of bronze

Z. Żółkiewicz[1], A. Gwiżdż[1], S. Pysz[1], M. Nowak[2]

[1,2]Foundry Research Institute, 73 Zakopiańska St., 30-418 Krakow, Poland, kzs@iod.krakow.pl
Fabryka Armatur JAFAR S.A., 30-200 Jasło ul. Kadyiego 12

Received January 17.2013; accepted March 14.2013

Summary. Currently an increase is observed in quality requirements from manufactured products and installations. This also applies to castings. One of methods of improving cast quality is using modern porosity sealing methods during the technological process. This method has found wide use in the world in order to not only improve the working parameters of foundry operations, but also the quality of welding, sintering, electronics, artificial materials. There are industries where 100% of the produced cast is sealed. The article shows the method of leak-tightness improvement in valve castings working in extreme conditions e.g. extreme temperatures or adverse chemical environment.
Key words: leak-tightness, defects, castings repair, sealant.

INTRODUCTION

In iron, which is not made of non-ferrous metals and alloys, there are often defects such as foundry losses, gas bubbles, porosity, and others which in extreme cases lead to castings rejection.

This problem is especially significant during working in extreme conditions where, e.g., resistance is required to:
– increased pressure, e.g. 1, 6 MPa,
– temperature (increased or reduced),
– chemical reagents, sea water.

Since these defects often are detected after additional treatment operations such as removal, heat treatment, the costs incurred adversely affect the company budget, by increasing costs of its activities.

Therefore, technical staff of the companies are seeking to find methods of repairing of those equipment items. The application of repair casting is required to obtain proper technical economic and aesthetic properties [1, 2, 3, 6, 7, 8, 9].

REPAIR METHODS

Currently an increase is observed in quality requirements from manufactured products and installations, which also applies to castings. One way of improving cast quality is application of modern methods, such as sealing porosity repair, in the implemented technological process.

The above-mentioned method has found wide use in the world, not only to improve the working parameters of foundry operations, but also the quality of welding, sintering, electronics, artificial materials. There are industries where during the technological process 100% of the product is being sealed. Currently an increase is observed in quality requirements posed in practice, not only for iron. There are various methods of sealing repair in castings concerning faults caused by gas porosity, cracks in the cold and other defects affecting the cast's seal-tightness [10, 11, 12, 13, 14].

Health hazardous industrial elements of casts are under control, using several tests, in order to ensure the required foundry quality. Part of quality requirements are determined by the national standards and part of them by the European norms.

To meet all the requirements, the standards should be observed not only in quality of castings, quality of the hazardous connective elements, leak-tightness and productivity, but also in a number of other aspects [4, 5, 15, 16, 17, 18, 19].

The research was factory-based (S.A. is a leading producer in the industrial fittings export).

In the experiments (for a certain group produced castings were made of copper alloys with the technical conditions reception), the required technical leak-tightness was sought.

Tests were carried out on sample castings to show leak-tightness of a certain percentage of castings, due to lack of porosity defects occurrence.

The world's leading solutions that have been adopted in the casts production involve the method which is required for tightness of castings, where the process of production is solved so that the technological process in the cycle of castings is amended in order to apply sealing-repair process in 100% castings.

Tightness test is carried out after the carried out repair on the randomly selected casts. The sealing method involves the

introduction deep into the casting wall of synthetic sealants which have been effective so far in the sealing of all the leeks in a casting and providing its seal-tightness required by the technical conditions of acceptance.

For the repair different sealants are used, prepared on the basis f epoxy resins, polyurethane, polyester, anaerobic [20, 21, 22, 23, 24].

The sealant may be forced deep into the casting wall in a mechanical, manual or enforced (increased pressure, vacuum) way.

There are many producers of sealants and devices for sealing.

Their parameters are different from the sustainability of the sealing, within the scope resistance to chemical agents, increased or reduced temperature, the type of chemical composition preparation way, parameters of application, the range of temperatures.

Some manufacturers shall ensure the system of automatic control of the sealing process.

The sealing process as well as the applied substances should be safe for the worker and the environment.

In foundries which have not undergone the above-described process (Figure1) there are leak defects caused by the presence of transverse porosity sections in wall casting. Repair of a cast working in increased pressure conditions is effective when gas pores sizes are small.

Together with an increase in pore size, bubbles and gas pressure are spoiling the effectiveness of castings repair by impregnation method.

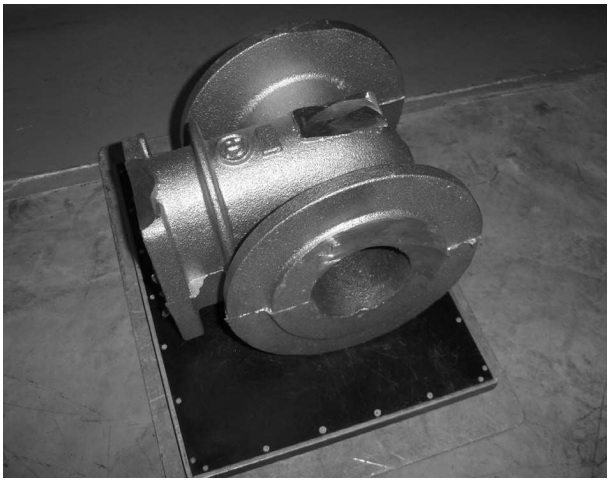

Fig. 1. Cast of corps DN 150 during preparation for an X-ray

In practice, not only for iron, there are various methods of sealing repair, in case of porosity presence caused by gas, cracks in the cold and under high pressure or other defects of castings affecting their seal-tightness.

The basic methods of repair can be:

– mechanical; (e.g. welding, reaming, high etc.). These methods do not ensure seal-tightness of casting affected by the presence porosity. They are applicable in articles where seal- tightness of casting is not required .
– chemical; (impregnation, diffusion, adsorption, application, immersion, necessitated by the sealants leaks in the area). These are methods recommended for the repair of leak defects in castings. These methods of casting repair are the so-called surface (wearing, immersion) ones, which do not fully ensure the required tightness of casting, the sealant does not fully get to the internal parts, on the surface of casting there is an additional layer cover which may not be accepted by the casting manufacturer.
– replenishment of losses, (for large losses). Used for the repair of large losses, especially occurring on surfaces of casting. Used for the commercial and aesthetic reasons. This method is not recommended for sealing of porosity castings requiring the determined parameters of seal-tightness [25, 26].

Choice of the repair method is dependent on technical requirements and economic considerations.

LEAK TEST OF CASTINGS

Factory “JAFAR” is a constructor, the producer of castings and valves which work in extreme conditions. Elements of valves are made of iron, bronze, brass. These are the water valves, gas, air, or valves on chemical agents. They work in the conditions of increased pressure, temperature or chemically active environment. The conditions of their technical reception statement indicate that they may not have defects involving external or internal leakage which eliminate devices part of which is formed by a cast. When developing new construction of valves, research activities were carried out related to development of assumptions of the technical and technological research using the methods of computer simulation. Acknowledgement of the adopted assumptions is their technical check in the current conditions. In drawing up of the technical assumptions, technological experiments on DN 80 valves and DN 150 computer simulations process were carried out on liquid metal movement in the form of seats which were at risk at porosity defects (Figure 2, 3) [27].

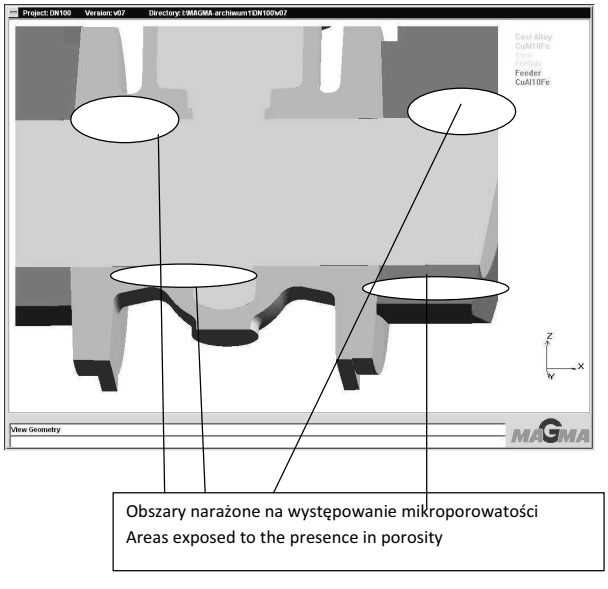

Fig. 2. Areas of porosity in the cast of valve corps

Areas in which the withdrawal is planned of foundry defects, gaseous bubbles, leaks, are characterized with areas of a variable thickness.

We have developed a number of solutions for technical and technological methods of castings repair. The chemical composition of sealants and construction of equipment used to process the sealing is the restricted information on the part of manufacturer.

After computer simulation and analysis, the carried out valve corps casts were tested in the candling position x (Figure 4) and the position to test leak of casting (Figure 5).

The obtained results were used to make a decision for the repair of defective cast by the method of sealing. (Figure 6). One of the principal technical solutions which are currently used in many countries for sealing castings was applied to the equipment, usually consisting of several tanks in which there are:

– process of preparing,
– forcing the sealants deep into the casting wall (high pressure, vacuum),
– chemical, thermal hardening
– washing
– cooling and removing cast from tank,
– technical inspection.

CONCLUSIONS

Sealing devices and technologies have many advantages but they also have defects.

The scope of these devices for the repair of casts is limited by their dimensions, quantity of produced castings (size series), diverse shapes and dimensions and the nature and characteristics plastic castings sealants, including:

– mechanical and thermal strength,
– resistance to chemical reagents' impact,
– ability to penetrate deep into the casting wall,
– resistance to the leaking of casting,
– bonding (reinforce) sealants,
– the ability and the way of the removal of external surface sealants from castings.

In the last period the knowledge has increased of the pros of the sealing process, its quality (pros and cons) and the opportunities for the application of sealants. The sealing process is now a tool to improve the quality of the manufactured products.

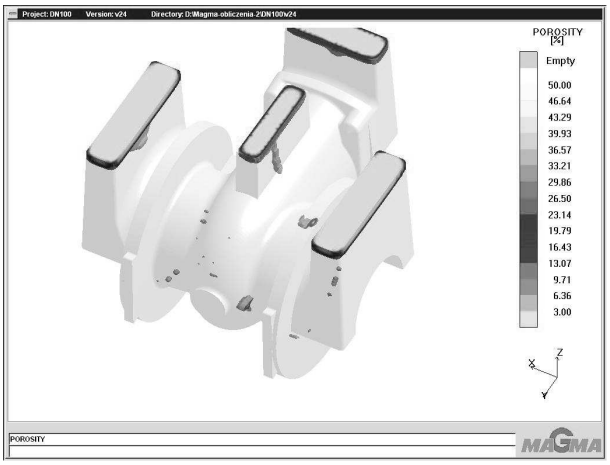

Fig. 3. The predicted sites of porosity in the valve corps cast DN 80

Fig. 5. Test of seal-tightness of the valve (in water)

Fig. 4. Corps cast DN 150 in the X-ray stand

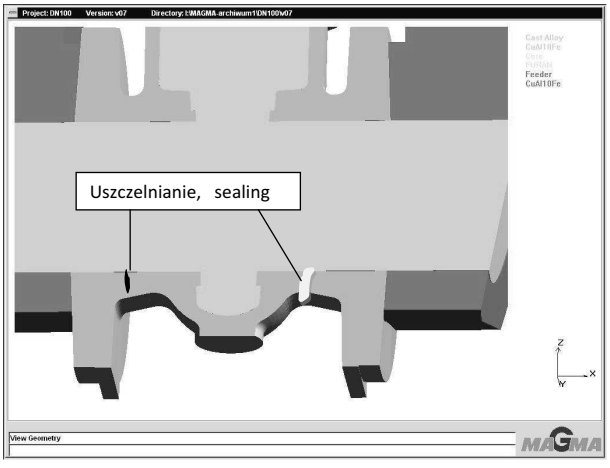

Fig. 6. Introduction of sealants deep into the wall of valve corps cast

REFERENCES

1. **Allison J.E., 2010.** Integrated Computational Materials Engineering (ICME) for Mg: International Pilot Project. Ford Motor Company, April.
2. **Bogacz T., Zbigniew Maniowski Z., Młyński M., Pysz S., Żółkiewicz Z. 2002.** Application of Computer Simulation at Metalodlew S.A. to aid the use of Expendable Polystyrene Patterns Used in Production of Castings from Ferrous Alloys. Acta Metallurgica Slovaca T. 8, nr. (1/2).
3. **Baliński A., Wisła-Walsh E. 2008.** Fly ash from hard coal combustion as a ceramic base material of moulding sands. "Polish Journal of Environmental Studies," vol.14, no. 3A.
4. **Gazda A., Homa M. 2009.** Określenie przewodnictwa cieplnego wybranych gatunków żeliwa sferoidalnego za pomocą pomiaru przewodnictwa temperaturowego metodą laser-flash. Prace Instytutu Odlewnictwa, t. XLIX, nr 2, s. 5-18, "Archives of Foundry Engineering", vol.8, no 2.
5. **Gazda A., Żółkiewicz Z. 2012.** Thermal and physical properties of some refractory layers used in lost foam technology. TEKA , V. 12, Lublin.
6. **Gazda A., 2007:** Kompleksowa baza danych właściwości termofizycznych metali ,stopów oraz materiałów formierskich i ceramicznych aspekcie projektowania odlewów. Innowacje w Odlewnictwie. Część I. Instytut Odlewnictwa. Kraków.
7. **Gwiżdż A ., Żuczek R. ,Nowak M. 2012.** Analiza stanu naprężeń w konstrukcjach odlewu korpusu, pokrywy i klina zasuw klinowych do gazu. Praca I.ODL. Tom LII, nr 4.
8. **Gwiżdż A., Żuczek R.:** Opracowanie modelu 3D zasuw klinowych do gazu, analiza stanu naprężeń w konstrukcjach odlewu korpusu, pokrywy i klina. Sprawozdanie z zadania nr 2 projektu celowego CI NOT ROW-III-209/2012.
9. **Gwiżdż A., Małysza M., Nowak M. 2012.** Badania modelowe i analiza rozpływu metalu I krzepnięcia w formach odlewniczych. Sprawozdanie z zadania nr 4 projektu celowego CI NOT ROW-III-209.
10. **Hindurao D.V., Chavan D.S. 2011.** Optimization of 16" plug valve body using FEA and Experimental Stress analysis method, International Journal of Mechanical Engineering, Vol. 1, No. 1.
11. **Ignaszak Z., Popielarski P., Hajkowski J., Prunier J.B. 2012.** Problem of Acceptability of Internal Prosity in Semi-Fisnished Cast Product as New Trend –"Tolerance of Damage" Present in Modern Desing Offise. Defect and Diffusion Forum Vols. 326-328 (2012) Online available since 2012 Apr /26 at www.sientific .net (2012)Trans Tech Publications, Switzerland. doi:10.4028/www.sientific.nrt.DDF.326-328.612.
12. **Karwiński A., Żółkiewicz Z. 2011.** Application of Modern Ecological Technology Lost Foam For The Implementation Of Machinery. TEKA, V. XIC 91-99, Lublin.
13. **Maj M., Piekło J., 2009.** MLCF-an optimised program of low – cycle fatigue test to determine mechanical properties of cast materials. Archives of Metallurgy and Materials, Vol. 54, No. 2.
14. **Madej W., Żółkiewicz Z., Maniowski Z., Pysz S., Milklaszewski J. 2002.** Simulation of the Feeding Process for Selected Castings of Brake Inserts Used in Railway System**.** Acta Metallurgica Slovaca T. 8, nr. (1/2).
15. **Z. Maniowski , M. Młyński , Z. Sierant, Z. Żółkiewicz. 2010.** Selected aspects of the piece production of iron alloy castings in terms of their environmental impact. Archives of Foundry Engineering. V. 10, nr. 3.
16. **Pirowski Z., Gościanski M. 2009.** Construction and technology of production of casted shares for rotating and firld plougs, TEKA , vol. IX.
17. **Pirowski Z. 2011.** Aplication of Nickiel Superalloys On Castings For Conventional Energy Equimpment Items. TEKA , vol. XIC.
18. Problem empirycznych parametrów pre-processingu na przykładzie symulacji krzepnięcia i zalewania odlewów z żeliwa sferoidalnego. 2007: Innowacje w Odlewnictwie .Część I. Instytut Odlewnictwa. Kraków.
19. **Pytel A., Stefański Z. 2011.** An Inovattive And Environmentally Safe Method To Manufacture High-Quality Iron Castings For Possible Use As elements Of Agriculture Machines. TEKA , vol. XIC.
20. **Pysz S., Żółkiewicz Z., Żuczek R., Maniowski Z., Sierant Z., Młyński M. 2010.** Badanie symulacyjne warunków wypełnienia wnęki formy ciekłym metalem w technologii modeli zgazowywanych. Transactions of the Foundry Research Institute. Volume L, nr 3.
21. **Pysz S., Karwiński A., Czekaj E. 2009.** An analyysis of the technical state of a stater Rusing the hall efekt--part II, TEKA , vol. IX.
22. **Warrick R.J., Althoff P., Druschitz A.P., Lemke J.P. 2000:** Zimmerman K.: Austempered Ductile Iron Castings for Chassis Applications. Society of Automotive Engineers, 2000 World Congress, Detroit, March 6–9.
23. **Wilk J., Żółkiewicz Z. 2006.** Detrmination of optimum Technology in Respect of the Required Values of Casting Quality Parameters by Aplication of the Weighted Variables Metric. Materials Enginering, vol. 13, nr. 3.
24. **Wilk W., Staniewicz-Brudnik B., Żółkiewicz Z. 2011.** Współczesne tendencje w obróbce ściernej wyrobów odlewanych. INNOWATIVE MSANUFACTURING TECHNOLGY. Kraków.
25. **Wowra S., 2010:** Obliczenia równoległe w ANSYS. Konferencja ANSYS – Symulacja 2010, Tarnowskie Góry.
26. **Żółkiewicz Z., Pysz S., Madej W., Wawrowska-Tomaszewska M. 2000.** An efekr of the metal mould pouring technique on porosity elimination in test castings. PAN, Krzepnięcie Metali i Stopów Rocznik 43, nr 2.
27. **Żółkiewicz Z., Jankowski W., 2012.** Badanie właściwości filtracyjnych doświadczalnych warstw ceramicznych. Transactions of the Foundry Research Institute. Kraków T. LII.

METODY ELIMINACJI POROWATOŚCI ODLEWU KORPUSU ZAWORU WYKONANEGO Z BRĄZU

Streszczenie. Aktualnie obserwuje się tak w kraju i za granicą wzrost wymagań jakościowych stawianym wytwarzanym produktom, urządzeniom. Dotyczy to również odlewów. Jedną z metod poprawy jakości odlewów jest wprowadzanie do procesu technologicznego ich wykonywania, nowoczesnych metod uszczelniania mikroporowatości. Metoda ta znalazła w świecie szerokie zastosowanie do poprawy własności, parametrów pracy nie tylko w odlewnictwie ale w miejscach spawanych, w elementach spiekanych, elektronice , mechanice, tworzywach sztucznych. Są gałęzie przemysłu gdzie 100% wyrobów, odlewów jest uszczelniane. W artykule przedstawiono metodę poprawy szczelności odlewów zaworów pracujących w ekstremalnych warunkach; temperatura, środowisko chemiczne.

Słowa kluczowe: szczelność, wady, naprawa odlewów, szczeliwo

Table of contents

List of the Reviewers

1. U. A. Abdulgazis
2. Kazimierz Dreszer
3. Mieczysław Dziubiński
4. Andrzej Kornacki
5. Elżbieta Kusińska
6. Andrzej Kusz
7. Andrzej Marciniak
8. Janusz Mysłowski
9. Ignacy Niedziółka
10. Mariusz Szymanek
11. Wojciech Tanaś
12. Janusz Wojdalski
13. Daniela Żuk

Editors of the „TEKA" quarterly journal of the Commission of Motorization and Energetics in Agriculture would like to inform both the authors and readers that an agreement was signed with the Interdisciplinary Centre for Mathematical and Computational Modelling at the Warsaw University referred to as "ICM". Therefore, ICM is the owner and operator of the IT system needed to conduct and support a digital scientific library accessible to users via the Internet called the "ICM Internet Platform", which ensures the safety of development, storage and retrieval of published materials provided to users. ICM is obliged to put all the articles printed in the "Motrol" on the ICM Internet Platform. ICM develops metadata, which are then indexed in the "Agro" database.

Impact factor of the TEKA quarterly journal according to the Commission of Motorization and Energetics in Agriculture is 3,01 (Vol. 13, No. 1).

GUIDELINES FOR AUTHORS (2013)

The journal publishes the original research papers. The papers (min. 8 pages) should not exceed 12 pages including tables and figures. Acceptance of papers for publication is based on two independent reviews commissioned by the Editor.

Authors are asked to transfer to the Publisher the copyright of their articles as well as written permissions for reproduction of figures and tables from unpublished or copyrighted materials.

Articles should be submitted electronically to the Editor and fulfill the following formal requirements:
- Clear and grammatically correct script in English,
- Format of popular Windows text editors (A4 size, 12 points Times New Roman font, single interline, left and right margin of 2,5 cm),
- Every page of the paper including the title page, text, references, tables and figures should be numbered,
- SI units should be used.

Please organize the script in the following order (without subtitles):
Title, Author(s) name (s), Affiliations, Full postal addresses, Corresponding author's e-mail
Abstract (up to 200 words), Keywords (up to 5 words), Introduction, Materials and Methods, Results, Discussion (a combined Results and Discussion section can also be appropriate), Conclusions (numbered), References, Tables, Figures and their captions

Note that the following should be observed:
An informative and concise title; Abstract without any undefined abbreviations or unspecified references; No nomenclature (all explanations placed in the text); References cited by the numbered system (max 5 items in one place); Tables and figures (without frames) placed out of the text (after References) and figures additionally prepared in the graphical file format jpg or cdr.

Make sure that the tables do not exceed the printed area of the page. Number them according to their sequence in the text. References to all the tables must be in the text. Do not use vertical lines to separate columns. Capitalize the word 'table' when used with a number, e.g. (Table1).

Number the figures according to their sequence in the text. Identify them at the bottom of line drawings by their number and the name of the author. Special attention should be paid to the lettering of figures – the size of lettering must be big enough to allow reduction (even 10 times). Begin the description of figures with a capital letter and observe the following order, e.g. Time(s), Moisture (%, vol), (%, $m^3m^{-3)}$ or (%, gg^{-1}), Thermal conductivity ($W\ m^{-1}K^{-1}$).

Type the captions to all figures on a separate sheet at the end of the manuscript.

Give all the explanations in the figure caption. Drawn text in the figures should be kept to a minimum. Capitalize and abbreviate 'figure' when it is used with a number, e.g. (Fig. 1).

Colour figures will not be printed.

Make sure that the reference list contains about 30 items. It should be numbered serially and arranged alphabetically by the name of the first author and then others, e.g.
7. Kasaja O., Azarevich G. and Bannel A.N. 2009. Econometric Analysis of Banking Financial Results in Poland. Journal of Academy of Business and Economics (JABE), Vol. IV. Nr 1, 202–210.

References cited in the text should be given in parentheses and include a number e.g. [7].

Any item in the References list that is not in English, French or German should be marked, e.g. (in Italian), (in Polish).

Leave ample space around equations. Subscripts and superscripts have to be clear. Equations should be numbered serially on the right-hand side in parentheses. Capitalize and abbreviate 'equation' when it is used with a number, e.g. Eq. (1). Spell out when it begins a sentence. Symbols for physical quantities in formulae and in the text must be in italics. Algebraic symbols are printed in upright type.

Acknowledgements will be printed after a written permission is sent (by the regular post, on paper) from persons or heads of institutions mentioned by name.